



agronomy

Special Issue Reprint

Agricultural Water Conservation

Tools, Strategies, and Practices - Series II

Edited by
Aliasghar Montazar

mdpi.com/journal/agronomy



**Agricultural Water Conservation:
Tools, Strategies, and Practices -
Series II**

Agricultural Water Conservation: Tools, Strategies, and Practices - Series II

Editor

Aliasghar Montazar



Basel • Beijing • Wuhan • Barcelona • Belgrade • Novi Sad • Cluj • Manchester

Editor

Aliasghar Montazar
University of California
Agriculture and Natural
Resources
Holtville
United States

Editorial Office

MDPI
St. Alban-Anlage 66
4052 Basel, Switzerland

This is a reprint of articles from the Special Issue published online in the open access journal *Agronomy* (ISSN 2073-4395) (available at: www.mdpi.com/journal/agronomy/special_issues/agri_water_series2).

For citation purposes, cite each article independently as indicated on the article page online and as indicated below:

Lastname, A.A.; Lastname, B.B. Article Title. <i>Journal Name</i> Year , <i>Volume Number</i> , Page Range.
--

ISBN 978-3-0365-9705-8 (Hbk)

ISBN 978-3-0365-9704-1 (PDF)

doi.org/10.3390/books978-3-0365-9704-1

Cover image courtesy of Aliasghar Montazar

© 2023 by the authors. Articles in this book are Open Access and distributed under the Creative Commons Attribution (CC BY) license. The book as a whole is distributed by MDPI under the terms and conditions of the Creative Commons Attribution-NonCommercial-NoDerivs (CC BY-NC-ND) license.

Contents

About the Editor	vii
Preface	ix
Gaurav Jha, Floyd Nicolas, Radomir Schmidt, Kosana Suvočarev, Dawson Diaz and Isaya Kisekka et al. Irrigation Decision Support Systems (IDSS) for California’s Water–Nutrient–Energy Nexus Reprinted from: <i>Agronomy</i> 2022 , <i>12</i> , 1962, doi:10.3390/agronomy12081962	1
Julia Urquijo-Reguera, María Teresa Gómez-Villarino, David Pereira and Lucia De Stefano An Assessment Framework to Analyze Drought Management Plans: The Case of Spain Reprinted from: <i>Agronomy</i> 2022 , <i>12</i> , 970, doi:10.3390/agronomy12040970	32
Abdullah Açık and Feride Öncan Sümer Foliar Application of Zinc Improves Agronomical and Quality Parameters and Biofortification of Cowpea (<i>Vigna sinensis</i>) under Deficit Irrigation Reprinted from: <i>Agronomy</i> 2023 , <i>13</i> , 1021, doi:10.3390/agronomy13041021	48
Daniela Cea, Claudia Bonomelli, Johanna Mártiz and Pilar M. Gil Response of Potted Citrus Trees Subjected to Water Deficit Irrigation with the Application of Superabsorbent Polyacrylamide Polymers Reprinted from: <i>Agronomy</i> 2022 , <i>12</i> , 1546, doi:10.3390/agronomy12071546	65
Essam F. El-Hashash, Moamen M. Abou El-Enin, Taia A. Abd El-Mageed, Mohamed Abd El-Hammed Attia, Mohamed T. El-Saadony and Khaled A. El-Tarabily et al. Bread Wheat Productivity in Response to Humic Acid Supply and Supplementary Irrigation Mode in Three Northwestern Coastal Sites of Egypt Reprinted from: <i>Agronomy</i> 2022 , <i>12</i> , 1499, doi:10.3390/agronomy12071499	74
Sebastiano Delfine, Violeta B. Velikova and Franco Mastrodonato Soil-Mulching Influence on Spearmint Oil Yield, Ecophysiological Activities and Essential-Oil Content in Rainfed Environment of Southern Italy Reprinted from: <i>Agronomy</i> 2022 , <i>12</i> , 1521, doi:10.3390/agronomy12071521	98
Muhammad Mansoor Javaid, Hussah I. M. AlGwaiz, Hasnain Waheed, Muhammad Ashraf, Athar Mahmood and Feng-Min Li et al. Ridge-Furrow Mulching Enhances Capture and Utilization of Rainfall for Improved Maize Production under Rain-Fed Conditions Reprinted from: <i>Agronomy</i> 2022 , <i>12</i> , 1187, doi:10.3390/agronomy12051187	112
Amanpreet Kaur, Kanwar Barjinder Singh, Rajeev Kumar Gupta, Abed Alataway, Ahmed Z. Dewidar and Mohamed A. Mattar Interactive Effects of Nitrogen Application and Irrigation on Water Use, Growth and Tuber Yield of Potato under Subsurface Drip Irrigation Reprinted from: <i>Agronomy</i> 2022 , <i>13</i> , 11, doi:10.3390/agronomy13010011	128
Yanfei Li, Xianying Feng, Yandong Liu, Xingchang Han, Haiyang Liu and Yitian Sun et al. Research on Hydraulic Properties and Energy Dissipation Mechanism of the Novel Water-Retaining Labyrinth Channel Emitters Reprinted from: <i>Agronomy</i> 2022 , <i>12</i> , 1708, doi:10.3390/agronomy12071708	147

Saurabh Tyagi, Rama Krishna Naresh, Rajan Bhatt, Mandapelli Sharath Chandra, Abdullah A. Alrajhi and Ahmed Z. Dewidar et al. Tillage, Water and Nitrogen Management Strategies Influence the Water Footprint, Nutrient Use Efficiency, Productivity and Profitability of Rice in Typic Ustochrept Soil Reprinted from: <i>Agronomy</i> 2022 , <i>12</i> , 1186, doi:10.3390/agronomy12051186	163
Mohammad Hossein Sedri, Ebrahim Roohi, Mohsen Niazian and Gniewko Niedbala Interactive Effects of Nitrogen and Potassium Fertilizers on Quantitative-Qualitative Traits and Drought Tolerance Indices of Rainfed Wheat Cultivar Reprinted from: <i>Agronomy</i> 2021 , <i>12</i> , 30, doi:10.3390/agronomy12010030	180
Lucía Vera-Herrera, Susana Romo and Juan Soria How Agriculture, Connectivity and Water Management Can Affect Water Quality of a Mediterranean Coastal Wetland Reprinted from: <i>Agronomy</i> 2022 , <i>12</i> , 486, doi:10.3390/agronomy12020486	197
Peirong Lu, Yujie Yang, Wan Luo, Yu Zhang and Zhonghua Jia Numerical Simulation of Soil Water–Salt Dynamics and Agricultural Production in Reclaiming Coastal Areas Using Subsurface Pipe Drainage Reprinted from: <i>Agronomy</i> 2023 , <i>13</i> , 588, doi:10.3390/agronomy13020588	216

About the Editor

Aliasghar Montazar

Dr. Aliasghar Montazar is currently Irrigation and Water Management Advisor at the University of California Cooperative Extension in Southern California. He has a PhD in Irrigation and Drainage; has more than 20 years of research, extension, teaching, and technical consulting experience; and has served in several leadership positions in agricultural water management and irrigation engineering in California and abroad. Before joining University of California in 2011, he was Associate Professor at the Department of Irrigation Engineering, University of Tehran. He runs a well-developed applied research and training program on irrigation and soil-water-related issues. His research interests include sensor-based irrigation management, water conservation, evapotranspiration, and the best irrigation and nutrient management practices.

Preface

Drought and climate change have decreased water availability for agriculture in arid and semiarid regions, and therefore efficiency enhancements in irrigation water management aimed at conserving water are key to adjust to limits in water supply, as well as improve the profitability and sustainability of agricultural production. Agricultural water management tools and practices that reduce water uses with acceptable impacts on crop production are viable strategies to cope with diminished water supplies and generate new sources of irrigation water. This Special Issue focuses on “Agricultural Water Conservation: Tools, Strategies, and Practices”, which aims to bring together a collection of recent cutting-edge research and advancements in applied agricultural water conservation. It provides a broad overview focusing on irrigation decision support systems, drought management plans, deficit irrigation strategies, soil mulching, surface and subsurface drip irrigation, conservation tillage, and optimal water and fertilizer management practices.

Aliasghar Montazar

Editor

Review

Irrigation Decision Support Systems (IDSS) for California's Water–Nutrient–Energy Nexus

Gaurav Jha ^{1,2,*} , Floyd Nicolas ³ , Radomir Schmidt ¹ , Kosana Suvočarev ¹, Dawson Diaz ¹, Isaya Kisekka ^{1,3} , Kate Scow ¹ and Mallika A. Nocco ¹ 

¹ Land, Air, and Water Resources, University of California, Davis, CA 95616, USA

² Agricultural and Technology Education, College of Agriculture, Montana State University, Bozeman, MT 59715, USA

³ Biological and Agricultural Engineering, University of California, Davis, CA 95616, USA

* Correspondence: gjha@ucdavis.edu

Abstract: California has unsustainable use of agricultural water and energy, as well as problems of severe drought, nitrate pollution and groundwater salinity. As the leading producer and exporter of agricultural produce in the United States, 5.6 percent of California's energy is currently used for pumping groundwater. These problems and new regulatory policies (e.g., Sustainable Groundwater Management Act, Irrigated Lands Regulatory Program) pressure growers to schedule, account and maintain records of water, energy and nutrients needed for crop and soil management. Growers require varying levels of decision support to integrate different irrigation strategies into farm operations. Decision support can come from the public or private sector, where there are many tradeoffs between cost, underlying science, user friendliness and overall challenges in farm integration. Thus, effective irrigation management requires clear definitions, decision support and guidelines for how to incorporate and evaluate the water–nutrient–energy nexus benefits of different practices and combinations of practices under shifting water governance. The California Energy Commission-sponsored Energy Product Evaluation Hub (Cal-EPE Hub) project has a mission of providing science-based evaluation of energy-saving technologies as a direct result of improved water management for irrigation in agriculture, including current and future irrigation decision support systems in California. This project incorporates end-user perceptions into evaluations of existing decision support tools in partnership with government, agricultural and private stakeholders. In this article, we review the policy context and science underlying the available irrigation decision support systems (IDSS), discuss the benefits/tradeoffs and report on their efficacy and ease of use for the most prevalent cropping systems in California. Finally, we identify research and knowledge-to-action gaps for incorporating irrigation decision support systems into new incentives and requirements for reporting water and energy consumption as well as salinity and nitrogen management in the state of California.

Keywords: food–water–energy nexus; nitrate leaching; precision agriculture; water productivity; irrigation management; soil moisture



Citation: Jha, G.; Nicolas, F.; Schmidt, R.; Suvočarev, K.; Diaz, D.; Kisekka, I.; Scow, K.; Nocco, M.A. Irrigation Decision Support Systems (IDSS) for California's Water–Nutrient–Energy Nexus. *Agronomy* **2022**, *12*, 1962. <https://doi.org/10.3390/agronomy12081962>

Academic Editor: Aliasghar Montazar

Received: 6 July 2022

Accepted: 12 August 2022

Published: 19 August 2022

Publisher's Note: MDPI stays neutral with regard to jurisdictional claims in published maps and institutional affiliations.



Copyright: © 2022 by the authors. Licensee MDPI, Basel, Switzerland. This article is an open access article distributed under the terms and conditions of the Creative Commons Attribution (CC BY) license (<https://creativecommons.org/licenses/by/4.0/>).

1. Introduction

Agricultural production in California includes the cultivation of approximately 400 crops accounting for one-third of vegetable and two-thirds of fruit and nut production in the United States [1]. According to California Agricultural Production Statistics (2019), this agricultural abundance makes California a leading US state accounting for over 13% of the country's total value in agricultural production. Some of California's leading crops include almonds, grapes, strawberries, pistachios, lettuce, walnuts and processing tomatoes [1]. In order to produce these crops for export across the country and other parts of the world, great amounts of water, fertilizer and energy are used. In California, agricultural water

use represents one-fifth of the electricity consumed for water use and four percent of total electricity consumption annually [2]. Approximately 75–80% of the total water pumped is used to irrigate three million hectares throughout the state [3,4]. The majority of the water and energy consumption is during the summer growing season (June to August), relying on groundwater that uses between 496 to 1750 Megajoules per Megaliter of water [5]. Declines in aquifer levels, increased land subsidence and loss of storage strain growers for energy efficiency improvements in drought years. The amplified demand for water and energy during drought also lowers stream flows and lake levels, which impact the production of hydroelectric power. In addition, the water table is lowered continually during these periods, as growers pump groundwater from deeper wells demanding more power. The California drought assessment of 2014 reported a loss of 8.1 million ML of surface water with a simultaneous increase of 6.3 million ML in groundwater pumped for an additional cost of USD 454 million [6]. Flood and furrow irrigation still account for approximately 40 percent of the total irrigated area in California, despite the advances and investments in irrigation systems. The adoption of the drip and micro-sprinkler irrigation significantly increased in acreage between 1991 (0.52 million hectares) and 2010 (16 million hectares) [7]. Figure 1 identifies the hydrologic regions across the state of California and the distribution of major crops, irrigation methods and levels of salinity in irrigation water.

California's increasing severity of droughts not only depletes groundwater but also increases the carbon footprint and greenhouse gas emissions from increased burning of fossil fuels to generate the power for pumping groundwater. After facing several severe drought years, state leaders implemented incentives, regulations and policies to manage groundwater that require record keeping and reporting of water use, nitrogen (N) leaching and energy consumption. Simple and scalable irrigation decision support systems are needed to facilitate base information for growers to manage and maximize irrigation water, energy and N use efficiency. On-farm water management using irrigation decision support systems coordinates the development and management of water, land and related resources aimed toward equitable economic welfare and sustainable water use for future generations [8,9]. Irrigation decision support systems (IDSS) are integrated solutions combining and interpreting real-time meteorological, soil moisture and/or crop water stress data using telemetric services to help growers make irrigation decisions. Most of the first IDSS developed in California ranged from spreadsheets to stand-alone software. With recent improvements in public weather-station networks, sensor technology, satellite and aerial imaging, wireless communications and cloud computing, web and smartphone applications automating a range of complex calculations involved in evapotranspiration-based irrigation scheduling, crop and soil nitrogen status IDSS have been developed.

The California Energy Product Evaluation Hub (or Hub) was proposed by the California Energy Commission to fill an information gap between energy sector manufacturers and large commercial and institutional customers. The purpose of the Hub is to accelerate the adoption of beneficial technologies by informing customers purchasing distributed energy resource products through procurement processes. The objectives of the Hub are to evaluate the selected distributed energy resource products (e.g., IDSS) in a rigorous and transparent manner and widely disseminate the evaluation results to large commercial and institutional customers. The evaluations will allow comparisons of similar technologies, as well as comparisons to existing government and industry standards. The evaluations, and the data behind them, will be distributed through the Hub's public web platform. The Hub is a cooperative effort among the University of California, Davis, Lawrence Berkeley National Laboratory, Energy Solutions and the Center for the Built Environment of the University of California, Berkeley.

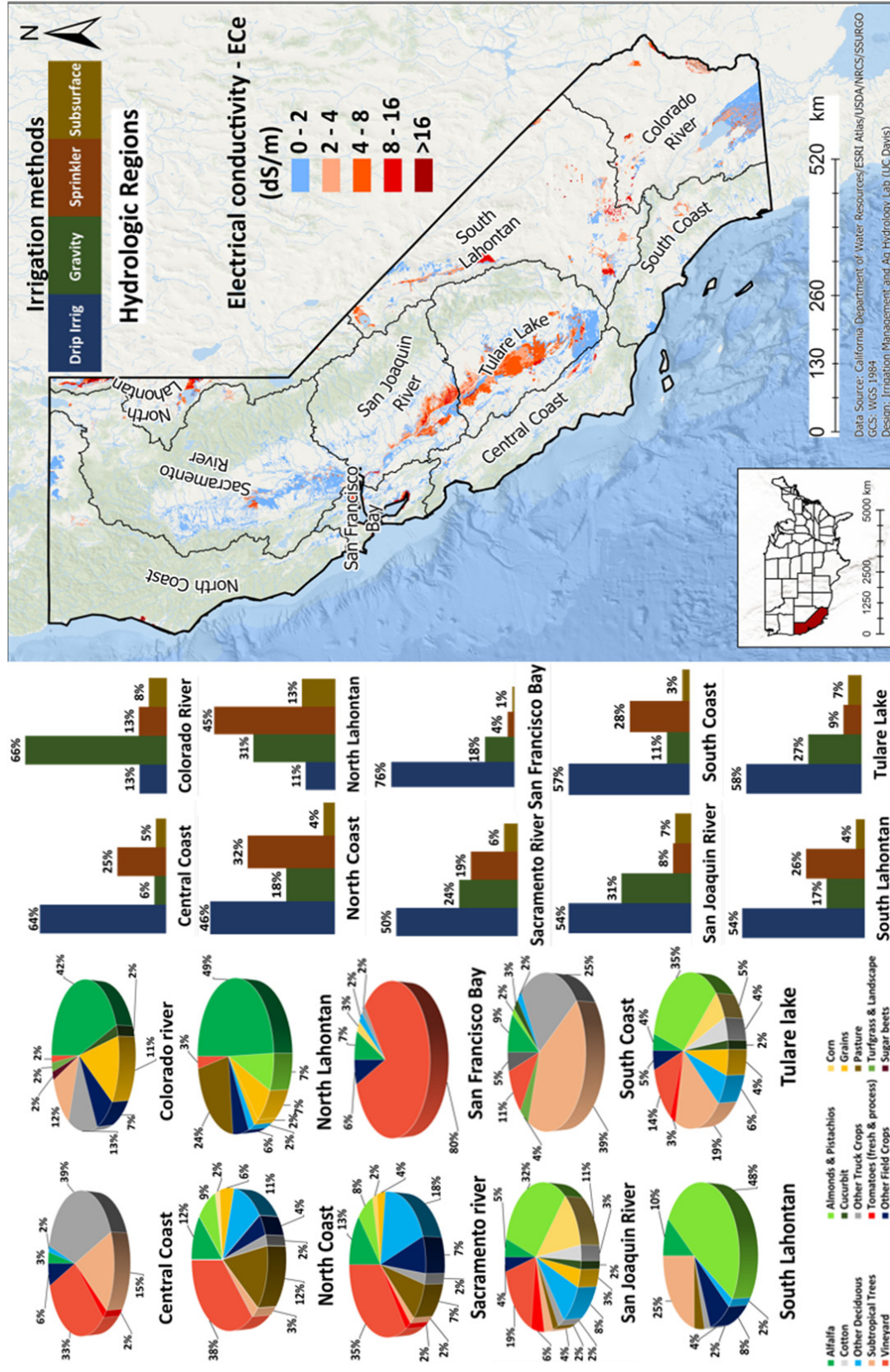


Figure 1. Distribution of irrigation methods, major crops and irrigation water salinity levels in hydrologic regions of California.

The overall goal of this narrative review is to identify, compile and assess the available IDSS in California and how they may serve multiple water, energy and nutrient management goals. Here, we discuss the different water budget components and measurements used in crop canopy, soil moisture, aerial reflectance and satellite-based IDSS. We also consider diverse California cropping and irrigation systems and how different IDSS are integrated into existing crop irrigation management as part of the ongoing research of the California Energy Product Evaluation Hub. Finally, we identify knowledge gaps in IDSS research and current available tools for integrating energy, nitrogen leaching and soil salinity management.

2. Objective and Review Methodology

We identified all active IDSS in California through a comprehensive search of all IDSS on the search engines and in consultation with a California IDSS product advisory group. The IDSS product advisory group consisted of growers, certified crop advisors, cooperative extension advisors, the California Department of Agriculture, California Agricultural Irrigation Association and additional government, industry and trade organizations. The advisory group helped define the IDSS needs for the California cropping system. This information was used to identify the commercially or freely available technologies and exclude the IDSS that have not yet been made available for widespread use.

Section 3 defines California's water management context and the need for IDSS under increasing drought, regulation and risk management. Section 4 provides a broad overview of soil–plant–atmosphere approaches for IDSS. Section 5 describes the commercially available IDSS based on soil tension, canopy temperature, stem water potential and remote-sensing techniques. Section 6 describes the science, policy and role of IDSS for integrated irrigation and energy management in agricultural systems. Section 7 describes the science, policy and role of IDSS for integrated irrigation and nitrogen (N) management to control the environmental problems or groundwater contamination due to excessive N fertilizer uses. Section 8 describes the science, policy and role of IDSS for integrated irrigation and salinity management. Sections 9 and 10 focus on IDSS as a holistic effort for water, nutrient and salinity management and consider the innovation, validation and adoption strategies.

3. Context for IDSS in California Agriculture

3.1. Water Scarcity

Overdrawn aquifers, decline in snowpack, frequent droughts and rising evaporative demand are increasing water scarcity in California. These water resource concerns have led to decreasing water availability for irrigation, increasing regulation (e.g., reduced allocations), increasing energy consumption, difficulty in water/fertilization co-management and increasing water and energy prices. Because the annual evaporative demand exceeds precipitation in the majority of California, irrigation is generally considered compulsory. While most of the precipitation falls in the winter, key economic crops have high water demands during the spring–summer–fall season. Additionally, there is a spatial disconnect between precipitation and agricultural water demand in California. Most of the surface water used for agriculture comes from precipitation in the northern part of the state, while the Central Valley and southern parts of the state have the greatest demand for agricultural water. These discrepancies in space and time have led to complex water conveyance, storage and transfer systems that are important for understanding the potential benefits of IDSS for California growers [10].

Although California spans a wide range of climates, much of the state, including some of the most productive farmland, occupies semi-arid regions of the Central and Imperial Valleys, which are characterized by a Mediterranean climate with hot, dry summers and mild, wet winters. Statewide, the average water use is roughly 50% environmental, 40% agricultural and 10% urban [11]. By necessity, California has adopted management strategies to deal with water shortages, such as reusing water, long-distance water con-

veyance and desalination technologies to complement local ground and surface water [12]. Unfortunately, water supply diversification strategies can also lead to increased energy use and, consequently, to increased greenhouse gas emissions [13]. California's water system is estimated to emit 10% of the state's greenhouse gas emissions [14]. Water–energy nexus approaches recognize the close connection between water and energy and the importance of considering all aspects of these complex systems [15,16]. As irrigation makes up a large portion of the water supply system in the state, it is under critical consideration by both government agencies and agricultural end users. Policy makers face the difficult task of balancing the needs of diverse stakeholders, protecting the environment and providing reliable, sustainable water supplies to agricultural, industrial and residential customers [16]. At the same time, California growers face more frequent and severe drought events, warmer temperatures and variable rainfall associated with climate change [17], leading to increasing dependence on irrigation [18].

Growers also face increasing competition for irrigation water and growing concerns about the environmental impacts of irrigation. Growers pay for water, energy and infrastructure to irrigate crops. California growers pay between USD 12/106 ML⁻¹ water in direct costs and USD 17/151 ML⁻¹ water in energy costs [19–21]. While growers are willing to adopt new technologies to reduce risks during periods of water shortage, the information provided by extension services and other educational sources plays an important role in new irrigation technology adoption [22].

3.2. Regulations

California growers identify the key barriers to water and energy conservation efforts as (1) cost, (2) a lack of return on investment (3) and uncertainty about the future of available water. Cost alone is not enough to increase IDSS adoption or agricultural water conservation [23]. In semi-arid regions, regulating surface water without regulating groundwater (or vice versa) increases pressure on the unregulated water source instead of increasing the use of IDSS [24]. However, approaches that involve cooperation across institutional ecosystems as well as multi-actor governance and participation to jointly regulate groundwater and surface water quantity, nutrient/pollutant transport and energy usage may increase IDSS adoption [23,25].

For the past century, California has been a demonstrative example where the regulation and governance of surface water quantity and quality have placed tremendous stress on groundwater supply and energy required to pump groundwater in years with limited surface water allocation. However, the legislation and policies adapted in 2014–2016 are attempting to jointly regulate groundwater and surface water quantity, quality and cooperation across institutions. In 2014, California passed the Sustainable Groundwater Management Act (SGMA), in which two state agencies (Department of Water Resources and State Water Resources Control Board) mandate and oversee communities self-organizing into groundwater sustainability agencies [26]. Each agency created groundwater sustainability plans to achieve sustainability goals by 2040–2042. Similarly, in 2014, the California Irrigated Lands Regulatory Program was expanded to regulate nitrates in discharge to both surface and groundwater from irrigated agricultural lands [27]. California's 2020 heat wave and widespread agricultural power outages have spurred agricultural trade organizations to consider the need for IDSS to accommodate off-peak energy usage and regulations imposed by utility companies [28]. However, there are not yet any direct statewide regulations on the energy used for groundwater pumping in California.

3.3. Loss and Risk Management

3.3.1. Infrastructure Failures

IDSS could help growers plan for water usage throughout the growing season when adjustments may be required to accommodate irrigation interruptions to avoid yield losses at critical moments. For example, in the 2018 Census on Irrigation and Water Management, 1792 CA growers (29,538 ha) reported yield losses because of irrigation interruptions related

to groundwater/surface water shortages, equipment failure, energy shortages, high salinity, loss of water rights or increase in water costs [29]. Having a formal IDSS in place does not prevent water, energy or infrastructure disruptions but instead could assist in identifying equipment failures and providing the projected data and calculations needed for difficult decisions—how best to prioritize the available water across the farm to the crops that will have the highest potential for short- and long-term revenue.

3.3.2. Disease-Based Losses and Water

Growers using intuitive, informal irrigation practices may err on the side of applying ‘extra’ water to ensure that crop water requirements are met. Additionally, some IDSS may also err on the side of overprediction of evapotranspiration and crop water requirements to match grower management practices. Although this logic may decrease the risk of underwatering or water stress, it can increase water logging, nitrate leaching, anoxia, denitrification, salinity, soil erosion and runoff, in addition to the wasted energy and water costs [30]. In California perennial crops, overirrigation or irrigating too soon can impact root development—especially of shallow, fine roots—which can lead to long-term yield losses, especially if the root zone oxygen concentration drops below 10% [31]. In both annual and perennial crops, overirrigation that increases soil and/or canopy moisture can often increase the survival, growth, infection and dispersal of pathogens, which ultimately leads to disease-based yield losses [32]. However, it is important to note that not supplying enough water to meet crop needs can also trigger many belowground diseases [32]. For a comprehensive review of irrigation–disease interactions, please see Swett (2020) [32]. Although IDSS could integrate crop-specific co-management of water and diseases in the future, to the best of our knowledge, no IDSS currently have this function for California cropping systems.

4. Soil–Plant–Atmosphere Approaches and Data for IDSS in California

4.1. Precipitation

Precipitation is an important component of the hydrologic cycle considered for all water budgets. In California, real-time rainfall data can be acquired from different sources, such as the Department of Water Resources California Irrigation Management Information System (CIMIS), National Oceanic and Atmospheric Administration’s California Nevada River Forecast Center (CNRFC) and United States Climate Data. For annual water budgeting, monthly precipitation data are often used. Several researchers have observed decreases in precipitation and increases in autumn temperatures since the 1980s [33,34]. In 2018, the delayed start of precipitation months resulted in the most destructive wildfires of California, burning about 766,439 hectares of land area [34,35]. This has not only disturbed water budget planning and estimation, but it has also impacted the contamination of groundwater and other available sources of irrigation by changing the pH due to debris and ash [36].

4.2. Evapotranspiration

Evapotranspiration depends on weather conditions, crop type, canopy density/development, stomatal conductance and regulation, irrigation system and management, soil management and soil type. In California, the estimates of reference evapotranspiration (ET_o) come from the 153 active CIMIS stations that are sited, maintained and equipped by the California Department of Water Resources to measure shortwave solar radiation (pyranometer), soil temperature (thermistor), air temperature (HMP35), relative humidity (HMP35), wind direction (wind vane), wind speed (anemometer) and precipitation (tipping bucket rain gauge). The state is divided into 18 ET_o climatic zones based on long-term monthly CIMIS averages. Additionally, a spatial CIMIS data product combines the network of available stations for ground measurement and satellite data in order to simulate the ET_o of the whole state. CIMIS estimates hourly ET_o for cool-season grass with a height of 0.10–0.15 m using the CIMIS Penman equation, which is modified from the Penman equation [37], with an approach for estimating net radiation from shortwave solar radiation,

temperature and relative humidity measurements developed and validated using 71 net radiometers across California [38]. The CIMIS Penman equation also uses different weights for wind speed in the hourly estimation of ET_o , depending on whether it is day or night time and a unique cloud factor obtained from each CIMIS station [39].

In addition to the CIMIS network, the National Oceanic and Atmospheric Administration (NOAA) Geostationary Operational Environmental Satellite (GOES) satellites have been used to predict incoming solar radiation as the main source energy for evapotranspiration. Satellite-based ET_o maps are calculated on a two-kilometer grid, which is an important contribution of data for decision making, given that the distance between the CIMIS stations can be tens of kilometers. These freely available estimates of ET_o can be paired with crop-specific coefficients (K_c) to estimate crop evapotranspiration (ET_c) during the growing season. It is important to note that evapotranspiration offers decision support as to how much water has been used by the crop based on meteorological data or will be used by the crop based on meteorological forecasting [40,41].

4.3. Irrigation Scheduling Resources

The quantity and timing of water application to irrigate a crop is a critical part of planning a growing season. Crop management activities are mainly dependent on the moisture present in the soil and root matrix. Scheduling depends on the combination of evaporative demand from the atmosphere, spatial and temporal heterogeneity in soil properties and changes in crop canopy during a growing season. California IDSS currently schedule irrigation by measuring, remotely sensing and/or modeling some combination of three different categories: (1) evapotranspiration, (2) allowable depletion of soil moisture and (3) canopy characteristics [42]. In this work, we discuss California IDSS and state specific data sources that can be used to ascertain data from these categories and represent these tools and sensors in Figure 2. These categories are used in IDSS throughout the world, and we recommend Gu et al. (2020) for an in-depth general review [43].

4.3.1. In Situ Calculation of Crop Coefficient Values

Crop coefficient (K_c) values can be obtained for the entire growing season from historical evapotranspiration databases for specialty crops (almonds, walnuts, pistachios, processing tomatoes, etc.) developed by the University of California under the drought management program. There are available databases maintained by the University of California Agriculture and Natural Resources (<https://www.sacvalleyorchards.com/et-reports/> (accessed on 20 August 2021)) Westlands Water Districts (<https://wwd.ca.gov/water-management/irrigation-guide/> (accessed on 20 August 2021)) that provide regional estimates of ET_o and ET_c for growers. Significant efforts have been made to measure actual evapotranspiration to derive the K_c values specific to California crops and management. Direct measurements using lysimetry, eddy covariance and surface renewal have estimated K_c values for almond, pistachio, walnut, processing tomato, wine grapes, lettuce, rice, corn, wheat, and alfalfa (Table 1) [44–68]. It is important to note that the K_c values derived from actual evapotranspiration studies have several assumptions and site-specific limitations for widespread adoption and water use projections. Attention should be given as to whether water stress had occurred during the actual evapotranspiration measurement periods as well as the uncertainty of actual evapotranspiration estimates by a methodological approach. The use of crop coefficients for irrigation of perennial crops is often more challenging than for annual crops. This is because there can be significant variability as a consequence of the crop density, crop load, row orientation, variety, irrigation system, pruning, floor management, soil type, salinity/sodicity and plant vigor between the two types.

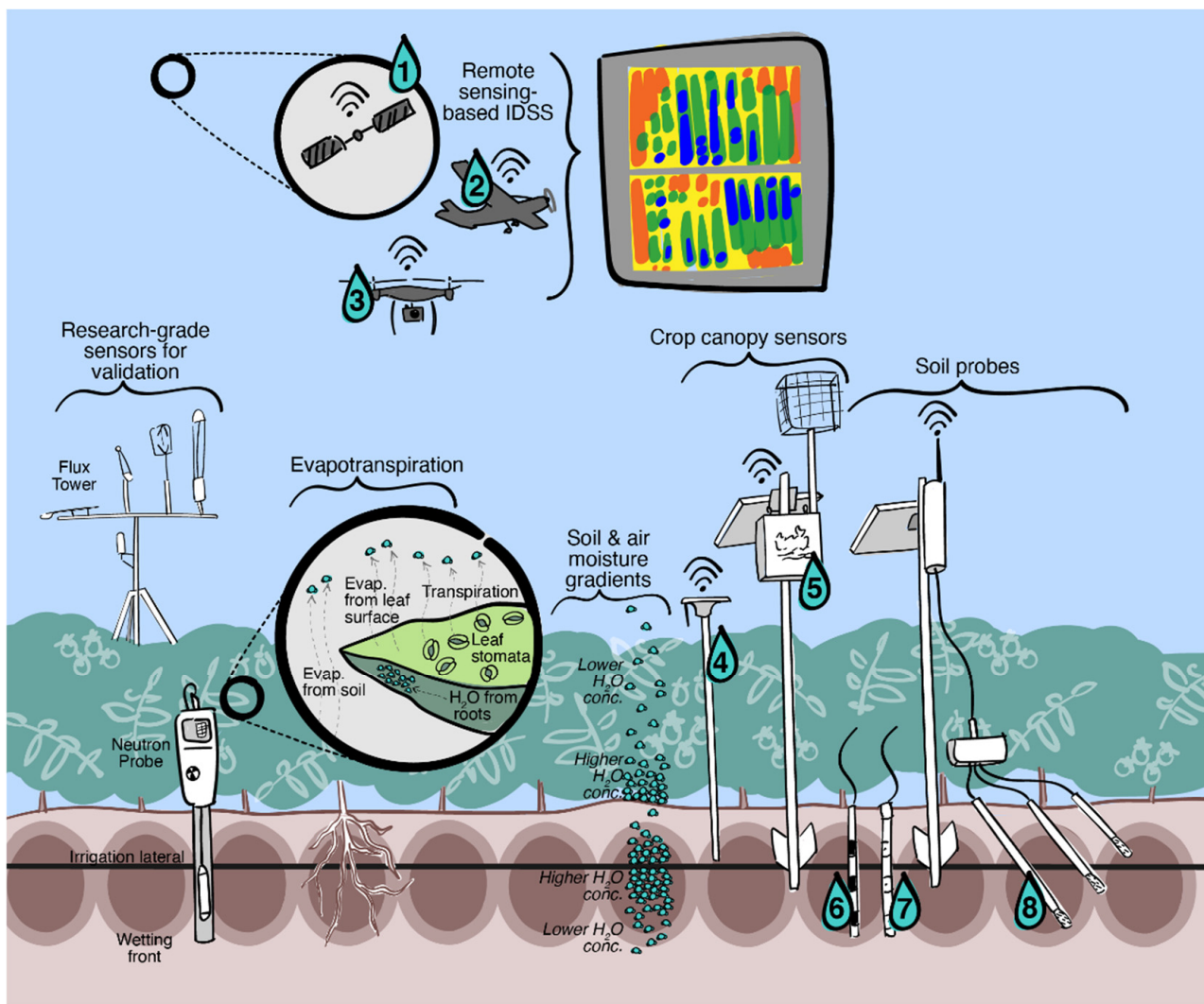


Figure 2. Conceptual illustration of integration and application of imagery (IDSS 1 is satellite imagery, 2 is aerial reflectance, and 3 is drone imagery using multispectral/thermal cameras), canopy (IDSS 4 and 5 based on crop evapotranspiration and other canopy-based parameters) and soil-based IDSS (IDSS 6 and 7 based on volumetric water content and 8 based on soil water potential) in a processing tomato field. Eddy covariance tower and neutron moisture probes are useful to estimate a complete water balance for validation of these available IDSS measurements. Artwork by Dr. Bonnie McGill.

Some California crops, such as processing tomato, wine grapes and olives for oil, can benefit from some degree of water stress in order to decrease the vegetative growth and/or improve the quality of the final product (e.g., sauce, wine, olive oil). Growing these crops can either benefit from constant water stress monitoring or development of K_c values that are multiplied by stress coefficients (K_s) after long-term data collection combined with fruit analysis and careful considerations with experienced growers and processors. The measurement of evapotranspiration values reveals much information about the irrigation needs; however, IDSS should also factor distribution uniformity, soil type, irrigation system efficiency, crop density, floor (interrow perennial cover crop) management, perennial stand density and variety when interpreting the published K_c values across California.

Table 1. Crop coefficient and seasonal water requirement ranges of major crops of California. Crop coefficient periods have been approximated for each crop, see notes column for more details.

Crop	Initial	Crop Coefficient * Developing	Late	Notes	Water Requirement (cm per Season)	References
Almonds	0.20–0.78	0.80–1.09	0.40–1.17	Mature trees; initial (hull, shell, integuments), developing (hardening, embryo growth), late (maturity, ripening, hull split).	104–112	[48–52]
Pistachios	0.07–0.79	0.82–1.19	0.35–1.19	Mature trees; initial (bloom, leafout, shell expansion), developing (shell hardening, nut fill), late (nut fill, shell split, hull split, harvest, post harvest).	76–127	[51,53–55]
Walnuts	0.12–0.93	1.00–1.10	0.28–0.97	Mature trees; initial (bloom, leafout, flowering, growth of hull), developing (shell and kernal development), and late (hull split).	104–112	[56,57]
Tomatoes	0.20–0.45	1.00–1.20	0.30–0.90	Processing and fresh market tomatoes; initial (planting, prebloom, bloom), developing (bloom, early fruit set, late fruit set), late (late fruit set, first color, red fruit, preharvest).	53–76	[51,56,58]
Grapes	0.30–0.37	0.62–0.85	0.45–0.75	Table, wine and rasin grapes; initial (shoot development, flowering), developing (berry formation, verasion), and late (berry ripening, harvest, senescence).	25–76	[51,59,60]
Lettuce	0.17–0.61	0.83–1.02	0.45–0.98	Lettuce grown year-round; initial (emergence to 40% canopy cover), developing (40% canopy cover to 80% canopy cover), and late (80% canopy cover to harvest).	30–61	[51,56,61,62]
Rice	0.95–1.05	1.20–1.25	0.60–0.95	For both paddy and non-paddy grown rice, initial (vegetative phase), developing (reproductive phase), and late (maturation phase).	61–122	[51,56,63]
Corn	0.18–0.26	1.06–1.17	0.30–0.55	Field and sweet corn; initial (vegetative stage), developing (reproductive stage), and end (maturity).	56–76	[56,64]
Wheat	0.26–0.70	1.09–1.15	0.25–0.41	Winter wheat; initial (tillering), developing (stem extension and heading), late (ripening, harvest).	46–53	[51,65,66]
Alfalfa	0.30–0.40	0.95–1.30	0.50–1.30	Initial (planting to 10% cover), developing (10% cover to senescence), and late (senescence to maturity).	51–117	[56,67,68]

* Periods of initial, developing, and late for crop coefficients have been approximated for each crop, see notes column for more details.

4.3.2. Scheduling with Allowable Depletion

The allowable depletion of soil moisture approach requires some knowledge or *a priori* assumption of the effective crop rooting depth, soil textural and hydrological properties and estimates of either soil volumetric water content or soil water potential. These parameters are used to estimate the plant available water content (AWC) as the difference between field capacity and permanent wilting point. The allowable depletion is established as a threshold based on a fraction of AWC or specific soil water potential at which water stress will occur without irrigation. The allowable depletion can differ by soil texture, crop type, as well as phenological stage. In California, the allowable depletion can range from 25% AWC in onions to 90% AWC in ripening wheat but generally runs in the 45–50% AWC range [69–71]. Allowable depletion, whether measured or modeled, offers decision support regarding how much to irrigate (e.g., refill the soil profile), as well as when to initiate irrigation. It is important to note that allowable depletion is not a direct assessment of plant water stress but rather assumes plant water stress based on empirical relationships between plant physiological stress (e.g., stem water potential, canopy temperature, reduced transpiration) and soil volumetric water content or soil water potential.

Soil cohesion and adhesion to water molecules determines the soil water potential (suction or negative pressure). Plants take up water when water potential is between the field capacity (−0.33 bar) and permanent wilting point (−15 bar). Therefore, irrigation scheduling is performed by maintaining the soil moisture within this range of soil water potential. The most commonly used methods for soil moisture or water potential

monitoring in California are tensiometers, electrical resistance block (watermark sensors) or capacitance-based sensors [72]. Recent developments in telemetric operations allow manufacturers to combine the soil moisture sensors with web or mobile applications as remote systems. Additionally, the user friendliness of remote telemetry and real-time moisture data in the field are now integrated with automated irrigation systems. Some of the common telemetric operators for soil moisture sensors in California are Wildeye, Farm(X), Hortau, Irriwatch and AquaSpy.

4.3.3. Scheduling with Crop Canopy Characteristics

Recent advancements in the capture and interpretation of remotely sensed vegetative indices (e.g., normalized difference vegetation index or NDVI) allow growers to empirically derive real-time values of crop coefficients throughout the growing season [73–75]. Remote sensing tools, such as directly or remotely piloted aerial vehicles or satellite imagery, aid in the use of algorithms to combine remotely sensed vegetative indices and soil reflectance maps [76–79]. This combination helps growers manage irrigation in orchard cropping systems where NDVI and other index values for individual trees can be calculated. In California, these services are widely provided by Ceres Imaging Inc. to specialty crop growers. Additionally, CropManage uses satellite-based estimates of phenology for irrigation scheduling [80–82].

5. IDSS for Crop Water Management in California

The use of IDSS has increased in California in the last decade, especially for efficient water application preparation for the SGMA regulatory standards. The most common IDSS in California integrate two major components: (1) data input/analysis and (2) user interface. The data input/analytical techniques acquire data based on soil, crop and/or weather parameters, and the user interface is based on telemetry that simplifies the acquired data using statistical interpretation, photogrammetry and/or simulation modeling. The ease of understanding or user friendliness of the acquired information depends on the use of graphics, color notations and approach to simplify the complex data [83]. The IDSS commonly used in cultivating specialty crops in California can be classified into three types (Table 2): (1) soil-based IDSS, (2) canopy-based IDSS and (3) remote-sensing IDSS. Irrigation strategies, such as deficit irrigation, subsurface drip irrigation, overhead linear move sprinkler irrigation, deep root irrigation, pressure-compensated drip irrigation, automated surface irrigation, and tail recovery systems may enhance water use efficiency for high-value crops in California [84].

5.1. Soil-Based IDSS

In IDSS, soil moisture is generally reported in inches of water per foot of soil or as a percentage of weight or volume [2,85], while soil water potential is usually reported in bars or kPa. The California IDSS based on soil moisture usually also estimate or infer soil hydrologic properties (e.g., texture, AWC) to contextualize the recommendations. Therefore, the soil sensors used as IDSS can be divided into two types.

Type 1—IDSS based on volumetric moisture content. These soil moisture sensors include time domain reflectometry, capacitance and frequency domain reflectometry sensors [80,86].

Type 2—IDSS based on soil water potential. These sensors include tensiometers and granular matrix sensors [87,88].

Table 2. List of commonly available IDSS for agricultural crops.

IDSS Type	Name of Device	Key Parameter (s)	Telemetry	Service Provider or Integration Partners
Soil-based	Sentek Drill and Drop Probes (Stepney, Australia)	Volumetric Moisture Content Soil temperature Soil salinity	IrriMax	Wildeye (Fresno, CA, USA) Wiseconn (Fresno, CA, USA)
	AquaCheck Sub-Surface probes (Perry, IA, USA)	Volumetric Moisture Content		Farm(X) (Mountain View, CA, USA)
	Hortau 1k sensors (Québec, QC, Canada)	Soil water potential	Irrolis 3	Hortau (Québec, Canada)
	Irrrometer tensiometer (Riverside, CA, USA)	Soil water potential	IRROcloud	Irrrometer (Riverside, CA, USA), Agri-Valley irrigation (Merced, CA, USA), Bennett and Bennett (Selma, CA, USA), Bi-County Irrigation (Yuba City, CA, USA), Wildeye (Fresno, CA, USA), Crouzet Irrigation Supply (Porterville, CA, USA), Hydratec, Inc. (Windham, NH), Reedley Irrigation (Reedley CA, USA)
Canopy-based	Watermark Sensor (Riverside, CA, USA)	Soil water potential	IRROcloud	
	Arable Mark 2 (San Francisco, CA, USA)	Crop Evapotranspiration Canopy temperature Precipitation Growing degree days Leaf wetness NDVI	Arable Open and Arable Mobile	Arable (San Francisco, CA, USA) Netafim (Tel Aviv-Yafo, Israel) (integrated data from Arable through NetBeat)
Imagery-based	Tule sensors (Davis, CA, USA)	Actual Evapotranspiration	Tule Web or mobile application	Tule Technologies (Davis, CA, USA)
	Ceres Imaging (Oakland, CA, USA)	Thermal imagery Water stress maps Color infrared maps Colorized NDVI	Ceres imaging web and mobile application	Ceres Imaging (Oakland, CA, USA) John Deere (Moline, IL, USA) ** Climate Field View (San Francisco, CA, USA) **
	Irriwatch (Maurik, The Netherlands)	Soil moisture and actual evapotranspiration using daily satellite imaging using SEBAL model	Irriwatch Portal web and mobile application	Vinduino Crop Optimization Technology (Temecula, CA, USA) **
	CIMIS *	Reference Evapotranspiration	153 CIMIS Stations through web and mobile applications	University of California, Davis WATERIGHT **
	CropManage *	Evapotranspiration using satellite imagery	CropManage Web Application	University of California Agriculture and Natural Resources (UCANR)
	Open ET *	Evapotranspiration and consumptive water use using satellite imagery	OpenET Web application	NASA, DRI, EDF, Google Earth Engine

* Available for free through web or mobile application. ** Integration partners.

Soil sensors are generally provided by IDSS vendors in combination with their telemetric services to access the data through cloud-based data storage applications. The selection of these sensors is based on evaluating water and energy savings, installation and maintenance, ease of use and suitability for specialty crops and soil type, data interpretation and additional services. Vendors have the capability of making recommendations to growers by integrating and installing in situ weather stations. However, the CIMIS weather stations are widely spread throughout the state and provide reliable and validated information on the required weather parameters for water budgeting. Some commonly used soil moisture sensors can be combined with telemetric services provided either by the sensor company or by a separate IDSS vendor.

Soil moisture probes are widely used to determine the real-time volumetric moisture content allowing user-friendly or site-specific calibrations. Measurements can be taken at the desirable depths throughout the soil profile. These sensors also provide additional information on soil temperature and salinity. These sensors, based on design, can also measure soil water potential up to -10 bars. The sensors are provided to growers as leased assets, and real-time irrigation recommendations are made through telemetry services. Examples include tensiometers that are designed to measure soil water potential in heavy ($0-1$ bar) and light soils ($0-0.3$ bar). Watermark sensors are based on electrical resistance in soils and are widely useful for measuring soil matric potential up to 2 bars.

5.2. Canopy-Based IDSS

The metabolic processes in a plant system are driven by its water content. Plant water status can be estimated by monitoring physiological and metabolic processes, such as stem or leaf water potential, relative moisture content, stomatal conductance, canopy temperature and xylem cavitation [2,73,89–92]. The most commonly measured water stress parameters in California are canopy temperature, canopy cover and stem water potential [2]. These plant water status indicators are most useful for irrigation timing and can be used to inform when irrigation is required, when crops are not receiving enough irrigation, when there are problems with irrigation systems (e.g., distribution uniformity), as a proxy for soil salinity stress and for applying controlled stress to improve crop quality or health. Plant water status indicators are less useful for understanding how much irrigation is needed, as they do not provide information about soil moisture or evaporative demand. Plant-based IDSS are generally combined with meteorological parameters and/or evapotranspiration data.

5.2.1. Canopy Cover

Radiation interception and evapotranspiration depend on the canopy cover and surface area of a crop. Canopy cover serves as an important parameter for several remote-sensing techniques used as IDSS. As crop canopies change throughout the growing season in terms of their size, area and reflectance properties, so do the values of the crop coefficient (K_c). The spectral reflectance of vegetation or crop canopy can help growers understand the variability in the field by assessing the plant vigor and chlorophyll content [93,94]. A key component of canopy-based IDSS is the crop and growth stage-specific K_c value. The K_c values are usually determined from field studies measuring actual evapotranspiration and ET_0 [95,96] but can also be assessed using measurements of leaf area index, light interception and percent canopy cover. Some of the commonly used IDSS based on evapotranspiration and canopy parameters include Arable Mark 2 sensors and Tule sensors. These sensors are leased by the respective vendors, and the irrigation recommendations based on canopy parameters are informed through web/mobile applications. Arable Mark 2 sensors are often combined with the soil moisture probes to apply the soil and canopy parameters to complete the water budget equation for irrigation decisions.

5.2.2. Canopy Temperature

Canopy temperature indirectly measures water deficit when it increases above the surrounding ambient temperature [97]. In general, the variability in canopy temperature

is also a result of solar radiation and air temperature. Different indices are used for irrigation scheduling using canopy temperatures. Some examples include the Crop Water Stress Index, Stress Degree Days, Stomatal Conductance Index, Degrees Above Canopy Threshold and Time Temperature Threshold (TTT) [98–101]. In California, the Crop Water Stress Index and Degrees Above Canopy Threshold have been evaluated for wine grapes, corn, pistachios and wheat growers using infrared thermal radiometry [102,103]. The Crop Water Stress Index is calculated by determining the canopy temperature minus the air temperature relative to a well-watered and non-transpiring reference crop [103]. Contrary to the Crop Water Stress Index, the Degrees Above Canopy Threshold only requires a single canopy temperature measurement for quantifying water stress [103,104]. For point-based measurements, canopy temperature can be acquired using an infrared thermal radiometer [103]. At larger spatial scales, thermal and spectral imagery IDSS (e.g., Ceres Imaging) using remote-sensing tools can be used for determining indices based on canopy temperature.

5.2.3. Stem Water Potential

Stem water potential is an indicator of how hard a plant is pumping to move water from the soil (−15 to 0 bars) through the xylem (−2 to −60 bars) to the atmosphere (−200 to −800 bars) [105]. In California, stem water potential is most commonly used and recommended for high-value perennial crops, such as grapes, almonds, walnuts and prunes [106,107]. Stem water potential is most often measured by a pressure chamber, which applies pressure to a sample leaf until the water is pushed out of the stem [90,106,108]. There are growing numbers of sensors available for measuring the stem water potential. These sensors can function as micro-chips or micro-tensiometers or dendrometers for installation in woody vines or trunks [108]. In order to be useful, stem water potential measurements need to be contextualized in relation to the environmental demand, as they are sensitive to temperature and vapor pressure deficit [105]. Local tools are available for growers to correct stem water potential readings in reference to the evaporative demand and compare the readings to baseline values when water is not limited. The use of stem water potential measurements is high in wine grapes, as growers are interested in maintaining specific levels of stress after veraison in order to maintain the quality (M. Cooper, personal communication). Larger California vineyards have ‘pressure bomb teams’ to constantly test stem water potential throughout the vineyards during the key time periods. Although there are disease management benefits to maintaining stress at hull split, nut growers have still been slow to adopt the pressure chambers to measure stem water potential, with adoption rates of under 20% among almond growers [109].

5.3. Remote-Sensing IDSS

Remote and proximal sensing tools can be used either independently or in conjunction with ground measurements to estimate actual evapotranspiration, ET_c , allowable depletion and plant water status. Remote sensing can use several modes of data collection, including satellite, aerial imaging and scanning towers. Remotely sensed measurements of evapotranspiration typically use thermal imaging as an indicator of canopy radiometric temperature, where higher temperatures indicate relatively lower rates of evapotranspiration (relatively higher partitioning to sensible heat flux), and relatively lower temperatures indicate higher rates of evapotranspiration (relatively higher partitioning to latent heat flux). Remotely sensed vegetation indices from multispectral data, such as NDVI, can be used as analogs for the leaf area index, canopy cover and height, which are also required for evapotranspiration mapping algorithms. All remotely sensed evapotranspiration models solve for sensible heat flux, soil heat flux and net radiation, which leaves the latent heat flux or the energy equivalent of evapotranspiration as the remainder of the energy budget. Some of the energy balance models commonly used in evapotranspiration estimation include Two-Source Energy Balance (TSEB), Surface Energy Balance Algorithm for Land (SEBAL), Surface En-

ergy Balance System (SEBS), Mapping EvapoTRanspiration using Internalized Calibration (METRIC) and High-Resolution Mapping of EvapoTranspiration (HRMET) [77,110–115].

These types of evapotranspiration maps and crop stress indices have been integrated into several IDSS that serve California, such as Ceres Imaging (Oakland, CA, USA), Iri-watch (Maurik, The Netherlands) and Open ET (a satellite-based water data resource launched by National Aeronautics and Space Administration (NASA) and United States Geological Services (USGS)). However, one potential concern or drawback is that detectable differences in evapotranspiration based on canopy radiometric temperature may be revealed too late for irrigation intervention, in that crops exhibiting this level of water stress have already suffered some yield loss from decreased photosynthesis [116]. This limitation of thermal imaging has led to new areas of development for IDSS that may involve combining a variety of spectral bands, solar-induced fluorescence and thermal imagery to provide additional information relating water status to yields [117,118].

Proximal sensing of soil apparent electrical conductivity can be a useful tool to develop high-resolution maps of AWC and other important soil physical and hydrological properties [119]. These soil maps can be used in conjunction with maps of evapotranspiration or stem water potential measurements to assess plant water status [77,78]. In many areas outside of California, commercial IDSS have been developed to assign management zones based on soil properties, especially in regions where center pivot irrigation systems dominate and can be retrofitted or designed with variable rate application technology. New opportunities for precision irrigation exist in California micro-irrigation systems using variable frequency drives to irrigate based on the management zones. However, there are not yet commercially available IDSS in California that rely primarily on soil apparent electrical conductivity mapping to delineate zone-based irrigation management.

6. IDSS for Energy Management in California

6.1. General Considerations

The California agricultural sector consumes 75% of total water use in California compared to 24% and 1% for municipal and industrial sectors, respectively [4]. During the most recent megadrought between 2012 and 2016, the groundwater contribution to total water use nearly doubled from 30–40% to 60%, with most of this being used for agricultural irrigation [120,121]. Agricultural groundwater consumption is directly linked with the energy required to pump groundwater from the aquifers. In California, 8% of total energy use is for agriculture, and 70% of the agricultural energy used is for groundwater pumping [122]. Agricultural water and energy demand surge in dry years and the summer months—especially in the afternoons during peak daily energy demand for water to cool both crops and humans [123]. Additionally, 60% of daily water-related energy demand is due to pumping irrigation water in California from surface and groundwater sources [124].

Most surface irrigation systems have an irrigation efficiency of 67.5–70%, while the traditional sprinkler system ranges between 70 and 82.5%. Drip and micro-sprinkler systems have the highest irrigation efficiency compared to sprinkler or surface systems, ranging between 87.5 and 90% [125]. Pressurized surface and subsurface drip or micro-sprinkler irrigation systems improve irrigation efficiency but require more energy than surface flood or gravity irrigation [121,126]. Because there has been a nearly commensurate conversion in half of California's irrigated lands from surface flood or gravity systems to pressurized systems since 1972 [127], California's irrigation infrastructure has unfortunately increased its overall energy consumption while increasing its overall water use efficiency.

6.2. Science

There are opportunities for coupled energy and water conservation in agriculture through improving irrigation system efficiency, application efficiency, as well as crop water use efficiency. Agricultural pumping of irrigation water uses approximately 10 TWh of electricity per year [128], and at least 1 TWh or 10% of this usage could be conserved through improved control of water with better water metering and improved distribution

uniformity [4]. Additionally, pumping reductions through science-based irrigation scheduling efforts on farm- or district-wide scales may also reduce energy consumption [123]. Additional energy savings may be available through increasing the pump efficiency to 55–65% and using variable frequency drives to facilitate changes in pump speeds when system pressure demands are not peaking [129]. Moreover, on-farm solar generation and solar or hybrid solar pumps can also curb peak energy demands that coincide with peak water demands [123].

Finally, either front loading pumping to on-farm water storage structures in advance of peak energy demand [123,130] or applying a larger magnitude of irrigation a week in advance of a predicted heat wave could mitigate peak energy usage during heat waves [126]. However, scheduling larger irrigation events in advance of a heat wave would have to ensure that soil properties facilitated storage rather than drainage of excess water. Similarly, deficit irrigation has been suggested for energy conservation; however, this would need to ensure that there either would not be a significant yield loss or that the yield losses would be low enough to justify an overall profit based on reduced energy and irrigation costs. Finally, there is an opportunity for collective and community-based action from irrigation districts and newly formed groundwater sustainability agencies to use and develop district-wide tools for common pool energy users to pump and store water in advance of peak times, as well as prioritize and optimize groundwater pumping based on the crop stage and need during droughts and heat waves [131].

6.3. Policy

The above coupled energy and water management measures require supportive policies and governance for success, in which California has made some promising progress. In response to the groundwater-pumping-related energy use and high greenhouse gas emissions during the megadrought of 2012–2016, California enacted the State Water Efficiency and Enhancement Program (SWEET) in 2014, which is the first and largest program of its kind in the United States to date. The SWEET program involves a competitive application process for growers to receive grants to make improvements that will reduce water and energy consumption, greenhouse gases, as well as improve drought resilience and air quality. Agricultural operations can receive grants for three project categories: (1) pump and motor enhancements, which include installing variable frequency drives and replacing or improving the efficiency of motors or pumps; (2) irrigation system enhancements for systems with pumps, which include system pressure reduction measures, soil moisture sensors, automating irrigation systems and IDSS; (3) fuel conversion and renewable energy, which include changing fuel types to low-carbon fuel, as well as the installation of on-site renewable energy sources to offset fuel use [132].

Applicants must quantify the baseline information about current energy, infrastructure efficiency and water use. Approximately one-third of applicants have been awarded SWEET at a maximum of USD 100,000 for 18 months [133]. The awardees must use baseline water and energy data, as well as the SWEET Irrigation Water Savings Assessment Tool and California Air Resources Board Greenhouse Gas Calculator tool, to quantify the projected water and energy savings. The SWEET program has invested USD 80 million in over 800 projects for an annual water saving of 88,496 Megaliters and GHG reduction of 80,077 MTCO_{2e} [134]. The program's challenges include the need for a stable, continuous funding source and increased accessibility for small and socially disadvantaged growers [133]. Specifically, although a third of projects have been located in disadvantaged communities, only 10% of the funds have gone to socially disadvantaged growers and ranchers [133,134]. Although the SWEET program has incentivized and improved the irrigation system infrastructure and design for energy optimization, there is still a need and large opportunity for IDSS and training related to coupled water and energy management in California [133].

6.4. Decision Support for Irrigation and Energy Management

Although there has been an identifiable need for co-management of irrigation and energy, there is currently only one decision support tool deployed for this purpose in California. The California Energy Commission funded the research and development of AgMonitor [135]. AgMonitor integrates irrigation schedules based on the crop coefficient approach and monthly aerial imagery with flow metering and all on-farm energy sources and sinks. This IDSS provides information on irrigation magnitude and timing events that will also optimize energy conservation across a farm and has been validated in key Californian crops, such as processing tomato, almond, pistachio and alfalfa. Although commercially available IDSS are limited in this area, there are currently research-level IDSS in development to optimize irrigation applications with photovoltaic power production [136,137].

7. IDSS for Nitrogen (N) Management in California

7.1. General Considerations

California's intensive irrigated agricultural production has led to the use of large amounts of nitrogen (N) fertilizers. In contrast, N over-application has been associated with water pollution and various human health concerns [138]. More than 50 years of tradeoffs between the use of N fertilizer and the health of the environment have been documented in California [139,140]. Over the past years, the volume of inorganic N fertilizer used in the state has expanded dramatically. The annual sales between 1980 and 2001 have exceeded 600,000 tons of N [141].

A significant increase in the N fertilizer application rate was observed in the Sacramento Valley, San Joaquin Basin and Tulare Basin of the Central Valley for the period 2002–2012 compared to 1991–2001 [142,143]. Nitrogen loading in the Sacramento Valley, San Joaquin Basin and Tulare Basin saw a significant increase in 2002–2012 compared to 1991–2001 [138]. More than 740,000 tons of N fertilizer was loaded on roughly 2.7 million hectares of irrigated farmland in California. The excess N fertilizer leaches to groundwater and affects the quality of drinking water [144]. Improper management of N fertilization in California has contributed to the unsustainability of agricultural production and has threatened the health of Central Valley communities whose drinking water relies on groundwater resources.

7.2. Science

Crop N needs have been investigated to provide growers with tools to determine proper fertilizer applications. Numerous quantitative and complex decision-making tools have been consistently used to achieve improved nutrient management and irrigation. Online spreadsheet models and IDSS that process large amounts of information have been implemented by the University of California to help growers determine the appropriate amounts of N fertilizers to apply (Table 3) [82]. Early season leaf sampling in tree crops was developed to estimate N status in tree tissues and make adjustments in fertilizer timing and amount. Brown et al. [145] developed online spreadsheet models for managing N in almonds and developed the four Rs of N management (right rate, right time, right place, right source). The right rate consists of applying N in appropriate proportion to tree demand. The right time is the N application with the accurate timing with tree uptake, which starts at 70% leaf out and stops soon after harvest. The right place encompasses variable rate irrigation and N application to address in-orchard soil and yield variability as well as N application to the tree's active root zone or foliage. The right source refers to using the type of fertilizer that optimizes other nutrients and suits the crop and the environment [146]. The Soil Nitrate Quick Test (SNQT), developed for vegetables, provides an estimate of the soil mineral N status capable of offsetting a fraction of the total N required by a crop. Hartz et al. [147] developed N requirements for processing tomatoes in the Central Valley. Nitrogen application guidelines were later modeled to help growers

optimize N application in processing tomato production [148] and across several key California crops [149].

Table 3. Principal decision support systems (DSS) for assisting with nitrate and salinity management of vegetable and tree crops in California.

IDSS Name	Operation Mode	Software Available	Reference
N management			
CropManage FARMS	Web-tool-based	https://cropmanage.ucanr.edu/ (accessed on 20 August 2021)	[82]
	Web-tool-based	https://ciswma.lawr.ucdavis.edu/ (accessed on 20 August 2021)	[81]
N budget calculator	Web-tool-based	http://fruitsandnuts.ucdavis.edu/N_Budget_Calculator/ (accessed on 20 August 2021)	[126]
Salinity management			
WARMF	Computer-based	-	[82]
SJRRTM	Web-tool-based	https://www.restoresjr.net/restoration-flows/water-quality/ (accessed on 20 August 2021)	[81]

7.3. Policy

To respond to California's nitrate issues, the State Water Board has evaluated the existing policies to determine if existing water regulations are sufficient and have improved the wastewater regulations to protect groundwater quality (www.cvsalinity.org (accessed on 20 August 2021)). The dischargers, such as growers, food processors, municipalities and ranchers, have to comply with new regulations (e.g., Salt and Nitrate Management Plan). Californian growers are under rising regulatory pressure to improve N use efficiency in agricultural production to decrease nitrate leaching. Therefore, they need the tools to accurately estimate crop N needs and availability to confidently adjust the N application rates. The federal and state agencies responsible for protecting air and water quality have been assessing the causes, consequences and costs of California's agriculture-wide N use. This concern explains the various regulatory initiatives, such as the Central Valley Regional Water Quality Control Board's Irrigated Lands Regulatory Program, the Central Coast Regional Water Quality Control Board's renewal process for the Irrigated Agricultural Lands Waiver, the Climate Action Reserve's N Fertilizer Reduction Protocol and the Central Valley Regional Water Quality Control Board's General Order for Dairy Waste Dischargers and the Central Valley Salinity Alternatives for Long-term Sustainability (CV-SALTS) program [150].

CV-SALTS is a collaborative program tasked to develop environmentally and economically sustainable management plans for nitrates and salts in the Central Valley. The Executive Committee encompasses diverse stakeholder groups, such as agricultural groups, cities, industry, regulatory agencies and community and environmental justice representatives. The Salt and Nitrate Management Plan (SNMP) developed by CV-SALTS is built on a range of existing water quality management policies. It proposes additional policies, mechanisms and tools to provide the Central Valley Water Board with the appropriate means for addressing the long-term loading of salt and nitrates in the different regions of the Central Valley. CV-SALTS is also tasked with developing an all-inclusive regulatory program with adequate strategies to address the management of salts and nitrates sustainably [151].

7.4. Decision Support for Irrigation and N Management

Numerous IDSS for irrigation + N have been developed by extension services, universities and other institutions involved in water management for states or regions [152]. Some IDSS that help manage N in CA include CropManage, Food, Agriculture, Resource Management System (FARMS) and the N Budget Calculator.

CropManage can help growers and farm managers determine watering and fertilizer N schedules on a field-by-field basis. All the required components to determine crop water needs, such as ET_0 and weather data (from CIMIS), estimated K_c , as well as adequate irrigation scheduling based on soil properties, are available without the need for in-field

sensors. CropManage is publicly available at: <https://cropmanage.ucanr.edu/> (accessed on 21 August 2021). The software automates all steps required to calculate crop water requirements, including N recommendations, based on soil crop N uptake models, nitrate quick test values and credits for nitrate in irrigation water and preceding crop residues. CropManage also helps growers track irrigation and fertilizer schedules on multiple fields and allows data sharing among users from the same farming operations. The web-based application record-keeping capability allows growers to review water and N applications on each field and maintain data required to comply with water quality regulations. CropManage can be integrated with other web applications and data sources to improve the accuracy of irrigation and fertilizer models [82].

FARMS is a user-friendly geospatial web-based application that simplifies the use of the decision support system for agrotechnology transfer (DSSAT) model by automating processes such as weather, climate and soil input. FARMS was developed using DSSAT-CSM and open-source GIS software. FARMS allows adaptive management to perform in-season yield predictions using both weather and climatic data to evaluate the potential impacts of management decisions on end-of-season yield. FARMS uses NASA POWER weather data integrated through an API [153]. FARMS simulates nitrogen cycling of the cropping systems and quantifies crop N stress based on nitrogen uptake versus available nitrogen and is expressed as a range between 0 (no stress) to 1 (maximum stress). FARMS also simulates the probability of nitrate leaching from a given irrigation and N management strategy.

The N Calculator is a predictive model that helps growers by advising on the timing and the appropriate amount of N fertilizer to meet yield-based demand [145]. The N Calculator has many functions, including calculating fertilization rates based on the newest UC N management research, applying the four Rs of nutrient management (right source, right rate, right timing and right location), enabling efficient fertilizer use, calculating N supplies from non-fertilizer sources, such as cover crops groundwater and compost, and cloning the N budget from one orchard to another within and between years.

For example, using this tool for almonds requires entering a yield estimate for pre- and post-bloom and adding early season tissue-sampling results. The N Calculator helps to meet much of the nutrients management required from the Irrigated Lands Regulatory Program. The Irrigated Lands Regulatory Program requires keeping an Irrigation and N Management Plan (INMP) worksheet onsite and submitting a summary report to one's coalition in post-harvest time.

8. IDSS for Salinity Management in California

8.1. General Considerations

About 40% of global irrigated land is located in arid/semi-arid zones, and this irrigation is often associated with salinization [154]. With the development of intensive irrigation practices, the Central Valley of California has become one of the world's most productive farming regions. The continuously increasing levels of crop production are threatened due to the deteriorating irrigation water quality. Clay layers impeding percolation to deeper groundwater regions have led to salt accumulation in drainage water in many Central Valley regions. One of the primary sources of salts is the water supply imported from the Sacramento–San Joaquin River Delta. About 250 tons of salt a day are imported into the San Joaquin Valley through the state and federal water project canals [155]. The soils of the Central Valley's western regions are sedimentary and alluvial from the origin and formed in an uplifted seabed. The native salts have mineralized and leached to the shallow water tables over time due to irrigation and flooding [156]. In the predominantly clay and silty clay soil textures, as plants extract water from the soil and transpire, the salt concentration level of the drainage water is likely to increase. As a result, salts are likely to concentrate in the root zone and accumulate in shallow water tables through leaching [157]. Excessive salt concentrations affect a plant's osmotic balance and trigger a reduction in plant water uptake and stomata closing, which causes transpiration inhibition to occur [158]. The increasing soil salinity slowly and steadily contaminates water supplies and reduces crop production.

Various factors, such as drought, climate change, water shortages and land-use changes, could exacerbate the salinity conditions.

More than 1.8 million hectares of irrigated cropland in Central Valley (primarily in the San Joaquin Valley) are affected either through saline irrigation water or saline soils, and tens of thousands of hectares of productive agricultural land are at risk (Figure 1) [159]. Salt accumulation has triggered more than 99957 hectares to be taken out of agricultural production, and another 0.6 million hectares are considered damaged by salinity [155]. Current management activities address only 15% of the annual salt load [150]. The direct annual costs from increasing salinity will range from USD 1 billion to USD 1.5 billion, and total annual income impacts to the State of California are predicted to range between USD 1.7 billion and USD 3 billion by 2030 [160]. The income reduction in the Central Valley will range between USD 1.2 billion and USD 2.2 billion [160]. In 2014, salinity reduced California's agricultural revenues by USD 3.7 billion, amounting to 8.0 million tons of crop production lost [161].

8.2. Science

The U.S. Salinity Laboratory (1954) classified five cases of agricultural soil salinity: non-saline ($0\text{--}2\text{ dS m}^{-1}$), slightly saline ($2\text{--}4\text{ dS m}^{-1}$), moderately saline ($4\text{--}8\text{ dS m}^{-1}$), strongly saline ($8\text{--}16\text{ dS m}^{-1}$) and extremely saline ($>16\text{ dS m}^{-1}$) [162]. Although this salinity system is the most commonly used, many other classification systems of salt-affected soils exist and are available in the literature [163]. The presence of salt in soil water may affect plant growth either through salt-specific or osmotic effects. The salt-specific or ion-excess effect of salinity occurs when excessive salt amounts enter the crop, accumulate and damage the transpiring leaves' cells and trigger plant growth reductions. The osmotic or water deficit effect of salinity occurs when salt in the soil solution decreases the plant's water uptake ability and leads to a decrease in the crop growth rate [164]. Salinity stress affects all the major plant processes, such as germination, growth, water uptake and yield [165].

Salinity can be classified as natural or primary salinity and second-hand salinity or human-induced salinity. Primary salinity comes from salts accumulation over long periods of time via natural soil or groundwater processes. Two natural processes contribute to primary salinity. The first is the weathering process that breaks down rocks and releases various types of soluble salts, including chlorides (of sodium, calcium and magnesium), sulfates and carbonates. The passive results from oceanic salt that the wind carries inland are deposited in the soil by rainfall. Passive salinity occurs due to human activities, leading to the modification of the soil's hydrologic balance [165].

8.3. Policy

The increase in salts concentration in the California Central Valley due to many factors, including intensive irrigation, has led to crises and political decisions toward remediation. High concentrations of selenium were found in fish in Kesterson National Wildlife Refuge, and vast numbers of deformed and dead waterfowl were discovered at the refuge [166]. In 2006, the Central Valley Regional Water Quality Control Board's Salt and Boron Total Maximum Daily Load for the San Joaquin River was approved, and a salinity control plan entitled 'Actions to Address the Salinity and Boron Total Maximum Daily Load Issues for the Lower San Joaquin River' was adopted in response to the Salinity and Boron Total Maximum Daily Loads [156]. Solutions for addressing salinity in the Central Valley water require considering innovative salt management strategies for both the short term and the long term to reach salt balance and restoration of the impacted areas. In 2015, the State Water Resources Control Board adopted Resolution No. 2015-0010 to approve Basin Plan amendments and to include the Salinity Variance Program, which applies to surface water under the Clean Water Act (CWA). The Salinity Variance Program follows water quality standards that include the following constituents: electrical conductivity, total dissolved solids, chloride, sulfate and sodium [155]. Recognizing the challenges of managing salinity in surface and ground waters, the Salt and Nitrate Management Plan

(SNMP) was implemented as part of the Central Valley Salinity Alternatives for Long-Term Sustainability (CV-SALTS).

The long-term salinity management strategies recommended by the SNMP are divided into three different phases, as described below.

- (i) Phase I focuses on developing a prioritization and optimization study for salinity management by using an interim salinity approach.
- (ii) Phase II is related to environmental permits, obtaining funding, engineering and design.
- (iii) Phase III consists of the implementation of physical projects to manage salt in the long term.

The interim salinity permitting approach is recommended by the SNMP to be set in place for 15 years. The interim salinity approach requires dischargers to participate in the prioritization and optimization study. However, the dischargers opting out of participating in the prioritization and optimization study would not be eligible for obtaining a variance under the Salinity Variance Program (<https://www.cvsalinity.org> (accessed on 29 August 2021)).

8.4. Decision Support for Irrigation and Salinity

Although there are not currently any California IDSS that also factor salinity management, there are several decision tools available to manage salinity in California. One of the water quality regulation tools used throughout the U.S. is the EPA-supported Total Maximum Daily Load (TMDL). The TMDL is a controlling tool for allocating responsibility for contamination in impaired waterbodies by assessing the assimilative capacity of the waterbody for the contaminant, determining the mass loading from non-point and point sources, which contribute to the pollution, and developing downstream water quality strategies reducing the excess of the pollutants in the waterbody. The implementation of the TMDL tool in the Central Valley of California has led to the development of decision support system tools, such as the Watershed Management Risk Management Framework (WARMF) and the San Joaquin River Real-Time Management (SJRRTM).

The Watershed Management Risk Management Framework (WARMF) model is a decision support system designed to guide stakeholders towards a comprehensive watershed management plan. The tool helps specifically to facilitate TMDL implementation at the watershed level. The embedded model uses a mass balance approach for an extensive suite of potential San Joaquin River pollutants, such as total dissolved solids (measured as EC), suspended solids, phosphates and nitrates. Models are also used to simulate agricultural and wetland drainage return flows and estimate the salts buildups from shallow groundwater. Components such as simulation models, graphical software and GIS software are incorporated into a graphical user interface (GUI) to easily visualize the model flow and salinity information. The WARMF model contains hydrologic routing that is capable of calculating flow and water quality at roughly one-mile intervals [156,167].

The SJRRTM is a web-based salinity DSS that combines WARMF and assimilative salt capacity forecasts information to increase stakeholder awareness of the unique opportunities and measures to improve water quality resource management in the San Joaquin River Basin. The decision support system was implemented using OpenNRM, an open-source software that systematically allows users to perform tasks such as creating, modifying and managing data and web content. One of the specific features of the SJRTM web portal has been the integration of WARMF model-generated flow with real-time SJR tributary flow and EC data with salt load assimilative capacity predictions [156].

In addition to decision support systems, various models are widely used for salinity management studies in the Central Valley. Models such as Westside Agricultural Drainage Economics (WADE) [168] and the Agricultural Production Salinity Irrigation Drainage Economics (APSIDE) [169] are examples of policy models used in the Central Valley. The APSIDE model has the specificity of simulating the agricultural production and projected income in response to irrigation water quality and drainage policy constraints [169].

9. IDSS for Irrigation System Management

Under increasing water deficit or drought conditions, distribution uniformity plays a critical factor in managing the available water efficiently while simultaneously improving and maintaining the yield and quality of specialty crops [170,171]. Distribution uniformity can be defined as the even distribution or spread of applied irrigation to avoid over- or under-watering at specific locations across the field. Non-uniform distribution can not only reduce the yield, but it affects the drainage, increases soil erosion risk through runoff, increases nitrate leaching and reduces the available nitrate content in the soil [172,173]. Under California's arid conditions, a reduced use of water and energy in the agricultural sector is largely dependent on efficient DU. Although it is impossible to attain 100% distribution uniformity, the goal is to maximize the uniform and efficient distribution of the applied irrigation water.

Application use efficiency is the ratio of the amount of water lost through evapotranspiration to the amount of water applied for crop production [174]. The joint initiative of the California Department of Food and Agriculture and Department of Water Resources has a goal of decreasing 1200–1220 ML of agricultural water use per year through on-farm efficiency improvements. The majority of California's crops are now cultivated using micro-irrigation systems, such as sprinkler, drip and subsurface drip irrigation. The distribution uniformity for drip and subsurface drip irrigation systems is determined by taking the ratio of average flow of the lowest quarter of emitters to all emitters sampled [130,175].

Decision support tools offer the potential for site-specific irrigation management, which optimizes distribution uniformity by delineating the fields into management zones [176,177]. The UCANR's Bilingual Emission Uniformity Calculator uses a bilingual (English and Spanish) interface with an Excel spreadsheet model to help growers calculate distribution uniformity based on emitter discharge measurements [178]. Using wireless sensor networks (soil and crop canopy-based), irrigation automation and telemetry control through mobile or cloud-based applications allows the growers to efficiently increase the distribution uniformity based on real-time data. Growers can use automation equipment to avoid over- or under-watering with remote access [179,180]. In California, many nut growers in the state are using an alternative method of determining transpiration uniformity rather than using distribution uniformity [181]. Transpiration uniformity describes the uniform loss of water from the field, in contrast to DU, which defines the spread across the field. Because transpiration is an indicator of plant metabolism, it can also be affected by nutrients, pests or soil heterogeneity, which would not be related to the uniformity of an application. Remote-sensing IDSS are useful in evaluating the distribution uniformity based on thermal and NDVI maps generated using multispectral imagery. In California, Ceres Imaging is widely used by orchard and vegetable growers to identify the water stress due to uneven distribution uniformity based on colorized NDVI and thermal maps, as shown in Figure 3. The identification of stressed areas at an early stage in a crop field allows growers to quickly identify, diagnose and correct irrigation system problems to avoid yield losses at the harvest stage.

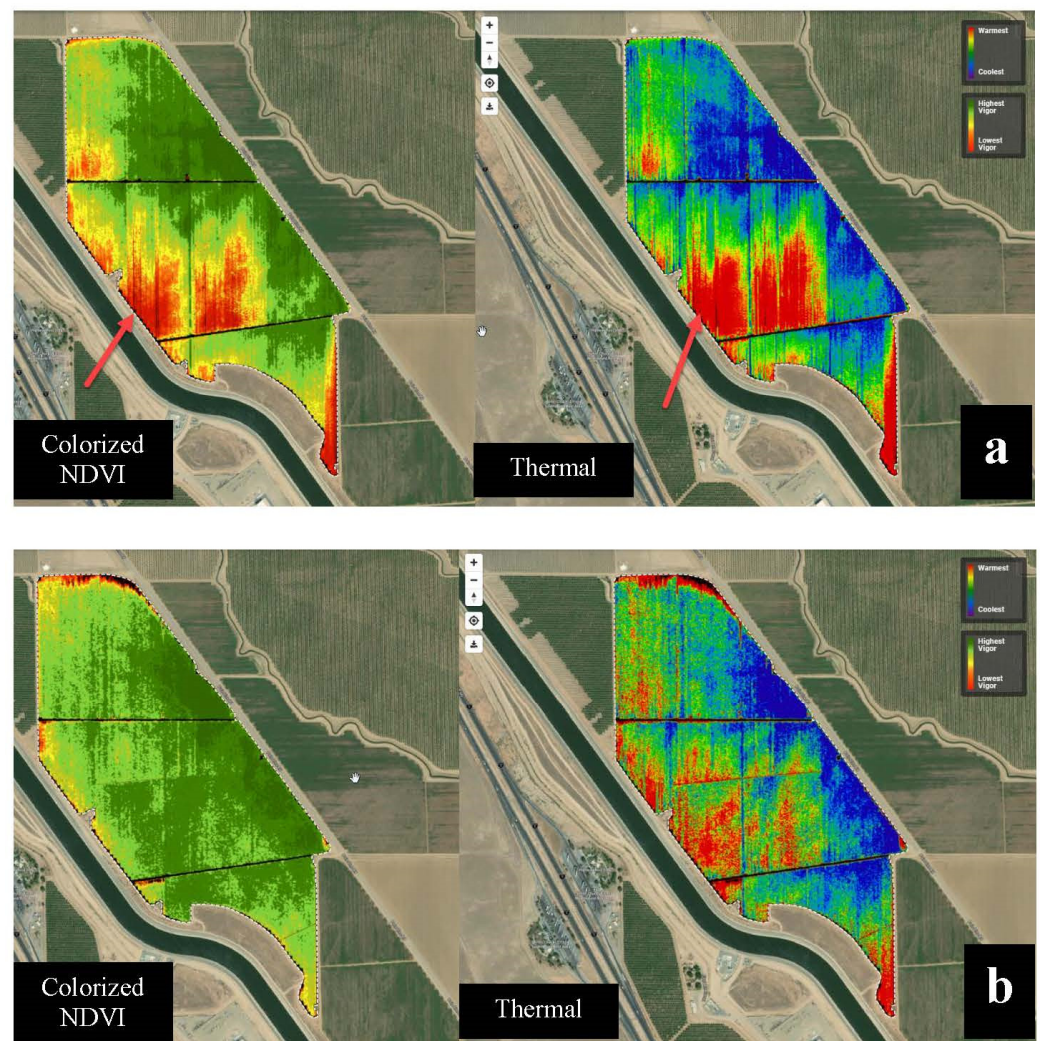


Figure 3. Remote-sensing imagery-based IDSS provided by Ceres Imaging Inc. (Oakland, CA, USA) for evaluating distribution uniformity using colorized NDVI and thermal maps. (a) Warmest areas of the field were under water stress and showed lowest vigor at early crop growth stage because of low dripline pressure due to topographical differences; (b) Increased pressure of driplines after identifying the stress led to more uniform distribution of water application with homogenous crop vigor saving an estimated yield worth USD 20,000.

10. IDSS Evaluation and Ongoing Work in California

In this rapidly growing field of products and services, detailed information on the utility, user friendliness, reliability, accuracy and precision of IDSS is of primary importance to the end user. The purpose of the Hub project is to evaluate the irrigation decision support systems to optimize irrigation water use efficiency and reduce energy use on farms for conveyance, pumping and distribution of irrigation water in California. The current evaluation of IDSS is based on scientific validation, user friendliness and inputs from advisory groups. User-friendly decision support tools are important for maximizing benefits by enhancing productivity and simplifying the spatiotemporal environmental parameters [182,183]. For IDSS, innovation, validation and adoption are cyclical, iterative processes engaged in by the agricultural technology industry, applied or Cooperative Extension researchers and growers (Figure 4). In the cyclical process of innovation–validation–adoption, it is helpful to form a project advisory group to achieve a more practical, secure and cohesive approach [179]. This user feedback is pivotal for implementing and improving new IDSS technologies [184]. The primary focus of the advisory group members is to assist in shaping the process of research that can simplify the later steps for adoption [185,186].

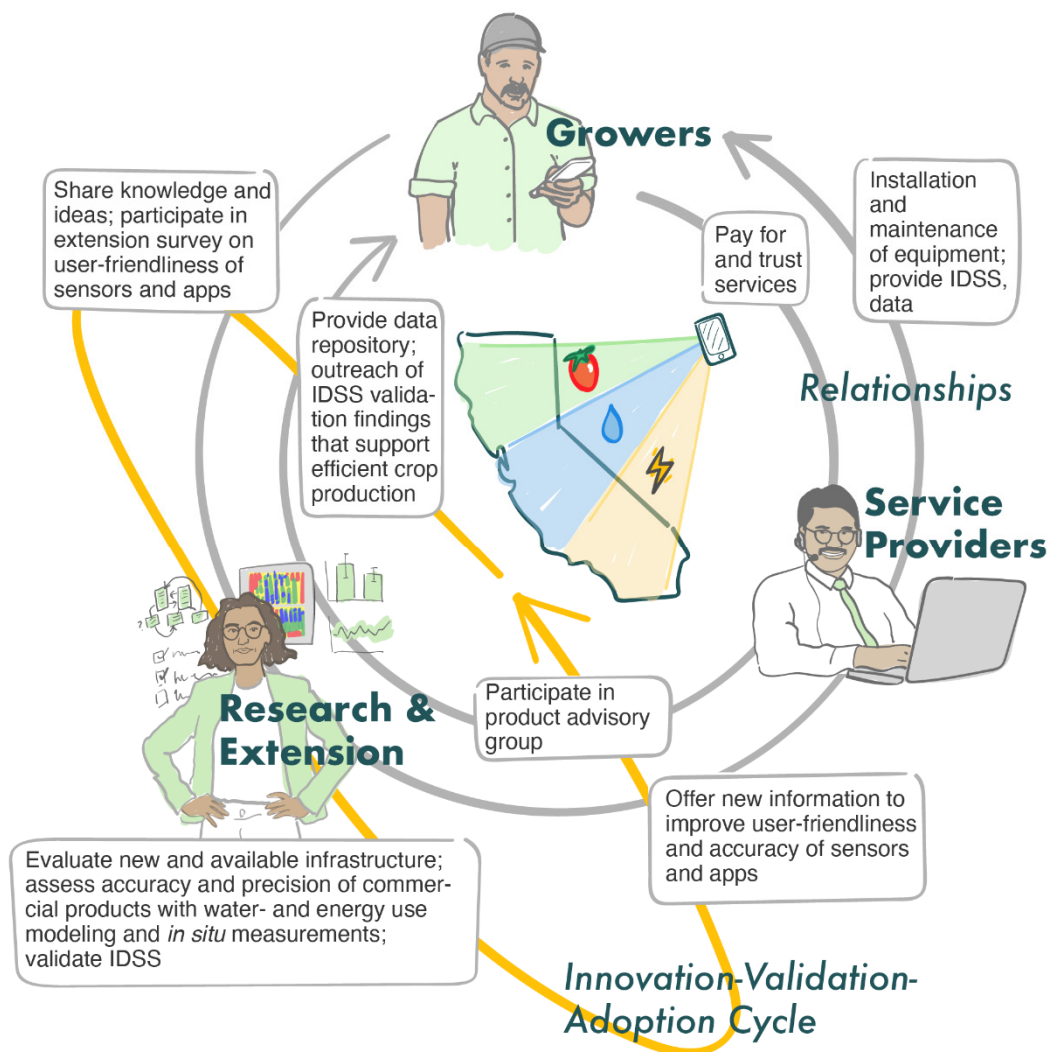


Figure 4. Innovation–adoption–validation cycle of irrigation decision support system. Artwork by Dr. Bonnie McGill.

Ideally, IDSS should be assessed for data accuracy, linearity, precision, response time and reliability [187,188]. This can be carried out using research-grade equipment with eddy covariance and neutron probe measurements of key water budget components, as well as estimates of leaf area index, to better understand and predict the K_c values. Different complexity may be required for different end users (i.e., farm manager versus irrigators). The system's user friendliness can be assessed by user interview or survey that generally focuses on: (a) graphic interface features, (b) graphic interface ease of use, (c) field placement decision support, (d) comprehensiveness, (e) update frequency, (f) reliability, (g) system value and (h) unanticipated costs [189,190]. In addition, the performance evaluation of IDSS is important based on soil and crop type. Performance evaluation should be based on statistical analysis and comparison based on root mean square error (RMSE), RMSE-observation-based standard deviation ratio (RSR), mean bias error and index of agreement [191].

11. Conclusions

Irrigation decision support systems (IDSS) may greatly benefit the >400 crops grown throughout the State of California to support diverse challenges, including drought, energy, nitrogen and salinity management. Here, we conducted a comprehensive review of existing IDSS available to California growers, their underlying science, incentive policies

and anticipated outcomes. Effective energy, water, nitrogen and salinity management in California under regulatory policies, such as the Sustainable Groundwater Management Act, require the integration of different strategies to improve precision irrigation scheduling, uniform water and nutrient application, and the soil–plant–water monitoring. In addition to water management, these policies also aim to manage groundwater and require the record keeping of water use, nitrogen (N) leaching, salinity management and energy consumption. Most of the irrigation decision support tools used in California are based on fewer components of the water budget, and none of the available IDSS provide estimation of all parameters together. For example, soil-based IDSS consider soil water potential or volumetric water content, while crop canopy IDSS are based on crop evapotranspiration. These IDSS can potentially be used in combination to obtain the overall inflow and outflow of water to and from the soil–plant–atmospheric continuum of the crops. However, heterogeneity in agronomic and field soils can lead to poor management practices at certain locations in agricultural fields. Remote sensing IDSS are useful in determining the spatial scale information based on spectral data, but the interpretation of multispectral/thermal imagery is complicated and difficult for growers to base decisions for water, nutrient and salinity hotspots. In a nutshell, there has been an identifiable need for the co-management of irrigation decision support, nitrogen and salinity management and energy efficiency. The integration of IDSS for nexus benefits is a cyclical process of innovation by service providers/researchers, validation by extension research professionals and adoption by growers. Therefore, for a widescale adoption of these tools, the synergetic evaluation of point-based and spatial IDSS needs to be studied and validated on different scales (farm to county). Not only is the information presentation and availability important; the integration within the farm management hierarchy is equally significant. The recommended information on water, nitrogen, salts and energy management must be clearly and simply transmitted to and from farm managers to individual irrigators.

Author Contributions: Conceptualization, G.J., R.S. and M.A.N.; writing—original draft, G.J., F.N., R.S., K.S. (Kosana Suvočarev) and D.D.; writing—reviewing and editing, G.J., K.S. (Kosana Suvočarev), D.D., I.K., K.S. (Kate Scow) and M.A.N.; visualization, G.J. and M.A.N.; funding acquisition, K.S. (Kate Scow) and M.A.N.; supervision, R.S. and M.A.N.; project administration, G.J., R.S. D.D. and M.A.N. All authors have read and agreed to the published version of the manuscript.

Funding: This research was funded by the California Energy Commission-sponsored Energy Product Evaluation Hub (Cal-EPE Hub) (Grant- EPC-17-034) and the California Department of Food and Agriculture.

Institutional Review Board Statement: Not applicable.

Informed Consent Statement: Not applicable.

Data Availability Statement: Not applicable.

Acknowledgments: The authors are thankful to the California Energy Commission-sponsored Energy Product Evaluation Hub and the IDSS Product Advisory Group for providing support in the planning of this research on decision support for water–nutrient–energy nexus in CA. The artwork in Figures 2 and 4 was created by Bonnie McGill.

Conflicts of Interest: The authors declare no conflict of interest.

Abbreviations

Nitrogen (N), ET_o (reference evapotranspiration over a grass surface), K_c (crop coefficient), ET_c (potential crop evapotranspiration based on ET_o and K_c), AWC (plant available soil water content), NDVI (Normalized Difference Vegetation Index).

References

1. CDFA—Statistics. Available online: <https://www.cdfa.ca.gov/Statistics/> (accessed on 5 July 2022).
2. Jerphagnon, O.; Knutson, S.; Geyer, R.; Scow, K. *Decision Support Tool to Reduce Energy and Water Consumption in Agriculture*; California Energy Commission: Sacramento, CA, USA, 2019.
3. California Department of Water Resources Agricultural Water Use Efficiency. Available online: <https://water.ca.gov/Programs/Water-Use-And-Efficiency/Agricultural-Water-Use-Efficiency> (accessed on 5 July 2022).
4. Berger, M.A.; Hans, L.; Piscopo, K.; Sohn, M.D. Exploring the Energy Benefits of Advanced Water Metering. *Energy Anal. Environ. Impacts Div. Energy Technol. Area* **2016**, *54*, 1005988.
5. Water & Energy—California Agricultural Water Stewardship Initiative. Available online: https://agwaterstewards.org/practices/water_energy/ (accessed on 5 July 2022).
6. Howitt, R.; Medellín-azuara, J.; Macewan, D. *Economic Analysis of the 2014 Drought for California Agriculture*; University of California Davis: Davis, CA, USA, 2014.
7. Johnson, R.; Cody, B.A. *California Agricultural Production and Irrigated Water Use*; Congressional Research Service: California, CA, USA, 2015; p. 28.
8. Bazzani, G.M. An Integrated Decision Support System for Irrigation and Water Policy Design: DSIRR. *Environ. Model. Softw.* **2005**, *20*, 153–163. [CrossRef]
9. Rinaldi, M.; He, Z. *Decision Support Systems to Manage Irrigation in Agriculture*, 1st ed.; Elsevier Inc.: Amsterdam, The Netherlands, 2014; Volume 123, ISBN 9780124202252.
10. Schwabe, K.; Nemati, M.; Landry, C.; Zimmerman, G. Water Markets in the Western United States: Trends and Opportunities. *Water* **2020**, *12*, 233. [CrossRef]
11. Mount, J.; Hanak, E. *Water Use in California: Just the Facts*; PPIC Water Policy Center: San Francisco, CA, USA, 2019.
12. California Department of Water Resources DWR Contributes \$16 Million to Support Desalination Research, Improved Energy Efficiency. Available online: <https://water.ca.gov/News/Blog/2021/September/DWR-Contributes-16-Million-to-Support-Desalination-Research> (accessed on 5 July 2022).
13. Willett, M.; Willett, M. *USF Scholarship: A Digital Repository @ Gleeson Library | Geschke Energy Intensity Variation among California Urban Water Supplies*; The University of San Francisco: San Francisco, CA, USA, 2020.
14. Escrivá-Bou, A.; Lund, J.R.; Pulido-Velazquez, M. Saving Energy from Urban Water Demand Management. *Water Resour. Res.* **2018**, *54*, 4265–4276. [CrossRef]
15. Fayiah, M.; Dong, S.; Singh, S.; Kwaku, E.A. A Review of Water–Energy Nexus Trend, Methods, Challenges and Future Prospects. *Int. J. Energy Water Resour.* **2020**, *4*, 91–107. [CrossRef]
16. Lofman, D.; Petersen, M.; Bower, A. Water, Energy and Environment Nexus: The California Experience. *Int. J. Water Resour. Dev.* **2002**, *18*, 73–85. [CrossRef]
17. Bedsworth, L.; Cayan, D.; Guido, F.; Fisher, L.; Ziaja, S. *California’s Fourth Climate Change Assessment Statewide Summary Report*; California Department of Parks & Recreation: Sacramento, CA, USA, 2018; p. 133.
18. English, M.J.; Solomon, K.H.; Huffman, G.J. A Paradigm Shift in Irrigation Management. *Perspect. Civ. Eng. Commem. Anniv. Am. Soc. Civ. Eng.* **2003**, *128*, 89–99. [CrossRef]
19. Baldocchi, D.; Agarwal, D.; Torn, M.; Humphrey, M. *Connecting AmeriFlux to the Globe, Extending the Partnership with Global Flux Network FLUXNET*; No. DOE-UCB-037357; University of California: Berkeley, CA, USA, 2018.
20. Younghein, M. Water and Energy Calculator 2.0 Project Report. 2022. Available online: <https://www.cpuc.ca.gov/-/media/cpuc-website/divisions/energy-division/documents/water-energy-nexus/we-calc20-project-report.pdf> (accessed on 20 June 2022).
21. CA Farm Bureau Federation Electricity Rates. 2022. Available online: <https://www.cfbf.com/> (accessed on 11 June 2022).
22. Koundouri, P.; Nauges, C.; Tzouvelekas, V. Technology Adoption under Production Uncertainty: Theory and Application to Irrigation Technology. *Am. J. Agric. Econ.* **2006**, *88*, 657–670. [CrossRef]
23. Berbel, J.; Expósito, A. The Theory and Practice of Water Pricing and Cost Recovery in the Water Framework Directive. *Water Altern.* **2020**, *13*, 659–673.
24. Portoghese, I.; Giannoccaro, G.; Giordano, R.; Pagano, A. Modeling the Impacts of Volumetric Water Pricing in Irrigation Districts with Conjunctive Use of Surface and Groundwater Resources. *Agric. Water Manag.* **2021**, *244*, 106561. [CrossRef]
25. Méndez-Barrientos, L.E.; DeVincentis, A.; Rudnick, J.; Dahlquist-Willard, R.; Lowry, B.; Gould, K. Farmer Participation and Institutional Capture in Common-Pool Resource Governance Reforms. The Case of Groundwater Management in California. *Soc. Nat. Resour.* **2020**, *33*, 1486–1507. [CrossRef]
26. Lubell, M.; Blomquist, W.; Beutler, L. Sustainable Groundwater Management in California: A Grand Experiment in Environmental Governance. *Soc. Nat. Resour.* **2020**, *33*, 1447–1467. [CrossRef]
27. *Water Resource Control Board Irrigated Lands Regulatory Program*; California Environmental Protection Agency: Sacramento, CA, USA, 2020; pp. 1–6.
28. Almond Board of California. Almond Irrigation Improvement Continuum., 1–6. 2020. Available online: <https://www.almonds.com/sites/default/files/2020-02/Almond-Irrigation-Improvement-Continuum.pdf> (accessed on 5 July 2022).
29. USDA-NASS 2018 Irrigation and Water Management Survey. Available online: https://www.nass.usda.gov/Publications/AgCensus/2017/Online_Resources/Farm_and_Ranch_Irrigation_Survey/index.php (accessed on 5 July 2022).

30. Ghafouri, N. WaterBit. 2019. Available online: <https://www.waterbit.app/over-irrigation/> (accessed on 5 July 2022).
31. Volder, A. Exploring the Black Box-Root Growth. In *Proceedings of the Tree Physiology: How Does an Almond Tree Grow*; Almond Board of California: Modesto, CA, USA, 2016.
32. Swett, C.L. Managing Crop Diseases under Water Scarcity. *Annu. Rev. Phytopathol.* **2020**, *58*, 387–406. [CrossRef]
33. Luković, J.; Chiang, J.C.H.; Blagojević, D.; Sekulić, A. A Later Onset of the Rainy Season in California. *Geophys. Res. Lett.* **2021**, *48*, e2020GL090350. [CrossRef]
34. Goss, M.; Swain, D.L.; Abatzoglou, J.T.; Sarhadi, A.; Kolden, C.A.; Williams, A.P.; Diffenbaugh, N.S. Climate Change Is Increasing the Likelihood of Extreme Autumn Wildfire Conditions across California. *Environ. Res. Lett.* **2020**, *15*, 094016. [CrossRef]
35. Peterson, T.C.; Stott, P.A.; Herring, S. Explaining Extreme Events of 2018 from a Climate Perspective. *Bull. Am. Meteorol. Soc.* **2020**, *93*, 1041–1067. [CrossRef]
36. Burton, C.A.; Hoefen, T.M.; Plumlee, G.S.; Baumberger, K.L.; Backlin, A.R.; Gallegos, E.; Fisher, R.N. Trace Elements in Stormflow, Ash, and Burned Soil Following the 2009 Station Fire in Southern California. *PLoS ONE* **2016**, *11*, e0153372. [CrossRef] [PubMed]
37. Pruitt, W.O.; Doorenbos, J. *Empirical Calibration: A Requisite for Evapotranspiration Formulae Based on Daily or Longer Mean Climate Data?* The Committee: Budapest, Hungary, 1977.
38. Dong, A.; Grattan, S.R.; Carroll, J.J.; Prashar, C.R.K. Estimation of Daytime Net Radiation over Well-Watered Grass. *J. Irrig. Drain. Eng.* **1992**, *118*, 466–479. [CrossRef]
39. Temesgen, B.; Eching, S.; Davidoff, B.; Frame, K. Comparison of Some Reference Evapotranspiration Equations for California. *J. Irrig. Drain. Eng.* **2005**, *131*, 73–84. [CrossRef]
40. Ben Hamouda, G.; Zaccaria, D.; Bali, K.; Snyder, R.L.; Ventura, F. Evaluation of Forecast Reference Evapotranspiration for Different Microclimate Regions in California to Enable Prospective Irrigation Scheduling. *J. Irrig. Drain. Eng.* **2022**, *148*, 04021061. [CrossRef]
41. Parker, L.; Pathak, T.; Ostoja, S. Climate Change Reduces Frost Exposure for High-Value California Orchard Crops. *Sci. Total Environ.* **2021**, *762*, 143971. [CrossRef] [PubMed]
42. Hanson, B.; Orloff, S.; Sanden, B. *Monitoring Soil Moisture for Irrigation Water Management*; University of California, Agriculture and Natural Resources: Davis, CA, USA, 2007; Volume 21635.
43. Gu, Z.; Qi, Z.; Burghate, R.; Yuan, S.; Jiao, X.; Xu, J. Irrigation Scheduling Approaches and Applications: A Review. *J. Irrig. Drain. Eng.* **2020**, *146*, 4020007. [CrossRef]
44. Montazar, A.; Rejmanek, H.; Tindula, G.; Little, C.; Shapland, T.; Anderson, F.; Inglese, G.; Mutters, R.; Linqvist, B.; Greer, C.A.; et al. Crop Coefficient Curve for Paddy Rice from Residual Energy Balance Calculations. *J. Irrig. Drain. Eng.* **2017**, *143*, 04016076. [CrossRef]
45. Hanson, B.R.; May, D.M. Crop Coefficients for Drip-Irrigated Processing Tomato. *Agric. Water Manag.* **2006**, *81*, 381–399. [CrossRef]
46. Hanson, B.; Bendixen, W. Drip Irrigation Evaluated in Santa Maria Valley Strawberries. *Calif. Agric.* **2004**, *58*, 48–53. [CrossRef]
47. Bellvert, J.; Adeline, K.; Baram, S.; Pierce, L.; Sanden, B.L.; Smart, D.R. Monitoring Crop Evapotranspiration and Crop Coefficients Over an Almond and Pistachio Orchard Throughout Remote Sensing. *Remote Sens.* **2018**, *10*, 2001. [CrossRef]
48. Steduto, P.; Hsiao, T.C.; Fereres, E.; Raes, D. *Crop Yield Response to Water*; Steduto, P., Ed.; FAO Irrigation and Drainage Paper; Food and Agriculture Organization of the United Nations: Rome, Italy, 2012; pp. 358–373. ISBN 978-92-5-107274-5.
49. Micke, W.C. *Almond Production Manual*; University of California, Division of Agriculture and Natural Resources: Oakland, CA, USA, 1996; ISBN 978-1-879906-22-8.
50. Sanden, B.; Brown, P.; Snyder, R. Insights on water management in almonds. In *2012 Conference Proceedings*; California Chapter; American Society of Agronomy: Madison, WI, USA, 2012; pp. 88–91.
51. FAO. Chapter 6-ETc-Single Crop Coefficient (Kc). Available online: <https://www.fao.org/3/x0490e/x0490e0b.htm> (accessed on 8 August 2022).
52. University of California Almonds. Available online: http://ucmanagedrought.ucdavis.edu/Agriculture/Crop_Irrigation_Strategies/Almonds (accessed on 7 August 2022).
53. Doll, D. *Pistachio Irrigation: Determining Water Needs and Managing Drought*; University of California, Agriculture and Natural Resources: Davis: Davis, CA, USA, 2017.
54. Goldhamer, D.A. Tree Water Requirements and Regulated Deficit Irrigation. *Pist. Prod. Man.* **2005**, *4*, 103–116.
55. Zaccaria, D. Updated Water Use Information for Irrigation Scheduling of Pistachio on Non-Saline and Increasingly Saline Soils. Available online: <https://ucanr.edu/sites/calasa/files/345175.pdf>. (accessed on 7 August 2022).
56. University of California Agriculture and Natural Resources. Using Reference Evapotranspiration (ETo) and Crop Coefficients to Estimate Crop Evapotranspiration (ETc) for Agronomic Crops, Grasses, and Vegetable Crops. Available online: <https://cimis.water.ca.gov/Content/PDF/21427-KcAgronomicGrassandVeg.pdf> (accessed on 7 August 2022).
57. University of California Agriculture and Natural Resources Walnuts. Available online: http://ucmanagedrought.ucdavis.edu/Agriculture/Crop_Irrigation_Strategies/Walnuts (accessed on 7 August 2022).
58. Irrigation of Processing Tomatoes/Tomato/Agriculture: Pest Management Guidelines/UC Statewide IPM Program (UC IPM). Available online: <https://www2.ipm.ucanr.edu/agriculture/tomato/Irrigation-of-Processing-Tomatoes/> (accessed on 7 August 2022).

59. López-Urrea, R.; Montoro, A.; Mañas, F.; López-Fuster, P.; Fereres, E. Evapotranspiration and Crop Coefficients from Lysimeter Measurements of Mature ‘Tempranillo’ Wine Grapes. *Agric. Water Manag.* **2012**, *112*, 13–20. [CrossRef]
60. Goldammer, T. *Grape Grower’s Handbook: A Guide to Viticulture for Wine Production*; APEX Publishers: Centreville, VA, USA, 2018; ISBN 978-0-9675212-5-1.
61. Hanson, B. Crop Coefficients: Irrigation Water Management: Science, Art, or Guess? Available online: https://ucanr.edu/sites/irrigation_and_soils_/files/93370.pdf (accessed on 7 August 2022).
62. Smith, R.; Cahn, M.; Daugovish, O.; Koike, S.; Natwick, E.; Smith, H.; Subbarao, K.; Takele, E.; Turini, T. *Leaf Lettuce Production in California*; University of California, Agriculture and Natural Resources: California, CA, USA, 2011; ISBN 978-1-60107-767-7.
63. Hardke, J.T. Water-Use Efficiency Options. In *Rice Farming*; One Grower Publishing: Memphis, TN, USA, 2013.
64. University of California Agriculture and Natural Corn. Available online: http://ucmanagedrought.ucdavis.edu/Agriculture/Crop_Irrigation_Strategies/Corn (accessed on 7 August 2022).
65. Gao, Y.; Duan, A.; Sun, J.; Li, F.; Liu, Z.; Liu, H.; Liu, Z. Crop Coefficient and Water-Use Efficiency of Winter Wheat/Spring Maize Strip Intercropping. *Field Crops Res.* **2009**, *111*, 65–73. [CrossRef]
66. Bauder, J. Wheat Irrigation—MSU Extension Water Quality | Montana State University. Available online: <https://waterquality.montana.edu/farm-ranch/irrigation/wheat/wheat-irrigation.html> (accessed on 8 August 2022).
67. Shewmaker, G.E.; Allen, R.G.; Neibling, W.H. *Alfalfa Irrigation and Drought 2013*; University of Idaho: Moscow, ID, USA, 2013.
68. Snyder, R.L.; Bali, K.M. Irrigation Scheduling of Alfalfa Using Evapotranspiration. In Proceedings of the 2008 California Alfalfa and Forage Symposium and Western Seed Conference, San Diego, CA, USA, 2–4 December 2008; pp. 2–4.
69. Hanson, B.; Schwankl, L.; Fulton, A. *Scheduling Irrigations: When and How Much Water to Apply*; Division of Agriculture and Natural Resources Publication: Oakland, CA, USA, 2004; p. 3396.
70. Devine, S.; Anthony Toby, O. Climate-Smart Management of Soil Water Storage: Statewide Analysis of California Perennial Crops. *Environ. Res. Lett.* **2019**, *14*, 44021. [CrossRef]
71. Sorooshian, S.; Li, J.; Hsu, K.; Gao, X. How Significant Is the Impact of Irrigation on the Local Hydroclimate in California’s Central Valley? Comparison of Model Results with Ground and Remote-sensing Data. *J. Geophys. Res. Atmos.* **2011**, *116*, D06102. [CrossRef]
72. Hanson, B.R.; Peters, D. Soil Type Affects Accuracy of Dielectric Moisture Sensors. *Calif. Agric.* **2000**, *54*, 43–47. [CrossRef]
73. Bausch, W.C. Remote Sensing of Crop Coefficients for Improving the Irrigation Scheduling of Corn. *Agric. Water Manag.* **1995**, *27*, 55–68. [CrossRef]
74. French, A.N.; Hunsaker, D.J.; Sanchez, C.A.; Saber, M.; Gonzalez, J.R.; Anderson, R. Satellite-Based NDVI Crop Coefficients and Evapotranspiration with Eddy Covariance Validation for Multiple Durum Wheat Fields in the US Southwest. *Agric. Water Manag.* **2020**, *239*, 106266. [CrossRef]
75. Horta, A.; Malone, B.; Stockmann, U.; Minasny, B.; Bishop, T.F.A.; McBratney, A.B.; Pallasser, R.; Pozza, L. Potential of Integrated Field Spectroscopy and Spatial Analysis for Enhanced Assessment of Soil Contamination: A Prospective Review. *Geoderma* **2015**, *241–242*, 180–209. [CrossRef]
76. Nocco, M.A.; Rouse, S.E.; Balster, N.J. Vegetation Type Alters Water and Nitrogen Budgets in a Controlled, Replicated Experiment on Residential-Sized Rain Gardens Planted with Prairie, Shrub, and Turfgrass. *Urban Ecosyst.* **2016**, *19*, 1665–1691. [CrossRef]
77. Nocco, M.A.; Zipper, S.C.; Booth, E.G.; Cummings, C.R.; Loheide, S.P.; Kucharik, C.J. Combining Evapotranspiration and Soil Apparent Electrical Conductivity Mapping to Identify Potential Precision Irrigation Benefits. *Remote Sens.* **2019**, *11*, 2460. [CrossRef]
78. McLennon, E.; Dari, B.; Jha, G.; Sihi, D.; Kankarla, V. Regenerative Agriculture and Integrative Permaculture for Sustainable and Technology Driven Global Food Production and Security. *Agron. J.* **2021**, *113*, 4541–4559. [CrossRef]
79. Jha, G.; Mukhopadhyay, S.; Ulery, A.L.; Lombard, K.; Chakraborty, S.; Weindorf, D.C.; VanLeeuwen, D.; Brungard, C. Agricultural Soils of the Animas River Watershed after the Gold King Mine Spill: An Elemental Spatiotemporal Analysis via Portable X-Ray Fluorescence Spectroscopy. *J. Environ. Qual.* **2021**, *50*, 730–743. [CrossRef]
80. Zhang, J.; Guan, K.; Peng, B.; Jiang, C.; Zhou, W.; Yang, Y.; Pan, M.; Franz, T.E.; Heeren, D.M.; Rudnick, D.R.; et al. Challenges and Opportunities in Precision Irrigation Decision-Support Systems for Center Pivots. *Environ. Res. Lett.* **2021**, *16*, 053003. [CrossRef]
81. Cahn, M.; Hartz, T.; Smith, R.; Noel, B.; Johnson, L.; Melton, F. CropManage: An Online Decision Support Tool for Irrigation and Nutrient Management. *West. Nutr. Manag. Conf. Proc.* **2015**, *11*, 9–15.
82. Cahn, M.; Brown, P.; Fulton, A. *Adapting CropManage Irrigation and Nitrogen Management Decision Support Tool for Central Valley Crops*; California Department of Food and Agriculture: Sacramento, CA, USA, 2020.
83. Khalid, S.; Sherzad, S. *Agricultural Extension Manual for Extension Workers*. Food and Agriculture Organization of United Nations Manual Book; FAO: Roma, Italy, 2019; pp. 1–42.
84. Montazar, A.; Bachie, O.; Corwin, D.; Putnam, D. Feasibility of Moderate Deficit Irrigation as a Water Conservation Tool in California’s Low Desert Alfalfa. *Agronomy* **2020**, *10*, 1640. [CrossRef]
85. Munoz-Carpena, R. Field Devices for Monitoring Soil Water Content. *Bull. Inst. Food Agric. Sci. Univ. Fla.* **2004**, *343*, 1–16. [CrossRef]
86. Busscher, W.J. Field Estimation of Soil Water Content: A Review. *J. Soil Water Conserv.* **2009**, *64*, 116A. [CrossRef]
87. Campbell, G.S. Soil Water Potential Measurement: An Overview. *Irrig. Sci.* **1988**, *9*, 265–273. [CrossRef]

88. Muñoz-carpena, R.; Dukes, M.D.; Li, Y.C.; Klassen, W. Field Comparison of Tensiometer and Irrigation on Tomato. *HortTechnology* **2005**, *15*, 584–590. [CrossRef]
89. Jha, G.; Choudhary, O.P.; Sharda, R.; Tejada Moral, M. Comparative Effects of Saline Water on Yield and Quality of Potato under Drip and Furrow Irrigation. *Cogent Food Agric.* **2017**, *3*, 1369345. [CrossRef]
90. Shackel, K.; Lampinen, B.; Sibbett, S.; Olson, W. The relation of midday stem water potential to the growth and physiology of fruit trees under water limited conditions. *Acta Hort.* **2000**, *537*, 425–430. [CrossRef]
91. Hu, T.; Kang, S.; Li, F.; Zhang, J. Effects of Partial Root-Zone Irrigation on Hydraulic Conductivity in the Soil-Root System of Maize Plants. *J. Exp. Bot.* **2011**, *62*, 4163–4172. [CrossRef]
92. Jha, G. A Review on Drip Irrigation Using Saline Irrigation Water in Potato (*Solanum tuberosum* L.). *J. Agroecol. Nat. Resour. Manag.* **2016**, *3*, 43–46.
93. Chen, A.; Orlov-Levin, V.; Meron, M. Applying High-Resolution Visible-Channel Aerial Imaging of Crop Canopy to Precision Irrigation Management. *Agric. Water Manag.* **2019**, *216*, 196–205. [CrossRef]
94. Hunt, E.R.; Doraiswamy, P.C.; McMurtrey, J.E.; Daughtry, C.S.T.; Perry, E.M.; Akhmedov, B. A Visible Band Index for Remote Sensing Leaf Chlorophyll Content at the Canopy Scale. *Int. J. Appl. Earth Obs. Geoinf.* **2012**, *21*, 103–112. [CrossRef]
95. Testa, G.; Gresta, F.; Cosentino, S.L. Dry Matter and Qualitative Characteristics of Alfalfa as Affected by Harvest Times and Soil Water Content. *Eur. J. Agron.* **2011**, *34*, 144–152. [CrossRef]
96. Green, S.; McNaughton, K.; Wünsche, J.N.; Clothier, B. Modeling Light Interception and Transpiration of Apple Tree Canopies. *Agron. J.* **2003**, *95*, 1380–1387. [CrossRef]
97. Massmann, A.; Gentine, P.; Lin, C. When Does Vapor Pressure Deficit Drive or Reduce Evapotranspiration? *J. Adv. Model. Earth Syst.* **2019**, *11*, 3305–3320. [CrossRef]
98. Greco, M.; Chiappetta, A.; Bruno, L.; Bitonti, M.B. Estimating Evapotranspiration and Drought Stress in DNA In Posidonia Oceanica Cadmium Induces Changes with Ground-Based Thermal Patterning Remote Sensing in Methylation and Chromatin Agriculture: A Review. *J. Exp. Bot.* **2012**, *63*, 4671–4712. [CrossRef]
99. Kisekka, I.; Aguilar, J.; Lamm, F.R.; Kansas, C.; Rogers, D. Using Soil Water and Canopy Temperature to Improve Irrigation Scheduling for Corn. In Proceedings of the 2014 Irrigation Association Conference, Phoenix, AZ, USA, 19–20 November 2014.
100. Aladenola, O.; Madramootoo, C. Response of Greenhouse-Grown Bell Pepper (*Capsicum annuum* L.) to Variable Irrigation. *Can. J. Plant Sci.* **2014**, *94*, 303–310. [CrossRef]
101. Bellvert, J.; Marsal, J.; Girona, J.; Gonzalez-Dugo, V.; Fereres, E.; Ustin, S.; Zarco-Tejada, P. Airborne Thermal Imagery to Detect the Seasonal Evolution of Crop Water Status in Peach, Nectarine and Saturn Peach Orchards. *Remote Sens.* **2016**, *8*, 39. [CrossRef]
102. Prueger, J.H.; Parry, C.K.; Kustas, W.P.; Alfieri, J.G.; Alsina, M.M.; Nieto, H.; Wilson, T.G.; Hipps, L.E.; Anderson, M.C.; Hatfield, J.L.; et al. Crop Water Stress Index of an Irrigated Vineyard in the Central Valley of California. *Irrig. Sci.* **2018**, *37*, 297–313. [CrossRef]
103. DeJonge, K.C.; Taghvaeian, S.; Trout, T.J.; Comas, L.H. Comparison of Canopy Temperature-Based Water Stress Indices for Maize. *Agric. Water Manag.* **2015**, *156*, 51–62. [CrossRef]
104. Kullberg, E.G.; DeJonge, K.C.; Chávez, J.L. Evaluation of Thermal Remote Sensing Indices to Estimate Crop Evapotranspiration Coefficients. *Agric. Water Manag.* **2017**, *179*, 64–73. [CrossRef]
105. Fulton, A.; Grant, J.; Buchner, R.; Connell, J. *Using the Pressure Chamber for Irrigation Management in Walnut, Almond and Prune*; University of California, Agriculture and Natural Resources: Davis, CA, USA, 2014.
106. Shackel, K.; Moriana, A.; Marino, G.; Corell, M.; Pérez-lópez, D.; Martín-palomo, M.J.; Caruso, T.; Marra, F.P.; Martín, L.; Alcaras, A.; et al. Establishing a Reference Baseline for Midday Stem Water Potential in Olive and Its Use for Plant-Based Irrigation Management. *Front. Plant Sci.* **2021**, *12*, 2715. [CrossRef] [PubMed]
107. CDFa. *Climate Change Consortium for Specialty Crops: Impacts and Strategies for Resilience*; CDFa: Sacramento, CA, USA, 2013; p. 76.
108. Chen, W.-H.; Shang, C.; Zhu, S.; Haldeman, K.; Santiago, M.; Stroock, A.D.; You, F. Theoretical Exploration of Irrigation Control for Stem Water Potential through Model Predictive Control. In Proceedings of the 2020 American Control Conference (ACC), Online, 1–3 July 2020; pp. 1992–1997.
109. 2020 Research Update—Almond Board of California. Available online: https://www.almonds.com/sites/default/files/2020-12/ResearchUpdate_121620202.pdf (accessed on 20 July 2021).
110. Knipper, K.R.; Kustas, W.P.; Anderson, M.C.; Alfieri, J.G.; Prueger, J.H.; Hain, C.R.; Gao, F.; Yang, Y.; McKee, L.G.; Nieto, H.; et al. Evapotranspiration Estimates Derived Using Thermal-Based Satellite Remote Sensing and Data Fusion for Irrigation Management in California Vineyards. *Irrig. Sci.* **2019**, *37*, 431–449. [CrossRef]
111. Semmens, K.A.; Anderson, M.C.; Kustas, W.P.; Gao, F.; Alfieri, J.G.; McKee, L.; Prueger, J.H.; Hain, C.R.; Cammalleri, C.; Yang, Y.; et al. Monitoring Daily Evapotranspiration over Two California Vineyards Using Landsat 8 in a Multi-Sensor Data Fusion Approach. *Remote Sens. Environ.* **2016**, *185*, 155–170. [CrossRef]
112. Roy, S.; Ophori, D.; Kefauver, S. Estimation of Actual Evapotranspiration Using Surface Energy Balance Algorithms for Land Model: A Case Study in San Joaquin Valley, California. *J. Environ. Hydrol.* **2013**, *21*, 1–13.
113. Zhao, J.; Chen, X.; Zhang, J.; Zhao, H.; Song, Y. Higher Temporal Evapotranspiration Estimation with Improved SEBS Model from Geostationary Meteorological Satellite Data. *Sci. Rep.* **2019**, *9*, 14981. [CrossRef]
114. Xue, J.; Bali, K.M.; Light, S.; Hessels, T.; Kisekka, I. Evaluation of Remote Sensing-Based Evapotranspiration Models against Surface Renewal in Almonds, Tomatoes and Maize. *Agric. Water Manag.* **2020**, *238*, 106228. [CrossRef]

115. Medellín-Azuara, J.; Paw, U.K.T.; Jin, Y.; Jankowski, J.; Bell, A.M.; Kent, E.; Clay, J.; Wong, A.; Alexander, N.; Santos, N.; et al. *A Comparative Study for Estimating Crop Evapotranspiration in the Sacramento-San Joaquin Delta—Appendix G. NASA Satellite Irrigation Management Support System (SIMS)*; University of California Davis: Davis, CA, USA, 2018; pp. 1–3.
116. Poirier-pocovi, M.; Volder, A.; Bailey, B.N. Modeling of Reference Temperatures for Calculating Crop Water Stress Indices from Infrared Thermography. *Agric. Water Manag.* **2020**, *233*, 106070. [CrossRef]
117. Magney, T.S.; Frankenberg, C.; Köhler, P.; North, G.; Harrington, A.; Hat, J.; Stutz, J.; Sun, Y.; Castell, A.P. Disentangling Changes in the Spectral Shape of Chlorophyll Fluorescence: Implications for Remote Sensing of Photosynthesis. *J. Geophys. Res. Biogeosci.* **2019**, *124*, 1491–1507. [CrossRef]
118. Nocco, M.A.; Smail, R.A.; Kucharik, C.J. Observation of Irrigation—Induced Climate Change in the Midwest United States. *Glob. Chang. Biol.* **2019**, *25*, 3472–3484. [CrossRef]
119. Yu, R.; Zaccaria, D.; Kisekka, I.; Kurtural, S.K. Soil Apparent Electrical Conductivity and Must Carbon Isotope Ratio Provide Indication of Plant Water Status in Wine Grape Vineyards. *Precis. Agric.* **2021**, *22*, 1333–1352. [CrossRef]
120. Brush, C.F.; Dogrul, E.C.; Kadir, T.N. *Development and Calibration of the California Central Valley Groundwater-Surface Water Simulation Model (C2VSim), Version 3.02-CG*; California Department of Water Resources Technical Memorandum: San Diego, CA, USA, 2013; p. 193.
121. PPIC. *Energy and Water Use in California Are Interconnected*; PPIC: San Francisco, CA, USA, 2016.
122. University of California Agriculture and Natural Resources. Agricultural Issues Center-Energy and Agriculture. Available online: <https://aic.ucdavis.edu/> (accessed on 20 June 2021).
123. Howes, D.J.; Freeman, B.; Jones, M. *Agricultural Water Energy Efficiency Final Report*; ITRC Report, No.R 11-007; Digital Commons @ Cal Poly: California, CA, USA, 2011.
124. House, L.W. *Water Supply Related Electricity Demand in California*; Public Interest Energy Research (PIER) Program: Sacramento, CA, USA, 2006; pp. 1–77.
125. Salas, W.; Green, P.; Frothing, S.; Li, C.; Boles, S. *Estimating Irrigation Water Use for California Agriculture: 1950s to Present*; California Energy Commission: Sacramento, CA, USA, 2006; p. 33.
126. Anderson, R.G. *Irrigation in California: Overview and Relation to Energy*; US Salinity Laboratory: Riverside, CA, USA, 2019.
127. Tindula, G.N.; Orang, M.N.; Snyder, R.L. Survey of Irrigation Methods in California in 2010. *J. Irrig. Drain. Eng.* **2013**, *139*, 233–238. [CrossRef]
128. Marks, G.; Wilcox, E.; Olsen, D.; Goli, S. *Opportunities for Demand Response in California Agricultural Irrigation: A Scoping Study*; Lawrence Berkeley National Lab. (LBNL): Berkeley, CA, USA, 2013.
129. Zoldoske, D. *Water & Energy Efficiency*; Colorado Water: Fort Collins, CO, USA, 2018; p. 35.
130. Burt, C.M. Rapid Field Evaluation of Drip and Microspray Distribution Uniformity. *Irrig. Drain. Syst.* **2004**, *18*, 275–297. [CrossRef]
131. Tarjuelo, J.M.; Rodriguez-Diaz, J.A.; Abadía, R.; Camacho, E.; Rocamora, C.; Moreno, M.A. Efficient Water and Energy Use in Irrigation Modernization: Lessons from Spanish Case Studies. *Agric. Water Manag.* **2015**, *162*, 67–77. [CrossRef]
132. California Air Resources Control Board. *Greenhouse Gas Quantification Methodology for the California Department of Food and Agriculture State Water Efficiency and Enhancement Program*; California Air Resources Control Board: Sacramento, CA, USA, 2017.
133. Shobe, B.; Merrill, J. *Climate Smart: Saving Water and Energy on California Farms Recommendations for California's State Water Efficiency and Enhancement Program (SWEEP)*; SWEEP: Sacramento, CA, USA, 2018.
134. California Climate and Agricultural Network. *Investing in California Agriculture's Climate Solutions*; California Climate and Agricultural Network: Sacramento, CA, USA, 2021.
135. Montazar, A.; Krueger, R.; Corwin, D.; Pourreza, A.; Little, C.; Rios, S.; Snyder, R.L. Determination of Actual Evapotranspiration and Crop Coefficients of California Date Palms Using the Residual of Energy Balance Approach. *Water* **2020**, *12*, 2253. [CrossRef]
136. Pardo, J.C.F.; Ramon, D.; Stefanelli-Silva, G.; Elegbede, I.; Lima, L.S.; Principe, S.C. Advancing Through the Pandemic from the Perspective of Marine Graduate Researchers: Challenges, Solutions, and Opportunities. *Front. Mar. Sci.* **2020**, *7*, 528. [CrossRef]
137. García, A.M.; García, I.F.; Poyato, E.C.; Barrios, P.M.; Díaz, J.A.R. Coupling Irrigation Scheduling with Solar Energy Production in a Smart Irrigation Management System. *J. Clean. Prod.* **2018**, *175*, 670–682. [CrossRef]
138. Galloway, J.N.; Aber, J.D.; Erisman, J.W.; Seitzinger, S.P.; Howarth, R.W.; Cowling, E.B.; Cosby, B.J. The Nitrogen Cascade. *BioScience* **2003**, *53*, 341–356. [CrossRef]
139. Rosenstock, T.S.; Liptzin, D.; Dzurella, K.; Fryjoff-Hung, A.; Hollander, A.; Jensen, V.; King, A.; Kourakos, G.; McNally, A.; Pettygrove, G.S.; et al. Agriculture's Contribution to Nitrate Contamination of Californian Groundwater (1945–2005). *J. Environ. Qual.* **2014**, *43*, 895–907. [CrossRef]
140. Harding, R.B.; Embleton, T.W.; Jones, W.W.; Ryan, T.M. Leaching and Gaseous Losses of Nitrogen from Some Nontilled California Soils. *Agron. J.* **1963**, *55*, 515–518. [CrossRef]
141. Reid, W.V.; Mooney, H.A.; Cropper, A.; Capistrano, D.; Carpenter, S.R.; Chopra, K.; Dasgupta, P.; Dietz, T.; Duraiappah, A.K.; Hassan, R.; et al. *Ecosystems and Human Well-Being-Synthesis: A Report of the Millennium Ecosystem Assessment*; Island Press: Washington, DC, USA, 2005.
142. Shrestha, A.; Luo, W. An Assessment of Groundwater Contamination in Central Valley Aquifer, California Using Geodetector Method. *Ann. GIS* **2017**, *23*, 149–166. [CrossRef]

143. Harter, T.; Dzurella, K.; Kourakos, G.; Hollander, A.; Bell, A.; Santos, N.; Hart, Q.; King, A.; Quinn, J.; Lampinen, G.; et al. *Nitrogen Fertilizer Loading to Groundwater in the Central Valley*; Final Report to the Fertilizer Research Education Program, Projects 11-0301 and 15-0454; University of California Davis: Davis, CA, USA, 2017; pp. 1–36.
144. Harter, T. Agricultural Impacts on Groundwater Nitrate, Nitrates in Groundwater. *Southwest Hydrol. Mag.* **2009**, *8*, 1–38.
145. Brown, P. Crop Nutrient Status & Demand in Almond. Available online: https://ucanr.edu/sites/scri/Crop_Nutrient_Status_and_Demand_Patrick_Brown (accessed on 5 July 2022).
146. Saa, S.; Peach-Fine, E.; Brown, P.; Michailides, T.; Castro, S.; Bostock, R.; Laca, E. Nitrogen Increases Hull Rot and Interferes with the Hull Split Phenology in Almond (*Prunus dulcis*). *Sci. Hortic.* **2016**, *199*, 41–48. [CrossRef]
147. Hartz, T.K.; Bottoms, T.G. Nitrogen Requirements of Drip-Irrigated Processing Tomatoes. *HortScience Horts* **2009**, *44*, 1988–1993. [CrossRef]
148. Geisseler, D.J. *Developing a Decision Support Tool for Processing Tomato Irrigation and Fertilization in the Central Valley Based on CropManage*; California Department of Food and Agriculture: California, CA, USA, 2018.
149. Geisseler, D.; Horwath, W.R. *California Crop Fertilization Guidelines*; UCANR Publication: Davis, CA, USA, 2018.
150. Rosenstock, T.T.; Liptzin, D.; Six, J.; Tomich, T. Fertilizer Use in California: Assessing the Data, Trends and a Way Forward. *Calif. Agric.* **2013**, *67*, 68. [CrossRef]
151. Walker, L. Central Valley Salt & Nitrate Management Plan Antidegradation Analysis. Available online: https://www.cvsalinity.org/_Archive/docs/ceqa/ceqa-documents/3524-central-valley-salt-and-nitrate-management-plan-antidegradation-analysis/file.html (accessed on 10 July 2021).
152. Gallardo, M.; Elia, A.; Thompson, R.B. Decision Support Systems and Models for Aiding Irrigation and Nutrient Management of Vegetable Crops. *Agric. Water Manag.* **2020**, *240*, 106209. [CrossRef]
153. Kim, J.S.; Kisekka, I. FARMS: A Geospatial Crop Modeling and Agricultural Water Management System. *ISPRS Int. J. Geo-Inf.* **2021**, *10*, 553. [CrossRef]
154. Smedema, L.K.; Shiati, K. Irrigation and Salinity: A Perspective Review of the Salinity Hazards of Irrigation Development in the Arid Zone. *Irrig. Drain. Syst.* **2002**, *16*, 161–174. [CrossRef]
155. CV-SALTS Central Valley Salinity Alternatives for Long-Term Sustainability. Available online: https://www.waterboards.ca.gov/centralvalley/water_issues/salinity/ (accessed on 10 July 2021).
156. Quinn, N.W.T. Policy Innovation and Governance for Irrigation Sustainability in the Arid, Saline San Joaquin River Basin. *Sustainability* **2020**, *12*, 4733. [CrossRef]
157. Mitchell, J.P.; Thomsen, C.D.; Graves, W.L.; Shennan, C. Cover Crops for Saline Soils. *J. Agron. Crop Sci.* **1999**, *183*, 167–178. [CrossRef]
158. Munns, R.; Tester, M. Mechanisms of Salinity Tolerance. *Annu. Rev. Plant Biol.* **2008**, *59*, 651–681. [CrossRef] [PubMed]
159. Letey, J. Soil Salinity Poses Challenges for Sustainable Agriculture and Wildlife. *Calif. Agric.* **2000**, *54*, 43–48. [CrossRef]
160. Howitt, R.E.; Kaplan, J.; Larson, D.; MacEwan, D.; Medellín-Azuara, J.; Horner, G.; Lee, N.S. *The Economic Impacts of Central Valley Salinity*; Final Report to the State Water Resources Control Board Contract; University of California Davis: Davis, CA, USA, 2009; pp. 5–417.
161. Welle, P.D.; Mauter, M.S. High-Resolution Model for Estimating the Economic and Policy Implications of Agricultural Soil Salinization in California. *Environ. Res. Lett.* **2017**, *12*, 094010. [CrossRef]
162. Richards, L.A. *Diagnosis and Improvement of Saline and Alkaline Soils*; US Department of Agriculture: Washington, DC, USA, 1954; Volume 160. [CrossRef]
163. Shahid, S.A.; Zaman, M.; Heng, L. Soil Salinity: Historical Perspectives and a World Overview of the Problem. In *Guideline for Salinity Assessment, Mitigation and Adaptation Using Nuclear and Related Techniques*; Zaman, M., Shahid, S.A., Heng, L., Eds.; Springer International Publishing: Cham, Switzerland, 2018; pp. 43–53. ISBN 978-3-319-96190-3.
164. Greenway, H.; Munns, R. Mechanisms of Salt Tolerance in Nonhalophytes. *Annu. Rev. Plant Physiol.* **1980**, *31*, 149–190. [CrossRef]
165. Parihar, P.; Singh, S.; Singh, R.; Singh, V.P.; Prasad, S.M. Effect of Salinity Stress on Plants and Its Tolerance Strategies: A Review. *Environ. Sci. Pollut. Res.* **2015**, *22*, 4056–4075. [CrossRef] [PubMed]
166. Kosloff, L.H. Tragedy at Kesterson Reservoir: Death of a Wildlife Refuge Illustrates Failings of Water Law. *Envtl. L. Rep. News Anal.* **1985**, *15*, 10386.
167. Chen, C.W.; Herr, J.; Ziemelis, L. *Watershed Analysis Risk Management Framework: A Decision Support System for Watershed Approach and Total Maximum Daily Load Calculation*; Topical Report; US Department of Energy Office of Scientific and Technical Information: Washington, DC, USA, 1998.
168. Hatchett, S.A.; Quinn, N.; Horner, G.L.; Howitt, R.E. A Drainage Economics Model to Evaluate Policy Options for Management of Selenium Contaminated Drainage. Toxic Substances in Agricultural Water Supply and Drainage. In Proceedings of the Second Pan American Regional Conference on Irrigation and Drainage, Denver, CO, USA, 1 June 1989.
169. Quinn, N.W.T.; Cronin, J. Use of the Hydro-Salinity, Crop Production Optimization Model APSIDE to Validate Results from an Updated Regional Flow Model of the San Joaquin River Basin. In *Proceedings of the Environmental Software Systems. Computer Science for Environmental Protection*; Hřebíček, J., Denzer, R., Schimak, G., Pitner, T., Eds.; Springer International Publishing: Cham, Switzerland, 2017; pp. 150–162.
170. Solomon, K.H. Yield Related Interpretations of Irrigation Uniformity and Efficiency Measures. *Irrig. Sci.* **1984**, *5*, 161–172. [CrossRef]

171. Abd El-Wahed, M.H.; Medici, M.; Lorenzini, G. Sprinkler Irrigation Uniformity: Impact on the Crop Yield and Water Use Efficiency. *J. Eng. Thermophys.* **2016**, *25*, 117–125. [CrossRef]
172. Liu, Y.; Wang, N.; Jiang, C.; Archer, L.; Wang, Y. Temporal and Spatial Distribution of Soil Water and Nitrate Content Affected by Surface Irrigation and Fertilizer Rate in Silage Corn Fields. *Sci. Rep.* **2020**, *10*, 8317. [CrossRef]
173. Wang, Z.; Li, J.; Li, Y. Effects of Drip Irrigation System Uniformity and Nitrogen Applied on Deep Percolation and Nitrate Leaching during Growing Seasons of Spring Maize in Semi-Humid Region. *Irrig. Sci.* **2014**, *32*, 221–236. [CrossRef]
174. Stanhill, G. Water Use Efficiency. *Adv. Agron.* **1986**, *39*, 53–85. [CrossRef]
175. Arya, C.K.; Purohit, R.C.; Dashora, L.K.; Singh, P.K.; Kothari, M. Performance Evaluation of Drip Irrigation Systems. *Int. J. Curr. Microbiol. App. Sci.* **2017**, *6*, 2287–2292. [CrossRef]
176. Zhu, X.; Chikangaise, P.; Shi, W.; Chen, W.H.; Yuan, S. Review of Intelligent Sprinkler Irrigation Technologies for Remote Autonomous System. *Int. J. Agric. Biol. Eng.* **2018**, *11*, 23–30. [CrossRef]
177. Khosla, R.; Westfall, D.G.; Reich, R.M.; Mahal, J.S.; Gangloff, W.J. Spatial Variation and Site-Specific Management Zones. In *Geostatistical Applications for Precision Agriculture*; Springer: Dordrecht, The Netherlands, 2010; pp. 195–219.
178. Oki, L. Measuring Distribution Uniformity and Calculating Run Time. University of California Davis California Center for Urban Horticulture. Available online: <https://ccuh.ucdavis.edu/measuring-DU-run-time> (accessed on 20 March 2021).
179. Huang, Y.; Thomson, S.J.; Brand, H.J.; Reddy, K.N. Development and Evaluation of Low-Altitude Remote Sensing Systems for Crop Production Management. *Int. J. Agric. Biol. Eng.* **2016**, *9*, 1–11. [CrossRef]
180. Yu, F.H.; Xu, T.Y.; Du, W.; Ma, H.; Zhang, G.S.; Chen, C.L. Radiative Transfer Models (RTMs) for Field Phenotyping Inversion of Rice Based on UAV Hyperspectral Remote Sensing. *Int. J. Agric. Biol. Eng.* **2017**, *10*, 150–157. [CrossRef]
181. McBride, J. *West Coast Nut*; JCS Marketing: Fresno, CA, USA, 2020.
182. Baja, S.; Arif, S.; Neswati, R. Developing a User Friendly Decision Tool for Agricultural Land Use Allocation at a Regional Scale. *Mod. Appl. Sci.* **2017**, *11*, 11–21. [CrossRef]
183. Aubert, B.A.; Schroeder, A.; Grimaudo, J. IT as Enabler of Sustainable Farming: An Empirical Analysis of Farmers' Adoption Decision of Precision Agriculture Technology. *Decis. Support Syst.* **2012**, *54*, 510–520. [CrossRef]
184. Fulton, A. *An Advisory Service for Optimum Irrigation Scheduling in California*; University of California, Agriculture and Natural Resources: Davis, CA, USA, 2011.
185. Porter, J.; Parsons, S.; Robertson, C. Time for Review: Supporting the Work of an Advisory Group. *J. Res. Spéc. Educ. Needs* **2006**, *6*, 11–16. [CrossRef]
186. Wolek, F.W. Advisory Groups. *J. Technol. Transf.* **2015**, *15*, 39–44. [CrossRef]
187. Torres-Sanchez, R.; Navarro-Hellin, H.; Guillamon-Frutos, A.; San-Segundo, R.; Ruiz-Abellón, M.C.; Domingo-Miguel, R. A Decision Support System for Irrigation Management: Analysis and Implementation of Different Learning Techniques. *Water* **2020**, *12*, 548. [CrossRef]
188. Kpienbaareh, D.; Kansanga, M.; Luginaah, I. Examining the Potential of Open Source Remote Sensing for Building Effective Decision Support Systems for Precision Agriculture in Resource-Poor Settings. *GeoJournal* **2019**, *84*, 1481–1497. [CrossRef]
189. Petrie, H.; Bevan, N. *The Evaluation of Accessibility, Usability, and User Experience*; CRC Press: Boca Raton, FL, USA, 2009; ISBN 9781420064995.
190. de Godoi, T.X.; Costa Valentim, N.M. Towards an Integrated Evaluation of Usability, User Experience and Accessibility in Assistive Technologies. In Proceedings of the XVIII Brazilian Symposium on Software Quality, Fortaleza, Brazil, 28 October–1 November 2019. [CrossRef]
191. Datta, S.; Taghvaeian, S.; Ochsner, T.E.; Moriasi, D.; Gowda, P.; Steiner, J.L. Performance Assessment of Five Different Soil Moisture Sensors under Irrigated Field Conditions in Oklahoma. *Sensors* **2018**, *18*, 3786. [CrossRef] [PubMed]

Article

An Assessment Framework to Analyze Drought Management Plans: The Case of Spain

Julia Urquijo-Reguera ¹, María Teresa Gómez-Villarino ^{1,*}, David Pereira ¹ and Lucia De Stefano ²

¹ Department of Agroforestry Engineering, School of Agricultural, Food and Biosystems Engineering, Universidad Politécnica de Madrid, 28040 Madrid, Spain; julia.urquijo@upm.es (J.U.-R.); d.pereira@upm.es (D.P.)

² Department of Geological Sciences, Universidad Complutense de Madrid, 28040 Madrid, Spain; luciads@geo.ucm.es

* Correspondence: teresa.gomez.villarino@upm.es

Abstract: Droughts affect all socio-economic sectors and have negative impacts on the environment. Droughts are expected to increase in frequency and severity due to climate change, which makes their effective management a high priority for policy makers and water managers. Drought Management Plans (DMPs) are a key instrument to deal with droughts and help to prepare for them in a proactive way as a framework for coordinated action before and during droughts. The development of DMPs is still incipient worldwide and their assessment remains limited. In Spain, DMPs at a river basin level were first approved in 2007. Following the legal obligation set in Spanish law, those plans were revised after ten years and a new version was approved in 2018. A content analysis was developed for assessing the 2018 DMPs of eight river basins managed by their corresponding River Basin Authorities, which depend on the Spanish central government. The evaluation criteria were set using the extant scientific literature and official guidelines on drought preparedness and management. The analysis showed that some aspects of the DMPs are especially well-developed, e.g., the distinction between drought and water scarcity, the definition of thresholds to trigger different levels of drought and water scarcity alerts and actions for drought management and coordination. Other issues still need further improvement, especially those related to the analysis of drought impacts, the assessment of vulnerability and the ex-post evaluation of DPM performance.

Keywords: drought; water scarcity; risk-based approach; drought management plan; assessment protocol; river basin scale



Citation: Urquijo-Reguera, J.; Gómez-Villarino, M.T.; Pereira, D.; De Stefano, L. An Assessment Framework to Analyze Drought Management Plans: The Case of Spain. *Agronomy* **2022**, *12*, 970. <https://doi.org/10.3390/agronomy12040970>

Academic Editors: Aliasghar Montazar and Dennis Gitz

Received: 2 March 2022

Accepted: 15 April 2022

Published: 17 April 2022

Publisher's Note: MDPI stays neutral with regard to jurisdictional claims in published maps and institutional affiliations.



Copyright: © 2022 by the authors. Licensee MDPI, Basel, Switzerland. This article is an open access article distributed under the terms and conditions of the Creative Commons Attribution (CC BY) license (<https://creativecommons.org/licenses/by/4.0/>).

1. Introduction

Droughts are expected to increase worldwide due to climate change [1,2], and “by the late twenty-first century, the global land area and population in extreme-to-exceptional terrestrial water storage drought could more than double, each increasing from 3% during 1976–2005 to 7% and 8%, respectively” [3]. Drought is a complex natural hazard that affects more people in relation to other disasters at a global level [4,5]. In Europe, the “overall economic impacts of droughts events in the past thirty years are estimated in a total of 100 billion € at EU level” [6] (p. 2) and are estimated at €9 billion per year currently but are projected to increase with climate change [7]. Moreover, FAO [8] estimates that there were USD29 billion in agricultural losses to developing countries between 2005 and 2015 from drought impacts alone. Our knowledge on drought impacts is still limited despite their characterization being essential to plan and manage drought episodes adequately [9–12]. Van Loon et al. [13] argues that feedbacks between drought and people are not fully understood, making drought management inefficient. Recently, Enenkel et al. [9] argued that that granularity of data on climate hazards such drought are increasing but it is not aligned with socio, economic and impact data, which is a priority for planning emergency as well as mitigation strategies.

To effectively mitigate such impacts, drought management should follow a proactive risk-based approach [8–11,14–16]. Moreover, preparedness and risk management reduce the cost of drought actions compared to crisis management or inaction [15]. This implies considering, at least, hazard characterization and drought event monitoring, vulnerability assessment and risk management including actions to address drought effects.

Despite a proactive risk-management approach being considered as the best way to mitigate drought impacts [8,14,17–22], drought management in many countries is still a reactive crisis management, instead of following a risk-management approach [23]. According to Fu et al. [24] (p. 53), “as drought directly and indirectly affects almost all aspects of a community, it appears there is not a holistic planning framework for droughts”, which can limit its development. Raikes et al. [23] found that planning and preparedness was less common for drought than for floods, and, for instance, in the USA, progress towards proactive and planned management for drought has been more limited than for other natural hazards [25,26].

Drought Management Plans (DMPs) are a major management tool for proactive risk-based drought management [27–32] and are still rather uncommon, as only 27 countries around the world are listed as having drought policies and plans under the Integrated Drought Management Programme initiative. An overview of the limited development of DMPs in the European Union (EU) was first provided by Benitez and Schmidt [32] and was recently updated by Vogt et al. [33]. Other studies report some relevant experiences, particularly in the USA, Australia, South Africa, Iraq, India, Brazil and Central America, among others [14,15,20,21,34]. Existing DMPs are quite heterogeneous in terms of the problems addressed and the legal and regulatory frameworks and sectors considered.

While numerous scholarly works have analyzed drought as a natural hazard, the literature on DMPs is much more limited [9,35]. There is a need for evidence on their adequacy and usefulness, which can be framed as analysis of DPM content and quality (ex-ante assessment) or as analysis of performance once applied (ex-post assessment). Ex-ante assessment implies obtaining a comprehensive understanding of DMPs characteristics and, more importantly, exploring to what extent they are designed for proactive drought management. This is the focus of this paper. The ex-post assessment analyzes the effectiveness of such plans in reducing drought impacts once the drought ends [35]. This type of assessment, however, is particularly challenging for at least three reasons: first, because it can be difficult to attribute observed impacts to a drought or to other concurrent non climate-driven factors; second, because the definition of a baseline against which to measure impacts and the capacity of measures to mitigate them can be controversial; and third, because it requires the systematic collection of impact data, which is rarely a priority.

From an evaluation perspective, in the last decade, some interesting efforts have emerged in the USA and Europe that can serve as a reference for analyzing the adequacy of the design and content of DMPs. In the USA, several authors [24,26,36,37] have assessed drought management initiatives at different levels. In the EU, two studies on water scarcity and drought set the basis for the analysis of DMPs across countries. The first one [32] provides an overview of the existence of DMPs, while the second one [38] focuses on how water scarcity and drought issues are considered in River Basin Management Plans (RBMP). Both studies were developed in the framework of the ‘Blueprint to Safeguard water in Europe’ [39], a European Commission initiative to assess the implementation of the EU water policy. Nonetheless, clear guidelines for the systematic assessment of DMPs using a risk-management approach are still lacking.

This study contributes to the field of DMPs evaluation by developing a framework for assessing the adequacy of the design and content of DMPs according to a risk-management approach. The purpose of this framework is to provide an ex-ante assessment tool to analyze the completeness of already existing DMPs in terms of a risk-management approach. The developed framework was applied to Spain to test its adequacy and to help to identify areas where DMPs can be improved and lessons for other countries where the use of this drought management tool is still incipient or absent.

The paper is structured as follows: the following section presents the assessment protocol developed, and Section 3 describes the case study based on drought characteristics and drought management experience in Spain. The results of the analysis and their discussion are presented in Sections 4 and 5, respectively. In Section 6, some research limitations are mentioned and, finally, conclusions are drawn in Section 7.

2. Materials and Methods

A conceptual framework was developed to organize and address relevant aspects for a DMP according to the literature on drought risk management (Figure 1). This includes three main components (drought hazard characterization, drought vulnerability and drought measures and management) originally proposed by Hayes et al. [11] and later adapted by Fu, et al. [24], WMO/GWP [14] and Vogt et al. [16]. In this framework, the first component looks at the hazard itself; the second characterizes the system exposed to the hazard, while the third component analyzes actions taken to minimize the impact of the hazard on the system.

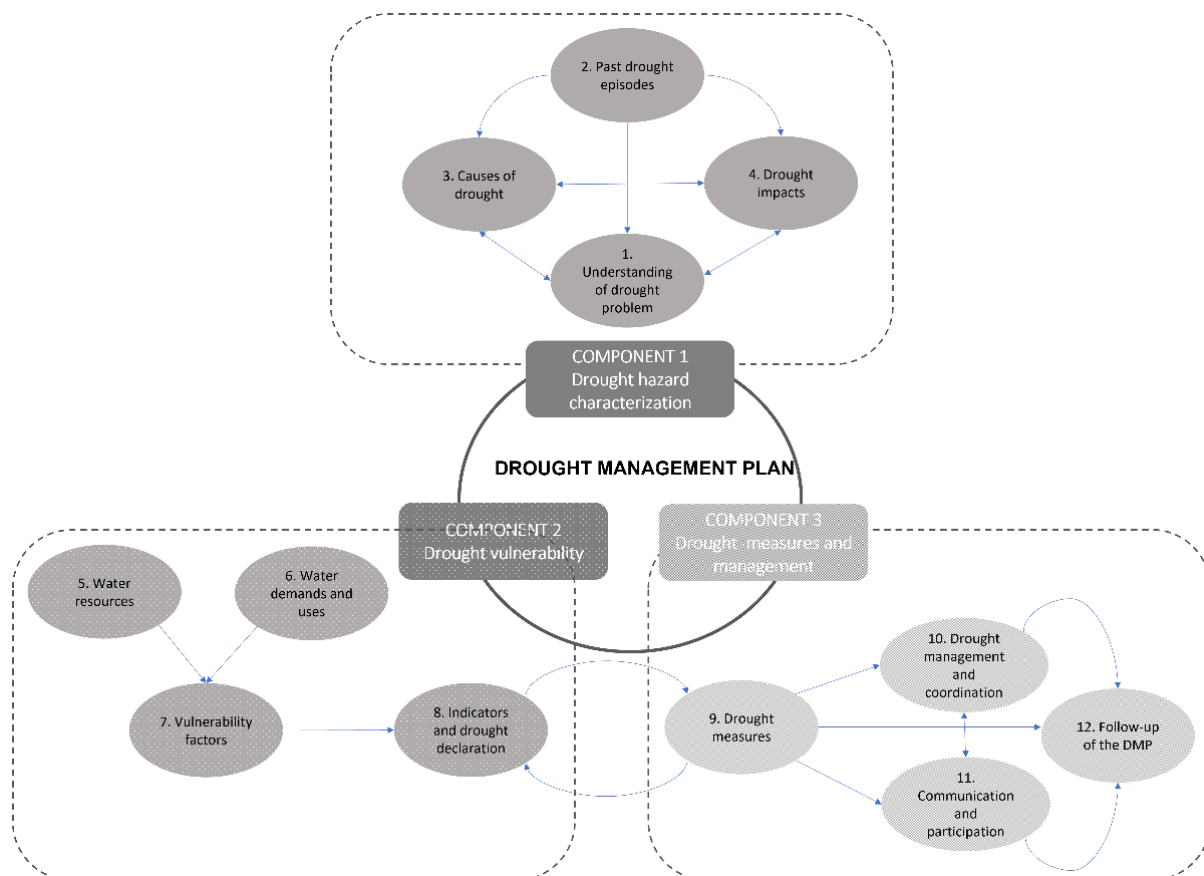


Figure 1. Conceptual framework for the assessment of drought management plans.

Assessment of these three components requires working with a set of criteria (12 in total), that, in turn, are made operative through specific indicators (43) (Table 1). They were selected or defined taking into account several sources: (a) extant literature on drought risk management [5,8,14,17,20,21,25,40–45]; (b) DMP guidelines developed in different geographical contexts [22,46–52]; and (c) applied assessments of DMPs from the literature [24,26,36,53].

Table 1. Assessment Protocol.

Component	Criteria	#	Indicators
1. Drought hazard characterization	1. Understanding of the problem	1	Definition of drought and drought types
		2	Definition of prolonged droughts
		3	Relation with other similar terms (water scarcity, aridity, desertification)
	2. Identification and assessment of past drought episodes	4	Identification of past drought episodes
		5	Number of episodes assessed
		6	Level of detail of the assessment
	3. Analysis of the causes of drought	7	Identification of the causes of drought
		8	Presence of references to climate change
		9	Identification of cause–effect relationship
	4. Analysis of drought impacts	10	Identification of type of impacts (social, economic, environmental)
		11	Identification of impacts by sectors
		12	Quantification of drought impacts
2. Drought Vulnerability	5. Analysis of water resources	13	Assessment of available water resources
		14	Analysis of water quality
		15	Assessment of environmental elements related to water resources
	6. Analysis of water demands and uses	16	Analysis of urban supply
		17	Analysis of agricultural demand
		18	Analysis of industry and/or hydroelectrical demand
		19	Analysis of other water demands
		20	Analysis of environmental water needs
	7. Analysis of vulnerability factors	21	Identification by areas or geographical references or systems
		22	Calculation of water balance
		23	Identification of vulnerable zones, sectors or groups
24		Identification of vulnerability factors	
25		Identification of measures or actions to reduce vulnerability	
8. Indicators and drought declaration	26	Identification of drought indicators	
	27	Establishment and calculation of indicators	
	28	Relationship between drought indicators and alert levels	
	29	Procedure for drought phase declaration	
3. Drought measures and management	9. Analysis of drought measures	30	Definition of drought measures
		31	Analysis of the effectiveness of measures
		32	Estimation of drought measures costs
		33	Relationship between measures and drought phases
		34	Implementation mechanism of the measures
	10. Drought management and coordination	35	Relation of the DMP with other plans
		36	Plan foundation and legal aspects
		37	Allocation of responsibilities
	11. Communication and participation	38	Identification of resources needs (means, staff and budget)
		39	Dissemination and communication of the DMP
	12. Follow-up of the DMP	40	Public participation
		41	Definition of follow-up indicators and tools
42		Ex-post assessment	
		43	Plan revision process

Source: Own elaboration based on [5,8,19–21,24,26,32,34,36,42,48,50–55].

The indicators are scored through a content analysis of the DMPs considered. Following the recommendations of the UN [56], a 1–4 scale was used. This type of scale allows for higher granularity than the absent/present (0–1) scale employed in [24] Fu et al. (2013b) and it is an alternative to the 0–2 scale used by Fu and Tang [26] which is linked to potential personal bias in the scoring process. In this assessment, the scoring values should

be understood as follows: very poorly described or absent (=1); insufficiently described and/or not supported by data (=2); well described and supported by some relevant data (=3); and well described and supported by data (=4).

The indicator scores are aggregated by criterion with equal weight and then by component. To reduce subjectivity in the coding process, at least two independent coders should score each DMP. When disagreements arise, the coders should discuss their scores to reach an agreement. This is a crucial step in content analysis, as it may show the clarity and adequacy of the coding protocol where a high level of disagreement between coders may reflect deficiencies in the scoring protocol [57]. Moreover, it helps reduce bias in the interpretation of the data [58]. However, there are limited standards and guidelines on how to report intercoder reliability [59].

3. The Case Study

3.1. Drought Management Context in Spain

Drought is a characteristic feature of Spain’s climate. Several droughts have occurred in the Iberian Peninsula since 1941, with significant spatial differences in terms of their severity, duration and time of occurrence [60,61]. The main episodes occurred in 1941–1945, 1979–1983, 1990–1995 and 2005–2008 [55].

Drought management in Spain is part of a broader water management system that is largely determined by the EU Water Framework Directive (WFD 2000/60/EC) [62]. According to this directive, water resources are managed with River Basin Management Plans (RBMPs), which should be drafted and revised by the River Basin Authorities (RBAs) every 6 years. In 2001, article 27 of the Spanish National Hydrological Plan (SNHP, Law 10/2001) [63] established that inter-regional RBAs should develop a DMP for the river district within two years of the approval of the law (i.e., 2003). It also required local governments in towns with populations over 20,000 inhabitants to develop their Drought Emergency Plans for urban water supplies. In 2005, the ministry in charge of water management drafted a guidance document [48] to support RBAs in the elaboration of drought management plans, which in the spirit of the WFD should complement RBMPs. Eventually, the first generation of DMPs was approved in March 2007 (ORDEN MAM/698/2007) [64], at the end of a prolonged drought (2004/05–2007/08) that affected most of Spain. Several authors analyzed the process of development of those DMPs in the context of the WFD implementation [27,28,31].

In 2017, the official DMP guidelines were upgraded [52] and a second generation of DPMs was approved at the end of the year 2018 (Orden TEC/1399/2018) [65]. Figure 2 summarizes the key milestones related to DMPs approval in Spain during recent decades.

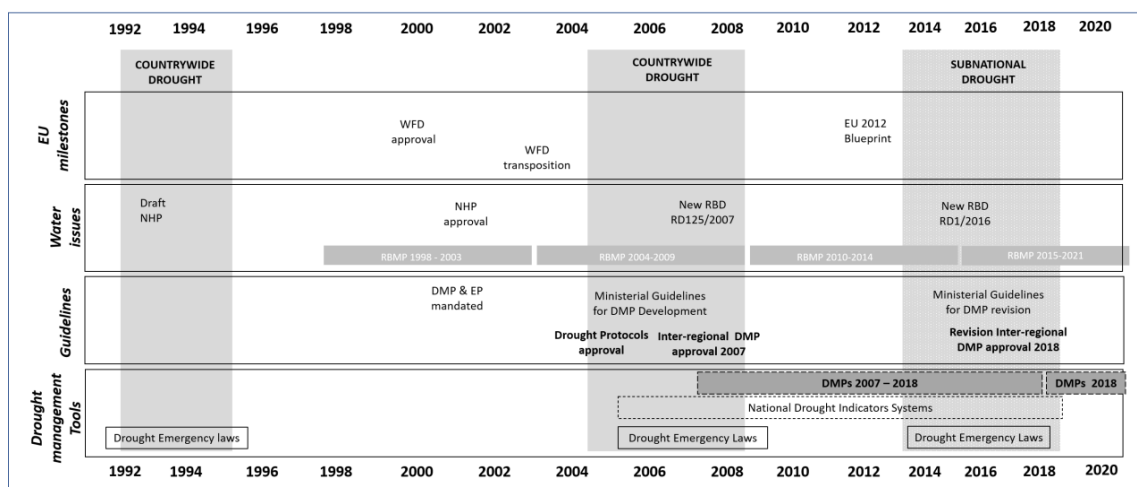


Figure 2. Timeline of the development of a drought management framework in Spain. Source. Adapted from Urquijo et al. [66].

The need for planning for drought has been present in the national legislation for almost two decades now, which puts Spain among the most advanced countries in the EU in the development of DMPs [32]. This and the following reasons make Spain an interesting case study to analyze drought planning practices at a river basin level: (a) It is a drought-prone country representative of drought risks in the Mediterranean region; (b) the approval of DMPs by RBDs has been compulsory since 2001; (c) DMPs were first developed during a prolonged and severe drought nation-wide, but since then, several droughts have occurred in different parts of the country; and (d) the 2018 DMPs are the result of a revision process, which should have led to a refinement and improvement of the original plans based on lessons from experience.

In Spain, the ministry in charge of water management undertook an assessment of drought management during the period of 2004–2008 [55] and, more recently, analyzed the DPMs approved in 2007 [67]. The latter study includes a descriptive review of the DMPs and focuses on monitoring procedures and results of the DMPs. However, no clear criteria of analysis were established to guide the assessment, which limits its ability to deliver a diagnosis and make recommendations for improvement. Additionally, a specific assessment of the 2007 DMP in the Segura River Basin was undertaken by Gómez Gómez and Pérez Blanco [68]. Other studies have explored current challenges in the integration of water resource management and drought risk management in Spain [30].

3.2. Geographical Scope of the Study

The proposed framework was applied to the DMPs developed in eight RBDs managed by River Basin Authorities belonging to the ministry in charge of water management and were approved in December 2018 (Figure 3, Table 2).

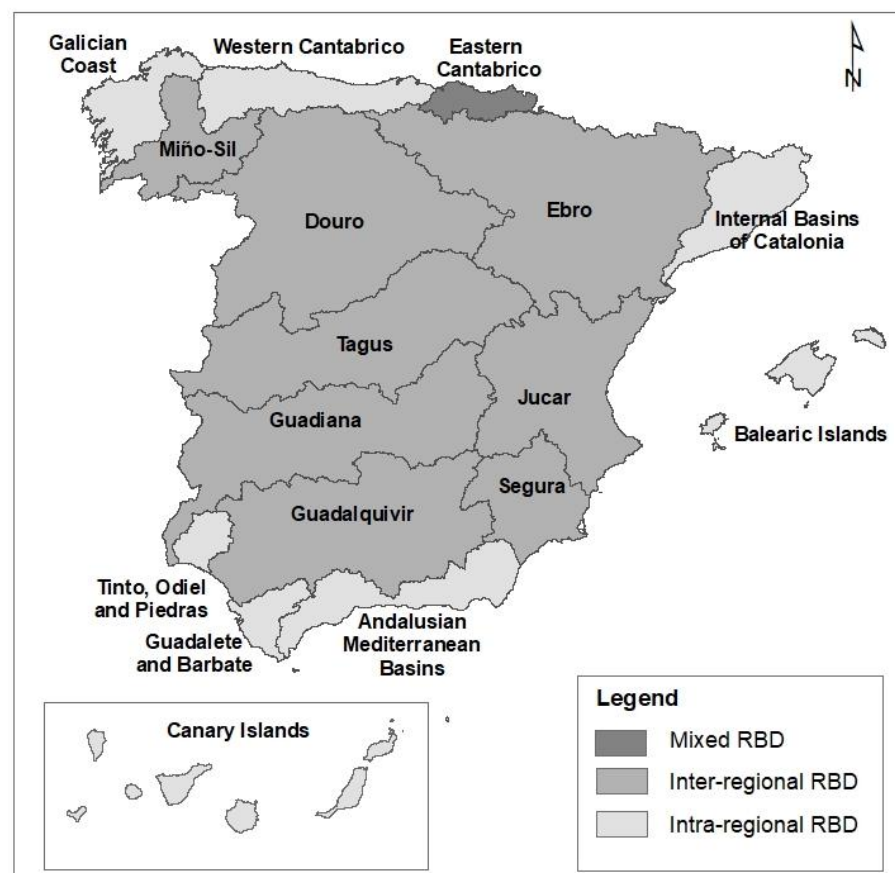


Figure 3. Spanish River Basin Districts.

Table 2. Spanish River Basin Districts: DMPs overview.

River Basin District		Sup. Km ²	Average Precipitation (mm/Year)	Available Resources (hm ³ /Year)
Douro	DOU	98,073	612	12,777
Tagus	TAG	55,781	636	7865
Guadiana	GUA	55,527	808	4869
Segura	SEG	20,234	385	1425
Ebro	EBR	85,362	622	14,340
Guadalquivir	GDQ	57,527	582	7071
Jucar	JUC	42,730	475	3194
Miño-Sil	MIN	17,619	1257	11,823

The analysis was applied to the main document of the DMPs (memoria in Spanish) and complementary documentation (Strategic Environmental Assessment report, public consultation process document, post-drought evaluation report) were analyzed only when clarification about specific topics was needed.

4. Results

4.1. Overall Drought Plan Content and Characteristics

The selected DMPs obtained a mean score of 3.04, which represents 76% of the maximum possible score (4), with a 0.16 standard deviation (Table 3).

Table 3. Results for each component and criteria by DMP.

	Min Score of a DMP	Max Score of a DMP	STDesv	Mean Score	% of Possible Max Score
Component 1. Drought hazard characterization	2.11	3.18	0.43	2.73	68%
1.1 Understanding of the problem	3	3.33	0.15	3.08	77%
1.2 Identification and assessment of past drought episodes	2.33	3.92	0.56	3.48	87%
1.3. Analysis of causes of drought	1.67	3.33	0.67	2.33	58%
1.4 Analysis of drought impacts	1.11	3.22	0.78	2.04	51%
Component 2. Drought vulnerability	3.44	3.65	0.10	3.53	88%
2.1 Analysis of water resources	3.44	3.65	0.1	3.17	79%
2.2 Analysis of water demands and uses	3	3.33	0.18	4.00	100%
2.3 Analysis of vulnerability factors	4	4	0	2.97	74%
2.4 Indicators and drought declaration	2.5	3.25	0.28	4.00	100%
Component 3. Drought measures and management	2.86	2.86	0.00	2.86	72%
3.1 Analysis of drought measures	2.86	2.86	0	2.42	60%
3.2 Drought management and coordination	2.42	2.42	0	3.20	80%
3.3 Communication and participation	3.2	3.2	0	3.00	75%
3.4 Follow-up of DMPs	3	3	0	2.83	71%

See Supplementary Materials Table S1.

The drought vulnerability component had the highest mean value (3.5/4 or 88% of the total possible score) followed by the component of drought measurement and manage-

ment (2.8/4 or 72% of the total possible score) and the drought hazard characterization component (2.7/4 or 68%).

4.2. Results by Component

4.2.1. Drought Hazard Characterization

All the DMPs include a clear definition of drought but do not distinguish among drought typologies (meteorological, agricultural, hydrological and socioeconomic), despite these operational definitions being considered important for drought management [38,50,69,70]. However, all the DMPs include a specific definition for prolonged drought, a key element [31] in the WFD, which states that prolonged droughts can justify the temporary non-compliance of the good status objective of the directive in the specific water body. Moreover, droughts are clearly defined as a natural phenomenon and differentiated from water scarcity caused by human water demands that exceed the availability of resources. Long-term water scarcity problems require different solutions as they have different causes, thus, a clear differentiation through an indicator-based monitoring system can have a positive practical implication for drought management. DMPs only tackle “temporary” water scarcity problems and leave “permanent” water scarcity problems to the ordinary planning in RBMPs. At times this distinction can be challenging, as temporary and permanent water scarcity situations may coexist within a territory or in time.

A detailed *Identification and assessment of past drought episodes* is included in all the plans. The *Analysis of the causes of drought*, water deficits or unsatisfied demands and drought impacts in general results in quite low scores. The plans that fare the lowest on this issue define and describe structural and conjunctural shortages but do not clearly identify their causes. Only two DMPs make a comprehensive analysis of drought causes, water deficits or unsatisfied demands, with the identification of drought causes and cause-effect relationships.

In general, references to climate change are generic, and even when some projections are provided, they are not downscaled to the specific RBD or are included in the DMPs only in terms of a relative reduction of natural runoff in 2027 and 2033 scenarios [30].

Similarly, the *Identification of drought impacts* is generic and qualitative. Only a small number of DMPs identify impacts by sectors and by type (social, economic and environmental). This criterion received the lowest scores in the component, which may be because limited information is available on impacts of past droughts. The literature on drought management widely acknowledges the need for a systematic inventory of environmental, economic and social impacts [10,71,72].

4.2.2. Drought Vulnerability

The DMPs obtained the highest global score in this component. All the DMPs include an extensive analysis of water availability, including surface water, groundwater and non-conventional resources (transfers, reuse, desalination) by territorial subunits within the river basin. This is complemented by the analysis of water quality and the assessment of associated environmental elements, which, in some DMPs, are insufficiently described and documented.

Most DMPs consider environmental flows, whose establishment is mandatory in the elaboration of the RBMP. Nonetheless, there is still a weak link between environmental flows and the operational system for drought management. Moreover, environmental concerns should not be limited to environmental flows if the recovery of the ecological status of water bodies after a drought is pursued [73].

All the DMPs obtain the highest possible score in the *Analysis of water demands and uses* (Table 3). This includes analysis of urban supply, agricultural, industry, hydropower, tourism and environmental needs, each identified by area or hydrological unit. As for the previous criterion, this information is easily available in the corresponding RBMP, which explains the high level of detail in the DMPs on this issue.

The scores received by the criterion of the *Analysis of vulnerability* factors vary widely across the assessed DMPs. The calculation of a water balance and the quantification of water deficits at different scales is present in all the plans and serves as a starting point for the identification of vulnerable zones. However, none of the plans relate those areas to specific factors of vulnerability [74] and concrete measures to reduce them. The analysis of vulnerability is often challenging but it is key in the adoption of a risk-management approach. The IPCC [75] proposed a conceptual framework that lays the foundation to develop a comprehensive analysis of vulnerability to drought within DMPs. The quantification of vulnerability should be context-specific and requires the integration of different types of data that are often not available at an RBD level [76].

All the DMPs received the maximum score in the criterion of the *Establishment and definition of indicators and a drought declaration process*. The system developed by RBAs to analyze and declare drought phases was established in 2007 for the first generation of DMPs, and since then it has been fine-tuned and homogenized across all the RBDs.

4.2.3. Drought Measures and Management

In this component, all the DMPs obtained the same scores (Table 3). This may be surprising at first, but, actually, it reveals an interesting pattern in the elaboration of the plans. As mentioned earlier, the DMPs were developed using an official guidance document [52] as a reference. In the case of three of the four criteria (*Drought management and coordination, Communication and participation, Follow-up of DMPs*) all the RBAs followed a similar approach for different reasons. In some cases, the legal framework defines intervention provisions and does not foresee basin-specific adjustments. In other cases, the score uniformity points to gaps shared across river basins, as is the case with the lack of availability of follow-up tools. Finally, the homogeneity reveals that RBAs in some instances have opted to just use standard information to fill in some sections of the DMP, without making an effort to consider the specific features of their basin.

The *Analysis of drought measures* criterion received the lowest score in this component and the second lowest value of all the indicators analyzed. Although all the plans identify drought measures and describe their implementation mechanisms, they do not make the criteria for the selection of measures explicit. In all DMPs, the definition of drought measures is associated with specific drought or water scarcity scenarios and is linked to a specific territorial unit within the RBD. In general, the planned measures are activated incrementally as the level of drought/water scarcity severity increases: (a) strategic planning and monitoring (non-drought/scarcity situation); (b) water saving, monitoring and public awareness (pre-alert); (c) demand and supply-side measures, monitoring and control (alert); and (d) intensification and exceptional actions (emergency). However, the DMPs do not assess the cost-effectiveness of each measure, which would allow for comparison across measures and the selection of the best option at each moment of the drought event.

The criterion *Drought management and coordination* is well rated. The allocation of responsibilities is described in detail in all the DMPs through the establishment of a drought task force and the definition of the role of each of the concerned actors during each stage of the drought event. Additionally, all the DMPs clearly identify the means, staff and budget needed for drought management in each RBD.

All the DMPs emphasize the importance and benefits of *Public participation* and highlight the need for effective communication. The plans present the participation process implemented during their revision, but they do not report results of consultation or how stakeholders' contributions have been taken into account. They state the need to undertake an assessment of the drought management performance after a drought episode (*Follow-up indicators*) but provide little detail on how to perform this in practice.

5. Discussion

The scoring produced by the application of the assessment framework can be useful for comparisons across similar management units (in this case, the river basin districts)

to identify best practices and gaps and to detect general patterns that point to common challenges or strengths.

The analysis of some of the issues in DMPs, which are disaggregated at smaller territorial units within the RBD, is supported by extensive data. These are mostly issues related to information already available in the RBMP, such as water resources availability, demand and uses, hydraulic balances or ecological flows.

All the DMPs include an innovative indicator system that distinguishes between prolonged drought as a natural event and water scarcity situations and links them to a set of phases and triggers that activate different sets of measures. This system has been adapted to the specific characteristics of each RBD, as each RBA defines the parameters to be used to calculate the indicators and the thresholds that trigger the activation of the drought management phases. This provides enough flexibility to monitor and manage different situations in a context-specific manner and, at the same time, allows for comparison across sub-units within an RBD or also across RBDs. This flexibility points to the potential of this indicator system in other countries, especially in an EU context, where, to date, “there is not a proposed common agreed indicator system to be used across the EU” [31] p.6. The Spanish drought indicator system could be particularly relevant for countries that have already developed drought policy initiatives and are interested in designing or refining their drought monitoring system. This could be the case of some EU countries such as Italy, Portugal or Greece [32,49], but also can apply for other countries in Asia, e.g., India, Iran and Iraq [20,21,34]; Africa, e.g., South Africa, Kenya, Ethiopia and Namibia [5,20,21]; Australia [77]; the USA, specifically in the Midwestern United States [14,24,36]; or countries of the Mesoamerican Dry Corridor such as Guatemala, Honduras, Nicaragua and El Salvador [78]. Even if, in general, this indicator system is positively valued by scholars and practitioners, it has also been criticized by some because it does not couple streamflow forecasting models and seasonal climate forecasts [31]. Moreover, several other drought and water scarcity indicators [79] could be considered in the existing indicator system to broaden its scope.

Several areas for improvement that should be included in the next generation of Spain’s DMPs were identified. DMPs should consider and analyze specific vulnerability factors. A better understanding of those factors is key to mitigate drought and water scarcity impacts at an RBD level and by sectors. Vulnerability is a complex issue and different conceptual frameworks already exist, but none of them has been systematically applied in the development of the DMPs analyzed in this study. This can limit the understanding of the root causes of vulnerability to drought in each territory, which in turn hampers the effective mitigation of impacts [35,41,46,71].

Climate change will aggravate the frequency, duration and intensity of drought episodes in the Mediterranean region [1,75], and this will affect several issues such as the characteristics of drought as well water availability and demands, and, hence, will determine the type of measures to be considered in each DPM. While some climate change considerations are included in the development of RBMPs, a specific analysis of the effect of climate change on drought characteristics would be key to understanding vulnerability to drought in the future.

The lack of a systematic analysis of drought impacts is one of the main weaknesses of the studied DMPs. The plans lack specific guidelines on how to characterize and register drought impacts. This is not an easy task, as the evaluation of drought impacts varies across sectors and territories. However, this type of information is crucial to complement the system of indicators related to the status of the availability of water resources and adequately inform decisions on drought management.

Another element that presents a great potential for improvement is related to the follow-up of the DMPs’ measures, as also stated by Hervás-Gómez and Delgado-Ramos [80]. This requires a comprehensive analysis of all the DMP elements that are implemented during a specific drought episode and should be based on a specific effort to monitor the development and the effects of the measures. Currently, DMPs focus on monitoring drought

and water scarcity conditions, and the measures to be implemented pivot on this indicator system. However, the systematic monitoring of the effectiveness of drought measures, the evolution of vulnerability factors and the characterization of drought impacts would contribute to more adaptive management. This should be done in coordination with the implementation and follow-up of the Emergency Plans for urban areas over 20,000 inhabitants. However, only a small number of Emergency Plans have been drafted and are operative (8.5% of those that should exist by law, according to Vargas and Paneque [30]), and, where they do exist, they are poorly coordinated with the corresponding DMP.

The analysis of the relation between drought and its impacts on environmental flows is still incipient. Despite the great progress made in the establishment of environmental flows in RBMPs, they are not still sufficiently integrated into DMPs as a variable for water demands analysis as well as a vulnerability factor-related to ecosystem. In future revisions of DMPs, this issue should receive larger attention. Moreover, more information on other relevant environmental issues and water quality parameters should be included in the next generation of DMPs.

In some cases, the RBAs have followed the official guidelines for the elaboration of DMPs with a limited effort to truly analyze and describe the mandated topics in the specific context of their RBD. Thus, some issues are dealt with superficially and their inclusion adds little to the actual management of drought (e.g., impacts analysis, ex post evaluation).

The assessment of DMPs is relevant to all the socioeconomic sectors that heavily depend on blue water, first among which is irrigated agriculture, which is responsible for 65% of water demand in Spain [81] and 70% worldwide [82]. In Spain, in case of prolonged drought, water rights for irrigation can be curtailed, and our study assesses the completeness of the legal and operational framework used to implement such restrictions. The analysis also reveals a bias that is present not only in Spain's DMPs but in the drought management literature in general. Drought management is mostly seen solely as a (blue) water management issue, whereas drought effects go far beyond a reduction in the amount of water available in reservoirs, streams or aquifers. Moreover, drought evolution over time largely depends on the conditions of land, soil and vegetation when the dry spell sets in and, more broadly, on how land and natural systems are managed. The view of drought management from a blue water perspective has several causes, the main possibly being that the lack of water for domestic water supply and economic uses is the most evident and severe consequence of a poorly-managed drought. While this is understandable, it misses the fact that drought is a complex, multifaceted phenomenon that would require a holistic approach in order to be managed in an effective way.

The analysis reveals that the studied DMPs have been developed using a reasonably complete, proactive risk-management based approach. Thus, the Spanish experience of drought management is worth being closely considered by countries that plan to develop or update their own DMPs. Our work also revealed aspects of drought management planning which are especially challenging in Spain and that will require special attention in future DMPs in Spain and may be bottlenecks in other countries.

The analysis of Spanish drought plans showcases the fact that having well-developed DMPs is no panacea. Those plans are intended to manage temporary situations of water stress in a structured way, with the ultimate goal of minimizing its negative effects. However, their existence or quality says little about the effectiveness of water policy to deliver a truly sustainable use of water resources, as shown by the fact that, currently, in Spain, 42.2% and 40.4% of surface and groundwater water bodies, respectively [83], fail to meet the good status requirements set by the EU Water Framework Directive. Moreover, since the effectiveness of drought management is rooted in water planning and in the daily management of water resources, it is possible to have well-developed DMPs and still suffer severe drought impacts.

6. Caveats and Future Research

This study develops and applies a framework to assess the content of eight DMPs in Spain in relation to a risk-management approach to drought management. The analysis of the actual performance of that approach during a drought event is beyond the scope of this paper and is a necessary next step in this research.

The analysis of public consultation documents may be of great value for further analysis of Spain's DMPs, as it may help identify controversial or critical issues as perceived by the different players who have a stake in how drought and water scarcity are managed.

The DMPs analyzed in this study have been developed by inter-regional RBAs to respond to a legal requirement. In order to comply with this, technical guidelines were provided by the Spanish Ministry in charge of water management. It would be interesting to expand the current analysis to Spain's intra-regional RBDs, where the development of DMPs is the responsibility of the regional water agency and there is no obligation to follow the Ministry's guidelines. The comparison of both types of DMPs could provide new insights into possible alternative approaches to manage drought in a similar geographical, legal and sociocultural context.

More research on specific issues related to drought management may contribute to the enhancement of DMPs. This includes (1) the role of groundwater resources as a buffer of drought impacts within a specific territory, (2) the integration of climatic and inflow forecast models more effectively and (3) the assessment of drought measures through, e.g., cost-benefit analysis that could help inform the selection of mitigation options during the drought event.

In Spain, drought management is mainly framed in terms of water policy and, as a result, DMPs have a strong emphasis on blue water. As highlighted in the previous section, our framework of analysis was developed using such a water-related focus and for this reason it does not assess the inclusion in DMPs of issues that are highly relevant in order to achieve holistic drought management (e.g., soil and land conditions, forest management, biodiversity conservation, public health, energy production). The analysis of how drought is considered in sectorial plans that do not fall under water management would be of great value in order to find synergies and gaps across sectors and therefore improve drought management in a transversal way.

7. Conclusions

During the past two decades, water authorities at different levels in Spain have made important efforts to shift from a reactive to a proactive risk-based management approach to deal with drought. This is reflected in the development of guidelines by the ministry in charge of water management for the elaboration of DMPs by different RBAs. As a result, all the DPMs analyzed in this study include, to some extent, the key elements of this approach according to the academic and specialized literature.

Some elements of the risk-management approach are well developed in the current DMPs. These are: the system of drought indicators and thresholds to trigger phased interventions to deal with drought and water scarcity, the analysis of past drought episodes and the characterization of water availability and demands, among other aspects. There is room for improvement in some other elements, namely: the identification and analysis of vulnerability factors, the inventory of past drought impacts, the relation of drought with climate change and environmental issues, the role of environmental flows and groundwater resources, the analysis of the effectiveness of drought measures options and the post-drought evaluation of management procedures.

The framework applied is a useful tool for the identification of possible gaps in and strengths of drought management plans, where they already exist. The resulting numerical scores help identify thematic and territorial trends and can contribute to the debate about the aspects of drought management that require special attention in the future. Moreover, the Spanish experience in this field can be considered as an interesting starting point for

the development of DMPs in other countries where drought management is still incipient or absent.

Supplementary Materials: The following supporting information can be downloaded at: <https://www.mdpi.com/article/10.3390/agronomy12040970/s1>, Table S1: Indicators scores byDMPs.

Author Contributions: Conceptualization, J.U.-R., M.T.G.-V., D.P. and L.D.S.; methodology, J.U.-R., M.T.G.-V., D.P. and L.D.S.; software, J.U.-R., M.T.G.-V., D.P. and L.D.S.; validation, J.U.-R., M.T.G.-V., D.P. and L.D.S.; formal analysis, J.U.-R., M.T.G.-V., D.P. and L.D.S.; investigation, J.U.-R., M.T.G.-V., D.P. and L.D.S.; resources, J.U.-R., M.T.G.-V., D.P. and L.D.S.; data curation, J.U.-R., M.T.G.-V., D.P. and L.D.S.; writing—original draft preparation, J.U.-R., M.T.G.-V., D.P. and L.D.S.; writing—review and editing, J.U.-R., M.T.G.-V., D.P. and L.D.S.; visualization, J.U.-R., M.T.G.-V., D.P. and L.D.S.; supervision, J.U.-R., M.T.G.-V., D.P. and L.D.S. All authors have read and agreed to the published version of the manuscript.

Funding: This research received no external funding.

Institutional Review Board Statement: Not applicable.

Informed Consent Statement: Not applicable.

Data Availability Statement: Data is contained within the article or supplementary material.

Conflicts of Interest: The authors declare no conflict of interest.

References

- Shukla, P.R.; Skea, J.; Buendia, E.C.; Masson-Delmotte, V.; Pörtner, H.-O.; Roberts, D.C.; Zhai, P.; Slade, R.; Connors, S.; van Diemen, R.; et al. (Eds.) IPCC, 2019: Summary for Policymakers. In *Climate Change and Land: An IPCC Special Report on Climate Change, Desertification, Land Degradation, Sustainable Land Management, Food Security, and Greenhouse Gas Fluxes in Terrestrial Ecosystems*; 2019; *in press*.
- Masson-Delmotte, V.; Zhai, P.; Pirani, A.; Connors, S.L.; Péan, C.; Berger, S.; Caud, N.; Chen, Y.; Goldfarb, L.; Gomis, M.I.; et al. (Eds.) IPCC, 2021: Summary for Policymakers. In *Climate Change 2021: The Physical Science Basis. Contribution of Working Group I to the Sixth Assessment Report of the Intergovernmental Panel on Climate Change*; 2021; *in press*.
- Pokhrel, Y.; Felfelani, F.; Satoh, Y.; Boulange, J.; Burek, P.; Gädeke, A.; Gerten, D.; Gosling, S.N.; Grillakis, M.; Gudmundsson, L.; et al. Global Terrestrial Water Storage and Drought Severity under Climate Change. *Nat. Clim. Chang.* **2021**, *11*, 226–233. [CrossRef]
- Guha-Sapir, D.; Below, R. *Hoyois Ph. EM-DAT: The CRED/OFDA International Disaster Database*; Www.Emdat.Be—Université Catholique de Louvain: Brussels, Belgium, 2010.
- UNISDR. *Revealing Risk, Redefining Development. Global Assessment Report on Disaster Risk Reduction*; United Nations for Disaster Risk Reduction (UNISDR): Geneva, Switzerland, 2011.
- European Commission Addressing the Challenge of Water Scarcity and Droughts in the European Union. *Communication from the Commission to the European Parliament and the Council. COM (2007) 414 Final*; European Commission: Brussels, Belgium, 2007.
- Naumann, G.; Cammalleri, C.; Mentaschi, L.; Feyen, L. Increased Economic Drought Impacts in Europe with Anthropogenic Warming. *Nat. Clim. Chang.* **2021**, *11*, 485–491. [CrossRef]
- FAO. Proactive Approaches to Drought Preparedness. Where Are We Now and Where Do We Go from Here? White Paper. 2019. Available online: <http://www.fao.org/3/ca5794en/ca5794en.pdf> (accessed on 1 November 2020).
- Enenkel, M.; Brown, M.E.; Vogt, J.V.; McCarty, J.L.; Reid Bell, A.; Guha-Sapir, D.; Dorigo, W.; Vasilaky, K.; Svoboda, M.; Bonifacio, R.; et al. Why Predict Climate Hazards If We Need to Understand Impacts? Putting Humans Back into the Drought Equation. *Clim. Chang.* **2020**, *162*, 1161–1176. [CrossRef]
- Wilhite, D.; Svoboda, M.; Hayes, M. Understanding the Complex Impacts of Drought: A Key to Enhancing Drought Mitigation and Preparedness. *Water Resour. Manag.* **2007**, *21*, 763–774. [CrossRef]
- Hayes, M.J.; Wilhelmi, O.V.; Knutson, C.L. Reducing Drought Risk: Bridging Theory and Practice. *Nat. Hazards Rev.* **2004**, *5*, 106–113. [CrossRef]
- Karavitis, C.A.; Tsesmelis, D.E.; Skondras, N.A.; Stamatakos, D.; Alexandris, S.; Fassouli, V.; Vasilakou, C.G.; Oikonomou, P.D.; Gregorič, G.; Grigg, N.S.; et al. Linking Drought Characteristics to Impacts on a Spatial and Temporal Scale. *Water Policy* **2014**, *16*, 1172–1197. [CrossRef]
- Van Loon, A.F.; Gleeson, T.; Clark, J.; Van Dijk, A.I.J.M.; Stahl, K.; Hannaford, J.; Di Baldassarre, G.; Teuling, A.J.; Tallaksen, L.M.; Uijlenhoet, R.; et al. Drought in the Anthropocene. *Nat. Geosci.* **2016**, *9*, 89–91. [CrossRef]

14. World Meteorological Organization. Global Water Partnership Directrices de Política Nacional Para La Gestión de Sequías: Modelo Para La Adopción de Medidas (D.A. Wilhite). Serie 1 de Herramientas y Directrices Del Programa de Gestión Integrada de Sequías. OMM, Ginebra (Suiza) y GWP, Estocolmo (Suecia). 2014. Available online: https://www.gwp.org/globalassets/global/gwp-sam_files/programas/directrices_de_politica_nacional_para_la_gestion_de_sequias.pdf (accessed on 1 November 2020).
15. World Meteorological Organization. *Global Water Partnership Benefits of Action and Costs of Inaction: Drought Mitigation and Preparedness—A Literature Review*; Gerber, N., Mirzabaev, A., Eds.; Integrated Drought Management Programme (IDMP) Working Paper 1; WMO: Geneva, Switzerland; GWP: Stockholm, Sweden, 2017.
16. Joint Research Centre (European Commission); Cammalleri, C.; Pischke, F.; Masante, D.; Barbosa, P.; Naumann, G.; Spinoni, J.; Erian, W.; Vogt, J.V.; Pulwarty, R. *Drought Risk Assessment and Management: A Conceptual Framework*; Publications Office of the European Union: Luxembourg, 2018; ISBN 978-92-79-97469-4.
17. Wilhite, D. *Moving Beyond Crisis Management*; Drought Mitigation Center Faculty Publications; University of Nebraska: Lincoln, NE, USA, 2001.
18. Kampragou, E.; Apostolaki, S.; Manoli, E.; Froebrich, J.; Assimacopoulos, D. Towards the Harmonization of Water-Related Policies for Managing Drought Risks across the EU. *Environ. Sci. Policy* **2011**, *14*, 815–824. [CrossRef]
19. UNISDR. *Drought Risk Reduction Framework and Practices: Contributing to the Implementation of the Hyogo Framework for Action*; United Nations Secretariat of the International Strategy for Disaster Reduction: Geneva, Switzerland, 2009; 214p. Available online: https://www.unisdr.org/files/11541_DroughtRiskReduction2009library.pdf (accessed on 1 November 2020).
20. UNISDR. *Drought Risk Reduction Framework and Practices Contributing to the Implementation of the Hyogo Framework for Action*; United Nations Secretariat of the International Strategy for Disaster Reduction (UNISDR) and World Bank: Geneva, Switzerland, 2007; 213p. Available online: https://www.unisdr.org/files/3608_droughtriskreduction.pdf (accessed on 1 November 2020).
21. FAO. *NDMC The Near East Drought Planning Manual: Guidelines for Drought Mitigation and Preparedness Planning*; Food and Agriculture Organization of the United Nations Regional Office for the Near East: Cairo, Egypt; National Drought Mitigation Center University of Nebraska: Lincoln, NE, USA, 2008; 59p.
22. UNDP. *Mainstreaming Drought Risk Management—A Primer*; United Nations Development Programme: New York, NY, USA, 2011; 73p.
23. Raikes, J.; Smith, T.F.; Jacobson, C.; Baldwin, C. Pre-Disaster Planning and Preparedness for Floods and Droughts: A Systematic Review. *Int. J. Disaster Risk Reduct.* **2019**, *38*, 101207. [CrossRef]
24. Fu, X.; Tang, Z.; Wu, J.; McMillan, K. Drought Planning Research in the United States: An Overview and Outlook. *Int. J. Disaster Risk Sci.* **2013**, *4*, 51–58. [CrossRef]
25. Combating Drought through Preparedness. Wilhite 2002 Natural Resources Forum—Wiley Online Library. Available online: <https://onlinelibrary.wiley.com/doi/abs/10.1111/1477-8947.00030> (accessed on 1 March 2022).
26. Fu, X.; Tang, Z. Planning for Drought-Resilient Communities: An Evaluation of Local Comprehensive Plans in the Fastest Growing Counties in the US. *Cities* **2013**, *32*, 60–69. [CrossRef]
27. Estrela, T.; Vargas, E. Drought Management Plans in the European Union. The Case of Spain. *Water Resour. Manag.* **2012**, *26*, 1537–1553. [CrossRef]
28. Estrela, T.; Sancho, T.A. Drought Management Policies in Spain and the European Union: From Traditional Emergency Actions to Drought Management Plans. *Water Policy* **2016**, *18*, 153–176. [CrossRef]
29. Vargas, J.; Paneque, P. Methodology for the Analysis of Causes of Drought Vulnerability on the River Basin Scale. *Nat Hazards* **2017**, *89*, 609–621. [CrossRef]
30. Vargas, J.; Paneque, P. Challenges for the Integration of Water Resource and Drought-Risk Management in Spain. *Sustainability* **2019**, *11*, 308. [CrossRef]
31. Hervás-Gámez, C.; Delgado-Ramos, F. Drought Management Planning Policy: From Europe to Spain. *Sustainability* **2019**, *11*, 1862. [CrossRef]
32. Benítez Sanz, C.; Schmidt, G. *Analysis of the Implementation of Drought Management Plans in the Wider Context of the River Basin Management Plans*; Report Drafted in the Framework of the Comparative Study of Pressures and Measures in the Major River Basin Management Plans. Task 3d: Water Abstraction and Water Use; Final Deliverable, Version: Draft 1.0. 2012. Available online: <https://ec.europa.eu/environment/archives/water/imp2007/pdf/Water%20abstraction%20and%20use%20-%20Drought%20management%20Plans.pdf> (accessed on 1 November 2020).
33. Vogt, J.V.; Barbosa, P.; Cammalleri, C.; Carrão, H.; Lavaysse, C. Drought Risk Management: Needs and Experiences in Europe. In *Drought and Water Crisis. Integrating Science, Management and Policy*, 2nd ed.; Wilhite, D.A., Pulwarty, R.S., Eds.; CRC Press: Boca Raton, FL, USA, 2017; Chapter 18; pp. 385–408. [CrossRef]
34. UNDP. *Preparation of Drought Vulnerability Assessment Study to Develop Iraq National Framework for Integrated Drought Risk Management (DRM)*; Inception Report. Prepared by ELARD; UNDP: New York, NY, USA, 2013.
35. Kallis, G. Droughts. *Annu. Rev. Environ. Resour.* **2008**, *33*, 85–118. [CrossRef]
36. Fu, X.; Svoboda, M.; Tang, Z.; Dai, Z.; Wu, J. An Overview of US State Drought Plans: Crisis or Risk Management? *Nat. Hazards* **2013**, *69*, 1607–1627. [CrossRef]
37. Fontaine, M.; Steinemann, A. Assessing Vulnerability to Natural Hazards: Impact-Based Method and Application to Drought in Washington State. *Nat. Hazards Rev.* **2009**, *10*, 11–18. [CrossRef]

38. Schmidt, G.; Benítez-Sanz, C.; Topic Report on: Assessment of Water Scarcity and Drought Aspects in a Selection of European Union River Basin Management Plans. Study by Intecsa-Inarsa for the European Commission (under Contract “Support to the Implementation of the Water Framework Directive (2000/60/EC)” (070307/2011/600310/SER/D.2)). 2012. Available online: <https://ec.europa.eu/environment/water/quantity/pdf/Assessment%20WSD.pdf> (accessed on 1 November 2020).
39. European Commission. *A Blueprint to Safeguard Europe’s Water Resources (COM(2012) 673 Final)*. Communication from the Commission to the European Parliament, the Council, the European Economic and Social Committee and the Committee of the Regions. SWD(2012) 381 Final, SWD(2012) 382 Final; European Commission: Brussels, Belgium, 2012.
40. European Commission. *Water Scarcity and Droughts. In-Depth-Assessment. Second Interim Report*. DG Environment; European Commission: Brussels, Belgium, 2007.
41. Knutson, C.; Hayes, M.; Phillips, T. *How to Reduce Drought Risk, Preparedness and Mitigation*; Working Group of the Western Drought Coordination Council: Lincoln, NE, USA, 1998.
42. Iglesias, A.; Cancelliere, S.; Gabiña, D.; López-Francos, A.; Moneo, A.; Rossi, G. (Eds.) *MEDROPLAN Drought Management Guidelines and Examples of Application (2 Volumes in 6 Languages)*; European Commission. MEDA-Water Programme: Zaragoza, Spain, 2007.
43. Garrido, A.; Rey, D. *Description and Analysis of Policy Approaches to Drought and Floods in Agriculture in Five OECD Countries. Joint Working Party on Agriculture and the Environment. Trade and Agricultural Directorate & Environmental Directorate*; Report COM/TAD/CA/ENV/EPOC(2014)2015; OECD: Paris, France, 2014.
44. Sivakumar, M.V.K.; Stefanski, R.; Bazza, M.; Zelaya, S.; Wilhite, D.; Magalhaes, A.R. High Level Meeting on National Drought Policy: Summary and Major Outcomes. *Weather Clim. Extrem.* **2014**, *3*, 126–132. [CrossRef]
45. Urquijo, J.; Pereira, D.; Dias, S.; Stefano, L.D. A Methodology to Assess Drought Management as Applied to Six European Case Studies. *Int. J. Water Resour. Dev.* **2017**, *33*, 246–269. [CrossRef]
46. Wilhite, D.; Hayes, M.; Knutson, C.; Smith, K. *Planning for Drought: Moving from Crisis to Risk Management*; Drought Mitigation Center Faculty Publications: Lincoln, NE, USA, 2000.
47. Wilhite, D.A.; Hayes, M.; Knutson, C. *Drought Preparedness Planning: Building Institutional Capacity*; Drought Mitigation Center Faculty Publications: Lincoln, NE, USA, 2005.
48. MMA-DGA—Ministry of Environment and Water. *General Directorate Guidelines for the Redaction of Special*; Drought Management Plans: Madrid, Spain, 2005.
49. European Commission. *Drought Management Plan Report: Including Agricultural; Drought Indicators and Climate Change Aspects*; Technical Report—2008—023. Water Scarcity and Drought Expert Network, DG Environment: Luxembourg, 2007.
50. MED EUWI. Mediterranean Water Scarcity and Drought Report; Mediterranean Water Scarcity and Drought Working Group—Med EUWI. Joint Mediterranean EUWI/WFD Process, EU Water Initiative. 2008. Available online: http://www.emwis.net/topics/WaterScarcity/PDF/MedWSD_FINAL_Edition (accessed on 1 November 2020).
51. National Institute of Disaster Management. *NIDM Manual for Drought Management*; Department of Agriculture and Cooperation, Ministry of Agriculture, Government of India: New Delhi, India, 2009.
52. MITECO—Ministry for the Ecological Transition. *Technical Instructions for the Elaboration of the Special Drought Plans and the Definition of Global System of Indicators of Prolonged Drought and Scarcity (Instrucción Técnica Para La Elaboración de Los Planes Especiales de Sequía y La Definición Del Sistema Global de Indicadores de Sequía Prolongada y de Escasez)*; Ministry for the Ecological Transition: Madrid, Spain, 2017.
53. Fontaine, M.; Steinemann, A.; Hayes, M. State Drought Programs and Plans: Survey of the Western United States. *Publ. Nat. Hazards Rev.* **2014**, *15*, 95–99. [CrossRef]
54. WSDEN. *Water Scarcity and Droughts Expert Network. Drought Management Plan Report, Including Agricultural, Drought Indicators and Climate Change Aspects. Technical Report 2008—023*; European Commission: Brussels, Belgium, 2007.
55. Ministerio de Medio Ambiente. *Medio Rural y Marino-MMA Gestión de La Sequía de Los Años 2004 a 2007*; Estrela, T y Rodriguez Fontal, A (Coord.): Madrid, Spain, 2008.
56. UN UN-SWAP Evaluation Performance Indicator Technical Note. Guidance Document. Revised August 2014. 2014. Available online: <http://unevaluation.org/document/download/2270> (accessed on 1 November 2020).
57. Kolbe, R.H.; Burnett, M.S. Content-Analysis Research: An Examination of Applications with Directives for Improving Research Reliability and Objectivity. *J. Consum. Res.* **1991**, *18*, 243–250. [CrossRef]
58. Neuendorf, K. *The Content Analysis Guidebook*; Sage: Thousand Oaks, CA, USA, 2002.
59. Lombard, M.; Snyder-Duch, J.; Bracken, C.C. Content Analysis in Mass Communication: Assessment and Reporting of Intercoder Reliability. *Hum. Commun. Res.* **2002**, *28*, 587–604. [CrossRef]
60. Vicente-Serrano, S.M.; Cuadrat, J.M. North Atlantic Oscillation Control of Droughts in North-East Spain: Evaluation since 1600 a.d. *Clim. Chang.* **2007**, *85*, 357–379. [CrossRef]
61. Domínguez-Castro, F.; Vicente-Serrano, S.M.; Tomás-Burguera, M.; Peña-Gallardo, M.; Beguería, S.; Kenawy, A.E.; Luna, Y.; Morata, A. High Spatial Resolution Climatology of Drought Events for Spain: 1961–2014. *Int. J. Climatol.* **2019**, *39*, 5046–5062. [CrossRef]

62. European Commission. Directive 2000/60/EC of the European Parliament and of the Council Establishing a Framework for the Community Action in the Field of Water Policy (EU Water Framework Directive), 2000 Official Journal (L 327) (EC). 2000. Available online: <https://eur-lex.europa.eu/legal-content/en/ALL/?uri=CELEX%3A32000L0060> (accessed on 1 November 2020).
63. Law 10/2001, of July 5th, of National Hydrological Plan. Available online: <https://www.boe.es/buscar/act.php?id=BOE-A-2001-13042> (accessed on 1 March 2022).
64. MMA ORDEN MAM/698/2007 de 21 de Marzo, por la que se aprueban los Planes Especiales de Actuación en situaciones de Alerta y Eventual Sequía en los ámbitos de los Planes Hidrológicos de Cuencas Intercomunitarias. 2007. Available online: <https://www.boe.es/buscar/doc.php?id=BOE-A-2007-6228> (accessed on 1 March 2022).
65. MITECO. *Ministry for the Ecological Transition ORDEN TEC/1399/2018, de 28 de Noviembre, Por La Que Se Aprueba La Revisión de Los Planes Especiales de Sequía*; MITECO: Madrid, Spain, 2018.
66. Urquijo, J.; De Stefano, L.; La Calle, A. Drought and Exceptional Laws in Spain: The Official Water Discourse. *Int. Env. Agreem.* **2015**, *15*, 273–292. [CrossRef]
67. MAGRAMA. Estudio de Seguimiento de Las Sequías En Las Cuencas Intercomunitarias Españolas, de Acuerdo Con Lo Establecido En Los Planes Especiales de Alerta y Eventual Sequía (Not Public). 2013. Available online: <https://www.iberhidra.es/portfolio/seguimiento-sequias-cuencas-intercomunitarias/> (accessed on 1 March 2022).
68. Gómez Gómez, C.M.; Pérez Blanco, C.D. Do Drought Management Plans Reduce Drought Risk? A Risk Assessment Model for a Mediterranean River Basin. *Ecol. Econ.* **2012**, *76*, 42–48. [CrossRef]
69. Wilhite, D.A.; Glantz, M.H. Understanding: The Drought Phenomenon: The Role of Definitions. *Water Int.* **1985**, *10*, 111–120. [CrossRef]
70. Mishra, A.K.; Singh, V.P. A Review of Drought Concepts. *J. Hydrol.* **2010**, *391*, 202–216. [CrossRef]
71. Stahl, K.; Kohn, I.; Blauhut, V.; Urquijo, J.; De Stefano, L.; Acácio, V.; Dias, S.; Stagge, J.H.; Tallaksen, L.M.; Kampragou, E.; et al. Impacts of European Drought Events: Insights from an International Database of Text-Based Reports. *Nat. Hazards Earth Syst. Sci.* **2016**, *16*, 801–819. [CrossRef]
72. Lackstrom, K.; Brennan, A.; Ferguson, D.; Crimmins, M.; Darby, L.; Dow, K.; Ingram, K.; Meadow, A.; Reges, H.; Shafer, M.; et al. *The Missing Piece: Drought Impacts Monitoring Report from a Workshop in Tucson, AZ MARCH 5–6, 2013*; Drought Mitigation Center Faculty Publications: Lincoln, NE, USA, 2013.
73. Paneque, P. Drought Management Strategies in Spain. *Water* **2015**, *7*, 6689–6701. [CrossRef]
74. De Stefano, L.; Tánago, I.; Ballesteros Olza, M.; Urquijo Reguera, J.; Blauhut, V.; Stagge, J.; Stahl, K. *Methodological Approach Considering Different Factors Influencing Vulnerability-Pan-European Scale*; Technical Report no. 26; DROUGHT-R&SPI Project: Madrid, Spain, 2015; 121p.
75. Field, B.C.; Barros, V.; Stocker, T.F.; Qin, D.; Dokken, D.J.; Ebi, K.L.; Mastrandrea, M.D.; Mach, K.J.; Plattner, G.-K.; Allen, S.K.; et al. (Eds.) *IPCC Managing the Risks of Extreme Events and Disasters to Advance Climate Change Adaptation: Special Report of Working Groups I and II of the Intergovernmental Panel on Climate Change*; Cambridge University Press: Cambridge, UK; New York, NY, USA, 2012; 582p.
76. González Tánago, I.; Urquijo, J.; Blauhut, V.; Villarroya, F.; De Stefano, L. Learning from Experience: A Systematic Review of Assessments of Vulnerability to Drought. *Nat. Hazards* **2016**, *80*, 951–973. [CrossRef]
77. Botterill, L.C. Uncertain Climate: The Recent History of Drought Policy in Australia. *Aust. J. Politics Hist.* **2003**, *49*, 61–74. [CrossRef]
78. FAO. *Drought Characteristics and Management in the Caribbean*; FAO Water Reports 42; FAO: Rome, Italy, 2016.
79. Pedro-Monzonis, M.; Solera, A.; Ferrer, J.; Estrela, T.; Paredes-Arquiola, J. A Review of Water Scarcity and Drought Indexes in Water Resources Planning and Management. *J. Hydrol.* **2015**, *527*, 482–493. [CrossRef]
80. Hervás-Gámez, C.; Delgado-Ramos, F. Critical Review of the Public Participation Process in Drought Management Plans. The Guadalquivir River Basin Case in Spain. *Water Resour. Manag.* **2019**, *33*, 4189–4200. [CrossRef]
81. OECD. *Agriculture and Water Policies: Main Characteristics and Evolution from 2009 to 2019*. Available online: <https://www.oecd.org/agriculture/topics/water-and-agriculture/documents/oecd-water-policies-country-note-spain.pdf> (accessed on 4 January 2021).
82. World Bank. *Water in Agriculture*. Available online: <https://www.worldbank.org/en/topic/water-in-agriculture#1> (accessed on 1 March 2022).
83. Miteco. *Síntesis de los Borradores de Planes Hidrológicos de las Demarcaciones Hidrográficas Intercomunitarias; Revisión Para el Tercer Ciclo 2021–2017*; Secretaria de Estado de Medio Ambiente, Dirección General del Agua: Madrid, Spain, 2021.

Article

Foliar Application of Zinc Improves Agronomical and Quality Parameters and Biofortification of Cowpea (*Vigna sinensis*) under Deficit Irrigation

Abdullah Aık¹ and Feride ncan Smer^{2,*} ¹ Graduate School of Natural and Applied Science, Aydın Adnan Menderes University, Aydın 09100, Turkey² Department of Field Crops, Faculty of Agriculture, Aydın Adnan Menderes University, Aydın 09100, Turkey

* Correspondence: fsumer@adu.edu.tr; Tel.: +90-256-220-63-00

Abstract: Due to climate changes, we encounter irregular and low rainfall. It is important to effectively use groundwater and to select crops that can be grown with deficit irrigation in the summer period. Restricted irrigation reduces water consumption but it may cause losses in terms of yield and quality. Different agronomic practices can be used to minimize these losses. One of these practices is the application of foliar zinc fertilizer. In previous studies, zinc application was found to increase the bioavailability of cowpea grain. In this study, the effects of the application of zinc fertilizer on yield, some yield components, physiological traits, and grain quality characteristics of three different cowpea genotypes (Akkız, Karagöz, and a Local variety) were investigated under full (100%) and deficit (50%) irrigation. The field experiment was conducted using a randomized complete block split-split plot design with irrigation rates (100% and 50%) and foliar zinc application (0 and 60 kg ha⁻¹) with three replicates used each season (2020 and 2021 growing seasons of cowpea) in the field crops trial fields of the Aydın Adnan Menderes University, at the Faculty of Agriculture, located in the western region of Turkey. Yield and quality characteristics such as grain yield, some yield components, grain protein content, grain mineral matter content, and grain amino acid content were measured. According to the data obtained, a 40% yield reduction was observed under restricted irrigation in the first year of the study. It was determined that zinc application under restricted irrigation increased the yield by approximately 10%. The second-year results found that the amount of essential amino acids such as histidine, phenylalanine, valine, and lysine increased with the zinc application. This study highlights that deficit irrigation conditions caused stress in the plant and caused losses in the yield and quality. Still, the severity of this stress was reduced by foliar zinc application, and it was determined that it positively affected grain yield and bioavailability in cowpea.

Keywords: cowpea; deficit irrigation; zinc; amino acid; biofortification

Citation: Aık, A.; ncan Smer, F. Foliar Application of Zinc Improves Agronomical and Quality Parameters and Biofortification of Cowpea (*Vigna sinensis*) under Deficit Irrigation.

Agronomy **2023**, *13*, 1021. <https://doi.org/10.3390/agronomy13041021>

Academic Editor: Aliasghar Montazar

Received: 2 March 2023

Revised: 21 March 2023

Accepted: 27 March 2023

Published: 30 March 2023



Copyright: © 2023 by the authors. Licensee MDPI, Basel, Switzerland. This article is an open access article distributed under the terms and conditions of the Creative Commons Attribution (CC BY) license (<https://creativecommons.org/licenses/by/4.0/>).

1. Introduction

Cowpea is a legume that is grown in tropical and subtropical areas, especially in Africa. Of the approximately 15 million ha of cultivation area in the world, 14.8 million ha are located on the African continent, and 8.6 million tons of cowpea production of 8.9 million tons are obtained from the African continent [1]. Cowpeas can adapt to low fertile soils and arid conditions. In this way, they can adapt to high temperatures and low rainfall due to recent climate changes.

The Aegean Region, which has a Mediterranean climate with mild and rainy winters and dry and hot summers, is the region with the largest cultivation area in Turkey.

Drought is one of the most important abiotic stress factors that negatively affects grain yield [2,3]. The adaptation of plants to water deficits and survival may occur with different responses [4,5]. Many morphological, physiological, and molecular changes may occur in drought stress [6,7]. The most important physiological responses are decreased chlorophyll content, photosynthesis, and evaporation [8–10]. Among legumes, the cowpea

is a plant that can tolerate these adverse conditions [5,9–12]. In addition, the cowpea experiences little change in its leaf water potential through osmotic adjustment under drought conditions [13]. Because of these characteristics, it is a product that can be utilized, especially in Mediterranean climate conditions where water scarcity is caused by high temperatures, irregular and low rainfall amounts, and global climate changes [13,14].

In recent years, longer drought periods and higher maximum temperature values have been observed in Mediterranean climate conditions compared to previous years. Climate change is felt more effectively in the region. Studies have predicted that the earth's average temperature will increase by 2–4.5 °C [15]. Long temperature periods and extremely hot conditions in semi-arid regions cause water scarcity in crop production [16]. Water scarcity negatively affects the plant's growth and development and thus, significantly reduces the grain yield. Under drought conditions, water is the most important factor determining the yield. It has been observed that water scarcity, especially during flowering and pod formation periods, negatively affects a plant's yield by causing a decrease in the number of pods in the plant due to a decrease in the flowering rate and inhibition of nitrogen fixation [17–19].

Cowpea plants tend to turn their leaves vertically to reduce the amount of light coming in and lessen the effect of sunlight on the leaves when there is drought in the field [20]. In this way, cowpea, unlike many other plants, can survive the vegetative period under drought conditions. This is achieved using as much soil water as possible by deepening the roots of some varieties that can handle not getting enough water [21].

One of the most important characteristics of the cowpea is that it consists of plant parts with high nutrient content [22–25]. The grain is rich in protein content (23–32%) and amino acids such as lysine (427 mg g⁻¹ N) and tryptophan (68 mg g⁻¹ N). The grain contains protein, fiber, and minerals such as zinc, iron, and magnesium [26]. The mineral substances contained in the cowpea gain importance in meeting the nutritional needs of the rapidly increasing world population. Zinc is the most important element associated with human health, especially in developing countries [27]. In previous studies, while the grain yield and grain zinc content increased with the zinc fertilizer application in cereals [28–31], it was also determined that the amount of zinc needed for nutrition was met [28,29,32–34]. It is known that the tryptophan content of plants decreases, protein synthesis stops, and free amino acids accumulate in a zinc deficiency. This situation naturally causes yield and quality losses. The zinc intake of plants may affect their sensitivity to drought stress. Zinc is involved in detoxifying reactive oxygen species (ROS) and it is also important for reducing the production of free radicals by superoxide radical-producing enzymes [35]. Under drought stress, the plant may die due to the production of reactive oxygen species during photosynthesis [36]. In addition, in zinc deficiency, photosynthetic carbon turnover is impaired, oxygen production and activity are reduced, and sensitivity to drought increases [37].

Zinc is an essential element in human nutrition [38]. It is known that 17% of the world's population suffers from inadequate zinc intake [39]. Many people do not receive adequate amounts of zinc in their diets [31,40]. Biofortification is the elimination of deficiencies in humans by increasing the concentrations of vitamins and minerals, which are widely deficient in society, in the products most consumed by society [41]. Increasing the amount of zinc in grains through fertilization has been observed in cereals and other crops [31,42]. Biofortification aims to improve zinc fertilizers' application and develop crop varieties that take up more zinc from outside and accumulate it in the edible parts [31]. The bioavailability of zinc varies between 18 and 34%. Compensating for this low bioavailability is important for biofortification [39], because zinc application is associated with cowpea's nitrogen metabolism and protein content [43]. Thus, zinc biofortification increases the zinc content in the cowpea grain, which is beneficial for human nutrition. As a result, exposure of the plant to zinc deficiency during drought may cause the drought sensitivity in the plant to become more pronounced.

Zinc is given to plants in two ways, through the soil, and through foliar application. Foliar application minimizes groundwater pollution [44–46]. In addition, zinc uptake from the soil is deficient in soils with high pH [47]. For these reasons, the foliar application of zinc becomes more attractive.

This study will provide information on deficit irrigation and the arid conditions that are expected to be experienced in many countries. The effect of zinc fertilizer applied under these conditions on grain yield and nutritional value will be determined. Some previous studies have been carried out on this subject, but detailed quality analyses, such as grain amino acid measurements in cowpea, have been lacking. This study aimed to determine the effects of foliar zinc application on grain yield, grain mineral matter content, and grain amino acid content under deficit irrigation conditions.

2. Materials and Methods

The study was conducted in 2020 and 2021 in the experimental field (27°51' E, 37°51' N, altitude 50 m) of the Department of Field Crops, at the Faculty of Agriculture, Adnan Menderes University, Aydin/Turkey.

According to Table 1, it has a sandy loamy characteristic in soil properties. The table shows that soil organic matter and potassium are low, while phosphorus and calcium are high. According to the results of soil analyses, it is observed that soil pH is high.

Table 1. Soil properties of the trial site.

Soil Texture			pH	Organic Matter (%)	Phosphorus (ppm)	Potassium (ppm)	Calcium (ppm)	Sodium (ppm)
Sand (%)	Silt (%)	Clay (%)						
72	16.7	11.3	8.0	2.0	21	176	2978	101
Sandy loam			High	Low	High	Low	High	Low

Figure 1 shows the experimental years' average temperature and total precipitation values. It can be observed that the average temperature values exceeded the long-term average in both years. In the first year of the experiment, the average temperature in June exceeded all previous years. Notably, the average temperature in July and August of the second year was higher than in the other years. When the total rainfall values were analyzed, it was determined that the total rainfall in the trial years was lower than the total of the long years, and the lowest rainfall was obtained from the second year of the trial.

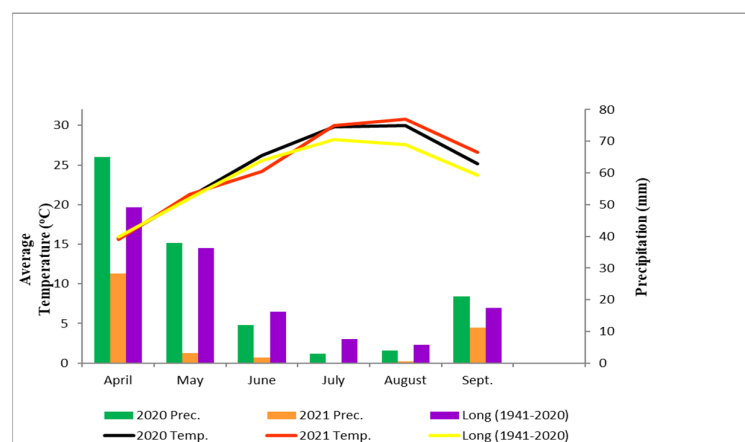


Figure 1. Climatic data for the years of the experiment.

Three cowpea varieties (Karagöz, Akkız, and a local variety) were used in the experiment. Akkız and Karagöz varieties are registered in Turkey; while the local variety is not a registered variety, it is a variety that farmers in the region have been planting in their

fields for many years to meet their consumption. The local variety was supplied by farmers producing in the region because it is not commercially produced. Two varieties (Akkız and Karagöz) were widely cultivated in the region. Local variety was supplied by farmers producing in the region. The experiment was conducted under normal irrigation (100%) and restricted irrigation (50%) conditions, with and without zinc (kg Zn ha^{-1} , ZnSO_4 as foliar spraying). Irrigation factor was used as the main plot, cultivar as sub-plot, and Zn treatments as split-split plot.

Before sowing, 40 kg ha^{-1} of nitrogen, phosphorus, and potassium were applied as 15-15-15 fertilizer. The weeds were controlled twice, at the beginning and post-flowering stages, by hand. After sowing, nitrogen fertilization (20 kg N ha^{-1}) was applied at a 10–15 cm plant height.

Sowing was performed by regina model sowing machine manufactured by the Italian company Maschio-Gaspardo on May 9 of the first year and on 10 May of the second year. Each plot was 70 cm wide with 6 rows (5 m long). The randomized complete block split-split plot design with three replicates was used each season. Before sowing, 40 kg ha^{-1} of nitrogen, phosphorus, and potassium were applied as 15-15-15 fertilizer. The weeds were controlled twice, at the beginning and post-flowering stages, by hand. After sowing, nitrogen fertilization (20 kg N ha^{-1}) was applied at a 10–15 cm plant height. Foliar zinc applications were applied at the beginning of the flowering period. Foliar treatments were applied with a portable, hand-held field plot sprayer at 250 kPa pressure using a water carrier volume of $400 \text{ L} \cdot \text{ha}^{-1}$.

The irrigation water to be applied to the plots was calculated based on the cumulative evaporation amount from the class A evaporation container multiplied (located near the experimental field) by different coefficients. In the study, 2 irrigation doses (full irrigation and deficit irrigation) were determined, in which different levels of cumulative evaporation were applied.

These are as follows:

1. Full irrigation (100%): Irrigation water applied for 7 days as much as possible for the cumulative evaporation measured with a screened US Weather Bureau Class A pan located at the meteorological station near the experimental field.
2. Deficit irrigation (50%): It was established that irrigation water was applied as 50% of full irrigation.

The equation given in [48] was utilized to apply to the plots.

$$I = K_{pc} \cdot E_p \cdot P \cdot A$$

I = amount of irrigation water to be applied to the plot (L); K_{pc} = evaporation container coefficient 100%; E_p = cumulative evaporation amount (mm); P = Plant cover (%); and A = Plot area (m^2) and drip irrigation method was used [49].

In the study, irrigation started when flowers were seen on the plants, and irrigation was carried out with a drip irrigation system every 7 days.

Plant height, number of pods per plant, number of grains per pod, leaf area index, leaf chlorophyll content, 100 grain weight, grain yield, grain protein content, grain mineral content, and grain amino acid content were measured.

Approximately 500 g samples were dried at $70 \text{ }^\circ\text{C}$ for 48 h. 100-seed weight (g) was determined by counting from dry seeds and weighing four replicates of 100 seeds.

Seed yield was calculated from 11.4 m^2 ($4 \text{ rows} \times 4 \text{ m} \times 0.7 \text{ m}$) harvested area in each plot (kg da^{-1}).

Seed protein content (%), seed ash content (%), seed fiber content (%), and seed oil content (%) were measured by using Near Infrared Reflected Spectroscopy (NIRS) method Bruker MPA, German at Adnan Menderes University Agricultural Biotechnology and Food Safety Application and Research Center (ADÜ-TARBIYOMER) [50].

The seed mineral content (mg kg^{-1}) was determined by atomic absorption spectrometry after ashing samples at $550 \text{ }^\circ\text{C}$ and dissolving ash in 3.3% HCl [51] (Aydin Adnan

Menderes University, Faculty of Agriculture, Department of Soil Science and Plant Nutrition Laboratory).

Seed amino acid content (g/100 g) and cowpea dry grains were ground after harvest, and random samples were prepared from each plot. A total of seventeen amino acids were measured. Seed. Amino acid analyses (high-performance liquid chromatography or high-pressure liquid chromatography, HPLC) were performed at Research and Application Center of Drug Development and Pharmacokinetics Laboratory in Ege University.

Statistical Analysis

Statistical analyses were conducted using JMP Statistical Analysis Software (version Pro 13) in the split-split plot design. The experimental data about each study parameter were subjected to statistical analysis using the variance analysis technique, and their significance was tested by the “F” test (Steel and Torrie, 1980). When differences were found in ANOVA, means were compared using Fisher’s protected least significant difference (LSD) test at $p \leq 0.05$.

3. Results

The heat map (Figure 2) was improved, including the averages of agronomic traits of three cowpea cultivars treated with zinc fertilizer under different irrigation conditions for two years of the experiment.

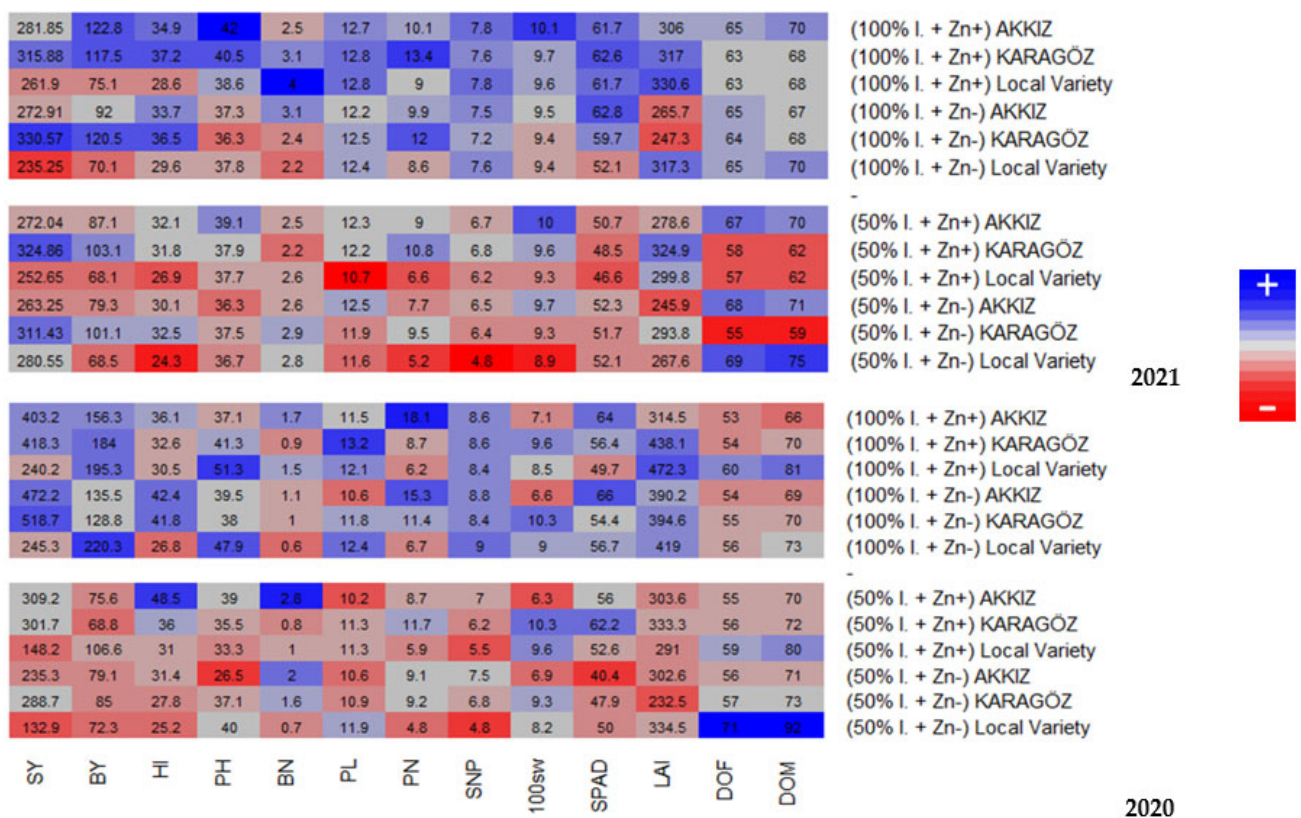


Figure 2. Mean values of grain yield and yield components.

Based on the results of the analysis of variance (Table 2), there was a significant difference between the years, so the averages for each year were evaluated separately. In the same way, the results of the analysis of variance showed that the mean values of the grain yield, biological yield, plant height, pod length, number of pods, number of grains in pods, 100 grain weight, and leaf area index were significantly better than those under deficit irrigation conditions in the first year.

Table 2. ANOVA of grain yield and yield components.

SOV	Df	Seed Yield		BY		HI		Plant H.		BN		Pod Length		PN	
Years	1	*		*		*		*		*		*		*	
		2020	2021	2020	2021	2020	2021	2020	2021	2020	2021	2020	2021	2020	2021
I	1	*	-	*	*	-	-	-	-	-	-	-	-	-	-
Zn	1	-	-	*	-	*	-	-	-	-	-	-	-	-	-
C	2	*	-	*	*	*	*	*	-	-	-	-	-	*	-
I*Zn	2	-	-	-	-	*	-	-	*	-	*	*	-	-	-
I*C	2	-	-	*	-	-	-	-	*	-	-	*	*	*	*
Zn*C	2	-	-	-	-	-	-	-	-	-	-	-	-	-	-
I*Zn*C	11	-	*	*	-	-	-	*	-	-	-	-	-	*	-
SOV	Df	Seed Number		100 Seed Weight		SPAD		LAI		DOS		DOM			
Years	1	*		*		*		*		*		*			
		2020	2021	2020	2021	2020	2021	2020	2021	2020	2021	2020	2021	2020	2021
I	1	-	-	-	-	-	*	*	-	-	-	-	-	-	-
Zn	1	-	-	-	-	-	-	-	-	-	-	-	-	-	-
C	2	*	-	*	-	-	-	-	-	*	-	*	-	-	-
I*Zn	2	-	-	-	-	*	-	-	-	-	-	-	-	-	-
I*C	2	*	*	-	*	-	-	-	-	-	-	-	-	-	*
Zn*C	2	-	-	-	-	-	-	-	-	-	-	-	-	-	*
I*Zn*C	11	-	-	-	-	-	-	*	-	-	*	*	-	-	-

SY: seed yield, BY: biological yield, HI: harvest index, PH: plant height, BN: branch number, PL: pod length, PN: pod number, SNP: number of seeds per pod, 100 SW: 100 seed weight, SPAD: chlorophyll meter, LAI: leaf area index, DOF: days of flowering, and DOM: days of maturity. (*; significant at 5% probability level *: significant -: nonsignificant).

The first-year irrigation dose \times zinc and variety interactions were significant for a plant's height. While 51.30 cm of the plant's height was obtained under full irrigation conditions, 26.51 cm was observed under restricted irrigation conditions. It was concluded that a limitation in the irrigation dose significantly decreased the plant height. Similarly, in our study, the plant heights were ranked as local variety > Karagöz > Akkız at a statistically significant level. The plant height performance of the local variety was observed to be higher than the other two varieties. In the second year of our study, irrigation dose \times zinc and variety \times irrigation interactions were significant regarding the plant's height. The difference between zinc application (40.37 cm) under full irrigation conditions and plant height (36.84 cm) of zinc-free plots under deficit irrigation conditions was significant. It was concluded that the response of plant height to zinc fertilization with full irrigation was positive. When the variety \times irrigation interaction was analyzed, the difference between irrigation doses was insignificant in Karagöz and local varieties. In contrast, the difference between both irrigation doses was significant in the Akkız variety. Therefore, we observed that deficit irrigation significantly affected the Akkız variety.

In the first year, the interactions did not make a difference in the number of side branches. However, in the second year, the irrigation dose \times zinc interaction made a difference in the number of side branches, and the plots with a zinc application and full irrigation had the most side branches (3.23).

In the first year, there was a significant interaction between the irrigation dose, zinc level, and variety in terms of the number of pods. Under conditions where there was not enough water, the number of pods went down by a lot. The number of pods of Akkız (8.88) and the local variety (5.20) decreased significantly under restricted irrigation conditions. Zinc application was not effective under full irrigation conditions, but it positively affected Karagöz and local varieties under deficit irrigation conditions and increased the number of pods.

In the second year, the variety \times irrigation interaction was found to be significant in terms of the pod number. The number of pods decreased significantly in Akkız, Karagöz, and local varieties under deficit irrigation conditions.

In the first year, the pod length was affected by the interactions between variety and irrigation and between irrigation and zinc. Using the variety \times irrigation interaction, it was found that the Karagöz variety (12.05) responded significantly to water doses, and the pod length decreased significantly when there was not enough water. There was no significant difference between irrigation doses of other varieties. Pod length was higher under full irrigation \times zinc application conditions than irrigation \times zinc interactions. In the second year, the variety \times irrigation interaction was determined to be significant. Among the varieties, the local variety was significantly affected by irrigation doses. The decrease in pod length of the local variety was found to be significant under deficit irrigation conditions.

The irrigation \times cultivar interaction significantly increased the number of grains in the pod in the first year. The number of grains in pods of all varieties decreased significantly under the restricted irrigation conditions. Zinc fertilizer application had no significant effect on the number of grains in the pods. While there was no significant difference between the mean values of the varieties under full irrigation conditions, the number of grains in the pods of the Akkız (7.23) variety was higher than the others under restricted irrigation conditions. In the second year, the variety \times irrigation interaction was significant. It was determined that the restricted irrigation conditions affected the local variety (5.17), which had lower grain numbers in the pods.

In terms of the weight of 100 grains, it was seen that the variety factor was important in the first year. The highest 100 grain weight among the varieties was observed in Karagöz (9.99 g) under full irrigation conditions. It was followed by local variety (8.79 g) and Akkız (6.81 g). The variety \times irrigation dose interaction was significant in the second year. The responses of the varieties to irrigation doses were found to be significant. In both irrigation doses, the order of the varieties changed to Akkız > Karagöz > local variety. The lowest value in the deficit irrigation was measured for the local variety (9.10 g).

When the SPAD values were analyzed, it was observed that cultivars had a significant effect in the first year, and irrigation had a significant effect in the second year. Looking at the average values, it is observed that the SPAD values decreased under deficit irrigation conditions.

The variety factor was significant in terms of days to flowering in the first year. It was observed that the local variety flowered later among the varieties under both irrigation conditions. Akkız and Karagöz varieties flowered earlier than the local variety. However, the average number of days of flowering for the local cultivar (65 days) under deficit irrigation conditions was longer than full irrigation (59.0 days). In the second year, cultivar \times irrigation \times zinc application was found to be significant. It was observed that the varieties generally flowered faster under deficit irrigation conditions, especially Karagöz (55 days), which flowered faster under deficit irrigation conditions, and the local variety (69 days), which was the variety with the latest flowering period.

When the number of days to maturity values was analyzed, it was determined that the cultivar \times irrigation \times zinc application interaction was significant in the first year. The earliest variety was determined to be Akkız under full irrigation and zinc application conditions. However, the variety most affected by deficit irrigation conditions was the local variety, and the days to flowering and ripening were found to be longer. In the second year, the variety \times irrigation \times zinc fertilizer interaction was found to be significant in days to the flowering values. Akkız was found to be earlier than the other varieties, and the local variety was found to be later than the others. Variety \times irrigation and variety \times zinc fertilizer interactions were found to be significant in the second year in terms of days to maturity. Among the varieties, Karagöz (59 days) was significantly affected by restricted irrigation and showed a shorter ripening period under restricted irrigation conditions. This was followed by the Akkız variety and then the local variety.

First-year irrigation \times zinc interaction was found to be significant for SPAD. According to the interaction, the zinc factor was significant under deficit irrigation conditions. The SPAD values of the zinc-free plots decreased significantly under restricted irrigation

conditions. The irrigation factor was found to be significant in the second year. It was revealed that the drought conditions affected the plants.

In the first year, the interaction of variety \times irrigation \times zinc was found to be significant for the leaf area index. According to this interaction, the leaf area index of the local variety (472.3) and Karagöz (438.1) was higher than Akkız (314.5) under full irrigation conditions. The responses of the varieties to restricted irrigation conditions were different, the local variety was significantly affected by restricted irrigation, and the leaf area index decreased. In addition, among the varieties, Karagöz was significantly affected by the zinc application, and the leaf area index increased with the zinc application in both irrigations. The variety \times irrigation interaction was found to be significant in the second year. Variety responses to irrigation were found to be different, and the local variety was significantly affected by deficit irrigation. For this reason, the leaf area index of the local variety decreased significantly under deficit irrigation.

The first-year irrigation \times zinc \times variety interaction was found to be significant in biological yield values. It was observed that deficit irrigation conditions significantly affected the biological yield values. Water limitations caused a decrease in biological yield values. Karagöz (68.84) gave the lowest biological yield value under restricted irrigation conditions. Under full irrigation conditions, the biological yield value of the local variety (220.3) was the highest. In the second year, the irrigation and variety factors were statistically significant. Deficit irrigation caused a decrease in the biological yield. Among the varieties of the Karagöz, 110 had a higher biological yield than the others.

In the harvest index values, the irrigation \times zinc application interaction was found to be significant in the first year. Under full irrigation conditions, the harvest index values were higher in zinc application (178.5). Under deficit irrigation and zinc-free conditions (78.8), the harvest index values decreased significantly. The variety factor was found to be significant in the second year. It was revealed that there was a ranking among the varieties, which was as follows: Karagöz > Akkız > local variety.

The variety and irrigation factors were significant in grain yield values in the first year. While 382.98 kg/da of yield was obtained under full irrigation conditions, 236.0 kg/da yield was measured under restricted irrigation conditions. Water limitations caused a significant decrease in the grain yield. All the varieties in the study showed a decrease in the grain yield under deficit irrigation conditions. However, Karagöz (292.2 kg/da) had the highest grain yield among the varieties, followed by Akkız (272.2 kg/da), and the local variety (140.5 kg/da). It was determined that the local variety had a lower yield than the other varieties at both irrigation doses. While zinc application was not found to be statistically significant, it was observed that the average grain yield values under deficit irrigation conditions increased with zinc application. Under stress conditions, the effect of zinc application on grain yield was found to be more significant. In the second year of the study, the irrigation \times zinc \times variety interaction was found to be significant. A decrease in the grain yield was observed under restricted irrigation conditions. The highest yield was obtained from Karagöz under restricted irrigation conditions. It was found that restricted irrigation conditions affected Akkız and local cultivars more. The yield values of the varieties under full irrigation and deficit irrigation conditions were ranked as Karagöz > Akkız > local variety. Zinc application had a positive effect on the grain yield under deficit irrigation conditions.

Figure 3 shows the mean of quality values. According to the results of variance analysis (Table 3), it was determined that grain copper, zinc, iron, potassium, magnesium, calcium, phosphorus, fiber, ash, oil, and protein contents were significantly superior to deficit irrigation under full irrigation conditions.

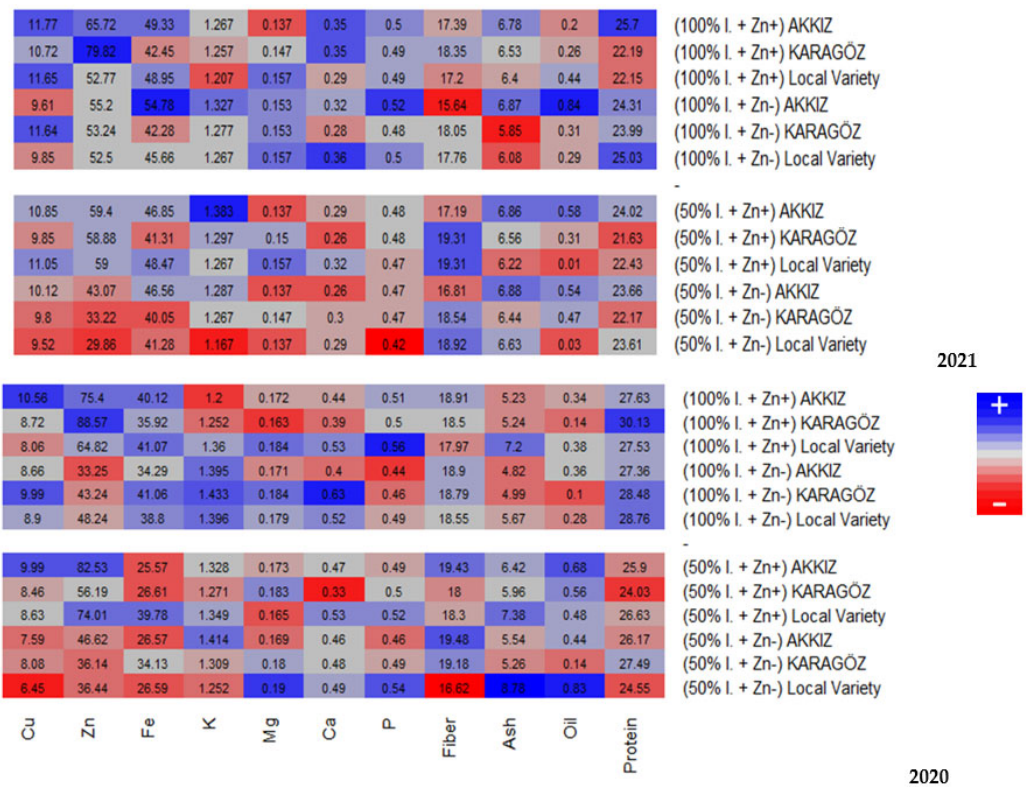


Figure 3. Mean values of grain quality components.

Table 3. ANOVA of grain quality components (*: significant -: nonsignificant).

SOV	Df	Cu		Zinc		Fe		Potassium		Magnesium		Calcium	
Years	1	*		*		*		*		*		*	
		2020	2021	2020	2021	2020	2021	2020	2021	2020	2021	2020	2021
I	1	*	-	-	-	*	*	-	*	-	*	-	*
Zn	1	*	-	*	*	-	*	-	*	-	-	-	*
C	2	-	-	-	*	-	*	-	*	-	*	-	*
I*Zn	2	*	-	-	*	-	*	-	*	-	*	-	-
I*C	2	-	-	-	-	-	*	-	*	-	-	-	*
Zn*C	2	*	-	-	-	-	*	-	*	*	*	-	*
I*Zn*C	11	-	-	-	-	-	*	-	*	-	-	-	*

SOV	Df	Phosphorus		Fibre		Ash		Oil		Protein	
Years	1	*		*		*		*		*	
		2020	2021	2020	2021	2020	2021	2020	2021	2020	2021
I	1	-	*	-	-	-	-	*	-	-	*
Zn	1	*	*	-	-	-	-	-	-	-	-
C	2	*	*	-	*	-	*	-	-	-	*
I*Zn	2	*	*	-	-	-	-	-	-	-	-
I*C	2	-	*	-	-	-	-	-	-	-	-
Zn*C	2	-	-	-	-	-	*	-	-	-	-
I*Zn*C	11	-	*	-	*	-	-	-	-	*	-

(cu: copper, zn: zinc, fe: iron, k: potassium, mg: magnesium, ca: calcium, and p: phosphorus). (*: significant at 5% probability level -: nonsignificant).

Regarding grain copper content, irrigation × variety, and zinc × variety interactions, were found to be significant in the first year. According to the irrigation × variety interactions, the grain copper content of the varieties was higher under full irrigation than under deficit irrigation. The varieties were ranked as Akkız > Karagöz > local variety in terms of the grain copper content. According to the zinc × variety interactions, zinc application positively affected the grain copper content in Akkız and local varieties. In the second

year, the factors in the experiment were not found to be significant. However, according to the average results, it can be observed in Table 2 that the values obtained from restricted irrigation are lower.

In terms of the grain zinc content, zinc application was a significant factor in both years of the study. It was observed that zinc application significantly affected the grain zinc content in both years of the study. The grain zinc content of all varieties with zinc application under full and deficit irrigation conditions was higher than the plots without zinc application.

In the first year of the study, the irrigation factor had a big effect on the amount of iron in the grain. It was determined that deficit irrigation negatively affected the grain's iron content. In the second year, the irrigation \times zinc \times variety interaction was found to be significant. The iron content was found to be higher under full irrigation conditions. Among the varieties, the order was Akkız > local variety > Karagöz. Zinc application was effective in the Akkız (39.78) variety under deficit irrigation conditions.

Regarding grain potassium content, interactions, and factors, they were insignificant in the first year. When the averages were evaluated, the data obtained from full irrigation were higher than from deficit irrigation. The local variety and Karagöz had the highest average grain potassium contents among the varieties. In the second year, irrigation \times zinc \times variety interactions were significant.

Regarding magnesium content, irrigation \times variety zinc interaction was found to be significant in the first year of the study. In the second year, irrigation \times zinc and irrigation \times variety interactions were significant. For the grain calcium content, the zinc \times irrigation interaction was found to be significant in the first year, while the irrigation \times zinc \times variety interaction was found to be significant in the second year. For the grain phosphorus content, the irrigation \times zinc interaction was significant in the first year, while the irrigation \times zinc \times variety interaction was significant in the second year. The interaction of the irrigation \times zinc \times variety was significant for the grain fiber content in the first year.

In contrast, the irrigation factor was significant in the second year. For the ash content, the irrigation \times zinc \times variety interaction was found to be significant in the first year. In the second year of the study, the zinc \times variety interaction was found to be significant.

Regarding the grain oil content, the irrigation factor was significant in the first year, while the irrigation \times variety interaction was significant in the second year. Regarding the grain protein content, the irrigation \times zinc \times variety interaction was found to be significant in the first year. In the second year, the interaction and all factors were found to be insignificant.

The average data of grain amino acid contents are indicated in Figure 4. Eight of the seventeen amino acids measured are essential (histidine, threonine, valine, methionine, phenylalanine, isoleucine, lysine, and leucine), which are not synthesized in the body and are only taken in from food. The essential amino acids in the study were evaluated. According to ANOVA, the experiment factors were found to be insignificant in the first year, while the irrigation and zinc factors were found to be significant in the second year (Table 4). In the first year, it was determined that restricted irrigation significantly affected histidine values. Histidine values were higher under full irrigation (0.86) than under deficit irrigation (0.80). However, it was determined that the histidine value increased with the zinc application.

The negative effect of restricted irrigation on histidine values in the second year was observed significantly. When the threonine values were analyzed, it was determined that the factors in the experiment in the first year were not effective on threonine, and the values obtained ranged between 0.78 and 0.85. In the second year, the water factor significantly affected threonine. It was determined that the amount of threonine obtained from full irrigation conditions (0.85) was higher than from deficit irrigation (0.78).

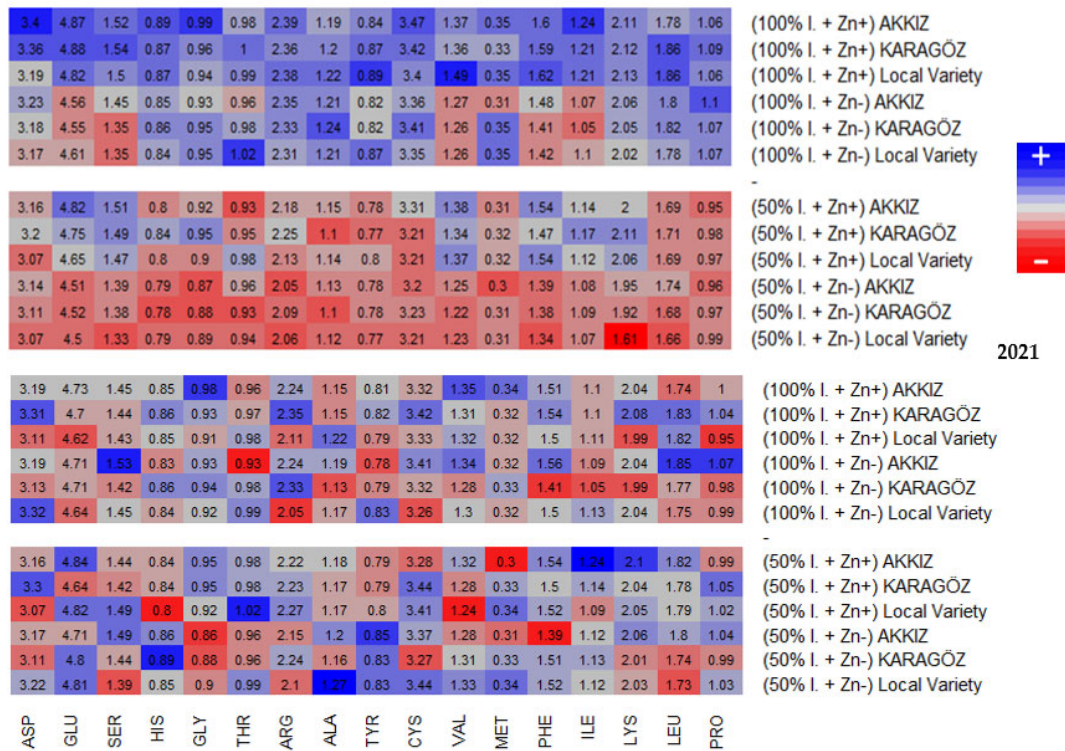


Figure 4. Mean values of grain amino acid contents.

Table 4. ANOVA of amino acids of cowpea cultivars (*: significant -: nonsignificant).

SOV	Df	ASP	GLU	SER	HIS	GLY	THR	ARG	ALA	TYR
Years	1	*	*	*	*	*	*	*	*	*
I	1	-	*	-	*	-	*	-	*	*
Zn	1	-	*	-	*	-	*	-	*	-
C	2	-	*	-	-	-	-	-	-	-
I*Zn	2	-	*	-	-	-	-	-	*	-
I*C	2	-	-	-	-	-	-	-	-	-
Zn*C	2	*	*	-	-	-	-	-	-	*
I*Zn*C	11	-	-	-	-	-	-	-	-	-

SOV	Df	CYS	VAL	MET	PHE	ILE	LYS	LEU	PRO
Years	1	*	*	*	*	*	*	*	*
I	1	-	*	-	-	*	-	*	*
Zn	1	-	-	*	*	*	*	-	-
C	2	-	-	-	-	-	-	-	-
I*Zn	2	-	*	-	-	*	-	-	-
I*C	2	-	-	*	-	*	-	-	-
Zn*C	2	-	-	-	-	-	-	-	-
I*Zn*C	11	-	-	-	-	-	-	-	-

(ASP: aspartic acid, GLU: glutamic acid, SER: serine, HIS: histidine, GLY: glycine, THR: threonine, ARG: Arginine, ALA: alanine, TYR: tyrosine, CYS: cysteine, VAL: valine, MET: methionine, PHE: phenylalanine, ILE: isoleucine, LYS: lysine, LEU: leucine, and PRO: proline). (*: significant at 5% and probability level *: significant -: nonsignificant).

Regarding the valine values, the irrigation × zinc application interaction was found to be significant in the first year. The highest value of valine (1.33) was obtained under full irrigation conditions and from zinc-treated plots. In the second year, the zinc factor was found to be significant. Zinc-treated plots (1.39) were higher than those without zinc treatment (1.25). It was observed that the values of the varieties were close to each other.

The irrigation \times variety factor was found to be significant for methionine. In the second year, zinc application was found to be significantly effective.

Regarding phenylalanine, the zinc factor was significantly effective in the first year. Phenylalanine values of zinc-treated samples (1.52) were higher than those of zinc-free samples (1.48). The irrigation \times zinc application interaction was significantly effective in the second year.

In terms of isoleucine values, it was observed that the treatments were not significant in the first year. In the second year, the irrigation \times variety and irrigation \times zinc application interactions were significantly effective.

Regarding lysine values, treatments were not significant in the first year, but the zinc application factor was found to be significant in the second year. It was determined that zinc-free plots had lower lysine values.

Regarding leucine values, treatments were not significant in the first year. In the second year, the irrigation factor was found to be significant.

The results obtained in non-essential amino acids were evaluated. In the first year, aspartic acid was found to be significantly affected by the cultivar \times zinc application interaction. In contrast, the effects of the treatments on glu, ser, gly, threonine, ala, cys, and pro were found to be insignificant, and the cultivar factor had a significant effect on arg. In the second year, the zinc \times variety, irrigation \times zinc application, and the variety \times irrigation application interactions on asp were found to be significant. The zinc application \times irrigation interactions on glutamic acid and SER were found to be significant. Irrigation factors significantly affected ala, thr, cys, and pro. For arg and gly, the irrigation \times variety interactions were found to be significant.

4. Discussion

When the traits in the study were analyzed, the results were evaluated. The varieties were found to be significant in terms of days of flowering in the first year, and it was observed that the local variety flowered and matured later than the others. In the second year, the irrigation conditions significantly affected these traits, and flowering and physiological maturity periods were prolonged under full irrigation conditions.

The amount of irrigation had a significant effect on the leaf area index values, and in both years, when irrigation was limited, the leaf area index values were lower. Additionally, zinc application was found to be effective in the second year, and zinc-free plots had lower leaf area index values. Under full irrigation conditions, plants grew better, and the leaf area index was higher because they did not compete [46,52]. Ref. [52] stated that the most critical period for the leaf area index is between the pod-setting and grain-filling periods. When the plant is exposed to zinc deficiency, auxin deficiency in the plant causes defoliation [53].

SPAD values decreased under deficit irrigation conditions in this study. However, according to some researchers, drought stress changes the leaves' anatomy, so leaves become smaller and thicker, and the SPAD value increases due to concentrated chlorophyll pigments in smaller cells [54,55]. Maintaining the chlorophyll concentration under drought stress helps stabilize photosynthesis [56]. The decrease in the chlorophyll content is associated with an increased production of oxygen radicals in the cell. The authors of [57] reported that with the decrease in chlorophyll concentration, the green color of the leaves decreases, and premature senescence of the plant occurs. The lowest SPAD values were obtained from a local variety under deficit irrigation conditions. In SPAD measurements made during the grain-filling period under high temperature and water stress conditions, 35.48 values were obtained under control conditions, 36.84 under high-temperature stress conditions, and 22.38 under water stress conditions, and it was determined that the chlorophyll content of the leaves decreased significantly in cases of water scarcity. Readings of the chlorophyll content (SPAD) during the grain-filling period in soybeans were said to be the best way to figure out how water stress hurts the plant's ability to use nitrogen [58]. It has been reported that SPAD measurements made at grain filling showed a significant positive correlation in yield estimation [59].

It was observed that pod length, number of pods per plant, number of grains per pod, and 100 grain weight among yield components were affected by deficit irrigation. It was determined that the mean values of these traits decreased under deficit irrigation conditions. Cowpea is generally sensitive to drought during pod-set and grain-setting periods [10]. In terms of pod length and pod number, the zinc \times irrigation interaction was significantly effective in some years. Zinc applied under restricted irrigation conditions had a positive effect on these traits. Concerning the grain yield, irrigation and variety factors in the first year and irrigation \times zinc \times variety interaction in the second year were found to be significant.

Drought applied five weeks after sowing was found to cause a flower drop and significantly reduce the grain yield by 67% [60]. Under post-flowering drought stress, the grain yield and forage yield of cowpea grown in the field both dropped by 65% and 40%, respectively [61]. It was also found that drought applied during the vegetative and flowering stages reduced the leaf area and affected the grain quality [62]. Drought stress reduces biomass production in many crops, including cowpea, by reducing photosynthesis, stomatal conductance, transpiration, and plant water status [63]. Drought reduces biomass production in cowpea [63]. Drought stress caused a reduction in the leaf area in cultivars [64]. Under drought conditions, cowpea is most susceptible to yield loss during flowering and grain filling [65]. Yield loss occurs due to reduced assimilation by the grain due to the inhibition of photosynthesis by closing stomata (stomatal limitations) [66]. In the cowpea water deficit, a 44.3% yield loss was determined [66]. Some studies determined that the soil zinc application did not affect the grain zinc content, and different cowpea cultivars responded differently in the grain yields, Melo et al., 2017.

The grain yield decreased under deficit irrigation conditions in the first year, and the lowest yield was obtained from the local variety. The highest average yield was obtained from the Karagöz variety in both years. In both years, zinc application under restricted irrigation conditions positively affected the grain yield of the varieties. Previous studies have shown that crop loss is higher in zinc deficiency and deficit irrigation conditions [67]. Oxidative stress conditions of plants under stress conditions such as drought and deficit irrigation limit the agricultural productivity. The inability to fully reduce oxygen causes active oxygen species to appear in the environment. Their damage to cellular structures is called "oxidative stress." Active oxygen species resulting from oxidative stress have toxic effects and can cause crop losses. Under stressful circumstances, the plant's antioxidant defense mechanisms that normally reduce active oxygen species start to increase them.

The scavenging effect of zinc on active oxygen species plays a key role here [35,67]. An adequate zinc supply under restricted irrigation conditions may cause the important components of the plant's antioxidative defense system, which contains zinc, to tolerate these conditions effectively [35]. The average values of the second-year grain yield were observed to be lower than the first year. The fact that the average temperature values in the second year were higher than the long-term average and the average of the second year may have caused a decrease in crop loss. In cowpea, increases in night temperatures cause a 4–14% decrease in pod set and grain setting for each 0 °C above the threshold of 16 °C [68,69].

The measured quality traits—irrigation \times zinc \times variety interaction—significantly affected the protein ratio. It was observed that the protein ratio was negatively affected under restricted irrigation conditions. Protein synthesis may be suppressed in legumes under restricted irrigation conditions, and protein accumulation in legume grains may decrease when nitrogen breakdown and fixation are prevented under deficit water conditions [70]. Ref. [67] determined that zinc promoted seedling growth in durum wheat under drought conditions. In another study, the N, P, Fe, and Zn levels and, thus, the total protein content decreased with drought in bean seeds [71].

Protein quality decreased under high temperatures or poor irrigation conditions [72]. Genotypic factors and the environment are effective together in improving the grain's protein content. In this study, it was observed that the average protein values increased

with zinc application. Most proteins in biological systems require zinc in their structures. Foliar application of zinc fertilizer is a fast and effective method to increase the grain's zinc content [73]. In cereals, the grain's zinc concentration was found to be correlated with the grain's protein content [70–72]. Foliar zinc applications have been observed to increase protein synthesis [74].

Increasing the micronutrient elements in the grain is the first step to making these foods a richer food source for humans. Foliar zinc application, it was found that the grain's zinc content, which is one of its micronutrients, was significantly increased in both years. There are differences among crop species in the zinc uptake and tissue utilization efficiency [75]. In general, the zinc content of cereal grains is lower than that of legumes. For this reason, zinc deficiency may occur in cereal-based diets [76]. It is important to include legumes in the diet. Zinc application significantly affected the grain iron and phosphorus contents in the second year of the experiment. This study supports the importance of foliar zinc application in reducing yield loss and contributing toward bioavailability by increasing the grain's micronutrient concentration, especially under restricted irrigation conditions.

In this study, a total of 17 amino acids were measured. Among these, eight are essential; that is, the eight amino acids that our body needs to take from outside. These are histidine, threonine, valine, methionine, phenylalanine, isoleucine, lysine, and leucine. When the results, especially those related to the essential amino acids, were analyzed, leucine and threonine were significantly affected only by deficit irrigation. All other essential amino acids were significantly affected by zinc application. In general, cowpea is low in sulfur-containing amino acids, and their consumption with cereals will make up for this deficiency. The low level of methionine in cowpeas can be overcome with such a diet. The relatively higher lysine content in cowpea will also help compensate for the cereals' deficiency [77].

Among other amino acids, cysteine is known to favor zinc bioavailability. In this study, deficit irrigation had a significant effect on cysteine.

Iron and zinc have many biological functions. More than half of the iron in the human body is bound to hemoglobin, so the most obvious consequence of an iron deficiency is anemia. Zinc is a cofactor with various structural and catalytic functions in 10% of human proteins.

The bioavailability of iron and zinc in basic foods is low because of some complicated interactions. Some minerals are thought to be absorbed by humans at about 5% for iron and 25% for zinc [40]. Some amino acids, such as cysteine and histidine, can increase zinc absorption. For this reason, they are also called fortifiers [78].

Drought, spreading over an ever-expanding area and affecting an increasing number of countries, has become a factor limiting agricultural production. To solve this problem, different farming systems or crops with an unknown value should be used in new ways. This study shows that cowpea are a very valuable crop because they are naturally tolerant to drought and they can be grown with less water. They are also very nutritious and bioavailable.

5. Conclusions

When looking at the study results, it was found that limited irrigation had a significant effect on grain yield and the components of yield. In the first year of the study, there was a 40 percent decrease in yield with limited irrigation (382.9 kg da^{-1}) compared to full irrigation (235.0 kg da^{-1}). However, the application of zinc fertilizer was effective in the manage stress, and yield increases were observed in zinc-applied plots under limited irrigation conditions. The yield performances of the varieties showed differences depending on the genotype. Among the cultivars, Karagöz has the highest yield in both years. This was followed by Akkız and local varieties, respectively. Local varieties developed vegetatively better than the other varieties.

In the second year of the study, the amount of zinc, iron, and copper in the grain changed because of the foliar zinc application. Grain bioavailability enriches the product in

terms of nutrients; it is also possible to say that grain bioavailability may be affected by the amount of essential amino acids.

Author Contributions: Data curation, A.A.; Project administration, F.Ö.S. All authors have read and agreed to the published version of the manuscript.

Funding: The first year of the study was financed within the scope of the Adnan Menderes University scientific research projects (ZRF-20026) master thesis project by Abdullah AÇIK. The master thesis was written in the first year of the study.

Conflicts of Interest: The authors declare no conflict of interest.

References

1. FAO. Food and Agriculture Organization of the United Nations. Rome. 2018. Available online: <http://faostat.fao.org> (accessed on 20 October 2022).
2. Jain, C.; Saxena, R. Varietal differences against PEG induced drought stress in cowpea. *Octa J. Environ. Res.* **2016**, *4*, 58–62.
3. Eftekhari, A.; Baghizadeh, A.; Yaghoobi, M.M.; Abdolshahi, R. Differences in the drought stress response of DREB2 and CAT1 genes and evaluation of related physiological parameters in some bread wheat cultivars. *Biotechnol. Biotechnol. Equip.* **2017**, *31*, 709–716.
4. Carvalho, M.; Muñoz-Amatriaín, M.; Castro, I.; Lino-Neto, T.; Matos, M.; Egea-Cortines, M.; Carnide, V. Genetic diversity and structure of Iberian Peninsula cowpeas compared to world-wide cowpea accessions using high density SNP markers. *BMC Genom.* **2017**, *18*, 891. [CrossRef] [PubMed]
5. Carvalho, M.; Muñoz-Amatriaín, M.; Castro, I.; Lino-Neto, T.; Matos, M.; Egea-Cortines, M.; Carnide, V. Response of water deficit-stressed *Vigna unguiculata* performances to silicon, proline or methionine foliar application. *Sci. Hort.* **2018**, *228*, 132–144.
6. Hayatu, M.; Muhammad, S.; Abdu, H.U. Effect of water stress on the leaf relative water content and yield of some cowpea (*Vigna unguiculata* (L) Walp.) genotype. *Int. J. Sci. Technol. Res.* **2014**, *3*, 148–152.
7. Toscano, S.; Farieri, E.; Ferrante, A.; Romano, D. Physiological and biochemical responses in two ornamental shrubs to drought stress. *Front. Plant Sci.* **2016**, *7*, 645. [CrossRef]
8. Kutama, A.S.; Hayatu, M.; Raliat, T.M.; Binta, U.B.; Abdullahi, I.K. Screening for some physiological mechanisms in some drought tolerant genotypes of cowpea (*Vigna unguiculata* (L.) Walp.). *Stand. Res. J. Agric. Sci.* **2014**, *2*, 59–64.
9. Agbicodo, E.M.; Fatokun, C.A.; Muranaka, S.; Visser, R.G.; Linden Van Der, C.G. Breeding drought tolerant cowpea: Constraints, accomplishments, and future prospects. *Euphytica* **2009**, *167*, 353–370. [CrossRef]
10. Turk, K.J.; Hall, A.E.; Asbell, C. Drought adaptation of cowpea. I. Influence of drought on seed yield 1. *Agron. J.* **1980**, *72*, 413–420. [CrossRef]
11. Timko, M.P.; Ehlers, J.D.; Roberts, P.A. Cowpea. In *Pulses, Sugar and Tuber Crops*; Springer: Berlin/Heidelberg, Germany, 2007; pp. 49–67.
12. Kröner, N.; Kotlarski, S.; Fischer, E.; Lüthi, D.; Zubler, E.; Schär, C. Separating climate change signals into thermodynamic, lapse-rate and circulation effects: Theory and application to the European summer climate. *Clim. Dyn.* **2017**, *48*, 3425–3440. [CrossRef]
13. Shackel, K.A.; Hall, A.E. Comparison of water relations and osmotic adjustment in sorghum and cowpea under field conditions. *Funct. Plant Biol.* **1983**, *10*, 423–435. [CrossRef]
14. Lionello, P.; Scarascia, L. The relation of climate extremes with global warming in the Mediterranean region and its north versus south contrast. *Reg. Environ. Chang.* **2020**, *20*, 31. [CrossRef]
15. Raza, A.; Razaq, A.; Mehmood, S.S.; Zou, X.; Zhang, X.; Lv, Y.; Xu, J. Impact of climate change on crops adaptation and strategies to tackle its outcome: A review. *Plants* **2019**, *8*, 34. [CrossRef]
16. Farré, I.; Faci, J.-M. Deficit irrigation in maize for reducing agricultural water use in a Mediterranean environment. *Agric. Water Manag.* **2009**, *96*, 383–394. [CrossRef]
17. Streeter, J. Effects of drought on nitrogen fixation in soybean root nodules. *Plant Cell Environ.* **2003**, *26*, 1199–1204. [CrossRef]
18. Hu, M.; Wiatrak, P. Effect of planting date on soybean growth, yield, and grain quality. *Agron. J.* **2012**, *104*, 785–790. [CrossRef]
19. He, J.; Du, Y.L.; Wang, T.; Turner, N.C.; Yang, R.P.; Jin, Y.; Li, F.M. Conserved water use improves the yield performance of soybean (*Glycine max* (L.) Merr.) under drought. *Agric. Water Manag.* **2017**, *179*, 236–245. [CrossRef]
20. Ehlers, J.; Hall, A. Cowpea (*Vigna unguiculata* L. walp.). *Field Crops Res.* **1997**, *53*, 187–204. [CrossRef]
21. Condon, A.; Hall, A. Adaptation to diverse environments: Variation in water-use efficiency within crop species. In *Agricultural Ecology*; Jackson, L.E., Ed.; Academic Press: San Diego, CA, USA, 1997; pp. 79–116. [CrossRef]
22. Tan, H.; Tie, M.; Luo, Q.; Zhu, Y.; Lai, J.; Li, H. A review of molecular markers applied in cowpea (*Vigna unguiculata* L. Walp.) breeding. *J. Life Sci.* **2012**, *6*, 1190.
23. Boukar, O.; Fatokun, C.A.; Roberts, A.; Abberton, M.; Huynh, B.L.; Close, T.J.; Ehlers, J.D. Cowpea. *Grain Legum.* **2015**, *10*, 219–250. [CrossRef]
24. Ravelombola, W.S.; Shi, A.; Weng, Y.; Clark, J.; Motes, D.; Chen, P.; Srivastava, V. Evaluation of salt tolerance at germination stage in cowpea [*Vigna unguiculata* (L.) Walp.]. *HortScience* **2017**, *52*, 1168–1176. [CrossRef]

25. Timko, M.P.; Singh, B. Cowpea, a multifunctional legume. In *Genomics of Tropical Crop Plants*; Springer: Berlin/Heidelberg, Germany, 2008; pp. 227–258.
26. Frota, K.M.G.; Mendonça, S.; Saldiva, H.N.; Cruz, R.J.; Arêas, J.A.G. Cholesterol-lowering properties of whole cowpea seed and its protein isolate in hamsters. *J. Food Sci.* **2008**, *73*, 235–240. [CrossRef] [PubMed]
27. Brown, K.H.; Rivera, J.A.; Bhutta, Z.; Gibson, R.S.; King, J.C.; Lönnerdal, B. International Zinc Nutrition Consultative Group (IZiNCG) technical document# 1. Assessment of the risk of zinc deficiency in populations and options for its control. *Food Nutr. Bull.* **2004**, *25* (Suppl. 2), S99–S203. [PubMed]
28. Cakmak, I. Enrichment of cereal grains with zinc: Agronomic or genetic biofortification? *Plant Soil* **2008**, *302*, 1–17. [CrossRef]
29. Joy, E.J.; Stein, A.J.; Young, S.D.; Ander, E.L.; Watts, M.J.; Broadley, M.R. Zinc-enriched fertilisers as a potential public health intervention in Africa. *Plant Soil* **2015**, *389*, 1–24. [CrossRef]
30. Wang, B.; Abdalla, E.; Atrio-Barandela, F.; Pavon, D. Dark matter and dark energy interactions: Theoretical challenges, cosmological implications and observational signatures. *Rep. Prog. Phys.* **2016**, *79*, 096901. [CrossRef]
31. White, P.J.; Broadley, M.R. Biofortification of crops with seven mineral elements often lacking in human diets—iron, zinc, copper, calcium, magnesium, selenium and iodine. *New Phytol.* **2009**, *182*, 49–84. [CrossRef]
32. Cakmak, I.; Kalayci, M.; Kaya, Y.; Torun, A.A.; Aydin, N.; Wang, Y.; Horst, W.J. Biofortification and localization of zinc in wheat grain. *J. Agric. Food Chem.* **2010**, *58*, 9092–9102. [CrossRef]
33. Welch, R.M.; Graham, R.D. Breeding for micronutrients in staple food crops from a human nutrition perspective. *J. Exp. Bot.* **2004**, *55*, 353–364. [CrossRef]
34. Zou, C.Q.; Zhang, Y.Q.; Rashid, A.; Ram, H.; Savasli, E.; Arisoy, R.Z.; Cakmak, I. Biofortification of wheat with zinc through zinc fertilization in seven countries. *Plant Soil* **2012**, *361*, 119–130. [CrossRef]
35. Cakmak, I. Tansley Review No. 111 Possible roles of zinc in protecting plant cells from damage by reactive oxygen species. *New Phytol.* **2000**, *146*, 185–205. [CrossRef]
36. Goodman, B.A.; Newton, A.C. Effects of drought stress and its sudden relief on free radical processes in barley. *J. Sci. Food Agric.* **2005**, *85*, 47–53. [CrossRef]
37. Marschner, H.; Cakmak, I. High light intensity enhances chlorosis and necrosis in leaves of zinc, potassium, and magnesium deficient bean (*Phaseolus vulgaris*) plants. *J. Plant. Physiol.* **1989**, *134*, 308–315. [CrossRef]
38. White, P.J.; Broadley, M.R. Biofortifying crops with essential mineral elements. *Trends Plant Sci.* **2005**, *10*, 586–593. [CrossRef]
39. Kumssa, D.B.; Joy, E.J.; Ander, E.L.; Watts, M.J.; Young, S.D.; Walker, S.; Broadley, M.R. Dietary calcium and zinc deficiency risks are decreasing but remain prevalent. *Sci. Rep.* **2015**, *5*, 10974. [CrossRef]
40. Bouis, H.E.; Welch, R.M. Biofortification—A sustainable agricultural strategy for reducing micronutrient malnutrition in the global south. *Crop Sci.* **2010**, *50*, S-20–S-32. [CrossRef]
41. Lividini, K.; Fiedler, J.L.; De Moura, F.F.; Moursi, M.; Zeller, M. Biofortification: A review of ex-ante models. *Glob. Food Secur.* **2018**, *17*, 186–195. [CrossRef]
42. Kumar, S.; Pandey, G. Biofortification of pulses and legumes to enhance nutrition. *Heliyon* **2020**, *6*, 03682. [CrossRef]
43. Moura, J.D.O.; Rocha, M.D.M.; Gomes, R.L.F.; Freire Filho, F.R.; Damasceno e Silva, K.J.; Ribeiro, V.Q. Path analysis of iron and zinc contents and others traits in cowpea. *Crop Breed. Appl. Biotechnol.* **2012**, *12*, 245–252. [CrossRef]
44. Liu, R.; Lal, R. Potentials of engineered nanoparticles as fertilizers for increasing agronomic productions. *Sci. Total Environ.* **2015**, *514*, 131–139. [CrossRef]
45. Noroozlo, Y.A.; Souri, M.K.; Delshad, M. Stimulation effects of foliar applied glycine and glutamine amino acids on lettuce growth. *Open Agric.* **2019**, *4*, 164–172. [CrossRef]
46. Vaghar, M.S.; Sayfzadeh, S.; Zakerin, H.R.; Kobraee, S.; Valadabadi, S.A. Foliar application of iron, zinc, and manganese nano-chelates improves physiological indicators and soybean yield under water deficit stress. *J. Plant Nutr.* **2020**, *43*, 2740–2756. [CrossRef]
47. Alloway, B.J. *Zinc in Soils and Crop Nutrition*; International Zinc Association: Brussels, Belgium; International Fertilizer Industry Association: Paris, France, 2008.
48. Kanber, R. Irrigation of first and second crop groundnut using open water surface evaporation under Çukurova conditions. *Reg. Soil Water Res. Inst. Publ.* **1984**, *114*, 64.
49. Efetha, A.; Harms, T.; Bandara, M. Irrigation management practices for maximizing seed yield and water use efficiency of Othello dry bean (*Phaseolus vulgaris* L.) in southern Alberta, Canada. *Irrig. Sci.* **2011**, *29*, 103–113. [CrossRef]
50. Gislum, R.; Micklander, E.; Nielsen, J. Quantification of nitrogen concentration in perennial ryegrass and red fescue using near-infrared reflectance spectroscopy (NIRS) and chemometrics. *Field Crops Res.* **2004**, *88*, 269–277. [CrossRef]
51. Cakmak, I.; Sari, N.; Marschner, H.; Kalayci, M.; Yilmaz, A.; Eker, S.; Gülüt, K.Y. Dry matter production and distribution of zinc in bread and durum wheat genotypes differing in zinc efficiency. *Plant Soil* **1996**, *180*, 173–181. [CrossRef]
52. Liu, X.; Jin, J.; Wang, G.; Herbert, S.J. Soybean yield physiology and development of high-yielding practices in Northeast China. *Field Crops Res.* **2008**, *105*, 157–171. [CrossRef]
53. Lacerda, J.S.; Martinez, H.E.; Pedrosa, A.W.; Clemente, J.M.; Santos, R.H.; Oliveira, G.L.; Jifon, J.L. Importance of zinc for arabica coffee and its effects on the chemical composition of raw grain and beverage quality. *Crop Sci.* **2018**, *58*, 1360–1370. [CrossRef]
54. Souri, M.K.; Hatamian, M. Aminochelates in plant nutrition: A review. *J. Plant Nutr.* **2019**, *42*, 67–78. [CrossRef]

55. Souri, M.K.; Sooraki, F.Y. Benefits of organic fertilizers spray on growth quality of chili pepper seedlings under cool temperature. *J. Plant Nutr.* **2019**, *42*, 650–656. [CrossRef]
56. Movahhedy-Dehnavy, M.; Modarres-Sanavy, S.A.M.; Mokhtassi-Bidgoli, A. Foliar application of zinc and manganese improves seed yield and quality of safflower (*Carthamus tinctorius* L.) grown under water deficit stress. *Ind. Crops Prod.* **2009**, *30*, 82–92. [CrossRef]
57. Zahra, Z.; Arshad, M.; Rafique, R.; Mahmood, A.; Habib, A.; Qazi, I.A.; Khan, S.A. Metallic nanoparticle (TiO₂ and Fe₃O₄) application modifies rhizosphere phosphorus availability and uptake by *Lactuca sativa*. *J. Agric. Food Chem.* **2015**, *63*, 6876–6882. [CrossRef]
58. Ahmed, S.U.; Senge, M.; Ito, K.; Adomako, J.T. Effects of water stress on soil plant analytical development (SPAD) chlorophyll meter reading and its relationship to nitrogen status and grain yield of soybean under different soil types. *J. Rainwater Catchment Syst.* **2010**, *15*, 33–38. [CrossRef]
59. Ergo, V.V.; Lascano, R.; Vega, C.R.; Parola, R.; Carrera, C.S.; Ergo, V.V. Heat and water stressed field-grown soybean: A multivariate study on the relationship between physiological-biochemical traits and yield. *Environ. Exp. Bot.* **2018**, *148*, 1–11. [CrossRef]
60. Fatokun, C.A.; Boukar, O.; Muranaka, S. Evaluation of cowpea (*Vigna unguiculata* (L.) Walp.) germplasm lines for tolerance to drought. *Plant Genet. Resour.* **2012**, *10*, 171–176. [CrossRef]
61. Belko, N.; Zaman-Allah, M.; Cisse, N.; Diop, N.N.; Zombre, G.; Ehlers, J.D.; Vadez, V. Lower soil moisture threshold for transpiration decline under water deficit correlates with lower canopy conductance and higher transpiration efficiency in drought-tolerant cowpea. *Funct. Plant Biol.* **2012**, *39*, 306–322. [CrossRef]
62. Hamidou, F.; Zombre, G.; Diouf, O.; Diop, N.N.; Guinko, S.; Braconnier, S. Physiological, biochemical and agromorphological responses of five cowpea genotypes (*Vigna unguiculata* (L.) Walp.) to water deficit under glasshouse conditions. *Biotechnol. Agron. Société Environ.* **2007**, *11*, 225–234.
63. Daryanto, S.; Wang, L.; Jacinthe, P.-A. Global synthesis of drought effects on cereal, legume, tuber and root crops production: A review. *Agric. Water Manag.* **2017**, *179*, 18–33. [CrossRef]
64. Tankari, M.; Wang, C.; Ma, H.; Li, X.; Li, L.; Sothar, R.K.; Wang, Y. Drought priming improved water status, photosynthesis and water productivity of cowpea during post-anthesis drought stress. *Agric. Water Manag.* **2021**, *245*, 106565. [CrossRef]
65. Hamidou, F.; Zombre, G.; Braconnier, S. Physiological and biochemical responses of cowpea genotypes to water stress under glasshouse and field conditions. *J. Agron. Crop Sci.* **2007**, *193*, 229–237. [CrossRef]
66. Daryanto, S.; Wang, L.; Jacinthe, P.-A. Global synthesis of drought effects on food legume production. *PLoS ONE* **2015**, *10*, e0127401. [CrossRef] [PubMed]
67. Candan, N.; Cakmak, I.; Ozturk, L. Zinc-biofortified seeds improved seedling growth under zinc deficiency and drought stress in durum wheat. *J. Plant Nutr. Soil Sci.* **2018**, *181*, 388–395. [CrossRef]
68. Hall, A.; Mutters, R.; Farquhar, G. Genotypic and drought-induced differences in carbon isotope discrimination and gas exchange of cowpea. *Crop Sci.* **1992**, *32*, 1–6. [CrossRef]
69. Hall, A.E.; Ismail, A.M.; Ehlers, J.D.; Marfo, K.O.; Cisse, N.; Thiaw, S.; Close, T.J. Breeding cowpea for tolerance to temperature extremes and adaptation to drought. In *Challenges and Opportunities for Enhancing Sustainable Cowpea Production*; International Institute of Tropical Agriculture: Ibadan, Nigeria, 2002; pp. 14–21.
70. Zhao, Y.; Takenaka, M.; Takagi, S. Comprehensive understanding of coulomb scattering mobility in biaxially strained-Si pMOSFETs. *IEEE Trans. Electron Devices* **2009**, *56*, 1152–1156. [CrossRef]
71. Cakmak, I. Biofortification of cereals with zinc and iron through fertilization strategy. In Proceedings of the 19th World Congress of Soil Science, Washington, DC, USA, 1–6 August 2010; CiteSeerX: Princeton, NJ, USA, 2010; pp. 329–346.
72. Guttieri, M.J.; McLean, R.; Stark, J.C.; Souza, E. Managing irrigation and nitrogen fertility of hard spring wheats for optimum bread and noodle quality. *Crop Sci.* **2005**, *45*, 2049–2059. [CrossRef]
73. Cakmak, I.; Hoffland, E. Zinc for the improvement of crop production and human health. *Plant Soil* **2012**, *361*, 1–2. [CrossRef]
74. Salih, H.O. Effect of Foliar Fertilization of Fe, B and Zn on nutrient concentration and seed protein of Cowpea "*Vigna unguiculata*". *J. Agric. Vet. Sci.* **2013**, *6*, 42–46. [CrossRef]
75. Cakmak, I. Plant nutrition research: Priorities to meet human needs for food in sustainable ways. *Plant Soil* **2002**, *247*, 3–24. [CrossRef]
76. Graham, A.; McDonald, G. Effect of zinc on photosynthesis and yield of wheat under heat stress. In Proceedings of the 10th Australian Agronomy Conference, Hobart, Australia, 29 January–1 February 2001.
77. Farinu, G.O.; Ingrao, G. Gross composition, amino acid, phytic acid and trace element contents of thirteen cowpea cultivars and their nutritional significance. *J. Sci. Food Agric.* **1991**, *55*, 401–410. [CrossRef]
78. Shahzad, Z.; Rouached, H.; Rakha, A. Combating mineral malnutrition through iron and zinc biofortification of cereals. *Compr. Rev. Food Sci. Food Saf.* **2014**, *13*, 329–346. [CrossRef]

Disclaimer/Publisher’s Note: The statements, opinions and data contained in all publications are solely those of the individual author(s) and contributor(s) and not of MDPI and/or the editor(s). MDPI and/or the editor(s) disclaim responsibility for any injury to people or property resulting from any ideas, methods, instructions or products referred to in the content.

Article

Response of Potted Citrus Trees Subjected to Water Deficit Irrigation with the Application of Superabsorbent Polyacrylamide Polymers

Daniela Cea, Claudia Bonomelli , Johanna Mártiz  and Pilar M. Gil * 

Departamento de Fruticultura y Enología, Facultad de Agronomía e Ingeniería Forestal, Pontificia Universidad Católica de Chile, Vicuña Mackenna 4860, Macul, Santiago 7820436, Chile; dfcea@uc.cl (D.C.); cbonomel@uc.cl (C.B.); jmartiz@uc.cl (J.M.)

* Correspondence: pmgil@uc.cl

Abstract: Searching for new strategies to mitigate the effects of low water availability for citrus production, a study was carried out on potted mandarin cv. W. Murcott, with the objective of evaluating the physiological and growth response of the plants to polyacrylamide gel application in the substrate in water restriction conditions. The following treatments were evaluated, T0 (control) with 100% ETc water replenishment, T1 with 50% ETc water replenishment, and T2 with 50% ETc water replenishment plus the application of polyacrylamide polymers to the substrate. Temperature and water volumetric content (θ : $\text{m}^3 \text{m}^{-3}$) were evaluated in the substrate. Plant water-status parameters such as stem water potential (SWP), stomatal conductance (gs), and chlorophyll fluorescence (Fv/Fm), as well as biomass, nutrients levels, and proline biosynthesis were measured in the plants in response to the treatments. The results showed that the substrate moisture for T2 was kept significantly higher than T0 and T1, despite receiving the same irrigation rate as T1 and a half of T0; however, this higher moisture availability in the substrate of T2 was not reflected in the plant's water status or growth. On the contrary, the T2 plants showed responses such as lower total biomass, lower vegetative development, and lower root biomass, as well as a higher concentration of proline in the root. According to these results, it is concluded that polymers such as polyacrylamide sodium allow the retention of water in the substrate, but do not necessarily release that water for plants, probably because that moisture is kept in the hydrogel and not released to the substrate media or the roots, or if released, in this case, this occurs with an increase in the concentration of sodium available to the plants, which could lead the citrus crop to a worse situation of water and/or osmotic stress.



Citation: Cea, D.; Bonomelli, C.; Mártiz, J.; Gil, P.M. Response of Potted Citrus Trees Subjected to Water Deficit Irrigation with the Application of Superabsorbent Polyacrylamide Polymers. *Agronomy* **2022**, *12*, 1546. <https://doi.org/10.3390/agronomy12071546>

Academic Editor:
Aliasghar Montazar

Received: 3 May 2022
Accepted: 24 June 2022
Published: 28 June 2022

Publisher's Note: MDPI stays neutral with regard to jurisdictional claims in published maps and institutional affiliations.



Copyright: © 2022 by the authors. Licensee MDPI, Basel, Switzerland. This article is an open access article distributed under the terms and conditions of the Creative Commons Attribution (CC BY) license (<https://creativecommons.org/licenses/by/4.0/>).

Keywords: hydrogel; irrigation deficit; mandarin; proline

1. Introduction

Drought is one of the major limiting factors for crop yields and causes important economic losses to the farmers. There is a constant search for tools to allow efficiency in the use of available water resources, save water, and increase crop productivity per unit of water used [1]. Climate change is threatening fruit production in several countries, mostly in Mediterranean countries where irrigation is necessary for agricultural production [1]. Under this context, several techniques and/or technologies have been evaluated in soil and/or plants in searching for strategies to deal with conditions of water shortage, without significantly affecting the yield and quality of fruit production.

In response to water stress, some tree species have a series of morphophysiological and physiological mechanisms that allow crop development despite stress conditions [2]. In citrus species, some forms of tolerance to water stress are based on increasing tissue elasticity, stomatal regulation [3], an adequate architecture of the canopy [4], and the adaptability of the rootstock [5]. Citrus rootstocks have different responses to water

stress, using different physiological strategies such as hydraulic redistribution, osmotic adjustment, and adjustment in stomatal opening [5].

Additionally, several authors have observed that under water-stress conditions, osmotic adjustment is a habitual physiological response in different plant species, whose mechanism consists in synthesizing osmoprotective substances such as proline [2]. In citrus, the osmotic adjustment occurs mainly in the root, finding accumulated inorganic solutes, such as soluble sugars, and organic solutes such as proline and glycine betaine [5].

Among the techniques and/or technologies used for increasing water productivity in citrus we can point out the use of biostimulants, irrigation strategies for reducing the applied water, and physical barriers for reducing crop evapotranspiration. In the case of biostimulant application, products are mainly foliar-applied and have a diverse origin, usually coming from different organic sources, such as seaweed extract [6,7]. These applications can increase the vigor of plants and increase the capacity to tolerate stresses with better use of water resources [6].

Irrigation strategies such as controlled deficit irrigation (CDI) and partial rootzone drying (PRD) have been evaluated in citrus, and in both cases, the results showed water saving but a significant decrease in yield and fruit quality [8]. In terms of the use of physical barriers to prevent water evapotranspiration, an example is the use of organic or plastic mulch over the soil to reduce water evaporation. In Eureka Lemon, the use of black polyethylene mulch showed a significant increase in soil moisture, improving plant growth and yield [9].

Some of the above-mentioned technologies and/or techniques have been demonstrated to significantly reduce crop water consumption. However, they involve high investments, and in some cases, negative effects on the production and/or fruit quality. Considering that in the fruit industry water saving without causing water stress in the crop is a big concern, other tools are continuously being sought. A tool of growing interest in agriculture to be used as a water-saving tool has been the use of water-retaining polymers called hydrogels, which have been reported by some authors as a clean and efficient alternative for retaining water in soil or substrate [10,11].

Hydrogels, hydro-retainers, or super-absorbent gels are hydrophilic acrylamide-based polymers with a three-dimensional structure, generally made up of long-chain, high-molecular-weight organic molecules, linked by cross-links between the chains [12]. Polyacrylamides have the property of being highly absorbent, with a storage capacity ranging from 400 to 1500 g of water per gram of product, which improves the absorption and retention capacity of water in the soil without affecting its availability to plants [13,14]. The authors of [10] observed that the highest percentage of water absorption by potassium polyacrylamide was in soils with a sandy texture, while the authors of [12], evaluated the effectiveness of sodium polyacrylate in soil water retention, concluding that it improved the water-retention capacity of different soil textures, promoting greater efficiency in the use of both irrigation and rainfall water by reducing percolation losses. On the other hand, acrylamide is considered a toxic element, and therefore it could contaminate soil, water, and food [15]. Another long-term negative effect of these gels is by altering the physiological activities of the plants through both the toxic effect of acrylamide and a physical negative effect in soil, clogging of pores due to their high viscosity and molecular weight [15].

Although the use of polyacrylamide-based water-retaining gels has been incorporated into crop management for several species, there is little information regarding their effect on water retention by soils or substrates and the effect on the physiology of agricultural species such as citrus. Considering that hydrogels could be an alternative tool for water saving in citrus orchards, in this study, the use of polyacrylamide gels in mandarin *W. Murcott* under pot conditions was evaluated, to determine their effect on plant water status, biomass, and nutritional effects when applied in water-restriction conditions.

2. Materials and Methods

2.1. Experimental Setup

The experiment was conducted under climate-controlled greenhouse conditions (the daily temperature fluctuated between 15 and 32 °C with a relative humidity between 65 and 75%), at the Facultad de Agronomía e Ingeniería Forestal, Central Zone of Chile (34°07'55" S and 70°43'15" W).

The plant material was a 2-year-old Tangor (*Citrus sinensis* × *Citrus reticulata*), cv. W. Murcott, grafted on clonal rootstock C35 Citrange, which was established individually in plastic containers of 20 L, containing compost as substrate. The substrate chemical characteristics were as follows: 20% organic matter content (Walkley–Black method); pH 7.2 (soil: water, 1:2.5); 45 mg kg⁻¹ P (Olsen method); 258 mg kg⁻¹ exchangeable K (ammonium acetate method); and adequate secondaries macronutrient and micronutrients. To keep similar evapotranspiration between treatments, a pruning was performed to homogenize the leaf area in a range of 1291 and 1306 cm².

The polymer used for this experiment was a sodium anionic polyacrylamide, with a pH of 8.2, and a sodium and HCO₃ content that corresponds to the copolymerization of acrylamide with sodium acrylate.

2.2. Experimental Design

The trial was conducted with a completely randomized design, with three treatments and four replications. The experimental unit was a potted plant. Treatments were applied as follows: Control (T0): irrigation with 100% of water replenishment according to crop evapotranspiration (ETc). ETc was calculated from the water-balance equation: $I + PP = ETc + Pc + \Delta\theta v$, in which I was irrigation (mm), PP was precipitation (mm), Pc was percolation (mm), and $\Delta\theta v$ corresponds to the difference of the volumetric soil moisture estimated through the daily weights of the pots. Treatment 1 (T1): 50% of water replenishment concerning Control. Treatment 2 (T2): 50% of water replenishment concerning Control plus the application of polyacrylamide polymers mixed in the substrate. To mix the polymer with the substrate, 40 g of polymer was hydrated in four liters of distilled water for one hour. This was then mixed with the substrate according to the protocol recommended by the manufacturer.

At the beginning of the experiment, all the plants were irrigated with the same amount of water until pot capacity was reached (−1 KPa of soil water tension). The frequency of irrigation varied according to the daily evapotranspiration of the control treatment, maintaining the water content of the T0 substrate near the pot capacity. To keep T0 at pot capacity, the irrigation moment was determined according to the matric potential measured with a tensiometer; when soil matric potential in T1 showed less than −1 KPa, irrigation was performed by replenishing the water volume according to the treatment. Water replenishment in the treatments was applied by keeping the same time and frequency of irrigation but using different flow drippers: 4 L/h for T0 and 2 L/h for T1 and T2. The total water volume applied for each plant during the study period was 24,6 L for T0, whereas, for T1 and T2, 12,3 L was applied.

2.3. Measurements

To know the atmospheric water demand, the vapor pressure deficit (VPD) was registered. VPD was determined by the equation: $VPD = 0.61078 \exp [(17.269 \times T)/(T + 237.3)] \times (1 - HR/100)$. Temperature (°C) and relative humidity HR (%) were recorded every 15 min with a Hobo Pro V2 Logger sensor.

2.3.1. Substrate Temperature

The substrate temperature was evaluated every 15 days. This measurement was made at a depth of 15 cm, with a thermometer RTD Thermometer, model 505 (CHY, Taiwan).

2.3.2. Soil Water Content

The soil volumetric water content (θ) (substrate in this case) was measured in all the potted plants at a depth of 20 cm every 7 days using a portable Frequency Domain Reflectometry (FDR) sensor (GS-1, Decagon Devices Inc., Pullman WA 00163, USA), whose equation to estimate θ in substrate is: $\theta = 4.33 \times 10^{-4} \times \text{RAW} - 0.611$, where RAW is the readily available water calculated from raw dielectric permittivity values that the device measures, with the Topp equation [16]. Prior to the measurement, the real θ of the substrate was obtained from the gravimetric method [17] and substrate bulk density [18]. With real θ values and estimated θ obtained from eight in situ measurements, a calibration curve was performed.

2.3.3. Plant Water Status Measurements

Midday stem water potential (SWP) was measured using the method described by the authors of [19]. Midday SWP was measured monthly in one shoot per plant between 11:00 and 15:00 h. Before each SWP measurement, the shoot was enclosed in a plastic bag covered with aluminum foil for 30 min. The shoot was then excised and SWP was measured with a Scholander pressure chamber.

Leaf relative water content (RWC) was measured between 11:00 and 15:00 h every 30 days according to [20].

2.3.4. Physiological Parameters

Chlorophyll fluorescence (F_v/F_m) was measured as described by the authors of [21] using a chlorophyll fluorometer (Pocket PEA, Hansatech, Norfolk, UK) and stomatal conductance (g_s) was evaluated with a Leaf porometer SC-1 (Decagon Devices Inc, Pullman, WA 00163, USA). Measurements were made every 30 days between 11:00 and 15:00 h.

2.3.5. Growth and Biomass of Plants

At the end of the experiment, the plants were harvested and separated into leaves, shoots, and roots. Fresh weight (FW) was recorded for each plant tissue. Vegetal samples from leaves, shoots, and roots were taken and oven-dried at 65 °C to obtain a constant weight, obtaining dry matter content.

2.3.6. Nutrition and Metabolites Analysis

Since drought reduces the absorption and transport of nutrients from the roots to shoots, each plant tissue was nutritionally analyzed for nitrogen (N), phosphorous (P), potassium (K), calcium (Ca), magnesium (Mg), and sodium (Na).

Dry samples were subsequently ground and analyzed to determine the total N concentration using a LECO CNS-2000 Macro Elemental Analyzer (Leco, MI, USA) in the Analytical Laboratory of the Pontificia Universidad Católica de Chile.

For Ca, K, Mg, P, and Na, ashed tissue samples were then dissolved in HCl (2 M), and concentrations were determined by inductively coupled plasma–optical emission spectroscopy (ICP–OES) (Agilent 720 ES axial—Varian, Victoria, Australia).

Additionally, the root proline concentration was analyzed as an indicator of water stress, through the protocol described by the authors of [22].

2.3.7. Statistical Analysis

Data analysis was undertaken by one-way analysis of variance (ANOVA) and Tukey's studentized range test at $p \leq 0.05$, by using SAS statistical software (SAS Institute, Cary, NC, USA).

3. Results

3.1. Substrate and Plant Water Status

The substrate temperature ranged from 15.2 to 20.3 °C during the study period, without differences between treatments (data not shown). On the other hand, the moisture

content θ ($\text{m}^3 \text{m}^{-3}$) in the substrate showed significant differences between treatments. From May to September, the θ ($\text{m}^3 \text{m}^{-3}$) of T2 was significantly higher than T0 and T1, despite receiving the same amount of water as T1 and 50% less water than T0 (Figure 1). During October and November, θ values for T2 were similar to T0 and significantly higher than T1. It should be noted that the calibration curve between the real and estimated moisture values gave a linear direct relationship, with an R^2 of 0.93 with an equation that expresses the following: $\text{FDR } \theta = 2.4516 \times \text{Real } \theta - 1.64$ (data not shown).

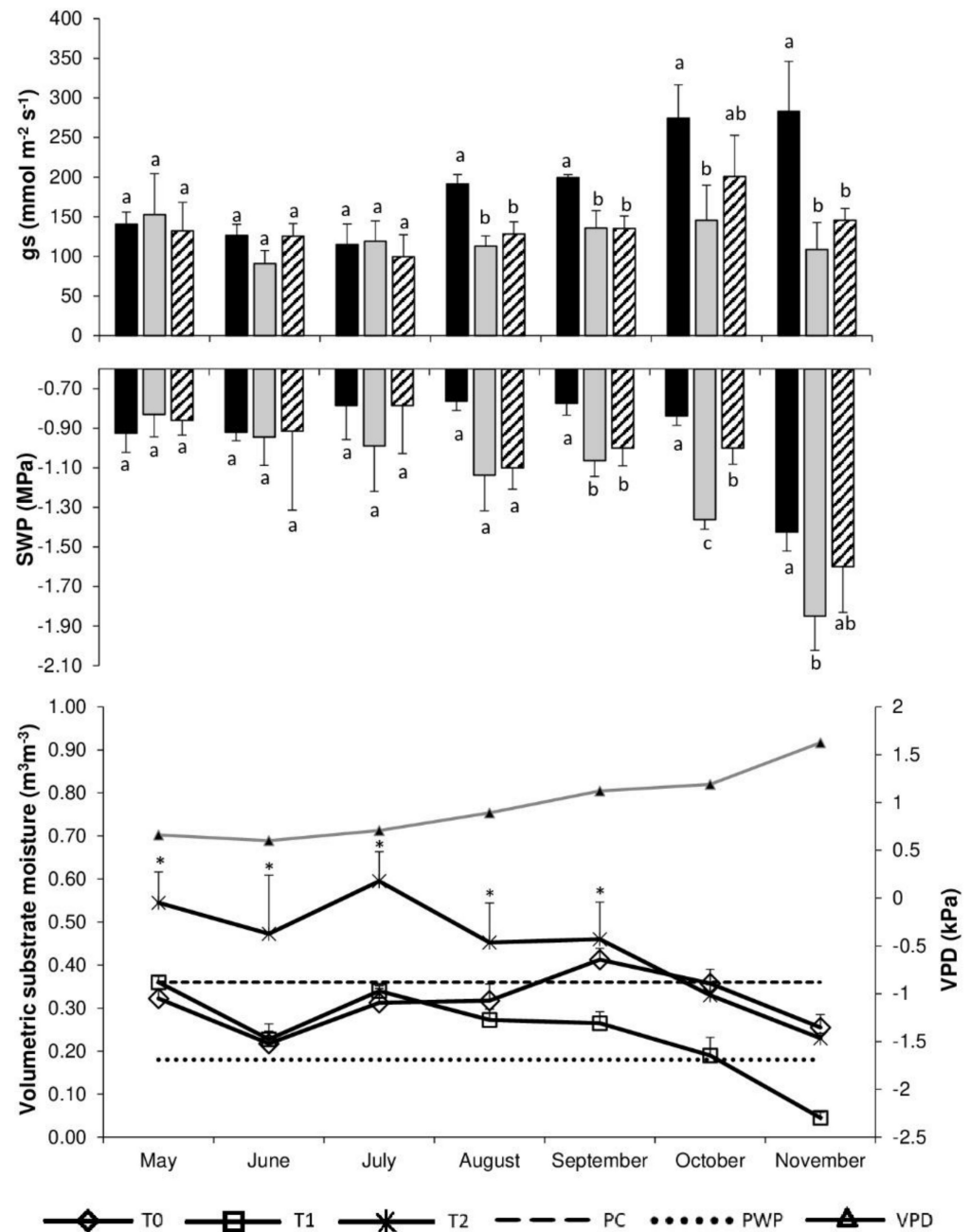


Figure 1. Stem-water potential (SWP), stomatal conductance (gs), and substrate moisture response to treatments: T0 (Control, 100% E_{Tc} water replenishment), T1 (50% of E_{Tc} water replenishment), and T2 (50% of E_{Tc} water replenishment + hydrogel). PC (pot capacity), PWP (permanent wilting point), and VPD (vapor pressure deficit). Different letters or asterisks indicate statistical differences ($p \leq 0.05$, Tukey test).

The difference in moisture content θ ($m^3 m^{-3}$) in the substrate between treatments was not reflected in physiological parameters during the first 3 months. No significant differences in g_s and SWP were observed between the treatments during May, June, and July (autumn and winter months). On the contrary, from August (the end of the winter season in SH), it was possible to observe a negative effect of treatments T1 and T2 (50% water restriction) on the physiological response of the citrus plants, both in g_s and SWP. In the case of fluorescence (F_v/F_m) and leaf RWC, plants did not show significant differences between the treatments (data not shown).

3.2. Growth and Biomass of Plants

The total biomass and shoot biomass of T0 plants were higher than the biomass of the T1 and T2 treatments. For roots and leaf biomass, no statistical differences were observed (Figure 2).

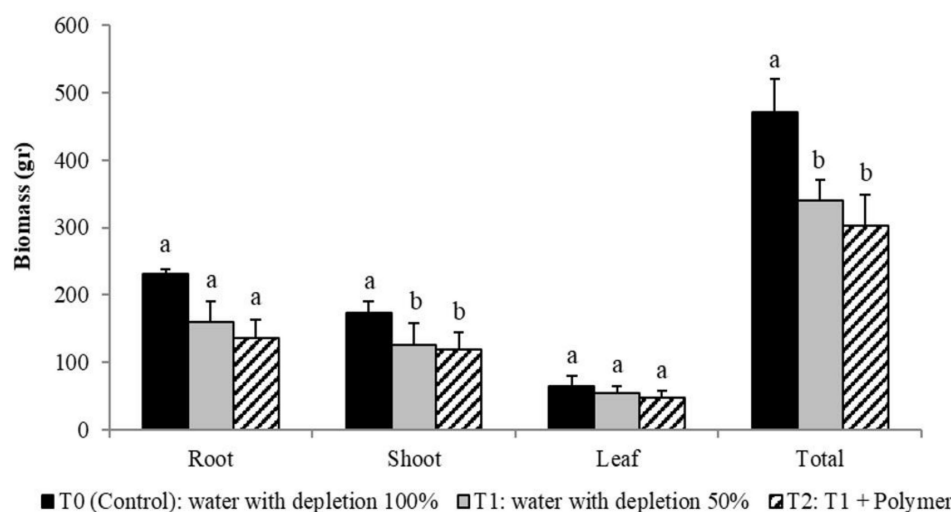


Figure 2. Total root, shoot, and leaf final biomass in W. Murcott trees subjected to T0 (black color) (Control, 100% of E_{Tc} water replenishment), T1 (grey color) (50% of E_{Tc} water replenishment) and T2 (hatched) (50% of E_{Tc} water replenishment + hydrogel). Different letters indicate statistical differences ($p \leq 0.05$, Tukey test).

3.3. Nutrition and Metabolites Analysis

Regarding the nutrient analyses, no significant differences in N, P, Ca, or Mg were observed. However, sodium content was significantly higher for T2 both in root and leaf, while potassium content was significantly higher only in leaves of T2 (Table 1).

Additionally, the proline concentration was significantly higher in the root of T2 plants compared to T1 and T0 (Table 2).

Table 1. Nutrient concentration in plant tissues. Total root, shoot, and leaf nutrient content in W. Murcott trees subjected to T0, T1, and T2. Different letters within the column indicate statistical differences ($p \leq 0.05$, Tukey test).

Organ	Tmt	% N	% P	% K	% Ca	% Mg	% Na	% Si
Root	T0	1.08 ±0.10 a	0.09 ±0.01 a	0.69 ±0.07 a	0.54 ±0.03 a	0.07 ±0.01 a	0.03 ±0.013 b	0.10 ±0.055 a
	T1	0.94 ±0.21 a	0.10 ±0.02 a	0.68 ±0.07 a	0.56 ±0.07 a	0.06 ±0.01 a	0.03 ±0.004 b	0.10 ±0.015 a
	T2	1.28 ±0.20 a	0.10 ±0.01 a	0.68 ±0.11 a	0.62 ±0.08 a	0.08 ±0.02 a	0.05 ±0.006 a	0.12 ±0.033 a
Shoot	T0	0.93 ±0.17 a	0.13 ±0.02 a	0.90 ±0.07 a	1.37 ±0.19 a	0.07 ±0.01 a	0.02 ±0.004 a	0.06 ±0.048 a
	T1	0.81 ±0.13 a	0.12 ±0.02 a	0.89 ±0.08 a	1.13 ±0.17 a	0.06 ±0.01 a	0.02 ±0.004 a	0.05 ±0.057 a
	T2	1.02 ±0.15 a	0.14 ±0.04 a	0.96 ±0.19 a	1.19 ±0.18 a	0.07 ±0.02 a	0.03 ±0.008 a	0.05 ±0.050 a
Leaf	T0	2.74 ±0.58 a	0.18 ±0.02 a	2.46 ±0.25 b	2.04 ±0.14 a	0.28 ±0.03 a	0.03 ±0.003 b	0.012 ±0.006 a
	T1	2.55 ±0.42 a	0.21 ±0.03 a	2.62 ±0.34 ab	2.10 ±0.20 a	0.29 ±0.03 a	0.04 ±0.004 b	0.004 ±0.002 b
	T2	3.29 ±0.19 a	0.20 ±0.02 a	3.08 ±0.27 a	1.94 ±0.36 a	0.28 ±0.02 a	0.12 ±0.068 a	0.003 ±0.001 b

Table 2. Proline concentration in fine (absorbent) roots in *W. Murcott* trees subjected to T0, T1, and T2. Different letters within the column indicate statistical differences ($p \leq 0.05$, Tukey test).

Treatments	Proline Fine Root (mg g ⁻¹)
T0	6.54 c
T1	9.42 b
T2	13.76 a

4. Discussion

The results obtained in this study indicated that the application of these water-retaining polymers effectively improved the water content in the substrate. The results showed that the substrate moisture for T2 was kept significantly higher than T0, and T1, despite receiving the same irrigation rate as T1 and a half of T0; however, this higher moisture availability in the substrate of T2 was not reflected in the plant's water status or growth. The higher water retention observed in the substrate with polyacrylamide gels was consistent with the information reported by the authors of [13], who pointed out that polyacrylamide-based polymers are highly absorbent and insoluble in water, a characteristic that allows one to increase the water-retention capacity in the soil and/or substrate. However, the difference observed in the water retention was not consistently reflected in the physiological parameters and biomass evaluated in the plants. It was only possible to observe the effect of 50% water restriction (T1 and T2) on the physiological response of the plants, expressing themselves through mechanisms such as g_s and SWP reduction [2], from August on. Other physiological responses such as chlorophyll fluorescence (F_v/F_m), indicated that the plants did not present severe stress limiting photosynthetic function (no significant differences between the treatments were observed) [23]; however, evident effects on growth and nutritional content were observed.

All these results do not coincide with what was observed by the authors of [10,12,13], who indicated that polymers favor the development of the crop. In our study, the hydrogel used demonstrated effective water retention, which is evidenced in the higher water content of the substrate compared to T1 and even T0 in some cases. If this retention capacity finally allows increases in the water available for the plants, T2 should have shown at least a greater growth than T1. However, it has no difference in biomass and has a smaller root compared to T1 and T0. The above-mentioned could indicate that the polymer has a high retention capacity but does not have a high capacity to deliver water to the plants as is required. It is probable that the observed behavior of this specific polyacrylamide gel may be given by its formulation.

A lower total biomass and root biomass for water restriction treatments, T1 and T2, was observed (Figure 2). An excess of moisture in the substrate could have reduced oxygenation, affecting the development of the roots in *W. Murcott* plants. This response was observed in the orange cv. Valencia [24]. On the other hand, the lower root development in T2 plants could be attributable to a lower root growth expression to seek water. Roots under little water availability respond through hydrotropism, a mechanism that modifies its growth, responding to a potential water gradient in the soil by growing towards areas with higher moisture content [25]. In this way, the lower growth of *W. Murcott* in the substrate with polyacrylamide hydrogel could be given by the high moisture presented in the substrate, making it unnecessary for the roots to search for areas with higher moisture. Additionally, citrus plants could have diverted photosynthates for the production of protective metabolites against saline or water stress (proline for example) instead of producing root biomass.

Nutritional analysis of the roots and leaves showed significantly higher Na content for T2. Authors such [12] observed similar results when using polyacrylamide polymers, obtaining a significant increase in sodium levels in crops such as wheat. From our results, it could be concluded that polyacrylamide hydrogels with high content of sodium could generate an accumulation of sodium in the rhizosphere, causing sodium absorption by

the roots and osmotic stress to the plants, which can cause a reduction in growth and/or osmotic adjustment if the species have the gene pool for expressing that strategy.

Proline is considered an osmotic stress indicator (water or salinity stress), as this osmolyte is commonly accumulated under abiotic stress conditions [2]. The authors of [26] indicate that citrus species under these stress conditions can respond through an osmotic adjustment, which means that cells respond by promoting the accumulation of compatible solutes (such as proline and others) to keep cellular functioning. However, this survival strategy has a negative effect on the growth of plants, since most of the energy is channeled towards the synthesis of these compatible solutes [27]. According to our results, proline concentration (mg g^{-1}) was significantly higher in T2 plants compared to those in T0 and T1, which may reflect an osmotic adjustment response of T2 plants, probably in response to the sodium content of the applied polyacrylamide, which probably generated saline stress. This possible adjustment response could also explain the lower growth of the shoots of the T2.

Although the addition of polyacrylamide polymers in this experiment significantly improved the retention of water in the substrate, it is questionable how much of this water was available to the W. Murcott plants. Our results showed that the plants expressed some signs of water and/or salt stress, which can be associated with a lack of water combined with a possible osmotic adjustment given by a high concentration of sodium, which leads to an increase in the concentration of osmolytes such as proline.

5. Conclusions

In conclusion, polymers such as sodium polyacrylamide allow water retention in the soil or substrate, but this is not necessarily released to plants. This can be explained insofar as that moisture is probably kept in the hydrogel and not released to the substrate media or the roots, or if released, in this case, this occurs with an increase in the concentration of sodium available to the plants, which could lead to the crop to a high-stress situation when the plant is subjected to water scarcity and increased growth and productivity problems. Our results also suggest that it is necessary to know the hydrogel-type product well and test it before applying it to commercial plantations.

Author Contributions: Conceptualization, P.M.G., C.B. and J.M.; methodology, D.C., C.B. and P.M.G.; software, D.C.; validation, D.C., C.B., J.M. and P.M.G.; formal analysis, D.C.; investigation, D.C.; resources, P.M.G. and C.B.; data curation, D.C. and P.M.G.; writing—original draft preparation, D.C.; writing—review and editing, P.M.G., C.B. and J.M.; visualization, D.C.; supervision, P.M.G.; project administration, P.M.G.; funding acquisition, D.C. and P.M.G. All authors have read and agreed to the published version of the manuscript.

Funding: This research received no external funding.

Data Availability Statement: Not applicable.

Acknowledgments: This work was supported by resources from the Laboratory of Water and Irrigation, of the Department of Fruit production and Oenology, Facultad de Agronomía e Ingeniería Forestal, Pontificia Universidad Católica de Chile. We thank Alejandro Campero, for contributing information and materials to this research.

Conflicts of Interest: The authors declare no conflict of interest.







References

1. Nikolaou, G.; Neocleous, D.; Christou, A.; Kitta, E.; Katsoulas, N. Implementing sustainable irrigation in water-scarce regions under the impact of climate change. *Agronomy* **2020**, *10*, 1120. [CrossRef]
2. Saxena, R.; Kumar, M.; Tomar, R.S. Plant responses and resilience towards drought and salinity stress. *Plant Arch.* **2019**, *19*, 50–58.
3. Syvertsen, J.P.; Lloyd, J.; Kriedemann, P.E. Salinity and drought stress effects on foliar ion concentration, water relations, and photosynthetic characteristics of orchard citrus. *Aust. J. Agric. Res.* **1988**, *39*, 619–627. [CrossRef]
4. Sánchez-Blanco, M.J.; Torrecillas, A.; Del Amor, F.; León, A. The water relations of Verna lemon trees from flowering to the end of rapid fruit growth. *Biol. Plant.* **1990**, *32*, 357–363. [CrossRef]

5. Miranda, M.T.; Da Silva, S.F.; Silveira, N.M.; Pereira, L.; Machado, E.C.; Ribeiro, R.V. Root osmotic adjustment and stomatal control of leaf gas exchange are dependent on citrus rootstocks under water deficit. *J. Plant Growth Regul.* **2021**, *40*, 11–19. [CrossRef]
6. Rodrigues, M.; Baptistella, J.L.C.; Horz, D.C.; Bortolato, L.M.; Mazzafera, P. Organic plant biostimulants and fruit quality—A review. *Agronomy* **2020**, *10*, 988. [CrossRef]
7. Bonomelli, C.; Celis, V.; Lombardi, G.; Mártiz, J. Salt stress effects on avocado (*Persea americana* Mill.) plants with and without seaweed extract (*Ascophyllum nodosum*) application. *Agronomy* **2018**, *8*, 64. [CrossRef]
8. Mossad, A.; Farina, V.; Lo Bianco, R. Fruit yield and quality of ‘Valencia’ orange trees under long-term partial rootzone drying. *Agronomy* **2020**, *10*, 164. [CrossRef]
9. Kumar, V.; Bhat, A.K.; Sharma, V.; Gupta, N.; Sohan, P.; Singh, V.B. Effect of different mulches on soil moisture, growth and yield of Eureka lemon (*Citrus limon burm*) under rainfed condition. *Indian J. Dryland Agric. Res. Dev.* **2015**, *30*, 83–88. [CrossRef]
10. Rivera, R.D.; Mesías, F. Water absorption hydrogel agricultural use and wetting of three soil types. *Rev. Fac. Cienc. Agrar. Univ. Nac. Cuyo* **2018**, *50*, 15–21.
11. Satriani, A.; Catalano, M.; Scalcione, E. The role of superabsorbent hydrogel in bean crop cultivation under deficit irrigation conditions: A case-study in Southern Italy. *Agric. Water Manag.* **2018**, *195*, 114–119. [CrossRef]
12. Geesing, D.; Schmidhalter, U. Influence of sodium polyacrylate on the water-holding capacity of three different soils and effects on growth of wheat. *Soil Use Manag.* **2004**, *20*, 207–209. [CrossRef]
13. López-Eliás, J.; Garza, S.; Jiménez, J.; Huez, M.A.; Garrido, O.D. Uso de un polímero hidrófilo a base de poli(acrilamida) para mejorar la eficiencia en el uso del agua. *Eur. Sci. J.* **2016**, *12*, 160. [CrossRef]
14. Cannazza, G.; Cataldo, A.; De Benedetto, E.; Demitri, C.; Madaghiale, M.; Sannino, A. Experimental assessment of the use of a novel superabsorbent polymer (SAP) for the optimization of water consumption in agricultural irrigation process. *Water* **2014**, *6*, 2056–2069. [CrossRef]
15. Thombare, N.; Mishra, S.; Siddiqui, M.Z.; Jha, U.; Singh, D.; Mahajan, G.R. Design and development of guar gum-based novel, superabsorbent and moisture-retaining hydrogels for agricultural applications. *Carbohydr. Polym.* **2018**, *185*, 169–178. [CrossRef] [PubMed]
16. Topp, G.C.; Davis, J.L.; Annan, A.P. Electromagnetic determination of soil water content: Measurements in coaxial transmission lines. *Water Resour. Res.* **1980**, *16*, 574–582. [CrossRef]
17. Reynolds, S.G. The gravimetric method of soil moisture determination part I: A study of equipment. And methodological problems. *J. Hydrol.* **1970**, *11*, 258–273. [CrossRef]
18. Blake, G.R.; Hartge, K.H. Bulk density. In *Methods of Soil Analysis, Part 1. Physical and Mineralogical Methods*, 2nd ed.; Klute, A., Ed.; Agronomy Monograph 9; American Society of Agronomy; Soil Science Society of America: Madison, WI, USA, 1986; pp. 363–382.
19. Scholander, P.F.; Bradstreet, E.D.; Hemmingsen, E.A.; Hammel, H.T. Sap Pressure in Vascular Plants: Negative hydrostatic pressure can be measured in plants. *Science* **1965**, *148*, 339–346. [CrossRef]
20. Weatherley, P.E. Studies in the water relations of the cotton plant I. The field measurements of water deficit in leaves. *New Phytol.* **1950**, *49*, 81–97. [CrossRef]
21. Rascher, U.; Liebig, M.; Lüttge, U. Evaluation of instant light-response curves of chlorophyll fluorescence parameters obtained with a portable chlorophyll fluorometer on site in the field. *Plant Cell Environ.* **2000**, *23*, 1397–1405. [CrossRef]
22. Bates, L.S.; Waldren, R.P.; Teare, I.D. Rapid determination of free proline for water-stress studies. *Plant Soil* **1973**, *39*, 205–207. [CrossRef]
23. Ribeiro, R.V.; Machado, E.C. Some aspects of citrus ecophysiology in subtropical climates: Re-visiting photosynthesis under natural conditions. *Braz. J. Plant Physiol.* **2007**, *19*, 393–411. [CrossRef]
24. Ben-Noah, I.; Nitsan, I.; Cohen, B.; Kaplan, G.; Friedman, S.P. Soil aeration using air injection in a citrus orchard with shallow groundwater. *Agric. Water Manag.* **2021**, *245*, 106664. [CrossRef]
25. Dietrich, D. Hydrotropism: How roots search for water. *J. Exp. Bot.* **2018**, *69*, 2759–2771. [CrossRef] [PubMed]
26. Núñez Vázquez, M.; Pérez Hernández, M.D.C.; Betancourt Grandal, M. Review water and saline stress on citrus. Strategies for reducing plant damages. *Cultiv. Trop.* **2017**, *38*, 65–74.
27. Munns, R. Comparative physiology of salt and water stress. *Plant Cell Environ.* **2002**, *25*, 239–250. [CrossRef]

Article

Bread Wheat Productivity in Response to Humic Acid Supply and Supplementary Irrigation Mode in Three Northwestern Coastal Sites of Egypt

Essam F. El-Hashash ¹, Moamen M. Abou El-Enin ¹, Taia A. Abd El-Mageed ²,
Mohamed Abd El-Hammed Attia ³, Mohamed T. El-Saadony ⁴, Khaled A. El-Tarabily ^{5,6,7,*}
and Ahmed Shaaban ⁸

¹ Department of Agronomy, Faculty of Agriculture, Al Azhar University, Cairo 11651, Egypt; dressamelhashash@azhar.edu.eg (E.F.E.-H.); magromodeller@azhar.edu.eg (M.M.A.E.-E.)

² Soil and Water Department, Faculty of Agriculture, Fayoum University, Fayoum 63514, Egypt; taa00@fayoum.edu.eg

³ Desert Research Center, Al Matera, Cairo 11753, Egypt; mattiadrc2017@gmail.com

⁴ Department of Agricultural Microbiology, Faculty of Agriculture, Zagazig University, Zagazig 44511, Egypt; m.talaatelsadony@gmail.com

⁵ Department of Biology, United Arab Emirates University, Al-Ain 15551, United Arab Emirates

⁶ Khalifa Center for Genetic Engineering and Biotechnology, United Arab Emirates University, Al-Ain 15551, United Arab Emirates

⁷ Harry Butler Institute, Murdoch University, Perth 6150, Australia

⁸ Agronomy Department, Faculty of Agriculture, Fayoum University, Fayoum 63514, Egypt; asm04@fayoum.edu.eg

* Correspondence: ktarabily@uaeu.ac.ae



Citation: El-Hashash, E.F.;
Abou El-Enin, M.M.;
Abd El-Mageed, T.A.;

Attia, M.A.E.-H.; El-Saadony, M.T.;
El-Tarabily, K.A.; Shaaban, A. Bread
Wheat Productivity in Response to
Humic Acid Supply and
Supplementary Irrigation Mode in
Three Northwestern Coastal Sites of
Egypt. *Agronomy* **2022**, *12*, 1499.
[https://doi.org/10.3390/
agronomy12071499](https://doi.org/10.3390/agronomy12071499)

Academic Editor: Aliasghar
Montazar

Received: 19 May 2022

Accepted: 17 June 2022

Published: 23 June 2022

Publisher's Note: MDPI stays neutral
with regard to jurisdictional claims in
published maps and institutional affil-
iations.



Copyright: © 2022 by the authors.
Licensee MDPI, Basel, Switzerland.
This article is an open access article
distributed under the terms and
conditions of the Creative Commons
Attribution (CC BY) license ([https://
creativecommons.org/licenses/by/
4.0/](https://creativecommons.org/licenses/by/4.0/)).

Abstract: Drought stress is a major factor limiting wheat crop production worldwide. The application of humic acid (HA) and the selection of the appropriate genotype in the suitable site is one of the most important methods of tolerance of wheat plants to drought-stress conditions. The aim of this study was achieved using a three-way ANOVA, the stress tolerance index (STI), the Pearson correlation coefficient (r_p), and principal component analysis (PCA). Three field experiments in three sites (Al-Qasr, El-Neguilla, and Abo Kwela) during the 2019/21 and 2020/21 seasons were conducted, entailing one Egyptian bread wheat variety (Sakha 94) with three HA rates (0, 30, and 60 kg ha⁻¹) under normal and drought-stress conditions (supplemental irrigation). According to the ANOVA, the sites, supplemental irrigation, HA rates, and their first- and second-order interactions the grain yield and most traits evaluated ($p \leq 0.05$ or 0.01) were significantly influenced in both seasons. Drought stress drastically reduced all traits registered in all factors studied compared with normal conditions. The wheat plants at the Al-Qasr site in both seasons showed significantly increased grain yield and most traits compared with that of the other sites under normal and drought-stress conditions. HA significantly promoted all studied traits under drought stress, and was highest when applying 60 kg HA ha⁻¹, regardless of the site. The greatest grain yield and most traits monitored were observed in wheat plants fertilized with 60 kg HA ha⁻¹ at the Al-Qasr site in both seasons under both conditions. Grain yield significantly ($p \leq 0.05$ or 0.01) correlated with water and precipitation use efficiency as well as the most studied traits under normal and drought-stress conditions. The results of STI, r_p , and PCA from the current study could be useful and could be used as a suitable method for studying drought-tolerance mechanisms to improve wheat productivity. Based on the results of statistical methods used in this study, we recommend the application of 60 kg HA ha⁻¹ to improve wheat productivity under drought conditions along the north-western coast of Egypt.

Keywords: correlation; environment; drought stress; humic acid; PCA analysis; rain-fed; wheat varieties

1. Introduction

Cereal crops are a major staple food worldwide, which directly contribute more than 50% of the total human calorie input. Among them, wheat (*Triticum aestivum* L.) occupies a prominent position as a source of dietary protein and calories for the ever-burgeoning population of the world [1]. Bread wheat is widely cultivated over the world because of its great demand and cultivars that are adaptable to various environmental conditions [2]. Wheat is the most significant cereal grain and a staple diet for millions of people in Egypt, where 1.40 million hectares were planted in 2021/2022, yielding 9.0 million tons [3]. Egypt is the world's largest wheat importer [4], and by expanding its output, it hopes to reduce its reliance on imports. Due to water constraints, inefficient irrigation systems, poor conservation, and low agricultural water efficiency, water availability per unit of irrigated area is decreasing in the Mediterranean regions [5,6].

Irrigation water scarcity is one of the most significant constraints on agricultural production [7], given that irrigated agriculture is the largest user of freshwater, accounting for approximately 79% of all water withdrawal in Egypt and 69% worldwide [8]. Increased water use efficiency (WUE) in both irrigated and rain-fed agriculture is required to meet the demand for food production while preserving freshwater resources [9]. Drought is the most serious issue affecting wheat output. As a result, improving drought resistance is of particular significance for long-term wheat production. Egypt's rain belt is confined to the coast, particularly in the north, which is categorized as semi-arid and has poor sandy or saline soil. Rain-fed agriculture is practiced in Egypt's North Sinai and Marsa Matrouh [10]. A substantial amount of the Egyptian North Coast's present economic activities is based on rain-fed agriculture. Rainfall in this area ranges from 130 to 150 mm on the northwest coast to 80 mm (west of Al-Arish) to 280 mm (near Rafah) in the northeast [11]. Drought-tolerant crops such as wheat, barley, fig, olive, and tiny patches of faba bean and lentils are the most widely grown crops in the area. Due to the lack of rain throughout the winter wheat-growing seasons, only 30% of the crop's water requirements are met, and over 70% of irrigation water is required to sustain winter wheat's potential output [10]. Long dry spells are common during important growth stages, such as flowering and grain filling, and have a significant impact on eventual production [12].

Rain-fed areas, where most of the land is farmed utilizing old, traditional, and rudimentary soil and agricultural practices, are facing several critical problems [13]. Because of their small canopy and low evaporative demands in the winter, all winter-sown crops are more vulnerable to drought in the spring or early summer when evaporative demand is high, especially during flowering and grain-filling stages, and are largely reliant on stored soil moisture to complete their growth cycles [14]. Supplemental irrigation (SI) with a limited amount of water can improve crop output while also increasing WUE [15]. Previous researchers found that increasing the soil water content at a depth of 40 cm to 65% of the field capacity after jointing and 70% of the field capacity after anthesis using SI boosted grain output and WUE by almost 40% and 15%, respectively. Many studies have found that varying quantities of SI at different stages of wheat growth considerably and significantly increased grain yield [16–20].

Under rain-fed conditions, fertilizer rates should be regulated because when excessive amounts of fertilizer are provided, the vegetative growth of the plants is stimulated much more in the early periods, and water stress may arise at later times, affecting the effective grain-filling period [21]. Fertilizer application improves the usage of stored water as well as boosts wheat yields by correcting nutritional deficiencies [22]. Therefore, increasing crop productivity under water scarcity is deliberated as the main purpose via hybridizing or genetic engineering plans [23]. To challenge this problem conventionally, chemical treatment and agronomical crop management practices have been applied to decrease the detrimental effects of water deficiency [24]. Alternatively, humic acid (HA) as organic fertilization plays an essential role in diminishing the utilization of chemical fertilizers and reducing its harmful impact on soil, the environment, and sustainable agriculture [25]. HA

is the active ingredient in organic fertilizers, and its use could be a viable alternative to traditional soil fertilization and a quick source of nitrogen, especially in semi-arid areas [26].

HA is a naturally occurring polymeric-heterocyclic organic molecule with carboxylic (COOH), phenolic (OH), alcoholic, and carbonyl fractions, and is used as an organic fertilizer [27]. HA has been shown to improve nutrient transport and availability [28,29]. Due to their effective components, humic compounds can alter biochemical processes in plants, resulting in higher photosynthesis and respiration rates, as well as increased hormone and protein production [28]. In general, the beneficial effects of HA on plant physiology are discussed in terms of root growth and nutrient uptake [30]. HA can be used as a low-cost organic fertilizer to boost plant growth and productivity, improve stress tolerance, and improve soil physical characteristics and complex metal ions, among other things [31]. Effect of HA on wheat seedling growth in the presence and absence of nitrogen (N) was also investigated. Small amounts of HA (54 mg L^{-1}) in the water medium resulted in a 500% increase in root length [32]. HA enhanced the fresh and dry weight of roots considerably. In the presence of 54 mg HA L^{-1} , the wheat dry matter yield of shoots rose by 22%. In addition to the improvement in the soil's physical structure, humic compounds in the soil boost nutrient absorption by increasing the availability of nutrients [32].

The main purpose of the current work was to evaluate the possible use of HA as a soil application to alleviate the harmful effects of water stress on wheat plants, explaining the role of HA in improving the growth and yield of water-stressed wheat plants and maximizing WUE for optimal crop production.

2. Materials and Methods

2.1. Geographic and Climatic Data of the Studied Sites

Field experiments (2019/2020 and 2020/2021 winter seasons) were carried out at three different sites along the north-western coast of Egypt: The Al-Qasr site (latitude: $31^{\circ}35'$ and longitude: $27^{\circ}16'$), the El-Neguilla site (latitude: $31^{\circ}43'$ and longitude: $26^{\circ}50'$), and the Abo Kwela site (latitude: $31^{\circ}57'$ and longitude: $25^{\circ}99'$), located in Marsa Matrouh, approximately 300 km west of Alexandria city, on the north-western coast of Egypt. Geographic coordinates for the three cultivated sites are presented in Figure 1. Climatic data of the three cultivated sites, such as the monthly average precipitation (mm), minimum and maximum temperature ($^{\circ}\text{C}$), solar radiation ($\text{Mj m}^{-2} \text{ d}^{-1}$), wind speed (m s^{-1}), and relative humidity (%) for the experimental duration (December–April) during both growing winter seasons (2019/2020 and 2020/2021), are presented in Table 1.

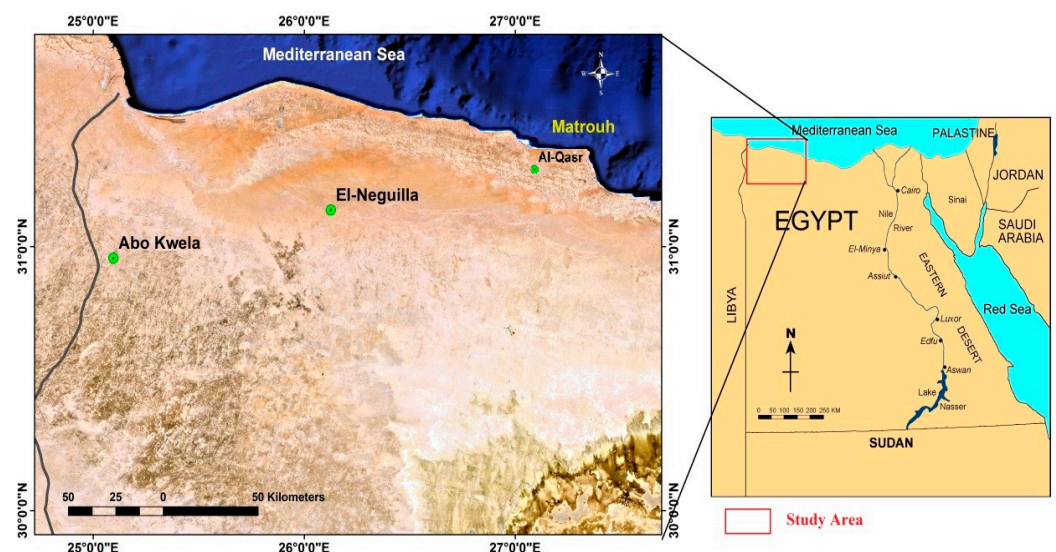


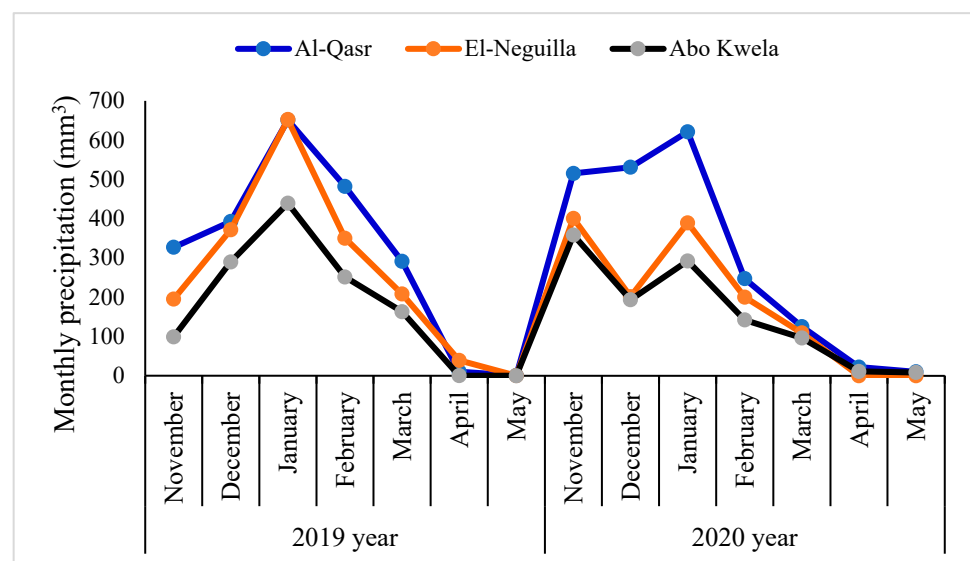
Figure 1. Geographic coordinates for Al-Qasr, El-Neguilla, and Abo Kwela sites, Marsa Matrouh, Egypt.

Table 1. Climatic data at Al-Qasr, El-Neguilla, and Abo Kwela sites, Egypt, during the 2019/2020 and 2020/2021 growing seasons.

Season	Al-Qasr					El-Neguilla					Abo Kwela					
	Temperature (°C)		RH (%)	WS (m s ⁻¹)	Solar Radiation (MJ m ⁻² d ⁻¹)	Temperature (°C)		RH (%)	WS (m s ⁻¹)	Solar Radiation (MJ m ⁻² d ⁻¹)	Temperature (°C)		RH (%)	WS (m s ⁻¹)	Solar Radiation (MJ m ⁻² d ⁻¹)	
	Min	Max				Min	Max				Min	Max				
2019/ 2020	November	9.65	28.3	66.1	2.40	13.2	10.01	28.9	62.6	5.23	15.3	9.16	29.9	56.2	2.45	8.6
	December	3.39	22.2	71.9	3.78	10.2	3.96	22.7	71.5	6.98	12.4	4.42	23.3	71.1	3.37	6.6
	January	3.37	17.8	74.0	3.98	11.3	3.49	17.7	74.3	5.74	11.1	3.83	17.9	75.9	3.21	6.8
	February	4.37	22.1	74.3	3.58	14.7	4.50	22.1	74.1	6.96	14.8	4.19	21.9	73.7	3.25	9.1
	March	4.91	25.7	67.4	3.98	20.8	4.99	27.3	64.6	6.38	20.6	4.97	29.1	61.6	3.73	12.0
	April	8.00	29.1	65.2	3.16	25.2	8.13	30.1	62.1	8.21	28.5	7.65	31.8	57.9	3.25	15.5
May	9.89	39.9	56.7	3.43	27.1	10.26	40.4	54.1	9.79	30.2	9.63	41.6	47.3	3.52	18.5	
2020/ 2021	November	7.22	24.0	79.6	2.88	12.3	7.33	23.9	77.8	12.01	29.8	6.37	24.8	76.4	2.61	7.9
	December	8.32	25.1	62.0	3.32	14.7	5.50	20.3	76.9	8.68	15.7	5.11	22.2	73.9	2.53	7.1
	January	5.08	19.7	79.3	2.51	10.8	10.8	17.1	63.0	4.89	7.12	6.87	25.8	68.2	2.87	7.8
	February	10.76	18.6	58.0	4.90	20.7	10.65	18.5	58.0	5.32	15.2	4.11	24.1	72.2	3.20	10.5
	March	10.92	26.8	57.0	4.88	25.9	12.91	22.2	57.0	4.94	22.1	6.12	15.6	74.3	3.98	8.0
	April	11.66	30.5	55.0	3.85	34.5	15.72	25.4	56.0	4.89	26.4	8.24	31.0	77.2	3.91	16.3
May	17.80	33.1	55.0	4.99	33.1	18.03	30.7	60.0	4.82	30.0	8.55	43.0	66.5	2.56	17.8	

RH = relative humidity and WS = wind speed.

The agriculture in the studied regions is mainly rain-fed, and these regions are characterized by a Mediterranean-type climate with cold wet winters and hot dry summers. The highest percentage of precipitation usually occurs in December and January in the three cultivated sites. The highest seasonal rainfall rates during the studied period (Figure 2) were recorded at the Al-Qasr site (4224 m³), followed by the El-Neguilla site (3115 m³), then the Abo Kwela site (2342 m³).

**Figure 2.** Monthly precipitation at each site during the two growing seasons.

2.2. Soil Characteristics of the Studied Field Sites

The soils of the studied area could be classified at the family level as Typic Torripsamments, siliceous, hyperthermic, and moderately deep. In addition, the suitability of the studied soils ranged between not suitable and marginally suitable [33]. The soil of the three sites where the experiments were carried out for the two seasons had topsoil (0–100 cm depth) characterized as sandy loam in texture. Table 2 shows the results of the soil analysis at the three study sites at a 0.0–0.50 cm depth before planting in both winter seasons (2019/2020 and 2020/2021) using [34,35] standard methods.

Table 2. Soil analysis of the studied experimental sites (0.0–0.5 m depth) before sowing during the 2019/2020 and 2020/2021 growing seasons.

Soil Property	Al-Qasr		El-Neguilla		Abo Kwela	
	2019/2020	2020/2021	2019/2020	2020/2021	2019/2020	2020/2021
Physical Characteristics						
Coarse sand (%)	45.78	36.97	38.76	35.22	42.87	37.11
Fine sand (%)	38.20	44.60	40.80	47.16	34.11	45.32
Silt (%)	14.30	16.32	19.46	15.74	21.04	15.21
Clay (%)	1.72	2.11	0.98	1.88	1.98	2.36
Texture class	SL	SL	SL	SL	SL	SL
Chemical properties:						
pH	8.35	8.27	8.50	8.11	8.40	7.25
EC _e (dS m ⁻¹)	2.40	6.00	4.50	9.30	3.10	8.80
Soluble Cations (meq 100⁻¹ g)						
Mg ²⁺	0.70	1.60	1.00	2.50	0.69	2.60
Ca ²⁺	0.81	2.60	1.50	3.16	1.30	3.90
Na ⁺	0.74	1.04	1.46	2.81	1.35	1.70
K ⁺	0.27	0.96	0.67	0.84	0.19	0.66
Soluble Anions (meq 100⁻¹ g)						
HCO ₃ ⁻	1.0	2.06	1.03	3.60	0.83	3.50
Cl ⁻	0.38	1.25	0.6	1.70	1.0	2.24
SO ₄ ²⁻	1.14	2.89	3.00	4.01	1.7	3.12

SL: Sandy loam; EC_e: Electrical conductivity of soil past extract (1:2.5 soil:H₂O, *w/v*).

2.3. Experimental Design and Treatment Details

The bread wheat Sakha 94 variety was bought from the central administration of seeds production of the Egyptian Ministry of Agriculture and Land Reclamation and was sown in different environments at three sites along the north-western coast of Egypt. The pedigree of the studied cultivar is OPATA/RAYON//KAUZ (CMBW90Y3180-OTOPM-3Y-010Y-10M-015Y-0Y-0AP-0S, the year of release was (2004). At each site, wheat grains were sown in a split-plot design in a randomized complete block design (RCBD) with three replicates. Each plot (3.5 × 4 m) included 13 rows 3.5 m long and 30 cm apart. Irrigation treatments were allocated to the main plots as rain-fed (drought) and SI (normal) (Table 3), and the water used for SI was groundwater (with EC_e = 1.2 ± 0.3 dS m⁻¹) pumped from a local well and provided via a sprinkler irrigation system. HA treatments were allocated in subplots and applied at three doses of 0 (HA₀), 30 (HA₃₀), and 60 (HA₆₀) kg ha⁻¹. The main constituents of the water-dissolvable HA compound used in this experiment (Alpha Chemika, Mumbai, Maharashtra, India) are listed in Table 4. Each HA dose was applied once during planting after being well mixed with fine sand (200 kg), then equally spread throughout the topsoil layer and blended in the rhizosphere zone where the root is active.

2.4. Agronomical Management Practices

After one chisel plow, grains of the Sakha 94 variety were sown at the rate of 167 kg ha⁻¹ in rows after the first effective rainfall precipitation on 10, 12, and 13 December in the first season and 15, 16, and 17 November in the second season for Al-Qasr, El-Neguilla, and Abo Kwela sites, respectively. The experimental field of each cultivated site was basally supplied with 52.5 kg of P₂O₅ ha⁻¹ (169.4 kg of calcium super monophosphate containing 15.5% P₂O₅) during the preparation of the field. Furthermore, nitrogen was applied with 180.4 kg of N ha⁻¹ (284.2 kg of ammonium nitrate 33.5% N), which was supplied in two or three equal doses with SI times. Meanwhile, the other recommended agricultural practices were applied as usual in bread wheat fields under Egyptian rain-fed conditions.

Table 3. Description of irrigation mode and humic acid treatments applied in the three research sites.

		A. Supplemental Irrigation (SI)											
		Total Amount of Supplemental and Rain Irrigation Water (m³ ha⁻¹)											
Treatment	Description	2019/2020						2020/2021					
		Al-Qasr		El-Neguilla		Abo Kwela		Al-Qasr		El-Neguilla		Abo Kwela	
		Rain	SI	Rain	SI	Rain	SI	Rain	SI	Rain	SI	Rain	SI
Normal	Wheat plants were irrigated with three supplemental irrigations at stages of stem elongation, flowering, and grain filling.	2154	1751	1815	2090	1242	2663	2070	1751	1300	2521	1100	2721
Drought	Wheat plants were irrigated with three supplemental irrigations (60% of water amount applied at normal level) at stages of stem elongation, flowering, and grain filling.	2154	189	1815	528	1242	1101	2070	223	1300	993	1100	1193
		B. Humic Acid (HA)											
HA ₀		0 kg ha ⁻¹ HA addition											
HA ₃₀		30 kg ha ⁻¹ of HA mixed well with 200 kg of fine sand was added once at planting for each site											
HA ₆₀		60 kg ha ⁻¹ of HA mixed well with 200 kg of fine sand was added once at planting for each site											

Table 4. The main components of humic acid (HA) substance applied in the three research sites on a dry weight basis.

Component	Concentration (%)	Component	Concentration (%)
Pure HA content	90.3	Iron (Fe)	0.61
Nitrogen (N)	0.94	Manganese (Mn)	0.09
Phosphorus (P)	1.04	Zinc (Zn)	0.32
Potassium (K)	1.46	Copper (Cu)	0.55
Calcium (Ca)	2.81	Sodium (Na)	0.04
Magnesium (Mg)	0.92	Others	0.44
Sulfur (S)	0.48		

2.5. Agronomic Traits, Grain Yield, and Its Components

At full maturity, wheat plants were manually harvested on 20, 21, and 27 April in the 2019/2020 season, and 9, 13, and 15 April in the 2020/2021 season for Al-Qasr, El-Neguilla, and Abo Kwela sites, respectively. Ten wheat plants were randomly collected from each plot to measure the plant height (PH; cm), spike length (SL; cm), and spikelet number per spike (SNS). The spikelet density was calculated by dividing SNS by SL. However, all wheat plants in one square meter area were manually harvested from each plot to measure the number of spike per m² (NSm²). The tillering index (%) was calculated by dividing the NSm²/tiller number per m² and the thousand-grain weight (T-GW; g). Meanwhile, the remaining wheat plants in each plot were harvested to determine the grain (GY), straw (SY), and biological (BY) yields and converted into t ha⁻¹. WUE was calculated by dividing GY (kg ha⁻¹) by growing season irrigation (m³ ha⁻¹). The precipitation use efficiency (PUE) was obtained by dividing GY (kg ha⁻¹) by growing season precipitation (m³ ha⁻¹) [36].

2.6. Statistical Analysis

Upon pre-running the variance analysis, Shapiro-Wilk's normality and Levene's homogeneity for all variables were verified using the normality and homogeneity tests according

to [37,38]. The outputs of the normality and homogeneity tests showed all variables to be statistically acceptable for further analysis of variance. Pooled data of all variables for both seasons were subjected to a three-way ANOVA using GenStat statistical software (12th edition, VSN International Ltd., Harpenden, UK) according to [39]. The coefficient of variation (C.V. %) was estimated and categorized as very high (C.V. % ≥ 21), high ($15 \leq$ C.V. % < 21), moderate ($10 \leq$ C.V. % < 15), and low (C.V. % < 10) according to [40]. The obtained data were expressed as the mean \pm standard error (SE), and multiple comparisons were determined using the least-significant-difference test (LSD) at the 0.05 level of probability [39]. The stress tolerance index was calculated according to [41]. Pearson's correlation coefficient and principal component analysis (PCA) were applied to assess the association among the studied traits using the Origin Pro 2021 version b 9.5.0.193 computer software program.

3. Results

3.1. Analysis of Variance (ANOVA) Results

Table 5 outlines the detailed results of the three-way ANOVA for the studied wheat traits. The results showed that the environment (E), SI, and HA treatments, as well as the first-order interactions (E \times SI, E \times HA, and SI \times HA), had a statistically significant effect ($p \leq 0.05$ or 0.01) on all studied traits. The second-order interaction (E \times SI \times HA) had statistically significant effects ($p \leq 0.05$ or 0.01) for most studied traits, while non-significant differences were observed between second-order interactions for the SNS trait. In Table 5, the C.V. % values registered for all evaluated traits across experimental factors are low (C.V. $\leq 10\%$), indicating the high precision and reliability of the field experiments carried out.

Table 5. Three-way ANOVA (p -values) for the impact of environment (E), supplemental irrigation (SI), humic acid (HA) treatment, and their interactions on the studied bread wheat traits.

S. O. V.	PH (cm)	TI (%)	SL (cm)	SNS	SD	NSm ²	SY	BY	GY	T-GW	WUE	PUE
							(t ha ⁻¹)			(g)	(kg m ⁻³)	
E	0.00 **	0.00 **	0.00 **	0.00 **	0.00 **	0.00 **	0.00 **	0.00 **	0.00 **	0.00 **	0.00 **	0.00 **
SI	0.00 **	0.00 **	0.00 **	0.00 **	0.02 *	0.00 **	0.00 **	0.00 **	0.00 **	0.00 **	0.03 *	0.00 **
HA	0.00 **	0.00 **	0.00 **	0.00 **	0.06 *	0.00 **	0.00 **	0.00 **	0.00 **	0.00 **	0.00 **	0.00 **
E \times SI	0.00 **	0.00 **	0.07 *	0.00 **	0.00 **	0.00 **	0.02 *	0.00 **	0.00 **	0.00 **	0.00 **	0.00 **
E \times HA	0.00 **	0.00 **	0.00 **	0.00 **	0.00 **	0.00 **	0.04 *	0.02 *	0.00 **	0.00 **	0.00 **	0.00 **
SI \times HA	0.00 **	0.00 **	0.00 **	0.00 **	0.02 *	0.00 **	0.00 **	0.00 **	0.00 **	0.00 **	0.00 **	0.00 **
E \times SI \times HA	0.00 **	0.00 **	0.00 **	0.32 ns	0.05 *	0.03 *	0.00 **	0.00 **	0.00 **	0.00 **	0.00 **	0.00 **
C.V. %	4.39	5.14	4.39	6.14	6.11	8.11	7.80	5.93	6.38	4.45	6.48	7.18

(*) and (**) significant for $p \leq 0.05$ and $p \leq 0.01$, respectively; ns: Indicates a non-significant difference. S.O.V.: Source of variance, PH: Plant height, TI: Tillering index, SL: Spike length, SNS: Spikelet number per spike, SD: Spikelet density, NSm²: Number of spike per m², SY: Straw yield, BY: Biological yield, GY: Grain yield, T-GW: Thousand-grain weight, WUE: Water use efficiency, and PUE: Precipitation use efficiency. C.V. %: Coefficient of variation (%).

3.2. Experimental Factors Effects on Wheat Traits

The results in Table 6 shows significant differences in the effects of the environment (site \times year), SI, and HA treatments on all studied wheat traits. PH, SNS, and SD were significantly higher at the El-Neguilla site in both seasons than at the Al-Qasr and Abo Kwela sites. Meanwhile, SL, SY, BY, GY, T-GW, WUE, and PUE increased significantly at the Al-Qasr site in both seasons compared with the Abo Kwela and El-Neguilla sites. Regarding the irrigation mode, all studied wheat traits were markedly higher under normal conditions compared to drought-stress conditions, except WUE, which was higher in drought conditions compared to normal conditions. Regarding HA treatments, all studied wheat traits in the current study were significantly higher in plants supplied with 60 kg HA ha⁻¹, moderate in plants fertilized with 30 kg HA ha⁻¹, and lower in non-fertilized wheat plants (0 kg HA ha⁻¹).

Table 6. Effects of the environment (E; location and year), supplemental irrigation (SI), and humic acid (HA) on the studied bread wheat traits.

Factor	PH (cm)	TI (%)	SL (cm)	SNS	SD	NSm ²
E						
Abo Kwela 2019/20	44.4 ± 3.9c	1.37 ± 0.07b	6.06 ± 0.37c	12.23 ± 0.53e	2.06 ± 0.06c	113.6 ± 5.40c
Abo Kwela 2020/21	44.0 ± 3.6d	1.39 ± 0.06a	6.22 ± 0.38b	12.55 ± 0.54d	2.07 ± 0.05c	116.4 ± 5.10b
El-Neguilla 2019/20	58.7 ± 2.2a	0.77 ± 0.01f	5.99 ± 0.29d	15.31 ± 1.01b	2.52 ± 0.07b	63.1 ± 2.29d
El-Neguilla 2020/21	58.4 ± 2.0a	0.89 ± 0.05e	5.95 ± 0.32d	15.67 ± 1.15a	2.57 ± 0.04a	57.5 ± 4.60e
AL-Qasr 2019/20	44.3 ± 0.8c	1.14 ± 0.03c	6.26 ± 0.19b	10.92 ± 0.38f	1.75 ± 0.03e	136.8 ± 8.28a
AL-Qasr 2020/21	45.6 ± 0.7b	1.06 ± 0.02d	6.79 ± 0.23a	13.20 ± 0.65c	1.94 ± 0.05d	137.6 ± 8.00a
SI						
Normal	54.3 ± 3.1a	1.14 ± 0.10a	7.01 ± 0.10a	15.25 ± 1.20a	2.18 ± 0.18a	117.8 ± 16.90a
Drought	44.2 ± 3.4b	1.08 ± 0.11b	5.42 ± 0.16b	11.37 ± 0.35b	2.12 ± 0.10b	90.5 ± 12.47b
HA						
0 kg ha ⁻¹ (HA ₀)	41.1 ± 3.5c	0.95 ± 0.08c	5.17 ± 0.30c	10.97 ± 0.35c	2.15 ± 0.13c	85.4 ± 10.72c
30 kg ha ⁻¹ (HA ₃₀)	49.8 ± 3.1b	1.11 ± 0.10b	6.30 ± 0.09b	13.28 ± 0.85b	2.12 ± 0.14b	102.8 ± 15.52b
60 kg ha ⁻¹ (HA ₆₀)	56.9 ± 3.4a	1.26 ± 0.14a	7.17 ± 0.21a	15.69 ± 1.08a	2.19 ± 0.16a	124.3 ± 17.23a
Factor	SY	BY	GY	T-GW (g)	WUE	PUE
	(t ha ⁻¹)				(kg m ⁻³)	
E						
Abo Kwela 2019/20	4.04 ± 0.25d	5.44 ± 0.42c	1.41 ± 0.20c	31.3 ± 2.5c	0.42 ± 0.10c	1.13 ± 0.30b
Abo Kwela 2020/21	4.49 ± 0.28b	5.90 ± 0.44b	1.43 ± 0.21c	32.3 ± 2.6b	0.43 ± 0.09c	1.28 ± 0.41a
El-Neguilla 2019/20	2.92 ± 0.27e	3.87 ± 0.39d	0.96 ± 0.12e	31.6 ± 1.1c	0.29 ± 0.07e	0.53 ± 0.06f
El-Neguilla 2020/21	2.93 ± 0.28e	3.89 ± 0.40d	0.98 ± 0.13d	32.4 ± 1.2b	0.30 ± 0.07d	0.75 ± 0.06e
AL-Qasr 2019/20	4.24 ± 0.31c	5.91 ± 0.50b	1.66 ± 0.20b	35.0 ± 2.9a	0.51 ± 0.16b	0.77 ± 0.34d
AL-Qasr 2020/21	4.67 ± 0.27a	6.45 ± 0.47a	1.78 ± 0.25a	35.1 ± 2.7a	0.54 ± 0.11a	0.86 ± 0.17c
SI						
Normal	4.64 ± 0.31a	6.63 ± 0.51a	1.99 ± 0.21a	38.5 ± 1.8a	0.52 ± 0.17a	1.30 ± 0.27a
Drought	3.12 ± 0.33b	3.86 ± 0.39b	0.74 ± 0.08b	27.4 ± 1.0b	0.32 ± 0.18b	0.48 ± 0.22b
HA						
HA ₀	2.88 ± 0.31c	3.85 ± 0.41c	0.97 ± 0.10c	25.6 ± 0.6c	0.30 ± 0.01c	0.63 ± 0.01c
HA ₃₀	4.09 ± 0.37b	5.40 ± 0.50b	1.30 ± 0.14b	32.4 ± 0.6b	0.40 ± 0.06b	0.85 ± 0.07b
HA ₆₀	4.66 ± 0.28a	6.49 ± 0.45a	1.83 ± 0.18a	40.8 ± 1.4a	0.55 ± 0.03a	1.19 ± 0.14a

Each value represents means ± standard error. Means sharing different letters in the same column indicate statistically significant ($p \leq 0.05$) differences according to the LSD test. PH: Plant height, TI: Tillering index, SL: Spike length, SNS: Spikelet number per spike, SD: Spikelet density, NSm²: number of spike per m², SY: Straw yield, BY: Biological yield, GY: Grain yield, T-GW: Thousand-grain weight, WUE: Water use efficiency, and PUE: Precipitation use efficiency. HA₀, HA₃₀, and HA₆₀ indicate the addition of 0, 30, and 60 kg ha⁻¹ humic acid, respectively.

3.3. The First-Order Interaction Effect on Wheat Traits

With respect to the E × SI interaction (Table 7), all studied wheat traits under normal conditions were higher than in drought conditions except for the TI trait at Abo Kwela and El-Neguilla sites in the 2019/2020 season and the SD trait at Abo Kwela in both seasons and AL-Qasr in the 2019/2020 season. The interaction effect between environments and normal conditions showed significant differences for all studied traits compared with the environments × drought stress interactions, except for WUE at the El-Neguilla site in both seasons and the AL-QASR site in the 2019/2020 season. The highest values of GY and most studied traits were registered by the Al-Qasr × SI interaction in the 2020/2021 season compared with their values in other E × SI interactions. A significant decrease was found in the El-Neguilla site × SI interaction than other E × SI interactions for GY and most studied traits under both conditions. Generally, the Al-Qasr site in both seasons showed more WUE, thus more GY and most traits comparatively than other sites under drought-stress conditions.

Table 7. The first-order interaction of environment (E) and supplemental irrigation (SI) for the studied bread wheat traits.

Factor		PH (cm)	TI (%)	SL (cm)	SNS	SD	NSm ²	
E	SI							
Abo Kwela 2019/2020	Normal	53.7 ± 12.5b	1.37 ± 0.14b	6.86 ± 1.11c	13.37 ± 1.7d	1.98 ± 0.10e	122.0 ± 16.4b	
	Drought	35.1 ± 2.8ab	1.38 ± 0.22b	5.27 ± 0.63h	11.09 ± 0.7g	2.14 ± 0.15d	105.1 ± 9.6e	
Abo Kwela 2020/2021	Normal	52.6 ± 11.3d	1.41 ± 0.16a	7.06 ± 1.14b	13.55 ± 1.7d	1.94 ± 0.09e	124.5 ± 14.4b	
	Drought	35.3 ± 3.0b	1.38 ± 0.21b	5.38 ± 0.63g	11.55 ± 0.8f	2.18 ± 0.12d	108.3 ± 11.3d	
El-Neguilla 2019/2020	Normal	63.3 ± 6.5f	0.76 ± 0.02j	6.76 ± 0.57d	18.33 ± 2.1b	2.70 ± 0.08b	68.8 ± 5.0f	
	Drought	54.1 ± 3.5d	0.79 ± 0.05i	5.21 ± 0.66h	12.29 ± 1.7e	2.35 ± 0.04c	57.4 ± 5.5g	
El-Neguilla 2020/2021	Normal	63.2 ± 5.4f	0.96 ± 0.17g	6.91 ± 0.67c	19.33 ± 2.3a	2.77 ± 0.09a	69.2 ± 5.6f	
	Drought	53.7 ± 3.9e	0.82 ± 0.09h	5.00 ± 0.54i	12.00 ± 1.7e	2.38 ± 0.13c	45.8 ± 10.0h	
AL-Qasr 2019/2020	Normal	46.4 ± 1.3i	1.20 ± 0.03c	6.98 ± 0.12bd	12.02 ± 0.7e	1.72 ± 0.08h	161.5 ± 19.9a	
	Drought	42.3 ± 1.8f	1.09 ± 0.05e	5.53 ± 0.15f	9.82 ± 0.5h	1.78 ± 0.06g	112.1 ± 11.0c	
AL-Qasr 2020/2021	Normal	46.6 ± 1.2i	1.12 ± 0.03d	7.48 ± 0.34a	14.91 ± 1.9c	1.98 ± 0.16e	160.6 ± 20.3a	
	Drought	44.7 ± 1.9h	1.01 ± 0.02f	6.11 ± 0.49e	11.50 ± 0.8f	1.89 ± 0.04f	114.5 ± 10.4c	
E	SI	SY		GY		T-GW (g)	WUE	
		BY		GY			PUE	
		(t ha ⁻¹)				(kg m ⁻³)		
Abo Kwela 2019/2020	Normal	4.59 ± 0.49c	6.69 ± 0.91d	2.10 ± 0.48c	37.8 ± 7.3d	0.54 ± 0.03b	1.69 ± 0.6b	
	Drought	3.49 ± 0.67e	4.20 ± 0.71i	0.71 ± 0.04h	24.8 ± 2.3j	0.31 ± 0.09f	0.58 ± 0.09g	
Abo Kwela 2020/2021	Normal	5.21 ± 0.26b	7.31 ± 0.73c	2.10 ± 0.47c	39.6 ± 7.2c	0.55 ± 0.04b	1.91 ± 0.2a	
	Drought	3.76 ± 0.81f	4.48 ± 0.86g	0.72 ± 0.05h	25.1 ± 3.0j	0.31 ± 0.09f	0.65 ± 0.03f	
El-Neguilla 2019/2020	Normal	3.74 ± 0.57f	5.10 ± 0.85e	1.36 ± 0.29e	32.9 ± 3.3f	0.35 ± 0.02e	0.75 ± 0.1e	
	Drought	2.10 ± 0.47h	2.65 ± 0.54j	0.55 ± 0.07i	30.2 ± 2.6g	0.24 ± 0.01g	0.30 ± 0.05j	
El-Neguilla 2020/2021	Normal	3.74 ± 0.59f	5.14 ± 0.88e	1.40 ± 0.29d	34.0 ± 3.7e	0.37 ± 0.03d	1.08 ± 0.5d	
	Drought	2.09 ± 0.48h	2.64 ± 0.55j	0.55 ± 0.07i	30.8 ± 2.7g	0.24 ± 0.01g	0.43 ± 0.073i	
AL-Qasr 2019/2020	Normal	5.13 ± 0.57b	7.43 ± 1.06b	2.30 ± 0.51a	43.7 ± 7.3a	0.59 ± 0.0b	1.07 ± 0.09d	
	Drought	3.36 ± 0.61g	4.38 ± 0.75h	1.03 ± 0.18f	26.2 ± 3.4i	0.44 ± 0.02c	0.48 ± 0.02h	
AL-Qasr 2020/2021	Normal	5.43 ± 0.09a	8.11 ± 0.58a	2.68 ± 0.50a	42.8 ± 6.7b	0.70 ± 0.10a	1.30 ± 0.60c	
	Drought	3.92 ± 0.78d	4.80 ± 0.83f	0.88 ± 0.06g	27.3 ± 3.7h	0.38 ± 0.03d	0.43 ± 0.05i	

Each value represents means ± standard error. Means sharing different letters in the same column indicate statistically significant ($p \leq 0.05$) differences according to the LSD test. PH: Plant height, TI: Tillering index, SL: Spike length, SNS: Spikelet number per spike, SD: Spikelet density, NSm²: number of spike per m², SY: Straw yield, BY: Biological yield, GY: Grain yield, T-GW: Thousand-grain weight, WUE: Water use efficiency, and PUE: Precipitation use efficiency.

In Table 8, compared with 0 and 30 kg of HA ha⁻¹, crops fertilized with 60 kg HA ha⁻¹ showed significantly increased interactions of E × HA for all studied traits under normal and drought-stress conditions. On the other hand, SD was significantly decreased with the 60 kg HA ha⁻¹ treatment at the Abo Kwela site in both seasons. Compared with sites and years in E × HA interactions, the Al-Qasr site across both years reached the maximum values of GY and most studied traits. Meanwhile, the highest PH, SNS, and SD were found at the El-Neguilla site in both seasons. Generally, the application of 60 kg HA ha⁻¹ at the Al-Qasr site during the 2020/2021 season comparatively produced more GY and most other traits than other applications of HA at other sites in both seasons under normal and drought-stress conditions.

Table 8. The first-order interaction of environment (E) and humic acid (HA) treatment for the studied bread wheat traits.

Factor		PH (cm)	TI (%)	SL (cm)	SNS	SD	NSm ²
E	HA						
Abo Kwela 2019/2020	HA ₀	30.8 ± 0.4k	1.07 ± 0.03g	4.54 ± 0.52g	10.36 ± 0.58j	2.30 ± 0.13e	91.7 ± 3.7d
	HA ₃₀	45.2 ± 10.4h	1.39 ± 0.10c	6.15 ± 0.49e	11.91 ± 0.67h	1.94 ± 0.04g	112.6 ± 6.3c
	HA ₆₀	57.2 ± 17.2c	1.66 ± 0.13b	7.49 ± 1.38a	14.42 ± 2.17f	1.94 ± 0.07g	136.5 ± 15.5b
Abo Kwela 2020/2021	HA ₀	31.1 ± 1.2k	1.08 ± 0.02g	4.67 ± 0.52g	10.50 ± 0.50j	2.27 ± 0.15e	95.4 ± 6.4d
	HA ₃₀	44.9 ± 9.1h	1.39 ± 0.11c	6.25 ± 0.65e	12.33 ± 0.50h	1.99 ± 0.13fg	114.3 ± 6.3c
	HA ₆₀	55.9 ± 15.5d	1.71 ± 0.08a	7.76 ± 1.35a	14.82 ± 2.01e	1.93 ± 0.08g	139.7 ± 11.7b
El-Neguilla 2019/2020	HA ₀	49.7 ± 2.4e	0.72 ± 0.02k	4.81 ± 0.87f	11.75 ± 2.75h	2.42 ± 0.14d	54.1 ± 6.9g
	HA ₃₀	59.7 ± 3.8b	0.80 ± 0.05i	6.26 ± 0.72e	16.00 ± 3.00c	2.54 ± 0.18c	63.3 ± 4.3f
	HA ₆₀	66.8 ± 7.8a	0.80 ± 0.01i	6.89 ± 0.72b	18.18 ± 3.32b	2.62 ± 0.21b	72.0 ± 6.0e
El-Neguilla 2020/2021	HA ₀	50.0 ± 3.5e	0.67 ± 0.02l	4.81 ± 0.86f	12.25 ± 3.25h	2.41 ± 0.26d	51.8 ± 7.8gf
	HA ₃₀	59.3 ± 7.8b	0.87 ± 0.04j	6.18 ± 0.88e	15.50 ± 3.50d	2.55 ± 0.15c	49.3 ± 19.8f
	HA ₆₀	66.00 ± 6.0a	1.12 ± 0.15e	6.88 ± 1.13a	19.25 ± 4.25a	2.77 ± 0.16a	71.5 ± 7.5e
AL-Qasr 2019/2020	HA ₀	41.75 ± 2.3j	1.12 ± 0.12efi	6.09 ± 0.86e	10.05 ± 0.74j	1.67 ± 0.11i	109.2 ± 16.9c
	HA ₃₀	44.15 ± 2.4h	1.14 ± 0.00efi	6.23 ± 0.57e	10.69 ± 1.26ij	1.71 ± 0.04hi	138.8 ± 24.8b
	HA ₆₀	47.0 ± 1.5g	1.18 ± 0.05d	6.45 ± 0.75d	12.02 ± 1.30h	1.86 ± 0.02h	162.5 ± 32.4a
AL-Qasr 2020/2021	HA ₀	43.0 ± 1.5i	1.03 ± 0.02h	6.12 ± 0.83e	10.91 ± 0.81i	1.81 ± 0.11h	110.5 ± 14.3c
	HA ₃₀	45.5 ± 1.0h	1.07 ± 0.09g	6.72 ± 0.66c	13.28 ± 1.55g	1.97 ± 0.03fg	138.5 ± 23.5b
	HA ₆₀	48.4 ± 0.4f	1.09 ± 0.06fg	7.55 ± 0.56a	15.42 ± 2.75d	2.03 ± 0.21fh	163.6 ± 31.4a
E	HA	SY	BY	GY	T-GW (g)	WUE	PUE
			(t ha ⁻¹)			(kg m ⁻³)	
Abo Kwela 2019/2020	HA ₀	2.90 ± 0.71h	3.89 ± 1.07j	0.99 ± 0.36i	23.4 ± 2.2k	0.31 ± 0.01h	0.80 ± 0.04l
	HA ₃₀	4.46 ± 0.59d	5.81 ± 1.21f	1.35 ± 0.62f	30.6 ± 6.5h	0.41 ± 0.02e	1.08 ± 0.06i
	HA ₆₀	4.75 ± 0.34c	6.63 ± 1.44c	1.88 ± 1.10c	39.9 ± 10.9c	0.55 ± 0.03c	1.51 ± 0.07e
Abo Kwela 2020/2021	HA ₀	3.48 ± 1.26f	4.47 ± 1.62h	0.99 ± 0.36i	24.4 ± 2.9j	0.31 ± 0.09i	0.90 ± 0.01o
	HA ₃₀	4.69 ± 0.58c	6.04 ± 1.19e	1.35 ± 0.61f	30.9 ± 8.1h	0.42 ± 0.04f	1.23 ± 0.50n
	HA ₆₀	5.30 ± 0.34a	7.18 ± 1.43b	1.89 ± 1.09c	41.7 ± 10.7b	0.56 ± 0.03d	1.71 ± 0.08m
El-Neguilla 2019/2020	HA ₀	2.00 ± 0.71i	2.68 ± 0.97k	0.68 ± 0.26l	26.3 ± 0.7i	0.21 ± 0.01j	0.38 ± 0.01m
	HA ₃₀	2.95 ± 0.88h	3.84 ± 1.21j	0.89 ± 0.33k	31.8 ± 1.5g	0.28 ± 0.14i	0.49 ± 0.03k
	HA ₆₀	3.80 ± 0.87e	5.10 ± 1.50g	1.30 ± 0.63g	36.5 ± 2.00e	0.39 ± 0.02g	0.72 ± 0.09g
El-Neguilla 2020/2021	HA ₀	1.99 ± 0.72i	2.67 ± 0.98k	0.69 ± 0.26l	26.5 ± 2.50i	0.22 ± 0.11j	0.53 ± 0.28m
	HA ₃₀	2.91 ± 0.85h	3.85 ± 1.25j	0.94 ± 0.39j	33.2 ± 2.33f	0.29 ± 0.08i	0.72 ± 0.05j
	HA ₆₀	3.85 ± 0.91e	5.15 ± 1.54g	1.30 ± 0.63g	37.5 ± 2.0d	0.40 ± 0.01eg	1.00 ± 0.04f
AL-Qasr 2019/2020	HA ₀	3.09 ± 0.95g	4.23 ± 1.31i	1.14 ± 0.36h	26.4 ± 5.7i	0.36 ± 0.02eg	0.53 ± 0.06fk
	HA ₃₀	4.66 ± 0.74c	6.19 ± 1.36d	1.53 ± 0.62e	33.8 ± 8.3f	0.47 ± 0.08d	0.71 ± 0.04c
	HA ₆₀	4.98 ± 0.97b	7.30 ± 1.90b	2.32 ± 0.93a	44.75 ± 12.3a	0.71 ± 0.08a	1.08 ± 0.04a
AL-Qasr 2020/2021	HA ₀	3.84 ± 1.43e	5.15 ± 1.95g	1.31 ± 0.52f	26.68 ± 5.3i	0.41 ± 0.01e	0.63 ± 0.06h
	HA ₃₀	4.89 ± 0.55c	6.65 ± 1.45c	1.76 ± 0.90d	34.0 ± 7.5f	0.54 ± 0.01c	0.85 ± 0.15d
	HA ₆₀	5.29 ± 0.28a	7.56 ± 1.56a	2.27 ± 1.28b	44.5 ± 10.5a	0.68 ± 0.02b	1.10 ± 0.29b

Each value represents means ± standard error. Means sharing different letters in the same column indicate statistically significant ($p \leq 0.05$) differences according to the LSD test. PH: Plant height, TI: Tillingering index, SL: Spike length, SNS: Spikelet number per spike, SD: Spikelet density, NSm²: Number of spike per m², SY: Straw yield, BY: Biological yield, GY: Grain yield, T-GW: Thousand-grain weight, WUE: Water use efficiency, and PUE: Precipitation use efficiency. HA₀, HA₃₀, and HA₆₀ indicate the addition of 0, 30, and 60 kg ha⁻¹ humic acid, respectively.

Regarding the SI \times HA interaction (Table 9), all studied wheat traits were increased with 60 kg HA ha⁻¹ applied, followed by a decrease with 30 and 0 kg HA ha⁻¹ treatments applied under the normal and drought conditions. All studied wheat traits with the three HA treatments were observed to be higher under normal conditions than drought conditions, although 0 kg HA ha⁻¹ had a higher value of SD in drought-stress conditions as compared to normal conditions. The SI \times HA interaction recorded the highest GY and other studied traits of wheat plants fertilized with 60 kg HA ha⁻¹ and the lowest values in wheat plants fertilized with 0 kg HA ha⁻¹ of HA under normal and drought-stress conditions, which was opposite to the SD trait. In all the first-order interactions, different tendencies were observed, but based on statistical evaluation, the highest values of GY, WUE, PUE, and other important traits were found in wheat plants fertilized with 60 kg HA ha⁻¹ at the Al-Qasr site in both seasons under normal and drought conditions.

Table 9. The first-order interaction of supplemental irrigation (SI) and humic acid (HA) treatment for the studied bread wheat traits.

Factor		PH (cm)	TI (%)	SL (cm)	SNS	SD	NSm ²
SI	HA						
Normal	HA ₀	42.9 \pm 3.9e	0.99 \pm 0.09e	5.91 \pm 0.34d	12.41 \pm 0.84d	2.13 \pm 0.18c	94.8 \pm 12.0d
	HA ₃₀	55.0 \pm 3.2b	1.16 \pm 0.12c	6.96 \pm 0.10b	15.03 \pm 1.32b	2.16 \pm 0.18b	116.9 \pm 17.3b
	HA ₆₀	64.9 \pm 5.2a	1.26 \pm 0.12a	8.15 \pm 0.30a	18.32 \pm 1.50a	2.26 \pm 0.21a	141.7 \pm 21.5a
Drought	HA ₀	39.2 \pm 3.1f	0.91 \pm 0.08f	4.43 \pm 0.26f	9.53 \pm 0.20f	2.16 \pm 0.11b	76.1 \pm 9.7f
	HA ₃₀	44.5 \pm 3.7d	1.06 \pm 0.08d	5.64 \pm 0.10e	11.54 \pm 0.48e	2.08 \pm 0.11d	88.6 \pm 14.6e
	HA ₆₀	48.8 \pm 3.6c	1.25 \pm 0.18b	6.18 \pm 0.19c	13.05 \pm 0.67c	2.12 \pm 0.13c	106.9 \pm 13.3c
SI	HA	SY	BY	GY	T-GW (g)	WUE	PUE
		(t ha ⁻¹)				(kg m ⁻³)	
Normal	HA ₀	3.85 \pm 0.43d	5.16 \pm 0.56c	1.32 \pm 0.14c	28.5 \pm 1.1d	0.34 \pm 0.01f	0.86 \pm 0.82c
	HA ₃₀	4.79 \pm 0.32b	6.67 \pm 0.53b	1.88 \pm 0.22b	38.1 \pm 1.4b	0.49 \pm 0.01d	1.22 \pm 0.09b
	HA ₆₀	5.28 \pm 0.21a	8.05 \pm 0.47a	2.77 \pm 0.28a	48.9 \pm 3.2a	0.72 \pm 0.02a	1.81 \pm 0.15a
Drought	HA ₀	1.92 \pm 0.21f	2.53 \pm 0.27f	0.61 \pm 0.07f	22.7 \pm 1.0f	0.27 \pm 0.05e	0.40 \pm 0.03f
	HA ₃₀	3.39 \pm 0.43e	4.12 \pm 0.48e	0.72 \pm 0.06e	26.7 \pm 1.4e	0.31 \pm 0.06c	0.47 \pm 0.04e
	HA ₆₀	4.04 \pm 0.38c	4.92 \pm 0.43d	0.88 \pm 0.11d	32.8 \pm 1.0 c	0.38 \pm 0.02b	0.56 \pm 0.06d

Each value represents means \pm standard error. Means sharing different letters in the same column indicate statistically significant ($p \leq 0.05$) differences according to the LSD test. PH: Plant height, TI: Tillering index, SL: Spike length, SNS: Spikelet number per spike, SD: Spikelet density, NSm²: Number of spike per m², SY: Straw yield, BY: Biological yield, GY: Grain yield, T-GW: Thousand-grain weight, WUE: Water use efficiency, and PUE: Precipitation use efficiency. HA₀, HA₃₀, and HA₆₀ indicate the addition of 0, 30, and 60 kg ha⁻¹ humic acid, respectively.

3.4. The Second-Order Interaction Effect on Wheat Traits

Table 10 depicts the effect of the second-order interactions of experimental factors on GY and other investigated wheat traits under normal and drought conditions. The interaction of E \times SI \times HA revealed significant differences between the single variations in experimental factors on GY and most studied traits under normal and drought conditions. The GY and some studied traits were increased in the studied environments and HA treatments in normal conditions compared to in drought-stress conditions. Compared with other interactions of E \times SI \times HA, the highest PH, SNS, and SD values under normal and drought conditions, as well as T-GW under drought conditions, were found in wheat plants fertilized with 60 kg HA ha⁻¹ at the El-Neguilla site in both seasons. Meanwhile, the highest SL, SN, SY, BY, GY, WUE, and PUE values under normal and drought conditions, as well as T-GW under normal conditions, were observed in wheat plants treated with 60 kg of HA ha⁻¹ at the Al-Qasr site in both seasons.

Generally, from the results of the effect of experimental factors and the first- and second-order interactions, the wheat plants fertilized with 60 kg HA ha⁻¹ showed increased GY and most measured traits, while this decreased in the plants fertilized with 30 and

0 kg HA ha⁻¹. Furthermore, the highest GY, WUE, PUE, and other studied traits were obtained in wheat plants treated with 60 kg HA ha⁻¹ at the Al-Qasr site in both seasons under drought conditions.

Table 10. The second-order interaction of environment, supplemental irrigation (SI), and humic acid (HA) treatment for the studied bread wheat traits.

E	Factor		PH (cm)	TI (%)	SL (cm)	SNS	SD	NSm ²
	SI	HA						
Abo Kwela 2019/2020	Normal	HA ₀	31.2 ± 0.4i	1.10 ± 0.01e	5.06 ± 0.18h	10.94 ± 0.40a	2.17 ± 0.15c	95.4 ± 2.7g
		HA ₃₀	55.6 ± 0.3e	1.49 ± 0.02c	6.65 ± 0.19e	12.58 ± 0.01a	1.90 ± 0.06d	118.8 ± 4.2e
		HA ₆₀	74.4 ± 3.1a	1.52 ± 0.03c	8.87 ± 0.06a	16.60 ± 0.55a	1.87 ± 0.05de	151.9 ± 11.5c
	Drought	HA ₀	30.5 ± 0.3j	1.05 ± 0.01ef	4.03 ± 0.10i	9.78 ± 0.33a	2.44 ± 0.14b	87.9 ± 2.8g
		HA ₃₀	34.8 ± 0.01i	1.29 ± 0.06d	5.66 ± 0.03g	11.24 ± 0.14a	1.99 ± 0.04d	106.3 ± 5.0fg
		HA ₆₀	40.0 ± 0.04h	1.79 ± 0.02a	6.11 ± 0.12f	12.25 ± 0.20a	2.01 ± 0.01d	121.0 ± 0.4e
Abo Kwela 2020/2021	Normal	HA ₀	32.3 ± 0.4i	1.10 ± 0.00ef	5.18 ± 0.10h	11.00 ± 0.00a	2.13 ± 0.04c	101.8 ± 1.0fg
		HA ₃₀	54.0 ± 1.2e	1.50 ± 0.01c	6.90 ± 0.06de	12.83 ± 0.04a	1.86 ± 0.02d	120.5 ± 3.2e
		HA ₆₀	71.4 ± 3.8b	1.62 ± 0.01b	9.11 ± 0.12a	16.83 ± 0.48a	1.85 ± 0.03d	151.3 ± 9.5c
	Drought	HA ₀	29.9 ± 0.6i	1.07 ± 0.00ef	4.15 ± 0.09i	10.00 ± 0.58a	2.42 ± 0.19b	89.0 ± 0.6g
		HA ₃₀	35.8 ± 0.1i	1.28 ± 0.05d	5.60 ± 0.06g	11.83 ± 0.10a	2.11 ± 0.00c	108.0 ± 4.6f
		HA ₆₀	40.4 ± 0.2h	1.79 ± 0.01a	6.40 ± 0.23e	12.82 ± 0.10a	2.01 ± 0.06d	128.0 ± 1.2e
El-Neguilla 2019/2020	Normal	HA ₀	52.0 ± 1.2e	0.74 ± 0.01k	5.68 ± 0.01g	14.50 ± 0.29a	2.55 ± 0.04b	61.0 ± 0.6i
		HA ₃₀	63.5 ± 2.0c	0.75 ± 0.00k	6.99 ± 0.00d	19.00 ± 0.00a	2.72 ± 0.00a	67.5 ± 0.3i
		HA ₆₀	74.5 ± 2.6a	0.79 ± 0.00jk	7.62 ± 0.29c	21.50 ± 0.87a	2.82 ± 0.01a	78.0 ± 0.6h
	Drought	HA ₀	47.3 ± 0.2f	0.70 ± 0.00k	3.94 ± 0.04i	9.00 ± 0.58a	2.28 ± 0.12c	47.2 ± 0.5j
		HA ₃₀	55.9 ± 0.3e	0.85 ± 0.01ij	5.54 ± 0.06g	13.00 ± 0.58a	2.35 ± 0.13b	59.0 ± 0.6i
		HA ₆₀	59.0 ± 0.6d	0.81 ± 0.03ij	6.17 ± 0.04f	14.87 ± 1.08a	2.41 ± 0.16b	66.0 ± 1.7i
El-Neguilla 2020/2021	Normal	HA ₀	53.5 ± 0.9e	0.69 ± 0.03k	5.68 ± 0.01g	15.50 ± 0.29a	2.67 ± 0.01a	59.5 ± 1.4i
		HA ₃₀	64.0 ± 0.6c	0.92 ± 0.09h	7.05 ± 0.03d	19.00 ± 0.00a	2.70 ± 0.01a	69.0 ± 0.6i
		HA ₆₀	72.0 ± 2.3b	1.27 ± 0.02d	8.00 ± 0.23b	23.50 ± 0.87a	2.94 ± 0.02	79.0 ± 0.6h
	Drought	HA ₀	46.5 ± 0.3f	0.66 ± 0.01k	3.95 ± 0.03i	9.00 ± 0.58a	2.15 ± 0.05c	44.0 ± 0.6j
		HA ₃₀	54.5 ± 0.9e	0.83 ± 0.02ij	5.30 ± 0.29h	12.00 ± 0.58a	2.40 ± 0.06b	29.5 ± 16.5k
		HA ₆₀	60.0 ± 0.01d	0.97 ± 0.01h	5.75 ± 0.03g	15.00 ± 0.58a	2.61 ± 0.09a	64.0 ± 1.7i
AL-Qasr 2019/2020	Normal	HA ₀	44.0 ± 0.6g	1.24 ± 0.09d	6.95 ± 0.39d	10.78 ± 0.10a	1.56 ± 0.07g	126.1 ± 7.8e
		HA ₃₀	46.6 ± 0.6f	1.14 ± 0.02e	6.80 ± 0.03de	11.95 ± 0.53a	1.76 ± 0.09e	163.6 ± 4.0b
		HA ₆₀	48.5 ± 0.3f	1.23 ± 0.01d	7.20 ± 0.26d	13.33 ± 0.96a	1.85 ± 0.07de	194.8 ± 2.8a
	Drought	HA ₀	39.5 ± 0.3h	1.00 ± 0.03gh	5.23 ± 0.04h	9.31 ± 0.33a	1.78 ± 0.08de	92.3 ± 1.3g
		HA ₃₀	41.8 ± 0.2h	1.14 ± 0.03e	5.66 ± 0.03g	9.44 ± 0.14a	1.67 ± 0.03g	114.0 ± 2.9ef
		HA ₆₀	45.5 ± 1.4f	1.13 ± 0.06e	5.70 ± 0.02ig	10.72 ± 0.03a	1.88 ± 0.00d	130.1 ± 5.4d
AL-Qasr 2020/2021	Normal	HA ₀	44.5 ± 0.9g	1.06 ± 0.06efg	6.95 ± 0.39d	11.73 ± 0.16a	1.70 ± 0.07ef	124.8 ± 8.6de
		HA ₃₀	46.6 ± 0.6f	1.16 ± 0.00e	7.38 ± 0.22c	14.83 ± 0.68a	2.01 ± 0.03d	162.0 ± 1.7b
		HA ₆₀	48.7 ± 0.2f	1.15 ± 0.02ef	8.11 ± 0.13b	18.17 ± 0.48a	2.24 ± 0.02c	195.0 ± 2.9a
	Drought	HA ₀	41.5 ± 0.9h	1.01 ± 0.01fg	5.28 ± 0.03h	10.10 ± 0.06a	1.91 ± 0.00d	96.3 ± 1.0g
		HA ₃₀	44.5 ± 1.4g	0.98 ± 0.02fh	6.06 ± 0.03f	11.74 ± 0.04a	1.94 ± 0.00d	115.0 ± 2.9e
		HA ₆₀	48.0 ± 1.2f	1.03 ± 0.01fgh	6.99 ± 0.00d	12.67 ± 0.19a	1.81 ± 0.03def	132.3 ± 4.2d
E	SI	HA	SY	BY	GY	T-GW (g)	WUE	PUE
			(t ha ⁻¹)		(kg m ⁻³)			
Abo Kwela 2019/2020	Normal	HA ₀	3.61 ± 0.29h	4.96 ± 0.30j	1.35 ± 0.01i	25.6 ± 1.2m	0.35 ± 0.01l	1.09 ± 0.15l
		HA ₃₀	5.06 ± 0.04c	7.02 ± 0.03e	1.96 ± 0.02f	37.1 ± 2.1g	0.50 ± 0.01j	1.58 ± 0.28i
		HA ₆₀	5.10 ± 0.30c	8.08 ± 0.32c	2.98 ± 0.02c	50.9 ± 0.6d	0.76 ± 0.02d	2.40 ± 0.46d
	Drought	HA ₀	2.18 ± 0.04k	2.82 ± 0.01m	0.64 ± 0.03m	21.3 ± 0.1o	0.27 ± 0.06j	0.52 ± 0.52q
		HA ₃₀	3.87 ± 0.18hi	4.60 ± 0.17j	0.73 ± 0.01l	24.1 ± 0.4n	0.31 ± 0.02j	0.59 ± 0.20pq
		HA ₆₀	4.41 ± 0.16f	5.19 ± 0.16i	0.78 ± 0.00l	29.0 ± 0.01j	0.33 ± 0.00i	0.63 ± 0.00op

Table 10. Cont.

E	SI	HA	SY	BY	GY	T-GW (g)	WUE	PUE
			(t ha ⁻¹)				(kg m ⁻³)	
Abo Kwela 2020/2021	Normal	HA ₀	4.73 ± 0.29e	6.08 ± 0.29g	1.35 ± 0.00i	27.4 ± 0.8l	0.35 ± 0.00l	1.23 ± 0.00q
		HA ₃₀	5.26 ± 0.01cd	7.23 ± 0.00e	1.97 ± 0.01f	39.0 ± 2.3f	0.52 ± 0.01j	1.79 ± 0.08o
		HA ₆₀	5.64 ± 0.15b	8.62 ± 0.18b	2.98 ± 0.03c	52.4 ± 0.9c	0.78 ± 0.03e	2.71 ± 0.27lm
	Drought	HA ₀	2.22 ± 0.17k	2.85 ± 0.14m	0.63 ± 0.02m	21.5 ± 0.9o	0.27 ± 0.04k	0.57 ± 0.19r
		HA ₃₀	4.11 ± 0.15hi	4.85 ± 0.14j	0.74 ± 0.01l	22.8 ± 0.4no	0.32 ± 0.02j	0.67 ± 0.07r
		HA ₆₀	4.96 ± 0.02ce	5.75 ± 0.03h	0.79 ± 0.01l	31.1 ± 0.6i	0.34 ± 0.02j	0.72 ± 0.09r
El-Neguilla 2019/2020	Normal	HA ₀	2.71 ± 0.03j	3.65 ± 0.00k	0.94 ± 0.03k	27.0 ± 0.01l	0.24 ± 0.02n	0.52 ± 0.67m
		HA ₃₀	3.83 ± 0.10h	5.05 ± 0.04ij	1.22 ± 0.06j	33.3 ± 0.8i	0.31 ± 0.05m	0.67 ± 1.34k
		HA ₆₀	4.67 ± 0.13ef	6.60 ± 0.16f	1.93 ± 0.03f	38.5 ± 0.3f	0.49 ± 0.03j	1.06 ± 0.74f
	Drought	HA ₀	1.29 ± 0.03l	1.71 ± 0.03n	0.43 ± 0.00o	25.7 ± 0.4m	0.18 ± 0.01m	0.24 ± 0.07q
		HA ₃₀	2.08 ± 0.08k	2.63 ± 0.08m	0.56 ± 0.01n	30.4 ± 1.0ij	0.24 ± 0.02k	0.31 ± 0.20pq
		HA ₆₀	2.93 ± 0.08j	3.60 ± 0.10k	0.67 ± 0.01lm	34.5 ± 0.3i	0.29 ± 0.03j	0.37 ± 0.27opq
El-Neguilla 2020/2021	Normal	HA ₀	2.71 ± 0.00j	3.65 ± 0.03k	0.95 ± 0.03k	27.0 ± 0.01l	0.25 ± 0.02n	0.73 ± 0.63m
		HA ₃₀	3.76 ± 0.08h	5.09 ± 0.06ij	1.33 ± 0.02i	35.5 ± 0.3h	0.35 ± 0.01lm	1.02 ± 0.42j
		HA ₆₀	4.77 ± 0.15e	6.69 ± 0.17f	1.93 ± 0.01f	39.5 ± 0.3f	0.51 ± 0.02j	1.48 ± 0.35e
	Drought	HA ₀	1.27 ± 0.04l	1.70 ± 0.04n	0.43 ± 0.01o	26.0 ± 0.6lm	0.19 ± 0.01m	0.33 ± 0.14q
		HA ₃₀	2.06 ± 0.07k	2.60 ± 0.06m	0.55 ± 0.01n	30.9 ± 0.2i	0.24 ± 0.03k	0.42 ± 0.35opq
		HA ₆₀	2.94 ± 0.09j	3.62 ± 0.11k	0.68 ± 0.01lm	35.5 ± 0.3h	0.30 ± 0.03j	0.52 ± 0.35o
AL-Qasr 2019/2020	Normal	HA ₀	4.04 ± 0.54g	5.54 ± 0.54h	1.50 ± 0.00h	32.00 ± 0.01ik	0.38 ± 0.00k	0.70 ± 0.00g
		HA ₃₀	5.40 ± 0.06bd	7.55 ± 0.03d	2.15 ± 0.03e	42.00 ± 1.7e	0.55 ± 0.02h	1.00 ± 0.82c
		HA ₆₀	5.95 ± 0.24a	9.20 ± 0.39a	3.25 ± 0.14b	57.00 ± 0.6a	0.83 ± 0.12c	1.51 ± 4.12a
	Drought	HA ₀	2.15 ± 0.03k	2.92 ± 0.05m	0.78 ± 0.01l	20.7 ± 0.01o	0.33 ± 0.03h	0.36 ± 0.41m
		HA ₃₀	3.91 ± 0.09g	4.83 ± 0.07j	0.92 ± 0.01k	25.5 ± 0.3m	0.39 ± 0.03f	0.43 ± 0.41l
		HA ₆₀	4.01 ± 0.24g	5.40 ± 0.23i	1.39 ± 0.01i	32.5 ± 0.3i	0.59 ± 0.02a	0.65 ± 0.25h
AL-Qasr 2020/2021	Normal	HA ₀	5.27 ± 0.08cd	7.10 ± 0.12e	1.83 ± 0.04g	32.0 ± 0.6ik	0.48 ± 0.03j	0.88 ± 0.86hi
		HA ₃₀	5.44 ± 0.00bd	8.10 ± 0.06c	2.66 ± 0.06d	41.5 ± 1.4e	0.70 ± 0.05f	1.29 ± 1.23d
		HA ₆₀	5.57 ± 0.07b	9.12 ± 0.13a	3.56 ± 0.19a	55.0 ± 0.6b	0.93 ± 0.16b	1.72 ± 4.12b
	Drought	HA ₀	2.41 ± 0.28k	3.20 ± 0.23l	0.79 ± 0.05l	21.4 ± 0.4o	0.34 ± 0.12h	0.38 ± 1.11no
		HA ₃₀	4.34 ± 0.25f	5.20 ± 0.17ij	0.86 ± 0.08k	26.5 ± 0.3lm	0.38 ± 0.18g	0.42 ± 1.72n
		HA ₆₀	5.01 ± 0.06de	6.00 ± 0.00gh	0.99 ± 0.06k	34.0 ± 0.6i	0.43 ± 0.14ef	0.48 ± 1.35m

Each value represents means ± standard error. Means sharing different letters in the same column indicate statistically significant ($p \leq 0.05$) differences according to the LSD test. PH: Plant height, TI: Tilling index, SL: Spike length, SNS: Spikelet number per spike, SD: Spikelet density, NSm²: Number of spike per m², SY: Straw yield, BY: Biological yield, GY: Grain yield, T-GW: Thousand-grain weight, WUE: Water use efficiency, and PUE: Precipitation use efficiency. HA₀, HA₃₀, and HA₆₀ indicate the addition of 0, 30, and 60 kg ha⁻¹ humic acid, respectively.

3.5. Stress Tolerance Index (STI)

The STI of wheat plants fertilized with HA under different environmental conditions is presented in Table 11. The wheat plants fertilized with 60 kg HA ha⁻¹ for all studied traits had the highest STI values at the three sites in both seasons, except the Abo Kwela site in the 2020/2021 season for the SD trait. Compared with that of the Abo Kwela and El-Neguilla sites, the STI increased for GY and most traits at the Al-Qasr site in both seasons. For GY and most traits, the wheat plants treated with 60 kg HA ha⁻¹ at the Al-Qasr site in both seasons recorded the highest STI.

3.6. Pearson's Correlation Coefficient

Pearson's correlation coefficient was employed to understand the relationships between the studied wheat traits across normal and drought-stress conditions (Figure 3). The statistical evaluation showed 25 and 31 positive and significant ($p \leq 0.05$ or 0.01) correlation coefficients among the traits under the normal and drought-stress conditions, respectively. Meanwhile, the other correlation coefficients were positive and non-significant as well as negative and non-significant or significant under the two conditions.

Table 11. Stress tolerance index for the studied bread wheat traits as affected by the environment (E) and humic acid (HA) treatment.

Factor		PH (cm)	TI (%)	SL (cm)	SNS	SD	NSm ²	SY	BY	GY	T-GW (g)	WUE	PUE
E	HA												
Abo Kwela 2019/2020	HA ₀	0.32	0.89	0.41	0.46	1.11	0.60	0.37	0.32	0.22	0.37	0.61	0.85
	HA ₃₀	0.66	1.49	0.77	0.61	0.79	0.91	0.91	0.74	0.36	0.60	1.01	1.02
	HA ₆₀	1.01	2.10	1.10	0.87	0.79	1.33	1.04	0.95	0.59	1.00	1.64	1.19
Abo Kwela 2020/2021	HA ₀	0.33	0.91	0.44	0.47	1.08	0.65	0.49	0.39	0.21	0.40	0.49	0.86
	HA ₃₀	0.66	1.48	0.79	0.65	0.82	0.94	1.00	0.80	0.37	0.60	0.83	1.01
	HA ₆₀	0.98	2.24	1.19	0.93	0.78	1.40	1.30	1.13	0.59	1.10	1.36	1.19
El-Neguilla 2019/2020	HA ₀	0.83	0.40	0.46	0.56	1.22	0.21	0.16	0.14	0.10	0.47	0.29	0.89
	HA ₃₀	1.20	0.49	0.79	1.06	1.34	0.29	0.37	0.30	0.17	0.68	0.49	0.88
	HA ₆₀	1.49	0.49	0.96	1.37	1.43	0.37	0.64	0.54	0.33	0.90	0.93	1.05
El-Neguilla 2020/2021	HA ₀	0.84	0.35	0.46	0.60	1.20	0.19	0.16	0.14	0.10	0.47	0.30	0.88
	HA ₃₀	1.18	0.59	0.76	0.98	1.36	0.15	0.36	0.30	0.18	0.74	0.53	0.95
	HA ₆₀	1.47	0.95	0.94	1.51	1.61	0.36	0.65	0.55	0.33	0.95	0.95	1.05
Al-Qasr 2019/2020	HA ₀	0.59	0.96	0.74	0.43	0.58	0.84	0.40	0.37	0.30	0.45	0.86	0.78
	HA ₃₀	0.66	1.00	0.78	0.48	0.62	1.34	0.98	0.83	0.50	0.72	1.46	0.93
	HA ₆₀	0.75	1.07	0.84	0.61	0.73	1.83	1.11	1.13	1.14	1.25	2.34	0.93
Al-Qasr 2020/2021	HA ₀	0.63	0.83	0.75	0.51	0.68	0.87	0.59	0.52	0.36	0.46	1.04	0.92
	HA ₃₀	0.70	0.88	0.91	0.75	0.82	1.34	1.10	0.96	0.58	0.74	1.63	1.09
	HA ₆₀	0.79	0.92	1.15	0.99	0.85	1.86	1.30	1.25	0.89	1.26	2.52	1.17

PH: Plant height, TI: Tillingering index, SL: Spike length, SNS: Spikelet number per spike, SD: Spikelet density, NSm²: Number of spike per m², SY: Straw yield, BY: Biological yield, GY: Grain yield, T-GW: Thousand-grain weight, WUE: Water use efficiency, and PUE: Precipitation use efficiency. HA₀, HA₃₀, and HA₆₀ indicate the addition of 0, 30, and 60 kg ha⁻¹ humic acid, respectively.

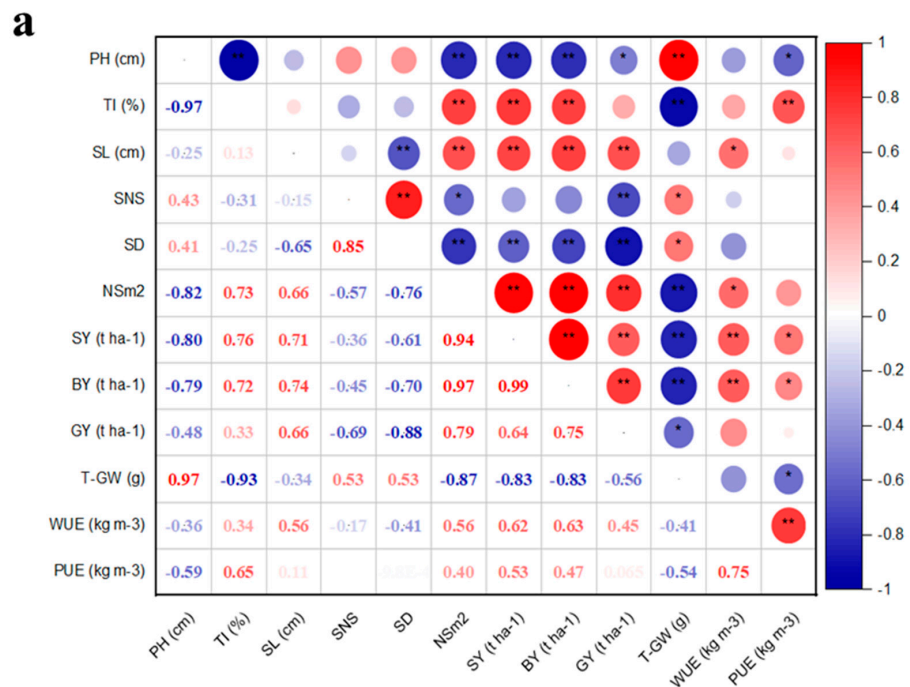


Figure 3. Cont.

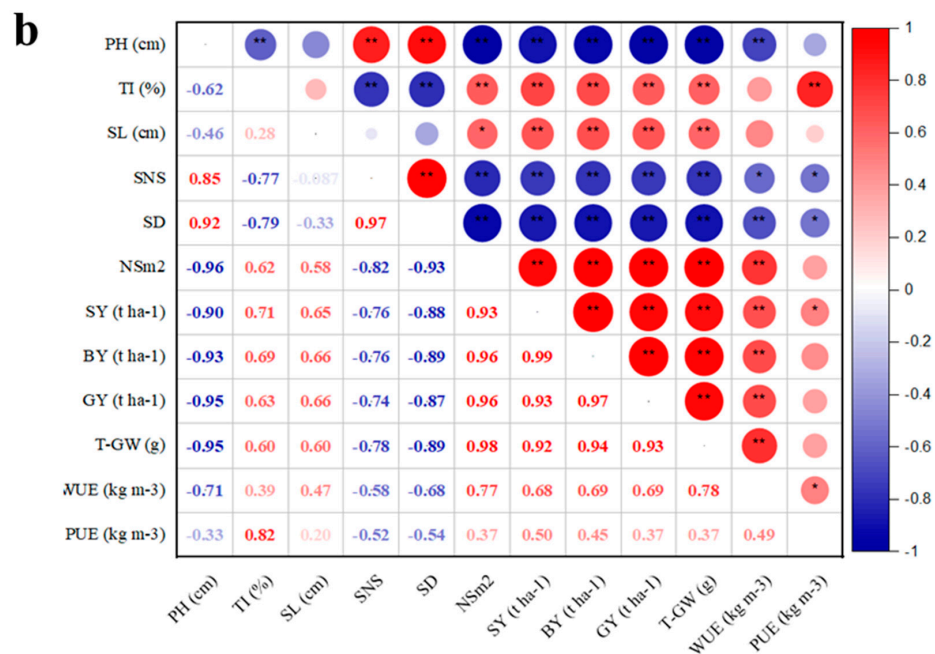


Figure 3. Plot describing Pearson’s correlation between studied traits in the normal (a,b) drought-stress conditions. PH: Plant height, TI: Tillingering index, SL: Spike length, SNS: Spikelet number per spike, SD: Spikelet density, NSm²: Number of spike per m², SY: Straw yield, BY: Biological yield, GY: Grain yield, T-GW: Thousand-grain weight, WUE: Water use efficiency, and PUE: Precipitation use efficiency. The large and medium blue (positive) and red (negative) circles indicate a significant (* $p \leq 0.05$) or highly significant (** $p \leq 0.01$) correlation, while the small blue (positive) and red (negative) circles indicate a non-significant correlation.

Under the normal conditions (Figure 3a), SL, SN, SY, BY, GY, and WUE, as well as SNS, SD, and T-GW, had positive and significant correlations ($p \leq 0.05$ or 0.01) across all factors studied. PH was significantly positively correlated with T-GW ($p \leq 0.01$). TI showed significant positive correlations ($p \leq 0.01$) with NS, SY, BY, and PUE. In this respect, PUE showed significant positive correlations ($p \leq 0.01$) with SY and BY ($p \leq 0.05$) and WUE ($p \leq 0.01$).

Regarding drought-stress conditions (Figure 3b), a high, significant, positive correlation ($p \leq 0.01$) was observed among all possible pairs for NS, SY, BY, GY, T-GW, and WUE, as well as for PH, SNS, and SD. TI and SL showed high, significant, positive correlations ($p \leq 0.01$) with NS, SY, BY, GY, and T-GW. PUE was significantly positively correlated with TI ($p \leq 0.01$), SY, and WUE ($p \leq 0.05$). Generally, the highest positive correlation was observed among the traits of SN, SY, BY, GY, and WUE under normal and drought conditions.

3.7. Principal Component Analysis (PCA)

The seven PCs for all bread wheat traits based on E, SI, and HA treatments are shown in Table 12. Out of all PCs, the two first main PCs (PC1 and PC2) extracted had eigenvalues larger than one (Eigenvalue > 1) with values of 7.57 and 3.39, respectively. Meanwhile, the rest of the other PCs had eigenvalues less than one (Eigenvalue < 1). Therefore, PC1 and PC2 were retained for the final analysis, in which these two PCs explain more variance than an individual attribute [42] and express more variability and support to select the trait with a positive loading factor. The first two PCs contributed 91.35% of the total variation existing among studied traits regarding E, SI, and HA variables. The contributions of PC1 to the total variance were higher than that of PC2 (28.27%), with PC1 describing approximately only 63.07% of the measured data total variability. The results of PC1 and PC2 may be used

to summarize the original variables in any further analysis of the data, as well as to explain the total variance and the collection of the PCs.

Table 12. Results of principal component analysis (PCA) in the first seven principal components (PCs) for the studied bread wheat traits as affected by the three experimental factors (i.e., environment, supplemental irrigation, and humic acid).

Trait	PC1	PC2	PC3	PC4	PC5	PC6	PC7
PH (cm)	−0.01	0.53	−0.05	0.34	−0.23	−0.42	0.32
TI (%)	0.25	−0.22	0.63	0.56	−0.04	0.14	0.29
SL (cm)	0.32	0.25	−0.13	0.08	0.34	−0.01	0.25
SNS	0.05	0.53	0.08	−0.04	0.29	0.31	0.05
SD	−0.21	0.42	0.28	−0.16	0.16	0.39	−0.06
N Sm^2	0.32	−0.23	−0.19	0.10	0.08	0.29	0.17
SY (t ha $^{-1}$)	0.36	−0.03	0.03	0.00	0.52	−0.36	−0.28
BY (t ha $^{-1}$)	0.36	0.00	−0.04	−0.16	0.20	−0.24	0.02
GY (t ha $^{-1}$)	0.35	0.06	−0.14	−0.45	−0.38	0.02	0.49
T-GW (g)	0.30	0.28	−0.16	0.32	−0.43	−0.02	−0.56
WUE (kg m $^{-3}$)	0.35	−0.01	−0.23	0.07	−0.11	0.52	−0.17
PUE (kg m $^{-3}$)	0.30	0.07	0.60	−0.43	−0.24	−0.12	−0.23
Eigenvalues	7.57	3.39	0.78	0.15	0.07	0.03	0.01
Variance (%)	63.07	28.27	6.50	1.26	0.61	0.22	0.05
Cumulative (%)	63.07	91.35	97.85	99.11	99.72	99.93	99.99

PH: Plant height, TI: Tilling index, SL: Spike length, SNS: Spikelet number per spike, SD: Spikelet density, N Sm^2 : Number of spike per m 2 , SY: Straw yield, BY: Biological yield, GY: Grain yield, T-GW: Thousand-grain weight, WUE: Water use efficiency, and PUE: Precipitation use efficiency.

Based on the data of E, SI, and HA variables (Table 12), PC1 had a high positive correlation with all studied traits, except PH and SD traits, while it was related to wheat GY, WUE, and PUE under both conditions in the present study. These variables of the wheat GY and its components contributed to PC1. PC2 identified all studied traits possessing positive loading factors and contributes to the variables except TI, SN, SY, and WUE traits, while the most variables studied had the highest positive loadings on PC3 and other PCs under experimental factors. Based on the studied traits (Table 13), the Al-Qasr and Abo Kwela sites in both years with 60 kg HA ha $^{-1}$ influenced PC1, while PC2 was affected by the El-Neguilla site and 60 kg HA ha $^{-1}$ in both seasons under normal conditions. During normal irrigation conditions, PC1 included 30 and 60 kg HA ha $^{-1}$ applications in the Al-Qasr and Abo Kwela sites in both seasons, while PC2 consisted of 60 kg HA ha $^{-1}$ application at the El-Neguilla site in both seasons.

Based on all measured data, PC1 and PC2 mainly distributed and distinguished the experimental factors and studied traits in different groups. Therefore, the first two PCs were employed to draw a biplot (Figure 4). The data of variables studied displayed a positive correlation between most studied traits, but they differed in their degree and consistency in quantity. The biplot diagram depicted the contribution of E, SI, and HA in creating variability of all traits measured.

In PC1 (Figure 4), GY and other investigated traits, excluding PH, SNS, and SD, were highly and positively associated with the Al-Qasr and Abo Kwela sites in both seasons, with 30 and 60 kg HA ha $^{-1}$ under normal irrigation conditions, which was located in the first and fourth quarters. Regarding PC2, PH, SD, and SNS traits had a positive correlation with the El-Neguilla site in both seasons with 0 kg HA ha $^{-1}$ under drought-stress conditions, which occupied the second and third quadrants. The 60 kg HA ha $^{-1}$ treatment at the Al-Qasr site in the 2020/21 season was located near GY and its component traits, as well as WUE and PUE parameters under the normal and drought-stress conditions. Regarding the relationships between all studied traits by PCA, WUE and PUE are strongly correlated with GY and its component traits under normal and drought-stress conditions. The PCA scree plot for E, SI, and HA on GY and other traits evaluated showed that the PC1 and PC2 eigenvalues correspond to the whole percentage of the variance in the dataset (Figure 5).

Table 13. Results of principal components (PCs) for the studied bread wheat traits as affected by the environment (E) and humic acid (HA) treatments under supplemental irrigation (SI) mode (i.e., normal and drought) conditions.

Factors	PC1	PC2	PC3	PC4	PC5	PC6	PC7
E							
Abo Kwela 2019/2020	0.76	−1.35	1.25	0.08	−0.11	0.08	0.17
Abo Kwela 2020/2021	1.53	−1.17	1.54	−0.09	0.19	−0.10	−0.13
El-Neguilla 2019/2020	−3.45	2.45	−0.57	0.01	0.09	−0.10	0.07
El-Neguilla 2020/2021	−3.07	2.62	0.34	0.00	−0.15	0.05	−0.08
Al-Qasr 2019/2020	1.73	−1.98	−1.31	0.27	−0.46	−0.17	−0.03
Al-Qasr 2020/2021	2.47	−0.55	−1.30	−0.32	0.46	0.19	0.00
SI							
Normal	3.11	1.69	0.11	−0.55	−0.17	−0.07	0.02
Drought	−3.06	−1.71	−0.09	0.59	0.16	0.11	−0.02
HA							
HA ₀	−3.43	−1.96	−0.06	−0.63	−0.21	0.12	−0.01
HA ₃₀	0.02	−0.04	−0.03	0.13	0.33	−0.31	0.04
HA ₆₀	3.41	2.01	0.12	0.51	−0.13	0.20	−0.02

HA₀, HA₃₀, and HA₆₀ indicate the addition of 0, 30, and 60 kg ha^{−1} humic acid, respectively.

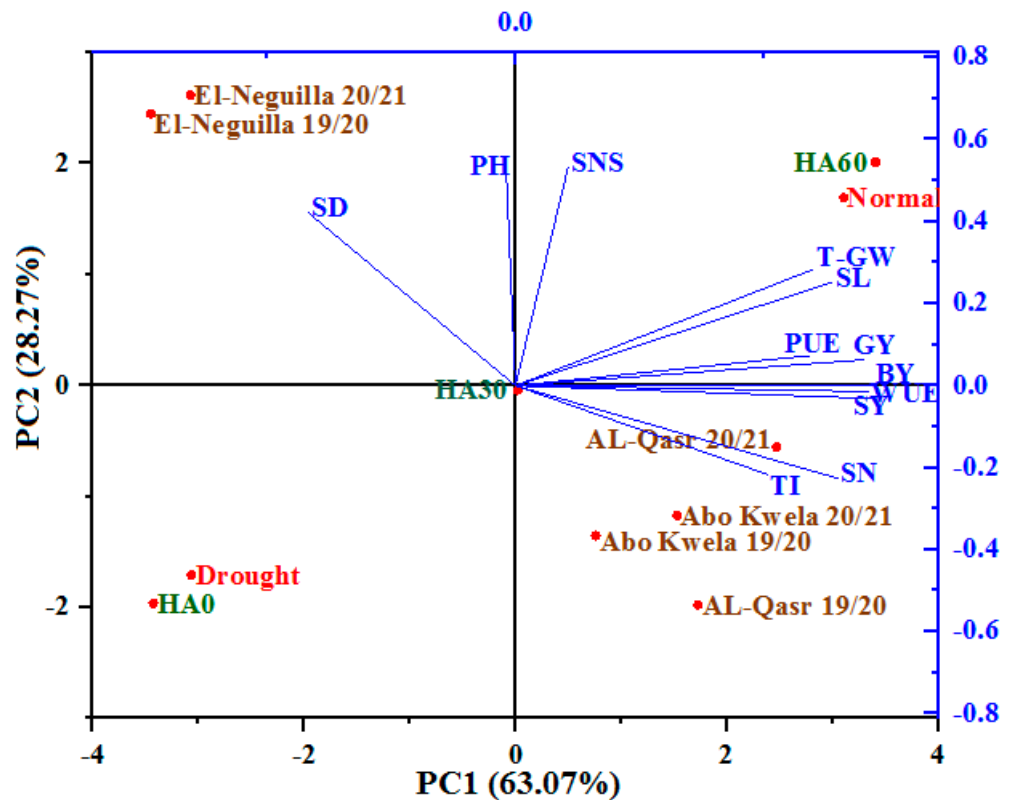


Figure 4. Biplot diagram of PC1 and PC2 shows similarities and dissimilarities in relationships between the studied traits for the studied factors under normal and drought conditions. HA₀, HA₃₀, and HA₆₀ indicate the addition of 0, 30, and 60 kg ha^{−1} humic acid, respectively. PH: Plant height, TI: Tillering index, SL: Spike length, SNS: Spikelet number per spike, SD: Spikelet density, Nsm²: number of spike per m², SY: Straw yield, BY: Biological yield, GY: Grain yield, T-GW: Thousand-grain weight, WUE: Water use efficiency, and PUE: Precipitation use efficiency.

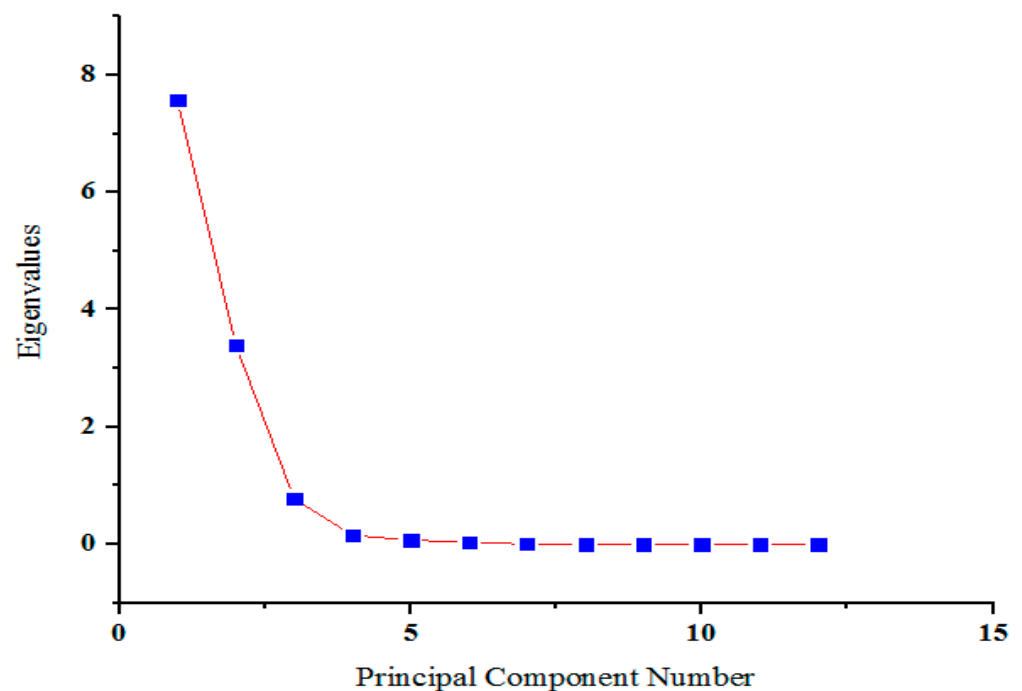


Figure 5. Scree plot of PCA between respective eigenvalues % and component number.

4. Discussion

The current study evaluated GY and other quantitative traits of the cultivar Sakha 94 fertilized with HA in different environments (three sites over two years) under normal and drought-stress conditions. Statistically, GY and most traits were significantly affected by E, SI, and HA, as well as first- and second-order interactions. These results indicated the existence of variability between our experimental factors for drought tolerance; thus, improvement can be achieved for wheat GY in Egypt. Some previous studies reported conclusions similar to our results; for example, [43–46] mentioned that HA and years had highly significant effects on all production components in wheat. Pačuta et al. [46] confirmed significant differences in the first- and second-order interactions for GY in wheat. The differences between years were oftentimes weather-related [43]. Thus, we can assume that weather conditions, HA, and SI were the causes of significant differences for all studied traits of bread wheat. Cultivar-specific differences can play an important role in helping wheat breeders to develop more climate-change-resistant wheat [47].

Based on C.V. % values, the environmental influence was low (<10%) for all studied traits, so this trial would be considered to have high precision. The SN, SY, and PUE traits showed that the C.V. % values ($10 > \text{C.V. \%} > 7\%$) were greater than that of the other traits measured. Thus, the environmental influence was high for these traits in the normal and drought-stress conditions when compared to the other traits. This would suggest the existence of substantial differences among experimental factors for the studied traits in their drought response. The magnitude of C.V. % indicated that the wheat plants fertilized with HA had exploitable variability during the selection of GY and other traits under the various environments. These findings were consistent with [48] and different from [49–51] in wheat. The values of C.V. % confirmed the existence of high diversity and it is a useful resource in providing the fundamentals for future breeding under stress conditions [51,52].

Mean values indicated that the interactions among experimental factors revealed that there was different behavior for studied traits in normal and drought-stress conditions. Thus, it is possible to use these data in the future to increase wheat GY in Egypt. Generally, the drought-stress conditions during critical stages of growth reduced all studied traits compared to normal conditions, with decreased values ranging from 1% for SD to 46% for GY. Our results are also in agreement with [47,48,50,53–55]. The decrease in GY and

its related traits under drought-stress conditions is a popular phenomenon and can be controlled by many complex morphological, physiological, and molecular factors during plant growth stages [56]. The largest impact of drought on the grain yield of wheat may be partially due to the accumulative effects that it exerts on grain yield-related characteristics [57], pre-anthesis, post-anthesis, anthesis, and booting stages [58], and the grain-filling duration [48].

Our study revealed that GY and most studied traits were significantly higher at the Al-Qasr site in both seasons than those at the Abo Kwela and El-Neguilla sites under normal and drought-stress conditions, regardless of HA rates. Wheat productivity and other traits increased at the Al-Qasr site due to the high seasonal rainfall rates during the studied seasons, and the extent of the increase was 10% and 20% in the 2019/2020 season, as well as 50% and 45% in the 2020/2021 season, compared to the El-Neguilla and Abo Kwela sites, respectively. Applying 60 kg HA ha⁻¹ led to a significant increase in wheat GY and its traits compared to 0 and 30 kg HA ha⁻¹ under the two conditions, regardless of the other factors studied. We also found that all studied traits of normal conditions were higher than that of drought-stress conditions, regardless of the other two factors studied. In the study by [45], the growing season affected the GY and T-GW of durum wheat differently; also, the behavior of the genotypes changed in relation to growing years. Wheat production varies greatly from year to year. Lower GY may be due to rainfall variability in the wheat-growing season [46]. As reported in [59], wheat plants respond to drought stress through changes in various metabolic and physiological processes. The significant increase in GY and other traits due to HA application compared to the control treatment was also reported previously by [27,46,60,61].

Regarding the first-order interactions, the highest GY and most traits were found in the interaction of E × SI (Al-Qasr in both seasons × normal conditions), the interaction of E × HA (Al-Qasr in both seasons × 60 kg HA ha⁻¹), and the interaction of SI × HA (normal conditions × 60 kg HA ha⁻¹). As for the second-order interaction, the highest GY and most studied traits were found for the interaction of Al-Qasr × normal conditions × 60 kg HA ha⁻¹ in both seasons under the two conditions. These results may be due to enabling the plants to adapt to drought conditions. The GY and other studied traits have been observed to increase via the combination of factors in an experiment that evaluated and recorded the highest values of every single factor, as already reported by [45,46].

STI is used for the identification of high-tolerance genotypes based on the ratio of means under normal and drought-stress conditions [41]. Compared with all experimental factors in our study, the wheat plants fertilized with 60 kg HA ha⁻¹ at the Al-Qasr site in both seasons recorded the highest STI for GY and most studied traits under normal and drought-stress conditions. The application of 60 kg HA ha⁻¹ differed from other HA rates by showing higher performance under drought conditions, hence having higher STI values. Thus, wheat plants under the 60 kg HA ha⁻¹ application had the lowest susceptibility to drought stress. STI was most useful to identify genotypes differing in their response to drought in wheat [50] and barley [62].

The reciprocal correlations among most studied traits were positive and insignificant or significant ($p \leq 0.05$ or 0.01) under normal and drought-stress conditions. Generally, the GY was positively and significantly correlated with the most studied traits under both conditions. Positive correlations for studied traits indicated that selection for the increased value of one trait will result in an increase in the value of the other [63], where the contrasting GY change is a consequence of the changes in yield components [64]. Statistically, a significant correlation was noted for GY and other traits under drought-stress conditions by [49,65]. Significant correlations between most of the traits were found under rainfed and water-stress conditions in different years, which also explained why an increase in these traits would further enhance GY under both conditions [50].

Principal component analysis (PC) has been used to estimate the similarities and dissimilarities in the relationships between the studied traits across environments, supplemental irrigation, and HA variables. Similarly, Koua et al. [51] reported that the first

two PCs explain the total variance under drought-stress conditions better than in rainfed conditions. In agreement with [66], PC1 and PC2 explain more than 90% of the total variance of all variables studied in both conditions. Meanwhile, both PCs explained lower values in our results than those in [44,49,50,67,68]. PC1 explained approximately <63% of the measured data total variability in the original variables under normal and drought-stress conditions in our study, similar to other studies [66–68]. It is evident that PC1 and PC2 can be interpreted as a response related to WUE and PUE, as well as GY and its components traits, which possess positive and negative contributions to the experimental factors. PC1 is considered very important to increase wheat GY under drought-stress conditions. Likewise, PC1 characterized GY and other agronomic traits under drought stress in winter wheat in both seasons [50], while PC2 seems to represent humic substances [67]. The biplot showed the degree of correlation amongst most studied wheat traits under E, SI, and HA variables. In other studies, the statistical analysis of PCA exhibited a strong correlation among the studied traits of wheat in both seasons under drought stress [49,50]. PC1 obtained higher loading values for all traits measured, except PH, SNS, and SD, and it also included wheat plants under the 60 kg HA ha⁻¹ application at the Al-Qasr site in both seasons under normal irrigation conditions. The results of the scree plot were harmonic with [69] who reported that there is a break in the plot that separates the meaningful components from the trivial components. Thus, most researchers would agree that PC1 and PC2 are likely meaningful.

The biplot analysis of the relationship between the variables studied revealed that wheat plants under 60 kg HA ha⁻¹ treatment at the Al-Qasr site in both seasons gave the highest wheat GY under normal and drought-stress conditions. In line with this study, Hegab et al. [70] have already stated that wheat GY and its components increased with an increasing the application of HA rates. It is worth noting that HA application in wheat promoted plant growth, yields (grain, straw, and biological), nutrient uptake in the soil, and resistance to biotic and abiotic stress. Furthermore, previous authors [59,71–73] mentioned that HA increased the levels of 40 compounds that are associated with the stress response. HA molecules promote the osmotic adjustment ability, increase leaf water retention, as well the photosynthetic and antioxidant metabolism of plants under drought stress [74,75]. The integration of HA application and a water deficit makes it possible to assess the precision and efficiency of the system in researching the effect of HA on drought tolerance [45,76]. Moreover, the traits may respond differently across genotypes, showing different types of drought tolerance [77]. Generally, our results showed that there is a divergence between environments (sites and seasons) and HA rates under normal irrigation and drought-stress conditions, and thus, these diversities can be used to improve wheat GY under drought-stress conditions.

5. Conclusions

Significant divergences between different environments (sites and seasons) and HA rates under normal irrigation and drought-stress conditions, as well as their interactions for wheat GY and most traits evaluated, were observed via a three-way ANOVA. Drought stress markedly decreased wheat GY and its components compared to normal conditions under the studied factors. The Al-Qasr site had the highest positive impact on GY and most studied traits in both seasons. The application of HA at a rate of 60 kg ha⁻¹ markedly increased all studied traits compared with 0 and 30 kg ha⁻¹. The highest level of GY and most of its traits was recorded when fertilizing wheat plants with 60 kg HA ha⁻¹ under normal and drought-stress conditions at the Al-Qasr site. The results of STI, Pearson's correlation coefficients, and PCA in our study could be useful and used as a suitable method for studying drought tolerance mechanisms and wheat GY improvement. Finally, the application of the 60 kg HA ha⁻¹ dose is recommended to obtain the maximum wheat productivity under drought-stress conditions in Egypt.

Author Contributions: Conceptualization: E.F.E.-H., M.M.A.E.-E., M.A.E.-H.A. and K.A.E.-T.; investigation, methodology, and data curation: M.A.E.-H.A. and M.M.A.E.-E.; preparing original draft: E.F.E.-H., M.M.A.E.-E., K.A.E.-T. and A.S.; review and final editing: A.S., E.F.E.-H., M.M.A.E.-E., K.A.E.-T.; M.T.E.-S. and T.A.A.E.-M. All authors have read and agreed to the published version of the manuscript.

Funding: This project was funded by the Abu Dhabi Research Award (AARE2019) for Research Excellence-Department of Education and Knowledge (ADEK; Grant #: 21S105) to Khaled A. El-Tarabily.

Data Availability Statement: The datasets used and/or analyzed during the current study are available from the corresponding author on reasonable request.

Acknowledgments: Khaled A. El-Tarabily would also like to thank the library at Murdoch University, Australia, for the valuable online resources and comprehensive databases. All authors give thanks and gratitude to the PRIMA project entitled Development and Optimization of Halophyte-based Farming systems in salt affected Mediterranean soils, for the availability of the requirements for conducting research in the study areas, and especially thank Hasan Mohamed El-Shaer, head of the project.

Conflicts of Interest: The authors declare that they have no competing interests.

References

1. FAO. 2019. Available online: <http://www.fao.org/3/cb1329en/CB1329EN.pdf> (accessed on 21 July 2021).
2. Ghasemi-Mobtaker, H.; Kaab, A.; Rafiee, S. Application of life cycle analysis to assess environmental sustainability of wheat cultivation in the west of Iran. *Energy* **2020**, *193*, 116768. [CrossRef]
3. USDA. United States Department of Agriculture. World Agricultural Production. March 2022. Available online: <https://apps.fas.usda.gov/psdonline/circulars/production.pdf> (accessed on 8 April 2022).
4. FAO. FAOSTAT Wheat Production Statistics 2016. Available online: www.fao.org/faostat/en/#data/TP (accessed on 20 June 2020).
5. Abd El-Mageed, T.A.; El-Sherif, A.M.; Abd El-Mageed, S.A.; Abdou, N.M. A novel compost alleviate drought stress for sugar beet production grown in Cd-contaminated saline soil. *Agric. Water Manag.* **2019**, *226*, 105831. [CrossRef]
6. Rady, M.O.A.; Semida, W.M.; Howladar, S.M.; Abd El-Mageed, T.A. Raised beds modulate physiological responses, yield and water use efficiency of wheat (*Triticum aestivum* L.) under deficit irrigation. *Agric. Water Manag.* **2021**, *245*, 106629. [CrossRef]
7. Rady, M.O.A.; Semida, W.M.; Abd El-Mageed, T.A.; Howladar, S.M.; Shaaban, A. Foliage applied selenium improves photosynthetic efficiency, antioxidant potential and wheat productivity under drought stress. *Int. J. Agric. Biol.* **2020**, *24*, 1293–1300.
8. Food and Agriculture Organization of the UN (FAO). AQUASTAT-FAO's Global Information System on Water and Agriculture. Available online: <http://www.fao.org/aquastat/en/> (accessed on 20 December 2019).
9. Shaaban, A.; Al-Elwany, O.A.; Abdou, N.M.; Hemida, K.A.; El-Sherif, A.; Abdel-Razek, M.A.; Semida, W.M.; Mohamed, G.F.; Abd El-Mageed, T.A. Filter mud enhanced yield and soil properties of water-stressed *Lupinus termis* L. in saline calcareous soil. *J. Soil Sci. Plant Nutr.* **2022**, *22*, 1572–1588. [CrossRef]
10. Ouda, S.; Noreldin, T.; Alarcón, J.J.; Ragab, R.; Caruso, G.; Sekara, A.; Abdelhamid, M.T. Response of spring wheat (*Triticum aestivum*) to deficit irrigation management under the semi-arid environment of Egypt: Field and modeling study. *Agriculture* **2021**, *11*, 90. [CrossRef]
11. Ouda, S.A.H.; Noreldin, T.; Amer, A. Rain fed areas in Egypt: Obstacles and opportunities. In *Management of Climate Induced Drought and Water Scarcity in Egypt*; Springer: Cham, Switzerland, 2016; pp. 27–46.
12. Agami, R.A.; Alamri, S.A.M.; Abd El-Mageed, T.A.; Abousekken, M.S.M.; Hashem, M. Salicylic acid and proline enhance water use efficiency, antioxidant defense system and tissues anatomy of wheat plants under field deficit irrigation stress. *J. Appl. Bot. Food Qual.* **2019**, *92*, 360–370. [CrossRef]
13. Kumar, A.; Verma, R.P.; Singh, A.; Sharma, H.K.; Devi, G. Barley landraces: Ecological heritage for edaphic stress adaptations and sustainable production. *Environ. Sustain. Indic.* **2020**, *6*, 100035. [CrossRef]
14. Cooper, P.J.M.; Gregory, P.J.; Keating, J.D.H.; Brown, S.C. Effects of fertilizer, variety and site on barley production under rainfed conditions in Northern Syria 2. Soil water dynamics and crop water use. *Field Crops Res.* **1987**, *16*, 67–84. [CrossRef]
15. Man, J.; Shi, Y.; Yu, Z.; Zhang, Y. Root growth, soil water variation, and grain yield response of winter wheat to supplemental irrigation. *Plant Prod. Sci.* **2016**, *19*, 193–205. [CrossRef]
16. Ilbeyi, A.; Ustun, H.; Oweis, T.; Pala, M.; Benli, B. Wheat water productivity and yield in a cool highland environment: Effect of early sowing with supplemental irrigation. *Agric. Water Manag.* **2006**, *82*, 399–410. [CrossRef]
17. Benli, B.; Pala, M.; Stockle, C.; Oweis, T. Assessment of winter wheat production under early sowing with supplemental irrigation in a cold highland environment using CropSyst simulation model. *Agric. Water Manag.* **2007**, *93*, 45–53. [CrossRef]
18. Xiao, G.; Zhang, Q.; Xiong, Y.; Lin, M.; Wang, J. Integrating rainwater harvesting with supplemental irrigation into rain-fed spring wheat farming. *Soil Till. Res.* **2007**, *93*, 429–437. [CrossRef]
19. Erekul, O.; Gotz, K.P.; Gurbuz, T. Effect of supplemental irrigation on yield and bread-making quality of wheat (*Triticum aestivum* L.) varieties under the Mediterranean climatical conditions. *Turk. J. Field Crops* **2012**, *17*, 78–86.

20. Tadayon, M.R.; Ebrahimi, R.; Tadayyon, A. Increased water productivity of wheat under supplemental irrigation and nitrogen application in a semi-arid region. *J. Agric. Sci. Technol.* **2012**, *14*, 995–1003.
21. Keatinge, J.D.H.; Neate, P.J.; Shepherd, K.D. The role of fertilizer management in the development and expression of crop drought stress in cereals under mediterranean environmental conditions. *Exp. Agric.* **1985**, *21*, 209–222. [CrossRef]
22. Singh, R.S.; Prihar, Y.S.S.; Singh, P. Effects of N fertilization on yield and water use efficiency of dryland wheat as affected by stored water and rainfall. *Agron. J.* **1975**, *67*, 599–603. [CrossRef]
23. Cattivelli, F.S.; Sayed, A.H.; Hu, X.; Lee, D.; Vespa, P. Mathematical models of cerebral hemodynamics for detection of vasospasm in major cerebral arteries. In *Acta Neurochirurgica Supplements*; Springer: Vienna, Austria, 2008; pp. 63–69.
24. Qiao, J.; Wang, J.; Zhao, D.; Zhou, W.; Schwenke, G.; Yan, T.; Li Liu, D. Optimizing N fertilizer rates sustained rice yields, improved N use efficiency, and decreased N losses via runoff from rice-wheat cropping systems. *Agric. Ecosys Environ.* **2022**, *324*, 107724. [CrossRef]
25. Mekdad, A.A.; El-Sherif, A.; Rady, M.M.; Shaaban, A. Culture management and application of humic acid in favor of *Helianthus annuus* L. oil yield and nutritional homeostasis in a dry environment. *J. Soil Sci. Plant Nutr.* **2021**, *22*, 71–86. [CrossRef]
26. Semida, W.M.; Abd El-Mageed, T.A.; Howladar, S.M.; Mohamed, G.F.; Rady, M.M. Response of *Solanum melongena* L. seedlings grown under saline calcareous soil conditions to a new organo-mineral fertilizer. *J. Anim. Plant Sci.* **2015**, *25*, 485–493.
27. Khan, R.U.; Khan, M.Z.; Khan, A.; Saba, S.; Hussain, F.; Jan, I.U. Effect of humic acid on growth and crop nutrient status of wheat on two different soils. *J. Plant Nutr.* **2018**, *41*, 453–460. [CrossRef]
28. Olk, D.C.; Dinnes, D.L.; Scoresby, J.R.; Callaway, C.R.; Darlington, J.W. Humic products in agriculture: Potential benefits and research challenges a review. *J. Soils Sediment* **2018**, *18*, 2881–2891. [CrossRef]
29. Rady, M.M.; Boriek, S.H.K.; Abd El-Mageed, T.A.; El-Yazal, M.A.S.; Ali, E.F.; Hassan, F.A.S.; Abdelkhalik, A. Exogenous gibberellic acid or dilute bee honey boosts drought stress tolerance in *Vicia faba* by rebalancing osmoprotectants, antioxidants, nutrients, and phytohormones. *Plants* **2021**, *10*, 748. [CrossRef] [PubMed]
30. Dinçsoy, M.; Sönmez, F. The effect of potassium and humic acid applications on yield and nutrient contents of wheat (*Triticum aestivum* L. var. Delfii) with same soil properties. *J. Plant Nutr.* **2019**, *42*, 2757–2772. [CrossRef]
31. Piccolo, A.; Nardi, S.; Concheri, G. Structural characteristics of humic substances as regulated to nitrate uptake and growth regulation in plant systems. *Soil Biol. Biochem.* **1992**, *24*, 373–380. [CrossRef]
32. Abdelrasheed, K.G.; Mazrou, Y.; Omara, A.E.; Osman, H.S.; Nehela, Y.; Hafez, E.M.; Rady, A.; El-Moneim, D.A.; Alowaiesh, B.F.; Gawayed, S.M. Soil amendment using biochar and application of K-humate enhance the growth, productivity, and nutritional value of onion (*Allium cepa* L.) under deficit irrigation conditions. *Plants* **2021**, *10*, 2598. [CrossRef]
33. IUSS Working Group WRB. *World Reference Base for Soil Resources 2014, Update 2015. International Soil Classification System for Naming Soils and Creating Legends for Soil Maps*; World Soil Resources Reports No. 106; FAO: Rome, Italy, 2015.
34. Page, A.I.; Miller, R.H.; Keeny, D.R. *Methods of Soil Analysis. Part II. Chemical and Microbiological Methods*, 2nd ed; American Society of Agronomy: Madison, WI, USA, 1982; pp. 225–246.
35. Klute, A. Water retention: Laboratory methods. *Methods Soil Anal. Part 1 Phys. Mineral. Methods* **1986**, *5*, 635–662. [CrossRef]
36. Sun, H.; Shen, Y.; Yu, Q.; Flerchinger, G.N.; Zhang, Y.; Liu, C.; Zhang, X. Effect of precipitation change on water balance and WUE of the winter wheat-summer maize rotation in the North China Plain. *Agric. Water Manag.* **2010**, *97*, 1139–1145. [CrossRef]
37. Razali, N.; Wah, Y.B. Power comparisons of Shapiro-Wilk, Kolmogorov-Smirnov, Lilliefors and Anderson-Darling tests. *J. Stat. Modeling Anal.* **2011**, *2*, 21–33.
38. Levene, H. Robust tests of equality of variances. In *Contributions to Probability and Statistics, Essays in Honor of Harold Hoteling*; Olkin, I., Ghurye, S.G., Hoeffding, W., Madow, W.G., Mann, H.B., Eds.; Stanford University Press: Stanford, CA, USA, 1960; pp. 278–292.
39. Steel, R.G.D.; Torrie, J.H. *Dickey DA Principles and Procedures of Statistics: A Biometrical Approach*, 3rd ed.; McGraw Hill: New York, NY, USA, 1997.
40. Gomes, F.P. *Curso de Estatística Experimental*, 15th ed.; Esalq: Piracicaba, Brazil, 2009; p. 477.
41. Fernandez, G.C. Effective selection criteria for assessing plant stress tolerance. In *Proceedings of the International Symposium on Adaptation of Food Crops to Temperature and Water Stress, Taiwan, China, 13–16 August 1992*; pp. 257–270.
42. Sharma, S. *Applied Multivariate Techniques*; Wiley: New York, NY, USA, 1996.
43. Delfine, S.; Tognetti, R.; Desiderio, E.; Alvino, A. Effect of foliar application of N and humic acids on growth and yield of durum wheat. *Agron. Sustain. Dev.* **2005**, *25*, 183–191. [CrossRef]
44. Vergara-Diaz, O.; Kefauver, S.C.; Elazab, A.; Nieto-Taladriz, M.T.; Araus, J.L. Grain yield losses in yellow-rusted durum wheat estimated using digital and conventional parameters under field conditions. *Crop J.* **2015**, *3*, 200–210. [CrossRef]
45. Gagliardi, A.; Carucci, F.; Masci, S.; Flagella, Z.; Gatta, G.; Giuliani, M.M. Effects of genotype, growing season and nitrogen level on gluten protein assembly of durum wheat grown under mediterranean conditions. *Agronomy* **2020**, *10*, 755. [CrossRef]
46. Pačuta, V.; Rašovský, M.; Michalska-Klimczak, B.; Wyszzyński, Z. Grain yield and quality traits of durum wheat (*Triticum durum* Desf.) treated with seaweed- and humic acid-based biostimulants. *Agronomy* **2021**, *11*, 1270. [CrossRef]
47. Shew, A.M.; Tack, J.B.; Nalley, L.L.; Petronella, C. Yield reduction under climate warming varies among wheat cultivars in South Africa. *Nat. Commun.* **2020**, *11*, 4408. [CrossRef]

48. Chowdhury, M.K.; Hasan, M.A.; Bahadur, M.M.; Islam, M.R.; Hakim, M.A.; Iqbal, M.A.; Javed, T.; Raza, A.; Shabbir, R.; Sorour, S.; et al. Evaluation of drought tolerance of some wheat (*Triticum aestivum* L.) genotypes through phenology, growth, and physiological indices. *Agronomy* **2021**, *11*, 1792. [CrossRef]
49. Taheri, S.; Jalal, S.; Farid, S.; Thohirah, L.A. Effects of drought stress condition on the yield of spring wheat (*Triticum aestivum*) lines. *Afr. J. Biotech.* **2011**, *10*, 18339–18348. [CrossRef]
50. Grzesiak, S.; Natalia, H.; Piotr, S.; Maciej, T.; Angelika, N.; Magdalena, S. Variation among wheat (*Triticum easativum* L.) genotypes in response to the drought stress: I—Selection approaches. *J. Plant Interact.* **2019**, *14*, 30–44. [CrossRef]
51. Koua, A.P.; Oyiga, B.C.; Baig, M.M.; Léon, J.; Ballvora, A. Breeding driven enrichment of genetic variation for key yield components and grain starch content under drought stress in winter wheat. *Front. Plant Sci.* **2012**, *12*, 684205. [CrossRef]
52. Oyiga, B.C.; Sharma, R.; Shen, J.; Baum, M.; Ogbonnaya, F.; Léon, J. Identification and characterization of salt tolerance of wheat germplasm using a multivariable screening approach. *J. Agron. Crop Sci.* **2016**, *202*, 472–485. [CrossRef]
53. Beltrano, J.; Ronco, M.G. Improved tolerance of wheat plants (*Triticum aestivum* L.) to drought stress and rewatering by the arbuscular mycorrhizal fungus *Glomus claroideum*: Effect on growth and cell membrane stability. *Braz. J. Plant Physiol.* **2009**, *20*, 29–37. [CrossRef]
54. Farooq, M.; Mubshar, H.; Kadambot, H.; Siddique, M. Drought stress in wheat during flowering and grain-filling periods. *Crit. Rev. Plant Sci.* **2014**, *33*, 331–349. [CrossRef]
55. Daryanto, S.; Wang, L.; Jacinthe, P.A. Global synthesis of drought effects on maize and wheat production. *PLoS ONE* **2016**, *11*, e0156362. [CrossRef] [PubMed]
56. Kadam, N.N.; Struik, P.C.; Rebolledo, M.C.; Yin, X.; Jagadish, S.K. Genome-wide association reveals novel genomic loci controlling rice grain yield and its component traits under water-deficit stress during the reproductive stage. *J. Exp. Bot.* **2018**, *69*, 4017–4032. [CrossRef] [PubMed]
57. Mohammadi, R. Breeding for increased drought tolerance in wheat: A review. *Crop Pasture Sci.* **2018**, *69*, 223–241. [CrossRef]
58. Mehraban, A.; Tobe, A.; Gholipouri, A.; Amiri, E.; Ghafari, A.; Rostaii, M. The effects of drought stress on yield, yield components, and yield stability at different growth stages in bread wheat cultivar (*Triticum aestivum* L.). *Pol. J. Environ. Stud.* **2019**, *28*, 739–746. [CrossRef]
59. Chandrasekar, V.; Sairam, R.K.; Srivastava, G.C. Physiological and biochemical responses of hexaploid and tetraploid wheat to drought stress. *J. Agron. Crop Sci.* **2000**, *185*, 219–227. [CrossRef]
60. Tahir, M.M.; Khurshid, M.; Khan, M.Z.; Abbasi, M.K.; Kazmi, M.H. Lignite-derived humic acid effect on growth of wheat plants in different soils. *Pedosphere* **2011**, *21*, 124–131. [CrossRef]
61. Manzoor, A.; Riaz, A.K.; Dost, M. Humic acid and micronutrient effects on wheat yield and nutrients uptake in salt affected soils. *Int. J. Agric. Biol.* **2014**, *16*, 991–995.
62. El-Hashash, E.F.; Agwa, A.M. Genetic parameters and stress tolerance index for quantitative traits in barley under different drought stress severities. *Asian J. Res. Crop Sci.* **2018**, *1*, 1–16. [CrossRef]
63. Yehia, W.M.B.; El-Hashash, E.F. Correlation and multivariate analysis across non-segregation and segregation generations in two cotton crosses. *Egypt. J. Agric. Res.* **2012**, *99*, 354–364. [CrossRef]
64. He, D.; Shibo, F.; Hanyue, L.; Enli, W.; Dong, W. Contrasting yield responses of winter and spring wheat to temperature rise in China. *Environ. Res. Lett.* **2020**, *15*, 124038. [CrossRef]
65. Zhang, Y.; Qiu, X.; Yin, T.; Liao, Z.; Liu, B.; Liu, L. The impact of global warming on the winter wheat production of China. *Agronomy* **2021**, *11*, 1845. [CrossRef]
66. Chen, X.; Wu, J.; Opoku-Kwanowaa, Y. Effects of returning granular corn straw on soil humus composition and humic acid structure characteristics in saline-alkali soil. *Sustainability* **2020**, *12*, 1005. [CrossRef]
67. Kotzé, E.; Loke, P.F.; Akhosi-Setaka, M.C.; Du Preez, C.C. Land use change affecting soil humic substances in three semi-arid agro ecosystems in South Africa. *Agric. Ecosys. Environ.* **2016**, *216*, 194–202. [CrossRef]
68. Júnior, G.A.; Pereira, R.A.; Sodré, G.A.; Gross, E. Humic acids from vermicompost positively influence the nutrient uptake in mangosteen seedlings. *Pesqui. Agropecuária Trop.* **2019**, *49*, 1–8. [CrossRef]
69. El-Hashash, E.F. Genetic diversity of soybean yield based on cluster and principal component analyses. *J. Adv. Biol. Biotech.* **2016**, *10*, 1–9. [CrossRef]
70. Hegab, R.H.; Fawy, H.A.; Habib, A.A.M. Evaluates effect of amino acids, humic acid and antioxidants as foliar application on the biochemical content and productivity of wheat under North Sinai soils conditions. *Am. J. Agric. Forest.* **2020**, *8*, 167–174. [CrossRef]
71. Elshabrawi, H.M.; Bakry, B.A.; Ahmed, M.A.; Abouellail, M. Humic and oxalic acid stimulates grain yield and induces accumulation of plastidial carbohydrate metabolism enzymes in wheat grown under sandy soil conditions. *Agric. Sci.* **2015**, *6*, 175–185. [CrossRef]
72. Van Oosten, M.J.; Pepe, O.; De Pascale, S.; Silletti, S.; Maggio, A. The role of biostimulants and bioeffectors as alleviators of abiotic stress in crop plants. *Chem. Biol. Technol. Agric.* **2017**, *4*, 5. [CrossRef]
73. Roomi, S.; Masi, A.; Conselvan, G.B.; Trevisan, S.; Quaggiotti, S.; Pivato, M. Protein profiling of arabidopsis roots treated with humic substances: Insights into the metabolic and interactome networks. *Front. Plant Sci.* **2018**, *871*, 1812. [CrossRef]

74. Abou Tahoun, A.M.; El-Enin, M.M.A.; Mancy, A.G.; Sheta, M.H.; Shaaban, A. Integrative soil application of humic acid and foliar plant growth stimulants improves soil properties and wheat yield and quality in nutrient-poor sandy soil of a semiarid region. *J. Soil Sci. Plant Nutr.* **2022**, *22*, 851–858. [CrossRef]
75. Shen, J.; Guo, M.J.; Wang, Y.G.; Yuan, X.Y.; Wen, Y.Y.; Song, X.; Dong, S.Q.; Guo, P.Y. Humic acid improves the physiological and photosynthetic characteristics of millet seedlings under drought stress. *Plant Signal. Behav.* **2020**, *15*, 8. [CrossRef] [PubMed]
76. Dalal, A.; Bourstein, R.; Haish, N.; Shenhar, I.; Wallach, R.; Moshelion, M. Dynamic physiological phenotyping of drought-stressed pepper plants treated with productivity-enhancing and survivability-enhancing biostimulants. *Front. Plant Sci.* **2019**, *10*, 905. [CrossRef] [PubMed]
77. Negin, B.; Moshelion, M. The advantages of functional phenotyping in pre-field screening for drought-tolerant crops. *Funct. Plant Biol.* **2016**, *44*, 107–118. [CrossRef]

Article

Soil-Mulching Influence on Spearmint Oil Yield, Ecophysiological Activities and Essential-Oil Content in Rainfed Environment of Southern Italy

Sebastiano Delfine ^{1,*} , Violeta B. Velikova ² and Franco Mastrodonato ³

¹ Dipartimento di Agricoltura, Ambiente ed Alimenti, Università degli Studi del Molise, Via De Sanctis, 86100 Campobasso, Italy

² Institute of Plant Physiology and Genetics, Bulgarian Academy of Sciences, Acad. G. Bonchev Street, Bldg. 21, 1113 Sofia, Bulgaria; violeta.velikova@gmail.com

³ Società Italiana Medicina Biointegrata, Variante Esterna, 86091 Bagnoli del Trigno, Italy; mastrodonato.f@gmail.com

* Correspondence: delfine@unimol.it

Abstract: The application of soil mulching is widely used to improve crop productivity within semiarid regions of Mediterranean environments. A field study was conducted during two consecutive cycles of spearmint (*Mentha spicata* L.) within the rainfed region of Southern Italy to evaluate the effects of straw mulch cultivation practices on crop yields and ecophysiological activities. Four treatments were evaluated: (1) rainfed with straw mulch (RM), (2) rainfed without straw mulch (R), (3) well-watered control plants (W) and (4) well-watered with straw mulch (WM). The rainfed mulch treatment (RM) significantly improved oil yields and ecophysiological activity of the spearmint in comparison with rainfed (R). The rainfed mulch treatment (RM) showed lower inhibition of photosynthesis and smaller diffusive limitations than control treatment, while in rainfed plants (R) photosynthetic activity and diffusive limitations strongly decreased at the end of crop cycle. The average essential-oil content was significantly lower under the W, WM and RM treatments, in comparison to the R treatment, during the full-bloom stages (40 DAT). Instead, at the end of crop cycle, the mulching practice (RM and WM) insignificantly changed the essential-oil content compared with non-mulched well-watered treatment (W), while in rainfed plants (R) the essential-oil content strongly decreased. In addition, rainfed conditions affected the percentage of the three major monoterpenes and decreased the formation of carvone from limonene. Therefore, the current study concluded that straw mulch is an effective management practice to improve growing conditions by decreasing groundwater consumption and to increase oil yields in spearmint within this Mediterranean rainfed region.

Keywords: mulching; spearmint; yield; ecophysiology; essential oil



Citation: Delfine, S.; Velikova, V.B.; Mastrodonato, F. Soil-Mulching Influence on Spearmint Oil Yield, Ecophysiological Activities and Essential-Oil Content in Rainfed Environment of Southern Italy. *Agronomy* **2022**, *12*, 1521. <https://doi.org/10.3390/agronomy12071521>

Academic Editors:
Aliasghar Montazar and Robert J. Lascano

Received: 13 May 2022

Accepted: 24 June 2022

Published: 24 June 2022

Publisher's Note: MDPI stays neutral with regard to jurisdictional claims in published maps and institutional affiliations.



Copyright: © 2022 by the authors. Licensee MDPI, Basel, Switzerland. This article is an open access article distributed under the terms and conditions of the Creative Commons Attribution (CC BY) license (<https://creativecommons.org/licenses/by/4.0/>).

1. Introduction

Spearmint (*Mentha spicata* L.), is a creeping rhizomatous, glabrous and herbaceous perennial plant, with a pungent smell. The commercial interest in spearmint essential oil, which is among the 10 most commercialized in the world, has increased the demand in mint cultivation. Spearmint indeed contributes greatly to the economy due to its extensive use in food, perfumery, toothpaste, the pharmaceutical industry and the production of essential oil (EO).

The EO of spearmint has antimicrobial [1], insecticidal [2], larvicidal [3], antioxidant [4] and mutagenic activity due to the abundance of terpenes [5].

The crop needs sufficient water availability during summer months to ensure good growth and high yields. In spearmint, sustained deficit irrigation, reducing water availability, clearly decreased mint hay yields and affected oil yield and quality [3,6,7].

The positive effect of water availability on herb yields of various mint species and aromatic grasses has been reported [8–10]. Meanwhile, in medicinal plants, a moderate water-stress condition, while reducing the accumulation of dry matter, increases the yield of essential oil and modifies its composition in respect to the well-watered plants [8,11–13].

Severe water deficit limits crop growth and yield with negative economic consequences [14]. In the last few years, rainfall has declined in some parts of the Mediterranean region due to a climatic change [15] causing substantial shortage in the available water resources for agricultural production. Furthermore, the uneven distribution of rainfall has become the main limitation to sustainable crop yields in drought-prone areas [16]. Thus, the improved utilization of limited seasonal rainfall resources through reduction in soil water loss and increased water-utilization efficiency is needed.

A number of proven mulching techniques exist to entrap and conserve rainwater, such as plastic film mulch, straw mulch and ridge-furrow mulch [17]. The use of plastic film mulch, however, leaves a large amount of plastic in the field, which has obvious negative effects on the environment and soil structure [18].

Instead, the application of straw in agriculture will improve the agricultural ecological environment, because the need for open-field straw burning will be reduced or eliminated. Straw mulch has also been shown to reduce the needed quantities of chemical fertilizers [19] as it increases soil organic matter and improves soil structure [20].

Organic mulching plays a vital role in sustainably conserving soil moisture under low water availability in a manner that enhances crop yields and water-use efficiency [16,21]. Furthermore, conserving moisture through mulching and reduction in the frequency of water supplies may subsequently reduce the losses of N through leaching and minimize NH_3 volatilization by restricting soil temperature rise.

In the present study, we investigated the effect of straw mulch on rainfed spearmint (*Mentha spicata* L.) in environmental conditions typical of the Mediterranean region. In particular, we focused on plant growth, photosynthesis and oil yield. We hypothesized that mulch is useful and necessary to support plant growth and activity, and to avoid oil-yield reduction in spearmint.

2. Materials and Methods

2.1. Experimental Site

The study was conducted during 2020 and 2021 growing season at an experimental field site in Baranello (Molise Region, Italy, latitude $41^{\circ}31'$ N, longitude $14^{\circ}33'$ E, altitude 630 m a.s.l.). The area has an average annual rainfall of 845 mm and mean annual temperature of 12.7°C . Molise Region is positioned on the eastern side of the Apennines watershed, and has a typical Mediterranean climate of southern Italy.

Before fertilizer applications, soil samples (0–30 cm) were taken from each block and analyzed according to standard procedures [8]. The soil was characterized by a clay-sand texture (45% clay, 10% silt and 45% sand) and the organic-matter content was 1.5%. The soil profile was overall uniform, containing medium amount of total N (nitrogen, 0.11%), medium amount of available P (phosphorous, $19.5 \mu\text{g g}^{-1}$) and medium quantity of exchangeable K (potassium, $133 \mu\text{g g}^{-1}$). Soil had very low active CaCO_3 , and pH was average neutral; salinity was low. Bean (*Phaseolus vulgaris* L.) was the previous crop within both years.

2.2. Plant Material and Experimental Design

Ten-month old spearmint seedlings were transplanted during mid-April in both years, followed by a light irrigation after planting in rows 50 cm apart (plant density of 10 plants m^{-2}). The field was surrounded by a buffer strip to allow for uniform growing conditions.

The experiment was arranged in a randomized block design with five replications (5 m^2 each plot). After tillage was completed, the land was smoothed and firmed using a roller harrow.

The recommended doses of N (100 kg ha^{-1}), P_2O_5 (70 kg ha^{-1}) and K_2O (100 kg ha^{-1}), were applied before planting [22].

The following treatments were designed: plants cultivated under natural rainfed conditions without mulch (hereafter, R plants), plants cultivated under natural rainfed conditions with straw mulch (hereafter, RM plants), plants grown under well-watered conditions, considered as control (hereafter, W plants) and plants grown under well-watered conditions with straw mulch (hereafter, WM plants). Within the straw mulch treatments, the wheat straw covered all the soil surface at the rates of 1 kg m^{-2} (5 cm straw length). The wheat straw was applied annually. Plants cultivated under well-watered conditions served as a control.

In the control plots, the crop evapotranspiration (ET) was fully restored by drip irrigation. After plant establishment (at 10 May, in both years), irrigation was withheld in R and RW plots [0 days after treatment (DAT)]. Briefly, potential evapotranspiration was calculated from micrometeorological data using the Penman–Monteith formula [23]. Weeds were manually controlled.

2.3. Meteorological Measurements and Yield Biomass

Main meteorological parameters were measured by means of a standard weather station, located 20 m from the experimental field. The daily mean temperature ranged between $9.1\text{--}23.5 \text{ }^\circ\text{C}$, while the corresponding minimum and maximum temperatures were 7.6 and $34.7 \text{ }^\circ\text{C}$, respectively. Only 10.3 mm and 11.5 mm rainfall were received during the entire spearmint growth season in the years 2020 and 2021, respectively.

The crop was harvested manually on 0, 20, 40, 60 and 80 DAT in both years. The herbal-yield biomass was weighed, after which the plant samples were heated at $105 \text{ }^\circ\text{C}$ for one hour and then dried at $75 \text{ }^\circ\text{C}$ to constant weight.

2.4. Photosynthetic Gas Exchange

Gas-exchange activities, as net photosynthesis (P_n , $\mu\text{mol m}^{-2} \text{ s}^{-1}$) and stomatal conductance (g_s , $\text{mol m}^{-2} \text{ s}^{-1}$) were measured using a portable photosynthesis system, at ambient CO_2 concentration and at time of maximum solar radiation (e.g., 12:00 to 2:00 pm) as described by Delfine [24]. Measurements were recorded on five fully expanded leaves selected randomly on different plants. For photosynthesis measurements, the leaf temperature was maintained at $30 \text{ }^\circ\text{C}$ as in the environmental conditions. Mesophyll conductance (g_m , $\text{mol m}^{-2} \text{ s}^{-1}$) of CO_2 was determined as described by Delfine [8]. Briefly, the electron-transport rate calculated by gas exchange (J_c) and that measured by chlorophyll fluorescence (J_f) were compared at an irradiance of $800 \mu\text{mol m}^{-2} \text{ s}^{-1}$ for accurate measurements of intercellular CO_2 concentration.

2.5. Relative Water Content

The relative water content (RWC) of leaves was measured according to Di Stasio [25]. The third fully expanded leaves from the top were measured. The fresh leaves were weighed (FW), then submerged in distilled water for 12 h to obtain turgid weight (TW). Finally, the leaves were kept at $105 \text{ }^\circ\text{C}$ for 24 h until a constant weight was reached (DW). The formula $\text{RWC} (\%) = (\text{FW} - \text{DW}) / (\text{TW} - \text{DW}) \times 100$ was used to calculate the relative leaf water content.

2.6. Soil Water Content

The water content to a depth of 1.0 m was measured every 20 days from the beginning of treatment (DAT) to observe the dynamics in soil water content of the 0–0.3 and 0.3–1.0 m layers. The soil was sampled at 0.1 m intervals by manual coring between adjacent plants in the same row, and the gravimetric water content of the soil samples was calculated on the basis of oven-dried weights (dried at $105 \text{ }^\circ\text{C}$).

2.7. Essential-Oil Analysis

Essential oil was extracted by hydrodistillation of fresh samples through Clevenger's apparatus. The steam distillation was performed for 60 min. The separated spearmint EO collected was dried over anhydrous sodium sulfate and stored in dark-brown vials at 4 °C until used. Three extractions were performed for each treatment [26]. Samples from every treatment and replicate were collected and analyzed separately for oil composition.

The leaf and stem dry biomass, RWC, photosynthesis, stomatal and mesophyll conductance, essential-oil content and essential-oil yield were recorded with interval of 20 days from 0 DAT.

2.8. GC and GC–MS Analysis

Analytical gas chromatography was carried out on a Perkin–Elmer Sigma 115 gas chromatograph fitted with a HP-5 MS capillary column (30 m × 0.25 mm), 0.25 µm film thickness. Helium was the carrier gas (1 mL/min). Column temperature was initially kept at 40 °C for 5 min, then gradually increased to 250 °C at 2 °C/min rate, held for 15 min and finally raised to 270 °C at 10 °C/min. Diluted samples (1/100 *v/v*, in *n*-pentane) of 1 µL were injected at 250 °C, manually and in the splitless mode. Flame-ionization detection (FID) was performed at 280 °C. Analysis was also run by using a fused silica HP Innowax polyethyleneglycol capillary column (50 m × 0.20 mm), 0.20 µm film thickness and operating as described above. GC–MS analysis was performed on an Agilent 6850 Ser. II apparatus, fitted with a fused silica DB-5 capillary column (30 m × 0.25 mm), 0.33 µm film thickness, coupled to an Agilent Mass Selective Detector MSD 5973; ionization voltage 70 eV; electron-multiplier energy 2000 V. Gas chromatographic conditions were as given; transfer line temperature, 295 °C.

2.9. Identification of Compounds

Most constituents were identified by gas chromatography by comparison of their retention indices (Ki) with those of the literature [27,28] or with those of authentic compounds available in our laboratories. The retention indices were determined in relation to a homologous series of *n*-alkanes (C8–C24) under the same operating conditions. Further identification was made by comparison of their mass spectra on both columns with those stored in NIST 02, Wiley 275 libraries and our home-made library or with mass spectra from literature [27,29]. Component relative percentages were calculated based on GC peak areas without using correction factors. The primary oil components that were compared were limonene, carvone, 1,8-cineole and myrcene.

2.10. Data Statistics

All data were presented as means of the five replicates, while the data for essential oil content and yield and primary oil components are presented as means of the three replicates. SPSS 18.0 was used to conduct a one-way analysis of variance, and significant differences between treatments were compared by the least-significant-difference test at $p < 0.05$.

3. Results

As the measured parameters did not show significant differences between growing seasons, data averaged over 2 years, 2020 and 2021, were presented.

3.1. Plant Phenology and Soil Water Contents

No differences in phenology were observed between the spearmint plants exposed to the different treatments up to 40 DAT. Specifically, at the beginning of the study (0 DAT) the plants, of all treatments, were in the pre-flowering stage. After 20 DAT, the plants were in early bloom, and at 40 DAT in full bloom, in all four overall treatments. At 60 DAT the W, WM and RM plants were at the end of flowering and at 80 DAT in flower withering;

while the R plants were already withering from 60 DAT until the end of the cropping cycle (80 DAT).

The soil water contents (SWC) (Figure 1) showed that the rainfed mulching treatments increased the SWC within the 0–0.3 m soil profile compared with the rainfed treatment during the growing seasons of spearmint plants.

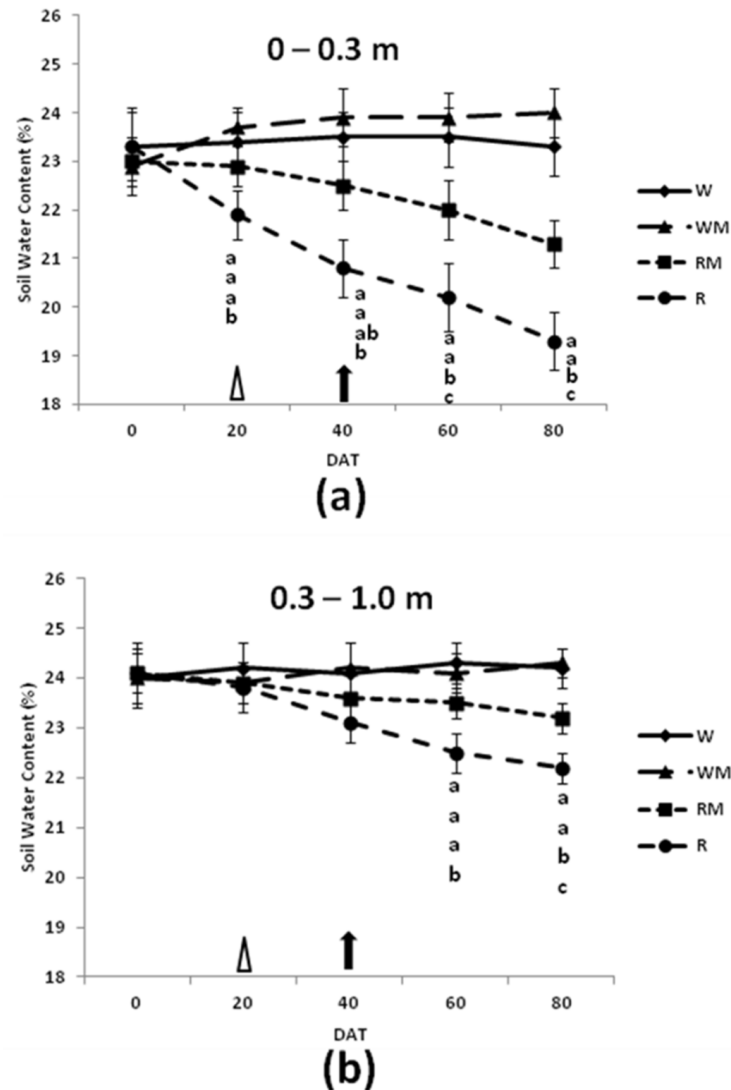


Figure 1. Changes in soil water content (%) in the 0–0.3 m (a) and 0.3–1.0 m (b) soil layers of spearmint exposed to the following treatments: R—rainfed without straw mulch, RM—rainfed with straw mulch, W—well-watered control plants and WM—well-watered with straw mulch. Measurements were performed 0, 20, 40, 60 and 80 days after the onset of the treatments (DAT). Vertical bars represent \pm SE of the mean ($n = 5$). Bars with different letters indicate significant differences among treatments in the given DAT at $p \leq 0.05$. Triangle at 20 DAT indicates the early bloom, and arrow at 40 DAT indicates the full bloom, in overall treatments.

At the end of the spearmint growth stage (flower-withering stage, 80 DAT), the SWC within the 0–0.3 m soil profile under the rainfed treatments was lower in comparison to the RM and control treatment. The SWC reductions indicated that under the mulching treatments, more water was stored within the 0–0.3 m soil profile compared with the rainfed treatment. Over the studied cropping cycle (0–80 DAT), there were no significant differences in SWC between well-watered and well-watered mulching treatments. The amplitude of the variation was much larger in the 0–0.3 m than the 0.3–1.0 m layer.

3.2. Biomass Yields

The dry herbal biomass yields of spearmint were significantly affected by the straw mulch treatment during the growth season (Figure 2).

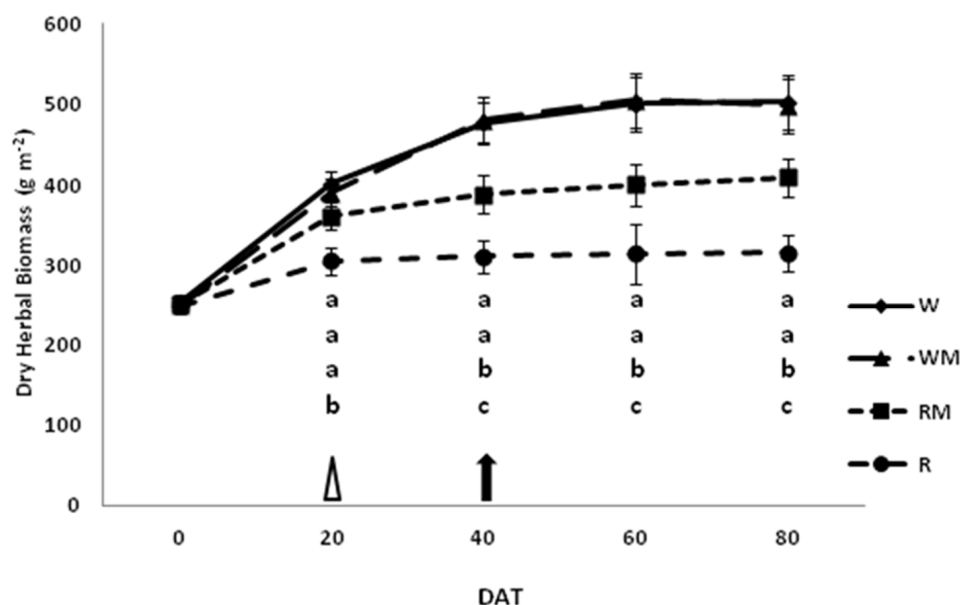


Figure 2. Changes in dry herbal biomass (g m^{-2}) of spearmint exposed to the following treatments: R—rainfed without straw mulch, RM—rainfed with straw mulch, W—well-watered control plants and WM—well-watered with straw mulch. Measurements were performed 0, 20, 40, 60 and 80 days after the onset of the treatments (DAT). Vertical bars represent \pm SE of the mean ($n = 5$). Bars with different letters indicate significant differences among treatments in the given DAT at $p \leq 0.05$. Triangle at 20 DAT indicates the early bloom, and arrow at 40 DAT indicates the full bloom, in overall treatments.

In W and WM plants, the dry herbal biomass content had increased over time, showing the maximum yield in full bloom (DAT 40) and no significant difference between the two treatments. The herbal yield of RM-treated plants tended to increase but significantly less than in WM plants, and the dry herbal biomass was about 20% less at the end of the experiments (DAT 80). Instead, the development of R plants stopped at the beginning of flowering, showing a reduction of about 38% at the end of the experiments compared to the control (W).

3.3. Photosynthesis, Stomatal and Mesophyll Conductances

The trends in photosynthesis (P_n), stomatal (g_s) and mesophyll (g_m) conductances among the different treatments are illustrated in Figures 3–5, respectively. The mean photosynthesis was 60% and 26% lower in R and RM plants compared to the corresponding controls (W and WM), respectively, at DAT 80. There were no significant differences in photosynthesis between the W and WM control plants over the studied cropping cycle (Figure 3).

The same trend was observed for stomatal conductance (Figure 4).

At the 20 DAT, mesophyll conductance was significantly lower only in the leaves of R plants with respect to control W (Figure 5).

On the contrary, the mesophyll conductance of the RM treatments decreased and was significantly lower ($p < 0.05$), with respect to control WM, only at the 80 DAT. Over the studied treatment cycle, the mesophyll conductance of control W was similar to those of plants grown under well-watered conditions with straw mulch (WM).

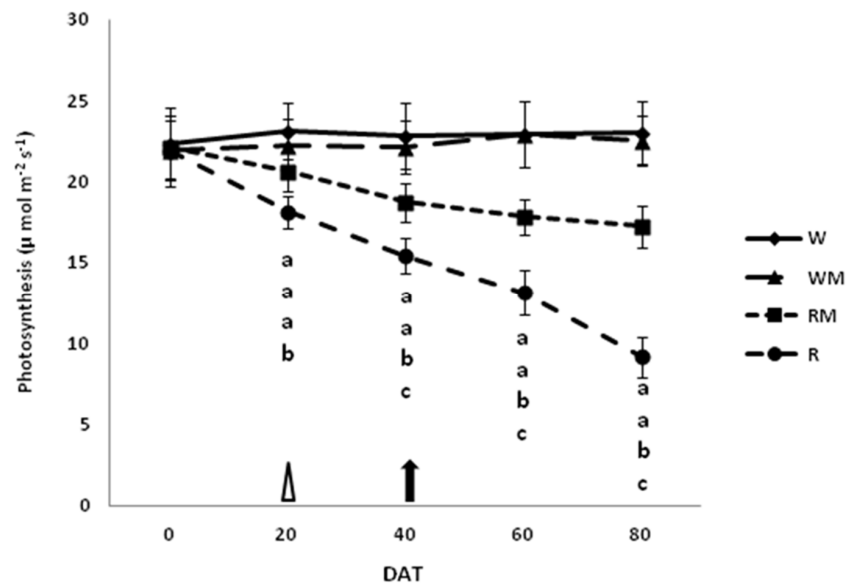


Figure 3. Changes in photosynthesis ($\mu\text{mol m}^{-2} \text{s}^{-1}$) of spearmint exposed to the following treatments: R—rainfed without straw mulch, RM—rainfed with straw mulch, W—well-watered control plants and WM—well-watered with straw mulch. Measurements were performed 0, 20, 40, 60 and 80 days after the onset of the treatments (DAT). Vertical bars represent \pm SE of the mean ($n = 5$). Bars with different letters indicate significant differences among treatments in the given DAT at $p \leq 0.05$. Triangle at 20 DAT indicates the early bloom, and arrow at 40 DAT indicates the full bloom, in overall treatments.

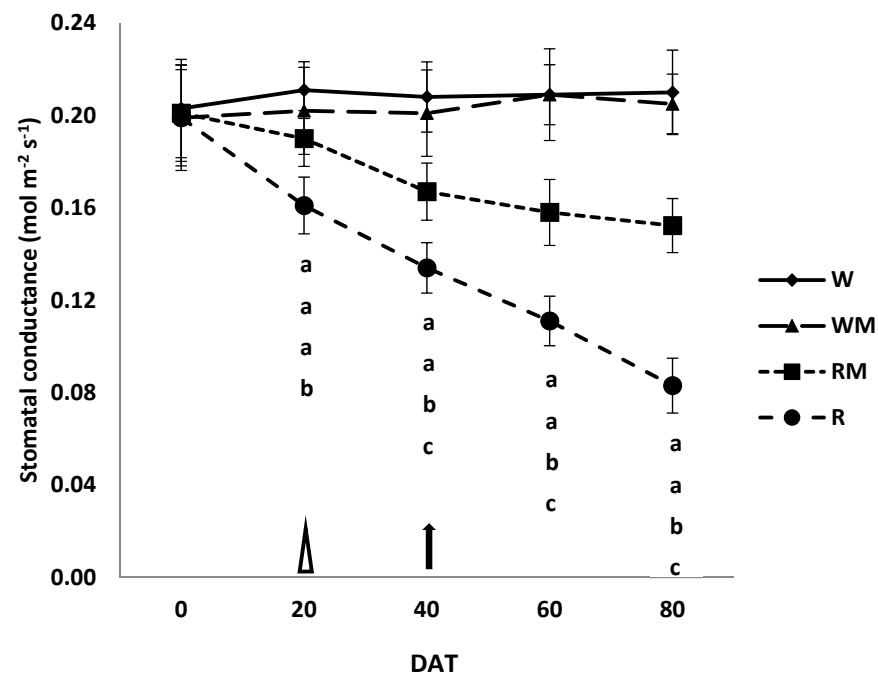


Figure 4. Changes in stomatal conductance ($\text{mol m}^{-2} \text{s}^{-1}$) of spearmint exposed to the following treatments: R—rainfed without straw mulch, RM—rainfed with straw mulch, W—well-watered control plants and WM—well-watered with straw mulch. Measurements were performed 0, 20, 40, 60 and 80 days after the onset of the treatments (DAT). Vertical bars represent \pm SE of the mean ($n = 5$). Bars with different letters indicate significant differences among treatments in the given DAT at $p \leq 0.05$. Triangle at 20 DAT indicates the early bloom, and arrow at 40 DAT indicates the full bloom, in overall treatments.

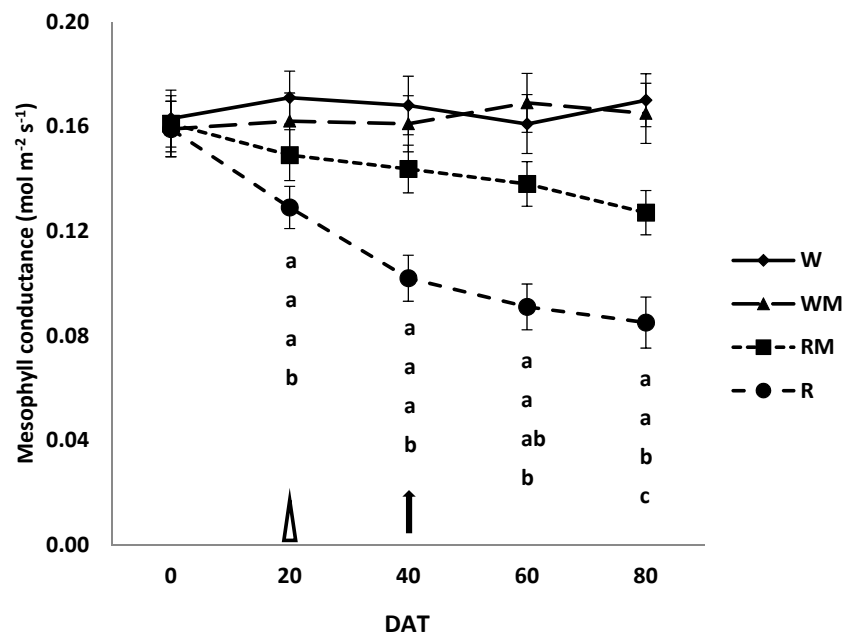


Figure 5. Changes in mesophyll conductance ($\text{mol m}^{-2} \text{s}^{-1}$) of spearmint exposed to the following treatments: R—rainfed without straw mulch, RM—rainfed with straw mulch, W—well-watered control plants and WM—well-watered with straw mulch. Measurements were performed 0, 20, 40, 60 and 80 days after the onset of the treatments (DAT). Vertical bars represent \pm SE of the mean ($n = 5$). Bars with different letters indicate significant differences among treatments in the given DAT at $p \leq 0.05$. Triangle at 20 DAT indicate the early bloom and arrow at 40 DAT indicate the full bloom, in overall treatments.

3.4. Relative Water Content

The results of the RWC indicated that RM plants generally had preserved tissue water content compared to R plants over the growing seasons (Figure 6).

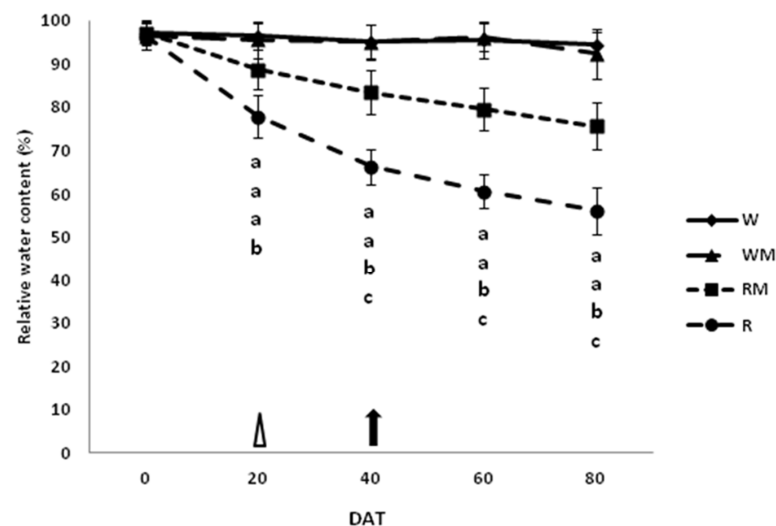


Figure 6. Changes in relative water content (%) of spearmint exposed to the following treatments: R—rainfed without straw mulch, RM—rainfed with straw mulch, W—well-watered control plants and WM—well-watered with straw mulch. Measurements were performed 0, 20, 40, 60 and 80 days after the onset of the treatments (DAT). Vertical bars represent \pm SE of the mean ($n = 5$). Bars with different letters indicate significant differences among treatments in the given DAT at $p \leq 0.05$. Triangle at 20 DAT indicates the early bloom, and arrow at 40 DAT indicates the full bloom, in overall treatments.

At the end of the spearmint growth stage (flower-withering stage, 80 DAT), the average RWC was significantly ($p < 0.05$) lower in R and RM plants, by about 40% and 20%, respectively, in comparison to the control W and WM plants. No significant differences in RWC between the W and WM control plants over the cropping cycle were observed (Figure 6).

3.5. Essential-Oil Content and Essential-Oil Yield

The mulching treatments increased the EO content (+16%) in the RM compared to WM plants during the full bloom (40 DAT) (Figure 7).

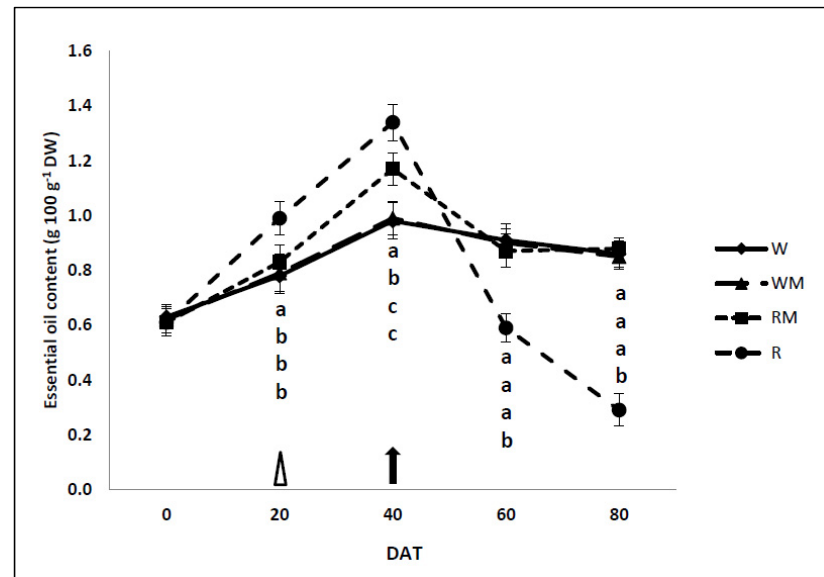


Figure 7. Changes in essential-oil content ($\text{g } 100 \text{ g}^{-1} \text{ d.w.}$) of spearmint exposed to the following treatments: R—rainfed without straw mulch, RM—rainfed with straw mulch, W—well-watered control plants and WM—well-watered with straw mulch. Measurements were performed 0, 20, 40, 60 and 80 days after the onset of the treatments (DAT). Vertical bars represent \pm SE of the mean ($n = 3$). Bars with different letters indicate significant differences among treatments in the given DAT at $p \leq 0.05$. Triangle at 20 DAT indicates the early bloom, and arrow at 40 DAT indicates the full bloom, in overall treatments.

There were no differences in EO content (EOC) between the W and WM plants over the cropping cycles. During the full-bloom stages (40 DAT), the EO content of the W (−26%), WM (−26%) and RM (−14%) plants were significantly lower in comparison to R plants. While EO content was strongly reduced in R plants (about 77%) compared to W plants at the last harvest (80 DAT). RM loses a negligible quantity of oils compared to WM. At 80 DAT, EO content in W and WM plants dropped by about 5% compared to full bloom (40 DAT). EOC of RM dropped by 3%, while in R plants EOC decreased by 51%, almost disappearing in leaf tissues.

The mean essential-oil yields (Figure 8) show significant decreases with increasing water deficit across the harvest time.

At 40 DAT, the essential-oil yield was significantly higher in W, WM and RM than in R, whereas the data did not differ significantly among W, WM and RM. The decrease in rainfed treatment at the end of harvest time (80 DAT) was much greater than rainfed mulching treatment compared to the respective control treatments (W and WM conditions). At the same time (80 DAT), the variation of essential-oil yields did not differ significantly between W and WM plants.

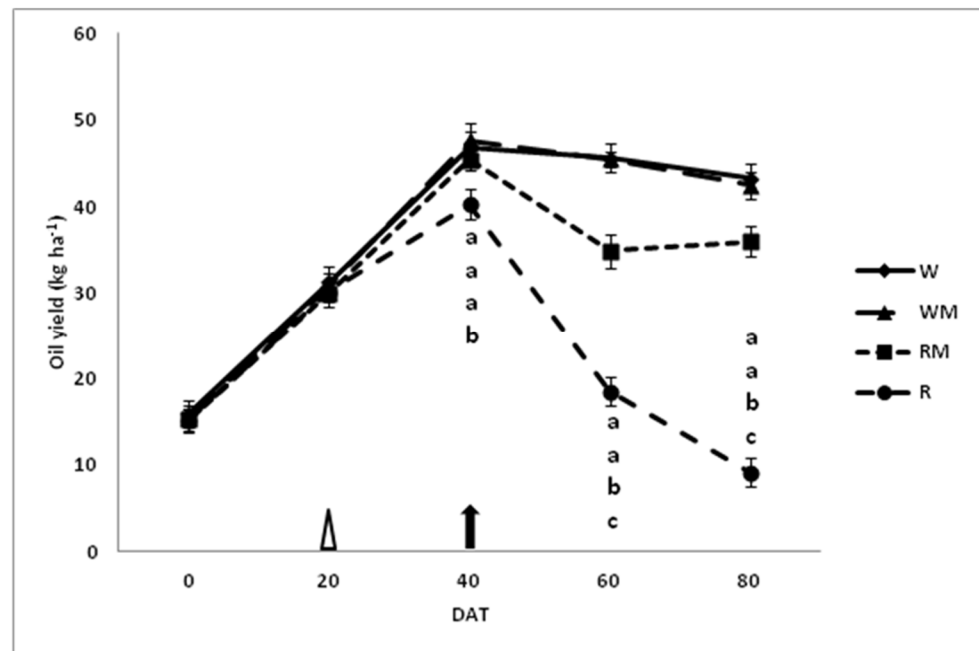


Figure 8. Changes in essential-oil yield (kg ha^{-1}) of spearmint exposed to the following treatments: R—rainfed without straw mulch, RM—rainfed with straw mulch, W—well-watered control plants and WM—well-watered with straw mulch. Measurements were performed 0, 20, 40, 60 and 80 days after the onset of the treatments (DAT). Vertical bars represent \pm SE of the mean ($n = 3$). Bars with different letters indicate significant differences among treatments in the given DAT at $p \leq 0.05$. Triangle at 20 DAT indicates the early bloom, and arrow at 40 DAT indicates the full bloom, in overall treatments.

3.6. Major Oil Components

The major oil components that were compared were myrcene, limonene, 1,8-cineole and carvone, which comprise over 75% of the significant monoterpenes (Table 1).

Table 1. The primary oil components (%) of spearmint exposed to the following treatments: R—rainfed without straw mulch, RM—rainfed with straw mulch, W—well-watered control plants and WM—well-watered with straw mulch. Measurements were performed 40 and 80 days after the onset of the treatments (DAT). 40 DAT indicates the full bloom, in overall treatments.

	Myrcene	Limonene	1,8-Cineole	Carvone
<i>DAT 40</i>				
W	5.11 a	17.51 b	9.56 b	41.25 a
WM	5.01 a	17.45 b	9.79 b	40.98 a
R	5.22 a	22.49 a	13.85 a	35.01 b
RM	4.99 a	17.77 b	9.61 b	41.05 a
<i>DAT 80</i>				
W	6.23 a	13.72 c	9.96 c	45.31 a
WM	6.31 a	13.69 c	10.06 c	44.86 a
R	6.27 a	19.91 a	14.56 a	40.55 c
RM	6.33 a	15.97 b	12.97 b	43.09 b
<i>Mean DAT 40</i>	5.08 b	18.81 a	10.70 b	39.57 b
<i>Mean DAT 80</i>	6.28 a	15.82 b	11.89 a	43.45 a

Different letters in columns indicate significant differences among treatments in the given DAT at $p \leq 0.05$. Data related to *Mean DAT 40* and *Mean DAT 80* are means for all treatments and different letters in columns indicate significant differences between 40 and 80 DAT at $p \leq 0.05$.

The percentage of myrcene did not differ significantly among treatments at 40 DAT. The percentages of limonene and 1,8-cineole, at 40 DAT, were significantly higher in R than

in W, WM and RM, which did not differ significantly from each other, whereas at 40 DAT, the percentage of carvone was significantly lower in R than in W, WM and RM, which did not differ significantly from each other.

Even after 80 DAT, the percentage of myrcene did not differ significantly among the treatments. The increase in the percentage of limonene and 1,8-cineole in rainfed treatment, at the end of harvest time (80 DAT), was much greater than rainfed mulching treatment compared to the respective control treatments (W and WM conditions). At the same time (80 DAT), the variation of percentage of limonene and 1,8-cineole did not differ significantly between W and WM. At 80 DAT, the decrease in the percentage of carvone in rainfed treatment was much greater than rainfed mulching treatment compared to the respective control treatments (W and WM). The variation of the percentage of carvone did not differ significantly between W and WM. From 40 to 80 DAT, the result showed a significant increase in the myrcene, 1,8-cineole and carvone, and a significant decrease in the limonene percentage over the ranges of applied treatments (Table 1).

4. Discussion

During the whole time of the experimentation, the scant precipitations occur in the form of low-intensity precipitation events. Thus, the precipitation quantities delivered in this manner cannot satisfy the normal growth of crops. Therefore, in these drought-prone environments, the soil-surface mulch practices may reduce the evaporation losses from the soil surface [16,21]. Thus, the improvement of the soil-moisture conditions of dry-land agriculture is of particular importance [30,31]. Our study indicated that rainfed mulching treatments increased the SWC within the 0–0.3 m soil profile compared with the rainfed conditions in the growing season of spearmint (Figure 1). The SWC for the rainfed treatment was even lower when compared with the mulching treatment from the full bloom (40 DAT) to the end of the cropping cycle (80 DAT). Moreover, already after 20 DAT, the SWC within the 0–0.3 m soil profile under the rainfed treatment was generally lower than under well-watered treatment.

In our study, the mulch treatments of rainfed plants significantly increased the dry herbal biomass yields during the crop-growing stages (Figure 2) in comparison to the rainfed treatment. Similar results have been reported on a menthol mint plants studied under different moisture regimes and nitrogen fertilization in the presence of sugarcane trash mulched [10]. Instead, there were no significant differences in the dry herbal biomass yields between W and WM plants. It should be noted that as expected, well-irrigated plants (W and WM) had higher dry herbal biomass yields than rainfed ones (R and RM). The rainfed mulching treatment conserves soil water and reduces soil evaporation, thus demonstrating that it is suitable in a rainfed climate for the utilization of water [32]. The dry herbal biomass accumulation was closely associated with photosynthetic gas-exchange parameters and leaf RWC during different crop-growth stages. There were no significant differences between W and WM plants during the entire spearmint growing season, which may be attributed to the similar tissue water content (Figures 3–6).

The mulching rainfed treatment likely enhanced the accumulation of biomass by improving the photosynthesis to accelerate crop growth compared to the rainfed treatment. The photosynthesis limitations highlighted in R and RM plants compared to W and WM plants were mostly due to diffusive resistances, including the mesophyll component [8]. Indeed, until 40 DAT, stomatal conductance in our study significantly decreased in R and RM plants in comparison to the well-watered controls (W and WM). To conclude that the reduction in photosynthesis observed until full bloom (40 DAT) is only attributable to stomatal closure, one should observe a consequent additional resistance to CO₂ diffusion toward the chloroplasts that is generally caused by the mesophyll components [24]. This additional resistance may increase under stress conditions [8]. However, mesophyll resistance is likely to be controlled by mesophyll anatomical structure and particularly by the chloroplast surfaces exposed to gas exchanges [33,34]. Mesophyll resistance was similar in controls (W and WM) and rainfed mulching treatment at 40 DAT (Figure 5). Thus, it

did not contribute to increasing resistance to CO₂ diffusion in RM leaves, indicating that mesophyll resistances to CO₂ diffusion did not directly affect photosynthesis [8]. In this condition, in which it is only the stomatal conductance that limits photosynthesis, it did not cause permanent damage to the carbon fixation apparatus, as has been observed in other studies [8,24], and therefore, it is possible to consider the stress condition as moderate. Moreover, contrary to what was found at 40 DAT, we observed that at 60 and mostly at 80 DAT, the CO₂ mesophyll conductance of R leaves was significantly lower than that of the rainfed mulching treatment. Thus, mesophyll resistance only contributed to the total resistance to CO₂ diffusion from 60 DAT [24]. During the harvesting period, when comparing R and RM plants it became clear that the total diffusive limitations were fewer in RM compared to R plants. Thus, the greater water availability increased the stomatal conductance, ensuring a greater input of carbon dioxide, which in turn increased photosynthetic activity in RM compared to R plants. These differences significantly accelerated the growth of the crop canopy and resulted in the significantly increased dry herbal biomass values that are shown in Figure 1 [35].

In our study, the rainfed treatments (without and with mulch) significantly increased the essential oil content, during the full bloom (40 DAT) (Figure 7). The rainfed treatment significantly increased the essential-oil content and storage in green tissues in comparison to the W, WM and RM treatments, before and during the early growth stage (20 DAT) [8]. During the withering stages, there were no significant differences in the essential-oil content between the well-watered control plants (W and WM) and RM plants, while the essential-oil content of R plants strongly decreased. Our study indicated that mulching rainfed treatment (RM) significantly increased the essential-oil content compared to the control treatment (WM) in the full-bloom phase and kept it constant until the end of the growing season during withering, extending the oil-extraction period (Figure 7).

Essential oil yield increased substantially with the increasing of bloom for all treatments (Figure 8). At 40 DAT, compared with rainfed treatment, mulching rainfed spearmint (RM) clearly yielded the same amount of essential oil as the W and WM controls. Moreover, after 80 DAT, the reduction in essential-oil yield in the mulching rainfed treatment (RM, −15%), although significant, was much less evident than in the rainfed treatment (R, −78%) compared to the respective controls (WM and W).

This indicates a possibility, at the full-bloom stage (40 DAT), for decreased grower costs through mulching rainfed treatment by cutting costs for water, harvesting, transportation and distilling spearmint hay; and for increasing profits if the oil yield and quality remain fairly constant. This encouraging result for mulching rainfed treatment (RM) is attributable to the presence of higher soil water contents compared to rainfed treatment (R), which helped sustain the crop at these rainfed conditions in mulching treatment.

The percentage of four major monoterpenes (limonene, carvone, 1,8-cineole and myrcene) showed a low sensitivity to rainfed conditions if at moderate stress levels (Table 1), or 40 DAT and in the presence of mulch (RM). Over time, from 40 to 80 DAT, the percentage of carvone significantly increased, whereas that of limonene decreased over the ranges of applied treatments (Table 1). Instead, at both 40 and 80 DAT, the result shows a significant decrease in the carvone and a significant increase in limonene percentage with the increase in water-stress conditions due to reduced water availability (R). This indicates that rainfed plants may show different metabolic maturity as limonene is a precursor to carvone [3,6].

5. Conclusions

The mulching treatment had significant and positive effects on rainfed spearmint yields. Spearmint yields were positively related to physiological activity. The beneficial effects of mulching on essential-oil content and yield primarily occurred during the early stages together with lower inhibition of photosynthesis and smaller diffusive limitations. This benefit was primarily reflected in the fact that mulching, in rainfed plants, regulated tissue water content, promoted the growth of spearmint plants in later growth stages and increased the essential-oil yields compared to rainfed treatment. Thus, the rainfed

mulching treatment may have helped decrease the consumption of groundwater by providing improved utilization of limited water availability and may have helped resolve the water-scarcity problem that limits sustainable agriculture production in rainfed environments. The findings of our investigation support the hypothesis that mulch is important for a more efficient and sustainable agricultural management.

Author Contributions: Conceptualization, S.D., V.B.V. and F.M.; methodology, S.D.; validation, S.D. and V.B.V.; investigation, S.D.; writing—original draft preparation, S.D.; writing—review and editing, S.D. and V.B.V.; supervision, F.M.; project administration, S.D.; funding acquisition, S.D. and F.M. All authors have read and agreed to the published version of the manuscript.

Funding: This research was funded by Dipartimento di Agricoltura, Ambiente ed Alimenti, Università degli Studi del Molise, and Società Agricola Officinali.

Institutional Review Board Statement: Not applicable.

Informed Consent Statement: Not applicable.

Data Availability Statement: The data presented in this study are available on request from the corresponding author.

Conflicts of Interest: The authors declare no conflict of interest. The funders had no role in the design of the study; in the collection, analyses, or interpretation of data; in the writing of the manuscript; or in the decision to publish the results.








References

1. Scherer, R.; Lemos, M.F.; Lemos, M.F.; Martinelli, G.C.; Martins, J.D.L.; Da Silva, A.G. Antioxidant and antibacterial activities and composition of Brazilian spearmint (*Mentha spicata* L.). *Ind. Crops Prod.* **2013**, *50*, 408–413. [CrossRef]
2. Kumar, P.; Mishra, S.; Malik, A.; Satya, S. Insecticidal properties of Mentha species: A review. *Ind. Crops Prod.* **2011**, *34*, 802–817. [CrossRef]
3. Chrysargyris, A.; Koutsoumpeli, E.; Xylia, P.; Fytrou, A.; Konstantopoulou, M.; Tzortzakakis, N. Organic Cultivation and Deficit Irrigation Practices to Improve Chemical and Biological Activity of Mentha spicata Plants. *Agronomy* **2021**, *11*, 599. [CrossRef]
4. Chrysargyris, A.; Xylia, P.; Botsaris, G.; Tzortzakakis, N. Antioxidant and antibacterial activities, mineral and essential oil composition of spearmint (*Mentha spicata* L.) affected by the potassium levels. *Ind. Crop. Prod.* **2017**, *103*, 202–212. [CrossRef]
5. Franzios, G.; Mirotsoy, M.; Hatziaepostolou, E.; Kral, J.; Scouras, Z.G.; Mavragani-Tsipidou, P. Insecticidal and genotoxic activities of mint essential oils. *J. Agric. Food Chem.* **1997**, *45*, 2690–2694. [CrossRef]
6. Okwany, R.O.; Peters, T.R.; Ringer, K.L.; Walsh, D.B.; Rubio, M. Impact of sustained deficit irrigation on spearmint (*Mentha spicata* L.) biomass production, oil yield, and oil quality. *Irrig. Sci.* **2012**, *30*, 213–219. [CrossRef]
7. Nakawuka, P.; Peters, T.R.; Gallardo, K.R.; Okwany, R.O.; Walsh, D.B. Effect of deficit irrigation on yield, quality, and costs of the production of native spearmint. *J. Irrig. Drain. Eng.* **2014**, *140*, 05014002. [CrossRef]
8. Delfine, S.; Loreto, F.; Pinelli, P.; Tognetti, R.; Alvito, A. Isoprenoids content and photosynthetic limitations in rosemary and spearmint plants under water stress. *Agric. Ecosyst. Environ.* **2005**, *106*, 243–252. [CrossRef]
9. Singh, V.P.; Kothari, S.K.; Singh, D.V. Effect of irrigation and nitrogen on herbage and essential oil yields of Japanese mint (*Mentha arvensis*). *J. Agric. Sci.* **1989**, *113*, 277–279. [CrossRef]
10. Ram, D.; Ram, M.; Singh, R. Optimization of water and nitrogen application to menthol mint (*Mentha arvensis* L.) through sugarcane trash mulch in a sandy loam soil of semi-arid subtropical climate. *Bioresour. Technol.* **2006**, *97*, 886–893. [CrossRef]
11. Tatar, Ö.; Konakchiev, A.; Tsonev, T.; Velikova, V.; Gesheva, E.; Bayram, E.; Vitkova, A.; Edreva, A. Plant-soil Water Status-induced Changes in Physiological and Biochemical Properties of Yarrow. *J. Essent. Oil-Bear Pl.* **2016**, *19*, 1776–1787. [CrossRef]
12. Formisano, C.; Delfine, S.; Oliviero, F.; Tenore, G.C.; Rigano, D.; Senatore, F. Correlation among environmental factors, chemical composition and antioxidative properties of essential oil and extracts of chamomile (*Matricaria chamomilla* L.) collected in Molise (South-central Italy). *Ind. Crop. Prod.* **2015**, *63*, 256–263. [CrossRef]
13. Selmar, D.; Kleinwächter, M. Stress Enhances the Synthesis of Secondary Plant Products: The Impact of Stress-Related Over-Reduction on the Accumulation of Natural Products. *Plant Cell Physiol.* **2013**, *54*, 817–826. [CrossRef] [PubMed]
14. Zurita, M.L.; Thomsen, D.C.; Holbrook, N.J.; Smith, T.F.; Lyth, A.; Munro, P.G.; De Bruin, A.; Seddaiu, G.; Roggero, P.P.; Baird, J.; et al. Global water governance and Climate Change: Identifying innovative arrangements for adaptive transformation. *Water* **2018**, *10*, 29. [CrossRef]
15. Lovelli, S.; Perniola, M.; Scalcione, E.; Troccoli, A.; Ziska, L.H. Future climate change in the Mediterranean area: Implications for water use and weed management. *Ital. J. Agron.* **2012**, *7*, 45–49. [CrossRef]
16. Bu, L.D.; Liu, J.L.; Zhu, L.; Luo, S.S.; Chen, X.P.; Li, S.Q.; Hill, R.L.; Zhao, Y. The effects of mulching on maize growth, yield and water use in a semi-arid region. *Agric. Water Manag.* **2013**, *123*, 71–78. [CrossRef]

17. Benincasa, P.; Massoli, A.; Polegri, L.; Concezzi, L.; Onofri, A.; Tei, F. Optimising the use of plastic protective covers in field grown melon on a farm scale. *Ital. J. Agron.* **2014**, *9*, 8–14. [CrossRef]
18. Liu, X.E.; Li, X.G.; Hai, L.; Wang, Y.P.; Li, F.M. How efficient is film fully-mulched ridge–furrow cropping to conserve rainfall in soil at a rainfed site? *Field Crops Res.* **2014**, *169*, 107–115. [CrossRef]
19. Wang, W.; Xie, X.L.; Chen, A.L.; Yin, C.M.; Chen, W.C. Effects of long-term fertilization on soil carbon, nitrogen, phosphorus and rice yield. *J. Plant Nutr.* **2013**, *36*, 551–561. [CrossRef]
20. Gami, S.K.; Lauren, J.G.; Duxbury, J.M. Soil organic carbon and nitrogen stocks in Nepal long-term soil fertility experiments. *Soil Till. Res.* **2009**, *106*, 95–103. [CrossRef]
21. Bechini, L.; Koenderink, N.; Ten Berge, H.; Corre, W.; Van Evert, F.; Facchi, A.; Gharsallah, O.; Gorriz-Mifsud, E.; Grignani, C.; Den Herder, M.; et al. Improving access to research outcomes for innovation in agriculture and forestry: The VALERIE project. *Ital. J. Agron.* **2017**, *12*, 85–95. [CrossRef]
22. Delfine, S. *La Coltivazione Delle Piante Officinali*; Appom: Isernia, Italy, 2009; ISBN 978-88-904-6660-1.
23. Doorenbos, J.; Kassam, A.H. *Yield Response to Water*; Irr. Drainage Paper; Food and Agricultural Organization (FAO): Rome, Italy, 1986; Volume 33, p. 257.
24. Delfine, S.; Loreto, F.; Alvito, A. Drought-stress effects on physiology, growth and biomass production of rainfed and irrigated bell pepper plants in the Mediterranean region. *J. Am. Soc. Hort. Sci.* **2001**, *126*, 297–304. [CrossRef]
25. Di Stasio, E.; Rouphael, Y.; Raimondi, G.; El-Nakhel, C.; De Pascale, S. Postharvest performance of cut rose cv. Lovely red as affected by osmoprotectant and antitranspirant compounds. *Adv. Hort. Sci.* **2018**, *32*, 311–318.
26. Delfine, S.; Marrelli, M.; Conforti, F.; Formisano, C.; Rigano, D.; Menichini, F.; Senatore, F. Variation of *Malva sylvestris* essential oil yield, chemical composition and biological activity in response to different environments across Southern Italy. *Ind. Crop. Prod.* **2017**, *98*, 29–37. [CrossRef]
27. Jennings, W.; Shibamoto, T. *Qualitative Analysis of Flavour and Fragrance Volatiles by Glass Capillary Gas Chromatography*; Academic Press: New York, NY, USA, 1980.
28. Davies, N.W. Gas chromatographic retention indices of monoterpenes and sesquiterpenes on methyl silicone and Carbowax 20M phases. *J. Chromatogr.* **1990**, *503*, 1–24. [CrossRef]
29. Adams, R.P. *Identification of Essential Oil Components by Gas Chromatography/Mass Spectroscopy*, 4th ed.; Allured Publishing Co.: Carol Stream, IL, USA, 2007.
30. Li, R.; Hou, X.Q.; Jia, Z.K.; Han, Q.F.; Ren, X.L.; Yang, B.P. Effects on soil temperature, moisture, and maize yield of cultivation with ridge and furrow mulching in the rainfed area of the Loess Plateau, China. *Agric. Water Manag.* **2013**, *116*, 101–109. [CrossRef]
31. Li, S.; Wang, Z.; Li, S.; Gao, Y.; Tian, X. Effect of plastic sheet mulch, wheat straw mulch, and maize growth on water loss by evaporation in dryland areas of China. *Agric. Water Manag.* **2013**, *116*, 39–49. [CrossRef]
32. Han, Q.F.; Li, X.T.; Wang, J.P.; Jiang, J.; Ding, R.X.; Liu, Z.H.; Jia, Z.K. Simulated study on soil moisture of field under water micro-collecting farming conditions. *Trans. Chin. Soc. Agric. Eng.* **2004**, *20*, 78–82.
33. Evans, J.R.; Von Caemmerer, S.; Setchell, B.A.; Hudson, G.S. The relationship between CO₂ transfer conductance and leaf anatomy in transgenic tobacco with a reduced content of Rubisco. *Austral. J. Plant Physiol.* **1994**, *21*, 475–495.
34. Delfine, S.; Alvito, A.; Zacchini, M.; Loreto, F. Resistances to CO₂ diffusion in salt stressed leaves. *Austral. J. Plant Physiol.* **1998**, *25*, 395–402.
35. Oweis, T.; Hachum, A. Water harvesting and supplemental irrigation for improved water productivity of dry farming systems in West Asia and North Africa. *Agric. Water Manag.* **2006**, *80*, 57–73. [CrossRef]

Article

Ridge-Furrow Mulching Enhances Capture and Utilization of Rainfall for Improved Maize Production under Rain-Fed Conditions

Muhammad Mansoor Javaid ^{1,*}, Hussah I. M. AlGwaiz ^{2,*}, Hasnain Waheed ¹, Muhammad Ashraf ³, Athar Mahmood ⁴, Feng-Min Li ⁵, Kotb A. Attia ^{6,7}, Muhammad Ather Nadeem ¹, Muneera D. F. AlKahtani ², Sajid Fiaz ⁸, Muhammad Nadeem ⁹ and Hafiz Bashir Ahmad ¹⁰

¹ Department of Agronomy, College of Agriculture, University of Sargodha, Sargodha 40100, Pakistan; hasnainwaheed90@yahoo.com (H.W.); ather.nadeem@uos.edu.pk (M.A.N.)

² Department of Biology, College of Science, Princess Nourah bint Abdulrahman University, P.O. Box 84428, Riyadh 11671, Saudi Arabia; mdfkahtani@pnu.edu.sa

³ Institute of Molecular Biology and Biotechnology, The University of Lahore, Lahore 54000, Pakistan; ashrafbot@yahoo.com

⁴ Department of Agronomy, University of Agriculture Faisalabad, Faisalabad 38000, Pakistan; athar.mahmood@uaf.edu.pk

⁵ State Key Laboratory of Grassland Agro-Ecosystems, School of Life Sciences, Lanzhou University, Lanzhou 730000, China; fmli@lzu.edu.cn

⁶ Center of Excellence in Biotechnology Research, King Saud University, P.O. Box 2455, Riyadh 11451, Saudi Arabia; kattia1.c@ksu.edu.sa

⁷ Rice Biotechnology Lab, Rice Department, Field Crops Research Institute, ARC, Sakha 33717, Egypt

⁸ Department of Plant Breeding and Genetics, The University of Haripur, Haripur 22620, Pakistan; sfiaz@uoh.edu.pk

⁹ Institute of Food Science and Nutrition, University of Sargodha, Sargodha 40100, Pakistan; nadeem.abdul@uos.edu.pk

¹⁰ Department of Forestry, College of Agriculture, University of Sargodha, Sargodha 40100, Pakistan; bashir.ahmad@uos.edu.pk

* Correspondence: mmansoorjavaid@gmail.com (M.M.J.); hugwaiz@pnu.edu.sa (H.I.M.A.)



Citation: Javaid, M.M.; AlGwaiz, H.I.M.; Waheed, H.; Ashraf, M.; Mahmood, A.; Li, F.-M.; Attia, K.A.; Nadeem, M.A.; AlKahtani, M.D.F.; Fiaz, S.; et al. Ridge-Furrow Mulching Enhances Capture and Utilization of Rainfall for Improved Maize Production under Rain-Fed Conditions. *Agronomy* **2022**, *12*, 1187. <https://doi.org/10.3390/agronomy12051187>

Academic Editor: Aliasghar Montazar

Received: 10 April 2022

Accepted: 10 May 2022

Published: 14 May 2022

Publisher's Note: MDPI stays neutral with regard to jurisdictional claims in published maps and institutional affiliations.



Copyright: © 2022 by the authors. Licensee MDPI, Basel, Switzerland. This article is an open access article distributed under the terms and conditions of the Creative Commons Attribution (CC BY) license (<https://creativecommons.org/licenses/by/4.0/>).

Abstract: The capture and utilization of rainwater by crops under various mulching conditions have great importance in agriculture production systems, especially in dry-prone regions. Understanding the effect of mulching on rainwater use efficiency growth and yield of a crop is very important. For this purpose, field experiments were conducted in 2017 and 2018 to evaluate the potential of ridge-furrow mulching on maize growth and development under rain-fed conditions. The field study compared four treatments, i.e., ridge-furrow without mulch (WM), black plastic mulch (BM), transparent plastic mulch (TM) and grass mulch (GM). The BM treatment consistently increased the soil moisture and temperature, resulting in earlier emergence, as well as increased plant height and plant biomass, compared to the WM treatment. Compared to WM, the two-years mean yield of maize with BM, TM and GM were recorded to be increased by 33.6%, 28.1% and 10.8%, respectively. The BM produced a maximal crop growth rate at 90 days after sowing (DAS) as specified by a greater leaf area index. Transpiration rate and leaf stomatal conductance were significantly higher with BM and TM than with WM, however, the BM treatment showed the highest net photosynthetic rate in both years. Net income for the BM treatment was the highest (USD 1226 ha⁻¹) of all the treatments and USD 335 ha⁻¹ greater than WM. As growth, yield and net income of maize were improved with BM, therefore this treatment was found to be the most effective for maize production in rain-fed conditions. This system is evaluated at a small scale, hence to maximize its effectiveness on a large scale, a simulation design needs to be developed.

Keywords: benefit-cost ratio; physiological traits; rainwater harvesting system; rain-fed conditions and ridge-furrow mulching

1. Introduction

Water is a crucial part of agricultural production [1,2]. Scarcity of irrigation water along with irregular and insufficient rainfall has significantly affected the agricultural productivity [3–5]. Inadequate water possessions are the key constraint for crop production [4,6,7]. The decline in future rainfall may cause a reduction in the yield of various crops and enhance the risk to food supply [8,9]. There is a dire need to develop strategies to capture and utilize the rainwater for optimum crop production in rain-fed, arid and semiarid areas [10].

Ridge-furrow covered with plastic mulch on flat land is one of the most viable approaches to maximize the rainfall usage [11,12]. It can enhance the availability of moisture in the crop root zone by reducing the surface runoff, reducing the unproductive evaporation and prolonging the water availability in dry conditions which enhanced the water use efficiency and yield of crops [13]. It also promotes rainfall penetration in deep soil and reduces the evaporation losses [14–16]. Each millimeter of rainwater collected, stored and conserved in the root zone has increased the yield of a crop up to 10 kg ha^{-1} [17]. It is documented that rainfall in maize crop ranging from 230–440 mm, ridge-furrow farming system increased the soil water contents in 0–100 topsoil by 5–12% when compared to that with conventional flat farming system [18]. In the northwest of China, ridge-furrow plastic film mulching and straw mulching increased the maize yield by 20% and 10%, respectively, when compared to that with conventional planting [18]. The main purpose of mulching is to improve the rainwater harvest over a small land area along with a reduction in water loss through soil evaporation [19]. Many researchers have suggested that there is a significant potential to increase agricultural productivity with a considerable increase in the rainwater use efficiency, particularly in rain-fed areas where crops depend only on rainfall [17,20,21]. Although the ridge-furrow mulching technique is considered very beneficial for achieving enhanced yield in rain-fed agriculture [22–24], there is still a need to understand the capture and utilization of rainwater under different mulches for clarifying physiological progression, growth and development of the crop. In general, crops are planted on the ridge in a ridge-furrow system that received little advantage from rain as rainwater makes a channel into the furrow areas, especially in the case of a light shower. However, in this study, the planting geometry was quite different than that in conventional methods of sowing, used in most areas of the world. In this study, we used furrows as planting zone and ridges served as water harvesting areas. Therefore, it is important to determine how different mulching practices affect crop growth, yield and resource utilization for maximizing the water management and enhancing the yield of maize. The main objective of this experiment was to investigate the role of the ridge-furrow mulching on the physiological, growth and yield of maize by collecting the rainwater and re-allocating it to the furrow where the crop was planted. This study could be helpful for water management approaches in maize production under rain-fed conditions.

2. Materials and Methods

2.1. Site Description

Experiments were conducted during the summer season of 2017 and 2018 at the Agronomic Research Area, College of Agriculture, University of Sargodha, Punjab Province, Pakistan (Latitude 31.41° N , Longitude 74.17° E and Altitude 194.4 m). The soil at the experimental site was clay loam with a pH of 7.7, organic matter 0.83%, 0.52% N, 10 mg/kg available P and 112 mg/kg available K. During the entire experimental phase, the daily maximum or minimum and rainfall distributions are shown in Figure 1. The total rainfall during the maize growing period was 443.76 mm in 2017 and 946.62 mm in 2018.

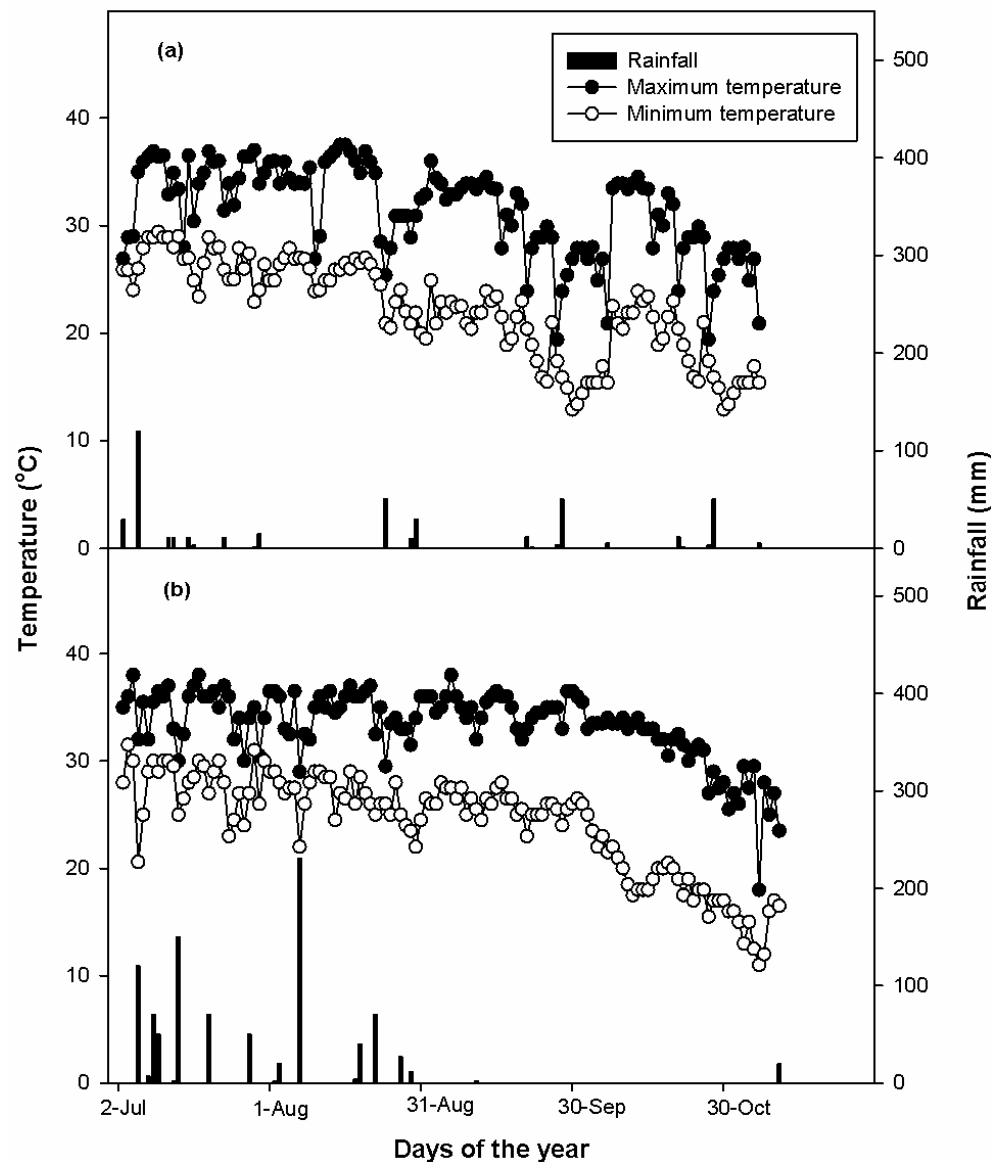


Figure 1. The daily maximum or minimum temperatures and rainfall during the maize growing seasons of the experimental site in 2017 (a) and 2018 (b).

2.2. Experimental Design and Field Management

Alternate ridge and furrow were set up on the flat land. There was a narrow ridge with a width of 30 cm and a height of 15 cm, whereas the wide ridge had a width of 60 cm and a height of 10 cm (Figure 2). The ridges served as rainwater harvesting zone and furrows served as planting zone. The treatments were comprised of ridge-furrow without mulching (WM), ridge-furrow covered with black plastic mulch (BM), transparent plastic mulch (TM) and grass mulch (GM). The experiment was carried out in a Randomized Complete Block Design with four replications. Each plot size was 5 m × 4.5 m. The thickness of the film was 0.008 mm. The edge of the plastic film was buried in the soil. Grass mulch was spread evenly on the ridges and furrows at a rate of 9000 kg ha⁻¹. The crop was sown in each furrow at the base of the ridge at 25 cm apart with a planting density of 88,888 ha⁻¹ (Figure 2). A fertilizer having 150 kg N ha⁻¹, 125 kg P₂O₅ ha⁻¹ and 125 kg K₂O ha⁻¹ was applied uniformly over the furrows and plowed into the soil layer. The maize seed was drilled with a hand push maize seeder with a dibbler wheel into the plastic mulch for all treatments except the grass cover mulch where mulching was done after sowing of the maize seed with the maize seeder.

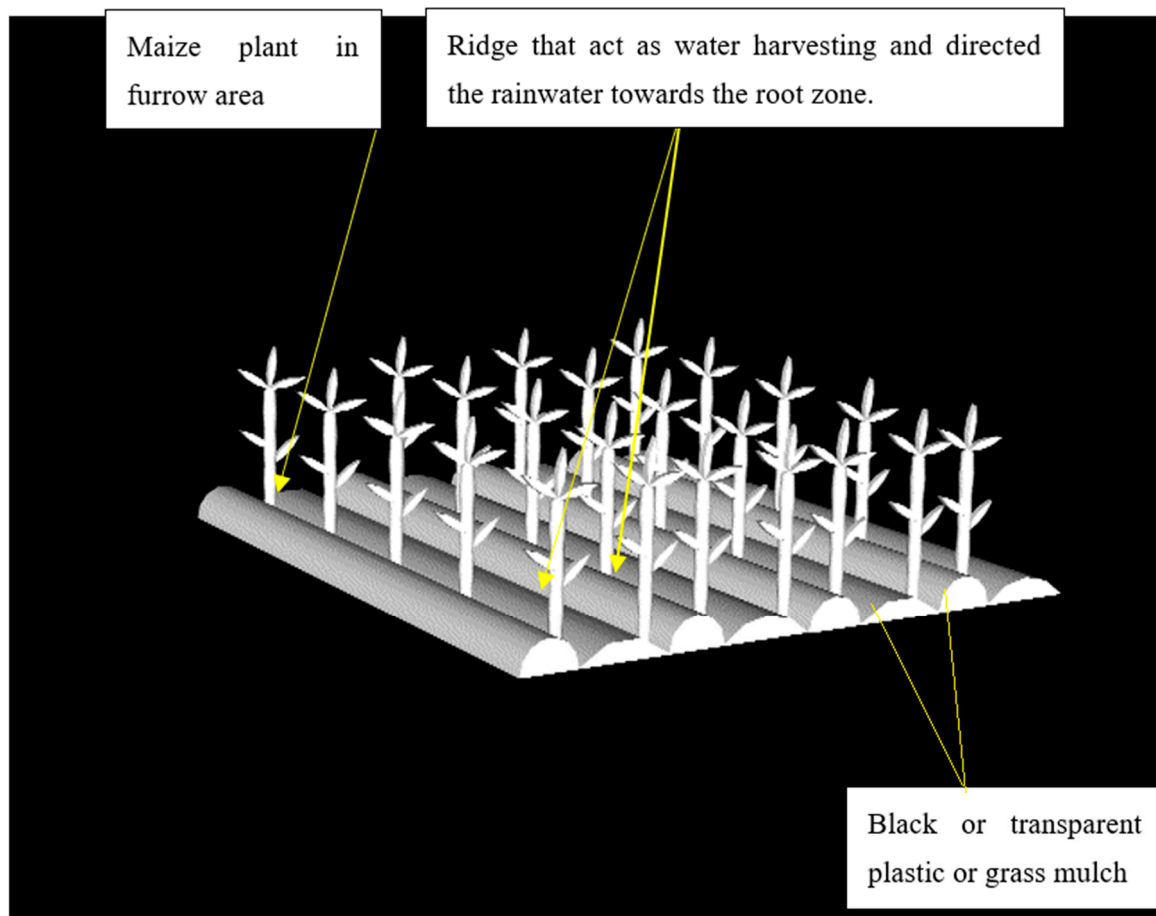


Figure 2. A schematic diagram of the field layout.

Maize (cv. DK-6525) was sown on 2nd and 6th July in 2017 and 2018, respectively, using a seed rate of 25 kg ha^{-1} with a drill. Thinning of the crop stand was performed at the 3 to 4 leaf stage to sustain one plant per hill. All other farming practices such as the use of natural and standard insecticides were done for all the treatments. If heavy rainfall occurs, the excess rainwater will be drained out through a drain at the end of the furrows. This means that at the end of each furrow, there is a small ridge about 10–15 cm high. When the rainfall is low, all the rainwater can be trapped in the furrow. If the rainfall is heavy, the excess water will drain out automatically and will not cause serious flooding problems. To prevent flooding, the mulch film can be punctured at the point of emergence, leaving a hole for emergence. This will ensure that there is no flooding risk.

2.3. Data Collection and Measurements

- **Growth and yield traits:** The number of plants grown in each plot was calculated from a selected area until a steady and constant number of plants was obtained. The mean days taken to emergence were determined from the time of sowing. Plant height and 1000-grain weight were measured from five indiscriminately selected plants from each plot at maturity and then the average was recorded. The leaf area from five consecutive plants randomly selected from a line in each plot was measured at 30, 60, 90 and 120 days after sowing [25] with the help of a leaf area meter (CI-202, CID, Bio-Science, Camas, WA, USA). The following formula was used to calculate the leaf area index (LAI):

$$LAI = \frac{\text{Leaf area}}{\text{Land area}} \quad (1)$$

To estimate the crop growth rate (CGR), five plants per plot were taken. Each plant was mocked, mixed well and then sun-dried. The samples were then subjected to an oven at $70\text{ }^{\circ}\text{C} \pm 5\text{ }^{\circ}\text{C}$ to record dry weight. The dry weight of each plant was measured and converted into dry matter per unit of land area (m^2). The CGR was calculated at 30, 60, 90 and 120 days after sowing according to the formula presented by Beadle [26]:

$$\text{CGR} = \frac{W2 - W1}{T2 - T1} \quad (2)$$

where $W2$ = Plant dry weight m^{-2} at 2nd harvest, $W1$ = Plant dry weight m^{-2} at 1st harvest, $T2$ = Time consistent to 2nd harvest, $T1$ = Time consistent to 1st harvest.

To obtain grain yield, the maize plants were harvested at maturity from every plot, dried in the sun and threshed manually. The biological yield was measured by collecting the total plant biomass from every plot, dried in the sun for several days and then transformed to t ha^{-1} .

The harvest index was determined using the following formula:

$$\text{Harvest Index (\%)} = \frac{\text{Grain yield}}{\text{Biological yield}} \times 100 \quad (3)$$

- *Soil moisture:* In every maize growing period, the water content in the soil was recorded at 30, 60, 90 and 120 days after sowing (DAS) to 100 cm soil depth at 20 cm intervals. By using a soil auger, the samples were arbitrarily collected at three locations in the middle of the furrow for every treatment [25]. The self-sealing plastic bags were used to collect the soil samples from the field. Upon arrival in the laboratory, each sample was placed directly in an aluminum box. To obtain fresh weights, all soil samples were weighed within one hour of collection and dried at $105\text{ }^{\circ}\text{C}$ to obtain a constant weight. The soil moisture was then calculated in the 0–100 cm soil from every plot and then estimated for the total soil water storage.
- *Physiological traits:* Net photosynthetic rate, transpiration rate and leaf stomatal conductance were recorded from five randomly selected flag leaves of maize plants from each treatment separately using a portable infrared gas analyzer (CI-340 Portable Photosynthesis System, CID Biosciences, Camas, WA, USA). The readings were taken between 9:00 to 11:00 am.
- *Economic analysis:* For economic analysis, the whole cost of production was estimated by the expenses incurred on all agronomic operations during both years and their average was determined. To determine the benefit–cost ratio, the total income of grains and stover was recorded [26].

2.4. Statistical Analysis

The statistical analysis was performed by the software Statistix 8.1 computer software (Statistix 8.1, Analytical Software, Tallahassee, FL, USA) to work out an analysis of variance (ANOVA) of each data set. The treatments' means were compared using Tukey's (HSD) test at a 5% probability level [27]. The graphical demonstration of the data was done using the Sigma plot 11.0 (Systat Software, Inc., San Jose, CA, USA).

3. Results

3.1. Plant Growth and Yield Attributes

Data showed that in BM and TM, maize emergence was two days earlier than that with WM in both years. Maize plant height was significantly influenced by various mulching treatments over the two years with the higher plant height observed in 2017 as compared with 2018 (Table 1). In 2017, higher plant height (186.5 cm) was observed with BM and lower plant height (169.2 cm) was measured with WM. In 2018, BM produced taller plants (188.2 cm) than did all other treatments. The lowest plant height (169.2 cm) of the maize crop was recorded in plots where not mulch material was used. The 1000-grain weight

of maize showed a substantial response to all mulch treatments. The BM exhibited a maximum 1000-grain weight (285.5 g) which was followed by TM in 2018. However, a minimum 1000-grain weight was recorded with WM during both growing seasons. All mulching treatments had a significant impact on grain yield as compared to WM in both years. The mulch treatments significantly influenced the grain yield of maize. The maize grain yield from every treatment was categorized as follows: BM > TM > GM > WM. Compared with WM, the mean grain yield of maize with BM, TM and GM was found to be improved significantly by 1.24 t ha⁻¹ (33.6%), 1.04 t ha⁻¹ (28.1%) and 0.40 t ha⁻¹ (10.8%), respectively (Table 2). As compared to WM, the ridge and furrow mulching improved the biological yield significantly. The mean biological yield with BM, TM and GM was markedly enhanced by 1.74, 1.42 and 0.81 t ha⁻¹, respectively. All tested treatments showed a variable harvest index (%) of maize, ranging from 42.1% to 48% in both growing seasons. The harvest index was higher (48%) in 2017 with BM and the difference of BM and TM vs. WM was significant during both years.

Table 1. Influence of different ridge-furrow mulching on days taken to emergence, plant height (cm) and 1000-grain weight of maize during 2017 and 2018.

Treatments	Days Taken to Emergence		Plant Height (cm)		1000-Grain Weight (g)	
	2017	2018	2017	2018	2017	2018
WM	6.7 a	6.5 a	169.2 d	171.5 b	237.5 c	243.2 c
BM	4.2 b	4.2 b	186.5 a	188.2 a	276.5 a	285.5 a
TM	4.7 b	4.5 b	181.2 b	187.0 a	260.0 b	278.0 ab
GM	5.2 b	5.0 b	174.2 c	177.0 b	252.0 b	260 bc
HSD (0.05)	1.16	1.38	4.51	5.53	10.47	19.27

Values within each column sharing the same letter did not differ significantly at a 5% level of probability. WM = Ridge-furrow without mulch, BM = black plastic mulch, TM = transparent plastic mulch, GM = grass mulch.

Table 2. Influence of different ridge-furrow mulches on grain yield (t ha⁻¹), biological yield (t ha⁻¹) and harvest index (%) of maize during 2017 and 2018.

Treatments	Grain Yield (t ha ⁻¹)		Biological Yield (t ha ⁻¹)		Harvest Index (%)	
	2017	2018	2017	2018	2017	2018
WM	3.73 c	3.65 c	8.55 c	8.66 c	43.7 b	42.1 b
BM	4.94 a	4.92 a	10.27 a	10.42 a	48.0 a	47.2 a
TM	4.71 a	4.76 a	9.83 ab	10.21 a	47.9 a	46.6 a
GM	4.11 b	4.08 b	9.46 b	9.37 b	46.4 b	43.5 b
HSD (0.05)	0.36	0.36	0.58	0.53	3.13	2.69

Values within each column sharing the same letter did not differ significantly at a 5% level of probability. WM = Ridge-furrow without mulch, BM = black plastic mulch, TM = transparent plastic mulch, GM = grass mulch.

In contrast to the WM treatment, all mulching treatments improved the leaf area index in both years (Figure 3). The leaf area index was significantly higher with BM and TM when compared with WM at each critical stage. The GM produced a slightly higher leaf area index than did the WM during both years at each developmental stage. Moreover, the major differences were perceived between the WM and GM treatments in 2018, mainly at 60 and 120 days after sowing (DAS). The variation in leaf area index was connected with a different crop growth rate under various mulch treatments (Figure 4). Of all the treatments, the ridge-furrow covered with BM or TM produced a higher crop growth rate in 2017 and 2018. At 30, 60, 90 and 120 DAS, the BM produced 27.6, 33.3, 49.3 and 33.2% higher crop growth rate, respectively, than WM in 2017 (Figure 4). The increase was 21.5% at 30 DAS, 30.8% at 60 DAS, 37.9% at 90 DAS and 26.4% at 120 DAS in 2018. However, TM produced a slightly higher crop growth rate over BM at 90 days after sowing in 2018 (Figure 4).

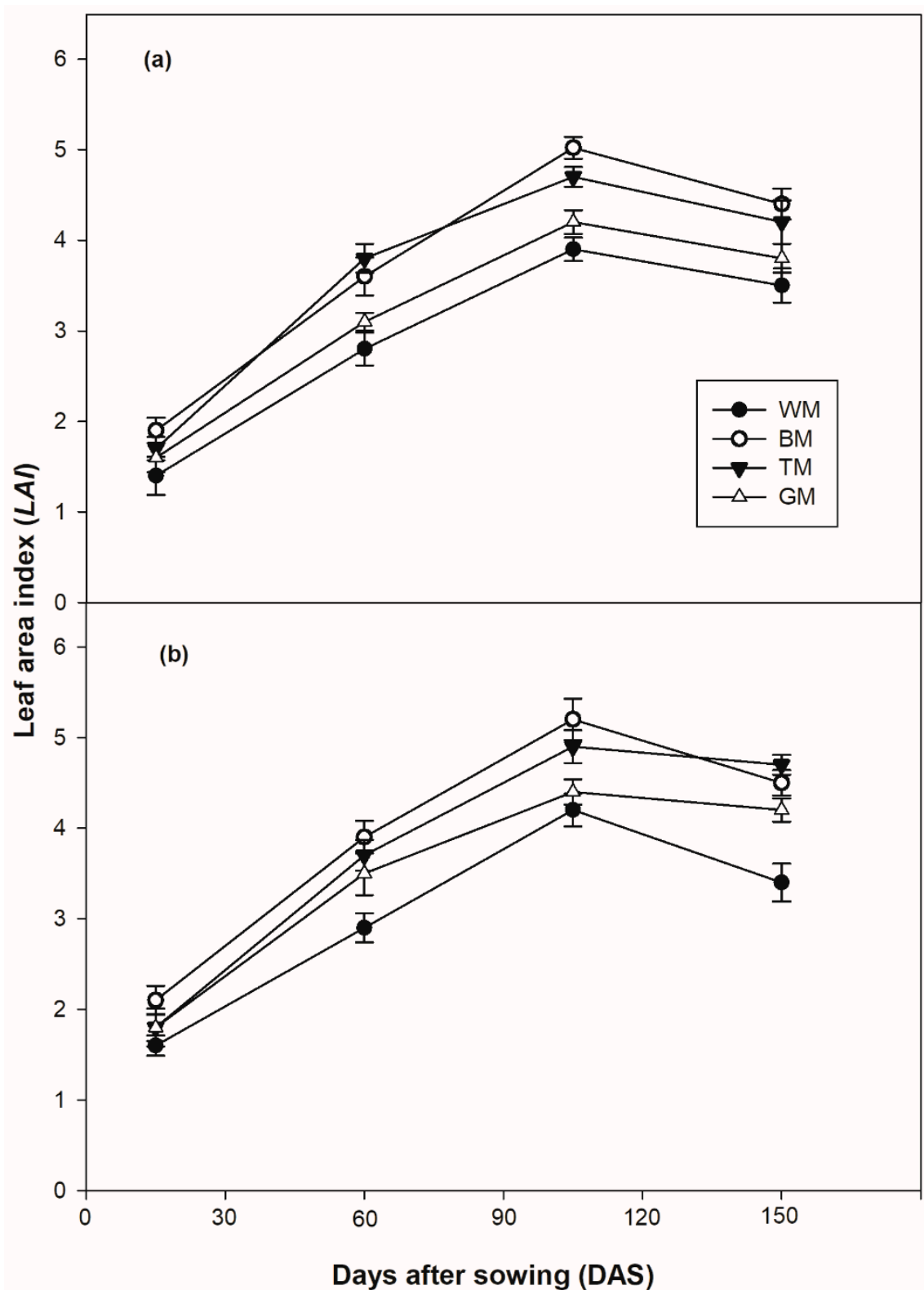


Figure 3. Leaf area index (LAI) of maize under ridge-furrow without mulching (WM), with black plastic mulch (BM), transparent plastic mulch (TM) and grass mulch (GM) in 2017 (a) and 2018 (b).

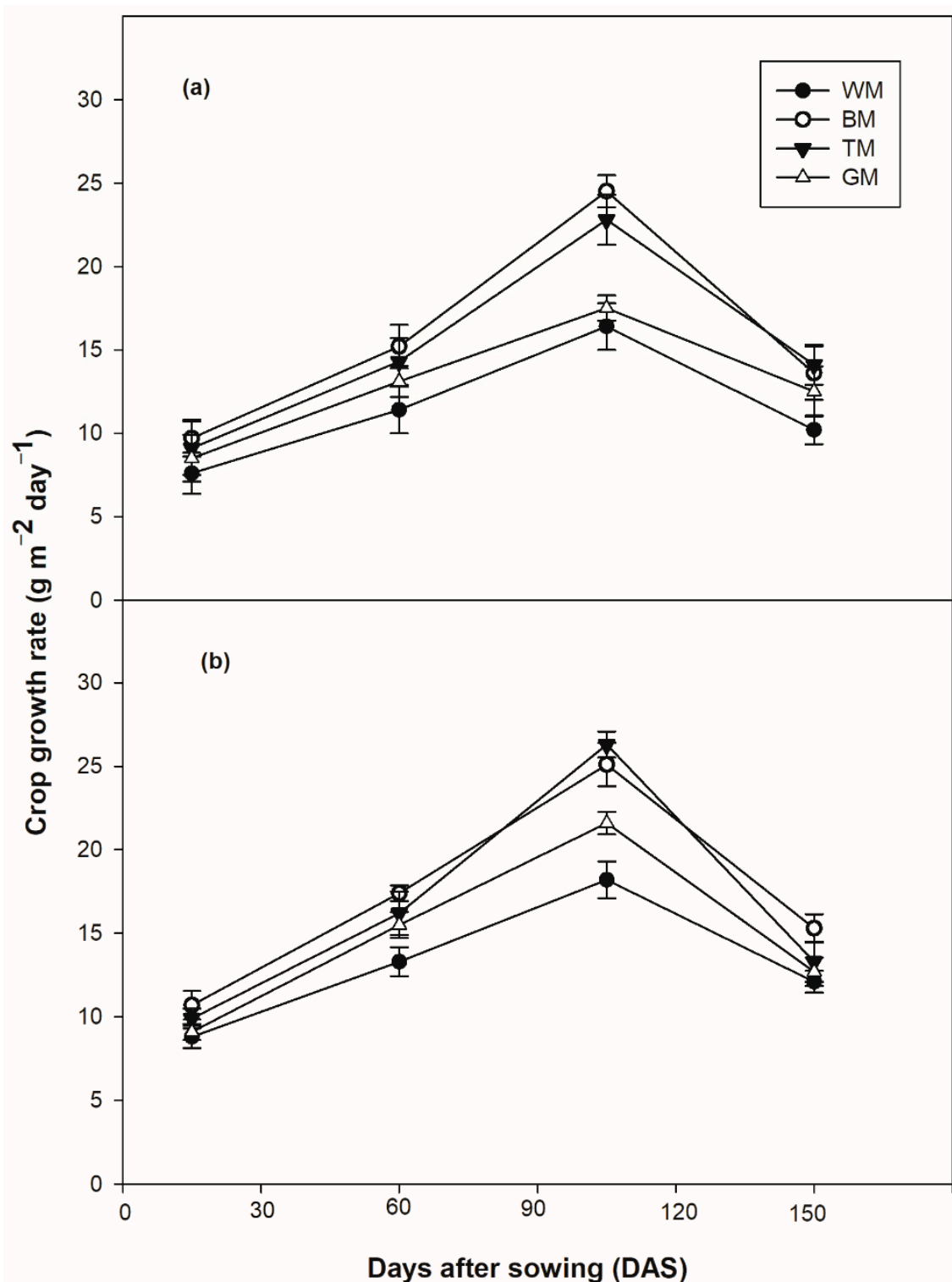


Figure 4. Crop growth rate (CGR) of maize under ridge-furrow without mulching (WM), with black plastic mulch (BM), transparent plastic mulch (TM) and grass mulch (GM) in 2017 (a) and 2018 (b).

Soil water storage (SWS) indicated a slight difference among the four treatments (Figure 5). Compared to the WM treatment, all mulching treatments augmented the SWS significantly during both growing seasons. The quantity of water storage from 1st (30 DAS) to 2nd (60 DAS) sampling was recorded to be improved with BM, TM and GM treatments in 2017 and 2018, as well as being the most vital water restoring time for crop growth. While, from the 2nd (60 DAS) to the 4th (120 DAS) sampling, differences between the treatments

in the value of SWS were very high in 2017, however, in 2018, the differences among the treatments were quite less. At the first sampling, higher soil water was stored in the WM treatment due to more rain in July in both growing seasons. The heavy rain caused the runoff in mulch treatments and WM facilitated the water penetration, which resulted in more soil water contents. The *p*-value showed that the effect of mulching was significant for leaf area index, crop growth rate and soil water storage at 30, 60, 90 and 120 DAS at a 5% level of probability (Table 3).

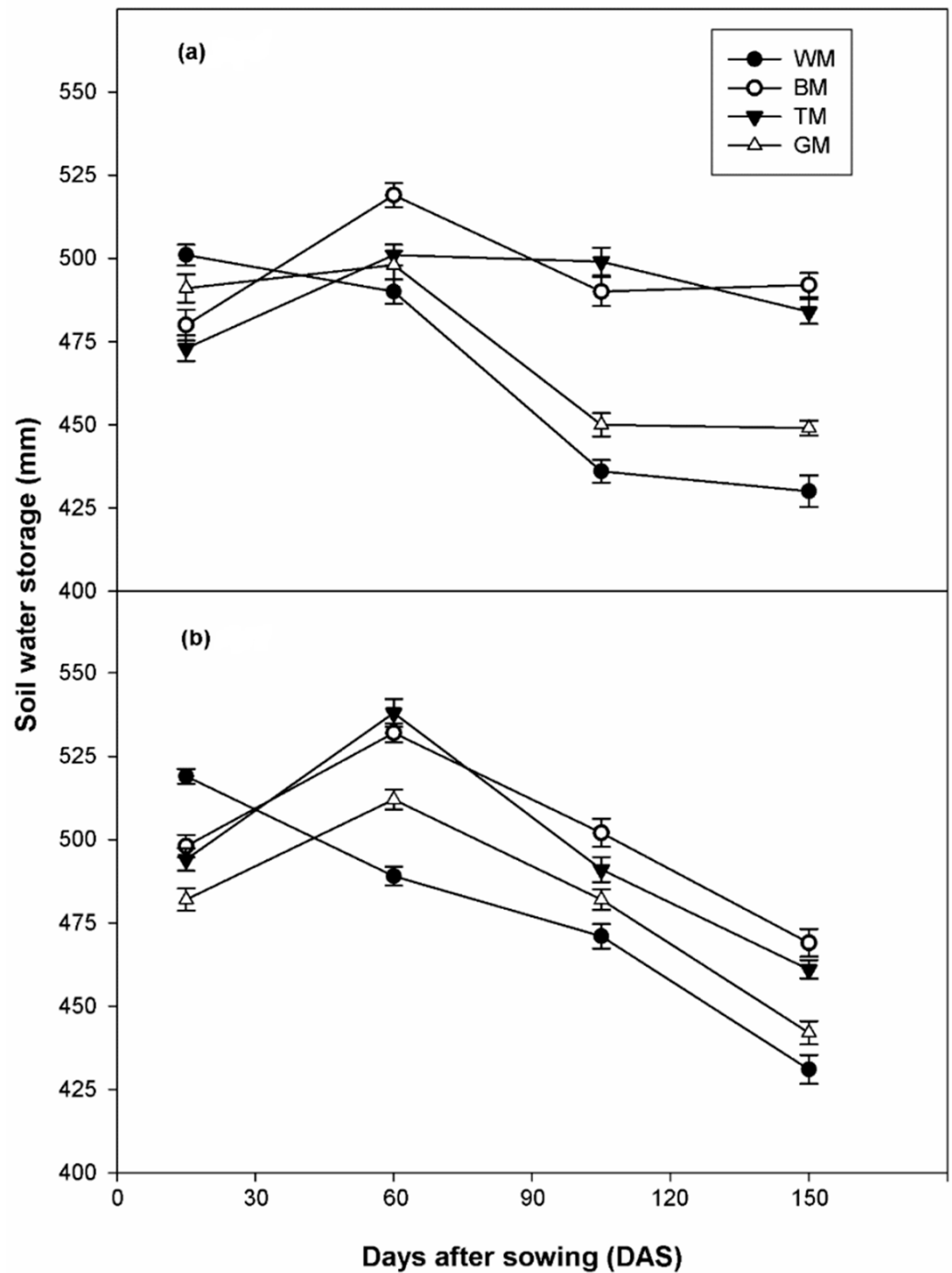


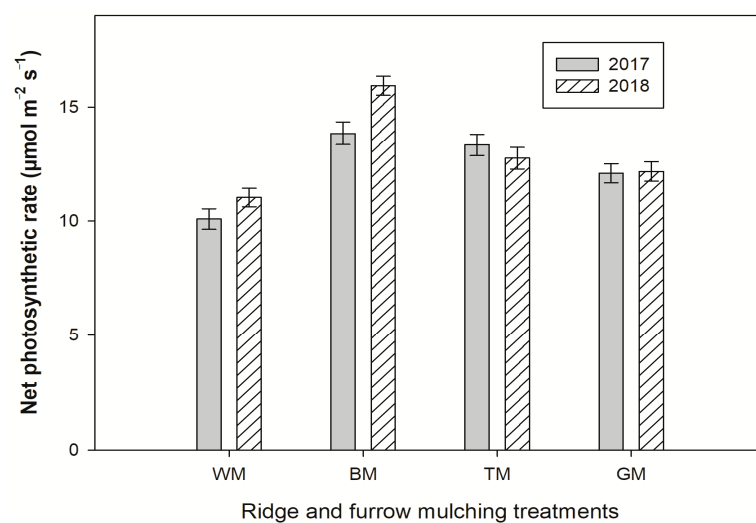
Figure 5. Average soil water storage (SWS, 0–100 cm) under ridge-furrow without mulching (WM), with black plastic mulch (BM), transparent plastic mulch (TM) and grass mulch (GM) in 2017 (a) and 2018 (b).

Table 3. Summary of the analysis variance for leaf area index, crop growth rate, soil water storage, net photosynthesis rate, transpiration rate and stomatal conductance of maize under different mulching materials.

Parameter	Mean Sum of Square		F-Value		p-Value (0.05)	
	2017	2018	2017	2018	2017	2018
Leaf area index at 30 DAS	0.17	0.17	8.67	5.67	0.003	0.012
Leaf area index at 60 DAS	0.77	0.75	23.2	24.9	<0.001	<0.001
Leaf area index at 90 DAS	1.00	0.84	37.1	19.3	<0.001	<0.001
Leaf area index at 120 DAS	0.65	1.31	21.7	39.2	<0.001	<0.001
Crop growth rate ($\text{gm}^{-2} \text{day}^{-1}$) at 30 DAS	2.92	2.91	44.9	54.7	<0.001	<0.001
Crop growth rate ($\text{gm}^{-2} \text{day}^{-1}$) at 60 DAS	10.54	12.82	148.00	46.8	<0.001	<0.001
Crop growth rate ($\text{gm}^{-2} \text{day}^{-1}$) at 90 DAS	62.34	52.68	156.00	152.00	<0.001	<0.001
Crop growth rate ($\text{gm}^{-2} \text{day}^{-1}$) at 120 DAS	12.30	7.42	46.70	47.10	<0.001	<0.001
Soil water storage at 30 DAS	599.72	2222.56	3.03	11.6	0.071	0.007
Soil water storage at 60 DAS	575.83	3043.23	2.51	32.2	0.108	<0.001
Soil water storage at 90 DAS	3749.06	650.72	32.6	7.97	<0.001	0.003
Soil water storage at 120 DAS	3479.50	2562.75	12.4	40.5	0.006	<0.001
Net photosynthesis rate ($\mu\text{mol m}^{-2} \text{s}^{-1}$)	11.21	17.69	13.1	23.7	<0.001	<0.001
Transpiration rate ($\text{mmol m}^{-2} \text{s}^{-1}$)	2.19	3.77	22.4	27.2	<0.001	<0.001
Leaf stomatal conductance ($\text{mmol m}^{-2} \text{s}^{-1}$)	23,631.9	3.77	18.2	27.2	<0.001	<0.001

3.2. Physiological Attributes

In both years of study, the net photosynthetic rate of maize was significantly affected by different ridge-furrow mulches (Figure 6). During both years, the net photosynthetic rate was consistently higher with BM, TM and GM as compared to that with WM. All mulching treatments markedly improved the transpiration rate of maize. The transpiration rate was observed higher in 2017 than that of 2018. The highest transpiration rate was recorded with BM and statistically at par with that of TM during both growing seasons. Compared to WM, GM showed a slightly higher transpiration rate (Figure 7). Figure 8 shows that compared to WM, other treatments, i.e., BM, TM and GM exhibited higher leaf stomatal conductance. Among all mulching treatments, BM produced slightly higher values of leaf stomatal conductance during both years. However, the lowest leaf stomatal conductance was recorded in plots with the ridge-furrow left uncovered (WM).

**Figure 6.** Influence of different ridge and furrow mulching treatments on net photosynthetic rate, of maize in 2017 and 2018. WM = Ridge-furrow without mulch, BM = Ridge-furrow covered with black plastic mulch, TM = Ridge-furrow covered with transparent plastic mulch, GM = Ridge-furrow covered with grass mulch.

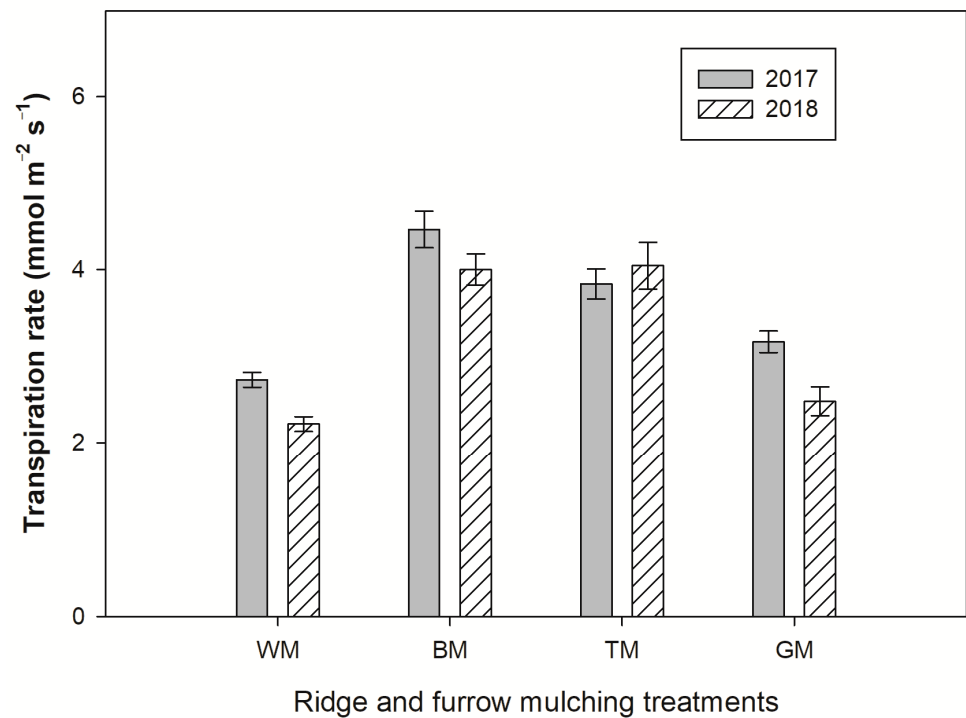


Figure 7. Influence of different ridge and furrow mulching treatments on the transpiration rate of maize in 2017 and 2018. WM = Ridge-furrow without mulch, BM = Ridge-furrow covered with black plastic mulch, TM = Ridge-furrow covered with transparent plastic mulch, GM = Ridge-furrow covered with grass mulch.

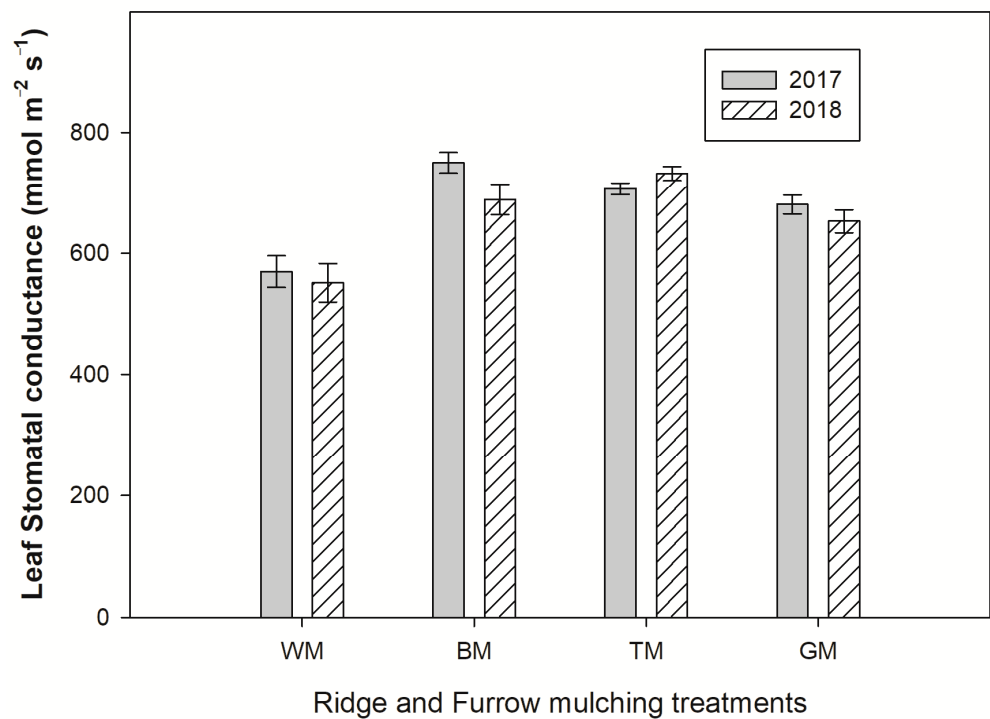


Figure 8. Influence of different ridge and furrow mulching treatments on leaf stomatal conductance of maize in 2017 and 2018. WM = Ridge-furrow without mulch, BM = Ridge-furrow covered with black plastic mulch, TM = Ridge-furrow covered with transparent plastic mulch, GM = Ridge-furrow covered with grass mulch.

3.3. Economic Analysis

Different mulching materials and treatments without mulch have a variable cost-benefit ratio (Table 4). The two-year average benefit–cost ratio was ranked as follows: BM > TM > GM > WM. The cost with different treatments followed the order: BM = TM > GM > WM. Net incomes of BM, TM and GM were higher than that of WM. Net income was highest (USD 1226 ha⁻¹) for the BM treatment and the benefit–cost ratio was improved by 16%, compared to WM. The net income difference for BM vs. WM was USD 335 ha⁻¹ (Table 3).

Table 4. Average economic benefit cost ratio (USD ha⁻¹) of maize production in 2017 and 2018.

Particulars	WM	BM	TM	GM
Fertilizer cost	258	258	258	258
Seed cost	97	97	97	97
Mulching material cost	-	109	109	58
Common cost ^a	238	238	238	238
Total cost	593	702	702	651
Grain yield (t ha ⁻¹)	3.69	4.93	4.73	4.09
Grain yield revenue (USD)	1069	1429	1371	1185
Fodder yield (t ha ⁻¹)	8.60	10.34	10.02	9.41
Fodder yield revenue (USD)	415	499	484	454
Gross income (USD)	1484	1928	1855	1639
Net benefit (USD)	891	1226	1153	988
Benefit-cost ratio	1.50	1.74	1.64	1.51
Net income differences (USD)	00	335	262	97

WM = Ridge-furrow without mulching, BM = Ridge-furrow covered with black plastic mulch, TM = Ridge-furrow covered with transparent plastic mulch, GM = Ridge-furrow covered with grass mulch, ^a Including labor cost was USD 4.34 per person per day, land preparation, pesticides and harvesting charges; cost of plastic film was USD 2.31 kg⁻¹, grass mulch USD 0.0063 kg⁻¹; maize seed price was USD 3.86 kg⁻¹. Cost was calculated in USD and paid in PKR.

4. Discussion

Our study showed that seedling emergence with TM was two days earlier than that with WM. It is believed that solar radiation passed through the transparent film mulch and reached the soil surface but this film prevents the entry of long-wave radiation, hence improving the soil thermal conditions. The early emergence under TM might be due to the thermal difference in the soil. Researcher also pointed out that straw mulch caused cooling effects and plastic film caused warming effects at the early growth stage of the crops. The reduction in the emergence days under mulch treatments might be due to the availability of more moisture compared to that under WM treatments. Mulch treatments reduced the days to emergence.

Consequently, the ridge-furrow mulching treatments produced higher plant height and biological yield than that with WM. The ridge-furrows covered with plastic film raised the soil moisture, which could increase the growth of maize during the early phase [14,28]. There were little differences between BM and TM in terms of improving maize growth and biological yield which may have been due to the availability of moisture at critical growth stages.

The productivity of maize appears to correlate closely with the successive distribution of detected resources [29], in particular, the uptake and absorption of sunlight, which were linked with the leaf area index [30,31]. The mulching treatments significantly improved stored soil water by retaining adequate levels of heat and water for plant growth at the seedling phase. Therefore, the increase in leaf area might have led to an increase in the effective intercepted radiation that was later available for the fast-growing maize crop. However, significant differences were observed between the treatments in terms of crop growth rate with respect to these properties. The BM and TM treatments exhibited a greater crop growth rate, which might have been due to the higher leaf area index, and improved radiation detention [32], which might have led to more biomass production compared

to the WM treatment. The possible reason for this is that covering the soil with mulches preserves the soil water by inhibiting the evaporation and enhancing the water. Further, it is reported that when plants were small, soil water was lost mainly through soil evaporation. As the maize crop grew vigorously, the water loss shifted from soil evaporation to plant transpiration, so better water conditions under mulch conditions improved the growth of the maize crop. Compared to the GM and WM treatments, the BM and TM symbolize a more operative exercise to respond to the scarcity of available water. Our findings showed that the ridge-furrow mulching enhanced the soil moisture and augmented the yield of maize with BM and TM at 33.6 and 28.1%, respectively. The improvement in the maize yield resulted from the more efficient single plants developed under BM and TM and could have been due to the exploitation of deep soil water effectively [33,34]. In our study, the ridge-furrow covered with mulches markedly enhanced the water storage of soil. The increased soil moisture contents under mulch conditions could improve the soil nitrogen availability. High N accumulation promotes maize growth by improving nitrogen use efficiency. The soil water storage was higher with BM, TM and GM than that with WM, which might have been due to the reason that mulches inhibit the evaporation from the soil surface and increase rainfall infiltration. According to Li et al. [31] and Wang et al. [35], plastic-covered ridge-furrow mulching can improve the soil moisture status by collecting water more efficiently from light rainfall, endorsing rainfall infiltration and reducing the evaporation. Ren et al. [18] also described that various intensities of rainfall (440, 340 and 230 mm) improved the mean water contents of soil by 4.5, 5.2 and 2.3%, respectively, with the plastic-covered ridge-furrow mulching than with the flat cultivation without ridges and plastic mulches. In addition, more harvested rainwater infiltrated deeper in the covered ridge system when compared to that with flat cultivation, hence increasing the availability of water to plant for a longer period of time as well as being less subject to evaporation [18]. However, for effectiveness on a large scale, this system needs simulation design with different rainfall amounts.

The physiological attributes such as net photosynthetic rate, transpiration rate and leaf stomatal conductance were found to be improved with BM, TM and GM treatments compared to that of WM, because photosynthetic capacity is highly linked with water availability, with maize crop at the early growth stage showing an increase in photosynthesis rate under the plastic film or grass mulch compared to that under non-mulch treatment [36–38]. In our experiment, the treatments of mulches resulted in increased retention of soil moisture as compared to that with WM treatment during the partial rainy season. These results might have been due to the loss of soil moisture from the WM treatment due to the strong evaporation from the soil surface by direct sun radiation and dry air during the early phases of maize growth. The BM, TM and GM treatments produced higher net photosynthetic, transpiration rate and leaf stomatal conductance than the WM treatment, because mulches directly inhibit water evaporation from the surface of soil [30] and provide more water to plants, increasing the gas exchange activity of plants by using solar radiation and enhanced canopy transpiration [39]. The plastic and grass mulches could enhance the soil moisture of dry arable land [14,15,35,40].

5. Conclusions

The ridge-furrow covered with plastic mulches accelerated the photosynthetic capacity, growth and development by capture and utilization of rainwater. The BM significantly increased the net photosynthesis and transpiration rate during both growing seasons over the other treatments. Consequently, as compared to all other treatments, BM was found to be the most effective approach to bring an increase in the farmer's income. Therefore, BM treatment must be encouraged and applied as an effective cultivation method in rain-fed areas.

6. Implication

Crop productivity in arid and semiarid regions of Pakistan is dependent on rainfall. Frequent drought is an important factor that limits crop production. Seasonal rainfall and distribution determine the success of crop in dry areas. This study indicates that ridge-furrow plastic film mulch has some advantages over conventional systems under the same volume of rainfall. First, the ridge-furrow configuration leads to capture and utilizing the small amount of rainfall, thus providing better conditions for maize growth and development. Secondly, the full cover of ridge-furrow with plastic film reduced the evaporation losses. This system is evaluated at a small scale, hence to maximize its effectiveness on a large scale in Pakistan, a simulation design needs to be developed. The cost of ridge-furrow plastic film is higher than the conventional system as the additional cost of plastic and labor is added every year. However, this cost can be compensated with higher productivity under plastic mulch, but plastic fate is a disadvantage in terms of recycling and environmental protection.

Author Contributions: Writing—original draft preparation and edition, M.M.J., H.W. and M.A.; project administration, F.-M.L. and M.A.; conceptualization, methodology and investigation, M.M.J., F.-M.L., A.M., H.I.M.A. and S.F.; writing—review and editing K.A.A., M.A.N., M.N., H.B.A. and M.D.F.A. All authors have read and agreed to the published version of the manuscript.

Funding: Princess Nourah bint Abdulrahman University Researchers Supporting Project Number (PNURSP2022R20), Princess Nourah bint Abdulrahman University, Riyadh, Saudi Arabia.

Institutional Review Board Statement: Not applicable as studies not involving humans or animals.

Data Availability Statement: Not applicable.

Acknowledgments: Princess Nourah bint Abdulrahman University Researchers Supporting Project Number (PNURSP2022R20), Princess Nourah bint Abdulrahman University, Riyadh, Saudi Arabia.

Conflicts of Interest: The authors declare no conflict of interest.

References

- Hanjra, M.A.; Qureshi, M.E. Global water crisis and future food security in an era of climate change. *Food Policy* **2010**, *35*, 365–377. [CrossRef]
- Basso, B.; Antle, J. Digital agriculture to design sustainable agricultural systems. *Nat. Sustain.* **2020**, *3*, 254–256. [CrossRef]
- Piao, S.; Ciais, P.; Huang, Y.; Shen, Z.; Peng, S.; Li, J.; Zhou, L.; Liu, H.; Ma, Y.; Ding, Y. The impacts of climate change on water resources and agriculture in China. *Nature* **2010**, *467*, 43–51. [CrossRef] [PubMed]
- Madushanki, R.; Wirasagoda, H.; Halgamuge, M. Adoption of the Internet of Things (IoT) in agriculture and smart farming towards urban greening: A review. *Int. J. Advan. Comp. Sci. Appl.* **2019**, *10*, 11–28. [CrossRef]
- Wasaya, A.; Abbas, T.; Yasir, T.A.; Sarwar, N.; Aziz, A.; Javaid, M.M.; Akram, S. Mitigating drought stress in sunflower (*Helianthus annuus* L.) through exogenous application of β -aminobutyric acid. *J. Soil Sci. Plant Nutr.* **2021**, *21*, 936–948. [CrossRef]
- Rockström, J.; Lannerstad, M.; Falkenmark, M. Assessing the water challenge of a new green revolution in developing countries. *Proc. Natl. Acad. Sci. USA* **2007**, *104*, 6253–6260. [CrossRef]
- Sarwar, R.A.; Ashraf, M.; Javaid, M.M. Response of foliar-applied nutrient solution with and without soil-applied fertilizers on growth and yield of mung bean. *J. Plant Nutr.* **2018**, *41*, 1083–1093. [CrossRef]
- Lobell, D.B.; Burke, M.B.; Tebaldi, C.; Mastrandrea, M.D.; Falcon, W.P.; Naylor, R.L. Prioritizing climate change adaptation needs for food security in 2030. *Science* **2008**, *319*, 607–610. [CrossRef]
- Dinar, A.; Tieu, A.; Huynh, H. Water scarcity impacts on global food production. *Glob. Food Secur.* **2019**, *23*, 212–226. [CrossRef]
- Zhao, H.; Xiong, Y.-C.; Li, F.-M.; Wang, R.-Y.; Qiang, S.-C.; Yao, T.-F.; Mo, F. Plastic film mulch for half growing-season maximized WUE and yield of potato via moisture-temperature improvement in a semi-arid agroecosystem. *Agric. Water Manag.* **2012**, *104*, 68–78. [CrossRef]
- Mak-Mensah, E.; Zhang, D.; Zhou, X.; Zhao, X.; Wang, X.; Zhao, W.; Wang, Q.; Ahiakpa, J.K. Effect of co-application of ridge-furrow rainwater harvesting and mulching on fodder yield, quality, and soil desiccation in alfalfa (*Medicago sativa*) production. *J. Soil Sci. Plant Nutr.* **2022**, *22*, 1–16. [CrossRef]
- Li, F.M.; Li, X.G.; Javaid, M.M.; Ashraf, M.; Zhang, F. Ridge-furrow plastic film mulching farming for sustainable dryland agriculture on the Chinese loess plateau. *Agron. J.* **2020**, *112*, 3284–3294. [CrossRef]
- Javaid, M.M.; Waheed, H.; Nazami, N.; Ashraf, M.; Li, F.-M.; Tanveer, A. Response of chickpea to foliar supply of Hoagland's solution under rain-fed condition. *Semin. Ciências Agrárias* **2020**, *41*, 3053–3066. [CrossRef]

14. Li, X.Y.; Gong, J.D.; Wei, X.H. In-situ rainwater harvesting and gravel mulch combination for corn production in the dry semi-arid region of China. *J. Arid Environ.* **2000**, *46*, 371–382. [CrossRef]
15. Xie, Z.K.; Wang, Y.J.; Li, F.M. Effect of plastic mulching on soil water use and spring wheat yield in arid region of northwest China. *Agric. Water Manag.* **2005**, *75*, 71–83. [CrossRef]
16. Zhang, J.; Sun, J.; Duan, A.; Wang, J.; Shen, X.; Liu, X. Effects of different planting patterns on water use and yield performance of winter wheat in the Huang-Huai-Hai plain of China. *Agric. Water Manag.* **2007**, *92*, 41–47. [CrossRef]
17. Siddique, K.H.; Johansen, C.; Turner, N.C.; Jeuffroy, M.-H.; Hashem, A.; Sakar, D.; Gan, Y.; Alghamdi, S.S. Innovations in agronomy for food legumes. *A review. Agron. Sustain. Dev.* **2012**, *32*, 45–64. [CrossRef]
18. Ren, X.; Jia, Z.; Chen, X. Rainfall concentration for increasing corn production under semiarid climate. *Agric. Water Manag.* **2008**, *95*, 1293–1302. [CrossRef]
19. Wang, Q.; Zhang, D.; Zhou, X.; Mak-Mensah, E.; Zhao, X.; Zhao, W.; Wang, X.; Stellmach, D.; Liu, Q.; Li, X. Optimum planting configuration for alfalfa production with ridge-furrow rainwater harvesting in a semiarid region of China. *Agric. Water Manag.* **2022**, *266*, 107594. [CrossRef]
20. Turner, N.C. Agronomic options for improving rainfall-use efficiency of crops in dryland farming systems. *J. Exp. Bot.* **2004**, *55*, 2413–2425. [CrossRef]
21. Farooq, N.; Sarwar, G.; Abbas, T.; Bessely, L.; Nadeem, M.A.; Javaid, M.M.; Matloob, A.; Naseem, M.; Ikram, N.A. Effect of drying-rewetting durations in combination with synthetic fertilizers and crop residues on soil fertility and maize production. *Pak. J. Bot.* **2020**, *52*, 2051–2058. [CrossRef]
22. Niu, J.Y.; Gan, Y.T.; Huang, G.B. dynamics of root growth in spring wheat mulched with plastic film. *Crop Sci.* **2004**, *44*, 1682–1688. [CrossRef]
23. Kong, M.; Jia, Y.; Gu, Y.-J.; Han, C.-L.; Song, X.; Shi, X.-Y.; Siddique, K.H.; Zdruli, P.; Zhang, F.; Li, F.-M. How Film Mulch Increases the Corn Yield by Improving the Soil Moisture and Temperature in the Early Growing Period in a Cool, Semi-Arid Area. *Agronomy* **2020**, *10*, 1195. [CrossRef]
24. Shahzad, T.; Ashraf, M.; Javaid, M.M.; Waheed, H.; Abbas, T.; Sattar, F. influence of field soil drought stress on some key physiological, yield and quality traits of selected newly-developed hexaploid bread wheat (*Triticum aestivum* L.) cultivars. *Sains Malays.* **2018**, *47*, 2625–2635. [CrossRef]
25. Zheng, J.; Fan, J.; Zhou, M.; Zhang, F.; Liao, Z.; Lai, Z.; Yan, S.; Guo, J.; Li, Z.; Xiang, Y. Ridge-furrow plastic film mulching enhances grain yield and yield stability of rainfed maize by improving resources capture and use efficiency in a semi-humid drought-prone region. *Agric. Water Manag.* **2022**, *269*, 107654. [CrossRef]
26. Abid, A.; Hussain, M.; Habib, H.S.; Kiani, T.T.; Anees, M.A.; Rahman, M.A. Foliar spray surpasses soil application of potassium for maize production under rainfed conditions. *Turk. J. Field Crops* **2016**, *21*, 36–43.
27. Steel, R.; Torrie, J.; Dicky, D. *Principles and Procedures of Statistics. Multiple Comparisons*, 3rd ed.; McGraw Hill: New York, NY, USA, 1997; pp. 178–198.
28. Deng, H.L.; Xiong, Y.C.; Zhang, H.J.; Li, F.Q.; Zhou, H.; Wang, Y.C.; Deng, Z.R. Maize productivity and soil properties in the Loess Plateau in response to ridge-furrow cultivation with polyethylene and straw mulch. *Sci. Rep.* **2019**, *9*, 1–13.
29. Mwale, S.; Azam-Ali, S.; Massawe, F. Growth and development of bambara groundnut (*Vigna subterranea*) in response to soil moisture: Dry matter and yield. *Eur. J. Agron.* **2007**, *26*, 345–353. [CrossRef]
30. Zhou, L.M.; Li, F.M.; Jin, S.L.; Song, Y. How two ridges and the furrow mulched with plastic film affect soil water, soil temperature and yield of maize on the semiarid Loess Plateau of China. *Field Crops Res.* **2009**, *113*, 41–47. [CrossRef]
31. Li, X.Y.; Gong, J.D.; Gao, Q.Z.; Li, F.R. Incorporation of ridge and furrow method of rainfall harvesting with mulching for crop production under semiarid conditions. *Agric. Water Manag.* **2001**, *50*, 173–183. [CrossRef]
32. Szota, C.; McCarthy, M.; Sanders, G.; Farrell, C.; Fletcher, T.; Arndt, S.; Livesley, S. Tree water-use strategies to improve stormwater retention performance of biofiltration systems. *Water Res.* **2018**, *144*, 285–295. [CrossRef] [PubMed]
33. Ma, S.; Wang, Q.; Luo, X. Effect of climate change on maize (*Zea mays*) growth and yield based on stage sowing. *Acta Ecol. Sin.* **2008**, *28*, 2131–2139.
34. Lu, H.; Xia, Z.; Fu, Y.; Wang, Q.; Xue, J.; Chu, J. Response of soil temperature, moisture, and spring maize (*Zea mays* L.) root/shoot growth to different mulching materials in semi-arid areas of northwest China. *Agronomy* **2020**, *10*, 453. [CrossRef]
35. Wang, Y.; Xie, Z.; Malhi, S.S.; Vera, C.L.; Zhang, Y.; Wang, J. Effects of rainfall harvesting and mulching technologies on water use efficiency and crop yield in the semi-arid Loess Plateau, China. *Agric. Water Manag.* **2009**, *96*, 374–382. [CrossRef]
36. Zhu, P.; Zhuang, Q.; Archontoulis, S.V.; Bernacchi, C.; Müller, C. Dissecting the nonlinear response of maize yield to high temperature stress with model-data integration. *Glob. Change Biol.* **2019**, *25*, 2470–2484. [CrossRef]
37. Wijewardana, C.; Henry, W.B.; Hock, M.W.; Reddy, K.R. Growth and physiological trait variation among corn hybrids for cold tolerance. *Canad. J. Plant Sci.* **2016**, *96*, 639–656. [CrossRef]
38. Javaid, M.M.; Wang, X.; Florentine, S.K.; Ashraf, M.; Mahmood, A.; Li, F.-M.; Fiaz, S. Effects on photosynthetic response and biomass productivity of *Acacia longifolia* subspecies *longifolia* under elevated CO₂ and water-limited regimes. *Front. Plant Sci.* **2022**, *13*, 817730. [CrossRef]

39. Jia, Y.; Li, F.-M.; Wang, X.-L.; Yang, S.-M. Soil water and alfalfa yields as affected by alternating ridges and furrows in rainfall harvest in a semiarid environment. *Field Crops Res.* **2006**, *97*, 167–175. [CrossRef]
40. Gu, C.; Liu, Y.; Mohamed, I.; Zhang, R.; Wang, X.; Nie, X.; Jiang, M.; Brooks, M.; Chen, F.; Li, Z. Dynamic changes of soil surface organic carbon under different mulching practices in citrus orchards on sloping land. *PLoS ONE* **2016**, *11*, e0168384. [CrossRef]

Article

Interactive Effects of Nitrogen Application and Irrigation on Water Use, Growth and Tuber Yield of Potato under Subsurface Drip Irrigation

Amanpreet Kaur¹, Kanwar Barjinder Singh¹, Rajeev Kumar Gupta^{1,*} , Abed Alataway², Ahmed Z. Dewidar^{2,3} and Mohamed A. Mattar^{2,3,4,5,*} 

¹ Department of Soil Science, Punjab Agricultural University, Ludhiana 141004, Punjab, India

² Prince Sultan Bin Abdulaziz International Prize for Water Chair, Prince Sultan Institute for Environmental, Water and Desert Research, King Saud University, Riyadh 11451, Saudi Arabia

³ Department of Agricultural Engineering, College of Food and Agriculture Sciences, King Saud University, Riyadh 11451, Saudi Arabia

⁴ Centre for Carbon, Water and Food, The University of Sydney, Camperdown, NSW 2570, Australia

⁵ Agricultural Engineering Research Institute (AEnRI), Agricultural Research Centre, Giza 12618, Egypt

* Correspondence: rkg1103@pau.edu (R.K.G.); mmattar@ksu.edu.sa (M.A.M.)

Abstract: Potatoes are a high-value crop with a shallow root system and high fertilizer requirements. The primary emphasis in potato production is minimizing nitrogen-leaching losses from the shallow root zone through fertigation. Therefore, a field experiment was conducted for two consecutive years, 2018–2019 and 2019–2020 to assess the effect of nitrogen and irrigation amount and frequency on tuber yield, water balance components and water productivity of potatoes under surface and subsurface drip irrigation. The experiment was laid out in a split-plot design with three nitrogen levels (187.5 kg N ha⁻¹ (N₁), 150 kg N ha⁻¹ (N₂) and 112.5 kg N ha⁻¹ (N₃)) in main plots and six irrigation levels in the subsurface (drip lines were laid at 20 cm depth) and one surface drip in subplots. Irrigation scheduling was based on 100% of cumulative pan evaporation at an alternate (I₁) and two-day interval (I₂), 80% of cumulative pan evaporation at an alternate (I₃) and two-day interval (I₄), 60% of cumulative pan evaporation at an alternate (I₅) and two-day interval (I₆) and 80% of cumulative pan evaporation at alternate days with surface drip (I₇). Our results showed that potato transpiration was higher in N₁ and N₂ compared to N₃, while soil evaporation was higher in N₃ over N₁ and N₂. Irrigation regimes I₅ and I₆ had lower transpiration than I₁, I₂, I₃ and I₇, while I₇ had more soil evaporation than I₁, I₂ and I₃. Leaf area index (LAI), dry matter accumulation (DMA), root mass density (RMD) and tuber yield in N₁ and N₂ were at par but significantly higher than N₃. The LAI and DMA were statistically at par in I₁, I₂ and I₃ but significantly higher than recommended irrigation (I₇). Tuber yield was statistically at par in I₁, I₂, I₃ and I₇ but I₃ and I₇ saved 20% irrigation water compared to I₁ and I₂. On the other hand, real water productivity (WP_{ET}) under N₁ and N₂ were comparable in I₃ and I₄ but significantly higher than recommended practice (I₇) as pooled evapotranspiration (ET) and soil evaporation (E) in I₇ were 19.5 and 20.6 mm higher, respectively, than in I₃. Among interactive treatment combinations, N₁I₁, N₁I₂, N₁I₃, N₁I₇, N₂I₁, N₂I₂ and N₂I₃ recorded the highest tuber yields without any significant differences among them. Treatment N₂I₃ saved 20% nitrogen and irrigation water compared to all other combinations. Water productivity in N₁ and N₂ was comparable in I₃ and I₄ but significantly higher than recommended practice (I₇).

Keywords: potato fertigation; leaf area index; root mass density; real water productivity; field water balance



Citation: Kaur, A.; Singh, K.B.; Gupta, R.K.; Alataway, A.; Dewidar, A.Z.; Mattar, M.A. Interactive Effects of Nitrogen Application and Irrigation on Water Use, Growth and Tuber Yield of Potato under Subsurface Drip Irrigation. *Agronomy* **2023**, *13*, 11. <https://doi.org/10.3390/agronomy13010011>

Academic Editors: Aliasghar Montazar and Junliang Fan

Received: 30 October 2022
Revised: 4 December 2022
Accepted: 16 December 2022
Published: 21 December 2022



Copyright: © 2022 by the authors. Licensee MDPI, Basel, Switzerland. This article is an open access article distributed under the terms and conditions of the Creative Commons Attribution (CC BY) license (<https://creativecommons.org/licenses/by/4.0/>).

1. Introduction

Potato (*Solanum tuberosum* L.) is the fourth-most-crucial vegetable crop, with a global production of 370 million tons [1]. India is the second-largest potato producer, with an

area of 2.17 million and a production of around 53.58 million metric tons [1]. Among the potato-growing zones of India, Punjab falls in the north-western plain, which accounts for about 5% of the total area under potato cultivation in India [2]. The main-season potato crop is popular among stakeholders in spring maize–rice–potato rotation. Spring maize and rice are high-water-requiring crops, and potato is sensitive to water stress which responds to frequent irrigation [3].

Moreover, potato is grown on raised beds and irrigated through furrows, accounting for significant water losses. Hence, the region's cultivation of water-guzzler rice and spring maize crops is becoming challenging as Punjab is already facing a water crisis [4]. The mean ground table has experienced a fall of 0.4 m year⁻¹ in 80% of irrigated areas in central Punjab [5] since 1990. Thus this scenario of water scarcity in the region has necessitated the adoption of improved water management technologies such as drip irrigation to improve the water productivity of cropping systems. Surface drip irrigation in potato is recommended by researchers worldwide [6–8], but studies on the feasibility of subsurface drip irrigation systems in potato are limited. Thus, this experiment was planned to study the growth and yield of subsurface-drip-irrigated potato sown after spring maize and rice on the same drip lines. Potato is a shallow-rooted crop and is highly affected by excessive water and stressed water conditions [9]. Although furrow irrigation is the most common irrigation method in the Indo-Gangetic plains, drip irrigation has proved to be a good option in managing the volumetric inefficiencies in irrigation regimes resulting from too frequent or too much irrigation [10]. Agronomic inadequacies occur when plants are stressed due to insufficient water being frequently applied or excessive water application resulting in water logging or increasing the incidence of diseases [11].

Potato production is highly dependent on nitrogen (N), phosphorous (P) and potassium (K) applications [12]. Nitrogen is a dominant nutrient determining potato's growth, development, productivity and quality, and its optimal application improves yields [13], while excessive N may contaminate groundwater [14]. Therefore, in potato, water and nutrient management through a drip irrigation system can be the best option for maximization of potato productivity. Studies [15,16] have shown that the maximum productivity of potato can be obtained while keeping the soil moist and ensuring the N available during periods of high demand, which can be managed well with drip irrigation and fertigation. This system is most economical in giving the highest water productivity and saving about 40–50% of irrigation water compared to the furrow method [17]. It gives uniform water distribution with a significant reduction in water losses by percolation and runoff. This system is also beneficial on frosty nights as it reduces frost damage in plants in main-season crops. We hypothesize that subsurface drip irrigation is also used globally for potato production [18–20], in which drip lines are buried below the soil surface, providing water and nutrients directly to the root zone. Therefore, it has the potential to save water by reducing evaporation losses compared to other methods of irrigation, particularly in sandy loam soil [21]. Therefore, this experiment was planned to study the interactive effects of nitrogen, irrigation amount and irrigation frequency on potato growth, evapotranspiration and yield under subsurface drip irrigation.

2. Materials and Methods

2.1. Climate Conditions

A field experiment was conducted at Research Farm, Soil and Water Engineering, Punjab Agricultural University, Ludhiana, India, during 2018–2019 and 2019–2020. The layout of the experiment is given in Figure S1. Ludhiana is situated at 30°56' N and 75°52' E at 247 m above sea level. The area has a sub-tropical to semiarid climate with a hot and dry summer (April to June), hot and humid monsoon (July to September), mild winter (October to November) and cold winter (December to February). The mean minimum and maximum temperatures show considerable fluctuation during summer and winter. Maximum air temperature above 38 °C is expected during summer and frequent frosty spells in December–January. The average annual rainfall at Ludhiana is 755 mm, 75%

of which is received in the summer monsoon (July to September), complemented by a few low- to medium-intensity showers in winter. During the 2018–2019 potato season, the highest mean maximum air temperature was observed during October and lowest during January, while the mean minimum air temperature was lowest during December and highest during October. The maximum relative humidity was 71% observed in January. 2018–2019 (Table 1). The potato crop during 2018–2019 received 68.6 mm of rainfall. During 2019–2020, the weekly mean maximum air temperature in October was 30.6 °C while the minimum temperature was observed during January. The mean maximum relative humidity was 78.4% observed in January. The total rainfall was 123 mm.

Table 1. Weather parameters during potato growing season.

	2018–2019 Growing Season						2019–2020 Growing Season					
	T _{max}	T _{min}	RF (mm)	Epan (mm)	RH (%)	ET ₀ (mm)	T _{max}	T _{min}	RF (mm)	Epan (mm)	RH (%)	ET ₀ (mm)
October	31.0	16.2	0	96.6	64	97.0	30.6	18.4	0	76.7	68.2	87.8
November	26.8	11.8	2.6	64.0	63	59.3	28.0	22.0	35.2	56.8	68.2	57.1
December	20.6	5.5	0	40.6	68	40.9	15.9	7.5	46.8	30.5	79.0	33.5
January	18.5	6.2	66.0	43.1	71	41.31	16.6	6.7	39.8	27.7	78.4	42.1

T_{max} is maximum air temperature, T_{min} is minimum air temperature, Epan is open pan evaporation, RF and RH are rainfall and relative humidity, respectively, and ET₀ is potential evapotranspiration.

2.2. Experimental Site Description

Soil samples were collected randomly from four depths (0–15, 15–30, 30–60 and 60–90 cm) and three different field sites before the experiment started with the help of a screw auger. A composite sample was made and brought to the soil and water testing laboratory in the Department of Soil and Water Engineering to analyze the initial status of physical and chemical properties. The analysis was performed according to standard laboratory procedures. The experimental field soil was sandy loam in texture with pH 8.1, electrical conductivity 0.23 dS m⁻¹, organic carbon 0.48%, nitrogen 170.2 kg ha⁻¹, phosphorous 37.4 kg ha⁻¹ and potassium 345 kg ha⁻¹ in 0–15 cm soil depth. The bulk density of the soil was 1.52 g cm⁻³. The physical properties of the soil are given in Table 2.

Table 2. Physical properties of experimental soil.

Soil Depth (cm)	Sand (%)	Silt (%)	Clay (%)	Soil Texture	Bulk Density (g cm ⁻³)	Saturated Hydraulic Conductivity (cm h ⁻¹)	Soil Moisture Retention (% v/v)	
							10 kPa	1500 kPa
0–15	70.8	20.4	10.8	Sandy loam	1.52	1.08	27.0	9.0
15–30	70.2	21.3	11.2	Sandy loam	1.61	0.64	27.2	9.2
30–60	69.7	22.2	11.7	Sandy loam	1.67	1.61	27.3	7.3
60–90	68.4	22.3	11.9	Sandy loam	1.64	1.27	23.0	6.0

In order to prepare good tilth before planting, the disc harrow was run twice, followed by two ploughings with a tractor-drawn cultivator. Drip lines were installed at a 20 cm depth below the soil surface with a tractor-drawn machine (as shown in the layout). The distance between the two drip lines was kept at 60 cm per row-to-row crop spacing. Ridges were made manually 60 cm apart in the east–west direction (Figure S1). The experiment was laid out in a split-plot design with three nitrogen levels of 187.5 kg N ha⁻¹ (N₁), 150 kg N ha⁻¹ (N₂) and 112.5 kg N ha⁻¹ (N₃) in the main plots. Seven irrigation levels (six subsurface drip lines and one surface drip) were kept in the subplots. The irrigations were 100% of Epan at alternate day (I₁) and two-day intervals (I₂), 80% of Epan at alternate (I₃) and two-day intervals (I₄), 60% of Epan at alternate day (I₅) and two-day intervals (I₆) in the subsurface and 80% of Epan at an alternate day in surface drip (I₇). The potato

variety *Kufri Pukhraj* was planted on 18 October, during 2018–2019 and on 15 October in 2019–2020 at 20 cm plant-to-plant distance and 7–8 cm soil depth from the top of the ridge in rows as per the layout. All the plants emerged between 14 and 18 days. All the crop management practices were followed as per the practice package for cultivating vegetable crops. Fertilizer N was applied as per treatments. The recommended doses of phosphorus ($62.5 \text{ kg P}_2\text{O}_5 \text{ kg ha}^{-1}$) and potassium ($\text{K}_2\text{O } 62.5 \text{ kg ha}^{-1}$) were applied along with N in 16 splits at weekly intervals. A water meter was installed on 63 mm PVC pipe to measure the irrigation water delivered to each plot. Tensiometers were installed at 10, 20, 30, 60 and 90 cm depths in I_1 , I_3 , I_5 and I_7 to monitor soil matric potential (SMP) daily at 8 am during 2018–2019. However, during 2019–2020 SMP was monitored only during three major rain events. Soil water content was determined 24 h, 48 h and 72 h after each irrigation from 0–10, 10–20, 20–30, 30–40, 40–60 and 60–100 cm profile depths with FDR (Frequency domain reflectometry). Actual crop evapotranspiration (ET_a) was estimated from the soil water balance equation.

$$I + P = ET_a + D + R \pm \Delta SW \quad (1)$$

where I is irrigation water applied (mm), P is precipitation (mm), R is surface runoff (mm), D is deep drainage (mm) and ΔSW is the change in soil profile moisture storage (mm). Runoff was absent as sufficient dikes were maintained. Deep drainage was considered zero when soil profile moisture storage was less than the field capacity. When soil moisture storage exceeded the field capacity storage after irrigation or rainfall, deep drainage was calculated as the difference between the field capacity storage and soil moisture storage plus irrigation/rainfall [22]. Evapotranspiration (ET_a) was partitioned into soil evaporation (E) and transpiration (T_p) [23]:

$$E = ET_a \times e^{-\alpha LAI} \quad (2)$$

$$T_p = ET_a - E_s \quad (3)$$

where α is the extinction coefficient of radiation set as 0.56 [24], and LAI is the leaf area index (measured with the Sunscan Plant Canopy Analyzer of Delta T Devices) at different crop growth stages. The following equation already calibrated for Potato LAI [23] was used to partition LAI during crop growth and senescence:

$$LAI_{(t)} = LAI_{max} \frac{1}{1 + e^{a_1(t - t_{inf})}} - e^{a_2(t - t_{end})} \quad (4)$$

where LAI_{max} is the maximum LAI value observed, a_1 and a_2 are shape factors controlling the growth and senescence rates, t_{inf} is the time at which the maximum growth rate is reached (inflexion point) and t_{end} is the time of complete senescence. The terms LAI_{max} , t_{inf} , and t_{end} were measured and a_1 and a_2 were fitted [23]. Whole plants and roots were uprooted, sun-dried and then dried in an oven at 60°C until they reached a constant weight for measuring dry matter accumulation at 60, 75 DAP and at harvest, which was expressed in Mg ha^{-1} . The leaf area index was recorded periodically (30, 60, 90 and 120 DAS) using Sunscan Plant Canopy Analyzer based on the principle of Beer–Lambert's law. After calibration, the leaf area index was recorded from 12:00 to 2:00 p.m. on a sunny day from two locations in each plot and then averaged for the final reading of the leaf area index. Root-mass density was determined by collecting root samples with the help of tubes having an internal diameter of 5 cm from 0–15, 15–30, 30–45 and 45–60 cm depths from three places, under the plant, 7 cm from the base of the plant towards row and 7 cm from the base of the plant towards furrow. These samples were mixed, passed through a 32 mm mesh and washed in a running water channel by providing gentle pulsing with the hand to make the roots free from soil. Then roots were transferred to Petri dishes to remove inert material. Then roots were dried in an oven and root mass density was calculated by dividing the mass of dry roots by the volume of the tube. N uptake in plant samples was determined at 90 days. The digestion process was performed for nitrogen determination in plant samples.

During digestion, complex structures were broken into simple structures, releasing nitrogen as ammonium radicals. For digestion, 0.5 g of plant sample was taken in a digestion tube and mixed with 6 mL of concentrated sulphuric acid. Then, one teaspoon of mix from a mixture of CuSO_4 (100 g), K_2SO_4 (10 g) and selenium oxide (1 g) was added to the digestion tube. The solution was retained at room temperature for 24 h. Then, the digestion tube was heated up to 410°C for 2 h. After completion of digestion, the sample turned to light green or colourless. After digestion, distillation with 4% boric acid and titration with 0.1 N H_2SO_4 was performed to determine the plant nitrogen as per the KEL PLUS manual. Nitrogen uptake was determined by multiplying the N content with biomass and tuber yield. Real water productivity (kg m^{-3}) was calculated as the ratio of grain yield and evapotranspiration as described by [5,25]:

$$\text{WP}_{\text{ET}} = \text{GY}/\text{ET}_a \times 10 \quad (5)$$

where WP_{ET} is real water productivity (kg m^{-3}), ET_a is crop evapotranspiration (mm) and GY is grain yield (Mg ha^{-1}).

2.3. Statistical Analysis

Analysis of variance was performed using the Proc GLM procedure of SAS version 9.4 (SAS Institute, Inc., Cary, NC, USA). Significant mean differences were tested using 54 Fisher's protected least significant difference (LSD) tests at $\alpha = 0.05$. For pooled analysis, the year was the main factor to increase the precision. In addition, the regression procedure was used to test the nature of the relationship between different parameters.

3. Results and Discussion

3.1. Soil Matric Potential and Soil Moisture Distribution at Different Depths

Soil matric potential (SMP) values for different treatments throughout cropping season 2018–2019 are shown in Figure 1. At 10 cm depth, SMP in I_1 and I_3 varied between -38 and -48 kPa, except for two significant rain events (Figure 1 at the same depth, SMP for I_5 was even less and varied between -48 and -55 kPa. However, under surface drip (I_7), SMP at the surface layer was high and varied between 18 and 24 kPa. At 20 and 30 cm depths, the SMP was higher at 60 and 90 cm depths in I_1 , I_3 and I_5 due to placement of the dripper at these depths. Between these treatments, the highest SMP was observed in I_1 , followed by I_3 and I_5 . However, in I_7 , higher SMP was observed at 10 cm and 20 cm depths compared to 30, 60 and 90 cm depths. In all these treatments, more changes in soil matric potential occurred in 10, 20 and 30 cm depths. However, fewer fluctuations were observed at 60 and 90 cm, even during the major rain events, indicating no drainage in our experiments. Mean seasonal volumetric soil moisture (MSVSM) during the growing season (except major events) is presented in Table 3. During 2018–2019, in 0–10 cm depth after 24 h of irrigation, MSVSM in I_1 , I_2 , I_3 , I_4 , I_5 , I_6 and I_7 was 11.1, 12.1, 10.9, 10.7, 9.6, 9.3 and 18.7%, respectively. It dropped to 9.2, 10.1, 8.8, 5.6, 9.1, 8.8, 8.5, and 15.8%, respectively, after 48 h of irrigation which indicated that, throughout the season, the surface soil layer remained relatively wet in surface drip and dry in subsurface drip irrigation. After 24 h in the 10–20 cm soil layer, the seasonal volumetric soil moisture was higher in I_1 and I_2 by 2.1 and 2.0%, respectively, over I_7 , while in I_5 and I_6 , it was lower than I_7 by 1.8 and 2.8%, respectively. Compared to I_7 , I_3 had 0.5% more, but I_4 contained less moisture content in this layer. After 24 h in the 20–30 cm soil layer, MSVSM was higher in I_1 , I_2 , I_3 , I_4 , I_5 and I_6 by 8.0, 6.2, 4.4, 3.7, 0.7, and 0.6%, respectively, over I_7 . A similar trend was observed after 48 h of irrigation. In 30–40 cm depth after 24 h of irrigation, MSVSM was higher in I_1 , I_2 , I_3 , I_4 , I_5 and I_6 than I_7 by 6.0, 5.8, 4.3, 3.8, 1.7 and 0.9%, respectively. A similar trend was observed after 48 h of irrigation. In 40–60 cm soil depth after 24 h of irrigation MSVSM was higher in I_1 , I_2 , I_3 , I_4 , I_5 and I_6 than in I_7 by 4.7, 4.0, 3.6, 3.2, 2.3 and 2.4%, respectively. Similarly, during 2019–2020 (Table 4), MSVSM in I_1 , I_2 , I_3 , I_4 , I_5 , I_6 and I_7 was 12.0, 11.8, 11.1, 10.8, 10, 9.9 and 20.2%, which dropped to 9.2, 10.1, 8.8, 9.1, 8.8, 8.5 and 15.8%, respectively, after 48 h and further dropped to 8.9, 8.1, and 8.3% after 72 h in treatments I_2 , I_4 and I_6 ,

respectively. In 10–20 cm depth, after 24 h, MSVSM was higher in I₁, I₂ and I₃ by 2.1, 1.7 and 0.6%, respectively, but I₄, I₅ and I₆ contained 0.5, 2.8 and 3.3% less moisture content, respectively, than I₇. After 48 h, the moisture content was highest in I₁, I₂, I₃ and I₄ over I₇ by 2.4, 1.6, 0.3 and 0.2%, respectively, but I₅ and I₆ contained 2.0 and 2.3% less moisture content, respectively. In 20–30 cm soil depth, all the subsurface drip treatments contained more MSVSM over surface irrigation (I₇). The percent difference of I₁ over I₂, I₃, I₄, I₅, I₆ and I₇ was 9.6, 8.7, 6.1, 5.3, 3.7 and 3.5%, respectively, after 24 h and 8.6, 8.7, 5.4, 5.2, 4.3 and 4.2%, respectively, after 48 h. Similarly, in 30–40 cm soil depth, the percent increase in MSVSM in I₁, I₂, I₃, I₄, I₅ and I₆ over I₇ was 6.9, 6.0, 4.0, 2.9, 1.7 and 0.8, respectively, after 24 h. This difference was 6.7, 5.2, 3.5, 2.4, 0.7 and 0.9%, respectively, after 48 h. A similar trend was observed in the 40–60 cm soil layer.

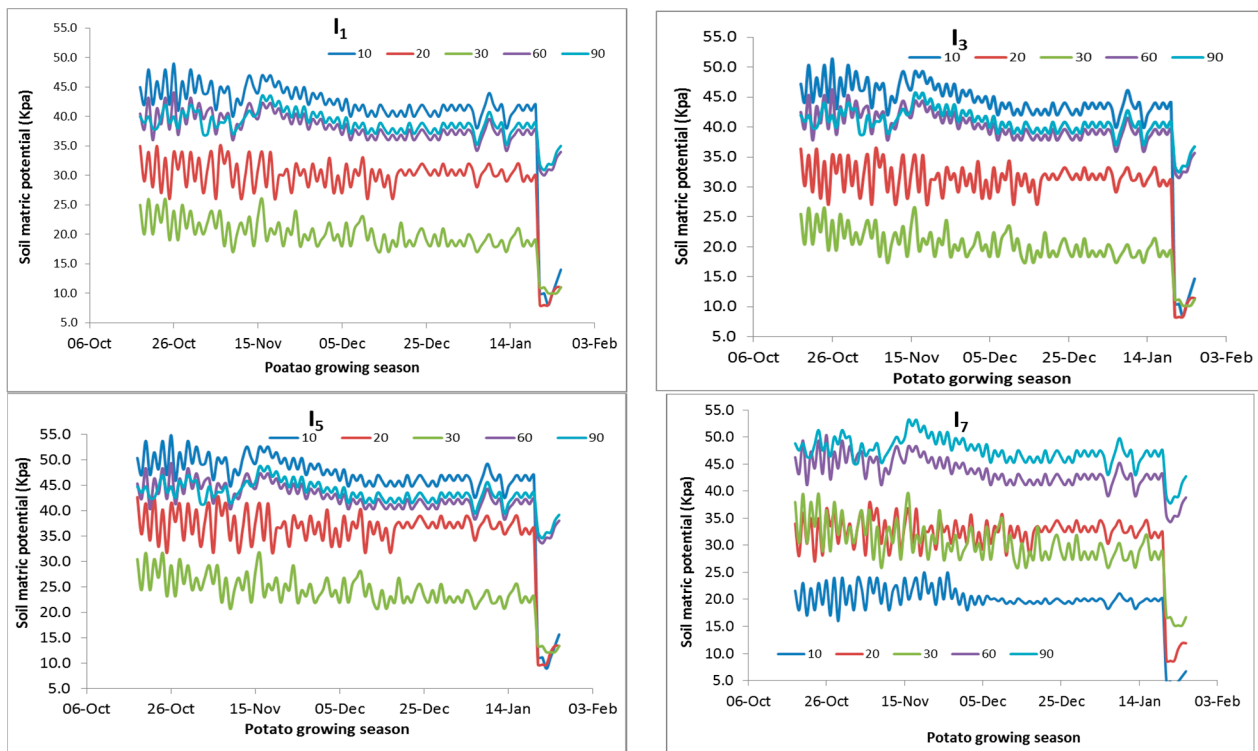


Figure 1. Soil moisture potential at different depths throughout the growing season of potato during the 2018–2019.

Table 3. Mean seasonal volumetric soil moisture content (%) in potato during 2018–2019.

Depth (cm)	Hours after Irrigation	I ₁	I ₂	I ₃	I ₄	I ₅	I ₆	I ₇
0–10	24	11.1 ^a	12.0 ^a	10.9 ^a	10.7 ^a	9.6 ^a	9.3 ^a	18.7 ^b
	48	9.2 ^a	10.1 ^a	8.8 ^a	9.1 ^a	8.8 ^a	8.5 ^a	15.8 ^b
	72		8.9 ^a		8.1 ^a		8.3 ^a	
10–20	24	17.2 ^a	18.1 ^a	15.7 ^{ab}	14.7 ^{ab}	13.3 ^b	12.3 ^b	15.1 ^{ab}
	48	12.5 ^a	12.5 ^a	12.1 ^a	11.3 ^a	10.1 ^a	10.2 ^a	11.5 ^a
	72		11.2 ^a		10.4 ^a	9.1 ^{ab}	8.5 ^b	
20–30	24	21.5 ^a	19.3 ^a	17.9 ^a	17.2 ^{ab}	14.2 ^b	14.1 ^b	13.5 ^b
	48	17.5 ^a	16.5 ^a	15.5 ^a	15.1 ^a	13.1 ^b	12.3 ^b	10.2 ^b
	72		14.4 ^a		13.1 ^a		10.1 ^b	
30–40 cm	24	17.1 ^a	16.9 ^a	15.4 ^a	14.9 ^{ab}	12.8 ^b	12.0 ^b	11.1 ^b
	48	16.4 ^a	15.1 ^a	14.2 ^{ab}	13.1 ^b	11.8 ^b	11.1 ^b	10.1 ^b
	72		14.8 ^a		12.5 ^b		10.8 ^c	

Table 3. Cont.

Depth (cm)	Hours after Irrigation	I ₁	I ₂	I ₃	I ₄	I ₅	I ₆	I ₇
40–60 cm	24	14.8 ^a	15.1 ^a	13.7 ^a	13.3 ^a	12.4 ^{ab}	12.2 ^{ab}	10.1 ^b
	48	14.1 ^a	13.8 ^a	13.2 ^a	12.5 ^a	12.1 ^a	12.1 ^a	9.9 ^b

Treatments with different lower case letters are significantly different at $p < 0.05$.

Table 4. Mean seasonal volumetric soil moisture content (%) in potato during 2019–2020.

Depth (cm)	Hours after Irrigation	I ₁	I ₂	I ₃	I ₄	I ₅	I ₆	I ₇
0–10	24	12 ^b	11.8 ^b	11.1 ^b	10.8 ^b	10 ^b	9.9 ^b	20.2 ^a
	48	11.3 ^b	10.8 ^b	10.5 ^b	9.9 ^b	8.5 ^b	8.1 ^b	16.9 ^a
	72		8.7 ^a	8.3 ^a	8.5 ^a		7.8 ^a	
10–20	24	18.2 ^a	17.8 ^a	16.7 ^{ab}	15.6 ^{ab}	13.3 ^b	12.8 ^b	16.1 ^{ab}
	48	15.5 ^a	14.7 ^{ab}	13.4 ^{ab}	13.3 ^{ab}	11.1 ^b	10.8 ^b	13.1 ^{ab}
	72		12.2 ^a		11.4 ^a		10.1 ^a	
20–30	24	22.4 ^a	21.5 ^a	18.9 ^{ab}	18.1 ^{ab}	16.5 ^b	16.3 ^b	12.8 ^c
	48	19.5 ^a	19.3 ^a	16.3 ^b	16.1 ^b	15.2 ^b	15.1 ^b	10.9 ^c
	72		15.1 ^a		14.1 ^a		12.9 ^b	
30–40	24	17.7 ^a	16.8 ^a	14.8 ^{ab}	13.7 ^{ab}	12.5 ^b	11.6 ^b	10.8 ^b
	48	16.8 ^a	15.3 ^a	13.6 ^{ab}	12.5 ^b	10.8 ^b	10.9 ^b	10.1 ^b
	72		14.1 ^a		11.4 ^b		10.1 ^b	
40–60	24	15.3 ^a	14.8 ^a	13.5 ^a	12.5 ^a	11.8 ^{ab}	11.2 ^{ab}	10.2 ^b
	48	15.1 ^a	14.1 ^a	13.2 ^{ab}	12.3 ^{ab}	11.5 ^{ab}	11.1 ^b	10.0 ^b
	72		13.2 ^a		11.1 ^a		9.8 ^a	

Treatments with different lower case letters are significantly different at $p < 0.05$.

3.2. Water Balance Components

3.2.1. Total Water Input

Irrigation was given to the crop based on E_{pan} according to the treatments (Tables 5 and 6). The potato crop during the growing season received 68.6 mm and 123.6 mm of rainfall during 2018–2019 and 2019–2020, respectively. During 2018–2019, total water input was 18.2% higher in I₁ or I₂ over I₃ and I₄ and 50.6% higher over I₅ and I₆, and the difference between I₃ and I₄ was 27% over I₅ and I₆. I₇ and I₃ treatments received a similar amount of total water. During 2019–2020, the percent difference between I₁ and I₂ over I₃ or I₄ was 9.8%, I₁ or I₂ over I₅ or I₆ was 24.8% and I₃ or I₄ over I₅ or I₆ was 13.3%.

Table 5. Water balance components of potato during 2018–2019.

Treatments	Irrigation (mm)	Rain (mm)	ET (mm)	Drainage (mm)	ΔS
N ₁ I ₁	160.8 ^a	68.6	223.2 ^a	0	6.4 ^a
N ₁ I ₂	158.6 ^a	68.6	215.2 ^a	0	10.0 ^a
N ₁ I ₃	126.0 ^b	68.6	208.4 ^a	0	−11.3 ^b
N ₁ I ₄	125.8 ^b	68.6	201.3 ^a	0	−11.6 ^b
N ₁ I ₅	83.7 ^c	68.6	186.3 ^b	0	−34.7 ^c
N ₁ I ₆	83.7 ^c	68.6	185.5 ^b	0	−36.2 ^c
N ₁ I ₇	126.0 ^b	68.6	230.2 ^a	0	−40.0 ^c
N ₂ I ₁	160.8 ^a	68.6	220.3 ^a	0	6.2 ^a
N ₂ I ₂	158.6 ^a	68.6	214.4 ^a	0	10.7 ^a
N ₂ I ₃	126.0 ^b	68.6	205.5 ^a	0	−10.3 ^b

Table 5. Cont.

Treatments	Irrigation (mm)	Rain (mm)	ET (mm)	Drainage (mm)	ΔS
N ₂ I ₄	121.0 ^b	68.6	199.9 ^a	0	−9.6 ^b
N ₂ I ₅	83.7 ^c	68.6	185.5 ^b	0	−33.2 ^c
N ₂ I ₆	80.7 ^c	68.6	183.3 ^b	0	−34.0 ^c
N ₂ I ₇	126.0 ^b	68.6	229.4 ^a	0	−39.1 ^c
N ₃ I ₁	160.8 ^a	68.6	219.9 ^a	0	9.5 ^a
N ₃ I ₂	158.6 ^a	68.6	211.5 ^a	0	23.1 ^b
N ₃ I ₃	126.0 ^b	68.6	201.2 ^a	0	−8.4 ^c
N ₃ I ₄	121.0 ^b	68.6	190.4 ^a	0	−0.8 ^c
N ₃ I ₅	83.7 ^c	68.6	174.4 ^b	0	−22.1 ^d
N ₃ I ₆	83.7 ^c	68.6	173.3 ^b	0	−23.9 ^d
N ₃ I ₇	126.0 ^b	68.6	225.4 ^a	0	−42.0 ^d

Treatments with different lower case letters are significantly different at $p < 0.05$.

Table 6. Water balance components of potato during 2019–20.

Treatments	Irrigation (mm)	Rain (mm)	ET (mm)	Drainage (mm)	ΔS
N ₁ I ₁	105.8 ^a	123	232.4 ^a	0	−3.6 ^a
N ₁ I ₂	104.3 ^a	123	230.1 ^a	0	−2.8 ^a
N ₁ I ₃	85.9 ^b	123	222.2 ^a	0	−13.3 ^b
N ₁ I ₄	84.8 ^b	123	220.4 ^a	0	−12.6 ^b
N ₁ I ₅	61.5 ^c	123	203.4 ^b	0	−18.9 ^b
N ₁ I ₆	60.7 ^c	123	201.3 ^b	0	−17.6 ^b
N ₁ I ₇	85.9 ^b	123	238.8 ^a	0	−29.9 ^c
N ₂ I ₁	105.8 ^a	123	232.4 ^a	0	−3.6 ^a
N ₂ I ₂	104.3 ^a	123	230.1 ^a	0	−2.8 ^a
N ₂ I ₃	85.9 ^b	123	221.1 ^a	0	−12.2 ^b
N ₂ I ₄	84.8 ^b	123	220.4 ^a	0	−12.6 ^b
N ₂ I ₅	61.5 ^c	123	203.4 ^b	0	−18.9 ^b
N ₂ I ₆	60.7 ^c	123	201.3 ^b	0	−17.6 ^b
N ₂ I ₇	85.9 ^b	123	236.2 ^a	0	−27.3 ^c
N ₃ I ₁	105.8 ^a	123	227.4 ^a	0	1.4 ^a
N ₃ I ₂	104.3 ^a	123	224.4 ^a	0	2.9 ^a
N ₃ I ₃	85.9 ^b	123	218.8 ^a	0	−9.9 ^a
N ₃ I ₄	84.8 ^b	123	220.4 ^a	0	−12.6 ^b
N ₃ I ₅	61.5 ^c	123	200.4 ^b	0	−15.9 ^b
N ₃ I ₆	60.7 ^c	123	198.8 ^b	0	−15.1 ^b
N ₃ I ₇	85.9 ^b	123	234.4 ^a	0	−25.5 ^c

Treatments with different lower case letters are significantly different at $p < 0.05$.

3.2.2. Evapotranspiration (ET) and Its Partitioning

During 2018–2019, the highest ET was observed in N₁ (207.2 mm), which was 0.8% and 3.9% higher than N₂ and N₃, respectively (Table 7). Transpiration in N₁ was 1.4 and 7.1% higher than N₂ and N₃, respectively. However, evaporation in N₃ was highest and was 10.8% and 9.4% higher than N₁ and N₂, respectively. During 2019–2020, the ET between nitrogen levels did not differ significantly, but in N₁ was higher by 0.4% and 7.8% than N₂ and N₃, respectively. However, evaporation in N₃ was higher by 15.6% and 14.3% than N₁ and N₂, respectively. ET and T in our experiment were comparable to another study conducted on drip irrigation [23]. The higher ET in N₁ and N₂ compared to N₃ may be due to more LAI in N₁ and N₂ than in N₃ (Table 8). The highest ET with a higher amount of nitrogen was also observed [26]. Among irrigation levels, during both years, ET was highest in I₇, with a difference of 23.3 and 15.6 mm over I₃ during 2018–2019 and 2019–2020, respectively. Despite receiving higher amounts of irrigation, lower ET was observed in I₁ and I₂ than recommended practice (I₇). However, the transpiration component was the

highest in I₁, and was higher by 6.9, 11.0, 18.4, 36.6, 41.3 and 9.8% over I₂, I₃, I₄, I₅, I₆ and I₇, respectively. Therefore, the highest ET in surface irrigated treatment (I₇) was due to an increase in evaporation (63.6 mm) which was 58.6, 43.8 and 51.7% higher than I₁, I₂ and I₃, respectively. The lowest evaporation in subsurface drip irrigation could be due to lower volumetric moisture content (%) in surface layers (Table 3) and higher leaf area index (Table 8) which resulted in higher transpiration. Similarly, during 2019–2020, transpiration was higher in I₁ by 3.5, 3.2, 9.2, 27.6, 32.5 and 8.5% than I₂, I₃, I₄, I₅, I₆ and I₇, respectively. The highest evaporation was recorded in I₇, followed by I₅ and I₆ and was the lowest in I₁. Amongst subsurface irrigation treatments, treatments with more frequent irrigation recorded more ET than deficit in less frequently irrigated treatments. It could be due to higher soil moisture availability, as also endorsed by [27].

Table 7. Evapotranspiration (ET_a) and its partitioning into soil evaporation (E) and transpiration (T_p).

Treatments	2018–19			2019–20		
	ET (mm)	T _p (mm)	E (mm)	ET (mm)	T _p (mm)	E (mm)
N ₁	207.2 ^a	160.2 ^a	46.9 ^a	221.8 ^a	169.5 ^a	52.3 ^a
N ₂	205.5 ^a	157.9 ^a	47.5 ^b	220.7 ^a	168.8 ^a	52.9 ^a
N ₃	199.4 ^b	149.5 ^b	52.0 ^b	217.2 ^a	157.2 ^b	60.5 ^b
Mean	204.0	155.9	48.8	219.9	165.2	55.3
I ₁	221.1 ^a	180.9 ^a	40.1 ^a	230.7 ^a	183.2 ^a	47.5 ^a
I ₂	213.7 ^a	169.3 ^{ab}	44.2 ^a	228.2 ^a	177.0 ^a	51.2 ^a
I ₃	205.0 ^a	169.9 ^{ab}	42.0 ^a	220.7 ^a	177.5 ^a	48.5 ^a
I ₄	197.2 ^{ab}	152.8 ^b	44.4 ^a	220.4 ^a	167.8 ^a	52.6 ^a
I ₅	182.1 ^b	132.4 ^c	49.7 ^b	202.4 ^b	143.6 ^b	58.8 ^{ab}
I ₆	180.7 ^b	128.0 ^c	57.7 ^{bc}	200.5 ^b	138.1 ^b	62.3 ^{ab}
I ₇	228.3 ^a	164.7 ^{ab}	63.6 ^c	236.5 ^a	168.9 ^a	67.6 ^b
Mean	204.0	155.9	48.8	219.9	165.2	55.3

Treatments with different lower case letters are significantly different at $p < 0.05$.

Table 8. Effect of nitrogen and irrigation on periodic leaf area index of potato.

Treatments	2018–2019				2019–2020			
	45 DAS	60 DAS	75 DAS	90 DAS	45 DAS	60 DAS	75 DAS	90 DAS
N ₁	3.45 (0.11)	4.97 (0.10)	4.98 (0.12)	4.31 (0.12)	2.96 (0.03)	4.87 (0.11)	4.89 (0.10)	4.33 (0.20)
N ₂	3.06 (0.13)	4.76 (0.11)	4.78 (0.11)	3.99 (0.11)	2.90 (0.02)	4.55 (0.11)	4.61 (0.11)	3.38 (0.18)
N ₃	2.65 (0.13)	4.40 (0.12)	4.38 (0.11)	3.45 (0.10)	2.78 (0.03)	4.16 (0.12)	4.19 (0.11)	2.62 (0.22)
Mean	3.05	4.71	4.71	3.86	2.88	4.54	4.56	3.34
LSD ($p = 0.05$)	0.39	0.29	0.31	0.32	0.06	0.31	0.29	0.66
I ₁	3.43 (0.13)	5.17 (0.05)	5.18 (0.04)	4.36 (0.05)	3.15 (0.02)	5.19 (0.03)	5.2 (0.02)	3.87 (0.01)
I ₂	3.22 (0.11)	5.11 (0.04)	5.13 (0.03)	4.24 (0.05)	2.90 (0.03)	5.08 (0.02)	5.11 (0.02)	3.81 (0.02)
I ₃	3.29 (0.14)	5.12 (0.05)	5.14 (0.05)	4.28 (0.06)	3.08 (0.02)	5.12 (0.04)	5.13 (0.03)	3.85 (0.01)
I ₄	2.99 (0.13)	4.72 (0.06)	4.78 (0.04)	3.92 (0.06)	2.80 (0.03)	4.35 (0.05)	4.38 (0.02)	3.22 (0.01)
I ₅	2.69 (0.11)	4.13 (0.05)	4.10 (0.03)	3.15 (0.05)	2.60 (0.02)	3.78 (0.02)	3.79 (0.03)	2.60 (0.02)
I ₆	2.58 (0.12)	3.71 (0.06)	3.60 (0.04)	2.92 (0.05)	2.54 (0.03)	3.45 (0.04)	3.44 (0.04)	2.47 (0.02)
I ₇	3.18 (0.13)	5.02 (0.06)	5.04 (0.05)	4.14 (0.04)	3.06 (0.04)	4.82 (0.03)	4.84 (0.03)	3.53 (0.01)
Mean	3.10	4.71	4.72	3.86	2.88	4.54	4.56	3.34
LSD ($p = 0.05$)	0.52	0.15	0.14	0.18	0.08	0.11	0.11	0.0
Interactions	NS	NS	NS	NS	NS	NS	NS	NS

Numbers given in parentheses indicate standard error.

3.2.3. Change in Seasonal Soil Moisture Storage

The seasonal change in soil moisture storage varied with nitrogen and irrigation during cropping seasons (Tables 5 and 6). During 2018–2019, in N₁, maximum extraction of profile water was found under I₇ (−40 mm) and I₆ (−36.2 mm) treatments followed by I₅

(−34.2 mm), I₃ (−11.3 mm) and I₄ (−11.6). However, the change in soil moisture storage was positive in I₁ (6.4 mm) and I₂ (10.0 mm). Under the N₂ level of irrigation, maximum extraction was observed under I₇ (−39.1 mm) followed by I₆ (−34.0 mm) and I₅ (33.2 mm), I₃ (−10.3 mm), I₄ (−9.6 mm), I₁ and I₂ (6.2 and 10.7 mm.). However, the profile storage was more under all the irrigation levels than N₁. Similarly, under N₃ treatment, maximum profile water extraction was observed in I₇ (−42.0 mm) followed by I₆ (−23.9 mm) and I₅ (−22.1 mm), I₃, I₄ (−8.4, 0.8 mm), I₃, I₁ (9.5 mm) and I₂ (23.1 mm). The profile moisture storage was more under the N₃ irrigation level, although a similar amount of irrigation was applied. It could be because of the significantly less biomass production and root development, which caused less water uptake by the crops and thereby less ET. Similarly, during 2019–20 (Table 6), profile moisture storage was negative. However, the profile was wetter than the first year, as rain events occurred after irrigation application. Higher extraction of moisture from profile under N₁ was observed in I₇ (−29.9 mm) followed by I₅ (−18.9 mm), I₆ (−17.6 mm), I₃ (−13.3 mm), I₄ (−12.6 mm), I₁ (−3.6 mm) and I₂ (−2.8 mm). A similar trend was observed in N₂ and N₃.

3.3. Plant Growth Parameters

Periodic Leaf Area Index (LAI), Total Dry Matter Accumulation and Root Growth

The leaf area index has been considered one of the prominent indicators of plant growth and yield, as it directly affects different eco-physiological processes in plants [28,29]. The leaf area index was significantly affected by different nitrogen and irrigation treatments throughout the crop growth period during both years (Table 8). LAI was at par in N₁ and N₂ at 45, 60, 75 and 90 DAS during 2018–2019. However, it decreased by 30.2, 12.9, 13.4 and 25.8% in N₃ at 45, 60, 75 and 90 DAP, respectively, during 2018–2019. The highest reduction in LAI was recorded with the reduction in nitrogen rate at 45 and 90 DAP. During 2019–2020, at 45 DAP, LAI did not differ in N₁ and N₂ treatments, but at 60, 75 and 90 DAP the highest LAI was observed in the N₁ treatment which was significantly higher than N₂ and N₃. It could be explained by the fact that this year, one fertigation at 60 DAP was delayed by three days due to continuous rains, and another was immediately followed by a major rain event. Rain might have leached the applied nitrogen. Among irrigation levels, the highest LAI was observed in I₁, which was at par with I₂, I₃ and I₇ at 45 DAP during both years. However, at 60, 75 and 90 DAP, LAI was at par in I₁, I₂ and I₃, which was significantly higher over I₇ and other treatments during both years. The highest LAI with the highest level of irrigation indicated higher photosynthesis due to higher radiation interception, as explained by [26,30]. The increase in LAI in I₁, I₂ and I₃ were also due to more root zone moisture (Tables 3 and 4).

The periodic dry matter accumulation (DMA) was significantly affected by nitrogen and irrigation regimes (Table 9). During 2018–2019, DMA did not differ significantly between N₁ and N₂ but decreased significantly with a further decrease in nitrogen level (N₃) at all the growth stages. A similar trend was observed during 2019–2020 except at 60 DAP, where biomass was significantly higher in N₁ compared to N₂ and N₃. Regardless of fertilizer application, the highest periodic DMA during both years was observed in I₁, which was followed by I₂, I₃ and I₇. The DMA was at par in I₁, I₂ and I₃ but significantly higher than recommended treatment (I₇) and all other treatments. Higher and frequent irrigation treatments under subsurface drip (I₁, I₂, I₃) favoured the improvement in plant vigour because of higher availability of moisture content in the root zone (Tables 3 and 4) and higher soil matric potential (−25 to −30 kPa) (Figure 1) compared to recommended (I₇) and other deficit irrigation treatments, which was further supported [31–34].

Table 9. Effect of nitrogen and irrigation on periodic dry matter accumulation (Mg ha^{-1}) of potato.

Treatments	2018–2019			2019–2020		
	60 DAS	75 DAS	90 DAS	60 DAS	75 DAS	90 DAS
N ₁	4.43 (0.11)	5.64 (0.13)	8.28 (0.15)	3.96 (0.01)	6.72 (0.03)	10.5 (0.13)
N ₂	4.17 (0.13)	5.27 (0.11)	8.04 (0.09)	3.72 (0.02)	6.66 (0.04)	10.1 (0.15)
N ₃	3.66 (0.15)	4.54 (0.16)	7.11 (0.11)	3.34 (0.04)	5.62 (0.06)	95.2 (0.19)
Mean	4.09	5.15	7.81	3.67	6.33	10.0
LSD						
(<i>p</i> = 0.05)	0.45	0.44	0.35	0.14	0.21	0.64
I ₁	4.55 (0.05)	5.77 (0.07)	8.53 (0.11)	4.19 (0.04)	7.04 (0.09)	10.7 (0.15)
I ₂	4.49 (0.03)	5.66 (0.06)	8.37 (0.10)	4 (0.05)	6.75 (0.10)	10.4 (0.16)
I ₃	4.32 (0.04)	5.6 (0.07)	8.27 (0.09)	4.06 (0.04)	6.8 (0.11)	10.1 (0.17)
I ₄	3.87 (0.04)	4.92 (0.08)	7.85 (0.11)	3.65 (0.03)	5.98 (0.08)	9.54 (0.14)
I ₅	3.7 (0.07)	4.52 (0.09)	7.04 (0.08)	3.15 (0.05)	5.7 (0.11)	8.92 (0.18)
I ₆	3.5 (0.07)	4.13 (0.08)	6.53 (0.11)	2.94 (0.06)	5.51 (0.10)	8.58 (0.17)
I ₇	4.2 (0.05)	5.46 (0.06)	8.09 (0.08)	3.94 (0.05)	6.56 (0.09)	10.0 (0.19)
Mean	4.06	5.15	7.81	3.7	6.33	9.75
LSD						
(<i>p</i> = 0.05)	0.23	0.26	0.29	0.18	0.31	0.54
Interactions	NS	NS	NS	NS	NS	NS

Numbers given in parentheses indicate standard error.

The distribution of root mass density of potato during both years is presented in Figure 2a,b. It was observed that a major portion of the roots was observed in 0–45 cm for all the treatments. Among different nitrogen levels, RMD was highest in N₁ in all the depths. During the first year (Figure 2a), RMD in N₁ was 17% and 26% higher over N₂ and N₃, respectively, in 0–15 cm depth. The difference was 16% and 31%, respectively, in 15–30 cm depth. In 30–45 cm depth, RMD in N₁ was 13% and 27.8% higher over N₂ and N₃, respectively. The difference between 45 and 60 cm depths was 12% and 26%, respectively. During 2019–2020 (Figure 2b), the mean RMD was 12.2% higher in N₁ over N₂ in all the depths. The difference between N₁ and N₃ was 38, 21.5, 24.0 and 26.6% in 0–15, 15–30, 30–45 and 45–60 cm depths, respectively. Among irrigation levels, all the subsurface drip irrigation treatments produced the highest RMD in 15–30 cm followed by 0–15 cm, 30–45 and 45–60 cm depths except I₇. In I₇, the highest RMD was observed in the 0–15 cm soil layer, followed by 15–30 and 30–45 cm depths. Mean RMD of I₇ was 1025.7, 398.0, 151.9 and 3.1 g m^{-3} in 0–15, 15–30, 30–45 and 45–60 cm soil depths, respectively. Respective values for I₁ and I₂ were 652.7, 721.6, 273.4 and 18.2 and 651.9, 720.9, 303.8 and 24.3 g m^{-3} . RMD of I₃ and I₄ was 641.9, 673.4, 287.1 and 21.3 and 629.5, 648.0, 278.0 and 6.1 g m^{-3} in 0–15, 15–30, 30–45 and 45–60 cm soil depths, respectively. The I₅ and I₆ treatments showed the lowest RMD in 0–15 and 15–30 cm soil depths but slightly more than I₁ and I₂ in 30–45 cm soil depth. Out of total the RMD of each subsurface irrigation treatment, 37–38% RMD was found in the 0–15 cm layer, 40–43% in 15–30 cm and 16–19% in the 30–45 cm layer. However, in the 45–60 cm soil layer, only 1–2% root mass density was found. On the other hand, in the surface drip irrigation treatment, 64.9% RMD was found in 0–15 cm depth, 25.2% in 15–30 cm, 9% in 30–45 cm and only 0.1% in 45–60 cm. These results are similar to those of [27,35]. Lu et al. [36] also reported that the 0–20 cm soil layer accounted for 62–68% of total root weight of potato under surface drip. Similar observations were observed in the second year of study (Figure 2b). However the difference between RMD of all the treatments in 0–15 cm and 15–30 cm soil layers was less than in the first year. RMD was more in 30–45 cm soil depth than in the first year. This may be because of more rain in the second year. Also, the overall total RMD was more in the second year of study than in the first year for all the treatments. A previous study [37] also reported decreased RMD in 0–30 cm depth in water-stressed conditions.

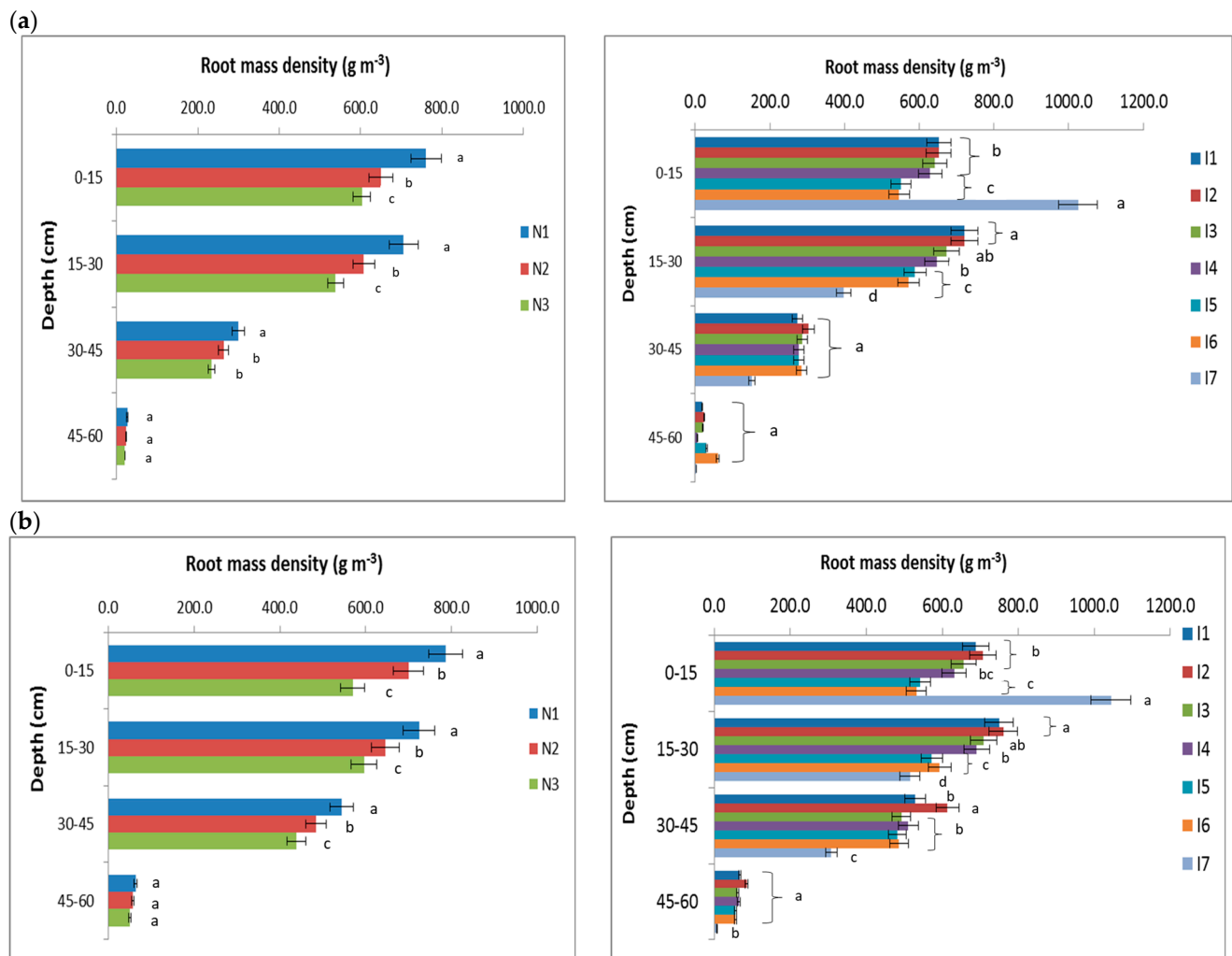


Figure 2. Root mass density of potato as affected by nitrogen and irrigation levels during 2018–2019 (a) and 2019–2020 (b). Treatments with different lower case letters are significantly different at $p < 0.05$.

3.4. Tuber Yield

Data on the tuber yield for both years are presented in Table 10. Tuber yield was affected significantly by nitrogen and irrigation during both years. During 2018–2019, tuber yield was at par in N_1 and N_2 but decreased (by 8.9% compared to N_1) significantly as the nitrogen level decreased to N_3 . However, during 2019–2020, the highest mean tuber yield was obtained in N_1 , which was significantly higher by 2.4 and 10.7% over N_2 and N_3 , respectively. It could be either due to the difference in rain amount during both years or due to a delay in one fertigation because of rain. In addition to this, another significant rain event occurred immediately after fertigation, which may have leached the soil nitrogen [14,16]. Due to its shallow root system, potato responds to high nutrition as nitrogen may leach with higher irrigation below the root zone [14]. The highest tuber yield with a higher dose (240 kg N ha^{-1}) of nitrogen has been reported earlier [38]. The pooled analysis also showed that the highest tuber yield was recorded with an N_1 level of nitrogen which was significantly higher than N_2 and N_3 . The tuber yield decreased with decrease in nitrogen (N_3), as a result of reduction in tuber weight by 21.31% and number of tubers per plant by 17.5% compared to N_1 (Tables 11–13) during 2018–2019. During 2019–2020, tuber weight was also reduced by 25.9% with a reduction in nitrogen level from N_1 to N_3 . However, it was at par in N_1 and N_2 . However, the number of tubers per plant decreased significantly (6.2%) with the decrease in nitrogen from N_1 to N_2 , and it further decreased

by 19.8% as the nitrogen level further decreased to N₃. The results are consistent with earlier findings [6,39], where drip irrigation significantly affected the weight of the tubers and the number of tubers per plant. Among various irrigation levels, the highest tuber yield was obtained in the I₁ treatment and was statistically similar to I₂ and I₃ during both years but was significantly higher than I₄, I₅, I₆ and I₇. It could be because of higher root mass density in 15–30 cm soil depth in I₁, I₂ and I₃ (Figure 2a) compared to I₇, which led to more N uptake by plants under I₁ and I₂. Higher water supply at frequent intervals caused increased transpiration (Table 7), which might have resulted in an enhanced tuber yield via gaseous exchange and photosynthesis [40]. However, tuber yield in I₇ and I₃ were also mutually at par. Decreased tuber yield with the reduction in irrigation amount below 50% of water depletion and SMP near –45 kPa [33,34,36,41,42] and the highest tuber yield with 100% ET_c was also reported [43]. Similar observations have also been reported in cereal [44]. The increase in potato yield with the highest level of irrigation was due to an increase in tuber weight, number of tubers per plant and evapotranspiration, as is clear from the potato production function (Figures 3–5). A linear relationship was found between tuber yield and tuber weight. The value of R² between tuber yield and tuber weight was 0.94 and 0.87 during 2018–2019 and 2019–2020, respectively. The R² value between tuber yield and number of tubers was 0.8782 and 0.9034 in 2018–2019 and 2019–2020, respectively. R² between tuber yield and ET (Figure 5) was 0.75 and 0.77 during 2018–2019 and 2019–2020, respectively. However, the R² between tuber yield and transpiration was 0.92 (Figure 6) during both years. Higher yield and yield attributes in I₁ could be because of more moisture at 30 cm depth and below compared to other treatments (Tables 4 and 5). Interaction results during both years revealed that at the highest nitrogen level (N₁), I₁, I₂ and I₃ produced statistically similar yields as recommended (I₇), but at the N₂ level, I₁, I₂ and I₃ produced statistically higher yields over I₇. The results are in line with a study conducted in our region [45], that found a higher response of potato to a frequently irrigated treatment (ratio of irrigation water to pan evaporation 1.0) compared to a less-frequently irrigated treatment (ratio of irrigation water to pan evaporation 0.8). During both years and in the pooled analysis, the highest tuber yield (average 34.44 Mg ha⁻¹) was recorded in seven treatment combinations (N₁I₁, N₁I₂, N₁I₃, N₁I₇, N₂I₁, N₂I₂ and N₂I₃) without any significant difference among them. Other treatment combinations recorded significantly lower tuber yield. The results align with other studies [20,46] in sandy loam soil.

Table 10. Effect of different nitrogen and irrigation levels on tuber yield (Mg ha⁻¹).

Treatments	2018–2019				2019–2020				Pooled Analysis			
	N ₁	N ₂	N ₃	Mean	N ₁	N ₂	N ₃	Mean	N ₁	N ₂	N ₃	Mean
I ₁	35.2	34.7	32.4	34.1 (0.27)	35.4	35.0	33.1	34.5 (0.22)	35.3	34.6	32.6	34.2
I ₂	34.9	34.2	32.1	33.7 (0.26)	35.3	34.7	32.7	34.2 (0.21)	35.1	33.9	32.4	33.8
I ₃	34.5	33.9	31.7	33.4 (0.25)	35.1	34.3	32.4	33.9 (0.19)	34.8	33.6	32.1	33.5
I ₄	33.1	32.2	29.4	31.6 (0.23)	34.2	33.8	30.6	32.9 (0.23)	33.7	33.0	30.0	32.2
I ₅	28.8	27.8	25.5	27.4 (0.22)	31.4	29.2	25.4	28.6 (0.20)	30.1	28.5	25.1	27.9
I ₆	28.0	26.7	25.0	26.6 (0.25)	27.7	27.4	24.9	26.7 (0.23)	27.9	27.1	24.4	26.5
I ₇	33.9	33.0	31.5	32.8 (0.26)	34.6	33.8	32.1	33.5 (0.22)	34.7	33.7	31.3	33.3
Mean	32.4	31.8	29.7	31.3	33.4	32.6	30.2	32.0	33.1	32.1	29.6	31.6
SE±	0.29	0.30	0.31		0.22	0.19	0.21					
LSD (<i>p</i> = 0.05)	N = 0.95 I = 0.83, I × N = 1.43				N = 0.57, I = 0.66, I × N = 1.15				Y = 0.21 N = 0.26, Y × N = ns, I = 0.44, I × N = 0.74, Y × N × I = ns			

Numbers given in parentheses indicate standard error.

Table 11. Effect of nitrogen and irrigation on tuber weight and No. of tubers per plant.

Treatments	2018–2019		2019–2020	
	Tuber Weight (g)	No. of Tubers/10 Plants	Tuber Weight (g)	No. of Tubers/10 Plants
N ₁	44.16 (1.58)	88.9 (1.22)	47.37 (2.12)	96.2 (1.93)
N ₂	41.54 (1.60)	86.0 (1.24)	44.01 (2.10)	90.5 (1.90)
N ₃	36.40 (1.63)	75.6 (1.26)	37.61 (2.28)	80.3 (1.96)
Mean	40.7	83.5	42.99	89.6
LSD (<i>p</i> = 0.05)	4.7	3.5	6.0	5.5
I ₁	44.9 (1.74)	96.8 (2.78)	48.61 (1.64)	104.7 (2.74)
I ₂	44.2 (1.73)	93.1 (2.81)	47.33 (1.61)	99.9 (2.75)
I ₃	43.5 (1.68)	90.7 (2.81)	45.31 (1.65)	97.0 (2.76)
I ₄	41.0 (1.71)	83.3 (2.88)	43.62 (1.64)	90.0 (2.73)
I ₅	35.6 (1.76)	70.5 (2.91)	37.29 (1.66)	74.8 (2.75)
I ₆	32.1 (1.77)	62.1 (2.93)	34.28 (1.65)	63.0 (2.76)
I ₇	43.5 (1.71)	88.1 (2.94)	44.50 (1.63)	93.7 (2.75)
Mean	40.7	83.5	42.99	89.6
LSD (<i>p</i> = 0.05)	5.0	8.4	4.9	8.3
Interactions	NS	NS	NS	NS

Numbers given in parentheses indicate standard error.

Table 12. N uptake by aboveground biomass and tubers (kg ha⁻¹) during 2018–2019.

Treatments	N Uptake by Biomass				Tuber N Uptake			
	N ₁	N ₂	N ₃	Mean	N ₁	N ₂	N ₃	Mean
I ₁	119.8	116.6	87.4	107.9 (2.31)	358.8	353.5	314.7	342.3 (2.80)
I ₂	113.6	109.5	84.4	102.5 (2.24)	355.6	349.0	308.3	337.6 (2.91)
I ₃	112.6	109.1	83.5	101.7 (2.45)	348.5	344.1	303.1	331.9 (2.51)
I ₄	103.6	95.4	73.6	90.9 (2.13)	331.4	318.3	276.4	308.7 (2.61)
I ₅	92.8	84.4	64.1	80.4 (2.34)	285.4	272.5	235.0	264.3 (2.55)
I ₆	86.6	77.8	55.3	73.2 (2.40)	274.8	256.7	230.1	253.9 (2.64)
I ₇	109.3	101.3	81.1	97.2 (2.23)	346.2	336.3	290.2	324.2 (2.60)
Mean	105.5	99.2	75.6		328.7	318.6	279.7	309.0
SE±	2.51	2.55	2.68		1.81	0.83	0.85	
LSD (<i>p</i> = 0.05)	N = 8.1 I = 6.5, I _x × N = 13.1				N = 5.5, I = 10.6, I _x × N = NS			

Numbers given in parentheses indicate standard error.

Table 13. N uptake by aboveground biomass and tubers (kg ha⁻¹) during 2019–2020.

Treatments	N Uptake by Biomass				Tuber N Uptake			
	N ₁	N ₂	N ₃	Mean	N ₁	N ₂	N ₃	Mean
I ₁	129.4	128.1	110.2	122.6 (1.29)	368.2	364.4	338.0	356.9 (1.51)
I ₂	127.4	125.6	109.1	120.7 (1.31)	367.4	360.6	329.8	352.6 (1.50)
I ₃	124.3	121.8	108.4	118.8 (1.34)	364.6	356.3	326.7	349.2 (1.52)
I ₄	107.7	102.3	85.1	98.4 (1.30)	349.1	344.4	302.5	332.0 (1.53)
I ₅	94.3	90.5	71.1	85.3 (1.28)	316.8	288.8	243.4	283.0 (1.50)
I ₆	86.1	76.5	65.2	75.9 (1.31)	274.2	263.1	236.7	258.0 (1.53)
I ₇	115.5	110.6	98.7	108.3 (1.32)	359.3	344.9	324.3	342.8 (1.52)
Mean	112.1	107.9	92.5		342.8	331.8	300.2	324.9
SE±	1.34	1.32	1.34		1.55	1.52	1.58	
LSD (<i>p</i> = 0.05)	N = 4.0, I = 4.1, I × N = 7.0				N = 4.7, I = 4.5, I × N = 7.2			

Numbers given in parentheses indicate standard error.

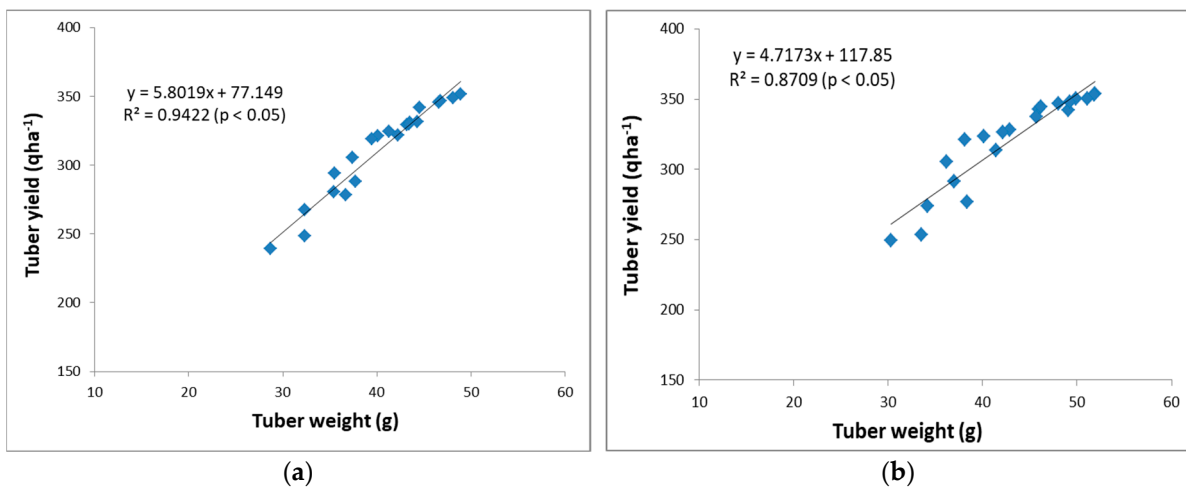


Figure 3. Relationship between tuber yield and tuber weight during (a) 2018–2019 and (b) 2019–2020.

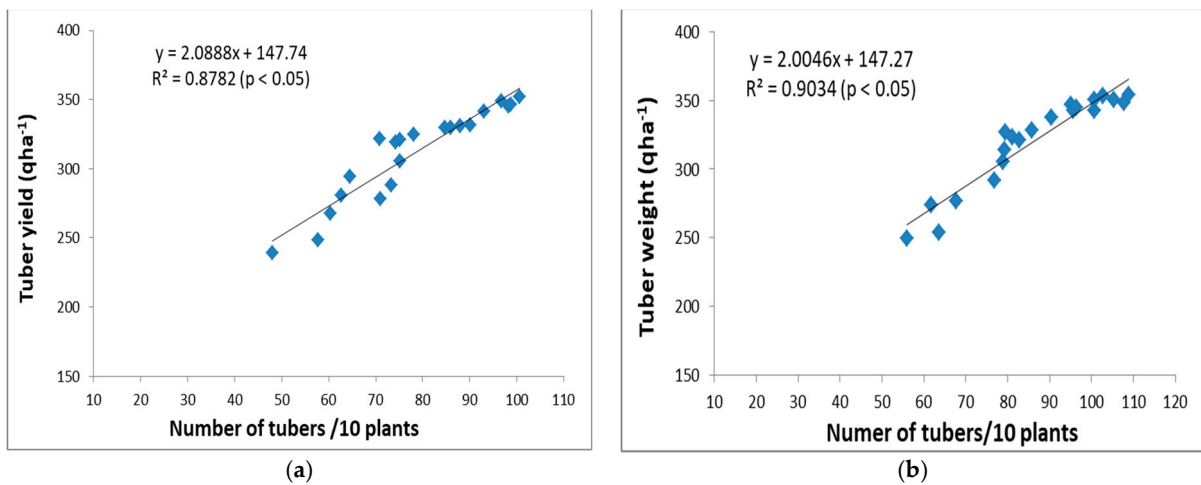


Figure 4. Relationship between tuber yield and number of tubers per 10 plants (a) 2018–2019 (b) 2019–2020.

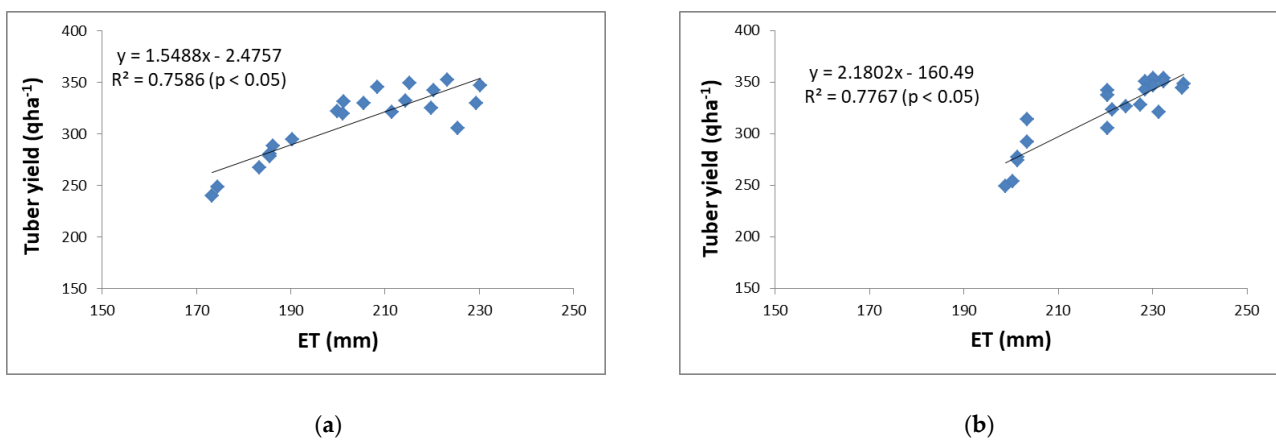


Figure 5. Relationship between tuber yield and ET (a) 2018–2019 (b) 2019–2020.

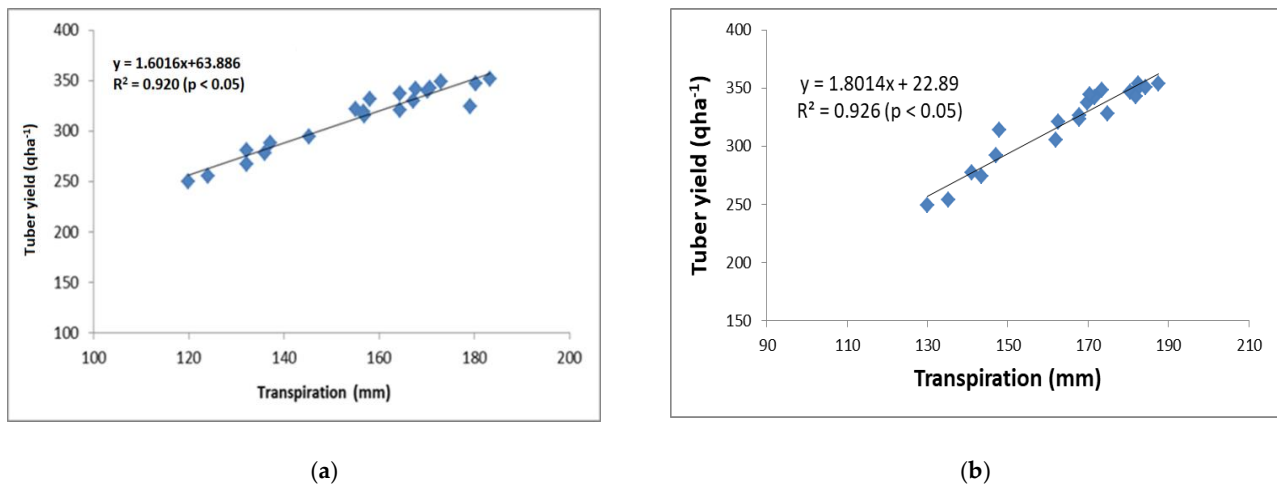


Figure 6. Relationship between tuber yield and transpiration (a) 2018–2019 (b) 2019–2020.

3.5. N Uptake by Aboveground Parts and Tubers

Nitrogen uptake at 90 DAP (days after planting) and tuber N uptake during both years are presented in Tables 12 and 13. During 2018–2019, N uptake aboveground was at par in N_1 and N_2 but significantly higher over N_3 . The difference between N_1 and N_3 was 39.5%. However, during 2019–2020, N uptake was significantly higher in N_1 than in N_2 and N_3 . This could be due to the difference in rain events in both years. Among irrigation levels, during both years, N uptake was at par among I_1 , I_2 and I_3 . The interaction between irrigation and nitrogen was also significant. The highest N uptake was observed in N_1I_1 , which was at par with N_1I_2 , N_1I_3 , N_1I_7 , N_2I_1 , N_2I_2 , N_2I_3 and N_2I_7 . N uptake by the tuber was also affected by nitrogen and irrigation during both years. During 2018–2019, the highest N uptake was observed in N_1 , significantly higher over N_2 and N_3 . It was higher by 4.2% and 30.4% over N_2 and N_3 , respectively. Similarly, during 2019–2020, N_1 recorded 3.8 and 14.2% higher N uptake over N_2 and N_3 , respectively. Among the irrigation levels, tuber N uptake was at par in I_1 , I_2 and I_3 but significantly higher than recommended practice and all other treatments. The highest tuber N uptake was observed during both years in N_1I_1 (358.8 and 368.2 kg ha⁻¹). It was at par with N_1I_2 , N_1I_3 , N_2I_1 and N_2I_2 . N uptake with an increase in N level from 160 to 340 kg N ha⁻¹ by aboveground biomass and tubers was also observed [20]. Singh et al. [45] on the same type of soil observed an increase in N uptake with increase in N rate from 135 kg ha⁻¹ to 225 kg ha⁻¹ and also reported an increase in mean N uptake by 13 and 24.9% in $I_{1.5}$ (1.5 ratios of irrigation to pan E) and $I_{2.0}$ (2.0 ratio of irrigation to pan E), respectively, over $I_{1.0}$ regime (1.0 ratio of irrigation to pan E). Similar effects of irrigation and N were observed on total N uptake in the sandy loam soil [47]. Higher N uptake by tubers in the highest level of nitrogen may have contributed towards the higher yield [48].

3.6. Real Water Productivity

Real water productivity (WP_{ET}) is the ratio of tuber yield and evapotranspiration. During both years (Table 14), the highest WP_{ET} (15.7 and 15.0 kg m⁻³) was obtained with N_1 and at par with N_2 (15.4 and 14.7 kg m⁻³) and significantly higher over N_3 (14.7 and 13.8 kg m⁻³). Higher water productivity by opting for drip irrigation and optimum nitrogen has also been found in potato and eggplant [20,48–50]. Among irrigation levels, the highest WP_{ET} was obtained with I_3 and I_4 (16.2 and 16.0 kg m⁻³, respectively), which was statistically higher than all the other treatments. During 2019–2020, WP_{ET} (15.3 kg m⁻³) was statistically higher in I_3 compared to all other treatments. The highest water productivity during the first year was obtained with N_1I_3 (16.6 kg m⁻³), followed by N_1I_4 and N_2I_3 (16.4 kg m⁻³). Similarly, in the second year, water productivity was highest

in N_1I_3 (15.8 kg m^{-3}), which was at par with N_2I_3 and N_1I_4 . Our findings agree with [20], who reported 16.7% higher water use by reducing 20% of applied water.

Table 14. Effect of irrigation and nitrogen on real water productivity (WP_{ET}) of potato (kg m^{-3}).

Treatments	2018–2019				2019–2020			
	N_1	N_2	N_3	Mean	N_1	N_2	N_3	Mean
I_1	15.8	15.7	14.8	15.4	15.2	15.1	14.4	14.9
I_2	16.2	16.0	15.2	15.8	15.4	15.1	14.5	15.0
I_3	16.6	16.4	15.9	16.2	15.8	15.5	14.8	15.3
I_4	16.4	16.1	15.4	16.0	15.5	15.3	13.9	14.9
I_5	15.5	15.0	14.6	15.0	15.4	14.3	12.6	14.1
I_6	15.1	14.6	14.4	14.7	13.8	13.6	12.5	13.3
I_7	14.7	14.4	14.0	14.4	14.6	14.6	13.7	14.3
Mean	15.7	15.4	14.9	115.4	15.1	14.8	13.8	14.5
LSD ($p = 0.05$)	N = 0.43, I = 0.26, I \times N = 0.48				N = 0.42, I = 0.21, I \times N = 0.40			

4. Conclusions

Under subsurface fertigation, lower nitrogen application (N_3) resulted in less LAI and DMA, which further reduced the transpiration and potato tuber yield compared to higher (N_1) and optimum nitrogen (N_2). The unproductive water losses of soil evaporation were much higher in surface than in subsurface drip irrigation. Tuber yield was statistically at par in combinations of N_1I_1 , N_1I_2 , N_1I_3 , N_1I_7 , N_2I_1 , N_2I_2 and N_2I_3 , which indicated that both 20% nitrogen and irrigation water could be saved with N_2I_3 compared to all other combinations. Therefore, subsurface drip irrigation with 80% of recommended nitrogen and irrigation can be a viable option for obtaining higher biomass, tuber yield and water productivity compared to surface drip irrigation with 100% recommended nitrogen and 80% irrigation water. Thus, statistically similar yield and higher real water productivity were obtained with the application of 20% less nitrogen with subsurface than surface fertigation.

Supplementary Materials: The following supporting information can be downloaded at: <https://www.mdpi.com/article/10.3390/agronomy13010011/s1>, Figure S1: Layout of the field experiment.

Author Contributions: Conceptualization, methodology, investigation, resources, data curation, project administration, formal analysis, writing—original draft preparation, A.K., K.B.S. and R.K.G.; funding acquisition, writing—review and editing, A.A., A.Z.D. and M.A.M. All authors have read and agreed to the published version of the manuscript.

Funding: This research was funded by the Deanship of Scientific Research, King Saud University through the Vice Deanship of Scientific Research Chairs; Research Chair of Prince Sultan Bin Abdulaziz International Prize for Water.

Institutional Review Board Statement: Not applicable.

Informed Consent Statement: Not applicable.

Data Availability Statement: The data presented in this study are available on request from the corresponding author.

Acknowledgments: The authors extend their appreciation to the Deanship of Scientific Research, King Saud University for funding through the Vice Deanship of Scientific Research Chairs; Research Chair of Prince Sultan Bin Abdulaziz International Prize for Water. Authors are thankful to ARS Mandor, AU Jodhpur and ICAR-CAZRI, Jodhpur and IC-AR-NRCSS, Ajmer for providing support during the research period.

Conflicts of Interest: The authors declare no conflict of interest.

References


1. FAOSTAT (2021) FAO Statistical Database. Available online: <http://faostat3.fao.org/home/index.htm> (accessed on 8 October 2021).
2. Rana, R.K. Status of Punjab state in Indian potato processing industry. *Indian J. Agric. Mktg* **2011**, *25*, 1–17.
3. Levy, D.; Coleman, W.K.; Veilleux, R.E. Adaptation of Potato to Water Shortage: Irrigation Management and Enhancement of Tolerance to Drought and Salinity. *Am. J. Potato Res.* **2013**, *90*, 186–206. [CrossRef]
4. Kumar, R.; Vaid, U.; Mittal, S. Water Crisis: Issues and Challenges in Punjab. In *Water Resources Management*; Singh, V., Yadav, S., Yadava, R., Eds.; Springer: Singapore, 2018; Volume 78. [CrossRef]
5. Brar, S.K.; Mahal, S.S.; Brar, A.S.; Vashisht, K.K.; Sharma, N.; Butter, G.S. Transplanting time and seedling age affect water productivity, rice yield and quality in north-west India. *Agric. Water Manag.* **2012**, *115*, 217–222. [CrossRef]
6. Rolbiecki, R.; Rolbiecki, S.; Figas, A.; Jagosz, B.; Stachowski, P.; Sadan, H.A.; Prus, P.; Pal-Fam, F. Requirements and Effects of Surface Drip Irrigation of Mid-Early Potato Cultivar Courage on a Very Light Soil in Central Poland. *Agronomy* **2021**, *11*, 33. [CrossRef]
7. Mokh, E.F.; Nagas, K.; Masmoudi, M.M.; Mechlia, N.B. Yield and Water Productivity of Drip-Irrigated Potato under Different Nitrogen Levels and Irrigation Regime with Saline Water in Arid Tunisia. *Am. J. Plant Sci.* **2015**, *6*, 501–510. [CrossRef]
8. Feng, Z.; Kang, Y.; Wan, S.; Liu, S. Effect of Drip Fertigation on Potato Productivity with Basal Application of Loss Control Fertilizer in Sandy Soil. *Irrig. Drain.* **2018**, *67*, 210–221. [CrossRef]
9. Fabio, C.; Olalla, F.M.S.; Juan, J.A. Yield size of deficit irrigated potatoes. *Agric. Water Manag.* **2001**, *48*, 255–266.
10. Sharma, V.; Sharma, I.P.; Spehia, R.S.; Kumar, P. Influence of irrigation methods and fertilizer levels on the productivity of Potato (*Solanum tuberosum*). *Indian J. Agric. Sci.* **2012**, *82*, 117–121.
11. Peerzada, S.H.; Najar, A.G.; Ahmad, M.; Dar, G.H.; Bhat, K.A. Effect of Irrigation Frequency on Potato Late Blight (*Phytophthora Infestans*). *Int. J. Curr. Microbiol. Appl. Sci.* **2013**, *2*, 125–132.
12. Davenport, J.R.; Milburn, P.H.; Rosen, C.J.; Thornton, R.E. Environmental impacts of potato nutrient management. *Am. J. Potato Res.* **2005**, *82*, 321–328. [CrossRef]
13. Ierna, A.; Pandino, G.; Lombardo, S.; Mauromicale, G. Tuber yield, water and fertilizer productivity in early Potato as affected by a combination of irrigation and fertilization. *Agri. Water Manag.* **2011**, *101*, 35–41. [CrossRef]
14. Jiang, Y.; Nyiraneza, J.; Khakbazan, M.; Geng, X.; Murray, B.J. Nitrate Leaching and Potato Yield under Varying Plow Timing and Nitrogen Rate. *Agrosyst. Geosci. Environ.* **2019**, *2*, 1–14. [CrossRef]
15. Ojala, J.C.; Stark, J.C.; Kleinkopf, G.E. Influence of irrigation and nitrogen management on potato yield and quality. *Am. Potato J.* **1990**, *67*, 29–43. [CrossRef]
16. Stark, J.C.; McCann, I.R.; Westermann, D.T.; Izadi, B.; Tindall, T.A. Potato response to split nitrogen timing with varying amount of excessive irrigation. *Am. Potato J.* **1993**, *70*, 765–777. [CrossRef]
17. Kaur, A.; Brar, A.S. Influence of mulching and irrigation scheduling on productivity and water use of turmeric (*Curcuma longa* L.) in north-western India. *Irrig. Sci.* **2016**, *34*, 261–269. [CrossRef]
18. Enciso-Molina, J.M.; Colaizzi, P.D.; Multer, W.L.; Stichler, C.R. Cotton response to phosphorus fertigation using subsurface drip irrigation. *Appl. Eng. Agric.* **2007**, *23*, 299–307. [CrossRef]
19. Laman, F.R.; Camp, C.R. Subsurface drip irrigation. In *Micro-Irrigation for Crop Production: Design, Operation and Management*; Developments in Agriculture Engineering; Elsevier: Amsterdam, The Netherlands, 2007; Chapter 13; pp. 473–551.
20. Badr, M.A.; El-Tohamy, W.A.; Zaghoul, A.M. Yield and water use efficiency of Potato grown under different irrigation and nitrogen levels in an arid region. *Agric. Water Manag.* **2012**, *110*, 9–15. [CrossRef]
21. Patel, N.; Rajput, T.B.S. Effect of drip tape placement depth and irrigation level on yield of Potato. *Agric. Water Manag.* **2007**, *88*, 209–223. [CrossRef]
22. Sahoo, P.; Brar, A.S.; Sharma, S. Effect of methods of irrigation and sulphur nutrition on seed yield, economic and bio-physical water productivity of two sunflower (*Helianthus annuus* L.) hybrids. *Agric. Water Manag.* **2018**, *206*, 158–164. [CrossRef]
23. Brar, A.S.; Buttar, G.S.; Thind, H.S.; Singh, K.B. Improvement of water Water Productivity, Economics and Energetics of Potato through Straw Mulching and Irrigation Scheduling in Indian Punjab. *Potato Res.* **2019**, *62*, 465–484. [CrossRef]
24. Singh, K.B.; Jalota, S.K.; Gupta, R.K. Soil water balance and response of spring maize (*Zea mays*) to mulching and differential irrigation in Punjab. *Indian J. Agron.* **2015**, *60*, 279–284.
25. Ali, M.H.; Talukdar, M.S.U. Increasing water productivity in crop production. A synthesis. *Agric. Water Manag.* **2008**, *95*, 1201–1213. [CrossRef]
26. Lerna, A.; Mauromicale, G. Tuber yield and irrigation water productivity in early potatoes as affected by irrigation regime. *Agric. Water Manag.* **2012**, *115*, 276–284.
27. Wang, F.X.; Kang, Y.H.; Liu, S.P. Effects of drip irrigation frequency on soil wetting pattern and potato growth in North China Plain. *Agric. Water Manag.* **2006**, *79*, 248–264. [CrossRef]
28. Yin, X.E.A.; Lantinga, C.M.; Schapendonk, X.; Zhong, X. Some relationships between leaf area index and canopy nitrogen content and distribution. *Ann. Bot.* **2003**, *91*, 893–903. [CrossRef]
29. Sadras, V.O.; Lemaire, G. Quantifying crop nitrogen status for comparisons of agronomic practices and genotypes. *Field Crops Res.* **2014**, *164*, 54–64. [CrossRef]

30. Zhao, H.; Wang, R.Y.; Ma, B.L.; Xiong, Y.C.; Qiang, S.C.; Wang, C.L.; Liu, C.A.; Li, F.M. Ridge-furrow with full plastic film mulching improves water use efficiency and tuber yields of Potato in a semiarid rainfed ecosystem. *Field Crops Res.* **2014**, *161*, 137–148. [CrossRef]
31. Nowacki, W. Water in potato production, problems and challenges. *Inżynieria Ekol.* **2018**, *19*, 14–25. [CrossRef]
32. Wang, F.X.; Wu, X.X.; Shock, C.C.; Chu, L.Y.; Gu, X.X.; Xue, X. Effects of drip irrigation regimes on potato tuber yield and quality under plastic mulch in arid Northwestern China. *Field Crops Res.* **2011**, *122*, 78–84. [CrossRef]
33. Kang, Y.; Wang, F.X.; Liu, H.J.; Yuan, B.Z. Potato evapotranspiration and yield under different drip irrigation regimes. *Irrig. Sci.* **2004**, *23*, 133–143. [CrossRef]
34. Ahuja, S.; Khurana, D.S.; Singh, K. Soil Matric Potential-Based Irrigation Scheduling to Potato in the Northwestern Indian Plains. *Agric. Res.* **2018**, *8*, 320–330. [CrossRef]
35. Lahlou, Q.; Ledent, J.F. Root mass and depth, stolons and roots formed on stolons in four cultivars of Potato under water stress. *Eur. J. Agron.* **2005**, *22*, 159–173. [CrossRef]
36. Wu, L.; Li, L.; Ma, Z.; Fan, M. Improving Potato Yield, Water Productivity and Nitrogen Use Efficiency by Managing Irrigation Based on Potato Root Distribution. *Int. J. Plant Prod.* **2022**, *16*, 547–555. [CrossRef]
37. Wang, F.X.; Kang, Y.H.; Liu, S.P. Effects of soil matric potential on potato growth under drip irrigation in North China Plain. *Agric. Water Manag.* **2007**, *88*, 34–42. [CrossRef]
38. Ferreira, T.C.; Carr, M.K.V. Responses of potatoes (*Solanum tuberosum* L.) to irrigation and nitrogen in a hot dry climate: I. water use. *Field Crops Res.* **2002**, *78*, 51–64. [CrossRef]
39. Rolbiecki, S.; Rolbiecki, R.; Kuśmierk-Tomaszewska, R.; Dudek, S.; Zarski, J.; Rzekanowski, C. Requirements and effects of drip irrigation of mid-early potato on a very light soil in moderate climate. *Fresenius Environ. Bull.* **2015**, *24*, 3895–3902.
40. Eid, M.A.M.; Abdel-Salam, A.A.; Salem, H.M.; Mahrous, S.E.; Seleiman, M.F.; Alsadon, A.A.; Solieman, T.H.I.; Ibrahim, A.A. Interaction Effects of Nitrogen Source and Irrigation Regime on Tuber Quality, Yield, and Water Use Efficiency of *Solanum tuberosum* L. *Plants* **2020**, *9*, 110. [CrossRef]
41. Zhou, S.; Li, F.; Zhang, H. Effect of Regulated Deficit Irrigation on Potato under-Mulched Drip Irrigation. *IOP Conf. Ser. Earth Environ. Sci.* **2020**, *615*, 012104. [CrossRef]
42. Kashyap, P.; Panda, R. Effect of irrigation scheduling on potato crop parameters under water stressed conditions. *Agric. Water Manag.* **2003**, *59*, 49–66. [CrossRef]
43. Ierna, A.; Mauromicale, G. Potato growth, yield and water productivity response to different irrigation and fertilization regimes. *Agric. Water Manag.* **2018**, *201*, 21–26. [CrossRef]
44. Ghorbani, M.; Neugschwandtner, R.W.; Konvalina, P.; Asadi, H.; Kopecký, M.; Amirahmadi, E. Comparative effects of biochar and compost applications on water holding capacity and crop yield of rice under evaporation stress: A two years field study. *Paddy Water Environ.* **2022**, *20*, 1–12. [CrossRef]
45. Singh, C.B.; Singh, S.; Arora, V.K.; Sekhon, N.K. Residue Mulch Effects on Potato Productivity and Irrigation and Nitrogen Economy in a Subtropical Environment. *Potato Res.* **2015**, *58*, 245–260. [CrossRef]
46. Yuan, B.Z.; Nishiyama, S.; Kang, Y. Effects of different irrigation regimes on the growth and yield of drip-irrigated Potato. *Agric. Water Manag.* **2003**, *63*, 153–167. [CrossRef]
47. Arora, V.K.; Nath, J.C.; Singh, C.B. Analyzing potato response to irrigation and nitrogen regimes in a subtropical environment using SUBSTOR-Potato model. *Agric. Water Manag.* **2013**, *124*, 69–76. [CrossRef]
48. Liang, S.; Abd El Baki, H.M.; An, P.; Fujimaki, H. Determining Irrigation Volumes for Enhancing Profit and N Uptake Efficiency of Potato Using WASH_2D Model. *Agronomy* **2022**, *12*, 2372. [CrossRef]
49. Aujla, M.S.; Thind, H.S.; Buttar, G.S. Fruit yield and water use efficiency of eggplant (*Solanum melongema* L.) as influenced by different quantities of nitrogen and water applied through drip and furrow irrigation. *Sci. Hort.* **2007**, *112*, 142–148. [CrossRef]
50. Unlu, M.; Kanber, R.; Senyigit, U.; Onaran, H.; Diker, K. Trickle and sprinkler irrigation of Potato (*Solanum tuberosum* L.) in Middle Anatolian Region in Turkey. *Agric. Water Manag.* **2006**, *79*, 43–71. [CrossRef]

Disclaimer/Publisher’s Note: The statements, opinions and data contained in all publications are solely those of the individual author(s) and contributor(s) and not of MDPI and/or the editor(s). MDPI and/or the editor(s) disclaim responsibility for any injury to people or property resulting from any ideas, methods, instructions or products referred to in the content.

Article

Research on Hydraulic Properties and Energy Dissipation Mechanism of the Novel Water-Retaining Labyrinth Channel Emitters

Yanfei Li ^{1,2}, Xianying Feng ^{1,2,*} , Yandong Liu ^{1,2}, Xingchang Han ^{1,2,3}, Haiyang Liu ^{1,2}, Yitian Sun ^{1,2,3}, Hui Li ^{1,2} and Yining Xie ^{1,2}

- ¹ School of Mechanical Engineering, Shandong University, Jinan 250061, China; yanfei-li@foxmail.com (Y.L.); liuyd2018@foxmail.com (Y.L.); 18678865298@126.com (X.H.); 18943653361@163.com (H.L.); sytde@163.com (Y.S.); lihuifs@sdu.edu.cn (H.L.); xieyining@mail.sdu.edu.cn (Y.X.)
- ² Key Laboratory of High Efficiency and Clean Mechanical Manufacture of Ministry of Education, Shandong University, Jinan 250061, China
- ³ Shandong Academy of Agricultural Machinery Sciences, Jinan 250100, China
- * Correspondence: fxying@sdu.edu.cn

Abstract: As a key component of a drip irrigation system, the performance of the drip irrigation emitters is mainly determined by the flow channel structures and structural parameters. In this study, a novel type of circular water-retaining labyrinth channel (CWRLC) structure emitter was proposed, inspired by the effect of roundabouts that make vehicles slow down and turn. Using the single-factor experiment method, the influence of the hydraulic performance of CWRLC emitters was researched under different circular radii. The internal flow characteristics and energy dissipation mechanism were analyzed by a computational fluid dynamics (CFD) simulation. It can be seen from the analysis that the energy dissipation abilities of the flow channel depend on the proportion of low-speed vortex areas. The larger the proportion of low-speed vortex areas, the smaller the flow index of the CWRLC emitter. Quadrate water-retaining labyrinth channel (QWRLC) and stellate water-retaining labyrinth channel (SWRLC) structures were obtained by structural improvements for increasing the proportion of low-speed vortex areas. The simulation results showed that the flow indexes of two improved structural emitters were significantly decreased. CWRLC, QWRLC, SWRLC, and widely used tooth labyrinth channel (TLC) emitters were manufactured by using technologies of electrical discharge machining (EDM) and injection molding (IM). The physical test results showed that the SWRLC emitter achieved the best hydraulic performance compared with the other three emitters. Therefore, the SWRLC emitter has a broad prospect of application in water-saving irrigation.

Keywords: irrigation emitter; hydraulic performance; energy dissipation mechanism; structural design; computational fluid dynamics



Citation: Li, Y.; Feng, X.; Liu, Y.; Han, X.; Liu, H.; Sun, Y.; Li, H.; Xie, Y. Research on Hydraulic Properties and Energy Dissipation Mechanism of the Novel Water-Retaining Labyrinth Channel Emitters. *Agronomy* **2022**, *12*, 1708. <https://doi.org/10.3390/agronomy12071708>

Academic Editor: Aliasghar Montazar

Received: 7 June 2022

Accepted: 17 July 2022

Published: 19 July 2022

Publisher's Note: MDPI stays neutral with regard to jurisdictional claims in published maps and institutional affiliations.



Copyright: © 2022 by the authors. Licensee MDPI, Basel, Switzerland. This article is an open access article distributed under the terms and conditions of the Creative Commons Attribution (CC BY) license (<https://creativecommons.org/licenses/by/4.0/>).

1. Introduction

Drip irrigation is an advanced and effective water-saving irrigation technology in modern agriculture [1]. It is widely used in the irrigation of economic crops such as melons, fruits, vegetables, and cotton. A drip irrigation emitter is the core component of the whole drip irrigation system [2]. Energy dissipation is realized by several flow channel structural units inside the emitter [3,4]. The flow channel structure units enable water flow under different pressures as uniform and stable small flows [5,6].

The hydraulic performance is one of the important indicators to evaluate the performance of drip irrigation emitters, which are generally expressed by the flow index [7]. The flow index reflects the sensitivity of the drip irrigation emitter flow to the inlet pressure [8]. The flow index of the drip irrigation emitter is a parameter that must be considered in the design and optimization of the flow channel structure [9]. The labyrinth channel emitter is

currently the most widely used drip irrigation emitter for the superior hydraulic performance of the labyrinth channel structure [10]. The structure of the labyrinth channel has been deeply researched by many scholars using the Computational Fluid Dynamics (CFD) simulation and Digital Particle Image Velocimetry (DPIV) experiment methods [11–13]. Liu et al. [14] used DPIV to measure the flow field in the flow channel section, the structural unit, and the local area near the sawtooth and found that there were flow stagnation areas and vortex areas in the structure of the labyrinth path section. Feng et al. [15] found that the near-wall velocity was lower than in the center of the flow path in a laminar labyrinth emitter and that the velocity along the depth of the flow path was relatively uneven when using CFD simulation and DPIV experiment methods. Al-Muhammad et al. [16] presented the mean velocity distribution and turbulence quantities within the cylindrical labyrinth channel drip irrigation emitter flow using the microparticle image velocimetry (micro-PIV) technique and found that the flow regime was turbulent and non-isotropic. Liu et al. [17] proposed a full-scale transparent model combining DPIV and planar laser-induced fluorescence (PLIF) technology to observe the motion characteristics of particles with different diameters in the flow channel of an embedded flat plate emitter. Yu et al. [18] explored the influence of the dentation angle of a sawtooth labyrinth channel drip emitter on the hydraulic performance by CFD simulation. Wang et al. [19] studied the reasons for structural changes in the hydraulic performance of the rectangular labyrinth emitter through the analysis of the vortex intensity using the CFD simulation method. The results showed that the relative error of the simulated results and experimental data was 1.02–2.11%. The internal flow characteristics of the labyrinth channel of a drip emitter have also been studied by some scholars through mathematical models. Falcucci et al. [20] proposed a numerical technique based on the Lattice Boltzmann Method (LBM) to model the water flow characteristics of a rectangular labyrinth channel drip emitter. The results for the simulation values were in good agreement with the experimental data. Wu et al. [21] applied the standard $k - \epsilon$ model and the Large Eddy Simulation (LES) model to analyze the internal flow characteristics in a cylindrical labyrinth channel drip irrigation emitter and found that the LES model was more effective in describing the flow characteristics of the fluid in the passage and optimizing the path structure. Based on the comprehensive consideration of the calculation accuracy and computational efficiency, Feng et al. [22] indicated that the RNG $k - \epsilon$ model was the most suitable for a flow field simulation of the flat labyrinth drip irrigation emitter.

In order to improve the hydraulic performance of the labyrinth channel emitter, some scholars have proposed several models for optimizing the flow channel structure. Feng et al. [22] proposed five different boundary optimization methods for improving the hydraulic performance of a sawtooth labyrinth channel drip emitter. Zhang et al. [23] proposed the pressure loss coefficient as an index of the hydraulic performance and developed a mathematical model that rapidly predicted the hydraulic performance for emitters with different geometries. Saccone et al. [24] analyzed the internal flow field of seven different sawtooth labyrinth channel drip emitters using the CFD method and calculated the relationship between the outlet flow rate and inlet working pressure to improve its hydraulic performance. In recent years, some researchers have put forward several new types of labyrinth channels. Zhangzhong et al. [25] constructed 13 M-type fractal flow paths with different geometrical parameters based on fractal theory and analyzed the influence of different geometrical parameters on the variation of the internal flow field and hydraulic performance characteristics using the CFD and PIV methods. Guo et al. [26] designed three kinds of two-way mixed flow drip irrigation emitter prototypes and established the evaluation method of the macroscopic flow rate index and microscopic flow velocity index. Xu et al. [27] proposed a pit drip irrigation emitter based on the pit structure in the water transport tracheids of bionic plants and designed the four optimized labyrinth flow channels. Xing et al. [28] also proposed a perforated drip irrigation emitter based on the structure of scalariform perforation plates in plant xylem vessels and established a numerical simulation method suitable for it. These provide new ideas for the structural design

and performance optimization of drip irrigation emitters. However, most studies focused on the relationship between the structure parameters of the sawtooth or a similar sawtooth labyrinth channel and the hydraulic performance. Although several new types of labyrinth channel structure models are designed and constructed, the reason for the mechanism and conversion of the water flow energy loss in the flow field are not consistently reported in the references.

In the design of the flow channel structure of the irrigation emitter, the increase in energy consumption and the generation of multiple local head losses can be achieved by increasing the diversity of the flow channel section structure types of the emitter. In this study, inspired by the effect of a roundabout that made vehicles slow down and turn, a new type of circular water-retaining labyrinth channel (CWRLC) structure was designed. The flow index variation and internal flow characteristics were analyzed using the CFD software package in CWRLC emitters with different radii of a circular water-retaining structure. The mechanism of energy loss and main factor affecting the energy dissipation of the CWRLC structure were revealed. The quadrate water-retaining labyrinth channel (QWRLC) structure and stellate water-retaining labyrinth channel (SWRLC) structure were obtained by structural improvement based on the energy dissipation mechanism. Finally, comparative analyses of numerical simulation and hydraulic performance tests were conducted. The relevant results of this study can be used as a reference for the structural design and application of drip irrigation emitters.

2. Materials and Methods

2.1. Structure Design and Physical Model

In this study, a novel flat drip irrigation emitter was made up of water inlets, water outlet, filter grids, and an energy dissipating flow channel structure. Inspired by the effect of a roundabout that makes vehicles slow down and turn, a new type of circular water-retaining labyrinth channel (CWRLC) structure was designed. The CWRLC unit was composed of a circular water-retaining structure and two symmetrical isosceles trapezoid structures without a baseline. The characteristics and parameters of the CWRLC unit were shown in Figure 1, where r represents the radius of the circular water-retaining structure, s represents the length of the trapezoid baseline, h represents the trapezoid height, and θ represents the angle between the hypotenuses of the adjacent trapezoids.

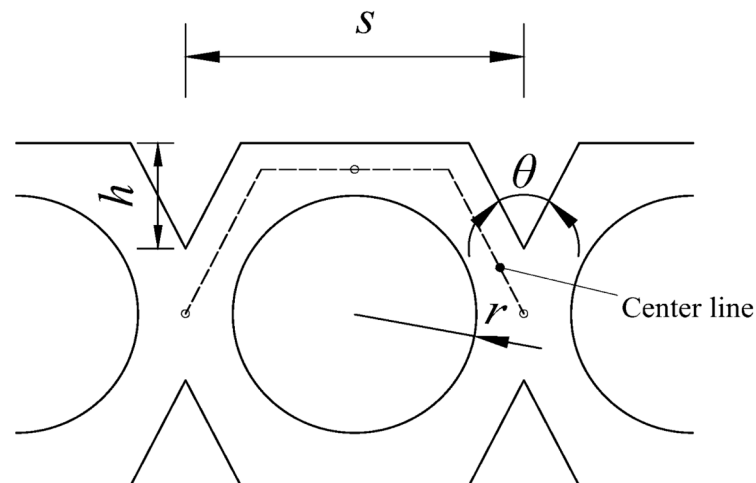


Figure 1. Schematic diagram of the CWRLC unit structure.

In order to reduce the research factors, the single-factor experimental way was adopted in this study. According to the literature [3,22], the values of the critical structural parameters of the CWRLC flow channel were as follows: s was 2.50 mm, h was 0.80 mm, θ as 54° , and r was 0.90–1.15 mm, with values of 0.05 mm at intervals. Similar values (2.50 mm, 0.80 mm, and 54°) are the parameters of most tooth labyrinth channel (TLC) emitters in the market. The 3D model of the CWRLC emitter was designed and constructed using

SolidWorks2018 software (Dassault Systemes, Waltham, MA, USA), as shown in Figure 2. The depth of the CWRLC flow channel was 1.50 mm, the number of the CWRLC units was 15, the height of the water inlets and filter grids was 1.20 mm, the width of the water outlet was 8.90 mm, and the thickness of the outer edge of the CWRLC emitter was 1.05 mm. The main structural parameters and settings for the CWRLC emitter flow channel are listed in Table 1.

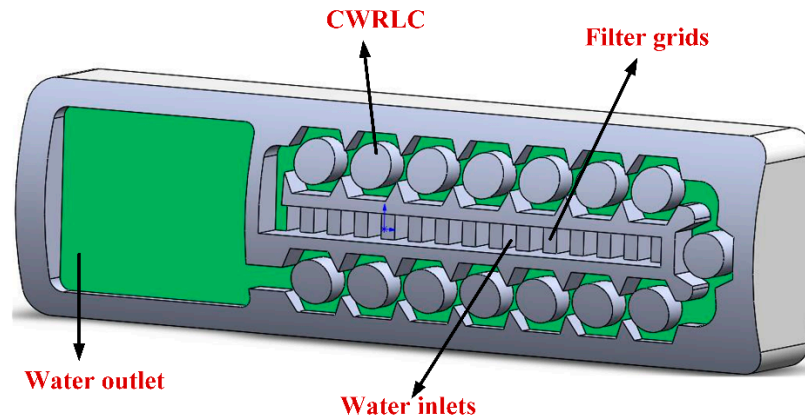


Figure 2. Three-dimensional physical model of the CWRLC emitter.

Table 1. Structural parameters and settings for the CWRLC emitter flow channel.

Trapezoid Baseline Lengths (mm)	Trapezoid Height <i>h</i> (mm)	Radius of Circular Water-Retaining <i>r</i> (mm)	Angle between Hypotenuses of Adjacent Trapezoids θ (°)	Channel Depth <i>d</i> (mm)	The Number of Channel Units <i>n</i>
2.50	0.80	0.90; 0.95; 1.00 1.05; 1.10; 1.15	54	1.50	15

2.2. Mathematical Model of the CWRLC Emitter

The water flow in the CWRLC emitter was considered a viscous, incompressible fluid. The heat exchange of the CWRLC emitter could be ignored. Therefore, only two basic governing equations: the continuity equation and the Navier–Stokes equations need to be considered.

Continuity equation:

$$\frac{\partial(u)}{\partial x} + \frac{\partial(v)}{\partial y} + \frac{\partial(w)}{\partial z} = 0 \tag{1}$$

Navier–Stokes equations:

$$\rho\left(\frac{\partial u}{\partial t} + u\frac{\partial u}{\partial x} + v\frac{\partial u}{\partial y} + w\frac{\partial u}{\partial z}\right) = \rho f_x - \frac{\partial p}{\partial x} + \mu\left(\frac{\partial^2 u}{\partial x^2} + \frac{\partial^2 u}{\partial y^2} + \frac{\partial^2 u}{\partial z^2}\right) \tag{2}$$

$$\rho\left(\frac{\partial v}{\partial t} + u\frac{\partial v}{\partial x} + v\frac{\partial v}{\partial y} + w\frac{\partial v}{\partial z}\right) = \rho f_y - \frac{\partial p}{\partial y} + \mu\left(\frac{\partial^2 v}{\partial x^2} + \frac{\partial^2 v}{\partial y^2} + \frac{\partial^2 v}{\partial z^2}\right) \tag{3}$$

$$\rho\left(\frac{\partial w}{\partial t} + u\frac{\partial w}{\partial x} + v\frac{\partial w}{\partial y} + w\frac{\partial w}{\partial z}\right) = \rho f_z - \frac{\partial p}{\partial z} + \mu\left(\frac{\partial^2 w}{\partial x^2} + \frac{\partial^2 w}{\partial y^2} + \frac{\partial^2 w}{\partial z^2}\right) \tag{4}$$

where *u*, *v*, and *w* are the components of the flow velocity in the *x*, *y*, and *z* directions, respectively; ρ represents the density of the water; f_x , f_y , and f_z are the components of the body force per unit in the *x*, *y*, and *z* directions, respectively; μ represents the dynamic viscosity coefficient; and *p* represents the pressure.

The $k - \varepsilon$ two-equation model is the most popular turbulence model. The Realizable $k - \varepsilon$ model was applied to the numerical calculations because of the curved wall structure of the CWRLC emitter and the strong eddy current in the internal flow field.

The Realizable $k - \varepsilon$ transport equations:

$$\frac{\partial(\rho k)}{\partial t} + \frac{\partial(\rho k \bar{u}_i)}{\partial x_i} = \frac{\partial}{\partial x_j} \left[\left(\mu + \frac{\mu_t}{\sigma_k} \right) \frac{\partial k}{\partial x_j} \right] + G_k - \rho \varepsilon \quad (5)$$

$$\frac{\partial(\rho \varepsilon)}{\partial t} + \frac{\partial(\rho \varepsilon \bar{u}_i)}{\partial x_i} = \frac{\partial}{\partial x_j} \left[\left(\mu + \frac{\mu_t}{\sigma_\varepsilon} \right) \frac{\partial \varepsilon}{\partial x_j} \right] + \rho C_1 S \varepsilon - \rho C_2 \frac{\varepsilon^2}{k + \sqrt{\mu \varepsilon}} \quad (6)$$

where k denotes the turbulent kinetic energy, ε denotes the turbulent dissipation rate, \bar{u}_i represents the time-averaged velocity, and μ_t represents the turbulent viscosity coefficient.

In transport Equation (5) of k , G_k is the turbulent generation term caused by the average velocity gradient. G_k can be represented as follows:

$$G_k = \mu_t \left(\frac{\partial \bar{u}_i}{\partial x_j} + \frac{\partial \bar{u}_j}{\partial x_i} \right) \frac{\partial \bar{u}_i}{\partial x_j} \quad (7)$$

In transport Equation (6) of ε :

$$S = \sqrt{2 S_{ij} S_{ij}} \quad (8)$$

$$S_{ij} = \frac{1}{2} \left(\frac{\partial \bar{u}_i}{\partial x_j} + \frac{\partial \bar{u}_j}{\partial x_i} \right) \quad (9)$$

μ_t can be expressed as a function of k and ε :

$$\mu_t = C_\mu \frac{k^2}{\varepsilon} \quad (10)$$

$$C_\mu = \frac{1}{A_0 + A_S U^* k / \varepsilon} \quad (11)$$

where we defined:

$$A_0 = 4.0, A_S = \sqrt{6} \cos \phi, \phi = \frac{1}{3} \cos^{-1}(\sqrt{6}W), W = \frac{S_{ij} S_{jk} S_{ki}}{\tilde{S}^3}, \tilde{S} = \sqrt{S_{ij} S_{ij}} \quad (12)$$

$$U^* = \sqrt{S_{ij} S_{ij} + \tilde{\Omega}_{ij} \tilde{\Omega}_{ij}}, \tilde{\Omega}_{ij} = \Omega_{ij} - 2\varepsilon_{ijk} \omega_k, \Omega_{ij} = \bar{\Omega}_{ij} - 2\varepsilon_{ijk} \omega_k \quad (13)$$

where $\bar{\Omega}_{ij}$ is the time-averaged rotation rate, and ω_k is the angular velocity.

The other parameters in the transport equations can be expressed as follows:

$$\sigma_k = 1.0, \sigma_\varepsilon = 1.2, C_2 = 1.9, C_1 = \max\left(0.43, \frac{\eta}{\eta + 5}\right), \eta = S \frac{k}{\varepsilon} \quad (14)$$

The relationship between the flow rate and pressure of the CWRLC emitter can be described as follows:

$$Q = K_d h^x \quad (15)$$

where Q represents the outlet average flow rate, K_d represents the flow coefficient, h represents the inlet pressure, and x represents the flow index. The smaller the flow index, the better the irrigation uniformity.

2.3. Meshing and Simulation Parameters Setting

The 3D fluid region model of the CWRLC emitter was created using SpaceClaim2020R2 software (ANSYS, Canonsburg, PA, USA). The three parts of the fluid region model of the

CWRLC emitter were set up for the inlet, outlet, and wall. The meshes were generated by Fluent Meshing 2020R2 software (ANSYS, Canonsburg, PA, USA). The minimum size, maximum size, and growth rate of the surface mesh were set to 0.01, 0.1, and 1.2, respectively. The curvature normal angle was set to 10° , and the proximity was selected. The volume grids were filled by Poly-Hexcore. Buffer layers, and the Peel Layers were set to 2 and 1, respectively. Finally, the total number of CWRLC emitter fluid domain calculation grids was about 946,000.

For the flow field calculations of the CWRLC emitter flow channel, the Realizable $k - \epsilon$ model and standard wall function were selected. The boundary conditions of the inlet were set to the pressure inlet, which was set as 20 KPa, 40 KPa, 60 KPa, 80 KPa, 100 KPa, 120 KPa, 140 KPa, 160 KPa, and 200 KPa, respectively. The boundary condition of the outlet was set to the pressure outlet that was set as 0. No slip boundary condition and stationary wall motion were adopted for the wall of the CWRLC emitter flow channel. The SIMPLE algorithm was used to couple the pressure and velocity. The governing equations were discretized by the finite volume method. The momentum term, turbulent kinetic energy, and turbulent dissipation rate were solved using the second-order upwind method. The relaxation factors were set by default, and the convergent accuracy was 10^{-5} .

2.4. Experimental Test

To validate the precision of the numerical simulations with respect to the hydraulic properties of the novel water-retaining labyrinth channel emitters, the technologies of electrical discharge machining (EDM) and injection molding (IM) were used in the manufacture of emitters. The manufacturing processes of the emitters were divided into two parts: mold manufacturing and injection molding production. EDM technology was used in the manufacture of emitter molds. The processes of EDM are shown in Figure 3. The discharge channels were generated by the breakdown of the working solution between the tool electrode and the work piece electrode using pulse voltage in the course of processing. The tiny corrosion pits on the work piece surface were formed by the instantaneous high temperature that was generated by the discharge channels. The molds of the emitters were processed by the servo system that automatically fed and adjusted the relative position of the tool electrode and the work piece electrode to ensure a normal pulse discharge. After the molds of the emitters were processed, injection molding technology was used to produce the emitter products.

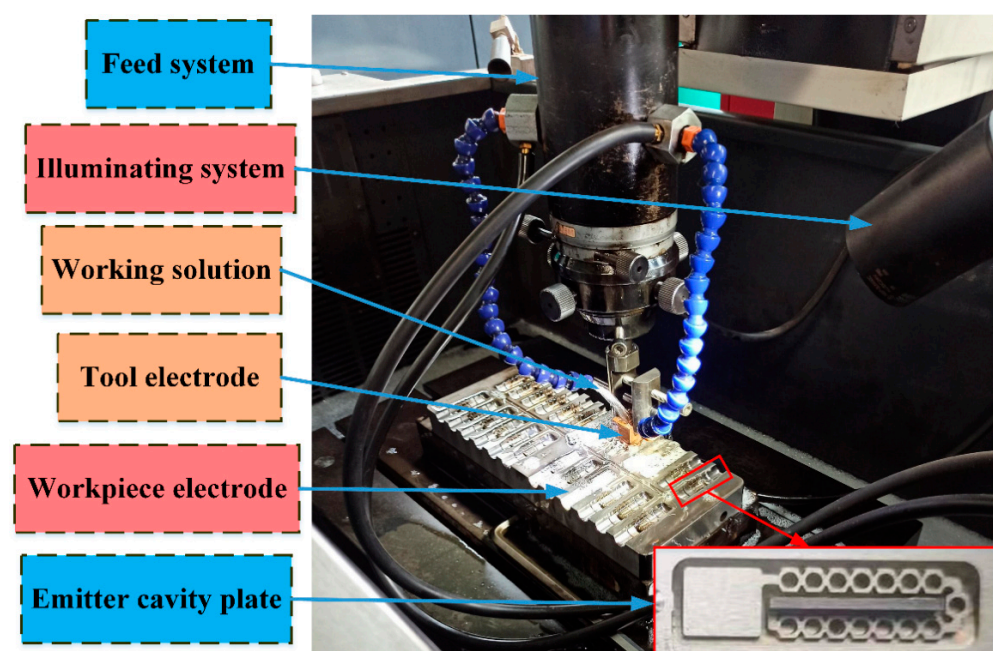


Figure 3. Processing of molds of the novel emitters using EDM.

The drip irrigation emitters flow experimental platform was used as the hydraulic properties of the novel water-retaining labyrinth channel emitters, as shown in Figure 4. This experimental platform consists of a pressure-regulating valve, a pressure gauge, a test area for the irrigation emitters, several measuring cups, an electronic weighing scale, and the data acquisition unit. Twenty-five novel water-retaining labyrinth channel emitters were randomly selected to be connected to the emitters test area for experimenting. In the experiment, tap water was utilized for the experimental water, and its temperature was about 18 °C. During the experiment, the outlet flow of the emitters was measured every three minutes under different pressures (20–200 KPa). The inlet pressures of the emitters were monitored by a pressure gauge. The experimental results took the average of the two measured flow results as the final value.



Figure 4. Drip irrigation emitters flow test platform.

3. Results

3.1. Influence of Hydraulic Performance

Flow rates of the simulation values of the CWRLC emitter with different parameters r under 20–200 KPa pressure are shown in Table 2. Under the same parameters r , the average outlet flow rate of the CWRLC emitter increased, but the growth rate decreased with the rise of the working pressure. For example, when the inlet pressure increased from 20 KPa to 40 KPa, the average outlet flow rate of CWRLC $_{r = 0.90 \text{ mm}}$ increased from 2.654 L/h to 3.850 L/h and the increment of 1.196 L/h with a growth rate of 45.08%; whereas, when the inlet pressure increased from 180 KPa to 200 KPa, the average outlet flow rate of CWRLC $_{r = 0.90 \text{ mm}}$ increased from 8.586 L/h to 9.082 L/h and only the increment of 0.496 L/h with a growth rate of 5.78%, the reason that the viscous resistance and impact force of water along the CWRLC emitter wall increased with the rise of the working pressure and the flow velocity, resulting in a large loss of flow energy and decrease in growth rate. For the same inlet pressure, the average outlet flow rate of the CWRLC emitter decreased with the increase in the parameters r . For each 0.05-mm increase in the parameters r , the average outlet flow rate decreased by about 0.35 L/h. This caused the flow in the cross-sectional area to be reduced with the increase in the parameters r , leading to a decrease in the average outlet flow rate.

The hydraulic performance is one of the important indexes to evaluate the merits and demerits of a drip irrigation emitter. It is generally quantified and evaluated by the flow index, which reflects the sensitivity of the drip irrigation emitter to the working pressure. The smaller the flow index, the better the hydraulic performance of the CWRLC emitter. In general, the flow index of the drip emitter with the optimal flow channel is about 0.5.

The flow index x of the CWRLC emitter with different parameters r was obtained by Equation (15) using Origin2018 software, as shown in Figure 5. The fitting correlation coefficients (R^2) of $CWRLC_{r=0.90\text{ mm}}$, $CWRLC_{r=0.95\text{ mm}}$, $CWRLC_{r=1.00\text{ mm}}$, $CWRLC_{r=1.05\text{ mm}}$, $CWRLC_{r=1.10\text{ mm}}$, and $CWRLC_{r=1.15\text{ mm}}$ were 0.99999, 0.99999, 0.99999, 0.99998, 0.99992, and 0.99982, respectively, which all reached a significant level ($R^2 > 0.8$). The flow index x of the CWRLC emitter increased with the rise of the parameters r , demonstrating that the average outlet flow rate became more sensitive to the change of the working pressure. When $r = 0.90\text{ mm}$, the flow index of the CWRLC emitter was 0.5334; when $r = 1.15\text{ mm}$, the flow index of the CWRLC emitter was 0.5719. The reason that the boundary wall constraint on the water flow decreased with the rise of the parameters r , leading to an increase in sensitivity of the average outlet flow rate to the working pressure. Therefore, it is necessary to further analyze the internal flow field in the flow channel.

Table 2. Simulation flow rate of the CWRLC emitter with different parameters r under 20–200 KPa.

r (mm)	Flow Rate (L/h)									
	20 KPa	40 KPa	60 KPa	80 KPa	100 KPa	120 KPa	140 KPa	160 KPa	180 KPa	200 KPa
0.90	2.654	3.850	4.781	5.573	6.277	6.917	7.509	8.063	8.586	9.082
0.95	2.335	3.393	4.216	4.915	5.536	6.101	6.623	7.113	7.575	8.014
1.00	2.006	2.925	3.638	4.244	4.782	5.270	5.722	6.144	6.542	6.921
1.05	1.670	2.451	3.056	3.570	4.026	4.440	4.821	5.178	5.515	5.834
1.10	1.319	1.962	2.461	2.885	3.260	3.600	3.914	4.208	4.484	4.746
1.15	0.946	1.440	1.828	2.158	2.451	2.718	2.963	3.193	3.409	3.614

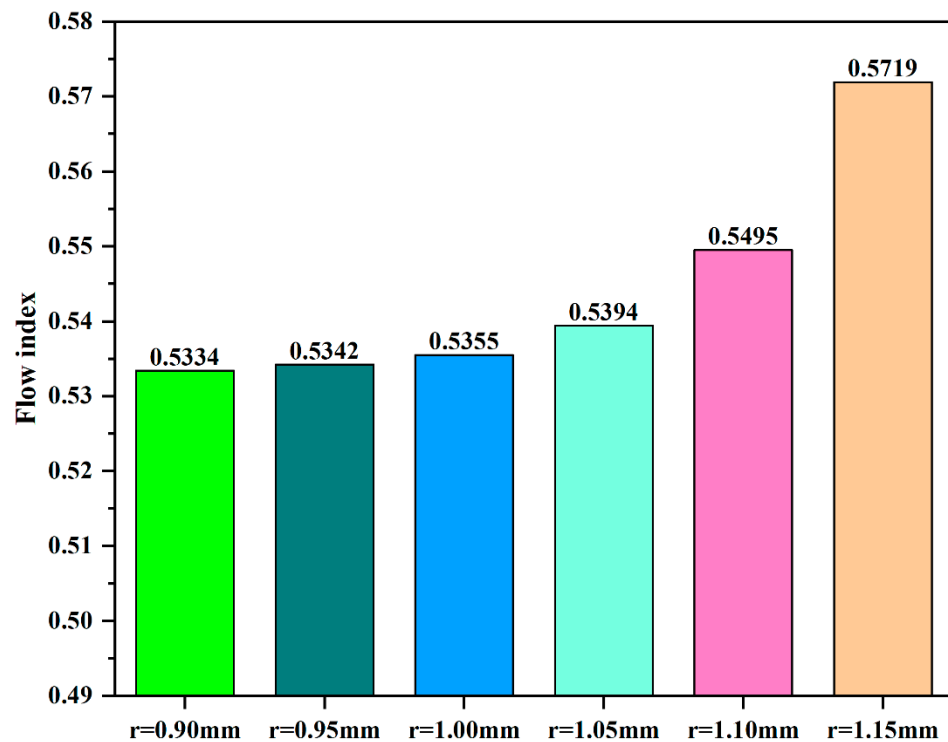


Figure 5. The flow indexes of the CWRLC emitter with different parameters r .

3.2. Analysis of Flow Channel Internal Flow Characteristics

The velocity vector distributions of the fourth flow channel unit at the mid-depth cross-section of flow channels with six different parameters r under 100 KPa are shown in Figure 6. Due to the symmetrical structure of the flow channel unit, only one side of the flow field distribution characteristics was analyzed. The velocity vector distributions of the six flow channels were similar. According to the relative position of the vector distribution features, the upper half of the flow field in the channel was divided into two

areas: upstream area of the circular water-retaining structure (A) and downstream area of the circular water-retaining structure (B). Depending on the velocity magnitude, area A or B was further separated into a high-speed mainstream area (C_A or C_B) and low-speed vortex area (D_A or D_B). The flow velocity in area C_A was obviously higher than that in area C_B . The maximum flow velocities of $CWRLC_r = 0.90$ mm, $CWRLC_r = 0.95$ mm, $CWRLC_r = 1.00$ mm, $CWRLC_r = 1.05$ mm, $CWRLC_r = 1.10$ mm, and $CWRLC_r = 1.15$ mm were 4.47 m/s, 4.32 m/s, 4.14 m/s, 4.02 m/s, 3.67 m/s, and 3.22 m/s, respectively. The maximum flow velocity decreased with the increase in the parameters r .

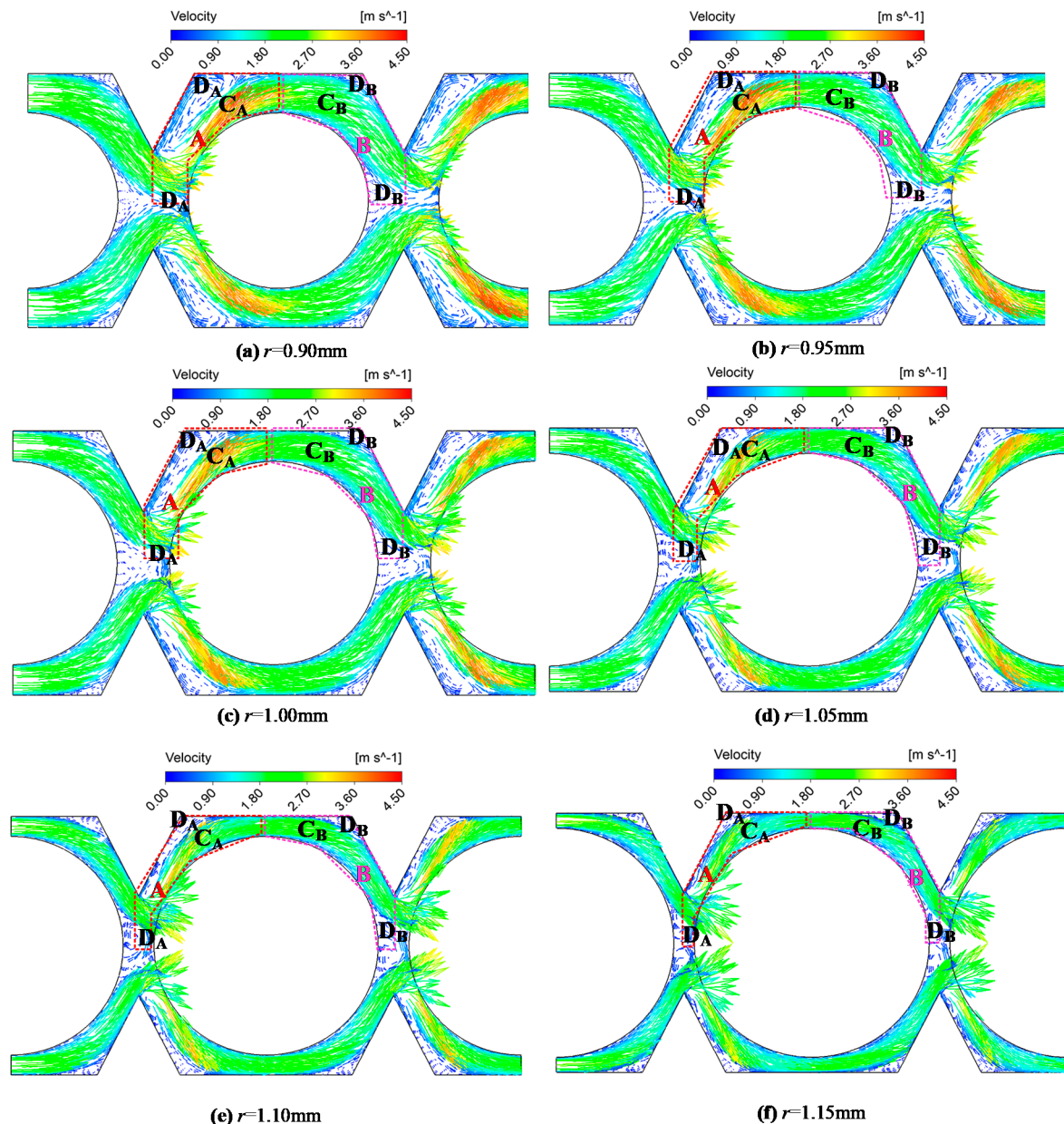


Figure 6. The mid-depth cross sectional velocity vector distributions of the fourth flow channel unit for six flow channels under 100 KPa.

In addition, the proportion of the low-speed vortex area (D_A or D_B) also decreased with the rise of the parameters r from the velocity vector distribution. The water flow in this area formed a large vortex and eddy between the boundary wall of the flow channel and mainstream area. The energy of the water flow in the flow channel was fully expended by the vortex flow. The proportion of the vortex area (D_A or D_B) determined the constraint ability of the boundary wall to the water flow. The larger the proportion of the vortex

area (D_A or D_B), the greater the constraint ability of the boundary wall to the water flow. Obviously, the proportion of the vortex area (D_A or D_B) of $CWRLC_{r=0.90\text{ mm}}$ in the flow channel was largest, and the $CWRLC_{r=1.15\text{ mm}}$ was the smallest.

The velocity line diagram of the center line of the mid-depth cross-section further confirmed this phenomenon, as shown in Figure 7. The center line passed through the D_A , C_A , D_A , C_A , C_B , D_B , C_B , and D_B areas successively. We defined the crests as C_{A1} , C_{AB} , and C_{B1} , respectively. The troughs were defined as D_{A1} , D_{A2} , D_{B1} , and D_{B2} , respectively. In the $CWRLC_{r=0.90\text{ mm}}$ internal flow field, the speed of C_{A1} (2.76 m/s) was greater than that of C_{AB} (2.25 m/s) due to the sufficient generation of low-speed vortex areas. However, the velocity of C_{A1} (2.12 m/s) was less than that of C_{AB} (2.65 m/s) in the $CWRLC_{r=1.15\text{ mm}}$ internal flow field. This means that the flow channel of $CWRLC_{r=0.90\text{ mm}}$ consumed more water flow energy than $CWRLC_{r=1.15\text{ mm}}$. It was also sufficient to indicate that the proportion of the low-speed vortex areas played a critical role in the energy consumption capacity of the flow channel. The larger the proportion of low-speed vortex areas, the more obvious the energy dissipation. This was a fundamental reason why the flow index increased with the rise of the parameters r . Therefore, the increase in the proportion of the low-speed vortex area (D) could reduce the flow index, thereby improving the hydraulic performance and energy dissipation of the drip irrigation emitter.

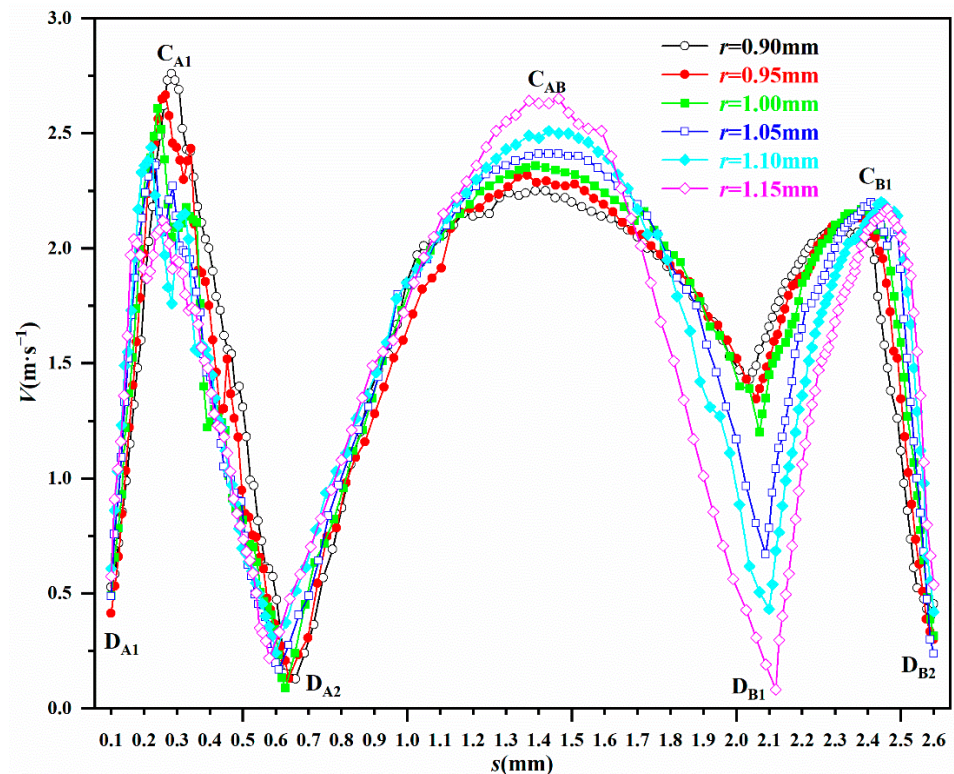


Figure 7. The velocity line diagram of the center line of the mid-depth cross-section for six flow channels.

3.3. Structure Optimization of the Flow Channel

On the basis of the analysis of the CFD numerical simulation and flow rate curve fitting in the CWRLC emitter flow channels of six different parameters r , the different parameters r had obvious influences on the velocity vector distribution, velocity magnitude, flow index, and hydraulic performance of the flow channel. The analysis results showed that a proportion of the low-speed vortex zones played a key role in the energy dissipation of the flow channel. If the flow channel structure of the drip emitter was optimized, the proportion of the low-speed vortex zones increased, and the energy expended in the internal flow field also increased, which could reduce the flow index and improve its hydraulic performance and energy dissipation. The simulation and analysis results also indicated that the CWRLC

emitter flow channel structure, when parameter $r = 0.9$ mm, yielded the minimum flow index value and best hydraulic performance compared with the others. Therefore, the following work of the optimization simulation analysis and experimental verification were carried out based on the CWRLC $_{r = 0.90}$ mm flow channel structure.

In order to increase the proportion of the low-speed vortex areas, consume more of the energy internal flow field, and reduce the sensitivity of the flow rate to the working pressure, the circular water-retaining structure was optimized. We tried hundreds of attempts and finally found two optimal ways to achieve that goal using solidworks2018 (Dassault Systemes, Waltham, MA, USA) and Fluent2020R2 software (ANSYS, Canonsburg, PA, USA). The two specific optimization methods were as follows: the first method was the diameters AB and CD were used as diagonals to make a cyclic quadrilateral ABCD, and the optimized flow channel structure was called the quadrate water-retaining labyrinth channel (QWRLC), as shown in Figure 8a; the second method was that the straight lines A'C', C'B', B'D', and D'A' were used as the symmetry axis to mirror the dotted arcs A'C', C'B', B'D', and D'A', respectively, which obtained solid arc structure A'B'C'D', and the optimized flow channel structure was named the stellate water-retaining labyrinth channel (SWRLC), as shown in Figure 8b.

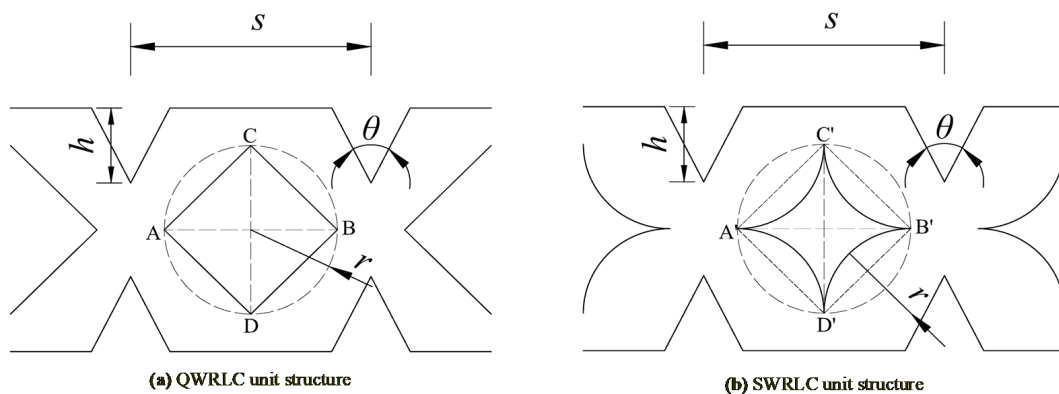


Figure 8. Schematic diagrams of two structural improvements.

All the parameters of the two improved structures were the same as those of the CWRLC structure. The 3D models and fluid domains of the two improved emitters were established by SolidWorks2018 (Dassault Systemes, Waltham, MA, USA) and SpaceClaim2020R2 software (ANSYS, Canonsburg, PA, USA), respectively. The internal flow characteristics of the two improved flow fields were analyzed using Fluent2020R2 software (ANSYS, Canonsburg, PA, USA). The velocity vector distributions of the fourth flow channel unit at the mid-depth cross-section of the two improved flow channels under 100 KPa are shown in Figure 9.

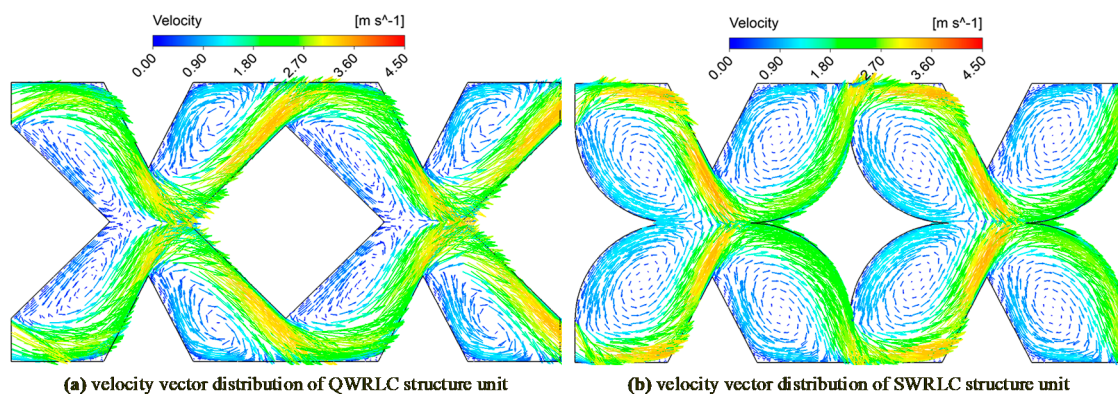


Figure 9. Simulation results of the velocity vector distributions in two improved flow channel structures under 100 KPa.

From the simulation results of the velocity vector distributions, the proportion of the low-speed vortex zones for two improved flow channel structures visibly increased compared with the CWRLC structure. The maximum flow velocity of QWRLC (3.94 m/s) and SWRLC (3.92 m/s) fell by 11.8% and 12.3% compared with CWRLC (4.47 m/s). Moreover, the proportion of the low-speed vortex zones of the SWRLC structure were larger than that of the QWRLC structure in the two improved structures. This means that the constraint abilities of the boundary wall of the two optimized structures to the water flow were stronger than that of the CWRLC structure, and the SWRLC structure was the strongest compared with the other structures. Therefore, the energy dissipation of the emitter was significantly improved through the above optimization methods.

In order to further verify the performance of the improved structures, the most widely used TLC drip irrigation emitter in the market was designed and analyzed. The parameters of the TLC emitter were the same as the QWRLC and SWRLC emitters, except for the parameters r . The schematic diagram of the TLC structure unit is shown in Figure 10a; the velocity vector distribution of the fourth flow channel unit at the mid-depth cross-section of the TLC structure under 100 KPa is shown in Figure 10b. The maximum velocity of TLC was 4.20 m/s, which was between the two improved flow channels and the CWRLC.

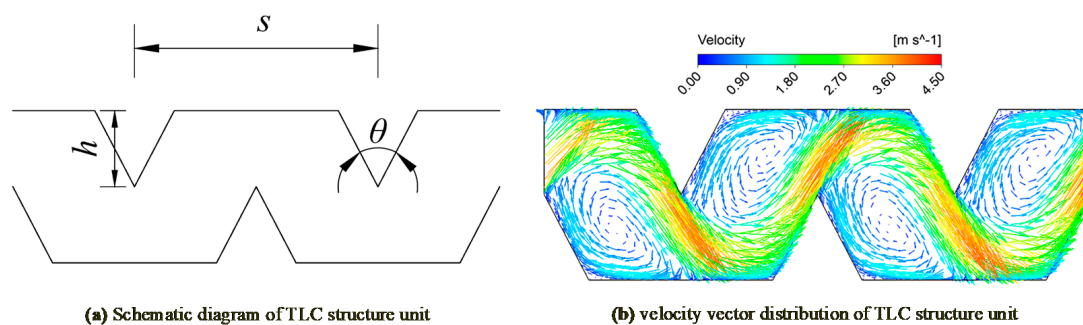


Figure 10. Schematic diagram and velocity vector distribution of the flow channel structures under 100 KPa.

The relationship curves between outlet flow rate and inlet pressure of four emitters were obtained by Equation (15) fitting, as shown in Figure 11. All four curves were fitted successfully, and the correlation coefficients (R^2) were 0.9999, 0.9999, 0.9999, and 0.9994, respectively. The flow indexes of the four emitters were 0.5334, 0.5041, 0.4796, and 0.4917, respectively. Among them, the SWRLC emitter had the lowest flow pattern index. The values of the flow index of the QWRLC and SWRLC emitters were decreased by 5.49% and 10.09%, respectively, compared with that of the CWRLC emitter by analyzing the internal flow field and optimizing the structure. In particular, the value of the flow index of the improved emitter SWRLC was 2.46% lower than that of the widely used emitter, TLC. Therefore, the novel SWRLC emitter had a better hydraulic performance and irrigation uniformity.

3.4. Experimental Verification of Hydraulic Performance for Drip Emitters

To further examine the reliability of the simulation results with respect to the hydraulic performance of the above emitters, four emitters (CWRLC, QWRLC, SWRLC, and TLC) were manufactured by EDM technology and the IM method. The physical models of the four emitters are shown in Figure 12. The drip irrigation belts with an inner diameter of 16 mm and a wall thickness of 0.3 mm corresponding to the four emitters were produced, and the distance between emitters on each drip irrigation belt was 40 cm. The hydraulic performance tests were carried out on the experimental bench.

The test results of the four emitters are listed in Table 3, from which the test flow rate of the four emitters increased with the increase of the inlet pressure. The statistical differences between the average flow rate of the four emitters at 20–200 KPa were verified using Tukey's test method. The average outlet flow rate of the four emitters had significant differences at 20–180 KPa. Except for no significant difference in the average flow rate

of the QWRLC and SWRLC emitters at 200 KPa, the other differences were significant, as shown in Table 4. The average errors between the actual flow and simulated flow of the CWRLC, QWRLC, SWRLC, and TLC emitters were 1.46%, 7.52%, 2.84%, and 5.62%, respectively. The comparison diagram of the flow index of the four emitters between the test and simulation is shown in Figure 13. The actual flow indexes of the CWRLC, QWRLC, SWRLC, and TLC emitters were 0.5559, 0.5008, 0.4719, and 0.4851, respectively. The flow index errors of the CWRLC, QWRLC, SWRLC, and TLC emitters were 4.05%, 0.66%, 1.69%, and 1.36%, respectively, as shown in Figure 14. In the test results, the SWRLC emitter had the lowest value of the flow index compared with the other three emitters. The flow index of the SWRLC emitter was 2.72% lower than that of the widely used TLC emitter under the same conditions. This showed that the flow channel structure of the novel SWRLC emitter with the optimized design had a strong constraint ability, which means the SWRLC emitter had a superior hydraulic performance. Therefore, the novel SWRLC emitter has broad application prospects in the field of water-saving irrigation.

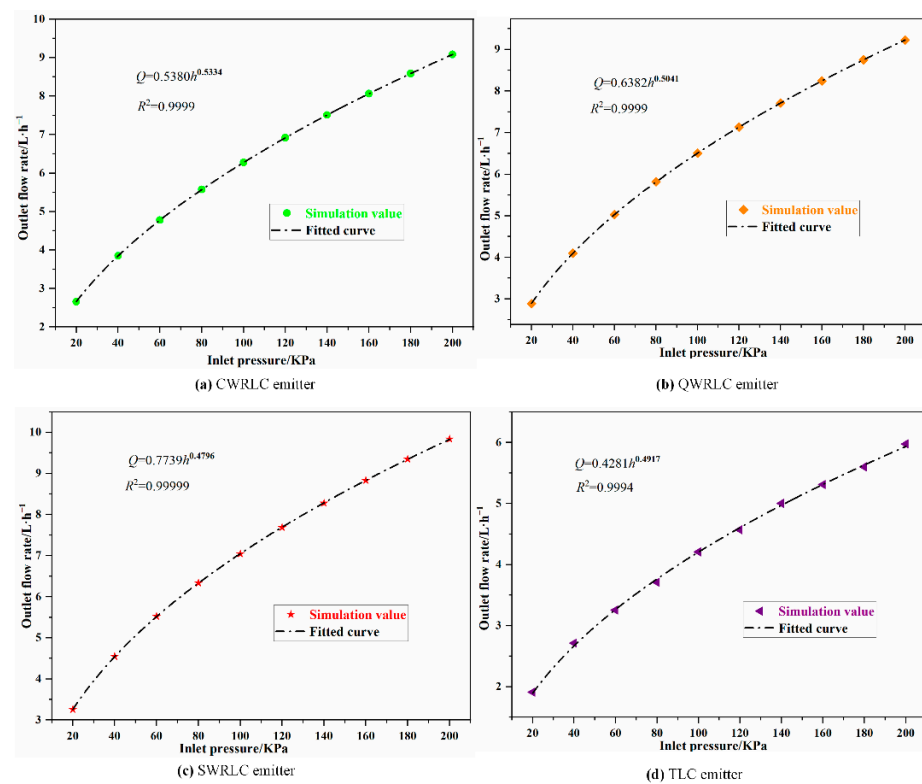


Figure 11. The outlet flow rate and inlet pressure fitted curves of the four emitters.

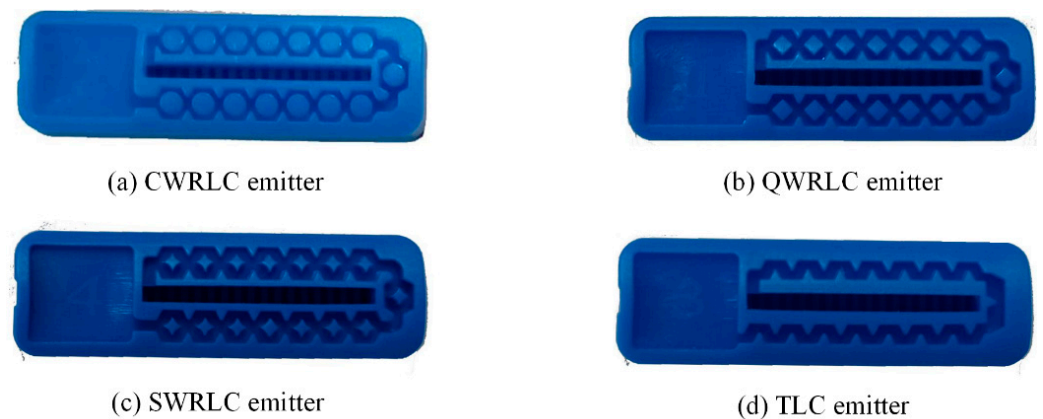


Figure 12. Four real emitters.

Table 3. Test flow rate statistics of the four emitters.

Emitters	Flow Rate (L/h)									
	20 KPa	40 KPa	60 KPa	80 KPa	100 KPa	120 KPa	140 KPa	160 KPa	180 KPa	200 KPa
CWRLC	2.588	3.716	4.721	5.491	6.237	6.922	7.571	8.180	8.706	9.207
QWRLC	3.150	4.428	5.467	6.245	7.037	7.688	8.328	8.906	9.463	9.950
SWRLC	3.449	4.641	5.651	6.483	7.237	7.880	8.499	9.106	9.626	10.09
TLC	2.054	2.826	3.498	3.992	4.443	4.860	5.255	5.615	5.942	6.230

Table 4. Statistical analysis of the differences of the emitter flow rate using Tukey’s method at 200 KPa.

Emitters (I)	Emitters (J)	Means (I)	Means (J)	Differences (I-J)	p-Value
CWRLC	QWRLC	9.207	9.950	−0.742	0.001
CWRLC	SWRLC	9.207	10.09	−0.882	0.001
CWRLC	TLC	9.207	6.230	2.978	0.001
QWRLC	SWRLC	9.950	10.09	−0.140	0.058
QWRLC	TLC	9.950	6.230	3.720	0.001
SWRLC	TLC	10.09	6.23	3.860	0.001

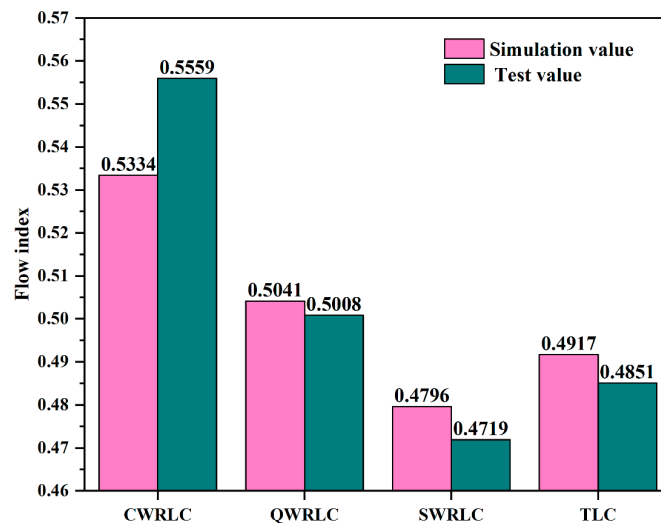


Figure 13. The histogram of the flow index of the four emitters.

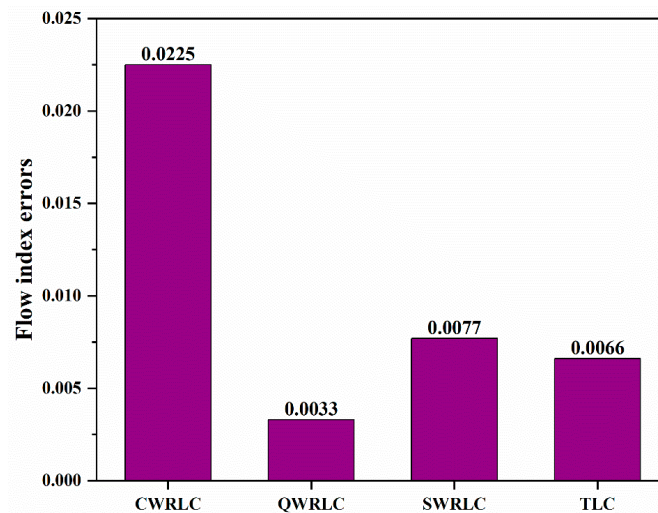


Figure 14. The histogram of the flow index errors of the four emitters.

4. Conclusions

In this study, a novel type of circular water-retaining labyrinth channel (CWRLC) structure was proposed, inspired by the effect of a roundabout that makes vehicles slow down and turn for eliminating excess energy in a flow channel. The hydraulic performance of the CWRLC emitters under different circular water-retaining radii were studied by the single-factor test. The results showed that, with the increase in the circular water-retaining radii of CWRLC, the flow index of the emitter increased, and the outlet flow became more sensitive to change in the inlet pressure. The water-retaining structure played an important role in energy dissipation of the CWRLC emitter. The analysis of the flow characteristics indicated that the energy dissipation of the CWRLC emitter was highly correlated with the proportion of low-speed vortex areas in the flow field. The larger the proportion of low-speed vortex areas, the more obvious the energy dissipation. The change in the proportion of low-speed vortex areas was the main reason that the flow index of the CWRLC emitter increased with the increase of the radius. The quadrature water-retaining labyrinth channel (QWRLC) structure and stellate water-retaining labyrinth channel (SWRLC) structure were obtained by structural improvement based on the energy dissipation mechanism. With the two improved flow channel structures, the proportion of the low-speed vortex areas in the flow channel field were increased. The SWRLC emitter had the largest proportion of low-speed vortex areas in the flow field compared with the CWRLC emitter and QWRLC emitter. For the improved flow channel structure, the test results showed that the flow index of the SWRLC emitter was increased by 15.11% compared with that of the CWRLC emitter, and the hydraulic performance of this emitter was significantly improved. The flow index of the SWRLC emitter was also lower than that of the widely used tooth labyrinth channel (TLC) emitter. Therefore, the SWRLC emitter can be recommended as a reference for the structural design optimization of the superior hydraulic performance of an emitter. It is expected that the SWRLC emitter has a fairly bright application foreground in the water-saving irrigation field.

Author Contributions: Conceptualization, Y.L. (Yanfei Li) and X.F.; methodology, Y.L. (Yanfei Li), X.H. and H.L. (Haiyang Liu); software, Y.L. (Yanfei Li); validation, Y.L. (Yanfei Li) and Y.X.; formal analysis, Y.L. (Yanfei Li) and X.F.; investigation, Y.L. (Yanfei Li), Y.L. (Yandong Liu), X.H., H.L. (Haiyang Liu), Y.S. and Y.X.; resources, X.F.; data curation, Y.L. (Yanfei Li) and Y.X.; writing—original draft preparation, Y.L. (Yanfei Li); writing—review and editing, Y.L. (Yanfei Li), X.F. and H.L. (Hui Li); visualization, Y.L. (Yanfei Li); supervision, X.F. and H.L. (Hui Li); project administration, X.F. and H.L. (Hui Li); funding acquisition, X.F. All authors have read and agreed to the published version of the manuscript.

Funding: This research was funded by [Key Research and Development Plan of Shandong Province] grant number [2019JZZY010443 and 2020CXGC010807] and the APC was funded by [Key Research and Development Plan of Shandong Province (2020CXGC010807)].

Institutional Review Board Statement: Not applicable.

Informed Consent Statement: Not applicable.

Data Availability Statement: The study did not report any data.

Conflicts of Interest: The authors declare no conflict of interest.

References

1. Lamm, F.R.; Colaizzi, P.D.; Sorensen, R.B.; Bordovsky, J.P.; Dougherty, M.; Balkcom, K.; Zaccaria, D.; Bali, K.M.; Rudnick, D.R.; Peters, R.T. A 2020 Vision of Subsurface Drip Irrigation in the U.S. *Trans. ASABE* **2021**, *64*, 1319–1343. [CrossRef]
2. Nogueira, V.H.B.; Diotto, A.V.; Thebaldi, M.S.; Colombo, A.; Silva, Y.F.; de Lima, E.M.; Resende, G.F.L. Variation in the Flow Rate of Drip Emitters in a Subsurface Irrigation System for Different Soil Types. *Agric. Water Manag.* **2021**, *243*, 106485. [CrossRef]
3. Yang, B.; Wang, J.; Zhang, Y.; Wang, H.; Ma, X.; Mo, Y. Anti-Clogging Performance Optimization for Dentiform Labyrinth Emitters. *Irrig. Sci.* **2020**, *38*, 275–285. [CrossRef]
4. De Sousa Pereira, D.J.; Lavanholi, R.; de Araujo, A.C.S.; Mouheb, N.A.; Frizzone, J.A.; Molle, B. Evaluating Sensitivity to Clogging by Solid Particles in Irrigation Emitters: Assessment of a Laboratory Protocol. *J. Irrig. Drain. Eng.* **2020**, *146*, 11. [CrossRef]

5. Gyasi-Agyei, Y. Validation of Dripline Emitter Characteristics and Pump Performance Curve for Network Analysis. *J. Irrig. Drain. Eng.* **2019**, *145*, 050190014. [CrossRef]
6. Solé-Torres, C.; Puig-Bargués, J.; Duran-Ros, M.; Arbat, G.; Pujol, J.; De Cartagena, J.R. Effect of Different Sand Filter Underdrain Designs on Emitter Clogging Using Reclaimed Effluents. *Agric. Water Manag.* **2019**, *223*, 105683. [CrossRef]
7. Al-Muhammad, J.; Tomas, S.; Ait-Mouheb, N.; Amielh, M.; Anselmet, M. Experimental and Numerical Characterization of the Vortex Zones Along a Labyrinth Milli-Channel Used in Drip Irrigation. *Int. J. Heat Fluid Flow* **2019**, *80*, 108500. [CrossRef]
8. Ait-Mouheb, N.; Schillings, J.; Al-Muhammad, J.; Bendoula, R.; Tomas, S.; Amielh, M.; Anselmet, F. Impact of Hydrodynamics on Clay Particle Deposition and Biofilm Development in a Labyrinth-Channel Dripper. *Irrig. Sci.* **2019**, *37*, 5. [CrossRef]
9. Zhou, W.; Zhang, L.; Wu, P.; Cai, Y.; Zhao, X. Hydraulic Performance and Parameter Optimisation of a Microporous Ceramic Emitter Using Computational Fluid Dynamics, Artificial Neural Network and Multi-Objective Genetic Algorithm. *Biosyst. Eng.* **2020**, *189*, 11–23. [CrossRef]
10. Yu, L.; Li, N.; Long, J.; Liu, X.; Yang, Q.-L. The Mechanism of Emitter Clogging Analyzed by CFD-DEM Simulation and PTV Experiment. *Adv. Mech. Eng.* **2018**, *10*, 2071943390. [CrossRef]
11. Lequette, K.; Ait-Mouheb, N.; Wery, N. Hydrodynamic Effect on Biofouling of Milli-Labyrinth Channel and Bacterial Communities in Drip Irrigation Systems Fed with Reclaimed Wastewater. *Sci. Total Environ.* **2020**, *738*, 139778. [CrossRef] [PubMed]
12. Chamba, D.; Zubezlu, S.; Juana, L. Determining Hydraulic Characteristics in Laterals and Drip Irrigation Systems. *Agric. Water Manag.* **2019**, *226*, 105791. [CrossRef]
13. Yu, L.; Li, N.; Liu, X.; Yang, Q.-L.; Long, J. Influence of Flushing Pressure, Flushing Frequency and Flushing Time on the Service Life of a Labyrinth-Channel Emitter. *Biosyst. Eng.* **2018**, *172*, 154–164. [CrossRef]
14. Liu, H.; Li, Y.; Liu, Y.; Yang, P.; Ren, S.; Wei, R.; Xu, H. Flow Characteristics in Energy Dissipation Units of Labyrinth Path in the Drip Irrigation Emitters with DPIV Technology. *J. Hydrodyn.* **2010**, *22*, 137–145. [CrossRef]
15. Feng, J.; Wang, W.; Liu, H. Study on Fluid Movement Characteristics Inside the Emitter Flow Path of Drip Irrigation System Using the Yellow River Water. *Sustainability* **2020**, *12*, 1319. [CrossRef]
16. Al-Muhammad, J.; Tomas, S.; Ait-Mouheb, N.; Amielh, M.; Anselmet, F. Micro-PIV Characterization of the Flow in a Milli-Labyrinth-Channel Used in Drip Irrigation. *Exp. Fluids* **2018**, *59*, 12. [CrossRef]
17. Liu, H.; Sun, H.; Li, Y.; Feng, J.; Song, P.; Zhang, M. Visualizing Particle Movement in Flat Drip Irrigation Emitters with Digital Particle Image Velocimetry. *Irrig. Drainage.* **2016**, *65*, 390–403. [CrossRef]
18. Yu, L.; Li, N.; Liu, X.; Yang, Q.-L.; Li, Z.; Long, J. Influence of Dentation Angle of Labyrinth Channel of Drip Emitters on Hydraulic and Anti-Clogging Performance. *Irrig. Drain.* **2019**, *68*, 256–267. [CrossRef]
19. Wang, C.; Li, Z.; Ma, J. Influence of Emitter Structure On its Hydraulic Performance Based on the Vortex. *Agriculture* **2021**, *11*, 508. [CrossRef]
20. Falcucci, G.; Krastev, V.K.; Biscarini, C. Multi-Component Lattice Boltzmann Simulation of the Hydrodynamics in Drip Emitters. *J. Agric. Eng.* **2017**, *48*, 175–180. [CrossRef]
21. Wu, D.; Li, Y.; Liu, H.; Yang, P.L.; Sun, H.; Liu, H. Simulation of the Flow Characteristics of a Drip Irrigation Emitter with Large Eddy Methods. *Math. Comput. Model.* **2013**, *58*, 497–506. [CrossRef]
22. Feng, J.; Li, Y.; Wang, W.; Xue, S. Effect of Optimization Forms of Flow Path on Emitter Hydraulic and Anti-Clogging Performance in Drip Irrigation System. *Irrig. Sci.* **2018**, *36*, 37–47. [CrossRef]
23. Zhang, J.; Zhao, W.; Lu, B. Rapid Prediction of Hydraulic Performance for Emitters with Labyrinth Channels. *J. Irrig. Drain. Eng.* **2013**, *139*, 414–418. [CrossRef]
24. Saccone, D.; De Marchis, M. Optimization of the Design of Labyrinth Emitter for Agriculture Irrigation Using Computational Fluid Dynamic Analysis. *AIP Conf. Proc.* **2018**, *2040*, 140013.
25. Zhangzhong, L.; Yang, P.; Li, Y.; Ren, S. Effects of Flow Path Geometrical Parameters on Flow Characteristics and Hydraulic Performance of Drip Irrigation Emitters. *Irrig. Drain.* **2016**, *65*, 426–438. [CrossRef]
26. Guo, L.; Bai, D.; Zhou, W.; Wang, J. Evaluation of Numerical Simulation Accuracy for Two-Ways Mixed Flow Drip Irrigation Emitter Based On CFD. *Int. J. Heat Technol.* **2017**, *35*, 384–392. [CrossRef]
27. Xu, T.; Zhang, L. Influence and Analysis of Structure Design and Optimization on the Performance of a Pit Drip Irrigation Emitter. *Irrig. Drain.* **2020**, *69*, 633–645. [CrossRef]
28. Xing, S.; Wang, Z.; Zhang, J.; Liu, N.; Zhou, B. Simulation and Verification of Hydraulic Performance and Energy Dissipation Mechanism of Perforated Drip Irrigation Emitters. *Water* **2021**, *13*, 171. [CrossRef]



Article

Tillage, Water and Nitrogen Management Strategies Influence the Water Footprint, Nutrient Use Efficiency, Productivity and Profitability of Rice in Typic Ustochrept Soil

Saurabh Tyagi ¹, Rama Krishna Naresh ², Rajan Bhatt ³ , Mandapelli Sharath Chandra ² ,
Abdullah A. Alrajhi ^{4,*} , Ahmed Z. Dewidar ^{5,6} and Mohamed A. Mattar ^{6,7,8}

- ¹ Department of Agriculture, School of Biological Engineering & Life Sciences, Shobhit University, Modipuram, Meerut 250110, Uttar Pradesh, India; srbhtyagi1@gmail.com
- ² Department of Agronomy, Sardar Vallabhbhai Patel University of Agriculture & Technology, Meerut 250110, Uttar Pradesh, India; r.knaresh@yahoo.com (R.K.N.); sharathagrigo@gmail.com (M.S.C.)
- ³ Regional Research Station, Kapurthala, Punjab Agricultural University, Ludhiana 141004, Punjab, India; rajansoils@pau.edu
- ⁴ King Abdulaziz City for Science and Technology (KACST), King Abdullah Road, Riyadh 11442, Saudi Arabia
- ⁵ Prince Sultan Bin Abdulaziz International Prize for Water Chair, Prince Sultan Institute for Environmental, Water and Desert Research, King Saud University, Riyadh 11451, Saudi Arabia; adewidar@ksu.edu.sa
- ⁶ Department of Agricultural Engineering, College of Food and Agricultural Sciences, King Saud University, Riyadh 11451, Saudi Arabia; mmattar@ksu.edu.sa
- ⁷ Centre for Carbon, Water and Food, The University of Sydney, Camperdown, NSW 2570, Australia
- ⁸ Agricultural Engineering Research Institute (AEnRI), Agricultural Research Centre, Giza 12618, Egypt
- * Correspondence: aalrajhi@kacst.edu.sa



Citation: Tyagi, S.; Naresh, R.K.; Bhatt, R.; Chandra, M.S.; Alrajhi, A.A.; Dewidar, A.Z.; Mattar, M.A. Tillage, Water and Nitrogen Management Strategies Influence the Water Footprint, Nutrient Use Efficiency, Productivity and Profitability of Rice in Typic Ustochrept Soil. *Agronomy* **2022**, *12*, 1186. <https://doi.org/10.3390/agronomy12051186>

Academic Editor: Aliasghar Montazar

Received: 2 April 2022
Accepted: 12 May 2022
Published: 14 May 2022

Publisher's Note: MDPI stays neutral with regard to jurisdictional claims in published maps and institutional affiliations.



Copyright: © 2022 by the authors. Licensee MDPI, Basel, Switzerland. This article is an open access article distributed under the terms and conditions of the Creative Commons Attribution (CC BY) license (<https://creativecommons.org/licenses/by/4.0/>).

Abstract: The current study was conducted to assess how optimal tillage water and nitrogen management system are adopted to reduce various field inputs, to improve water footprint (WF), nutrient use efficiency (NUE), rice productivity and profitability. The W_1 (CS to a depth of 5 cm) achieved significantly higher total water footprint (TWFP) compared to all other irrigation strategies. When N_1 (control) and N_2 (80 kg N ha⁻¹) was used, the highest TWFP was observed. The rice transplanted on wide raised beds (WBed-TPR) (0.71 kg m⁻³) yielded the greatest water productivity (WP_{IRRI}), followed by reduced tillage transplanted rice (RT-TPR) and conventional tillage puddled transplanted rice (CT-TPR). The physiological NUE values ranged from 33.3 to 50.6 kg grain/kg N absorption, the values decreasing as the N doses rose. According to the findings, WBed-TPR and RT-TPR plots similarly drank more moisture from the deeper profile layer than CT-TPR practice. In plots of CT-TPR and WBed-TPR, the yield contributing characteristics of rice all increased, while grain yield increased by 16.8% and 10.6% over NBed-TPR technique, respectively. Finally, CT-TPR reported with maximum cultivation costs, followed by NBed-TPR and the lowest in RT-TPR plots, although WBed-TPR had the highest net profit, B: C ratio.

Keywords: rice; water footprint; nutrient use efficiency; productivity; profitability

1. Introduction

Rice (paddy) is a staple food crop that feeds more than half of the world's population and provides approximately 19% of the world's nutritional energy [1]. Food production will need to increase by roughly 60% to meet global food demand in 2050 according to estimates [2]. Freshwater demands for food production are expected to rise dramatically in the coming decades as a result of population expansion, urbanisation and economic development [3]. Agriculture, on the other hand, consumes the most land and freshwater, accounting for about 37.5% of the world's land area [4] and 85% of global freshwater consumption [5]. Water is an important aspect of sustainable development and plays a key role in today's environmental concerns. Water scarcity, on the other hand, is becoming a global issue [6].

Water footprint is recognized as a technique for assessing the relationship between agricultural production, water resources and environmental consequences in order to improve water use efficiency, watershed sustainability, water impact mitigation and water resource management [7–9]. In India, the water footprint of per unit rice production and percolation was 1403 ($\text{m}^3 \text{t}^{-1}$) and 432.9 ($\text{m}^3 \text{t}^{-1}$), respectively. Thailand has a higher per capita water footprint ($547 \text{ m}^3 \text{ cap}^{-1} \text{ yr}^{-1}$) than India ($239 \text{ m}^3 \text{ cap}^{-1} \text{ yr}^{-1}$) [10,11], with water footprints related to rice consumption of 63, 364 and 250, 305 ($\text{Mm}^3 \text{ yr}^{-1}$), respectively. According to Chapagain and Hoekstra [12], India's rice cultivation had a total water footprint of $2020 \text{ m}^3 \text{ t}^{-1}$ and a percolation volume of $1403 \text{ m}^3 \text{ t}^{-1}$, whereas Pakistan claimed the highest water footprint ($2874 \text{ m}^3 \text{ t}^{-1}$). Water footprints in crop production must be reduced to make effective use of the available water by replacing conventional faulty crop establishment and irrigation techniques with new RCTs, and the saved water could then be used on to the other competitive sectors [13]. Rice production has become a challenge due to changing global weather trends and reduced per capita availability of surface and ground water quantum. Different components of soil water balance such as evaporation, transpiration, seepage, percolation and drainage, must be calculated in order to determine which component should be prioritized for enhancing the water use efficiency and productivity under a specific irrigation management system [14,15]. Footprints of water can be used to assess, directly and indirectly, groundwater resource requirements [16,17]. They are described as the ratio of the volume of consumptive water usage to the quantity of produce obtained.

Reduction tillage benefits a variety of soil qualities, but excessive and unnecessary tillage activities have the reverse effect, causing soil degradation. As a result, there is a lot of focus right now on changing from extreme tillage to conservation tillage to control erosion [18,19]. Traditional tillage activities change the bulk density and moisture content of the soil, altering its structure. In addition, conventional tillage produces in a finer and looser setting soil structure, whereas conservation and no-tillage methods preserve the soil [20]. Conversely, conservation tillage increases soil quality indicators over time [21]. Another issue is the degradation of soil (land) health, which is particularly prevalent in intensive agriculture, such as that practiced in northwest India. Poor agronomic management, water logging, acidification, salinization and alkalization, among others, lead to land degradation, low input use efficiency, water productivity, etc.

Nitrogen (N) is one of the most important inputs for rice growth and development, although soil N availability is often a constraint [22]. As a result, the application of nitrogen fertilizer has been a major component in increasing crop production over the last five decades, whereas excessive nitrogen fertilizer may not lead to crop benefits but may cause serious environmental and economic problems [23]. Rapid nitrogen losses in the soil flood water system due to ammonia volatilization, denitrification, surface runoff and leaching lead to lower nitrogen usage efficiency (NUE) when high N fertilizer input is used. As a result, major environmental issues such as soil acidification, air pollution and water eutrophication have occurred [22,24]. New strategies to increase yields while maintaining or decreasing optimally applied N are urgently needed to achieve higher crop productivity and NUE under well-fertilized conditions [25]. Depending on the soil quality and socioeconomic scenario, farmers in northern India apply 80 to 150 kg N ha^{-1} . However, in order to increase rice farmer income, more research into a sustainable N rate with various irrigation management options is still needed in the region [26]. Keeping this in mind, the aforementioned research study was conducted to investigate tillage, water and nitrogen management strategies for enhancing water footprint, nitrogen use efficiency, productivity and profitability of wet rice under *Typic Ustochrept* soil.

2. Materials and Methods

2.1. Investigational Location

The investigation was initiated during 2016 at the Sardar Vallabhbhai Patel University of Agriculture and Technology's Meerut research farm situated at $29^{\circ} 04' \text{ N}$ latitude,

770 42' E longitude, 237 meters above mean sea level in Uttar Pradesh, India. The investigation location was reported with semi-arid sub-tropical climate with an average yearly temperature of 16.8 °C. For the years 2016 and 2017, data on climatic parameters such as rainfall (mm), mean maximum and minimum temperatures, evaporation, air velocity and relative humidity were collected at the meteorological observatory of the Sardar Vallabhbhai Patel University of Agriculture and Technology Meerut (U.P.). The average maximum weekly temperature in 2016 and 2017 ranged between 27.7 and 35.9 °C, while the average minimum weekly temperature ranged between 11.9 and 26.1 °C, according to the meteorological data depicted graphically in Figure 1. In both years, there is a modest increase in mean daily temperature in June, reaching as high as 2.1 °C, and then a gradual decrease, reaching as low as 33.6 and 32.8 °C in October 2016 and 2017, respectively. The mean relative humidity is highest in July and lowest in June. During the crop period, minimum evaporation was recorded 10.5 mm in the second week of November and maximum evaporation was recorded at 52.3 mm in the fifth week of June in 2016 and minimum evaporation was recorded at 7.9 mm in the second week of November and maximum evaporation was recorded at 52.4 mm in the fourth week of June in 2017. The maximum temperature was highest in the fifth week of June during 2016 and the fourth week of June during 2017. Rainfall was recorded at 427.7 mm and 607.5 mm during the crop period in 2016 and 2017. The most prevalent soil type found at the test location is Typic Ustochrept. Before applying treatments, surface soil samples were collected and analyzed. The basic properties are poor accessible nitrogen, low in organic carbon, accessible phosphorus, accessible potassium medium and alkali in response.

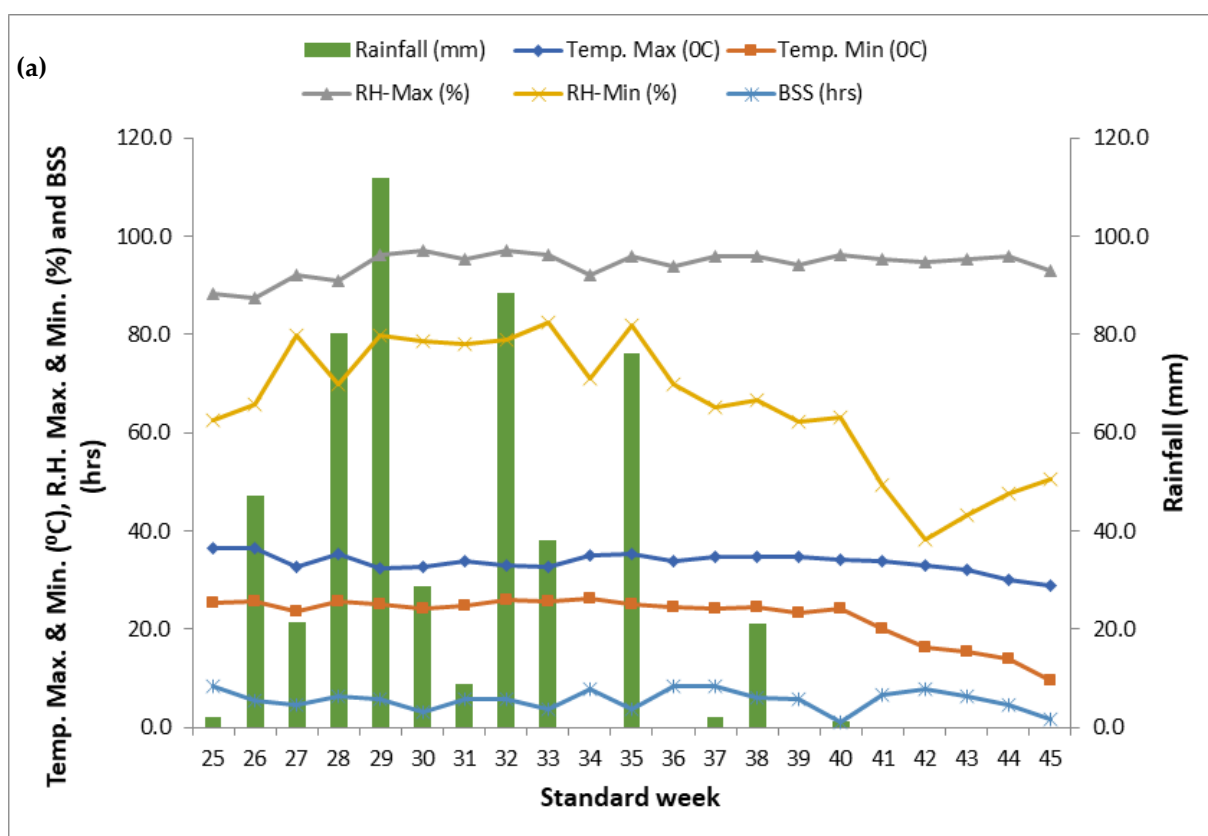


Figure 1. Cont.

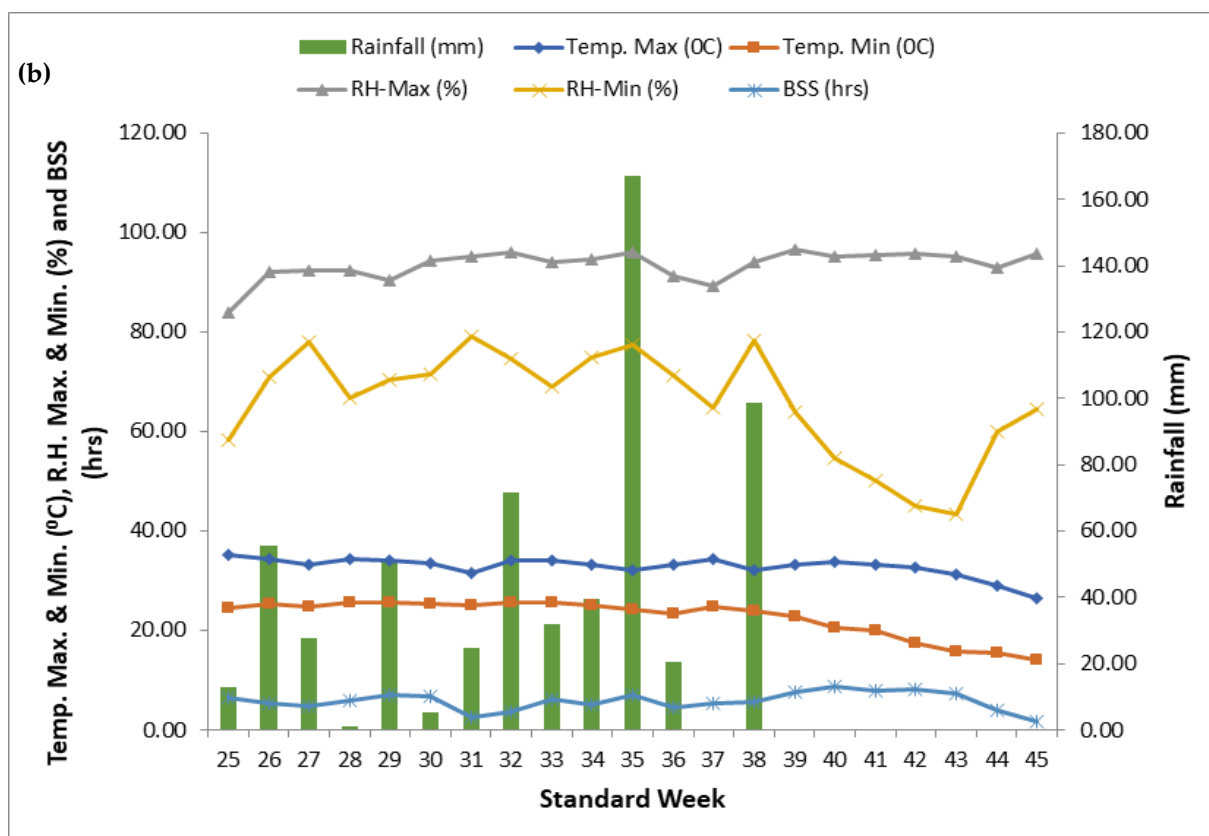


Figure 1. Mean weekly agro-meteorological data during the crop growing *kharif* season: (a) 2016 and (b) 2017.

2.2. Experimental Invent and Organization

A detailed description of different tillage systems is required to compare the effect of tillage techniques on environmental performance [27]. There are four different tillage crop establishing methods: T_1 is transplanted rice after reduced tillage (RT-TPR), T_2 is transplanted rice on narrow raised beds (N Bed-TPR), T_3 is transplanted rice on wide raised beds (W Bed-TPR) and T_4 is conventional tillage puddled transplanted rice in main plots (CT-TPR). There were three water management/alternate wetting drying (AWD) practices: W_1 is continuously submerged (CS) of 5 cm depth, W_2 is irregular submergence (IS) of 5 cm and irrigation after 2 days of water vanishing from the surface and W_3 is alternating submergence of 5 cm and irrigation after 5 days of water vanishing from the soil surface allotted to sub-plots; five nitrogen levels: N_1 is N0P0K0 (control), N_2 is 80 kg N ha⁻¹, N_3 is 120 kg N ha⁻¹, N_4 is 160 kg N ha⁻¹ and N_5 is 200 kg N ha⁻¹ allotted to sub-subplots in a split-split-plot design and replicated three times.

Treatments were layered on the same plot every year to evaluate their cumulative effect. The gross and net plot sizes were 8 m × 3.2 m and 6.0 m × 2.0 m, respectively. In traditional tillage, there were three tillage operations. The primary tillage took place during the pre-monsoon season (April/May), while the second took place 20–25 days later, in May/June. The third tillage was carried out in June with a tractor-drawn cultivator at a deeper depth (>15 cm). Nitrogen was applied in accordance with the protocols. Except for N_1 , all treatments received soil application 60 kg phosphorus (P), 40 kg potassium (K) and 25 kg zinc (Zn) ha⁻¹ in the form of di-ammonium phosphate, potash sulphate and 21 percent zinc sulphate, respectively. P, K and Zn, as well as 1/3 of nitrogen, were all applied at the time of transplanting and seed bed preparation. In terms of treatment, the remaining nitrogen fertilizer dose was split in half at the time of booting (3 weeks after transplantation) and panicle commencement (6 weeks after transplantation). On 1 July, three-week-old nursery seedlings were manually plucked and replanted into the main field

with a distance of 20 cm from row to row. When the crop reached physiological maturity, watering was stopped two weeks before harvest and the crop was harvested.

2.3. Weed Management

For the rest of the growing season, the plots would remain weed-free. Butachlor at 1300 ga.i.ha⁻¹ should be applied 2 days after transplanting (DAT), followed by a spray treatment of bispyribac sodium (Nomne gold) at 25 ga.i.ha⁻¹ one month later. Additionally, weeds were manually removed in the transplanted rice plots to keep it weed-free.

2.4. Water Footprints

The total amount of water used for producing agricultural goods is known as water footprint (WFP) [28]. The unit is commonly stated in m³ t⁻¹ or L kg⁻¹.

$$\text{WFP}_{\text{total}} = (\text{WFP}_{\text{green}}) + (\text{WFP}_{\text{blue}}) + (\text{WFP}_{\text{grey}}) = \frac{\text{CWU}_{\text{green}} + \text{CWU}_{\text{blue}} + \text{CWU}_{\text{grey}} \left(\text{m}^3 \text{ha}^{-1} \right)}{\text{Economic yield of the crop} \left(\text{t ha}^{-1} \right)} \quad (1)$$

Water productivity (WP_{I+R}) (kg m⁻³) was computed as follows

$$\text{WP}_{\text{I+R}} = \frac{\text{Grain yield}}{\text{Irrigation water applied} + \text{Rainfall received by the crop}} \quad (2)$$

Rice Water Footprints

Under conventional systems, total water inputs for the rice–wheat cropping sequence involved total water required to meet various components of soil water balance with extra water required for puddling, especially for rice. However, only evapotranspiration (ET) and evaporation (E) during land preparation were taken into consideration for water footprint calculations, and attempts mostly were made to reduce E. As a result, the amount of water evaporated to produce a specific set of yields equals the WFP (m³ t⁻¹) of rice–wheat production. Percolation is not considered a watershed loss, but it was left out of the farm-wide water footprint estimation because it occurs during crop development and field preparation. On the other hand, the crop’s grey WF due to N pollution was calculated and merged with the blue and green WF.

2.5. Nutrient Use Efficiency

The nitrogen harvest index (NHI) measures the ability of a crop to divide total N intake among different plant parts [29]. As a result, the NHI was defined as the ratio of seeds to total biomass nitrogen intake. The nitrogen usage efficiency (NUE) is categorized in various methods. The total N uptake by seed and straw as well as the amount of applied N as fertilizer are used to calculate the apparent N recovery (NUE) for various N treatments (Equation (3)). The term “nitrogen yield efficiency” (NYE) or “agronomic nitrogen efficiency” is preferred to characterize how well N inputs are used in relation to the amount of nitrogen applied [30]. Equation (4) [31] was used to compute the NYE in various N treatments using the applied nitrogen as fertilizer and seed yield. Equation (5) also determined the physiological nitrogen efficiency (NPE).

$$\text{NUE} = \frac{\text{Nui} - \text{Nuc}}{\text{Nfi} - \text{Nfc}} \quad (3)$$

$$\text{NYE} = \frac{\text{Yi} - \text{Yc}}{\text{Nfi} - \text{Nfc}} \quad (4)$$

$$\text{NPE} = \frac{\text{Yi} - \text{Yc}}{\text{Nui} - \text{Nuc}} \quad (5)$$

where NUE, Nuc, Nfi, Nfc, Yi and Yc represents nitrogen use efficiency, total N uptake by seed and straw (kg ha⁻¹), applied N (kg ha⁻¹), rice grain yields in N treatments and control (kg ha⁻¹), respectively.

2.6. Statistical Investigation

The SPSS application, which runs on Windows, was used to conduct the statistical analysis (Version 10.0, SPSS, 1996, Chicago, IL, USA). For analysis of variance, the SPSS technique was utilized to establish the statistical significance of treatment effects. Duncan’s multiple range test was used to compare the means using the least significant difference (LSD) method. Statistically significant values are considered at a probability level of 5%.

3. Results and Discussion

3.1. Soil Moisture Studies

Results revealed that surface soil pertaining to 0–15 cm of soil mined a higher proportion of the moisture as compared to the other three layers, viz., 15–30, 30–60 and 60–90 cm, where 60–90 cm extracted the least moisture (Figure 2).

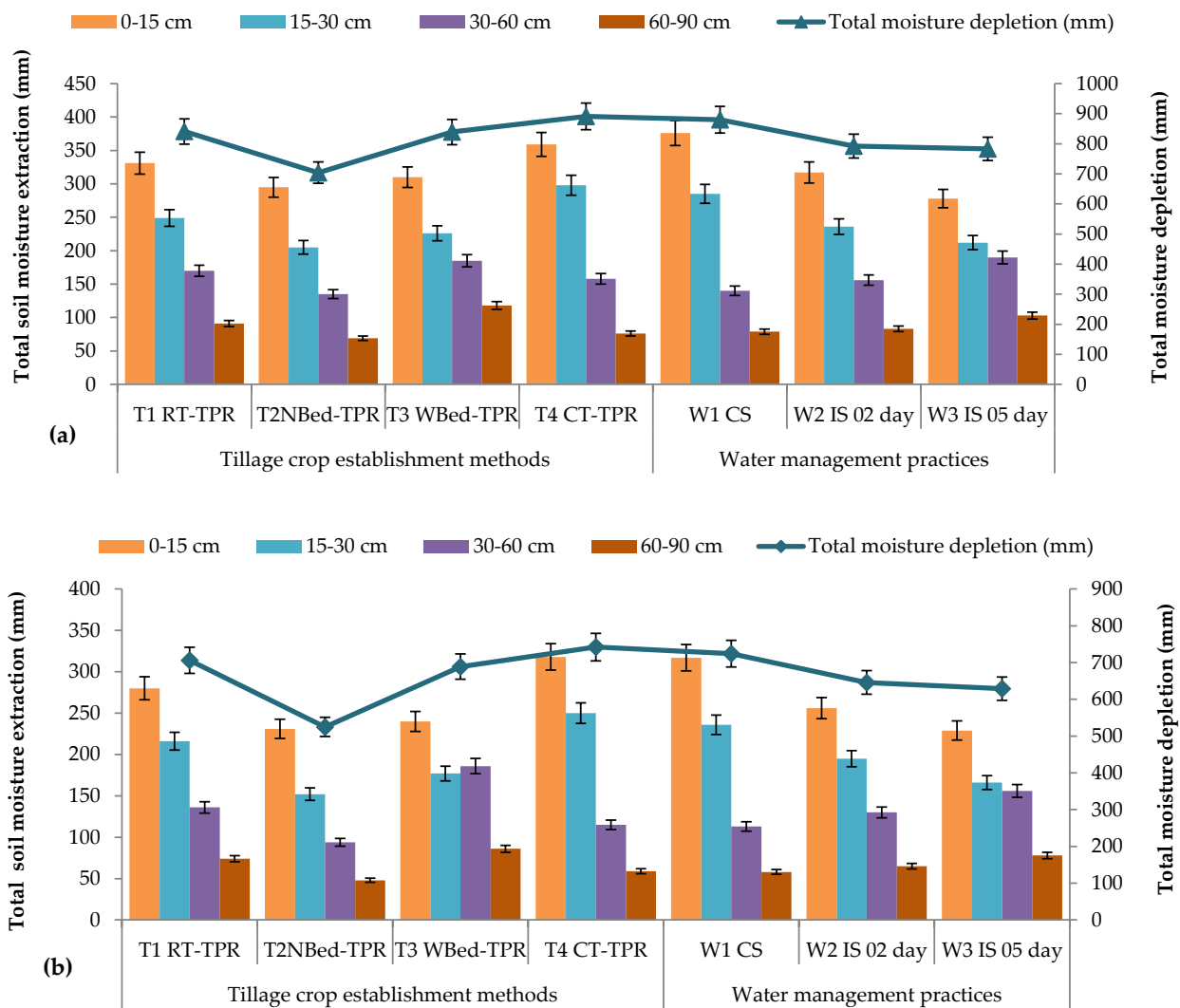


Figure 2. Tillage, water and nitrogen interactive effects on water extraction patterns in soil profile in both years: (a) 2016 and (b) 2017.

Moisture extraction from the surface layer (0–15 cm) was slightly increased using conventional tillage and reduced tillage techniques. Similarly, the moisture extraction

was marginally reduced as the profile depth and furrow irrigated raised beds increased during 2016 and 2017, respectively. Furthermore, rice transplanted on wide raised beds and in reduced tillage plots had higher moisture removal from deeper profile layer than rice transplanted using the conventional method. Throughout the experimentation period, moisture mined from 0–15 cm rose marginally as irrigation frequency increased. Similarly, as the profile depth and irrigation frequency increased in both years, moisture extraction reduced marginally of W_1 's water management technique decreased moisture extraction as profile depth increased. During the experimentation, however, moisture extraction was increased in profile depth for W_2 and W_3 treatments compared to W_1 treatment.

In 2016 and 2017, the seasonal variation in average profile moisture in all treatments ranged from 27.1 to 21.4% and 27.9 to 19.7%, respectively, which might be due to the variation in tillage practices adopted to establish the crop and receive rainfall. However, under irrigation, the soil upper profile was recharged to field capacity, but its moisture content decreased over time due to evapotranspiration losses, which are dependent on the weather parameters such as air maximum temperatures.

In both years, the lowest moisture content was found at the time of crop maturity, which could be because irrigation was stopped three weeks before harvesting. Furthermore, well-fertilized plots, i.e., N_4 or N_5 treatment, had lower moisture than the control plots with no fertilizers, etc., which could be attributed to better crop growth and higher transpiration losses in the previous plots. Similar observations are also reported by [32].

The amount of moisture extracted from various soil profile layers decreased as profile depth increased, which could be due to reduced root mass density (RMD) as we moved down the profile (Figure 2). However, in reciprocal of this, surface soil layers received better moisture, nutrients, and RMD, which further extracted higher soil moisture. No doubt, weather parameters also affected these quantum volumes. In both years, moisture was extracted from the 30–60 cm layer at around 19.9%, with 39.8 and 29.8% of water used from the 0–15 and 15–30 cm layers, respectively. Measuring moisture usage cm^{-1} of soil depth in the 0–15 cm layer can further support this argument. When compared to deeper layers, such as the 30–60 cm layer, T_1 and T_3 treatments had respective values of 0.35 and 0.23 cm cm^{-1} in T_2 treatment and 0.29 cm cm^{-1} in T_4 treatment. When irrigation scheduling mode was used, moisture removal from the upper layers increased by 1–2%, with a decline in similar values in the deepest soil layers. The reason for the recorded observation might be that the previous layers received higher solar radiation, which further resulted in higher ET losses than the respected lower layers, as also explained by [33–35].

However, moisture in the soil profile was reported to be around 40% higher during transplanting time than harvesting time, which might be due to the fact that transplantation was carried out in flooded conditions during both years. The enhancements in profile moisture content seen from the peaks under various tillage practices were linked to moisture conservation due to irrigation frequency application as per treatments.

Furthermore, during both years of experimentation, T_4 treatment at a deeper depth remained on the lower side as compared to T_1 and T_3 treatments, respectively, with the exception of peaks, where recharging of the profile by irrigation or rainfall made constant soil profile moisture. The average soil moisture content of the typical till crop was 1.5% lower than that of the broad raised bed plots throughout the crop season, excluding after the recharging of the soil profile by irrigation or rainfall.

3.2. Footprints and Productivity of Irrigation Water

During both years, T_4 treatment had the highest total water footprint (TWFP) with a value of 1894.4 and 1899.6 $\text{m}^3 \text{t}^{-1}$ whereas T_1 , T_3 and T_2 plots reported 1738.0, 1697.0 and 1659.6 and 1834.0, 1738.0 and 1659.6 $\text{m}^3 \text{t}^{-1}$, respectively. The irrigation technique of W_1 treatment had a TWFP of 1785.2 $\text{m}^3 \text{t}^{-1}$ in 2017 and 1821.9 $\text{m}^3 \text{t}^{-1}$ in 2018. That was significantly higher than all other irrigation strategies and statistically equivalent to W_2 treatment. During both years of the study, however, W_3 treatment had the lowest TWFP of 1709.3 and 1744.3 $\text{m}^3 \text{t}^{-1}$. The highest TWFP was reported in 2016 and 2017

when “control” fertilizer was not used and only 80 kg N ha⁻¹ was broadcast in N₁ and N₂ treatments during both years, with values of 1817.0, 1776.3 and 1825.2 and 1807.2 m³ t⁻¹, respectively. Furthermore, N₃, N₄ and N₅ plots recorded the lowest TWFP of 1768.3, 1743.6 and 1631.5 m³ t⁻¹ in 2017 and 1774.0, 1766.0 and 1741.3 m³ t⁻¹ in 2018. Hence, from control plots to fertilized plots, TWFP was reduced to better crop growth and higher transpiration losses, which only met with the used higher irrigation water quantum, which clearly explains why TWFP was lower in fertilized plots as compared to control plots. In addition, T₄ plots were recorded with significantly higher values of TWFP as compared to T₁, T₂ and T₃ plots during both experimental years (Tables 1 and 2).

Table 1. The impact of various treatments on footprints and productivity of applied irrigation water in the 2016 year.

Treatments	BWFP (m ³ t ⁻¹)	GWFP (m ³ t ⁻¹)	Gr WFP (m ³ t ⁻¹)	TWFP (m ³ t ⁻¹)	PERC_V (m ³ t ⁻¹)	TWU_V (m ³ t ⁻¹)	WP _{IRRI} (kg m ⁻³)	WP _{TCW} (kg m ⁻³)	WP _{ETC} (kg m ⁻³)
<i>Tillage crop establishment methods</i>									
T ₁ (RT-TPR)	1627	108.8	2.2	1738.0	1288	2919.2	0.68	0.42	0.37
T ₂ (NBed-TPR)	1554	105.3	0.7	1659.6	1325	2646.5	0.65	0.40	0.39
T ₃ (WBED-TPR)	1588	107.2	1.8	1697.0	1303	2804.5	0.70	0.43	0.44
T ₄ (CT-TPR)	1782	109.7	2.7	1894.4	1265	3080.8	0.66	0.38	0.42
LSD (<i>p</i> ≤ 0.05)	78.70	1.38	0.03	24.52	17.56	37.88	0.08	0.04	0.04
<i>Water management practices</i>									
W ₁ (CS)	1674	109.1	2.2	1785.2	1315	3135.3	0.61	0.39	0.36
W ₂ (IS 02 day)	1638	107.5	1.9	1747.3	1296	2846.5	0.63	0.39	0.43
W ₃ (IS 05 day)	1601	106.8	1.6	1709.3	1274	2606.5	0.64	0.42	0.44
LSD (<i>p</i> ≤ 0.05)	63.67	1.81	0.03	29.88	22.54	51.08	0.08	0.07	0.07
<i>Nitrogen levels</i>									
N ₁ (Control)	1709	106.4	2.1	1817.0	1366	3006.3	0.46	0.54	0.32
N ₂ (80 kg N ha ⁻¹)	1667	107.2	2.0	1776.3	1355	2984.7	0.49	0.41	0.38
N ₃ (120 kg N ha ⁻¹)	1659	107.8	1.9	1768.3	1342	2958.2	0.53	0.39	0.52
N ₄ (160 kg N ha ⁻¹)	1633	108.4	1.8	1743.6	1223	2717.1	0.56	0.35	0.64
N ₅ (200 kg N ha ⁻¹)	1521	109.2	1.7	1631.5	1189	2647.5	0.55	0.34	0.63
LSD (<i>p</i> ≤ 0.05)	NS	NS	0.06	52.75	38.71	86.12	0.07	0.08	0.13

BWFP, GWFP, Gr WFP stood for blue, green and grey water footprints while TWFP, PERC_V, TWU_V, WP_{IRRI}, WP_{TCW} and WP_{ETC} stands for total water footprint, percolation water volume, total water use volume, water productivity, water productivity of total crop water needs and water productivity as evapotranspiration only.

The ratio of percolation losses to grain yields was reported to be the highest in the control plots with no broadcasted N fertilizers, while it was reduced to 1366 and 1355 m³ t⁻¹ in 2017 and 1434 and 1423 m³ t⁻¹ in 2018 reported for the N₁ and N₂ treatments, respectively. During the years 2016 and 2017, N₃, N₄ and N₅ plots reported 1342, 1223 and 1189 m³ t⁻¹ and 1410, 1292 and 1258 m³ t⁻¹, respectively.

The highest grain yield was attributed to a lower volume of percolation water with higher fertilizer doses, but decreased infiltration volume was mostly due to shorter standing water duration under N₄ and N₅ treatments. Because of the continuous submergence under the previous treatment, the WFs are reported to be greater for W₁ (3135.3 and 3048.3 m³ t⁻¹) than for W₂ (2846.5 and 2877.6 m³ t⁻¹) and W₃ (2606.5 and 2745.7 m³ t⁻¹) than for W₂ (2846.5 and 2877.6 m³ t⁻¹) and W₃ (2606.5 and 2745.7 m³ t⁻¹) (Tables 1 and 2). These results indicate that agricultural administration (tillage crop establishment methods and irrigation techniques) had a greater impact on the water footprint and amount of water infiltration than the agro-climate in which the crop was grown. Through improved agro-management techniques, this opens up the option of improving production and water productivity. It is also determined that the optimal use of fertilizers has the potential to improve yield and, as a consequence, reduce water footprints in rice cultivation in the region.

Table 2. The impact of various treatments on footprints and productivity of applied irrigation water in 2017 year.

Treatments	BWFP (m ³ t ⁻¹)	GWFP (m ³ t ⁻¹)	Gr WFP (m ³ t ⁻¹)	TWFP (m ³ t ⁻¹)	PERC_V (m ³ t ⁻¹)	TWU_V (m ³ t ⁻¹)	WP _{IRRI} (kg m ⁻³)	WP _{TCW} (kg m ⁻³)	WP _{ETC} (kg m ⁻³)
<i>Tillage crop establishment methods</i>									
T ₁ (RT-TPR)	1718	113.9	2.4	1834.0	1370	2946.5	0.69	0.41	0.41
T ₂ (NBed-TPR)	1548	109.5	1.9	1659.6	1397	2683.5	0.67	0.39	0.42
T ₃ (WBED-TPR)	1624	111.8	2.3	1738.0	1356	2837.1	0.72	0.42	0.44
T ₄ (CT-TPR)	1781	115.5	2.9	1899.6	1330	3094.9	0.68	0.38	0.42
LSD ($p \leq 0.05$)	17.16	1.41	0.03	22.84	18.16	38.90	0.05	0.04	0.06
<i>Water management practices</i>									
W ₁ (CS)	1706	114.1	2.1	1821.9	1386	3048.3	0.40	0.39	0.42
W ₂ (IS 02 day)	1667	112.8	2.3	1782.3	1364	2877.6	0.42	0.39	0.45
W ₃ (IS 05 day)	1631	111.2	2.6	1744.3	1340	2745.7	0.43	0.42	0.46
LSD ($p \leq 0.05$)	23.73	1.90	0.05	30.70	23.75	51.4	NS	NS	NS
<i>Nitrogen levels</i>									
N ₁ (Control)	1713	111.3	2.4	1825.2	1434	3040.4	0.41	0.53	0.32
N ₂ (80 kg N ha ⁻¹)	1695	112.1	2.3	1807.2	1423	3017.2	0.42	0.41	0.33
N ₃ (120 kg N ha ⁻¹)	1660	112.7	2.2	1774.0	1410	2989.6	0.54	0.38	0.34
N ₄ (160 kg N ha ⁻¹)	1652	113.3	2.1	1766.0	1292	2738.8	0.58	0.35	0.38
N ₅ (200 kg N ha ⁻¹)	1626	114.1	2.5	1741.3	1258	2666.7	0.57	0.36	0.35
LSD ($p \leq 0.05$)	41.25	NS	0.07	53.43	40.76	86.74	0.08	0.07	0.08

BWFP, GWFP, Gr WFP stood for blue, green and grey water footprints while TWFP, PERC_V, TWU_V, WP_{IRRI}, WP_{TCW} and WP_{ETC} stands for total water footprint, percolation water volume, total water use volume, water productivity, water productivity of total crop water needs and water productivity as evapotranspiration only.

WP_{IRRI} was lower in T₁ (0.69 kg m⁻³) and T₄ (0.68 kg m⁻³) treatments, while it was the highest in T₃ (0.71 kg m⁻³) treatment (Tables 1 and 2). Despite having a 9.5% lower production, T₃ treatment had a 7.5% higher WP_{IRRI} than T₄ treatment. WP values of T₃ plots were recorded on the higher side as compared to T₄ plots, though yields were reported to be significantly different in the above plots. From control to N fertilized plots, the corresponding values of WP_{IRRI} jumped to 0.44, 0.46, 0.54, 0.57 and 0.56 kg m⁻³, respectively, for N₁, N₂, N₃, N₄ and N₅. Furthermore, in T₄, T₂, T₁ and T₃ treatments, the respective values of WP were recorded as 0.38, 0.40, 0.41 and 0.42 kg m⁻³. The reason for better WP is assumed to be poor vegetation and hence less transpiration loss in these plots. As a result, WPTCW yields were comparable to the other three tillage crop establishment treatments, whereas T₂ treatment yields were lower. Although the expected water productivity was comparable to that of N₃, N₄ and N₅ treatments, the WPTCW grew gradually as the nitrogen dose was increased. A similar pattern was observed when water productivity was evaluated only on the basis of evapotranspiration (Tables 1 and 2) as recorded earlier by [36–39].

3.3. Nitrogen Use Efficiency

Under various tillage, water and nitrogen treatments, ANUE values ranged from 13.5–24.1%. Over the course of the N treatments, alternate wetting and drying treatments (W₂ and W₃) had a higher ANUE than continuous submergence (W₁). The average ANUE was also found to be higher (24.1%) at N₂ treatment, but not at higher doses of N (14.6% at N₅ treatment). In water management treatments, the NHI was quite consistent, ranging from 47.7 to 50.7%. The level of significance for NHI was similarly inconsistent between N treatments (Figure 3).

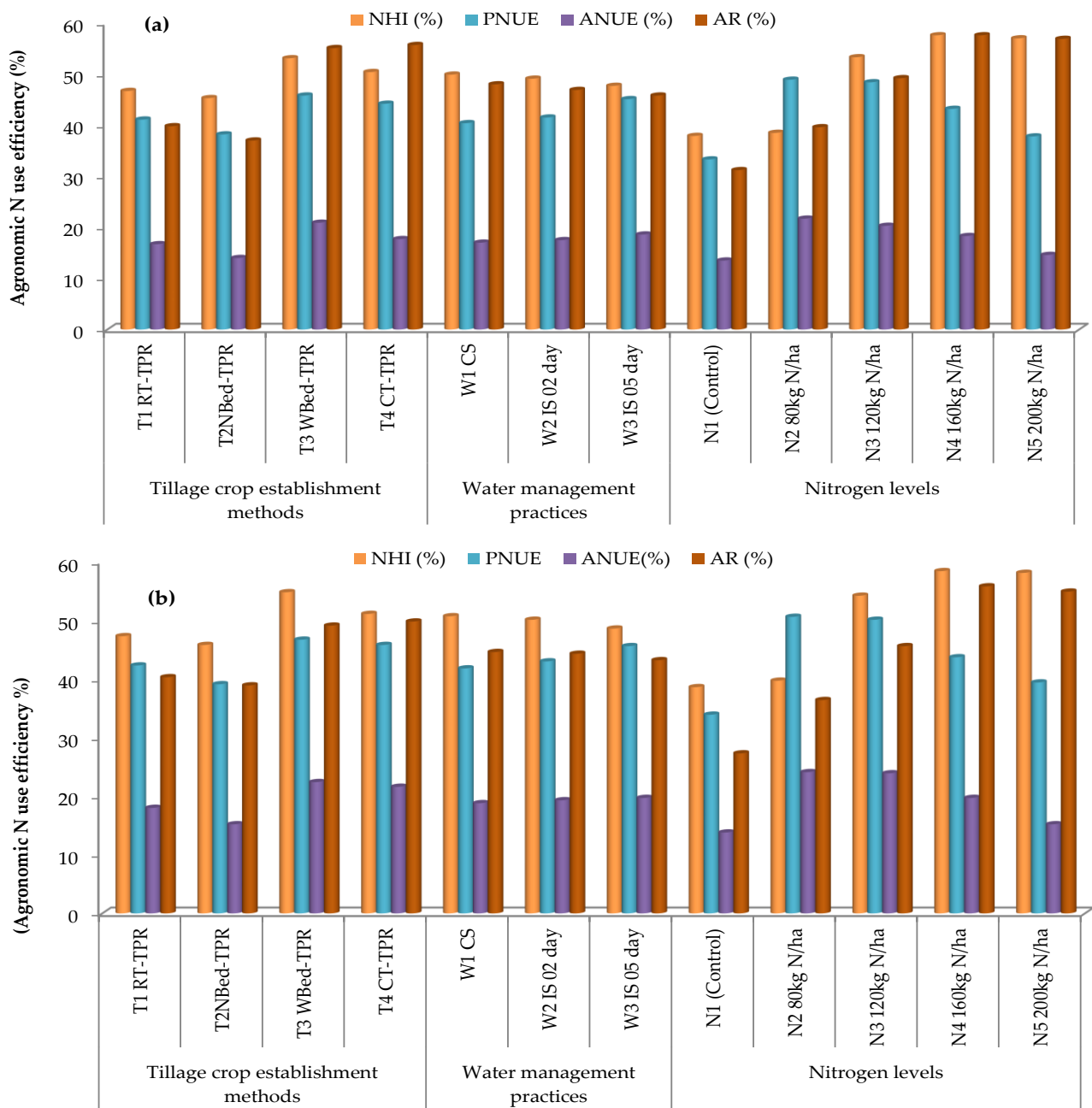


Figure 3. Tillage, water and nitrogen interactive effects on nitrogen use efficiency parameters in both years: (a) 2016 and (b) 2017.

The PNUE limits ranged from 33.3 to 50.6 kg grain kg⁻¹ N uptake, with decreasing values as the N dosages increased (Figure 3). As N doses increase, PNUE values tend to decrease due to higher N uptake and higher N concentrations in both the grain and straw. However, the PNUE values in W₁, W₂ and W₃ treatments were similar and statistically insignificant. Different N and water management procedures resulted in AR values ranging from 27.3 to 57.6%. Because of the larger grain output, the AR was higher at N₄ treatment. This was due to the greater yield difference between the N₁ and N₄ treatments (about 1.92 t ha⁻¹).

3.4. Yield Contributing Characteristics and Yield

Tillers m⁻², effective tillers m⁻², spike length and spikelets per panicle⁻¹ and number of grains per panicle⁻¹ all varied with tillage strategies, with the T₄ treatment having signifi-

cantly more effective tillers m^{-2} than all other land configurations. During the years of study, however, T_3 treatment recorded considerably greater yield in contributing metrics than the other treatments, compared to T_1 and T_2 , during testing, respectively (Figures 4 and 5).

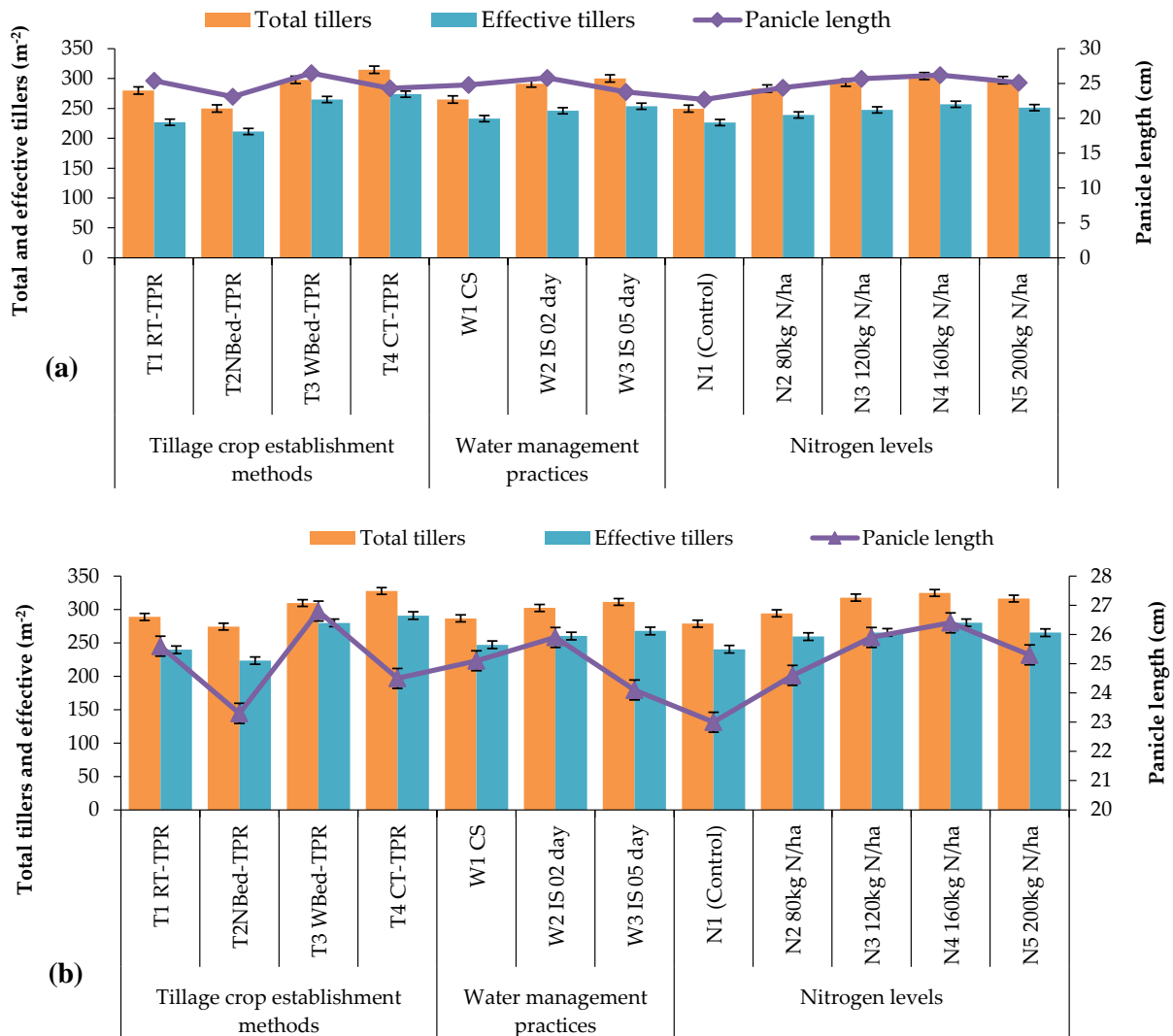


Figure 4. Interactive effects of tillage, water and nitrogen on total and effective tillers and panicle length of rice in both years: (a) 2016 and, (b) 2017.

Irrigation management differences were also shown to be significant in terms of average effective tillers m^{-2} . During both years of study, W_2 and W_3 treatments produced significantly higher yield contributing parameters than W_1 treatment. Differences in nitrogen management were also discovered to be significant in terms of yield contributing parameters. In 2016 and 2017, the N_1 and N_2 treatments produced significantly lower yield contributing parameters than the rest of the nitrogen management. In both the years of study, N_4 treatment produced significantly higher yield contributing parameters than all other treatments except N_3 treatment (Figures 4 and 5). This was due to a 25.2 and 25.9% increase in the quantity of grains per panicle, respectively, during the research years. Similarly, the increase in test weight during the experiment was between 25.8 and 26.2%. The current study's findings on the interactive effects of tillage, water and nitrogen on total and effective tillers, panicle length, spikelets, and grains/panicle and 1000 grain weight of rice were also corroborated by previous studies [39–43].

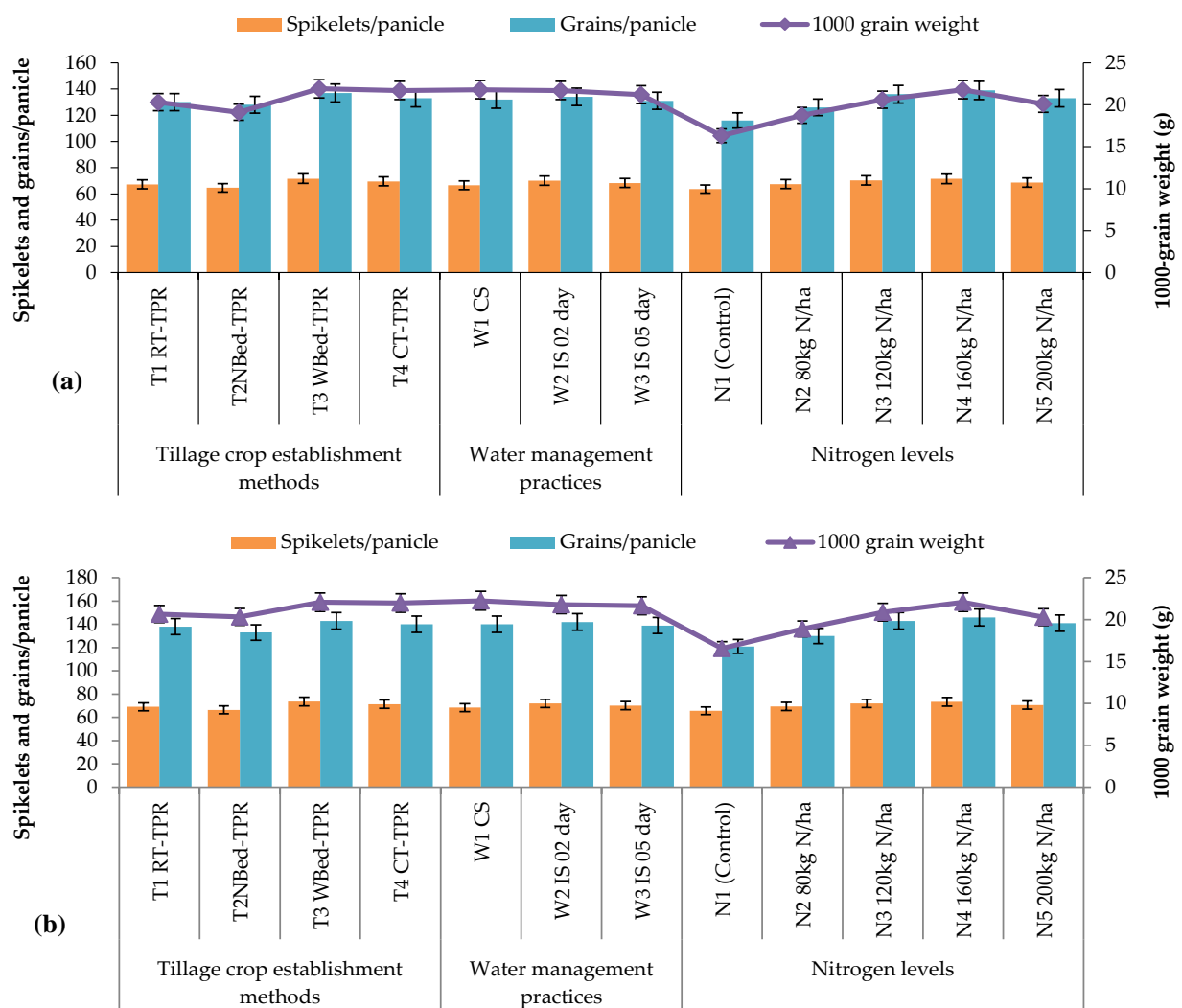


Figure 5. Interactive effects of tillage, water and nitrogen on spikelets and grains/panicle and 1000 grain weight of rice in both years: (a) 2016 and, (b) 2017.

During the study period, T₄ treatment (rice transplanted on wide raised beds) yielded the highest grain and straw yield (48.10 and 64.7 q ha⁻¹) and T₃ treatment (rice transplanted on narrow raised beds) (45.2 and 60.9 q ha⁻¹) remained statistically similar (Figure 6). The decline in grain and straw yield due to unpuddled tillage, i.e., reduced tillage and narrow raised bed practices, was 16.1, 9.8; 10.6, 3.9 and 17.2, 11.9, 12.1, 6.6% compared to T₄ and T₃ practices, respectively. However, rice transplanted on widespread raised beds of 4.1% recorded a significant increase in yield compared to the reduced tillage options.

Yields pertaining to grain and straw are reported to be significantly influenced by the interactive effects of water and N management. During both experimental years, W₁ treatment (continuously submerged to a depth of 5 cm) had a significantly higher grain yield (45.92, 46.89 and 63.16, 63.97 q ha⁻¹) when compared to all other water management treatments (Figure 6a,b). Moreover, W₂ treatment (intermittent submergence of 5 cm and irrigation after 2 days of disappearance of water from soil surface) was significantly superior to W₃ treatment (intermittent submergence of 5 cm and irrigation after 5 days of disappearance of water from soil surface), which recorded minimum grain yield during the years of study.

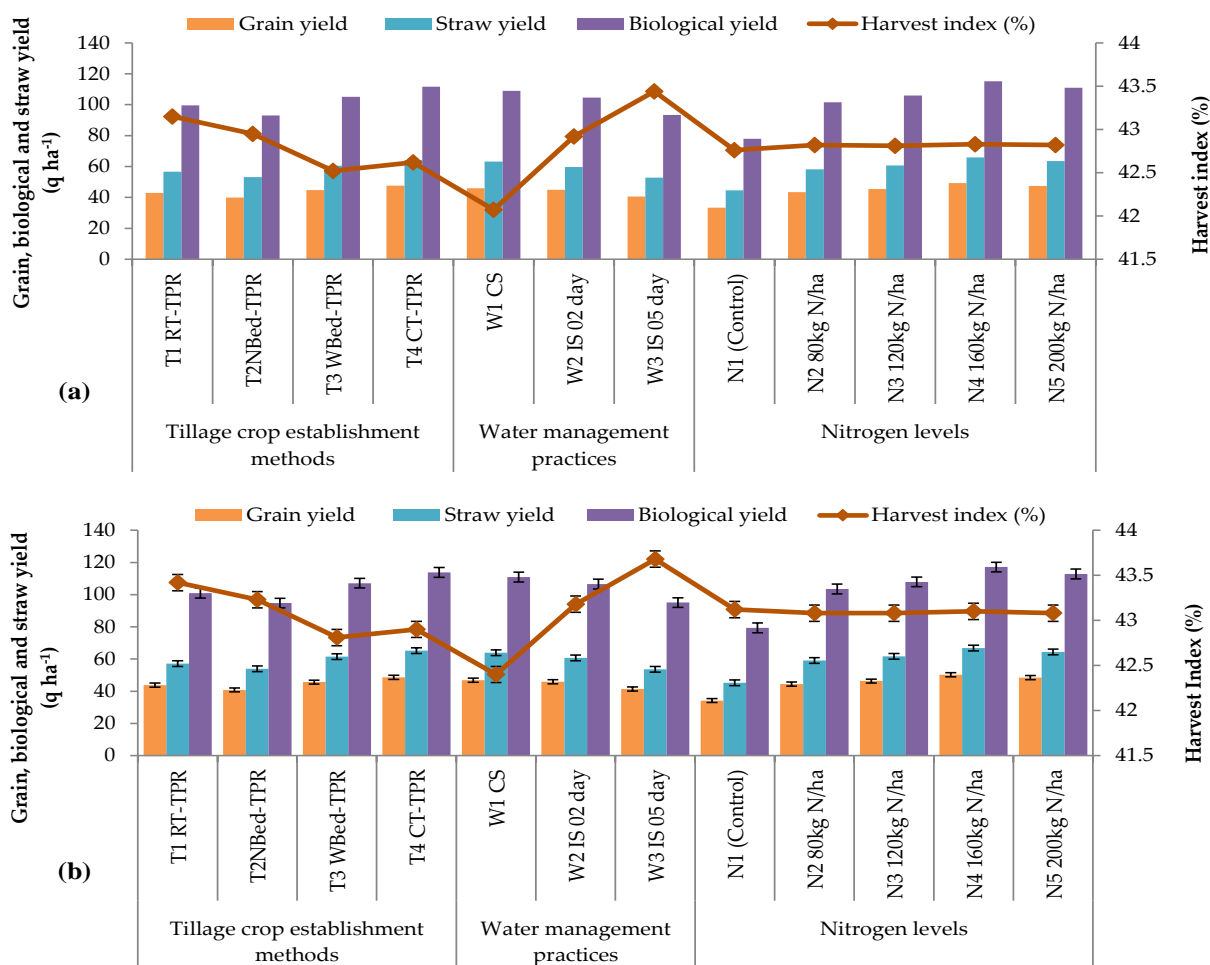


Figure 6. Interactive effects of tillage, water and nitrogen on grain, biological and straw yield, and harvest index (%) of rice in both years: (a) 2016 and (b) 2017.

Furthermore, grain yields of 49.30, 50.26 and 65.93 and 66.88 q ha^{-1} were significantly improved in the N_4 treatment, which remained statistically comparable to the N_5 treatment. The yield of N_3 treatment (120 kg N ha^{-1}) was much higher than that of N_2 and N_1 “control” treatments (Figure 6a,b). During the experimentation, the same yield behavior was observed for biological yield.

Due to favorable weather conditions, crop performance was somewhat higher in 2017 than in 2016. On the other hand, inorganic nitrogen sources may provide increased nutritional availability, allowing for improved growth and development. Because there were more nutrients accessible for crop growth, N_4 treatment (160 kg N ha^{-1}) had significantly greater grain (62.3 and 61.8%), straw (34.9 and 35.5%) and biological yield (36.1 and 48.7%) than N_1 treatment (Figure 6a,b). Poor nutrition had a greater impact on grain yield, as evidenced by [40–46], resulting in a significant drop in harvest index.

The harvest index is a critical criterion for evaluating how well dry matter is partitioned to the crop’s economic component. In irrigation and nutrient management treatments, all the treatments proved higher than W_3 and N_1 treatments during both years of study. However, all treatments were comparable to one another. There was no discernible trend in terms of planting techniques on the harvest index. However, during the experimental period, the T_1 treatment had the largest harvest index while the T_4 treatment had the lowest (Figure 6a,b).

3.5. Profitability

The year 2017 was reported with better profitability indices such as rice grain yield with reduced cultivation costs compared to 2016 (Figure 7). Various tillage operations increase total farming costs, gross income, net profit and B:C ratio due to better grain yields and hence gross income than the cost of cultivation. Of all the tillage techniques, the T₃ treatment had the highest net profit, gross income and B:C ratio. This could be owing to the better proficiency of FIRB systems compared to other tillage methods, as well as a better production gain when compared with other treatments. Among the various nitrogen doses, N₄ treatment had the highest net profit, gross income and B:C ratio. This could be attributed to the N₄ treatment's superior efficiency compared to the other N treatments, as well as the better rice grain yield hike compared to other treatments. As also reported by [47,48], lower nitrogen doses may not have satisfied crop requirements during the great growth period when bigger levels were required, causing crop growth and output to suffer.

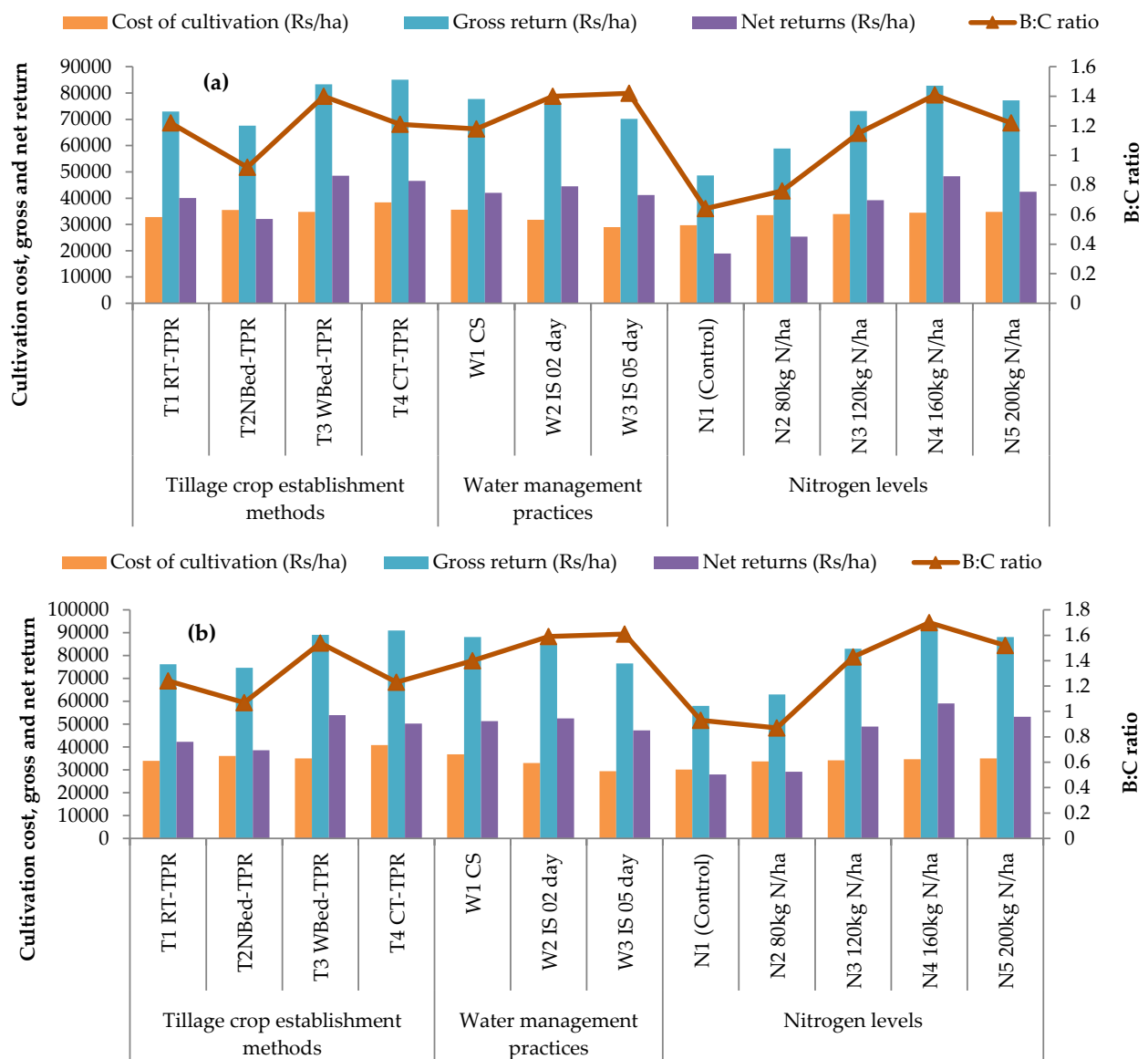


Figure 7. Interactive effects of tillage, water and nitrogen on the profitability of rice in both years: (a) 2016 and (b) 2017.

4. Conclusions

Finally, a two-year study covering tillage, water and nitrogen interactive effects on wet rice conclude that puddling is the most popular and commonly utilized crop establishment technique on the Indo-Gangetic Plain of India. However, it causes significant limits to production and sustainability of rice–wheat systems. Puddling is not necessary to produce high grain yields, according to two years of research in western Uttar Pradesh, India. Transplanting in unpuddled wide raised beds may be a viable option, and farmers can accept them if they are provided with the right information and recommendations. Rice transplanting under unpuddled wide raised beds is cost effective and can match conventional planting yields if weed control is accomplished. According to the findings, water footprints, crop water productivity and yield attributes of rice crops grown with optimal tillage, water and nitrogen management strategies improved significantly. In addition, if irrigation scheduling is reworked to accommodate these tactics, irrigation water can be saved. Hence, computation of the water balance parameters as affected by tillage, water and nitrogen management strategies to grow rice must be discovered for texturally divergent soils and under various agro-climatic conditions. Green water is important in rice cultivation and there is a lot of room to enhance water productivity by increasing yield levels within the existing water balance. The plots under WBed-TPR had significantly higher nutrient use efficiency, rice productivity and profitability than NBed-TPR and RT-TPR plots. The findings indicate that conservation tillage would enhance grain quality and yield while also being environmentally friendly. Although nitrogen fertilizer increases the probability of intensive agriculture, it does so at the expense of environmental protection. This study indicates that optimum tillage, water and nitrogen management strategies or technologies appear to be viable solutions for long-term rice productivity. However, local governments should encourage farmers to manage water and nutrients based on conservation tillage to improve their water footprint, profitability and crop quality and increase their crop water productivity for the long term.

Author Contributions: Conceptualization, data curation, methodology, formal analysis and writing—original draft, S.T. and R.K.N.; project administration, supervision, formal analysis and writing—review and editing, R.B. and M.S.C.; funding acquisition and writing—review and editing, A.A.A., A.Z.D. and M.A.M. All authors have read and agreed to the published version of the manuscript.

Funding: This research was financially supported by the Vice Deanship of Research Chairs at King Saud University.

Institutional Review Board Statement: Not applicable.

Informed Consent Statement: Not applicable.

Data Availability Statement: Data recorded in the current study are available in all tables and figures of the manuscript.

Acknowledgments: The authors extend their appreciation to the financial support given by the Vice Deanship of Research Chairs at King Saud University. Furthermore, the authors would like to acknowledge the Sardar Vallabhbhai Patel University of Agriculture and Technology in Meerut, Uttar Pradesh, India for facilitating necessary requirements for field experimentation and sample analysis.

Conflicts of Interest: The authors declare no conflict of interest.

References

1. IRRI. Rice Facts. Available online: <http://www.sustainable-rice.org/Resources/> (accessed on 1 January 2022).
2. Food and Agriculture Organization of the United Nations (FAO). *Energy-Smart for People and Climate*; Issue Paper; FAO: Rome, Italy, 2011.
3. Hoff, H. Understanding the Nexus. In Proceedings of the Bonn 2011 Conference: The Water, Energy and Food Security Nexus, Stockholm, Sweden, 16–18 November 2011; Stockholm Environment Institute (SEI): Stockholm, Sweden, 2011.
4. Silalertruksa, T.; Gheewala, S.H.; Mungkung, R.; Nilsalab, P.; Lecksiwilai, N.; Sawaengsak, W. Implications of Water Use and Water Scarcity Footprint for Sustainable Rice Cultivation. *Sustainability* **2017**, *9*, 2283. [CrossRef]

5. Hoekstra, A.Y.; Chapagain, A.K. Water footprints of nations: Water use by people as a function of their consumption pattern. *Water Resour. Manag.* **2007**, *21*, 35–48. [CrossRef]
6. Johannes, H.P.; Priadi, C.R.; Herdiansyah, H.; Novalia, I. Water footprint saving through organic rice commodity. *AIP Conf. Proc.* **2020**, *2255*, 040002. [CrossRef]
7. Mekonnen, M.M.; Hoekstra, A.Y. Water footprint benchmarks for crop production: A first global assessment. *Ecol. Indic.* **2014**, *46*, 214–223. [CrossRef]
8. Pfister, S.; Bayer, P. Monthly water stress: Spatially and temporally explicit consumptive water footprint of global crop production. *J. Clean. Prod.* **2014**, *73*, 52–62. [CrossRef]
9. Lovarelli, D.; Bacenetti, J.; Fiala, M. Water Footprint of crop productions: A review. *Sci. Total Environ.* **2016**, *548–549*, 236–251. [CrossRef]
10. Chukalla, A.D.; Krol, M.S.; Hoekstra, A.Y. Green and blue water footprint reduction in irrigated agriculture: Effect of irrigation techniques, irrigation strategies and mulching. *Hydrol. Earth Syst. Sci.* **2015**, *19*, 4877–4891. [CrossRef]
11. Naresh, R.K.; Timsina, J.; Dwivedi, A.; Kumar, V.; Singh, V.; Shukla, A.K.; Singh, S.P.; Gupta, R.K. Water footprint of rice from both production and consumption perspective assessment using remote sensing under subtropical India: A review. *Int. Chem. Stud.* **2017**, *5*, 343–350.
12. Chapagain, A.K.; Hoekstra, A.Y. The blue, green and grey water footprint of rice from production and consumption perspectives. *Ecol. Econ.* **2011**, *70*, 749–758. [CrossRef]
13. Cai, X.L.; Sharma, B.R. Integrating remote sensing, census and weather data for an assessment of rice yield, water consumption and water productivity in the Indo-Gangetic river basin. *Agric. Water Manag.* **2010**, *97*, 309–316. [CrossRef]
14. Jat, M.L.; Gathala, M.K.; Ladha, J.K.; Saharawat, Y.S.; Jat, A.S.; Kumar, V.; Sharma, S.K.; Kumar, V.; Gupta, R. Evaluation of precision land levelling and double zero-till systems in the rice–Wheat rotation: Water use, productivity, profitability and soil physical properties. *Soil Tillage Res.* **2009**, *105*, 112–121. [CrossRef]
15. Naresh, R.K.; Singh, S.P.; Singh, A.; Khilari, K.; Shahi, U.P.; Rathore, R.S. Evaluation of precision land leveling and permanent raised bed planting in maize–wheat rotation: Productivity, profitability, input use efficiency and soil physical properties. *Indian J. Agric. Sci.* **2012**, *105*, 112–121.
16. Keys, W.P.; Barnes, E.A.; van der Ent, R.J.; Gordon, L.J. *Variability of Moisture Recycling Using a Precipitation Shed Framework*; Copernicus Publications on behalf of the European Geosciences Union: Göttingen, Germany, 2012.
17. Zang, C.F.; Liu, J.; vander Velde, M.; Kraxner, F. Assessment of spatial and temporal patterns of green and blue water flows under natural conditions in inland river basins in North West China. *Hydrol. Earth Syst. Sci.* **2012**, *16*, 2859–2870. [CrossRef]
18. Lal, R.; Stewart, B.A. (Eds.) *Principles of Sustainable Soil Management in Agro-Ecosystems*; CRC Press: Boca Raton, FL, USA, 2013; Volume 20.
19. Naresh, R.K.; Gupta, R.K.; Gajendra, P.; Dhaliwal, S.S.; Kumar, D.; Kumar, V. Tillage Crop Establishment Strategies and Soil Fertility Management: Resource Use Efficiencies and Soil Carbon Sequestration in a Rice–Wheat Cropping System. *Ecol. Environ. Conserv.* **2015**, *21*, 127–134.
20. Naresh, R.K.; Gupta, R.K.; Rathore, R.S.; Singh, S.P.; Dwivedi, A.; Singh, V. Effects of tillage and residue management on soil aggregation, soil carbon sequestration and yield in rice–wheat cropping system. *J. Pure Appl. Microbiol.* **2016**, *10*, 1987–2003.
21. Cook, R.L.; Trlica, A. Tillage and Fertilizer Effects on Crop Yield and Soil Properties over 45 Years in Southern Illinois. *Agron. J.* **2016**, *108*, 415–426. [CrossRef]
22. Huang, S.; Zhao, C.; Zhang, Y.; Wang, C. *Nitrogen Use Efficiency in Rice, Nitrogen in Agriculture-Updates, Amanullah and Shah Fahad*; IntechOpen: London, UK, 2017. [CrossRef]
23. Lee, S. Recent Advances on Nitrogen Use Efficiency in Rice. *Agronomy* **2021**, *11*, 753. [CrossRef]
24. Li, P.; Lu, J.; Wang, Y.; Wang, S.; Hussain, S.; Ren, T.; Cong, R.; Li, X. Nitrogen losses, use efficiency, and productivity of early rice under controlled-release urea. *Agric. Ecosyst. Environ.* **2018**, *251*, 78–87. [CrossRef]
25. Guo, J.; Hu, X.; Gao, L.; Xie, K.; Ling, N.; Shen, Q.; Hu, S.; Guo, S. The rice production practices of high yield and high nitrogen use efficiency in Jiangsu, China. *Sci. Rep.* **2017**, *7*, 2101. [CrossRef]
26. Kar, G.; Kumar, A.; Sahoo, N.; Mohapatra, S. Radiation utilization efficiency, latent heat flux and crop growth simulation in irrigated rice during post-flood period in east coast of India. *Paddy Water Environ.* **2013**, *12*, 285–297. [CrossRef]
27. Derpsch, R.; Franzluebbers, A.J.; Duiker, S.W.; Reicosk, D.C.; Koeller, K.; Friedrich, T.; Sturny, W.G.; Sá, J.C.M.; Weiss, K. Why do we need to standardize no-tillage research? *Soil Tillage Res.* **2014**, *137*, 16–22. [CrossRef]
28. Hoekstra, A.Y.; Chapagain, A.K. *Globalization of Water: Sharing the Planet’s Freshwater Resources*; Blackwell Publishing: Oxford, UK, 2008.
29. Albrizio, R.; Todorovic, M.; Matic, T.; Stellacci, A.M. Comparing the interactive effects of water and nitrogen on durum wheat and barley grown in a Mediterranean environment. *Field Crops Res.* **2010**, *115*, 179–190. [CrossRef]
30. Fageria, N.K.; Baligar, V.C. Enhancing nitrogen use efficiency in crop plants. *Adv. Agron.* **2005**, *88*, 97–185.
31. Craswell, E.T.; Godwin, D.C. The efficiency of nitrogen fertilizers applied to cereals in different climates. *Adv. Plant Nutr.* **1984**, *1*, 1–55.
32. Sandhu, S.S.; Mahal, S.S.; Vashist, K.K.; Buttar, G.S.; Brar, A.S.; Singh, M. Crop and water productivity of bed transplanted rice as influenced by various levels of nitrogen and irrigation in northwest India. *Agric. Water Manag.* **2012**, *104*, 32–39. [CrossRef]

33. Ingle, A.V.; Shelke, D.K.; Aghav, V.D.; Karad, M.L. Effect of irrigation schedules and nutrient management on WUE and nutrient uptake of wheat on vertisol. *J. Soils Crops* **2007**, *17*, 188–190.
34. Yadav, S.; Humphreys, E.; Kukal, S.S.; Gill, G.; Rangarajan, R. Effect of water management on dry seeded and puddled transplanted rice part 2: Water balance and water productivity. *Field Crops Res.* **2011**, *120*, 123–132. [CrossRef]
35. Nalley, L.L.; Linqvist, B.; Kovacs, K.F.; Anders, M.M. The economic viability of alternate wetting and drying irrigation in Arkansas rice production. *Agron. J.* **2015**, *107*, 579–587. [CrossRef]
36. Pastor, A.V.; Ludwig, F.; Biemans, H.; Hoff, H.; Kabat, P. Accounting for environmental flow requirements in global water assessments. *Hydrol. Earth Syst. Sci. Discuss.* **2013**, *10*, 14987–15032. [CrossRef]
37. Karimi, P.; Bastiaanssen, W.G.M.; Molden, D.; Cheema, M.J.M. Basin-wide water accounting based on remote sensing data: An application for the Indus Basin. *Hydrol. Earth Syst. Sci.* **2013**, *17*, 2473–2486. [CrossRef]
38. Kiptala, J.K.; Mul, M.L.; Mohamed, Y.A.; van der Zaag, P. Modelling stream flow and quantifying blue water using a modified STREAM model for a heterogeneous, highly utilized and data-scarce river basin in Africa. *Hydrol. Earth Syst. Sci.* **2014**, *18*, 2287–2303. [CrossRef]
39. Naresh, R.K.; Arup, G.; Vivak, K.; Gupta, R.K.; Singh, S.P.; Purushottam; Vineet, K.; Vikrant, K.; Mahajan, N.C.; Arun, K.; et al. Tillage Crop Establishment and Organic Inputs with Kappaphycus-Sap Effect on Soil Organic Carbon Fractions and Water Footprints. *Int. J. Curr. Res. Acad. Rev.* **2017**, *5*, 57–69.
40. Mahajan, G.; Bharaj, T.S.; Timsina, J. Yield and water productivity of rice as affected by time of transplanting in Punjab, India. *Agric. Water Manag.* **2009**, *96*, 525–532. [CrossRef]
41. Jat, R.K.; Sapkota, T.B.; Singh, R.G.; Jat, M.L.; Kumar, M.; Gupta, R.K. Seven years of conservation agriculture in a rice–wheat rotation of Eastern Gangetic Plains of South Asia: Yield trends and economic profitability. *Field Crops Res.* **2014**, *164*, 199–210. [CrossRef]
42. Naresh, R.K.; Tomar, S.S.; Samsher, P.; Singh, S.P.; Kumar, D.; Dwivedi, A.; Kumar, V. Experiences with rice grown on permanent raised beds: Effect of water regime and planting techniques on rice yield, water use, soil properties and water productivity. *Rice Sci.* **2014**, *21*, 170–180. [CrossRef]
43. Carrijo, D.R.; Lundy, M.E.; Linqvist, B.A. Rice yields and water use under alternate wetting and drying irrigation: A meta-analysis. *Field Crops Res.* **2017**, *203*, 173–180. [CrossRef]
44. Singh, G.; Walia, S.S. Influence of FYM, brown manuring and levels of nitrogen on yield and soil properties of direct seeded and transplanted rice. *Geobios* **2010**, *37*, 210–216.
45. Kumar, S.; Sundaram, S.S.; Shivani, P.K.; Bhatt, B.P. *Agronomic Management and Production Technique of Unpuddled Mechanical Transplanted Rice*; Technical bulletin no. R-37/Pat-24; ICAR-RCER: Patna, India, 2015.
46. Mylavarapu, K.R.S.; Li, Y.C.; Reddy, G.B.; Reddy, M.D. Impact of aerobic rice cultivation on growth, yield, and water productivity of rice–maize rotation in semiarid tropics. *Agron. J.* **2012**, *104*, 1757–1765. [CrossRef]
47. Naresh, R.K.; Bhatt, R.; Chandra, M.S.; Laing, A.M.; Gaber, A.; Sayed, S.; Hossain, A. Soil organic carbon and system environmental footprint in sugarcane-based cropping systems are improved by precision land leveling. *Agronomy* **2021**, *11*, 1964. [CrossRef]
48. Naresh, R.K.; Rathore, R.S.; Dhaliwal, S.S.; Yadav, R.B.; Kumar, D.; Singh, S.P.; Nawaz, A.; Kumar, N.; Gupta, R.K. Crop Establishment Methods: Foliar and Basal Nourishment of rice (*Oryza sativa*) Cultivation Affecting Growth Parameters, Water Saving, Productivity and Soil Physical Properties. *Paddy Water Environ.* **2015**, *14*, 373–386. [CrossRef]

Article

Interactive Effects of Nitrogen and Potassium Fertilizers on Quantitative-Qualitative Traits and Drought Tolerance Indices of Rainfed Wheat Cultivar

Mohammad Hossein Sedri ^{1,*}, Ebrahim Roohi ² , Mohsen Niazian ²  and Gniewko Niedbała ³ 

¹ Soil and Water Research Department, Kurdistan Agricultural and Natural Resources Research and Education Center, Agricultural Research, Education and Extension Organization (AREEO), Sanandaj 6616936311, Iran

² Crop and Horticultural Science Research Department, Kurdistan Agricultural and Natural Resources Research and Education Center, Agricultural Research, Education and Extension Organization (AREEO), Sanandaj 6616936311, Iran; roohiebrahim@yahoo.com (E.R.); mniazian@ut.ac.ir (M.N.)

³ Department of Biosystems Engineering, Faculty of Environmental and Mechanical Engineering, Poznań University of Life Sciences, Wojska Polskiego 50, 60-627 Poznań, Poland; gniewko.niedbala@up.poznan.pl

* Correspondence: sedri_mh@yahoo.com; Tel.: +98-9181732273

Abstract: Increasing global food requirements and global warming are two challenges of future food security. Water availability and nutrient management are two important factors that affect high-yield and high-quality wheat production. The main and interactive effects of nitrogen and potassium fertilizers on quantitative-qualitative properties and drought tolerance of an Iranian rainfed cultivar of wheat, Azar-2, were evaluated. Four rates of nitrogen (N0, N30, N60, and N90 kg/ha), along with four concentrations of potassium (K0, K30, K60, and K90 kg/ha), were applied in rainfed (drought stress) and non-stress conditions. The interactive effect of N × K was significant on nitrogen and protein contents of grains at 5% and 1% probability levels, respectively. Different trends of SSI, STI, K1STI, and K2STI indexes were observed with the interactive levels of nitrogen and potassium. The lowest SSI index (0.67) was observed in N30K30, whereas the highest STI (1.07), K1STI (1.46), and K2STI (1.51) indexes were obtained by N90K60 and N90K90. The obtained results could be useful to increase yield and quality of winter rainfed wheat cultivars under drought stress with cool-rainfed areas. N60K30 and N90K60 can be recommended to increase the grain yield and protein content of rainfed wheat under drought stress and non-stress conditions, respectively.

Keywords: drought stress; protein content; rainfed; yield stability; wheat



Citation: Sedri, M.H.; Roohi, E.; Niazian, M.; Niedbała, G. Interactive Effects of Nitrogen and Potassium Fertilizers on Quantitative-Qualitative Traits and Drought Tolerance Indices of Rainfed Wheat Cultivar. *Agronomy* **2022**, *12*, 30. <https://doi.org/10.3390/agronomy12010030>

Academic Editor: Aliasghar Montazar

Received: 24 November 2021

Accepted: 22 December 2021

Published: 24 December 2021

Publisher's Note: MDPI stays neutral with regard to jurisdictional claims in published maps and institutional affiliations.



Copyright: © 2021 by the authors. Licensee MDPI, Basel, Switzerland. This article is an open access article distributed under the terms and conditions of the Creative Commons Attribution (CC BY) license (<https://creativecommons.org/licenses/by/4.0/>).

1. Introduction

Increasing the grain yield and quality of wheat (*Triticum aestivum* L.), as the most widely distributed cereal crop and major staple food crop in the world, is crucial to meet the growing demands of increasing human population [1,2]. Drought stress is a very important abiotic stress that constricts wheat production, especially in arid and semi-arid regions of the world, such as Iran [3]. Significant decreased net photosynthesis, stomatal conductance, relative water contents, 100-grain weight, and grain yield have been reported for 14 bread wheat genotypes under drought stress [4]. Low amounts of mineral nutrients in the soil is the second important constraint for wheat production in arid and semi-arid regions [5]. For an increasing human population, ever increasing global food requirements, and global warming, the development of basic and applied research on drought stress—as one of the most important treats of world food security—is very important [6–8]. Finding plant genotypes with high yield under drought stress and/or enhancing tolerance of drought sensitive genotypes are the proficient approaches to deal with drought stress-induced losses [9]. Selection and breeding of plants are the most economic and effective ways to overcome abiotic stresses [10]. Direct selection of drought

tolerance is not effective, as it is a quantitative character with low heritability. Drought tolerance indices (DTI), such as tolerance (TOL) [11], mean productivity (MP) [11], stress susceptibility index (SSI) [12], geometric mean productivity (GMP) [13], harmonic mean (HARM) [14], relative drought index (RDI) [15], stress tolerance index (STI) [13], yield index (YI) [16], and yield stability index (YSI) [17], which provide a measure of drought based on yield loss under drought condition in comparison to normal condition, are useful tools to assess the tolerance of different genotypes to stressful conditions [18]. Yield-based DTI have been widely applied by researchers to assess the drought tolerance of various important crops, such as oilseed rape (*Brassica napus* L.) [19], teff (*Eragrostis tef* (Zucc.) Trotter) [20], upland cotton (*G. hirsutum* L.) [21], and wheat [3,9,22–24].

As aforementioned, enhancing tolerance of drought sensitive genotypes is the second breeding strategy to cope with detrimental outcomes of drought stress. There are some adjuvants that their exogenous supply can increase the plant's ability to protect itself under stressful conditions [25]. The exogenous supply of some nutrient elements can reduce the inhibitory effects of drought stress on different plants. Nitrogen (N), phosphorous (P), and potassium (K) are three important plant stress ameliorants [26]. Creation of favorable growing conditions buffers plant stress, and long-term grain yield stability of winter wheat can be obtained through balanced nutrient supply [27]. Nitrogen (N)—as vital structural component of proteins, Rubisco, nucleic acids, chlorophyll system, and some hormones [28]—is an important nutrient that has a significant role in stimulating plant growth, development, and increasing crop productivity under environmental stresses [26]. In addition to drought stress, nitrogen deficiency is one of the primary factors limiting productivity of wheat [29]. Agami et al. [30] investigated the effect of exogenous nitrogen supply, N-fertilizer (0.3 and 0.6 g N/kg soil), on drought tolerance of wheat plants and reported that under deficit irrigation condition (60% of ETc), nitrogen-treated plants had higher growth and yield characteristics compared to the untreated plants. They also reported that nitrogen-treated plants were significantly better than untreated plants in terms of grain yield, photosynthetic pigments, and antioxidant enzymes activities. Applied N-fertilizer alleviated the adverse effects of drought stress in wheat plants through keeping higher relative water content and water use efficiency, higher osmoprotectants (soluble carbohydrates, soluble proteins, total soluble phenols, and free proline) and antioxidant systems (peroxidase, superoxide dismutase, glutathione reductase, and catalase) [30]. Sedri et al. [3] assessed the effect of different concentrations of nitrogen fertilizer (0, 30, 60, 90, and 120 kg/ha) on DTI of mean productivity (MP), GMP, TOL, SSI, STI, and modified stress tolerance index (MSTI), in a rainfed wheat cultivar and reported that drought tolerance of nitrogen-treated plants was significantly more than control plants, and STI was the best index for drought tolerance assessment. Potassium is another important nutrient element involved in grain weight, yield, and drought resistance of cereals [31,32]. The significantly higher content of endogenous K in a drought-resistant variety than a drought-sensitive variety of wheat has been reported previously [33]. Potassium is also involved in biotic stress tolerance of wheat [34]. Therefore, it seems that exogenous supply of this nutrient element can lead to positive results in wheat under water deficiency conditions. The positive effects of K fertilizer on grain filling and drought resistance of wheat have been reported [35,36]. Potassium (K⁺) has significant effects on enzyme activation, protein synthesis, photosynthesis, stomatal movement, and water-relation (turgor regulation and osmotic adjustment) in plants [37]. The co-application of N and K can prevent the harmful effects of drought stress through different routes. Application of potassium-nitrate-containing chitosan/montmorillonite microparticles led to significant increased root and shoot length, shoot fresh and dry weight, chlorophyll a, carotenoids, total soluble proteins, soluble sugars, potassium, and phosphorous concentrations of spinach (*Spinacia oleracea* L.) under severe drought stress [5].

In addition to the crop yield, there is an increasing attention to grain quality, especially the grain protein content, in modern intensive agricultural production [38]. In arid and semi-arid environments, wheat grain quality could be greatly affected by drought stress [39].

One of the major challenges in producing high-quality wheat is inconsistency and instability of wheat grain quality during grain filling [40]. Drought stress has an adverse effect on wheat grain development through affecting booting and anthesis stages, disrupting meiosis, reducing pollination efficiency, aborting ovules and seeds, reducing days to anthesis and maturity, and resulting in early seed maturity [41].

Decreased grain yield and quality are the most important challenges of wheat production under drought stress in arid and semi-arid regions. In addition to alleviating the adverse effects of drought stress, the co-application of nitrogen with phosphorus, potassium, and sulfur nutrients can reduce the rates of N fertilizer required by wheat, improve grain yield and protein content, grain yield and grain protein content stability, and subsequently reduce environmental pollution [42]. The present study was conducted to investigate the main and interactive effects of nitrogen and potassium fertilizers on yield components, qualitative characteristics, and yield-based DTI of an Iranian rainfed cultivar (Azar-2) of wheat and find the best interacting levels of N and K on mentioned characteristics under non-stress and drought stress conditions. We hypothesized that yield components, qualitative characteristics, and DTI of Azar-2 would all be affected by the interactions of N and K fertilizers.

2. Materials and Methods

2.1. Experimental Design and Treatments

Two field experiments were conducted, under rainfed (drought stress) and supplemental irrigation (non-stress) conditions, to assess the main and interactive effects of different concentrations of N × K fertilizers on quantitative-qualitative properties, and drought tolerance of Azar-2 rainfed cultivar of wheat, in two continuous growing seasons (2014–2015 and 2015–2016). The treatments consisted of four rates of N (N0, N30, N60, and N90 kg/ha) and K (K0, K30, K60, and K90 kg/ha) fertilizers. Factorial experiments, based on randomized complete block design (RCBD), were conducted in Arid Land Agricultural Research Station of Qamloo in Kurdistan province, Iran (47°29' E longitudes and 35°9' N latitude). The climate of this region is dry and cool [3].

For soil test, soil samples (6 samples, each being a combination of 10 samples) were taken from 0–30 cm depth, before planting. The physico-chemical soil analysis of experimental sites is presented in Table 1. Urea (46% N) and potassium chloride (60% K₂O) fertilizers were used as the source of N and K nutrients, respectively. Half of the mentioned concentrations of N and K fertilizers were broadcasted uniformly in experimental plots; before cultivation in fall, and remaining half was broadcasted in plots at tillering stage of wheat in spring as top-dress fertilizer. Azar-2 rainfed cultivar of wheat was sown at 150 kg seed per ha in plots of size 4 m × 5 m.

Table 1. Soil chemical and physical properties at arid land agricultural research station of Qamloo.

Environment	SP (%)	Ec × 10 ⁻³ (ds/m)	pH	T.N.V (%)	OC (%)	Total.N (%)	P.ava (mg/kg)	K.ava (mg/kg)	Texture
Drought stress	37.820	0.590	7.900	14.380	0.700	0.080	15.900	210.000	Clay
	37.930	0.570	7.900	25.140	0.650	0.080	16.700	200.000	Clay
	39.760	0.620	7.950	15.000	0.670	0.070	16.400	180.000	Clay
Non-stress	39.190	0.600	7.900	15.250	0.670	0.080	16.100	160.000	Clay
	38.320	0.580	7.900	14.880	0.680	0.070	14.700	170.000	Clay
	39.080	0.590	7.900	15.250	0.690	0.080	14.700	160.000	Clay

In non-stress conditions, supplemental irrigations were conducted in flowering and grain filling developmental steps. The volumetric soil water contents at depth 0–30 cm (rooting zone) and 30–60 cm were calculated using a time domain reflectometry (TDR)

probe in different phenological stages. The net depth of irrigation (mm) to bring the soil to field capacity was calculated using Equation (1) [43].

$$I_n = (\theta_{FC} - \theta_i) \times D_z \quad (1)$$

where, I_n is the net depth of irrigation (mm), θ_{FC} is the volumetric soil water content at field capacity ($\text{cm}^3/\text{cm}^{-3}$), θ_i is the volumetric soil water content before irrigation ($\text{cm}^3/\text{cm}^{-3}$), and D_z is the rooting depth (mm).

2.2. Measurements

The main and interactive effects of N and K fertilizers were assessed on quantitative (grain yield, straw yield, and 1000-seed weight) and qualitative (nitrogen and potassium concentrations in flag leaves, nitrogen, potassium, and protein content of seeds) characteristics of Azar-2 cultivar under both drought stress and non-stress conditions. Flag leaf samples were gathered at the heading stage to measure their nitrogen and potassium concentrations. Kjeldahl method was applied to determine the nitrogen content in flag leaf and combined seed samples. Protein content (%) of seed samples was determined by multiplying N content by 6.25 [25]. Atomic absorption spectrum using a flame photometer was applied to estimate the potassium concentration of flag leaf and combined seed samples according to Yoshida et al. [44].

Grain yield, straw yield, and 1000-seed weight (TSW) were measured from randomly selected samples at harvest stage.

2.3. Grain Yield and Grain Protein Content Stability

Stability of grain yield and protein content under interactive effects of applied N and K fertilizers was evaluated using coefficient of variation (CV) index (Equation (2)) [45].

$$\text{Coefficient of variance (CV)} = (\sigma/\bar{Y}) \times 100 \quad (2)$$

where, CV is the coefficient of variance, σ is the standard deviation (t/ha), and \bar{Y} is the average crop yield (t/ha).

2.4. Drought Tolerance Assessment

To assess the interactive effects of applied N and K fertilizers on drought tolerance of Azar-2 cultivar of wheat, different yield-based DTI—including *MP*, *GMP*, *TOL*, *SSI*, *STI*, and modified stress tolerance index (MSTI)—were calculated. Potential yield in normal (the obtained seed yield in non-stress condition) (Y_p) and drought stress condition (Y_s), the average performance in non-stress condition (\bar{Y}_p), and drought stress condition (\bar{Y}_s), were measured and then the mentioned DTI were calculated according to the following Equations (3)–(7) [11–13].

$$MP = \frac{Y_p + Y_s}{2} \quad (3)$$

$$GMP = \sqrt{Y_p \times Y_s} \quad (4)$$

$$TOL = Y_p - Y_s \quad (5)$$

$$SSI = \frac{1 - (Y_s/Y_p)}{1 - (\bar{Y}_s/\bar{Y}_p)} \quad (6)$$

$$STI = \frac{Y_s \times Y_p}{\bar{Y}_p^2} \quad (7)$$

Modified stress tolerance index were calculated for non-stress (defined as K1STI), and drought stress (defined as K2STI) conditions, according to Equations (8) and (9) [46], respectively

$$K1 = Y_{2p}/\bar{y}^2P \quad (8)$$

$$K2 = Y2s/\bar{y}^2s \quad (9)$$

2.5. Statistical Analysis

Statistical analyses, including the analysis of variance (ANOVA) and means comparison analysis were carried out using the MSTATC software. Least significant difference (LSD) test at 1% ($p \leq 0.01$) and 5% ($p \leq 0.05$) probability levels was used for means comparison analysis. The coefficient of variance and drought tolerance indices were calculated using Excel 2010 software. Simple correlation analysis was conducted using SAS[®] software (SAS Institute Inc., Cary, NC, USA).

3. Results and Discussions

3.1. Effect of the Mineral Content of the Soil on Morphological and Qualitative Parameters of the Azar-2 Wheat Cultivar

The correlation coefficient analysis of measured mineral contents of field soil with quantitative and qualitative characteristics of Azar-2 wheat cultivar showed that soil minerals such as N, P, and K had significant correlation with grain yield and grain protein content of Azar-2 cultivar in both stress and non-stress condition (Table 2). As the present study was conducted in an open field, the obtained results are valuable for the future field experiments to predict the grain yield and quality of the cultivated crop.

Table 2. Correlation coefficients of basic mineral content of the field soil with the quantitative and qualitative parameters of the Azar-2 wheat cultivar.

Plant Characteristics	Soil Mineral Contents			
	Total.N (%)	P.ava (mg/kg)	K.ava (mg/kg)	Total Neutralizing Value (T.N.V)
Grain yield	0.745 **	0.591 **	0.432 *	0.081 ns
Straw yield	0.230 ns	0.415 *	0.123 ns	0.341 ns
1000-seed weight	0.653 **	0.471 *	0.215 ns	0.182 ns
Grain N content	0.823 **	0.302 ns	0.243 ns	0.214 ns
Grain K content	0.146 ns	0.214 ns	0.732 **	0.124 ns
Grain protein content	0.516 **	0.504 **	0.361 ns	0.632 **

** , * : Significant at 1% and 5% probability level, respectively. ns: Not significant.

3.2. Main and Interactive Effects of N and K Fertilizers on Quantitative Properties of Wheat under Non-Stress and Drought Stress Conditions

The results of combined ANOVA showed that, under drought stress condition, the main effect of year was significant on grain yield and straw yield at 1% probability level; however, it was not affected 1000-seed weight trait (Table 3). Under non-stress condition, the main effect of year was significant on grain yield, straw yield, and 1000-seed weight of Azar-2 cultivar of wheat at 1% probability level (Table 3). Assessing yield trends in wheat dryland farming and under different fertilization conditions is important to recommend the best fertilizer rates and keep yield increases [47]. Crop yield stability can be assessed through the CV, sustainable yield index (SYI), and some statistical methods such as additive main effects and multiplicative interactions (AMMI). Obtained CV percentage of grain yield under drought stress condition (15.59) was more than that of non-stress condition (10.75) (Table 3). These results indicate higher variation degree and lower stability of average grain yield of Azar-2 cultivar of wheat during 2014–2015 and 2015–2016 growing seasons under drought stress conditions. Unlike grain yield, the CV percentage of straw yield under drought stress conditions (22.6) was lower than calculated CV under non-stress condition (23.25) (Table 3). It is obvious that environmental factors, such as water availability and nutrients, can affect both crops yield and yield stability. In regions with variable water-deficit years, additional water inputs led to more stable yield productivity in different crops, such as wheat, maize, rice, and soybean, with [48]. Balanced nutrient supply can also support long-term crop yield stability [27].

Table 3. Combined analysis of variance of the main and interactive effects of nitrogen and potassium fertilizers on quantitative characteristics of Azar-2 cultivar of wheat under drought stress and non-stress environments.

Source of Variation	df ^a	Mean Squares					
		Drought Stress			Non-Stress		
		Grain Yield	Straw Yield	1000-Seed Weight	Grain Yield	Straw Yield	1000-Seed Weight
Year (Y)	1	25,043,094.000 **	463,457,153.760 **	0.076ns	6,043,077.042 **	306,159,695.010 **	283.800 **
Year × Block	4	235,071.146 *	753,715.948 ns	11.898*	1,941,093.104 **	4,435,583.292 **	25.351 **
Nitrogen (N)	3	1,570,010.069 **	186,390.955 ns	63.570**	4,827,021.917 **	945,981.038 ns	14.306 *
Y × N	3	171,841.917 ns	328267.622 ns	4.778 ns	642,481.125 **	503,941.872 ns	4.887 ns
Potassium (K)	3	20,432.819 ns	547,642.955 ns	2.226 ns	5886.944 ns	1,035,804.233 ns	17.604 ns
Y × K	3	143,145.944 ns	1,253,567.399 ns	5.846 ns	31,186.819 ns	2,319,904.622 ns	0.608 ns
N × K	9	79,243.440 ns	163,752.890 ns	5.099 ns	55,293.694 ns	1,114,630.612 ns	5.808 ns
Y × N × K	9	111,048.639 ns	808,701.927 ns	1.765 ns	125,138.421 ns	2,078,221.446 ns	5.968 ns
Error	60	80,213.690	1,003,141.292	4.206	66,966.582	1,063,045.258	4.356
CV (%)		15.590	22.600	5.170	10.750	23.250	4.380

^a degree of freedom; **, *: Significant at 1% and 5% probability level, respectively. ns: Not significant.

The trend of wheat grain yield stability, based on calculated CV (%), with interactive effects of different rates of N and K fertilizers is depicted in Figure 1a. The highest and lowest CV percentages were obtained from N0 × K30 (30.14%) and N90 × K60 (18.17%) (Figure 1a). These results indicate positive effect of combined use of N and K fertilizers on grain yield stability of rainfed Azar-2 wheat. Azar-2 is a well-known dryland wheat cultivar in Iran, with acceptable levels of water use efficiency, grain yield, and biomass production under water-limited conditions [49]. At present, Azar-2 has the second rank of cultivated area in dryland conditions of cold and temperate regions of Iran. This cultivar can be useful for cultivation in arid and semi-arid regions of the world. The present study conducted in two constitute years to assess the drought response of this cultivar under the effect of N and K fertilizers. Azar-2 cultivar in rotation with a plant species that enriches the soil with nitrogen, such as chickpea (*Cicer arietinum*), is ideal for rainfed agriculture in countries with water scarcity. This rotation can improve nitrogen uptake, grain protein, soil nitrogen, soil properties, and elevated availability of nutrients [50]. Liu et al. [51] investigated the effects of different rates of N fertilizer (100%, 75%, 50%, 25%, and 0%) and two tillage patterns (conventional tillage and no-tillage) on wheat and maize productivity in a long-term experiment (10-year). Authors concluded that higher yield stability, according to the calculated SYI, in both wheat and maize cropping system were obtained by application of 75% and 50% N [51]. In terms of yield stability, the combined use of different fertilizers can be more effective than application of one kind of fertilizer alone [52]. In rainfed winter wheat, using a long-term fertilization experiment (20-year), it was revealed that higher grain yield and sustaining the productivity were obtained by integrated use of N and phosphor (P) fertilizers than the sole application of N and/or P [47]. Han et al. [45] assessed the effects of inorganic fertilizers (N, NP, NPK) and organic manure (M) on the yield stability of rice and wheat during a long term (34-year) field experiment and reported that the combined use of both organic manure and inorganic fertilizer led to lower CV of wheat yield and straw biomass. The yield stability analysis of winter wheat in a long-term fertilization experiment (36-year), using AMMI method, it was revealed that 62.3%, 26.3%, and 11.4% of sums of squares were attributable to fertilization effect, environmental effect, and fertilization × environmental interaction effect, respectively. In addition, authors concluded that the combination of organic and inorganic fertilization led to more stable yields than applied organic or inorganic fertilization alone [53].

In both drought stress and non-stress conditions, the main effect of N fertilizer on grain yield was significant at 1% probability level (Table 3). The main effect of N fertilizer on 1000-seed weight trait was significant under both drought stress and non-stress conditions, at 1% and 5% probability levels, respectively (Table 3). However, this effect was not significant on straw yield under non-stress and drought stress environments (Table 3). Results of means comparison analysis using LSD test showed that grain yield of Azar-2 cultivar of wheat was increased with increasing levels of N fertilizer, under both drought stress and

non-stress environments. However, obtained grain yields in the non-stress environment were more than those obtained under drought stress conditions (Table 4).

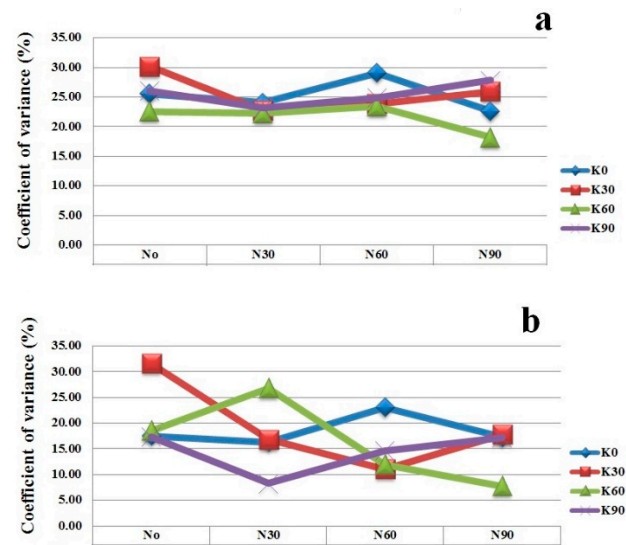


Figure 1. Grain yield and grain protein content stability of rainfed Azar-2 cultivar of wheat. (a) Trend of grain yield stability of wheat Azar-2 cultivar under interaction effects of different rates of nitrogen and potassium fertilizers. (b) Trend of grain protein content stability of wheat Azar-2 cultivar under interaction effects of different rates of nitrogen and potassium fertilizers.

Table 4. Means comparison analysis of the main effect of applied concentrations of nitrogen fertilizer on quantitative characteristics of Azar-2 cultivar of wheat under drought stress and non-stress environments.

Nitrogen (kg/ha)	Drought Stress		Non-Stress	
	Grain Yield (kg/ha)	1000-Seed Weight (g)	Grain Yield (kg/ha)	1000-Seed Weight (g)
N0	1473.000	41.580	1893.000	48.820
N30	1788.000	40.320	2279.000	47.500
N60	1941.000	39.000	2657.000	27.250
N90	2066.000	37.820	2857.000	47.160
LSD (5%)	163.500	1.184	149.400	1.205
LSD (5%)	217.500	1.575	198.700	1.603

Zhang et al. [54] assessed the effect of irrigation and nitrogen application on grain yield and quality of winter wheat over three cropping seasons and reported that N fertilizer significantly increased grain yield, grain protein and the total, essential, and non-essential amino acid content. The results of a long-term (20-years) evaluation of effects of N fertilizer on durum wheat revealed that grain yield was remarkably increased by N fertilizer application [55]. It has been reported that the effect of nitrogen fertilization on grain yield variation of winter wheat is more important than annual weather conditions [27]. Nitrogen affects canopy formation, photosynthesis, and subsequently wheat grain yield. Although growth, grain yield, and quality of wheat absolutely depend upon substantial N inputs [56], finding the optimum concentration and avoid over and under-use of N fertilizer is very important to keep maximum productivity with reduced costs, resource waste, and environmental pollution [51].

The interaction effect of N × K was not significant on grain yield, straw yield, and 1000-seed weight of wheat under both drought stress and non-stress environments (Table 3). These results may relate to the K deficiency in the soil of experimental site (Table 1). In soils with high concentrations of P, K, and S, less N fertilizer might be required for crops to reach rainfall-limited yield potentials. In addition, genetic variation and weather conditions can

also affect N \times nutrient(s) interactions [42]. In addition, water deficiency and drought stress may prevent the absorption of potassium in wheat plants. In comparison with control treatment (N0K0), grain yield of Azar-2 cultivar of wheat increased by 52% with application of N90K60 (Figure 2a). The highest positive increases were then obtained by N90K90 (46%) and N90K0 (42%) interactive effects, respectively (Figure 2a).

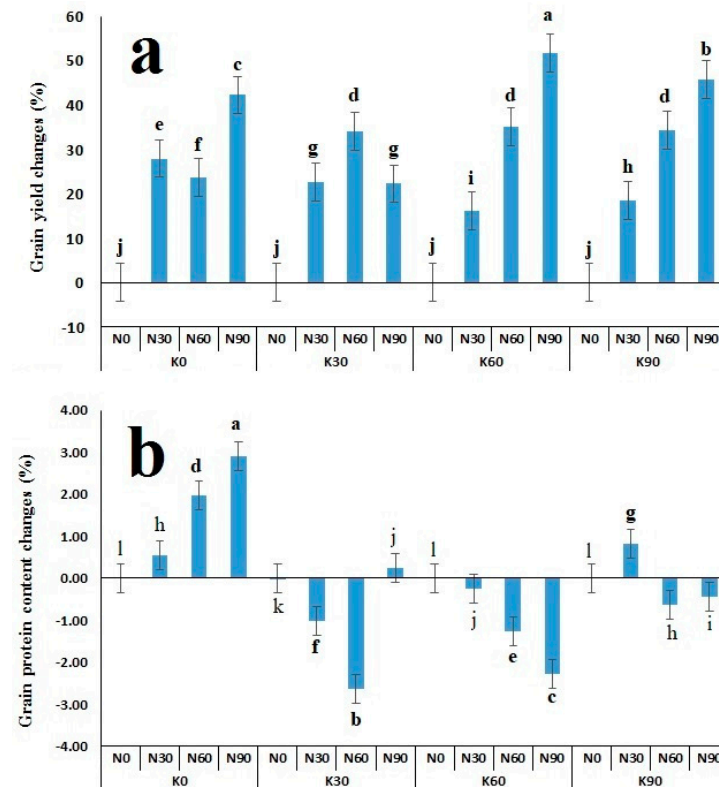


Figure 2. Changes of grain yield and protein content of wheat Azar-2 cultivar under applied interactive rates of N and K fertilizers versus control treatment. (a) Differences of grain yield achieved by interactive effects of N and K fertilizers versus control treatment. (b) Differences of grain protein content achieved by interactive effects of N and K fertilizers versus control treatment. Means followed by the same letters within columns are not significantly different at the 5% level.

Based on the results of combined ANOVA, the main effect of K fertilizer, its interactive effects with year (year \times potassium) and with N fertilizer (nitrogen \times potassium), were not significant on all investigated quantitative characteristics of Azar-2 cultivar of wheat neither in drought stress nor in non-stress environments (Table 3). In addition, the interactive effect of year \times nitrogen \times potassium was not significant on grain yield, straw yield, and 1000-seed weight traits, under both drought stress and non-stress conditions (Table 3). It can be related to the non-significant main effect of potassium. In the hierarchy of nutrients for wheat, carbon, N and P are more important than K [57]. Although it has been reported that K fertilizer can affect grain filling and grain yield of wheat under drought stress conditions [32]; however, the main effect of K and its interactive effect with N fertilizer were not significant on grain yield and 1000-seed yield of wheat in the present study. It can be related to the cool condition of the present study, as the previous study was conducted in a controlled dry condition [32]. Assessing the interactive effects of N fertilizer with other components involved in tolerance to cold and chilling stresses, such as brassinosteroids [58], could be more helpful to increase both drought-cold tolerance in wheat under the environments similar to the present study.

3.3. Main and Interactive Effects of N and K Nutrients on Qualitative Properties of Wheat under Non-Stress and Drought Stress Conditions

According to the results of combined ANOVA, potassium concentration of flag leaves and nitrogen and protein contents of grains were changed during to evaluated growing seasons, under drought stress condition (Table 5). Vazquez et al. [59] also reported the significant effect of the year on grain yield and grain protein concentration of wheat in two growing seasons of 2012 and 2013. The obtained CV percentage of grain protein concentration under drought stress (16.35) was lower than that of non-stress conditions (20.42) (Table 5). These results indicate the higher stability of grain protein content of Azar-2 cultivar of wheat under drought stress environment. Giunta et al. [60] evaluated grain protein stability in old and modern durum wheat cultivars, grown under different cropping systems in terms of soil fertility, sowing date, sowing rate, and nitrogen rate, and reported that the greatest genotype and year interaction ($G \times Y$) was obtained by the more favorable years. They also reported that the interaction of rainfall, during post-anthesis, with nitrogen availability was the main cause of $G \times Y$ interaction for grain protein percentage [60].

Table 5. Combined analysis of variance of the main and interactive effects of nitrogen and potassium fertilizers on qualitative characteristics of Azar-2 cultivar of wheat under drought stress and non-stress environments.

Source of Variation	df ^a	Mean Squares									
		Drought Stress					Non-Stress				
		Flag Leaves		Grain			Flag Leaves		Grain		Protein
N	K	N	K	Protein	N	K	N	K	Protein		
Year (Y)	1	0.013 ns	4.263 **	4.438 **	0.001 ns	144.158 **	3.323 **	0.672 **	3.046 **	0.015 ns	105.169 **
Year \times Block	4	0.957 **	0.090 ns	1.475 **	0.045 **	47.927 **	1.042 **	0.336 **	3.674 **	0.012 ns	120.638 **
Nitrogen (N)	3	0.068 ns	0.058 ns	0.093 ns	0.003 ns	3.073 ns	0.436 ns	0.280 *	0.092 ns	0.006 ns	2.435 ns
Y \times N	3	0.098 ns	0.140 *	0.029 ns	0.012 ns	0.932 ns	0.303 ns	0.064 ns	0.187 ns	0.008 ns	7.067 ns
Potassium (K)	3	0.113 ns	0.047 ns	0.084 ns	0.002 ns	2.722 ns	0.184 ns	0.044 ns	0.057 ns	0.001 ns	2.584 ns
Y \times K	3	0.070 ns	0.021 ns	0.003 ns	0.003 ns	0.083 ns	0.222 ns	0.073 ns	0.280 ns	0.003 ns	10.751 ns
N \times K	9	0.131 ns	0.039 ns	0.271 **	0.006 ns	8.820 **	0.271 ns	0.070 ns	0.126 ns	0.003 ns	3.992 ns
Y \times N \times K	9	0.199 ns	0.082 ns	0.206 *	0.007 ns	6.638 *	0.151 ns	0.050 ns	0.205 ns	0.004 ns	7.533 ns
Error	60	0.196	0.044	0.099	0.005	3.199	0.208	0.091	0.197	0.006	6.405
CV (%)		15.40	16.61	16.360	24.320	16.350	14.090	23.170	20.350	20.740	20.420

^a degree of freedom; **, *: Significant at 1% and 5% probability level, respectively. ns: Not significant.

The main effects of N and K fertilizers were not significant on investigated qualitative characteristics, except in non-stress condition that the main effect of N fertilizer on potassium content of flag leaves was significant at 5% probability level (Table 5). Flag leaves are an important source of N metabolites, including amino acids, which then transport them into the developing kernels [61]. Under drought stress conditions, the interactive effect of N \times K fertilizers was significant on nitrogen and protein contents of wheat grain at a 1% probability level; however, this effect was not significant on all investigated qualitative characteristics under non-stress condition (Table 5). The interactive effect of year \times N \times K was only significant on nitrogen and protein contents of wheat grains at a 5% probability level under drought stress conditions (Table 5). These results indicate the importance of applied fertilizers on qualitative characteristics of wheat grain under water deficiency condition. The use of different nutrients is one of the practical strategies to maintain wheat flour quality. Tao et al. [40] investigated the effect of sulfur fertilization on wheat grain production and wheat flour proteins and reported that grain and protein yields; grain weight; total protein, albumin, gliadin, glutenin, and globulin contents; and total starch were increased using sulfur fertilization. In terms of grain protein concentration stability, the lowest calculated CV was obtained from interaction of N90 \times K60 (7.77); however, the highest CV percentage was obtained from the sole application of K fertilizer (N0 \times K30) (31.52) (Figure 1b). Therefore, the co-application of N and K fertilizers led to the higher grain protein content stability than the individually applied fertilizers (Figure 1b). Balanced nutrition—co-application of N, P, and K, nutrients—may protect proteins against protein dilution as yields increase [42]. Water availability and nutrients supply both can affect the grain N concentration and grain protein content of wheat. Yan et al. [62] reported the

different responses of the grain N concentration of winter wheat to the changing rates of fertilization and irrigation. Authors stated that the grain N concentration was firstly increased and then decreased with increasing rate of fertilization, whereas increasing irrigation rate first led to decrease and then increase of this trait.

Based on the means comparison analysis of the combined data of 2014–2015 and 2015–2016 growing seasons, using LSD test, the highest means of nitrogen and protein contents of wheat grains were obtained from interactive effects of N60 × K0 treatment (Figure 3a,b). The lowest means of these two qualitative characteristics were obtained from N0 × K0 treatment (Figure 3a,b). These results indicate the superiority of N than K in wheat grain quality. In comparison with control treatment (N0K0), protein content of wheat grains increased by 2.90% with application of N90K0 (Figure 2b). However, in contrast to N0K0, protein content changes were 0.24%, −2.28%, and −0.44% with N90K30, N90K60, and N90K90 fertilizers, respectively (Figure 2b). The reduced protein content of wheat grains with increasing levels of K fertilizer, in a constant level of N fertilizer (N90), can be related to the disturbed nutritional balance of wheat under drought stress conditions.

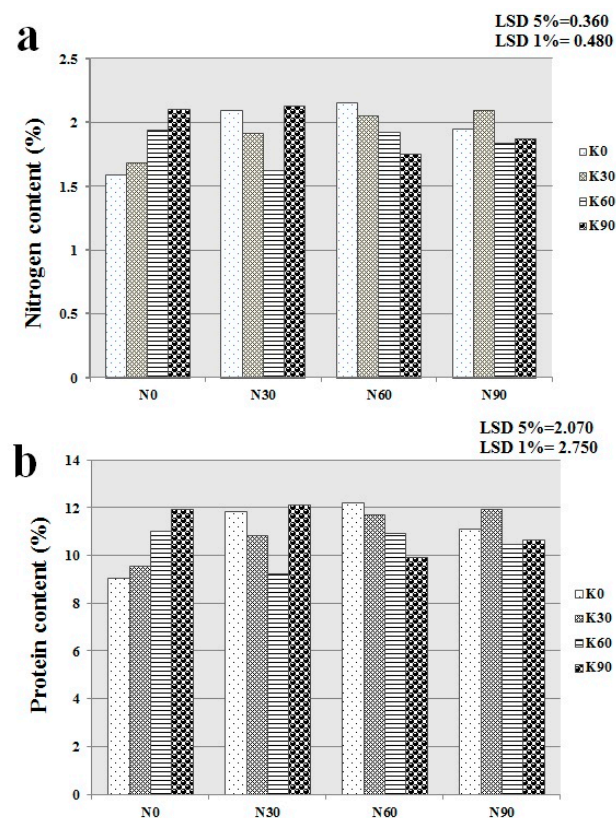


Figure 3. The means comparison analysis of the interactive effects of nitrogen and potassium fertilizers on qualitative characteristics of Azar-2 cultivar of wheat under drought stress condition using LSD test at 5% and 1% probability levels. (a) The interactive effects of nitrogen and potassium fertilizers on nitrogen content of grains. (b) The interactive effects of nitrogen and potassium fertilizers on protein content of grains.

The positive effect of nitrogen fertilization on nitrogen and protein content of wheat grain has been reported previously [63]. Evaluation of long-term (1966–2016) experimental data revealed that grain-nitrogen concentration of wheat increased linearly with increases in N, whereas it reduced with increases in P and K rate [64]. Nitrogen regime has important role in the concentration of storage protein in wheat grains and bread-making quality [59]. Increasing grain protein concentration with increasing levels of N fertilizer has been reported in wheat [65]. Zhang et al. [66] reported that expression of glutamine synthetase genes (*GS1* and *GS2*) in wheat cultivars were significantly increased with applied high

levels of N fertilizer. They also reported that high nitrogen resulted in increased grain yield, grain protein content, and protein fraction. Grain protein concentration is an important factor that determines baking quality of wheat flour. The protein content of wheat grains is more than other important cereals—such as maize (*Zea mays*), millet (*Pennisetum glaucum*), rice (*Oryza sativa*), and rye (*Secale cereale*)—which makes wheat flour valuable for the production of bread, pasta, and other bakery products [56]. Obtained grain protein concentration under drought stress condition (12.24%) (Figure 3b) is suitable for bakery products, as recently it has been reported that baking volume of wheat varieties with a 1–2% lesser protein content than varieties with high raw protein content (13–16%) was similar [56].

3.4. Main and Interactive Effects of N and K Nutrients on Yield-Based Drought Tolerance Indices of Wheat

Estimated values of YP, YS, MP, GMP, TOL, SSI, STI, K1STI, and K2STI in Azar-2 cultivar of wheat under the interactive effects of N and K fertilizers are presented in Table 6. The highest YP and YS values were obtained from N90 × K90 and N90 × K60, respectively (Table 6). The highest MP, GMP, STI, K1STI, and K2STI drought tolerance indices were obtained from the interaction of N90 × K60; whereas the lowest values of the mentioned DTI were obtained from N0 × K60 interactive effect (Table 6). The highest and lowest estimated TOL and SSI values were obtained from the N90 × K30 and N0 × K90 interactive effects, respectively (Table 6). The obtained results indicate the greater importance of N fertilizer than K fertilizer in drought tolerance of wheat. These results also showed the high interaction effects of investigated concentrations of N and K fertilizers on DTI of Azar-2 cultivar of wheat. Correlation coefficient of drought tolerance indices and grain yield is a suitable criterion for screening the best indices [67].

Table 6. Drought indexes in different rates of nitrogen and potassium fertilizers in rainfed wheat over two years.

Nitrogen (kg/ha)	Potassium (kg/ha)	Ys (kg/ha)	Yp (kg/ha)	MP	GMP	TOL	SSI	STI	K2STI	K1STI
N0	K0	1483	1881	1682	1670	398	0.86	0.48	0.31	0.29
	K30	1537	1853	1695	1688	317	0.70	0.49	0.35	0.28
	K60	1411	1924	1667	1648	512	1.08	0.47	0.28	0.29
	K90	1461	1700	1580	1576	238	0.57	0.43	0.27	0.21
N30	K0	1898	2356	2127	2114	458	0.79	0.77	0.83	0.72
	K30	1885	2254	2070	2061	369	0.67	0.73	0.78	0.63
	K60	1638	2230	1934	1911	592	1.08	0.63	0.50	0.53
	K90	1731	2278	2005	1986	547	0.98	0.68	0.61	0.59
N60	K0	1835	2731	2283	2238	896	1.34	0.86	0.87	1.08
	K30	2060	2646	2353	2335	585	0.90	0.94	1.19	1.10
	K60	1906	2514	2210	2189	609	0.99	0.83	0.89	0.88
	K90	1962	2737	2350	2317	775	1.15	0.93	1.06	1.17
N90	K0	2110	2748	2429	2408	638	0.95	1.00	1.33	1.27
	K30	1880	2880	2380	2327	1000	1.41	0.93	0.98	1.30
	K60	2142	2896	2519	2491	754	1.06	1.07	1.46	1.51
	K90	2129	2903	2516	2486	774	1.09	1.07	1.44	1.51
	Mean	1817	2408	2112	2090	591	0.98	0.77	0.82	0.83

Yp: grain yield under non-stress condition; Ys: grain yield under drought-stress condition; MP: mean productivity; GMP: geometric mean productivity; TOL: tolerance; SSI: stress susceptibility index; STI: stress tolerance index; K1STI: modified stress tolerance index in non-stress condition; K2STI: modified stress tolerance index in drought stress condition.

The simple correlation of calculated yield-based drought tolerance indices with grain yield under the non-stressed (Yp) and moisture-stressed (Ys) conditions are shown in Table 7. K2STI showed the highest positive correlation with grain yield under drought stress

condition ($r = 0.96^{**}$), following with GMP and STI indices ($r = 0.94^{**}$) (Table 7). K1STI, MP, GMP, and STI showed the highest positive correlation with grain yield under non-stress condition (Table 7). Nitrogen can improve drought tolerance of wheat through affecting physiological and biochemical processes such as accumulation of osmoprotectants and activity of antioxidant enzymes [26]. There is a positive correlation between water deficit stress and accumulation of reactive oxygen species (ROS) in cellular organelles [1,68]. Some cellular components, such as osmoprotectants and antioxidants, can stabilize cell membrane and proteins under stressful conditions through scavenging cellular ROS accumulation and keeping cell osmotic pressure [7,69]. In other hands, it has been reported that exogenous nitrogen supply led to higher osmoprotectants, antioxidant system, and lower relative membrane permeability in wheat plants [30]. Therefore, ROS detoxification and osmotic adjustment are the possible physiological mechanisms through which N-fertilizer can alleviate damages of drought stress in wheat and other plants.

Table 7. Simple correlations of yield-based drought tolerance indices and grain yield of Azar-2 cultivar of wheat.

	Ys	Yp	MP	GMP	TOL	SSI	STI	K2STI	K1STI
Ys	1								
Yp	0.85 **	1							
MP	0.92 **	0.97 **	1						
GMP	0.94 **	0.95 **	0.99 **	1					
TOL	0.56 *	0.86 **	0.77 **	0.75 **	1				
SSI	0.23 ns	0.63 **	0.48 ns	0.45 ns	0.90 **	1			
STI	0.94 **	0.95 **	0.99 **	0.99 **	0.75 **	0.45 ns	1		
K2STI	0.96 **	0.94 **	0.98 **	0.99 **	0.73 **	0.43 ns	0.99 **	1	
K1STI	0.89 **	0.99 **	0.98 **	0.97 **	0.83 **	0.57 *	0.97 **	0.96 **	1

Yp: grain yield under non-stress condition; Ys: grain yield under drought-stress condition; MP: mean productivity; GMP: geometric mean productivity; TOL: tolerance; SSI: stress susceptibility index; STI: stress tolerance index; K1STI: modified stress tolerance index in non-stress condition; K2STI: modified stress tolerance index in drought stress condition. **, *: Significant at 1% and 5% probability level, respectively. ns: not significant.

Estimated SSI values from the interaction of different rates of N fertilizer across applied rates of K fertilizer showed decreasing trend in interaction of lowest concentration of N (N30) with increased concentration of K (K0 to K30), and then it was increased with increasing levels of K (Figure 4a). Estimated STI values during two investigated growing seasons showed an increasing trend with increasing rates of N fertilizer across applied rates of K fertilizer (Figure 4b). The intersection point of STI trend curve was observed in N60 × K30 and N90 × K30 (Figure 4b). Therefore, there is no significant difference between these two interactive treatments in terms of grain yield under drought stress condition. However, the highest STI values were obtained by N90K60 and N90K90. K1STI was also had uniform trends with changing rates of N fertilizer across different rates of K fertilizer (Figure 4c). Unlike K1STI, K2STI showed variable trends, especially with N60 and N90 across different concentrations of K fertilizer (Figure 4d). The highest values of K1STI and K2STI were also obtained by interactive rates of N90K60 and N90K90 (Figure 4c,d). At all, it can be concluded that N90K60 and N90K90 were the best interactive rates of N and K fertilizers in terms of drought tolerance indices. However, N90K60 is the best, as the intersection point of SSI was also obtained in K60 (Figure 4a).

Drought stress indices are mainly applied by researchers to find most tolerant genotypes among huge number of studied genotypes. However, in the present study, DTI were applied to find the best interaction(s) of N and K fertilizers for enhance drought tolerance of a rainfed cultivar, Azar-2, cultivar of wheat. Sedri et al. [3] used drought stress indices of MP, GMP, TOL, SSI, STI, K1STI, and K2STI to evaluate effect of different concentrations of N fertilizer on drought tolerance of rainfed wheat and reported that application of 60 kg/ha N fertilizer improved both grain yield and drought tolerance of wheat. Khan and Mohammad [70] used stress tolerance indices of TOL, MP, harmonic mean (HM), SI, GMP,

STI, YI, YSI, low nitrogen tolerance index (LNTI), nitrogen stress index (NSI), nitrogen index (NI), stress susceptibility percentage index (SSPI), K1STI, K2STI, and relative nitrogen index (RNI) to assess grain yield of wheat varieties under with (N+) and without nitrogen (N0) conditions. They reported that only NI had a positive correlation with grain yield under stress conditions [70].

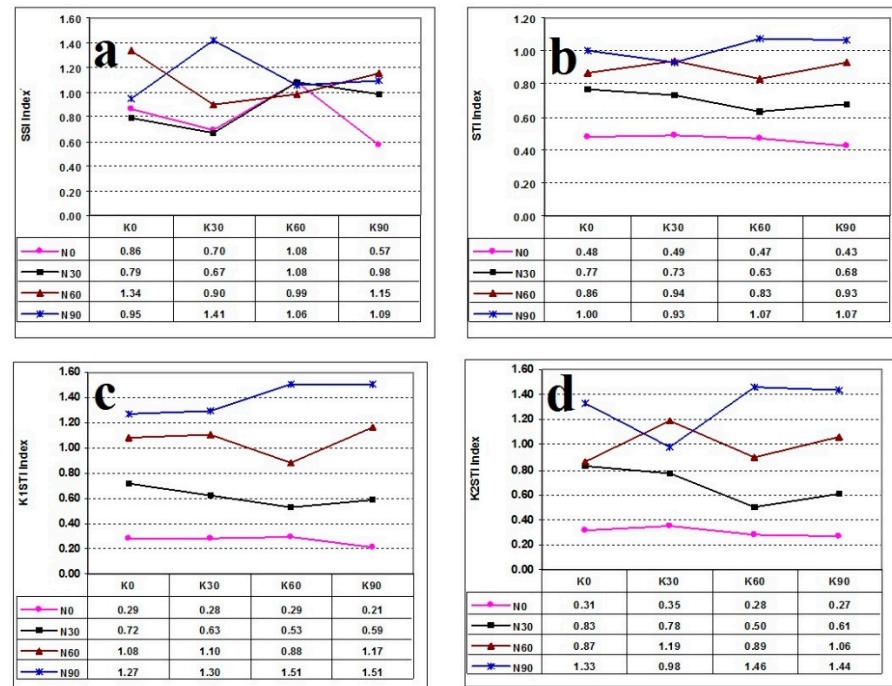


Figure 4. Trend of drought tolerance indices of Azar-2 cultivar of wheat under interactive effects of nitrogen and potassium fertilizers. (a) Trend of estimated SSI values under interactive effects of different concentrations of nitrogen and potassium fertilizers. (b) Trend of estimated STI values under interactive effects of different concentrations of nitrogen and potassium fertilizers. (c) Trend of estimated K1STI values under interactive effects of different concentrations of nitrogen and potassium fertilizers. (d) Trend of estimated K2STI values under interactive effects of different concentrations of nitrogen and potassium fertilizers.

Although yield-based DTI are most applied tools to identify tolerant genotypes in different crops, however, their discrimination efficiency depends on stress severity. Mohammadi [71] applied STI, GMP, MP, TOL, SSI, YSI, and YI drought tolerance indices to identify tolerant genotypes of durum wheat under mild, moderate, and severe levels of drought stress and reported that, under severe stress, discrimination among the genotypes was better than mild stress condition.

4. Conclusions

The exogenous supply of some nutrients, especially nitrogen, can improve grain yield, grain quality, and yield stability of wheat. In addition, these nutrients can alleviate drought stress-induced yield loss of wheat. The interactive effects of N and K fertilizers were not significant on grain yield trait, under both drought stress and non-stress environments; however, the main effect of N was significant on grain yield in both investigated environments. The interactive effects of N and K fertilizers, under drought stress conditions, significantly affected the grain protein content. In comparison with control treatment (N0K0), the highest increases of grain yield and grain protein content were obtained from the interactive rates of N90K60 and N90K0, respectively. The grain yield stability, based on calculated CV percentage of grain yield, of Azar-2 rainfed cultivar of wheat in drought stress condition was lower than non-stress condition. Calculated CV percentage of grain protein content under drought stress was lower than that obtained from non-stress con-

dition. In terms of grain yield and grain protein content stability, the combined use of N and K fertilizers (interaction of N90 × K60) was better than N and K fertilizers individually. The interaction of N90 × K60 led to the highest estimated MP, GMP, STI, K1STI, and K2STI drought tolerance indices. K2STI, GMP, and STI had the highest positive correlation with grain yield of Azar-2 rainfed cultivar of wheat under drought stress condition.

The positive effect of N fertilizer on yield and drought tolerance of wheat was significant in the present study. However, using other components involved in chilling tolerance—such as brassinosteroids and hydrogen sulfide—along with N fertilizer could enhance drought-chilling tolerance of wheat and increase its productivity under environments similar to the environment of the present study (cool and dry).

The present study could be expanded to include other types of fertilizers (individually or combined) and other wheat genotypes in future experiments. Different tolerance-enhancing components could be used along with conventional fertilizers to enhance biotic and abiotic stress tolerance of wheat genotypes. However, there are some limitations for both in-door and open filed assessments in this regard. Genotype × environment interaction is an important influencing factor that should be considered in stress tolerance assessment experiments. Many phenological, morphological, physiological, and biochemical characteristics must be assessed to find the best interaction(s) of applied stress tolerance-enhancers. This creates a multi-factorial condition, which is difficult to interpret. Advanced machine learning algorithms could be useful to make the right decisions in these situations.

Author Contributions: Conceptualization, M.H.S., E.R. and G.N.; Methodology, M.H.S. and G.N.; Software, M.H.S. and E.R.; Validation, M.H.S., E.R. and G.N.; Formal analysis, M.H.S. and G.N.; Investigation, M.H.S. and E.R.; Resources, M.H.S.; Data curation, M.H.S., E.R., and G.N.; Writing—original draft preparation, M.N. and G.N.; Writing—review and editing, G.N.; Visualization, M.N.; Supervision, M.H.S. and G.N.; Project administration, M.H.S. and E.R.; Funding acquisition, M.H.S. All authors have read and agreed to the published version of the manuscript.

Funding: This research (Grant Code: 3-052-182300-00-0000-84121) was funded by Dryland Agricultural Research Institute (DARI) of Iran.

Data Availability Statement: The datasets generated during and/or analyzed during the current study are available from the corresponding author on reasonable request.

Conflicts of Interest: The authors declare no conflict of interest.

References

1. Ma, D.; Sun, D.; Wang, C.; Ding, H.; Qin, H.; Hou, J.; Huang, X.; Xie, Y.; Guo, T. Physiological Responses and Yield of Wheat Plants in Zinc-Mediated Alleviation of Drought Stress. *Front. Plant Sci.* **2017**, *8*, 860. [CrossRef]
2. Niedbała, G.; Nowakowski, K.; Rudowicz-Nawrocka, J.; Piekutowska, M.; Weres, J.; Tomczak, R.J.; Tyksiński, T.; Pinto, A.Á. Multicriteria prediction and simulation of winter wheat yield using extended qualitative and quantitative data based on artificial neural networks. *Appl. Sci.* **2019**, *9*, 2773. [CrossRef]
3. Sedri, M.H.; Amini, A.; Golchin, A. Evaluation of Nitrogen Effects on Yield and Drought Tolerance of Rainfed Wheat using Drought Stress Indices. *J. Crop Sci. Biotechnol.* **2019**, *22*, 235–242. [CrossRef]
4. Wasaya, A.; Manzoor, S.; Yasir, T.A.; Sarwar, N.; Mubeen, K.; Ismail, I.A.; Raza, A.; Rehman, A.; Hossain, A.; EL Sabagh, A. Evaluation of Fourteen Bread Wheat (*Triticum aestivum* L.) Genotypes by Observing Gas Exchange Parameters, Relative Water and Chlorophyll Content, and Yield Attributes under Drought Stress. *Sustainability* **2021**, *13*, 4799. [CrossRef]
5. Bukhari, S.A.B.H.; Lalarukh, I.; Amjad, S.F.; Mansoor, N.; Naz, M.; Naeem, M.; Bukhari, S.A.; Shahbaz, M.; Ali, S.A.; Marfo, T.D.; et al. Drought Stress Alleviation by Potassium-Nitrate-Containing Chitosan/Montmorillonite Microparticles Confers Changes in *Spinacia oleracea* L. *Sustainability* **2021**, *13*, 9903. [CrossRef]
6. Farooq, M.; Wahid, A.; Kobayashi, N.; Fujita, D.; Basra, S.M.A. Plant Drought Stress: Effects, Mechanisms and Management. In *Sustainable Agriculture*; Springer: Dordrecht, The Netherlands, 2009; pp. 153–188.
7. Niazian, M.; Sadat-Noori, S.A.; Tohidfar, M.; Galuszka, P.; Mortazavian, S.M.M. Agrobacterium-mediated genetic transformation of ajowan (*Trachyspermum ammi* (L.) Sprague): An important industrial medicinal plant. *Ind. Crops Prod.* **2019**, *132*, 29–40. [CrossRef]
8. Arafa, S.A.; Attia, K.A.; Niedbała, G.; Piekutowska, M.; Alamery, S.; Abdelaal, K.; Alateeq, T.K.; Ali, M.A.M.; Elkelish, A.; Attallah, S.Y. Seed Priming Boost Adaptation in Pea Plants under Drought Stress. *Plants* **2021**, *10*, 2201. [CrossRef]



9. Anwaar, H.A.; Perveen, R.; Mansha, M.Z.; Abid, M.; Sarwar, Z.M.; Aatif, H.M.; ud din Umar, U.; Sajid, M.; Aslam, H.M.U.; Alam, M.M.; et al. Assessment of grain yield indices in response to drought stress in wheat (*Triticum aestivum* L.). *Saudi J. Biol. Sci.* **2020**, *27*, 1818–1823. [CrossRef]
10. Noori, S.A.S. Assessment for salinity tolerance through intergeneric hybridisation: *Triticum durum* × *Aegilops speltoides*. *Euphytica* **2005**, *146*, 149–155. [CrossRef]
11. Rosielle, A.A.; Hamblin, J. Theoretical Aspects of Selection for Yield in Stress and Non-Stress Environment. *Crop Sci.* **1981**, *21*, 943–946. [CrossRef]
12. Fischer, R.; Maurer, R. Drought resistance in spring wheat cultivars. I. Grain yield responses. *Aust. J. Agric. Res.* **1978**, *29*, 897. [CrossRef]
13. Fernandez, G.C.J. Effective selection criteria for assessing stress tolerance. In *Proceedings of the International Symposium on Adaptation of Vegetables and Other Food Crops in Temperature and Water Stress, Taipei, Taiwan, 13–16 August 1992*; Kuo, C.G., Ed.; AVRDC Publication: Tainan, Taiwan, 1992; pp. 257–270.
14. Schneider, K.A.; Rosales-Serna, R.; Ibarra-Perez, F.; Cazares-Enriquez, B.; Acosta-Gallegos, J.A.; Ramirez-Vallejo, P.; Wassimi, N.; Kelly, J.D. Improving Common Bean Performance under Drought Stress. *Crop Sci.* **1997**, *37*, 43–50. [CrossRef]
15. Fischer, R.; Wood, J. Drought resistance in spring wheat cultivars. III.* Yield associations with morpho-physiological traits. *Aust. J. Agric. Res.* **1979**, *30*, 1001. [CrossRef]
16. Gavuzzi, P.; Rizza, F.; Palumbo, M.; Campanile, R.G.; Ricciardi, G.L.; Borghi, B. Evaluation of field and laboratory predictors of drought and heat tolerance in winter cereals. *Can. J. Plant Sci.* **1997**, *77*, 523–531. [CrossRef]
17. Bouslama, M.; Schapaugh, W.T. Stress Tolerance in Soybeans. I. Evaluation of Three Screening Techniques for Heat and Drought Tolerance. *Crop Sci.* **1984**, *24*, 933–937. [CrossRef]
18. Mitra, J. Genetics and genetic improvement of drought resistance in crop plants. *Curr. Sci.* **2001**, *80*, 758–763.
19. REZA RAMAZANI, S.H.; KALANTARI, R.T. Evaluating the effect of sowing date and drought stress on morphological and functional characteristics of three genotypes of winter oilseed rape (*Brassica napus* L.). *Acta Agric. Slov.* **2019**, *113*, 63. [CrossRef]
20. Ferede, B.; Mekbib, F.; Assefa, K.; Chanyalew, S.; Abraha, E.; Tadele, Z. Evaluation of Drought Tolerance in Tef [*Eragrostis Tef* (Zucc.) Trotter] Genotypes Using Drought Tolerance Indices. *J. Crop Sci. Biotechnol.* **2020**, *23*, 107–115. [CrossRef]
21. Singh, C.; Kumar, V.; Prasad, I.; Patil, V.R.; Rajkumar, B.K. Response of upland cotton (*G.hirsutum* L.) genotypes to drought stress using drought tolerance indices. *J. Crop Sci. Biotechnol.* **2016**, *19*, 53–59. [CrossRef]
22. Boussakouran, A.; Sakar, E.H.; El Yamani, M.; Rharrabti, Y. Morphological Traits Associated with Drought Stress Tolerance in Six Moroccan Durum Wheat Varieties Released Between 1984 and 2007. *J. Crop Sci. Biotechnol.* **2019**, *22*, 345–353. [CrossRef]
23. Mickky, B.; Aldesuquy, H.; Elnajar, M. Uni- and Multi-Variate Assessment of Drought Response Yield Indices in 10 Wheat Cultivars. *J. Crop Sci. Biotechnol.* **2019**, *22*, 21–29. [CrossRef]
24. Elkelish, A.; El-Mogy, M.M.; Niedbała, G.; Piekutowska, M.; Atia, M.A.M.; Hamada, M.M.A.; Shahin, M.; Mukherjee, S.; El-Yazied, A.A.; Shebl, M.; et al. Roles of Exogenous α -Lipoic Acid and Cysteine in Mitigation of Drought Stress and Restoration of Grain Quality in Wheat. *Plants* **2021**, *10*, 2318. [CrossRef]
25. El-Saadony, F.M.A.; Mazrou, Y.S.A.; Khalaf, A.E.A.; El-Sherif, A.M.A.; Osman, H.S.; Hafez, E.M.; Eid, M.A.M. Utilization Efficiency of Growth Regulators in Wheat under Drought Stress and Sandy Soil Conditions. *Agronomy* **2021**, *11*, 1760. [CrossRef]
26. Shabbir, R.N.; Waraich, E.A.; Ali, H.; Nawaz, F.; Ashraf, M.Y.; Ahmad, R.; Awan, M.I.; Ahmad, S.; Irfan, M.; Hussain, S.; et al. Supplemental exogenous NPK application alters biochemical processes to improve yield and drought tolerance in wheat (*Triticum aestivum* L.). *Environ. Sci. Pollut. Res.* **2016**, *23*, 2651–2662. [CrossRef] [PubMed]
27. Macholdt, J.; Honermeier, B. Stability analysis for grain yield of winter wheat in a long-term field experiment. *Arch. Agron. Soil Sci.* **2019**, *65*, 686–699. [CrossRef]
28. Abid, M.; Tian, Z.; Ata-Ul-Karim, S.T.; Cui, Y.; Liu, Y.; Zahoor, R.; Jiang, D.; Dai, T. Nitrogen Nutrition Improves the Potential of Wheat (*Triticum aestivum* L.) to Alleviate the Effects of Drought Stress during Vegetative Growth Periods. *Front. Plant Sci.* **2016**, *7*. [CrossRef] [PubMed]
29. Wang, X.; Wang, L.; Shangguan, Z. Leaf Gas Exchange and Fluorescence of Two Winter Wheat Varieties in Response to Drought Stress and Nitrogen Supply. *PLoS ONE* **2016**, *11*, e0165733. [CrossRef] [PubMed]
30. Agami, R.A.; Alamri, S.A.M.; Abd El-Mageed, T.A.; Abousekken, M.S.M.; Hashem, M. Role of exogenous nitrogen supply in alleviating the deficit irrigation stress in wheat plants. *Agric. Water Manag.* **2018**, *210*, 261–270. [CrossRef]
31. Wani, J.A.; Malik, M.A.; Dar, M.A.; Akhter, F.; Raina, S.K. Impact of method of application and concentration of potassium on yield of wheat. *J. Environ. Biol.* **2014**, *35*, 623–626.
32. Lv, X.; Li, T.; Wen, X.; Liao, Y.; Liu, Y. Effect of potassium foliage application post-anthesis on grain filling of wheat under drought stress. *Field Crop. Res.* **2017**, *206*, 95–105. [CrossRef]
33. Damon, P.M.; Ma, Q.F.; Rengel, Z. Wheat genotypes differ in potassium accumulation and osmotic adjustment under drought stress. *Crop Pasture Sci.* **2011**, *62*, 550. [CrossRef]
34. Jeer, M.; Yele, Y.; Sharma, K.C.; Prakash, N.B. Exogenous Application of Different Silicon Sources and Potassium Reduces Pink Stem Borer Damage and Improves Photosynthesis, Yield and Related Parameters in Wheat. *Silicon* **2021**, *13*, 901–910. [CrossRef]
35. Hu, W.; Jiao, Z.; Wu, F.; Liu, Y.; Dong, M.; Ma, X.; Fan, T.; An, L.; Feng, H. Long-term effects of fertilizer on soil enzymatic activity of wheat field soil in Loess Plateau, China. *Ecotoxicology* **2014**, *23*, 2069–2080. [CrossRef]

36. Raza, M.A.; Saleem, M.; Shah, G.; Khan, I.; Raza, A. Exogenous application of glycinebetaine and potassium for improving water relations and grain yield of wheat under drought. *J. Soil Sci. Plant Nutr.* **2014**, *14*, 348–364. [CrossRef]
37. Kant, S.; Kafkafi, U.; Pasricha, N.; Bansal, S. Potassium and abiotic stresses in plants. *Potassium Sustain. Crop Prod. Gurgaon* **2002**, *233*, 251.
38. Luo, L.; Wang, Z.; Huang, M.; Hui, X.; Wang, S.; Zhao, Y.; He, H.; Zhang, X.; Diao, C.; Cao, H.; et al. Plastic film mulch increased winter wheat grain yield but reduced its protein content in dryland of northwest China. *Field Crop. Res.* **2018**, *218*, 69–77. [CrossRef]
39. Seleiman, M.F.; Al-Suhaibani, N.; Ali, N.; Akmal, M.; Alotaibi, M.; Refay, Y.; Dindaroglu, T.; Abdul-Wajid, H.H.; Battaglia, M.L. Drought Stress Impacts on Plants and Different Approaches to Alleviate Its Adverse Effects. *Plants* **2021**, *10*, 259. [CrossRef]
40. Tao, Z.; Chang, X.; Wang, D.; Wang, Y.; Ma, S.; Yang, Y.; Zhao, G. Effects of sulfur fertilization and short-term high temperature on wheat grain production and wheat flour proteins. *Crop J.* **2018**, *6*, 413–425. [CrossRef]
41. Zahra, N.; Wahid, A.; Hafeez, M.B.; Ullah, A.; Siddique, K.H.M.; Farooq, M. Grain development in wheat under combined heat and drought stress: Plant responses and management. *Environ. Exp. Bot.* **2021**, *188*, 104517. [CrossRef]
42. Duncan, E.G.; O’Sullivan, C.A.; Roper, M.M.; Biggs, J.S.; Peoples, M.B. Influence of co-application of nitrogen with phosphorus, potassium and sulphur on the apparent efficiency of nitrogen fertiliser use, grain yield and protein content of wheat: Review. *Field Crop. Res.* **2018**, *226*, 56–65. [CrossRef]
43. Hesami, A.; Amini, A. Changes in irrigated land and agricultural water use in the Lake Urmia basin. *Lake Reserv. Manag.* **2016**, *32*, 288–296. [CrossRef]
44. Yoshida, S.; Forno, D.A.; Cock, J.H. *Laboratory Manual for Physiological Studies of Rice*; CAB International: Los Banos, Philippines, 1971.
45. Han, X.; Hu, C.; Chen, Y.; Qiao, Y.; Liu, D.; Fan, J.; Li, S.; Zhang, Z. Crop yield stability and sustainability in a rice-wheat cropping system based on 34-year field experiment. *Eur. J. Agron.* **2020**, *113*, 125965. [CrossRef]
46. Farshadfar, E.; Sutka, J. Screening drought tolerance criteria in maize. *Acta Agron. Hungarica* **2002**, *50*, 411–416. [CrossRef]
47. HAO, M.-D.; FAN, J.; WANG, Q.-J.; DANG, T.-H.; GUO, S.-L.; WANG, J.-J. Wheat Grain Yield and Yield Stability in a Long-Term Fertilization Experiment on the Loess Plateau. *Pedosphere* **2007**, *17*, 257–264. [CrossRef]
48. Müller, C.; Elliott, J.; Pugh, T.A.M.; Ruane, A.C.; Ciaia, P.; Balkovic, J.; Deryng, D.; Folberth, C.; Izaurralde, R.C.; Jones, C.D.; et al. Global patterns of crop yield stability under additional nutrient and water inputs. *PLoS ONE* **2018**, *13*, e0198748. [CrossRef]
49. Miranzadeh, H.; Emam, Y.; Piletskiy, P.; Seyyedi, H. Water Use Efficiency of Four Dryland Wheat Cultivars under Different Levels of Nitrogen Fertilization. *J. Agric. Sci. Technol.* **2011**, *13*, 843–854.
50. Fateh, H.; Toubé, A.; Gholipuri, A.Q. The feasibility of reducing yield gap by improving crop management. *Ukr. J. Ecol.* **2019**, *9*, 21–30. [CrossRef]
51. Liu, Z.; Sun, K.; Liu, W.; Gao, T.; Li, G.; Han, H.; Li, Z.; Ning, T. Responses of soil carbon, nitrogen, and wheat and maize productivity to 10 years of decreased nitrogen fertilizer under contrasting tillage systems. *Soil Tillage Res.* **2020**, *196*, 104444. [CrossRef]
52. Macholdt, J.; Piepho, H.-P.; Honermeier, B. Mineral NPK and manure fertilisation affecting the yield stability of winter wheat: Results from a long-term field experiment. *Eur. J. Agron.* **2019**, *102*, 14–22. [CrossRef]
53. Chen, H.; Deng, A.; Zhang, W.; Li, W.; Qiao, Y.; Yang, T.; Zheng, C.; Cao, C.; Chen, F. Long-term inorganic plus organic fertilization increases yield and yield stability of winter wheat. *Crop J.* **2018**, *6*, 589–599. [CrossRef]
54. Zhang, P.; Ma, G.; Wang, C.; Lu, H.; Li, S.; Xie, Y.; Ma, D.; Zhu, Y.; Guo, T. Effect of irrigation and nitrogen application on grain amino acid composition and protein quality in winter wheat. *PLoS ONE* **2017**, *12*, e0178494. [CrossRef]
55. Seddaiu, G.; Iocola, I.; Farina, R.; Orsini, R.; Iezzi, G.; Roggero, P.P. Long term effects of tillage practices and N fertilization in rainfed Mediterranean cropping systems: Durum wheat, sunflower and maize grain yield. *Eur. J. Agron.* **2016**, *77*, 166–178. [CrossRef]
56. Zörb, C.; Ludewig, U.; Hawkesford, M.J. Perspective on Wheat Yield and Quality with Reduced Nitrogen Supply. *Trends Plant Sci.* **2018**, *23*, 1029–1037. [CrossRef]
57. Pettigrew, W.T. Potassium influences on yield and quality production for maize, wheat, soybean and cotton. *Physiol. Plant.* **2008**, *133*, 670–681. [CrossRef]
58. Fang, P.; Yan, M.; Chi, C.; Wang, M.; Zhou, Y.; Zhou, J.; Shi, K.; Xia, X.; Foyer, C.H.; Yu, J. Brassinosteroids Act as a Positive Regulator of Photoprotection in Response to Chilling Stress. *Plant Physiol.* **2019**, *180*, 2061–2076. [CrossRef] [PubMed]
59. Vazquez, D.; Berger, A.; Prieto-Linde, M.L.; Johansson, E. Can nitrogen fertilization be used to modulate yield, protein content and bread-making quality in Uruguayan wheat? *J. Cereal Sci.* **2019**, *85*, 153–161. [CrossRef]
60. Giunta, F.; Pruneddu, G.; Motzo, R. Grain yield and grain protein of old and modern durum wheat cultivars grown under different cropping systems. *Field Crops Res.* **2019**, *230*, 107–120. [CrossRef]
61. Barneix, A.; Guitman, M.R. Leaf regulation of the nitrogen concentration in the grain of wheat plants. *J. Exp. Bot.* **1993**, *44*, 1607–1612. [CrossRef]
62. Yan, S.; Wu, Y.; Fan, J.; Zhang, F.; Zheng, J.; Qiang, S.; Guo, J.; Xiang, Y.; Zou, H.; Wu, L. Dynamic change and accumulation of grain macronutrient (N, P and K) concentrations in winter wheat under different drip fertigation regimes. *Field Crop. Res.* **2020**, *250*, 107767. [CrossRef]
63. Vrignon-Brenas, S.; Celette, F.; Amossé, C.; David, C. Effect of spring fertilization on ecosystem services of organic wheat and clover relay intercrops. *Eur. J. Agron.* **2016**, *73*, 73–82. [CrossRef]

64. Lollato, R.P.; Figueiredo, B.M.; Dhillon, J.S.; Arnall, D.B.; Raun, W.R. Wheat grain yield and grain-nitrogen relationships as affected by N, P, and K fertilization: A synthesis of long-term experiments. *Field Crop. Res.* **2019**, *236*, 42–57. [CrossRef]
65. Xue, C.; auf'm Erley, G.S.; Rossmann, A.; Schuster, R.; Koehler, P.; Mühling, K.-H. Split Nitrogen Application Improves Wheat Baking Quality by Influencing Protein Composition Rather Than Concentration. *Front. Plant Sci.* **2016**, *7*. [CrossRef]
66. Zhang, M.; Ma, D.; Ma, G.; Wang, C.; Xie, X.; Kang, G. Responses of glutamine synthetase activity and gene expression to nitrogen levels in winter wheat cultivars with different grain protein content. *J. Cereal Sci.* **2017**, *74*, 187–193. [CrossRef]
67. Naghavi, M.; Pour-Aboughadareh, A.; Marouf, K. Evaluation of Drought Tolerance Indices for Screening Some of Corn (*Zea mays* L.) Cultivars under Environmental Conditions. *Not. Sci. Biol.* **2013**, *5*, 388–393. [CrossRef]
68. Batra, N.G.; Sharma, V.; Kumari, N. Drought-induced changes in chlorophyll fluorescence, photosynthetic pigments, and thylakoid membrane proteins of *Vigna radiata*. *J. Plant Interact.* **2014**, *9*, 712–721. [CrossRef]
69. Chen, H.; Hao, H.; Han, C.; Wang, H.; Wang, Q.; Chen, M.; Juan, J.; Feng, Z.; Zhang, J. Exogenous l-ascorbic acid regulates the antioxidant system to increase the regeneration of damaged mycelia and induce the development of fruiting bodies in *Hypsizygus marmoreus*. *Fungal Biol.* **2020**, *124*, 551–561. [CrossRef] [PubMed]
70. Khan, F.U.; Mohammad, F. Application of stress selection indices for assessment of nitrogen tolerance in wheat (*Triticum aestivum* L.). *J. Anim. Plant Sci.* **2016**, *26*, 201–210.
71. Mohammadi, R. Efficiency of yield-based drought tolerance indices to identify tolerant genotypes in durum wheat. *Euphytica* **2016**, *211*, 71–89. [CrossRef]

Article

How Agriculture, Connectivity and Water Management Can Affect Water Quality of a Mediterranean Coastal Wetland

Lucía Vera-Herrera ^{1,*} , Susana Romo ² and Juan Soria ³ 

¹ Food and Environmental Safety Research Group, University of Valencia (SAMA-UV), Desertification Research Centre—CIDE (CSIC-UV-GV), Moncada-Naquera Road Km 4.5, 46113 Moncada, Spain

² Department of Microbiology and Ecology, Campus Burjassot, University of Valencia, 46100 Burjassot, Spain; susana.romo@uv.es

³ Campus Paterna, Cavanilles Institute of Biodiversity & Evolutionary Biology (ICBiBE), University of Valencia, 46980 Paterna, Spain; juan.soria@uv.es

* Correspondence: vehelu@uv.es

Abstract: The Natural Park of Albufera (Valencia, Spain) is an important Mediterranean coastal wetland that suffers continuous environmental effects from human activities and water uses, mainly related to agriculture and urban/industrial sewage discharges. The aim of this research was to assess the water quality of the different aquatic environments of this wetland, taking into account the connection between them, the agricultural impact and the management of irrigation water. The UE Water Framework Directive was followed in order to evaluate the ecological and trophic status of water systems. Spatial approaches were used to integrate physicochemical data into GIS vector layers to map the more problematic points of pollution. The results showed a globally eutrophic system with poor ecological potential. The wetland is nutrient-overloaded during the entire rice cultivation period. Good-quality water inputs are deficient, since the river network already has high levels of nutrients and pollutants, especially in the northern area, where river water is mixed with inappropriate effluents from wastewater treatment plants. Agriculture and water management affected the area intensively up to the Albufera lake, modulating most of the studied variables. The information gathered here can help to optimize the global study and management of the coastal Mediterranean wetlands, which are highly linked to agriculture.

Keywords: water quality; agro-ecological wetland; irrigation; nutrients; ecological status



Citation: Vera-Herrera, L.; Romo, S.; Soria, J. How Agriculture, Connectivity and Water Management Can Affect Water Quality of a Mediterranean Coastal Wetland. *Agronomy* **2022**, *12*, 486.

<https://doi.org/10.3390/agronomy12020486>

Academic Editor:
Aliasghar Montazar

Received: 5 January 2022
Accepted: 14 February 2022
Published: 16 February 2022

Publisher's Note: MDPI stays neutral with regard to jurisdictional claims in published maps and institutional affiliations.



Copyright: © 2022 by the authors. Licensee MDPI, Basel, Switzerland. This article is an open access article distributed under the terms and conditions of the Creative Commons Attribution (CC BY) license (<https://creativecommons.org/licenses/by/4.0/>).

1. Introduction

The impact of human activity on nature is already known to constitute a new geological epoch, the Anthropocene [1,2]. The main current environmental problems, such as climate change, the loss of biodiversity, water pollution and desertification, are rooted in the impact of populations on natural resources and ecosystems. Wetlands are among the most important freshwater aquatic ecosystems, although they are also among the most vulnerable on the planet. They are considered indispensable for the ecosystem services they provide to humanity, including natural reserves of fresh water, the supply of essential foods, flood control and groundwater recharge and discharge, as well as being natural areas of great biological diversity [3]. Furthermore, more recently, many studies have confirmed that wetlands play a significant role in the permanent sequestration of carbon, acting as important buffers to climate change [4–8]. However, despite their importance, these aquatic ecosystems are currently at risk of disappearing due to the overexploitation of their resources and the continuous anthropogenic pressure to which they are subjected. Major anthropogenic activities include the conversion of natural wetlands into land for intensive agriculture or for industrial and urban development. As a result, it is now known that from 1970 to 2015, about 35% of the natural wetlands have disappeared and 36% of coastal wetland-dependent species have decreased. In addition, the quality of wetland water bodies

has experienced negative trends due to nutrient run-off from intensive agriculture and the release of urban pollutants from wastewater treatment plants (WWTPs) and untreated wastewater discharges [9,10].

In this context, Mediterranean coastal wetlands are examples of the fragility of these areas. Ecologically, these wetlands are recognized as biodiversity hotspots, especially for birds, serving as a refuge during migratory processes. In addition, they have a high economic value, as they are linked to important economic activities such as fishing, salt production and rice farming [11,12], but in contrast they have undergone several anthropogenic effects [13,14]. These wetlands have experienced dramatic changes in recent years, which could worsen in the coming decades [15–17]. Climate change has increased mean temperatures by 1.4 °C in the region since the preindustrial period and has also increased the frequency of severe drought events, contributing to the desertification of these natural areas [11,18]. Overall, it is estimated that 50% of Mediterranean wetlands have been lost in the last century [19]. Moreover, they all depend on complex hydrological cycles, determined mainly by groundwater and irrigation networks [11]. All these factors imply the complexity of managing of these ecosystems, which makes challenging to develop monitoring, conservation and environmental restoration strategies [9,11,20].

In recent decades, many environmental agencies around the world have established policy instruments to protect inland, transitional and coastal waters, as well as procedures to evaluate their status based mainly on large-scale assessments [9,21]. In 1991, the European Union (EU) developed the Nitrates Directive (91/676/EEC), which deals with pollution caused by nitrates from agricultural sources. It requires Member States to identify polluted waters and “Nitrate Vulnerable Zones” and establish Codes of Good Agricultural Practice and effective Action Programmes [22]. That same year, the EU developed the Urban Wastewater Treatment Directive (91/271/EEC), which sets out a number of obligations in relation to collection systems, with further restrictions in areas sensitive to eutrophication [23]. In 2000, the EU introduced the most ambitious and influential ecological legislative framework, the Water Framework Directive (2000/60/EC). This European Directive, based on a new approach to water policy, had as its first objective the achievement of a good status for EU waters by 2015 [24], and clearly involves the assessment, protection and restoration of wetlands as part of its purpose. This directive, together with the Birds Directive (2009/147/EC) and Habitats Directive (92/43/EEC), aim to achieve the sustainable use of wetlands resources and the conservation of their ecological functions and attributes [24].

The trophic state index is commonly used to determine the trophic degree of water bodies [25]. The Water Framework Directive has water quality indicators that also take into account the complexity of each aquatic ecosystem: the human pressures to which they are exposed and the spatio-temporal variation of its physicochemical characteristics, among other features [21,26–28]. The most important index is the ecological potential: “an expression of the quality of the structure and functioning of aquatic ecosystems associated with surface waters” [24]. This approach is based on thresholds assigned to specific physicochemical, hydrological and biological indices [29] and allows the assessment of the chemical status of water bodies and reversing deterioration trends.

In addition, recently new tools and methodologies have emerged for the environmental assessment of wetlands, such as remote sensing [30], which can evaluate the state of water bodies at spatial and temporal levels at different resolutions, and algorithms have been developed to measure limnological parameters [31–34]. Moreover, geographic information systems (GIS) have allowed new approaches in recent years different environmental compartments incorporating into environmental studies (known as landscape functional areas, LFAs) [35], as well as the hydrological connectivity between zones. The modeling approach [36] is often specific for an aquatic system [37], but can simulate wetland characteristics under different scenarios, frequently related to climate change [26,38–40].

The Natural Park of Albufera (Valencia, Spain) is an important Mediterranean coastal wetland (RAMSAR and NATURA 2000 site), which includes the largest Iberian coastal

lagoon. This wetland, the Doñana National Park and the Ebro Delta Natural Park represent three relevant natural reserves and areas for Spanish rice production. The present work evaluates for the first time the water quality of the different aquatic environments of this Mediterranean wetland, taking into account their connectivity, the agricultural impact and the management of irrigation water. The study will assess the current ecological status of the wetland water systems depending on the different agricultural activities and the origin of the irrigation water. The main aims of our study are to (1) analyze the differences in the water quality of the aquatic ecosystems at the beginning and the end of rice cultivation, (2) study the spatial heterogeneity of the variables using GIS approaches to assess water quality differentially according to agricultural activities in the catchment area and in relation to the management of the irrigation water and (3) determine the ecological and trophic status of the water systems of the wetland. The results can contribute to improving global databases on Mediterranean coastal wetlands, as well as helping to develop adequate management and assessment plans for these complex ecosystems.

2. Methods

2.1. Study Area

The study area is an extensive zone that includes part of the main rivers, irrigation channels and inflows and outflows related to the Natural Park of Albufera, which is located in eastern Spain ($39^{\circ}20' N$, $0^{\circ}21' W$) (Figure 1A). It is delimited by the rivers Turia (to the north) and Júcar (to the south). This wetland is near the city of Valencia and it is surrounded mostly by rice fields, as well as some industries. For this reason, the area presents a complex relationship between its intrinsic natural importance and human activities. The wetland has an area of 210 km² and is an important coastal Mediterranean wetland, protected by the Ramsar Convention and the European Habitat List NATURA 2000 [41].

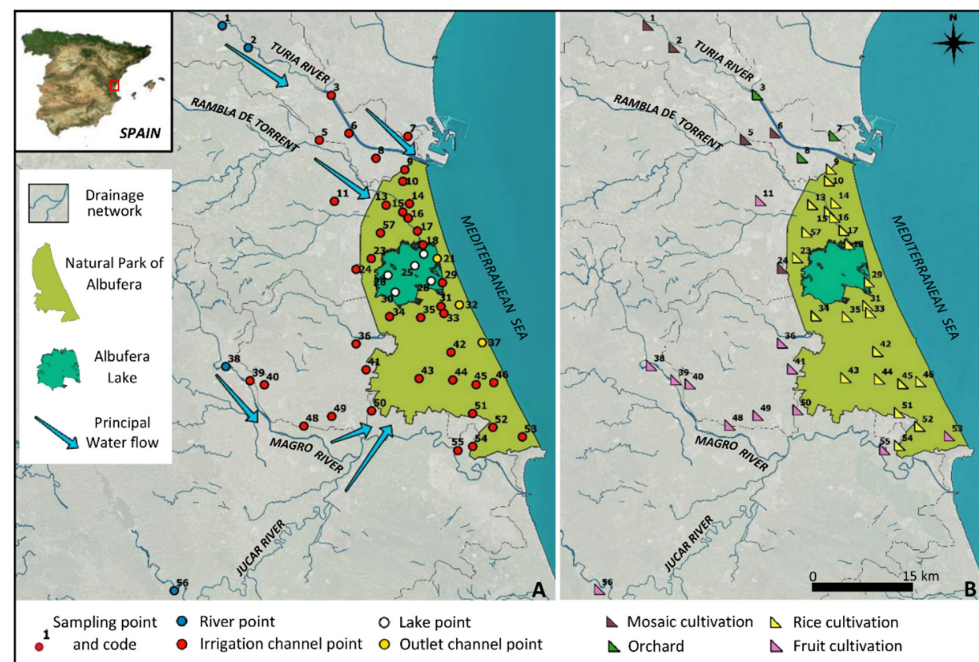


Figure 1. Study area with the principal river networks, the limit of the Natural Park of Albufera and the area of Albufera Lake. (A) Sampling points classified according to their corresponding aquatic habitats and arrows showing the principal water flow to the natural park. (B) Sampling points classified according to the agricultural activity carried out in their vicinity. Base image: OrtoPNOA 2018 CC-BY 4.0 scne.es.

In the study area there are three main types of crops (Figure 1B). On the one hand, the rainfed farming that once covered the western lands has been replaced by crops of fruit trees, especially citrus [42]. Since 1979, this area has been crossed from south to north by the Jucar-Turia Canal, which was designed to transport water from the Jucar to the Turia River and supply water to all the irrigated fields on both sides of the canal [43]. On the other hand, we can also find vegetable crops located near small towns in the border of the natural park. Finally, the farming activity of greatest interest to our study is rice cultivation, due to the fact that it has developed practically throughout the entire extent of the natural park, covering 73% of its surface area [21]. To achieve the effective irrigation of rice paddies, the entire study area supports a dense structure of overland artificial canals for the irrigation of 59.7 km and a density of 323 m/km² that connect the water from the Rivers Jucar and Turia with the crops [44]. However, this complex irrigation system connects many of the canals with the sewerage infrastructures of the surrounding municipalities, receiving industrial and urban discharges. These sewage effluents are considered sources of nutrients [45,46] and emerging pollutants, such as perfluoroalkyl substances, organophosphorus flame retardants and pharmaceuticals and personal care products, among others [47–50].

In the center of the Natural Park is the Albufera Lake, a shallow (mean depth of 1 m) and oligohaline (salinity 1–2‰) lagoon, that represents the largest Spanish coastal lake, with a surface area of 23.2 km², covering approximately 11% of the wetland area [51,52]. The hydrology of the lake combines natural contributions (seasonal rainfall) with complex water management for rice cultivation [53]. The lake's hydrological cycle has two periods of low water renewal from November to December and from April to September during rice sowing and growing. The higher lake water renovation takes place between January and March after the emptying of the paddy fields and by September–October after harvesting [34,51,54]. The lake water level is regulated by three artificial outlet canals, which flow into the Mediterranean Sea [51]. The lake has been eutrophic since the 1970s due to the urban and industrial discharges and nitrogen-rich effluents from rice fields. These discharges turned the lake rapidly into a turbid microalga-dominated site, whereas the richness of aquatic plants and fauna severely decreased after the first half of 20th century [51,55–58]. The plans for the reduction of nutrient-rich sewage discharges over the last three decades have failed to change the trophic state of the lake [51,59,60]. More detailed information about the lake is given elsewhere [51,61].

2.2. Sampling Points and Water Collection

A total of 51 water bodies were studied, located in four different aquatic systems: in sections of the rivers Turia, Jucar and Magro; in the most important ditches that irrigate the Natural Park; in the Albufera Lake and in the outlet canals that connect the lake with the Mediterranean Sea (Figure 1A). All these water systems were sampled twice, at the start and the end of rice cultivation in the wetland, during May and June 2019 and September and October 2019, respectively. A total of 100 samples were studied. During the first sampling campaign, 51 freshwater samples were taken, whereas in the second one there were 49 samples, because two irrigation channel points were dried.

Sampling points were classified for further analysis (Supplementary Material, Table S1). Firstly, they were identified with their corresponding aquatic habitat: rivers, irrigation channels or lake points (including outlet canals) (Figure 1A). Secondly, thanks to the digital layer “Corine Land Cover 2018 Classification” provided by the Copernicus Global Land Service (CGLS) [62], each sampling point was classified according to the agricultural activity carried out in its vicinity. The activities identified were traditional orchards, mosaic cultivation, rice cultivation (carried out inside the Natural Park) and fruit tree cultivation (Figure 1B). The water samples taken from the lake, outlet canals and *tancats* were excluded from this classification as they are not associated with any crop. Finally, the sampling points were also classified according to their irrigation zones [63] (Figure 2). The irrigation zones sampled were the following: Mislata, Benager and Faitanar (included in a single zone called “Huerta Oeste”), Favara, Oro, Acequia Real del Júcar (abbreviated as ARJ),

Sueca and Cullera. The Turia and Magro river points are not located in any irrigation zone and were classified separately, as happened with the lake points, also including the *tancats*.

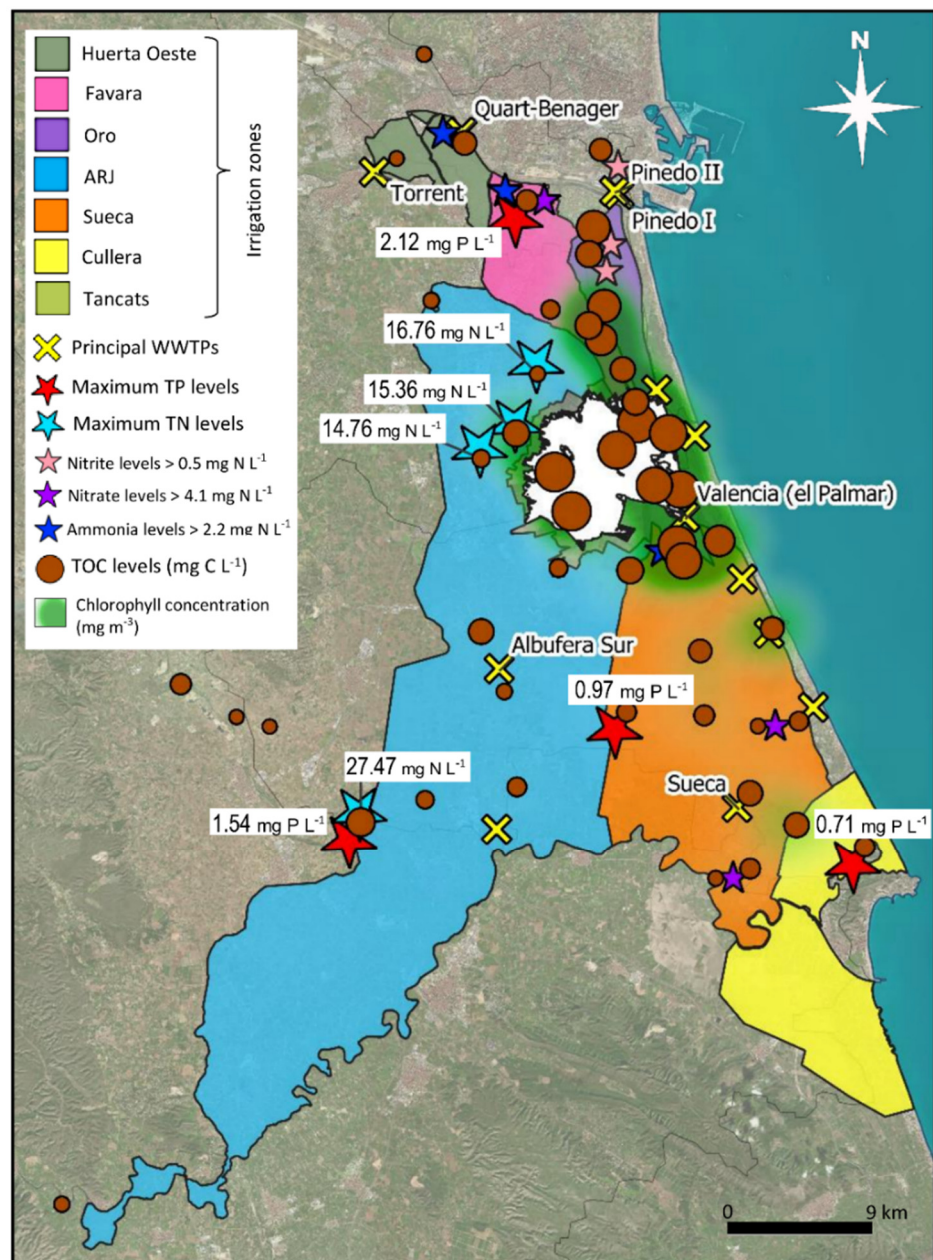


Figure 2. Agricultural (irrigation zones) and urban contextualization of the study area and spatial representation of the maximum levels of TP, TN, nitrite, nitrate and ammonium nitrogen together with the average concentrations of TOC and phytoplanktonic chlorophyll a. Base image: OrtoPNOA 2018 CC-BY 4.0 scne.es.

Water samples were taken in clean polyethylene bottles (capacity 0.5 L and 1 L). At each sampling point, the bottles were pre-rinsed with the sample water three times. The bottles were maintained at 4 °C until reaching the laboratory. Once there, samples were filtered through 0.45 µm glass microfiber GF/F filters (Whatman, UK) and the filters were stored in glass tubes in the dark at −20 °C for pigments extractions.

2.3. Water Analyses

Turbidity, pH and conductivity were measured in situ directly from the water bodies whenever possible, using an AquaFluor[®] Handheld Turbidimeter from Turner Designs (San Jose, CA, USA), and a pH and EC waterproof testers from Hannah Instruments[®] (Woonsocket, RI, USA), respectively. When direct data collection was not possible, 1 L of water was taken from the sampling point, using clean polyethylene beakers, pre-washed with the sample water three times. Organic matter, dissolved inorganic nitrogen (DIN: nitrate, nitrite and ammonium nitrogen) and phosphorus concentrations (SRP) were analyzed according to the standard methods [64]. For the analyses of total inorganic carbon (TIC), total organic carbon (TOC) and total nitrogen (TN), unfiltered water samples were first treated in an ultrasonic bath for 15 min in order to achieve an optimal mixture of dissolved and particulate components. Then, determinations were made using a carbon and nitrogen analyzer (a TOC-V combustion catalytic oxidation/NDIR system in combination with an ASI-V sampler from Shimadzu; Kyoto, Japan) according to ISO-CEN EN 1484:1997 [65]. Specifically, TIC was detected as CO₂ using a non-dispersive infrared detector (NDIR), from the acidification of the sample and its subsequent catalytic oxidation. After removal of the TIC fraction from the sample, TOC was determined as non-volatile organic carbon (NPOC) through catalytic oxidation of the remaining carbon (TOC by acidification/sparging method). TN was decomposed to nitrogen monoxide using a thermal decomposition catalyst and detected using a chemiluminescence detector. The total dissolved organic carbon (DOC) and the total dissolved nitrogen (DN) were analyzed in filtered water samples following the same methods described above, except for the previous step with the ultrasonic bath. Total phosphorus (TP) concentrations were determined in unfiltered samples by means of the molybdate-blue method after acid persulfate digestion [66]. Particulate phosphorus (P_{part}) and dissolved organic nitrogen (DON) were calculated by subtracting the respective SRP portion from the TP concentration, and subtracting the DIN portion from the DN concentration, respectively. The total carbon (TC) was calculated as the sum of NPOC and TIC. Chlorophyll *a* and carotene were extracted with acetone 90% and determined according to APHA [64] and Jeffrey and Humphrey [67]. LOD and LOQ information is provided in Table S2 (Supplementary Material).

2.4. Water Quality Assessment

The average of each study variable per sampling point was calculated and subjected to different evaluations. The trophic statuses of water bodies were calculated according to Chlorophyll *a*, TP [68] and TN levels [69]. The ecological potential was studied based on biological and physicochemical quality elements [24,70]. For this ecological assessment of water bodies, the sampling points were first classified according to their water body typology, applying the Water Framework Directive and following the requirements of Decree 1/2016. Information about the water body typologies included in our study is available in Table S1 (Supplementary Material).

All the results obtained were integrated into different digital vector layers using QGIS (3.12) software. The maps developed were delimited according to surface waters distribution, combining natural and irrigation networks. The GIS covers allowed us to carry out studies using different spatial approaches.

2.5. Meteorological Data

The daily and monthly meteorological data recorded in the basin during the study period (May–June and September–October 2019) were obtained from two different stations: one located in the city of Valencia (Penya-Roja station) and another located on the shore of the Albufera Lake (Tancat de la Pipa station) [71].

2.6. Statistical Analyses

Univariate statistical analyses were used to obtain descriptive statistics for each variable and sampling period and for the average values of the variables. The assumptions

of normality of the data were checked prior to statistical analyses, and non-parametric tests were used when variables were not normally distributed (Shapiro–Wilk test, $p < 0.05$). Student's t -test was used to identify statistically significant differences between the two sampling periods and the unequal variance t -test was used as an alternative when variances between pairs of data were very different. The average of each study variable per sampling point was then calculated, transformed and subjected to a principal components analysis (PCA) using the correlation matrix. Multidimensional clustering using Euclidean distance was calculated to detect relationships between groups of points and main driving factors. Spearman's rank-order correlation coefficient was used to obtain the correlation between study variables. In addition, the average data were subjected to some Kruskal–Wallis and PERMANOVA tests (with the Mann–Whitney post hoc test) to identify significant differences between the different clustering factors (zoning study). Analyses were performed using PAST (3.22) software [72].

3. Results

The study area has a Mediterranean climate. During the period of May–June 2019, the average temperature recorded was 20.4 °C, with a standard deviation of 2.9 °C; an absolute daily maximum of 31.6 °C and minimum of 10.2 °C. The total precipitation recorded was 26.6 mm, with an absolute daily maximum of 7.6 mm. During the second study period, September–October 2019, the average temperature recorded was 22.1 °C, the standard deviation was 2.8 °C; the absolute daily maximum was 33.7 °C and the minimum was 12.0 °C. The total precipitation recorded was 247.2 mm, with an absolute daily maximum of 52.3 mm. In accordance with the climate of the study area, the highest rainfall was recorded during the second study period, during autumn, when half of the total rainfall of the year is usually recorded. No extraordinary drought events were recorded.

3.1. Effects of Rice Cultivation on Water Quality

Table S3 (Supplementary Material) shows the results obtained for the variables analyzed in all the water bodies at different phases of rice cultivation. In general, the values ranged similarly at the start and the end of the cultivation. By considering the whole study system (referred to henceforth as the “wetland”) we found only significant differences in pH, EC, alkalinity and TC ($p < 0.05$) (Figure 3), with no significant changes observed in photosynthetic pigment concentrations or nutrient levels ($p > 0.05$). The rivers samples only increased their pH significantly and had a significant carbon decrease (TIC and TC) ($p < 0.05$) (Figure 3). The irrigation canals studied experienced the same significant changes as the wetland system and a decrease in ammonium nitrogen (NH₄-N) concentrations ($p < 0.05$) (Figure 3). The lake was the aquatic ecosystem that experienced the greatest changes during the cultivation period, with alkalinity, pH, TIC and TC increasing significantly ($p < 0.05$) (Figure 3). In contrast, the lake experienced a significant decrease in turbidity, EC, pigment concentrations and some nutrient levels ($p < 0.05$) (Figure 3) as a result of the dilution of the lake water after the emptying of the rice fields before harvesting.

3.2. Global Wetland Approach

For an evaluation of the wetland, the average values of the physicochemical and biological variables were studied per sampling point. In relation to the physical variables, turbidity reached a mean value of 11.57 NTU \pm 1.46 and the EC reached a mean of 1550.3 μ S cm⁻¹ \pm 86.7 (Table 1). Regarding dissolved nutrients, in general, the mean concentrations of NH₄-N and nitrite nitrogen were relatively moderate (Table 1). Nitrate nitrogen reached higher concentrations in water systems, with a mean concentration of 1.947 mg N L⁻¹ \pm 0.188 (Table 1). Phosphate concentrations were significant and reached a maximum value of 1.451 mg P L⁻¹ (Table 1). The mean concentrations of TN, TP and TC were 6.30 mg N L⁻¹ \pm 0.67, 0.226 mg P L⁻¹ \pm 0.05 and 35.82 mg C L⁻¹ \pm 1.48, respectively (Table 1). About 60–90% of TN was dissolved forms and about 50–90% of TP was particulate. TC was mainly inorganic, with TIC reaching a mean concentration of

29.90 mg C L⁻¹ ± 1.43 (Table 1). In relation to the biological variables, Chl-a and carotenes reached a mean concentration of 25.3 mg m⁻³ ± 3.9 and 11.2 mg m⁻³ ± 1.8, respectively (Table 1).

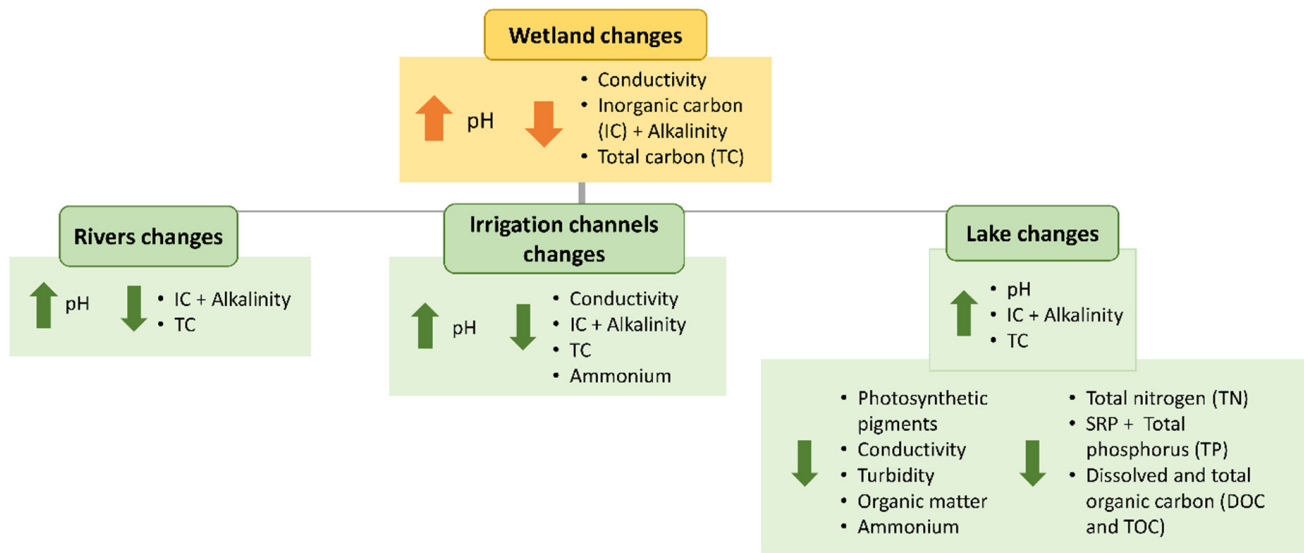


Figure 3. Statistically significant differences observed in the aquatic systems when comparing the beginning and ending of the rice cultivation period according to Student’s *t*-test results (*p* < 0.05).

Table 1. Mean, standard error, maximum and minimum values of the physico-chemical and biological variables studied in the water bodies during rice cultivation (May to October 2019), together with the results obtained for the Kruskal–Wallis tests to observe differences between (A) aquatic habitats, (B) agricultural activities and (C) irrigation zones. Probabilities are: * *p* < 0.05, ** *p* < 0.01; ns = not significant differences.

Variable	Mean	SE	Maximum	Minimum	(A) <i>p</i> -Value	(B) <i>p</i> -Value	(C) <i>p</i> -Value
Turbidity (NTU)	11.57	1.46	50.80	0.60	ns	**	ns
pH	7.86	0.04	8.80	7.30	ns	*	ns
Conductivity (µS cm ⁻¹)	1550.3	86.7	5136.0	663.0	**	*	**
Organic matter (mg L ⁻¹)	1.240	0.095	3.449	0.340	**	**	**
Ammonium nitrogen (mgN L ⁻¹)	0.551	0.123	3.920	0.005	**	**	**
Nitrite nitrogen (mgN L ⁻¹)	0.141	0.021	0.600	0.001	**	**	**
Nitrate nitrogen (mgN L ⁻¹)	1.947	0.188	4.705	0.013	ns	*	**
Dissolved inorganic nitrogen (DIN; mgN L ⁻¹)	2.639	0.247	7.155	0.358	*	**	**
Dissolved organic nitrogen (DON; mgN L ⁻¹)	2.972	0.675	26.075	0.021	ns	*	ns
Dissolved nitrogen (DN; mgN L ⁻¹)	5.61	0.67	26.51	0.70	**	ns	ns
Total nitrogen (TN; mgN L ⁻¹)	6.30	0.67	27.47	1.07	ns	*	ns
Soluble reactive phosphorus (SRP; mgP L ⁻¹)	0.073	0.029	1.451	0.001	**	ns	**
Particulate phosphorus (Ppart; mgP L ⁻¹)	0.153	0.043	2.018	0.004	ns	**	**
Total phosphorus (TP; mgP L ⁻¹)	0.226	0.052	2.121	0.009	*	**	**
Chlorophyll-a (Chl-a; mg m ⁻³)	25.3	3.9	84.3	1.0	**	**	**
Carotene (mg m ⁻³)	11.2	1.8	42.7	1.0	**	**	**
Inorganic carbon (TIC; mgC L ⁻¹)	29.90	1.43	53.05	12.84	*	ns	**
Dissolved organic carbon (DOC; mgC L ⁻¹)	5.16	0.45	12.02	1.32	**	**	**
Total organic carbon (TOC; mgC L ⁻¹)	5.91	0.54	13.94	1.94	**	**	**
Total carbon (TC; mgC L ⁻¹)	35.82	1.48	59.76	22.33	ns	*	**
Alkalinity (meq L ⁻¹)	2.49	0.12	4.42	1.07	*	ns	**

The nitrogen and phosphorus levels of the rivers to the wetland were taken as reference values to evaluate the balance of nutrients (Table 2). The assessment of the average nutrient concentration achieved in the wetland indicated that 16% of the sampling points had TN concentrations above 10 mg N L⁻¹ and 90% exceeded 2 mg N L⁻¹, whereas 4% of the sites had TP concentrations higher than 1 mg P L⁻¹ and 61% exceeded 0.1 mg P L⁻¹ (Table 3). Analyzing the results according to the aquatic habitats, none of the rivers sampled exceeded an average TN concentration of 10 mg N L⁻¹ and an average TP concentration of

1 mg P L⁻¹ (Tables 2 and 3), although the Turia River had TN concentrations higher than 5 mg N L⁻¹ (Table 2). Regarding the irrigation channels, 21% and 72% exceeded by one order of magnitude the average concentrations of TN and TP reached by the Júcar River (Table 2). In addition, 21% of the irrigation channels studied exceeded TN concentrations of 10 mg N L⁻¹ and 69% had TP concentrations above 0.1 mg P L⁻¹ (Table 3). Finally, for the Albufera lake (and outlet canals), 100% of the points had TN and TP concentrations higher than 2 mg N L⁻¹ and 0.05 mg P L⁻¹, respectively (Table 3).

Table 2. Average concentrations of TN and TP reached in the Turia, Magro and Júcar rivers during the rice cultivation period (May 2019–October 2019).

TN and TP Concentrations in the Rivers Sampled		
	Mean TN (mg N L ⁻¹)	Mean TP (mg P L ⁻¹)
Turia River-Masía Traver	5.66	0.01
Turia River-La Presa	5.44	0.02
Magro River	2.80	0.11
Júcar River	1.08	0.01

Table 3. Percentages of TN and TP for the different studied aquatic systems respect to the limits referenced.

% Ecosystems According to Nutrients Levels *					
Habitats	n Total	Total Nitrogen (TN)			
		>10 mgN L ⁻¹ [73]	>2 mgN L ⁻¹ [74]	>0.65 mgN L ⁻¹ [69]	
Global	51	16%	90%	100%	
River	4	0%	75%	100%	
Irrigation channel	39	21%	90%	100%	
Lake	8	0%	100%	100%	
Habitats	n Total	Total Phosphorus (TP)			
		>1 mgP L ⁻¹ [73]	>0.1mgP L ⁻¹ [63]	>0.05 mgP L ⁻¹ [75]	>0.035 mgP L ⁻¹ [68]
Global	51	4%	61%	82%	86%
River	4	0%	25%	25%	75%
Irrigation channel	39	5%	69%	85%	90%
Lake	8	0%	38%	100%	100%

* Percentages obtained from the calculated averages of TN and TP.

3.3. Spatial Mapping of the Variables

None of the variables studied presented a normal distribution (Shapiro–Wilk test, $p < 0.05$; Figure S1, Supplementary Material). There were significant differences in physicochemical and biological variables for the different irrigation zones in our study (PERMANOVA, $F = 8.973$, $p < 0.001$). No significant differences were observed with respect to different aquatic habitats and agricultural activities (PERMANOVA, $p > 0.05$).

Most of the variables studied had significant differences between the zoning groups independently (Kruskal–Wallis, $p < 0.05$) (Table 1). Turbidity, pH, nitrates, DON, TN, Ppart and TC did not differ significantly between the different aquatic habitats ($p > 0.05$) (Table 1). The lake group had the highest conductivity values and the highest concentration of pigments and organic carbon (Mann–Whitney post hoc tests, $p < 0.05$). The irrigation channels group showed the highest values of NH₄-N, nitrites nitrogen and phosphates (Mann–Whitney post hoc tests, $p < 0.05$).

According to the agricultural activities, DN, SRP, TIC and alkalinity were the only variables that did not differ significantly ($p > 0.05$) (Table 1). The rice group was associated with the highest concentrations of photosynthetic pigments and also differed statistically from the mosaic and fruit groups due to its having the highest values of conductivity, turbidity, organic matter and organic carbon (Mann–Whitney post hoc tests, $p < 0.02$). In ad-

dition, the rice and vegetable groups were those with higher concentrations of phosphorus compounds (Mann–Whitney post hoc tests, $p < 0.05$).

Geographical average values of the physicochemical and biological variables of the water bodies were well identified using GIS layers (Figure 2). In the north of the natural park, the groups of the Huerta Oeste, Favara and Oro irrigation zones were related to higher concentrations of $\text{NH}_4\text{-N}$ and nitrite nitrogen (Mann–Whitney post hoc tests, $p < 0.05$) (Figures 2 and 4). Turia River, Huerta Oeste and Favara were also the irrigation zones with the highest levels of nitrate nitrogen (Mann–Whitney post hoc tests, $p < 0.02$). Furthermore, Oro was the group with the highest concentrations of organic matter and total carbon (Mann–Whitney post hoc tests, $p < 0.05$) (Figures 2 and 4). Finally, turbidity, pH, DON, DN and TN did not differ significantly between irrigation zones ($p > 0.05$) (Table 1).

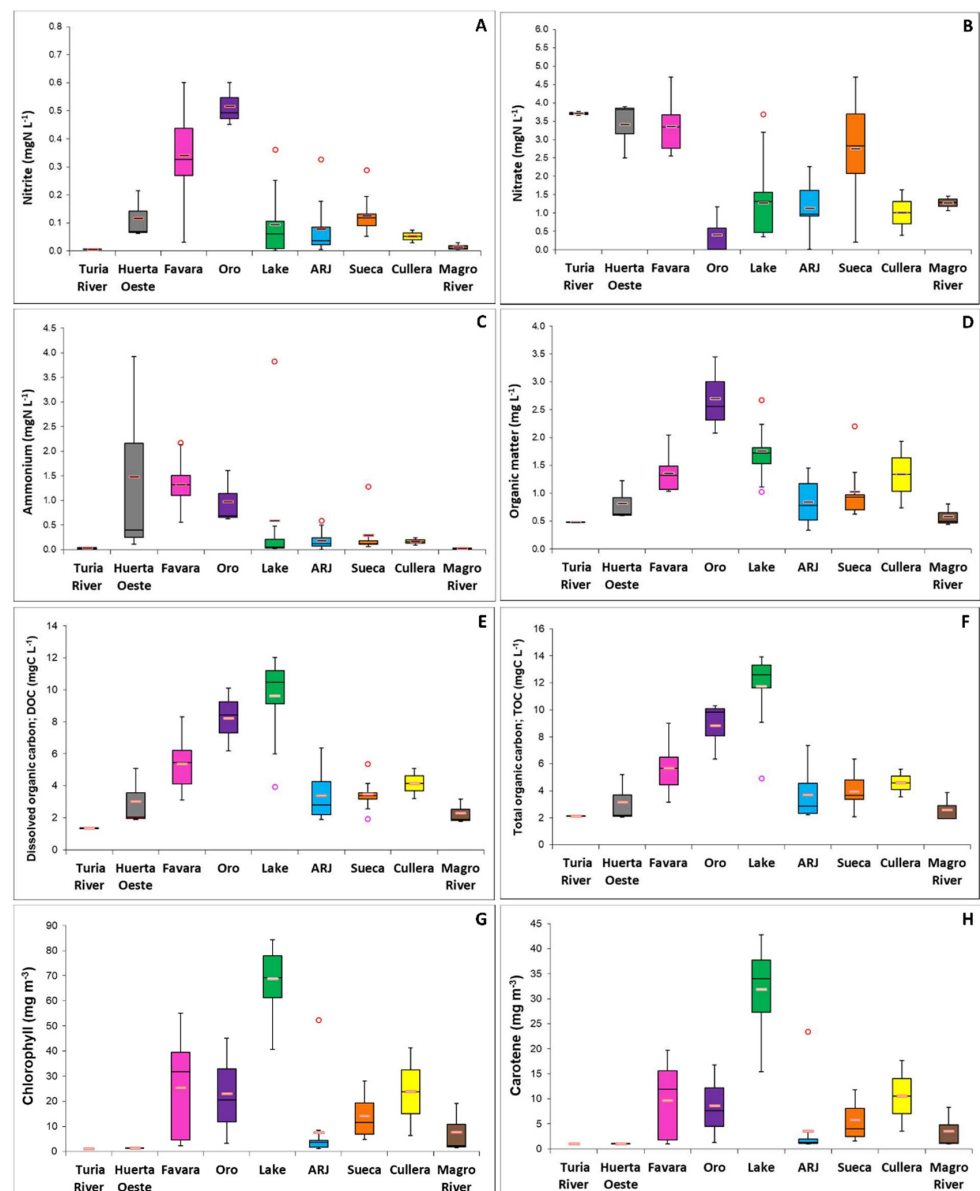


Figure 4. Some of the variables that showed statistical differences between the studied zones (Kruskal–Wallis test, $p < 0.05$). Box-plots with medians, percentiles and outlier values. (A) Nitrite, (B) nitrate, (C) ammonium, (D) organic matter, (E) dissolved organic carbon, (F) total organic carbon, (G) chlorophyll *a*, (H) carotene.

When we used multivariate analyses for a spatial approach to the studied points, the two first axes of the PCA analysis explained 52% of the variability in the data. The first axis accounted for most of the variance (31%) and clearly segregated the points sampled according to the concentrations of dissolved nutrients (especially phosphates, $\text{NH}_4\text{-N}$ and nitrite nitrogen). The second axis (21%) distributed the water bodies according to the concentration of photosynthetic pigments and turbidity. The cluster analysis grouped the points mainly according to conductivity and chlorophyll concentration, and showed greater variability among the water systems, with the lowest values for both variables.

The main variables that correlated significantly ($p < 0.05$) and positively with phytoplanktonic chlorophyll *a* were TOC ($r = 0.768$), DOC ($r = 0.754$), turbidity ($r = 0.711$) and organic matter ($r = 0.650$). All statistically significant correlations obtained for the main studied variables can be found in Supplementary Material, Figures S2 and S3.

3.4. Trophic State and Ecological Potential of the Wetland

The trophic status of water bodies was calculated first according to TP and Chl-*a* limits established by OECD [68]. Most of the aquatic systems (75%) were classified as hypertrophic, 12% eutrophic and 12% mesotrophic. Only 2% presented meso-oligotrophic conditions (Figure 5A). Secondly, trophic state was also calculated according to TN limits established by Nürnberg [69]. Almost all aquatic ecosystems (94%) were defined as hypertrophic, with the remaining 6% being eutrophic (Figure 5B).

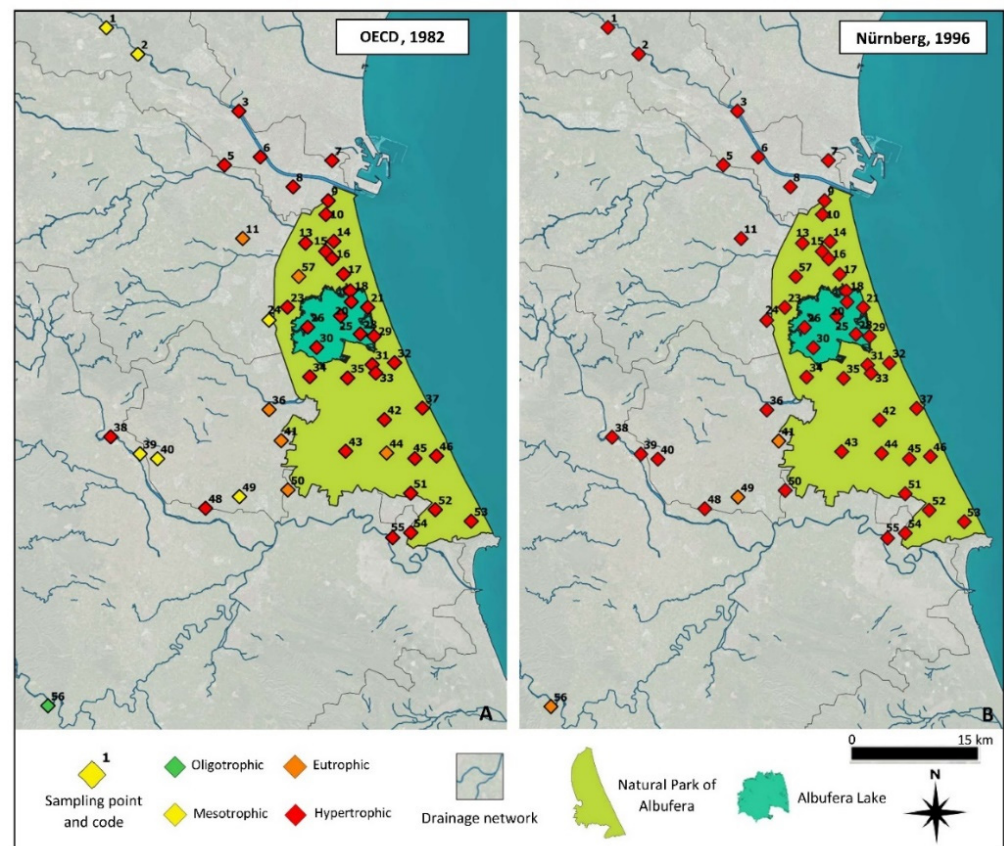


Figure 5. Study area with the spatial distribution of the sampling points classified according to their trophic status. (A) Evaluation according to OECD [68], (B) evaluation according to Nürnberg [69]. Base image: OrtoPNOA 2018 CC-BY 4.0 scne.es.

In relation to the ecological potential, 39% of the water systems had the worst quality category of “bad” ecological potential, followed by 6% and 25% of the sites classified with “poor” and “moderate” ecological potential, respectively. Only a small percentage

of 14% of the aquatic systems had a “high” ecological potential (Figure 6 and Figure S4, Supplementary Material).

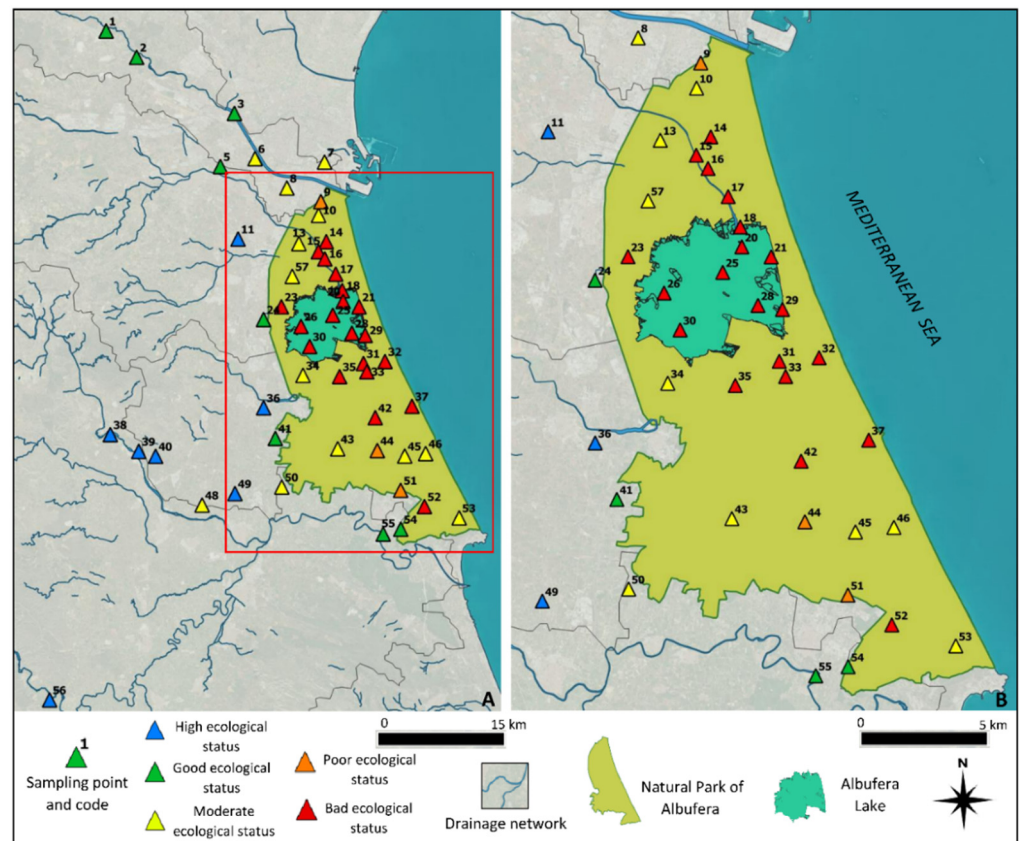


Figure 6. Study area and spatial distribution of the sampling points classified according to their ecological potential [24,70]. Results for (A) entire study area, (B) natural park area. Base image: OrtoPNOA 2018 CC-BY 4.0 scne.es.

Ecological potential was also assessed according to the different grouping criteria for aquatic ecosystems. Analyzing the water systems according to their water typologies, 59% of the sampling points located inside the natural park (categorized as L-T18-HM) had a “bad” ecological status, 9% presented a “poor” status and 26% a “moderate” status. The sampling points located in the north of the study area (classified as R-T14) generally presented the worst ecological potential compared to those located in the south (classified as R-T17). According to the aquatic habitats, 100% of lake sampling points had a “bad” ecological potential. The irrigation channels group was represented by all categories and globally had a “poor” ecological potential. The river group was the group with the best quality, with a “good” ecological potential (50% “high” and 50% “good”). According to the different agricultural activities, the groups with the best global ecological potential were fruit crops and mosaic (“good”), whereas rice was the group with the worst quality (“bad”). Finally, in relation to the irrigation zones the groups with the best global ecological potential were Magro and Jucar (“high” and “good”, respectively). The irrigation zones with the worst water quality were Favara, Oro, ARJ and Cullera, with a “poor” ecological potential. The percentages obtained from these analyses are shown in the Supplementary Material, Figure S4.

4. Discussion

In this study, the analysis of the physicochemical and biological variables of the different aquatic systems allowed us to evaluate the effect of agriculture and the irrigation water management, the wetland heterogeneity and the locations with a higher pollution

impact according to the different human activities. In the study wetland, the cultivation of rice severely modulates water management and affected water pH and conductivity. The average conductivity of the aquatic systems found during this study defines this Mediterranean wetland as brackish with a moderate marine influence due the water management for agriculture. This is similar to the results reported by Soria et al. [76] in a specific study on the conductivity of Lake Albufera, with certain oscillations due to fluvial contributions.

The second effect observed due to agriculture in the wetland was the decrease in water turbidity, microalgae concentrations and levels of some nutrients, mainly affecting the lake at the end of the rice cultivation as a consequence of drainage of the rice fields before harvesting. At this period, rapid flushing of the system has also been reported, together with negative consequences for the water quality of the nearby coastal sea [51,52,77].

An interesting result of our study is that the system is continuously overloaded with nutrients during the whole rice cultivation period and the water discharges from the main rivers are too poor to contribute positively to the water quality of this coastal ecosystem. The average levels of TN and TP clearly indicate the impact of nutrient loadings in the wetland. About 16% and 4% of the sampling points exceeded the concentration limits of TN and TP, respectively, established by the legislation that regulates the discharges of treated urban wastewater in sensitive areas [73] (Table 3). More specifically, all the rivers studied, with the exception of the Jucar River, presented TN concentrations above the recommended limit [74] and all of them were eutrophic (Tables 2 and 3). When we analyzed the irrigation channels, 21% and 5% exceeded the TN and TP limits established by law and TP was even 69% higher than the recommended values [63].

Therefore, the obtained results show a nutrient-rich hydrographic network, where the entry of good quality water is not guaranteed. Furthermore, it is confirmed that the concentrations of nutrients present in the lake interfere with the recovery process of its biological richness. For instance, 90% and 82% of the water bodies studied exceeded the levels of TN and TP recommended for the recovery of submerged aquatic plants, which are key species required to shift the trophic states of shallow lakes [74,75]. The intensive uses of pesticides in the park also prevents colonization by submerged plants [78]. Interestingly, the average concentrations of dissolved nutrients in the wetland greatly exceeded those reached in the Mar Menor lagoon (Murcia, Spain) during the break phase of 2016–2017 [79]. In contrast, dissolved nutrients were lower than those attained in the main streams feeding the Doñana National Park, which is also affected by intensive agriculture [80].

The trophic status and ecological potential clearly showed the severe degradation of the wetland water systems. About 59% of the sampling points located inside the natural park had a “bad” ecological status and almost all sampling points (94%) were hypertrophic. The level of TN in the wetland is one order of magnitude higher than the limit for a eutrophic system ($650 \mu\text{g N L}^{-1}$ vs. $6300 \mu\text{g N L}^{-1}$). In terms of the ecological potential, the natural park’s water bodies are classified as poor, especially its lake and the surrounding ditches (Figure 6). In regard to photosynthetic pigment levels, the average chlorophyll concentration in the wetland exceeds the limit established by the OECD [68] to describe a water body as hypertrophic (25.3 vs. 25.0 mg m^{-3}), which is remarkable, considering that this value includes all the different aquatic habitats studied. Although the maximum values were reached in the lake points, it is relevant to indicate that in several irrigation ditches the concentration of microalgae exceeded 50 mg m^{-3} . This eutrophication in irrigation systems is similar to the levels detected in the three sub-catchments that feed the Doñana marsh [80]. As a comparison, in the artificial Lake Nasser (Egypt) fed by the Nile River, chlorophyll levels never exceeded 12 mg m^{-3} , representing a very different system, free from the impact of agriculture [81]. Algal biomass in our study wetland was related to turbidity, DOC and TOC (Supplementary Material, Figure S2). Turbidity in lake Albufera can be also related to punctual precipitations [82] and sediment resuspension by wind [83]. In particular, a positive gradient of organic carbon and microalgae was observed, which

starts in the north area of the Natural Park (nearby Pinedo I and II treatment plants and the Rambla de Torrent) and reaches the lake (Figure 2).

Mapping by different approaches the heterogeneity of the Natural Park of the Albufera has showed the complexity of this agroecosystem. The results show clear spatial differences in the water quality between the northern and southern aquatic systems. The north part has a greater influence of the metropolitan area of Valencia, wastewater treatment plants and industry pollution. The southern part is more affected by the extension of agriculture (mainly paddy fields). The evaluation of the ecological potential by areas provided further information about the irrigation sectors and the reuse of wastewater for agricultural activities.

The digital covers provided by QGIS were used to integrate the results obtained from the analytical analyses and allowed a detailed spatial assessment of the aquatic ecosystems of the wetland and part of the river catchment area. Firstly, the already rich nutrient waters in the irrigation channels are mixed and enriched by effluents from different wastewater treatment plants (WWTPs), especially those located in the north. The water taken from the River Turia circulates, mixed with effluents from various WWTPs and industrial treatment plants [45,84]. The WWTPs of Quart de Benager and Pinedo had the maximum values of $\text{NH}_4\text{-N}$ and nitrite nitrogen, whereas the maximum nitrate nitrogen and TP values were also found in an irrigation ditch of this zone (Favara, Figures 2 and 4). The pollution with TP was also punctual in different irrigation sectors. The maximum TN values (exceeding 14 mg N L^{-1}) were found mainly in the northwest of the lake, in irrigation ditches used for fruit and rice crops (Figure 4), but there were also some points of high dissolved organic nitrogen in the south (Figures 2 and 4). The diffuse and punctual discharges of nitrogen and phosphorus affected to the entire wetland. It is relevant that no significant differences were observed between agricultural activities, suggesting that the environmental impact depended on the water management in the wetland.

The multivariate statistical study of the irrigation sectors corroborated the location of the sites for dissolved nutrients in the northern part of the wetland (Turia River and up to the Huerta Oeste, Favara and Oro sectors). The latter two sectors and the Albufera Lake also accumulated the highest levels of organic matter, DOC and TOC (Figure 5). All these sectors are characterized by the reuse of treated wastewaters in the rice fields during the cultivation period [85]. The results pointed out that the quality of the effluents from the WWTPs is deficient in removing nutrients [45–48] and additionally can also be rich in emerging contaminants [48–50]. Overall, it seems inappropriate to use effluents from these WWTPs for agriculture in the Natural Park of the Albufera. As a possible practical solution, hybrid treatments could be included during the secondary treatment phase of the WWTPs, which keep activated sludge and biofilms in the same reactor, ensuring a higher nutrient removal efficiency [86]. More innovative proposals such as the inoculation of microalgae associated with ZnO nanoparticles into the bioreactor, or the installation of an osmotic dynamic membrane bioreactor/nanofiltration (OsMBR/NF) system, can be considered for the near future [87,88]. With a successful reduction of the nutrient levels, the use of the WWTP effluents to flood the rice fields could be considered, with no ecological risk to the Albufera lake or to the rest of the water bodies.

The Mediterranean Spanish coastal systems seem to be severely impacted by agriculture and the use of the limited water resources, which has become especially complicated in relation to rice crops, for example, in the Albufera Natural Park and the Ebro Delta [89,90]. In the Doñana National Park, the loss of water quality was related in equal parts to industrial and urban pressures (WWTPs) and also to rice cultivation [80,91]. In the Mar Menor, nitrates derived from irrigation water in the orchards shifted a whole marine ecosystem in a very short period [92]. Furthermore, in recent years other studies focusing on water quality and the correct management of Mediterranean coastal wetlands have reported the fragility and complexity of these ecosystems when they are impacted by agriculture [11,19,38,93,94].

5. Conclusions

In the present study, we evaluated the current ecological status of the Natural Park of Albufera, one of the main Spanish coastal wetlands, taking into account the anthropogenic impacts derived from agriculture, water management and the connectivity of the irrigation network. The results show that the aquatic ecosystems of the wetland are in eutrophic conditions, with poor ecological potential. The wetland is nutrient (phosphorus and nitrogen)-overloaded during the entire rice cultivation period. The input into the wetland of good quality water is deficient, since the river network already contains high levels of nutrients and pollutants, especially in the northern area, where, in addition, the poor water quality from the main river is mixed with inappropriate effluents from WWTPs.

The extensive spatial study carried out allowed the mapping of the problematic points of pollution. These locations should become focuses of attention for environmental measures. We could not help but question the sustainability of the intensive rice cultivation in the wetland. This is a reasonable concern when considering climate change scenarios.

The impact of agriculture and the water management intensively affected the lake Albufera within the Natural Park, modulating most of its studied variables. This is a sensitive habitat of flux and the accumulation of pollutants could end up in the Mediterranean Sea. The connectivity of the hydrological system in this coastal ecosystem implies a complex cause-and-effect effect from the water catchment areas to the sea.

For all these reasons, the implementation of appropriate environmental measures is considered necessary for the Albufera Natural Park. This could involve extensive and continuous monitoring of the human uses and activities in the wetland and taking action on the sources of pollution. It is important to emphasize the need to increase the ecological inputs provided by fluvial systems with higher water quality and the importance of optimizing WWTPs. It seems inappropriate to use effluents from WWTPs for agriculture in the Natural Park of the Albufera. Finally, it is clear from the results that the recovery of an adequate ecological potential requires more restrictive nutrient thresholds and legislation. The information gathered in the Albufera Park can help to optimize the global study and management of coastal Mediterranean wetlands.

Supplementary Materials: The following supporting information can be downloaded at: <https://www.mdpi.com/article/10.3390/agronomy12020486/s1>. Table S1: Classification of sampling points according to their corresponding aquatic habitat, the agricultural activity carried out in its vicinity, the irrigation zone and the water body typology. Water body typology established according to the Water Framework Directive [24] and Decree 1/2016 (reference: BOE-A-2016-439); Table S2: Limit of detection (LOD) and limit of quantification (LOQ) of the main physico-chemical and biological variables determined in the laboratory, studied in the water bodies during rice cultivation (May to October 2019); Table S3: Mean, standard error, maximum and minimum values of the physico-chemical and biological variables studied in the wetland for the two sampling campaigns at the beginning and the end of rice cultivation (see Section 2 for more details); Figure S1: Frequency distribution and adjustment curves of turbidity, pH, conductivity, total nutrients, organic matter and phytoplanktonic chlorophyll for the values of the two sampling periods; Figure S2: Significant linear relationships ($p < 0.01$) of the study variables related to chlorophyll (A) and nitrogen (B), together with the values of Spearman's correlation coefficient; Figure S3: Significant linear relationships ($p < 0.01$) of the study variables related to phosphorus (A) and carbon (B), together with the values of Spearman's correlation coefficient; Figure S4: Percentages of the ecological potential for the different aquatic ecosystems and typologies [24,70]. Results for (A) the global study of the wetland and for the distinct water body typologies, (B) considering aquatic habitats, (C) according to agricultural activities and (D) according to irrigation zones.

Author Contributions: Conceptualization: S.R. and L.V.-H.; methodology: L.V.-H.; formal analysis: L.V.-H., S.R. and J.S.; investigation: L.V.-H., S.R. and J.S.; data curation: L.V.-H., S.R. and J.S.; writing—original draft preparation: L.V.-H.; writing—review and editing: S.R. and J.S.; visualization: L.V.-H.; supervision: S.R. and J.S. All authors have read and agreed to the published version of the manuscript.

Funding: This research was funded by the Spanish Ministry of Science, Innovation and Universities and the European Regional Development Fund (ERDF) through the project WETANPACK (grant number RTI2018-097158-B-C31) and by the Generalitat Valenciana through the project ANTROPOCEN@ (PROMETEO/2018/155).

Institutional Review Board Statement: Not applicable.

Informed Consent Statement: Not applicable.

Data Availability Statement: Not applicable.

Acknowledgments: We are grateful to all our collaborators for their valuable help and support during field and laboratory work, especially to our colleges from the CIDE-UV-GV Institute during sampling. We also thank to the Sara Calvo for her help during the research and the Valencia Environmental Agency for the facilities given during the study.

Conflicts of Interest: The authors declare no conflict of interest. The funders had no role in the design of the study; in the collection, analyses, or interpretation of data; in the writing of the manuscript, or in the decision to publish the results.

References

1. Chiaia-Hernández, A.C.; Günthardt, B.F.; Frey, M.P.; Hollender, J. Unravelling Contaminants in the Anthropocene Using Statistical Analysis of Liquid Chromatography–High-Resolution Mass Spectrometry Nontarget Screening Data Recorded in Lake Sediments. *Environ. Sci. Technol.* **2017**, *51*, 12547–12556. [CrossRef] [PubMed]
2. Yuan, X.; Zhang, M.; Wang, L.; Zhou, T. Understanding and Seasonal Forecasting of Hydrological Drought in the Anthropocene. *Hydrol. Earth Syst. Sci.* **2017**, *21*, 5477–5492. [CrossRef]
3. Mitsch, W.J.; Gosselink, J.G. *Wetlands*, 4th ed.; John Wiley & Sons: Hoboken, NJ, USA, 2007.
4. Moss, B. Fresh Waters, Climate Change and UK Nature Conservation. *Freshw. Rev.* **2014**, *7*, 25–75. [CrossRef]
5. Raymond, P.A.; Hartmann, J.; Lauerwald, R.; Sobek, S.; McDonald, C.; Hoover, M.; Butman, D.; Striegl, R.; Mayorga, E.; Humborg, C. Global Carbon Dioxide Emissions from Inland Waters. *Nature* **2013**, *503*, 355–359. [CrossRef]
6. Romo, S.; Soria, J.; Olmo, C.; Flor, J.; Calvo, S.; Ortells, R.; Armengol, X. Nutrients and Carbon in Some Mediterranean Dune Ponds. *Hydrobiologia* **2016**, *782*, 97–109. [CrossRef]
7. Shaltout, K.; El-Bana, M.; Galal, T. Coastal Lakes as Hot Spots for Plant Diversity in Egypt. In *Egyptian Coastal Lakes and Wetlands: Part II*; Negm, A.M., Beck, M.A., Abdel-Fattah, S., Eds.; Springer: Berlin/Heidelberg, Germany, 2017; pp. 129–146.
8. Were, D.; Kansime, F.; Fetahi, T.; Cooper, A.; Jjuuko, C. Carbon Sequestration by Wetlands: A Critical Review of Enhancement Measures for Climate Change Mitigation. *Earth Syst. Environ.* **2019**, *3*, 327–340. [CrossRef]
9. Gardner, R.C.; Finlayson, C.M. *Global Wetland Outlook: State of the World's Wetlands and Their Services to People 2018*; Secretariat of the Ramsar Convention: Gland, Switzerland, 2018.
10. Pascual-Aguilar, J.A.; Andreu Pérez, V.; Gimeno-García, E.; Picó, Y. Current Anthropogenic Pressures on Agro-Ecological Protected Coastal Wetlands. *Sci. Total Environ.* **2015**, *503*, 190–199. [CrossRef]
11. Leberger, R.; Geijzendorffer, I.R.; Gaget, E.; Gwelmami, A.; Galewski, T.; Pereira, H.M.; Guerra, C.A. Mediterranean Wetland Conservation in the Context of Climate and Land Cover Change. *Reg. Environ. Chang.* **2020**, *20*, 67. [CrossRef]
12. Myers, N.; Mittermeier, R.A.; Mittermeier, C.G.; da Fonseca, G.A.B.; Kent, J. Biodiversity Hotspots for Conservation Priorities. *Nature* **2000**, *403*, 853–858. [CrossRef]
13. Cuttelod, A.; García, N.; Malak, D.A.; Temple, H.J.; Stuart, S.N. The Mediterranean: A Biodiversity Hotspot under Threat. In *Wildlife in a Changing World: An Analysis of the 2008 IUCN Red List of Threatened Species*; Vié, J.C., Hilton-Taylor, C., Stuart, S.N., Eds.; IUCN: Gland, Switzerland, 2009.
14. Li, Y.; Zhu, X.; Sun, X.; Wang, F. Landscape Effects of Environmental Impact on Bay-Area Wetlands under Rapid Urban Expansion and Development Policy: A Case Study of Lianyungang, China. *Landsc. Urban Plan.* **2010**, *94*, 218–227. [CrossRef]
15. García-Ruiz, J.M.; López-Moreno, J.I.; Vicente-Serrano, S.M.; Lasanta-Martínez, T.; Beguería, S. Mediterranean Water Resources in a Global Change Scenario. *Earth-Sci. Rev.* **2011**, *105*, 121–139. [CrossRef]
16. Guiot, J.; Cramer, W. Climate Change: The 2015 Paris Agreement Thresholds and Mediterranean Basin Ecosystems. *Science* **2016**, *354*, 465–468. [CrossRef] [PubMed]
17. Klausmeyer, K.R.; Shaw, M.R. Climate Change, Habitat Loss, Protected Areas and the Climate Adaptation Potential of Species in Mediterranean Ecosystems Worldwide. *PLoS ONE* **2009**, *4*, e6392. [CrossRef]
18. Mariotti, A.; Zeng, N.; Yoon, J.-H.; Artale, V.; Navarra, A.; Alpert, P.; Li, L.Z. Mediterranean Water Cycle Changes: Transition to Drier 21st Century Conditions in Observations and CMIP3 Simulations. *Environ. Res. Lett.* **2008**, *3*, 044001. [CrossRef]
19. Geijzendorffer, I.; Chazée, L.; Gaget, E.; Galewski, T.; Gwelmami, A.; Perennou, C.; Davidson, N.; McInnes, R. *Mediterranean Wetlands Outlook 2: Solutions for Sustainable Mediterranean Wetlands*; Secretariat of the Ramsar Convention: Arles, France, 2018.
20. Jégou, A.; Sanchis-Ibor, C. The Opaque Lagoon. Water Management and Governance in l'Albufera de València Wetland (Spain). *Limnetica* **2019**, *38*, 503–515. [CrossRef]

21. Pascual-Aguilar, J.A.; Campo, J.; Meneu, S.N.; Gimeno-García, E.; Andreu, V. Analysis of Existing Water Information for the Applicability of Water Quality Indices in the Fluvial-Littoral Area of Turia and Júcar Rivers, Valencia, Spain. *Appl. Geogr.* **2019**, *111*, 102062. [CrossRef]
22. EEC. Council Directive 91/676/EEC, of 12 December 1991, concerning the protection of waters against pollution caused by nitrates from agricultural sources. *Off. J. Eur. Comm.* **1991**, L375, 1–8. Available online: <https://eur-lex.europa.eu/legal-content/EN/TXT/?uri=OJ:L:1991:375:TOC> (accessed on 10 May 2021).
23. EEC. Council Directive 91/271/EEC, of 21 May 1991, concerning urban wastewater. *Off. J. Eur. Comm.* **1991**, L135, 40–52. Available online: <https://eur-lex.europa.eu/legal-content/EN/TXT/?uri=OJ:L:1991:135:TOC> (accessed on 10 May 2021).
24. EC. Council Directive 2000/60/EC, of 23 October 2000, establishing a framework for Community action in the field of water policy. *Off. J. Eur. Comm.* **2000**, L327, 1–73. Available online: <https://eur-lex.europa.eu/legal-content/EN/TXT/?uri=OJ:L:2000:327:TOC> (accessed on 9 May 2021).
25. Carlson, R.E. A Trophic State Index for Lakes. *Limnol. Oceanogr.* **1977**, *22*, 361–369. [CrossRef]
26. Li, B.; Yang, G.; Wan, R.; Hörmann, G. Dynamic Water Quality Evaluation Based on Fuzzy Matter–Element Model and Functional Data Analysis, a Case Study in Poyang Lake. *Environ. Sci. Pollut. Res.* **2017**, *24*, 19138–19148. [CrossRef] [PubMed]
27. Şener, Ş.; Şener, E.; Davraz, A. Evaluation of Water Quality Using Water Quality Index (WQI) Method and GIS in Aksu River (SW-Turkey). *Sci. Total Environ.* **2017**, *584–585*, 131–144. [CrossRef]
28. Sun, W.; Xia, C.; Xu, M.; Guo, J.; Sun, G. Application of Modified Water Quality Indices as Indicators to Assess the Spatial and Temporal Trends of Water Quality in the Dongjiang River. *Ecol. Indic.* **2016**, *66*, 306–312. [CrossRef]
29. Escribano-Francés, G.; Quevauviller, P.; San Martín González, E.; Vargas Amelin, E. Climate Change Policy and Water Resources in the EU and Spain. A Closer Look into the Water Framework Directive. *Environ. Sci. Policy* **2017**, *69*, 1–12. [CrossRef]
30. Hestir, E.L.; Brando, V.E.; Bresciani, M.; Giardino, C.; Matta, E.; Villa, P.; Dekker, A.G. Measuring Freshwater Aquatic Ecosystems: The Need for a Hyperspectral Global Mapping Satellite Mission. *Remote Sens. Environ.* **2015**, *167*, 181–195. [CrossRef]
31. Dominguez, J.A. Estudio de La Calidad Del Agua de Las Lagunas de Gravera Mediante Teledetección. Doctoral Thesis, Universidad de Alcalá, Alcalá de Henares, Spain, 2003.
32. Osorio, R.J.; Linhoss, A.; Dash, P. Evaluation of Marsh Terraces for Wetland Restoration: A Remote Sensing Approach. *Water* **2020**, *12*, 336. [CrossRef]
33. Sòria-Perpinyà, X.; Vicente, E.; Urrego, P.; Pereira-Sandoval, M.; Tenjo, C.; Ruíz-Verdú, A.; Delegido, J.; Soria, J.M.; Peña, R.; Moreno, J. Validation of Water Quality Monitoring Algorithms for Sentinel-2 and Sentinel-3 in Mediterranean Inland Waters with In Situ Reflectance Data. *Water* **2021**, *13*, 686. [CrossRef]
34. Vera-Herrera, L.; Soria, J.; Pérez, J.; Romo, S. Long-Term Hydrological Regime Monitoring of a Mediterranean Agro-Ecological Wetland Using Landsat Imagery: Correlation with the Water Renewal Rate of a Shallow Lake. *Hydrology* **2021**, *8*, 172. [CrossRef]
35. Foltête, J.-C.; Vuidel, G. Using Landscape Graphs to Delineate Ecologically Functional Areas. *Landsc. Ecol.* **2017**, *32*, 249–263. [CrossRef]
36. Wang, X.; Zhang, J.; Babovic, V.; Gin, K.Y.H. A Comprehensive Integrated Catchment-Scale Monitoring and Modelling Approach for Facilitating Management of Water Quality. *Environ. Model. Softw.* **2019**, *120*, 104489. [CrossRef]
37. Roche, K.R.; Aubeneau, A.F.; Xie, M.; Aquino, T.; Bolster, D.; Packman, A.I. An Integrated Experimental and Modeling Approach to Predict Sediment Mixing from Benthic Burrowing Behavior. *Environ. Sci. Technol.* **2016**, *50*, 10047–10054. [CrossRef] [PubMed]
38. Çevirgen, S.; Elwany, H.; Pesce, M.; Zirino, A. Managing Nutrient Pollution in Venice Lagoon (Italy): A Practical Tool for Assessment of Water Quality. *Sustain. Water Resour. Manag.* **2020**, *6*, 33. [CrossRef]
39. Elshemy, M.; Zeidan, B.; Assar, W. Water Quality Mitigation Scenarios for Burullus Coastal Lake, Egypt. In *Estuaries and Coastal Zones in Times of Global Change*; Nguyen, K.D., Guillou, S., Gourbesville, P., Thiébot, J., Eds.; Springer: Berlin, Germany, 2020; pp. 89–110.
40. Shalby, A.; Elshemy, M.; Zeidan, B.A. Assessment of Climate Change Impacts on Water Quality Parameters of Lake Burullus, Egypt. *Egypt. Environ. Sci. Pollut. Res.* **2020**, *27*, 32157–32178. [CrossRef]
41. Generalitat Valenciana. Parc Natural de l’Albufera. 2015. Available online: <http://www.parquesnaturales.gva.es/es/web/pn-l-albufera> (accessed on 10 January 2021).
42. Pascual-Aguilar, J.A. Cambios de Usos del Suelo y Régimen Hídrico en la Rambla de Poyo y el Barranc de Carraixet. Doctoral Thesis, Universitat de València, Valencia, Spain, 2004.
43. Gil Olcina, A.; Rico, A. *El Problema Del Agua En La Comunidad Valenciana*; Fundación de la Comunidad Valenciana Agua y Progreso: Valencia, Spain, 2007; ISBN 84-611-5317-0.
44. Pascual-Aguilar, J.A.; Andreu, V.; Vázquez, P.; Picó, Y. Presence and Spatial Distribution of Emerging Contaminants (Drugs of Abuse) in Protected Agroecological Systems (L’Albufera de Valencia Coastal Wetland, Spain). *Environ. Earth Sci.* **2014**, *71*, 31–37. [CrossRef]
45. Martín, M.; Hernández-Crespo, C.; Andrés-Doménech, I.; Benedito-Durá, V. Fifty Years of Eutrophication in the Albufera Lake (Valencia, Spain): Causes, Evolution and Remediation Strategies. *Ecol. Eng.* **2020**, *155*, 105932. [CrossRef]
46. Aznar, R.; Sánchez-Brunete, C.; Albero, B.; Moreno-Ramón, H.; Tadeo, J.L. Pyrethroids Levels in Paddy Field Water under Mediterranean Conditions: Measurements and Distribution Modelling. *Paddy Water Environ.* **2017**, *15*, 307–316. [CrossRef]
47. Campo, J.; Masiá, A.; Picó, Y.; Farré, M.; Barceló, D. Distribution and Fate of Perfluoroalkyl Substances in Mediterranean Spanish Sewage Treatment Plants. *Sci. Total Environ.* **2014**, *472*, 912–922. [CrossRef]

48. Lorenzo, M.; Campo, J.; Morales Suárez-Varela, M.; Picó, Y. Occurrence, Distribution and Behavior of Emerging Persistent Organic Pollutants (POPs) in a Mediterranean Wetland Protected Area. *Sci. Total Environ.* **2019**, *646*, 1009–1020. [CrossRef]
49. Sadutto, D.; Andreu, V.; Ilo, T.; Akkanen, J.; Picó, Y. Pharmaceuticals and Personal Care Products in a Mediterranean Coastal Wetland: Impact of Anthropogenic and Spatial Factors and Environmental Risk Assessment. *Environ. Pollut.* **2021**, *271*, 116353. [CrossRef]
50. Sadutto, D.; Andreu, V.; Ilo, T.; Akkanen, J.; Picó, Y. Dataset of Pharmaceuticals and Personal Care Products in a Mediterranean Coastal Wetland. *Data Brief* **2021**, *36*, 106934. [CrossRef]
51. Romo, S.; Villena, M.-J.; Sahuquillo, M.; Soria, J.M.; Giménez, M.; Alfonso, T.; Vicente, E.; Miracle, M.R. Response of a Shallow Mediterranean Lake to Nutrient Diversion: Does It Follow Similar Patterns as in Northern Shallow Lakes? *Freshw. Biol.* **2005**, *50*, 1706–1717. [CrossRef]
52. Soria, J.; Vicente, E.; Miracle, M. The Influence of Flash Floods on the Limnology of the Albufera of Valencia Lagoon (Spain). *SIL Proc.* **2000**, *27*, 2232–2235. [CrossRef]
53. Soria, J.M.; Vicente, E. Estudio de Los Aportes Hídricos al Parque Natural de La Albufera de Valencia. *Limnetica* **2002**, *21*, 105–115. [CrossRef]
54. Soria, J.; Vera-Herrera, L.; Calvo, S.; Romo, S.; Vicente, E.; Sahuquillo, M.; Sòria-Perpinyà, X. Residence Time Analysis in the Albufera of Valencia, a Mediterranean Coastal Lagoon, Spain. *Hydrology* **2021**, *8*, 37. [CrossRef]
55. Arévalo, C. *Introducción al Estudio de Los Cladóceros Del Plankton de La Albufera de Valencia*; Anales del Instituto General y Técnico de Valencia, 1; Imprenta Hijos de Francisco Vives Mora: Valencia, Spain, 1916.
56. Blanco, C. Estudio de La Contaminación de La Albufera de Valencia y de Los Efectos de Dicha Contaminación Sobre La Fauna y Flora Del Lago. Doctoral Thesis, Universitat de València, Valencia, Spain, 1974.
57. Dafaue Ruiz, C. La Albufera de Valencia: Un Estudio Piloto. In *Monografías*; Instituto para la Conservación de la Naturaleza (ICONA): Valencia, España, 1975; Volume 4, pp. 1–127.
58. Pardo, L. *La Albufera de Valencia. Biología de Las Aguas Continentales II*; Instituto Forestal de Investigaciones y Experiencias: Madrid, Spain, 1942.
59. Onandia, G.; Gudimov, A.; Miracle, M.R.; Arhonditsis, G. Towards the Development of a Biogeochemical Model for Addressing the Eutrophication Problems in the Shallow Hypertrophic Lagoon of Albufera de Valencia, Spain. *Ecol. Inform.* **2015**, *26*, 70–89. [CrossRef]
60. Segura, J.B.M.; Ibor, C.S.; Vázquez, A.V. Regadío y Saneamiento Urbano En l'Albufera de València: Análisis Cartográfico. *Cuad. Geogr.* **1999**, *65*, 61–80.
61. Romo, S.; Soria, J.; Fernández, F.; Ouahid, Y.; Barón-Solá, Á. Water Residence Time and the Dynamics of Toxic Cyanobacteria. *Freshw. Biol.* **2013**, *58*, 513–522. [CrossRef]
62. Copernicus Land Monitoring Service. CORINE Land Cover 2018. Available online: <https://land.copernicus.eu/pan-european/corine-land-cover/clc2018> (accessed on 30 December 2020).
63. Mondría, M. *Estudio Para El Desarrollo Sostenible de L'Albufera de Valencia. Síntesis de Los Estudios Técnicos*; Confederación Hidrográfica Del Júcar: Madrid, Spain, 2004.
64. APHA. *Standard Methods for the Examination of Water and Wastewater*; General Books LLC: Memphis, TN, USA, 2011.
65. UNE-EN 1484:1998; Water Analysis—Guidelines for the Determination of Total Organic Carbon (TOC) and Dissolved Organic Carbon (DOC). European Committee for Standardization: Bruxelles, Belgium, 1997.
66. Murphy, J.; Riley, J.P. A Modified Single Solution Method for the Determination of Phosphate in Natural Waters. *Anal. Chim. Acta* **1962**, *27*, 31–36. [CrossRef]
67. Jeffrey, E.; Humphrey, G.F. New Spectrophotometric Equations for Determining Chlorophyll a, b, c1 and c2 in Higher Plants, Algae and Natural Phytoplankton. *Biochem. Physiol.* **1975**, *167*, 91–194. [CrossRef]
68. OECD. Organisation for Economic Co-Operation and Development. 1982. Available online: <http://www.oecd.org/> (accessed on 10 March 2021).
69. Nürnberg, G.K. Trophic State of Clear and Colored, Soft-and Hardwater Lakes with Special Consideration of Nutrients, Anoxia, Phytoplankton and Fish. *Lake Reserv. Manag.* **1996**, *12*, 432–447. [CrossRef]
70. Decret 817/2015. BOE. Real Decreto 817/2015, de 11 de Septiembre, Por El Que Se Establecen Los Criterios de Seguimiento y Evaluación Del Estado de Las Aguas Superficiales y Las Normas de Calidad Ambiental. Available online: https://www.boe.es/diario_boe/txt.php?id=BOE-A-2015-9806 (accessed on 12 April 2021).
71. AVAMET Meteorological Historical Database. Available online: <https://www.avamet.org/> (accessed on 10 February 2021).
72. Hammer, Ø.; Harper, D.A.; Ryan, P.D. PAST: Paleontological Statistics Software Package for Education and Data Analysis. *Palaeontol. Electron.* **2001**, *4*, 9.
73. Decret 509/1996. BOE. Real Decreto 509/1996, de 15 de Marzo, de Desarrollo Del Real Decreto-Ley 11/1995, de 28 de Diciembre, Por El Que Se Establecen Las Normas Aplicables al Tratamiento de Las Aguas Residuales Urbanas. Available online: https://www.boe.es/diario_boe/txt.php?id=BOE-A-1996-7159 (accessed on 10 April 2021).
74. Jeppesen, E.; Søndergaard, M.; Meerhoff, M.; Lauridsen, T.L.; Jensen, J.P. Shallow Lake Restoration by Nutrient Loading Reduction—Some Recent Findings and Challenges Ahead. *Hydrobiologia* **2007**, *584*, 239–252. [CrossRef]
75. Romo, S.; Miracle, M.R.; Villena, M.; Rueda, J.; Ferriol, C.; Vicente, E. Mesocosm Experiments on Nutrient and Fish Effects on Shallow Lake Food Webs in a Mediterranean Climate. *Freshw. Biol.* **2004**, *49*, 1593–1607. [CrossRef]

76. Soria, J.; Romo, S.; Vera-Herrera, L.; Calvo, S.; Sòria-Perpinyà, X. Evolución de la conductividad en la Albufera de Valencia entre 1985 y 2018. *Limnetica* **2021**, *40*, 223–232. [CrossRef]
77. Sòria-Perpinyà, X. Remote Sensing Application for the Study of Rapid Flushing to Remediate Eutrophication in Shallow Lagoons (Albufera of Valencia). *Hydrobiologia* **2019**, *829*, 125–132. [CrossRef]
78. Calvo, S.; Romo, S.; Soria, J.; Picó, Y. Pesticide Contamination in Water and Sediment of the Aquatic Systems of The Natural Park of the Albufera of Valencia (Spain) during the Rice Cultivation Period. *Sci. Total Environ.* **2021**, *774*, 145009. [CrossRef]
79. Pérez-Ruzafa, A.; Campillo, S.; Fernández-Palacios, J.M.; García-Lacunza, A.; García-Oliva, M.; Ibañez, H.; Navarro-Martínez, P.C.; Pérez-Marcos, M.; Pérez-Ruzafa, I.M.; Quispe-Becerra, J.I.; et al. Long-Term Dynamic in Nutrients, Chlorophyll a, and Water Quality Parameters in a Coastal Lagoon During a Process of Eutrophication for Decades, a Sudden Break and a Relatively Rapid Recovery. *Front. Mar. Sci.* **2019**, *6*, 26. [CrossRef]
80. Paredes Losada, I. Anthropogenic Pressures and Eutrophication in the Doñana Marsh and Its Watershed. Doctoral Thesis, Universidad de Sevilla, Sevilla, Spain, 2020.
81. Rizk, R.; Juzsakova, T.; Cretescu, I.; Rawash, M.; Sebestyén, V.; Le Phuoc, C.; Kovács, Z.; Domokos, E.; Rédey, Á.; Shafik, H. Environmental Assessment of Physical-Chemical Features of Lake Nasser, Egypt. *Environ. Sci. Pollut. Res.* **2020**, *27*, 20136–20148. [CrossRef]
82. Sebastián-Frasquet, M.-T.; Aguilar-Maldonado, J.A.; Santamaría-Del-Ángel, E.; Estornell, J. Sentinel 2 Analysis of Turbidity Patterns in a Coastal Lagoon. *Remote Sens.* **2019**, *11*, 2926. [CrossRef]
83. Soria, J.; Jover-Cerdá, M.; Gómez, J. Influence of Wind on Suspended Matter in the Water of the Albufera of Valencia (Spain). *J. Mar. Sci. Eng.* **2021**, *9*, 343. [CrossRef]
84. Mondría, M. Infraestructuras y Eutrofización en L'Albufera de València. El Modelo Cabhal. Doctoral Thesis, Universidad Politécnica de Valencia, Valencia, Spain, 2010.
85. Vazquez-Roig, P.; Andreu, V.; Blasco, C.; Picó, Y. SPE and LC-MS/MS Determination of 14 Illicit Drugs in Surface Waters from the Natural Park of L'Albufera (València, Spain). *Anal. Bioanal. Chem.* **2010**, *397*, 2851–2864. [CrossRef] [PubMed]
86. Rodríguez-Hernández, L.; Esteban-García, A.L.; Lobo, A.; Temprano, J.; Álvaro, C.; Mariel, A.; Tejero, I. Evaluation of a Hybrid Vertical Membrane Bioreactor (HVMBR) for Wastewater Treatment. *Water Sci. Technol.* **2012**, *65*, 1109–1115. [CrossRef] [PubMed]
87. Vasistha, S.; Khanra, A.; Rai, M.P. Influence of Microalgae-ZnO Nanoparticle Association on Sewage Wastewater towards Efficient Nutrient Removal and Improved Biodiesel Application: An Integrated Approach. *J. Water Process. Eng.* **2021**, *39*, 101711. [CrossRef]
88. Nguyen, N.C.; Nguyen, H.T.; Duong, H.C.; Chen, S.-S.; Le, H.Q.; Duong, C.C.; Trang, L.T.; Chen, C.-K.; Nguyen, P.D.; Bui, X.T.; et al. A Breakthrough Dynamic-Osmotic Membrane Bioreactor/Nanofiltration Hybrid System for Real Municipal Wastewater Treatment and Reuse. *Bioresour. Technol.* **2021**, *342*, 125930. [CrossRef]
89. Cerralbo, P.; F-Pedrerá Balsells, M.; Mestres, M.; Fernandez, M.; Espino, M.; Grifoll, M.; Sanchez-Arcilla, A. Use of a Hydrodynamic Model for the Management of Water Renovation in a Coastal System. *Ocean Sci.* **2019**, *15*, 215–226. [CrossRef]
90. Mañosa, S.; Mateo, R.; Guitart, R. A Review of the Effects of Agricultural and Industrial Contamination on the Ebro Delta Biota and Wildlife. *Environ. Monit. Assess.* **2001**, *71*, 187–205. [CrossRef]
91. Camacho-Muñoz, D.; Martín, J.; Santos, J.; Aparicio, I.; Alonso, E. Distribution and Risk Assessment of Pharmaceutical Compounds in River Sediments from Doñana Park (Spain). *Water Air Soil Pollut.* **2013**, *224*, 1665. [CrossRef]
92. Álvarez-Rogel, J.; Jiménez-Cárceles, F.; Nicolás, C.E. Phosphorus and Nitrogen Content in the Water of a Coastal Wetland in the Mar Menor Lagoon (SE Spain): Relationships with Effluents from Urban and Agricultural Areas. *Water Air Soil Pollut.* **2006**, *173*, 21–38. [CrossRef]
93. Day, J.W.; Ibañez, C.; Pont, D.; Scarton, F. Status and Sustainability of Mediterranean Deltas: The Case of the Ebro, Rhône, and Po Deltas and Venice Lagoon. In *Coasts and Estuaries*; Wolanski, E., Day, J.W., Elliot, M., Ramachandran, R., Eds.; Elsevier: Amsterdam, The Netherlands, 2019; pp. 237–249.
94. Tórz, A.; Bonisławska, M.; Rybczyk, A.; Nędzarek, A.; Tański, A. Susceptibility to Degradation, the Causes of Degradation, and Trophic State of Three Lakes in North-West Poland. *Water* **2020**, *12*, 1635. [CrossRef]

Article

Numerical Simulation of Soil Water–Salt Dynamics and Agricultural Production in Reclaiming Coastal Areas Using Subsurface Pipe Drainage

Peirong Lu, Yujie Yang, Wan Luo, Yu Zhang and Zhonghua Jia *

College of Hydraulic Science and Engineering, Yangzhou University, Yangzhou 225009, China

* Correspondence: jiazh@yzu.edu.cn

Abstract: Soil salinization induced by shallow saline groundwater in coastal areas can be managed using subsurface pipe drainage (SPD) for agricultural land reclamation. However, a reasonable SPD system layout should comprehensively consider local hydrological conditions and crop physiological characteristics based on long-term model evaluations. The objectives of this study were to test the applicability of a crop growth model (AquaCrop) for simulating winter wheat growth in SPD-applied fields by employing the water table behaviors predicted by the soil hydrologic model HYDRUS. Model calibration and validation based on field observations suggested that HYDRUS accurately predicted the distributions of soil water–salt dynamics, and the seasonal variations of canopy cover and biomass production predicted by AquaCrop were close to the measured values. The simulation scenarios considering the long-term effect of groundwater salinity (10.53, 21.06, and 31.59 g L⁻¹ for low, medium, and high levels), drain spacing (10, 20, 30, 40 m, and no-SPD), and precipitation category (dry, normal, and wet year) on soil solute transport, grain yield (GY), water productivity (WP), and groundwater supply (GS) were further explored using a combination of HYDRUS and AquaCrop. The simulation results indicated that narrowing the drain spacing could improve the desalination performance of SPD, but there was no continuous downward trend of soil solute concentration during the long-term application of SPD when groundwater salinity was constant. The SPD application could improve grain yield by 0.81–1.65 t ha⁻¹, water productivity by 0.13–0.35 kg m⁻³, and groundwater supply by 6.06–31.03 mm compared to the no-SPD scenarios, but such increases would be less pronounced in dry years with groundwater salinity at the low level. This study demonstrated that the co-application of hydrologic and crop growth models is a feasible method for revealing the effects of SPD on agricultural land reclamation in coastal areas.

Keywords: subsurface pipe drainage; soil salinity; saline groundwater; winter wheat; numerical simulation



Citation: Lu, P.; Yang, Y.; Luo, W.; Zhang, Y.; Jia, Z. Numerical Simulation of Soil Water–Salt Dynamics and Agricultural Production in Reclaiming Coastal Areas Using Subsurface Pipe Drainage. *Agronomy* **2023**, *13*, 588. <https://doi.org/10.3390/agronomy13020588>

Academic Editors: Aliasghar Montazar and Belen Gallego-Elvira

Received: 3 January 2023

Revised: 9 February 2023

Accepted: 16 February 2023

Published: 18 February 2023



Copyright: © 2023 by the authors. Licensee MDPI, Basel, Switzerland. This article is an open access article distributed under the terms and conditions of the Creative Commons Attribution (CC BY) license (<https://creativecommons.org/licenses/by/4.0/>).

1. Introduction

By the end of the 21st century, the global extent of coastal marshes is predicted to increase by 60% compared to the current area (approximately 2×10^5 km²), under the present level of fluvial sediment supply [1]. Therefore, coastal land reclamation is widely regarded as a sustainable strategy for meeting the increasing land resource demand for urbanization, industrialization, and agriculture [2]. However, the hydrological and hydrochemical conditions in the freshwater–seawater-interacting coastal stratum are controlled by land–ocean hydraulic gradients [3,4], which are likely to induce seawater intrusion and cause soil salinization in low-lying terrain (such as salt marshes or mudflats), which is often considered to be land resources reserved for cultivation [5]. The salinity dynamics in the soil surface layer of the coastal area are affected by precipitation, phreatic water evaporation, surface ecosystems, topography, and seawater intrusion [6–8], but the root cause of soil salinization is capillary-driven upward solute transport from saline groundwater, which

may cause salt stress that severely constrains the development of crop-based agriculture when adequate soil leaching and reasonable drainage management are lacking [9].

Subsurface pipe drainage (SPD) has been reported as a suitable method for the desalinization process during land reclamation in coastal areas with a shallow groundwater table and low-permeability soil texture [10,11]. By increasing the lateral discharge of soil water, SPD can control the groundwater table in a timely manner and further limit the capillary-driven upward solute build-up in the upper layers, thereby persistently protecting crop growth from salt stress [12,13]. As numerous previous studies have suggested, the drainage performance of SPD is highly dependent on the layout pattern of the subsurface drainpipe, including drain spacing, buried depth, and drainpipe diameter. The drain spacing can vary from a few to hundreds of meters based on different application requirements, and is the most researched factor during SPD system design [14–16]. Reasonable drain spacing usually corresponds to the optimal efficiency of water table control or salt discharge under a specific agricultural condition. Notably, blindly pursuing an SPD with high drainage capacity can induce excessive soil nutrient loss and restricted groundwater supply, which in turn affects crop growth and limits water use efficiency [17]. Therefore, the response of crop growth could be the most intuitive indicator for evaluating land reclamation status under the application of SPD, and the salt dynamics in the soil profile should be analyzed in the long term concerning groundwater salinity and SPD layout patterns.

Multiple factors (e.g., soil properties, weather, crop species, and field management) influence the performance of SPD systems, making it challenging to fully assess their interactions through limited field experimentation. A hydrologic numerical model, HYDRUS, is widely reported to be a powerful tool for integrating various environmental and management factors that influence soil water and solute transport under different SPD system designs [18–20]. The HYDRUS model has the advantage of providing flexible boundary conditions and great applicability to variably saturated media, which is convenient for establishing the scenario simulations that take varying rainfall and water table behaviors into account [21]. Additionally, the HYDRUS model uses an osmotic-pressure-related equation to calculate root water uptake [22], and incorporates a compensatory mechanism for the simulation of root-level physiological responses subject to salt and water stress situations [23]. However, the HYDRUS model lacks the ability to predict stress-affected crop biomass development and final grain yield, limiting the model application prospect in the evaluation of land reclamation for agricultural purposes. Therefore, the HYDRUS model has been recommended to be co-applied with crop growth models such as WOFOST, DSSAT, and AquaCrop to predict the crop development in fields with particular fertilization or irrigation regimes [24–26]. In terms of the crop-based model, the canopy-level AquaCrop model, based on the conservative relationship between crop biomass and transpiration, has been extensively studied to guide field-scale water or fertilizer management by estimating crop biomass progression, grain yield, and associated water productivity [27–29]. Meanwhile, in AquaCrop, the effect of soil salinity on biomass production is described by a salinity stress–crop response curve which consists of a lower and an upper threshold of soil salt content that corresponds to the extent of salt stress from no effect to full effect [30]. However, the drainage process in the soil profile is simplified in AquaCrop and is uniformly classified as deep percolation [31], which causes AquaCrop to be unable to calculate the lateral flow in drained fields or further simulate water table behaviors affected by SPD [32,33]. So far, AquaCrop has not been combined with HYDRUS to simulate the crop growth response to SPD in a coastal reclamation area where soil salinization is mainly caused by capillary-raised solutes from saline groundwater.

Thus, the main objectives of this study were to: (1) verify the feasibility of the AquaCrop model for simulating the response of crop growth in SPD-applied fields based on HYDRUS-predicted water table behaviors; (2) explore the evolution of soil solute concentration under long-term (30 years) application of the SPD system; and (3) investigate the variability of crop grain yield, water productivity, and groundwater upward supply as a function of groundwater salinity and drain spacing in different precipitation years.

2. Materials and Methods

2.1. Experimental Site Description and Data Collection

This study was conducted from 2020 to 2021 at the Coastal Area Research Station of Jiangsu Hydraulic Research Institute, located in Dongtai, Jiangsu Province, Eastern China (120°53' E, 32°51' N, mean altitude 4 m above sea level, approximately 5 km away from the Yellow Sea). Formed by sedimentation, the topography in this area is extremely flat (slope ranging from 0.1/1000 to 1/1000), and the dominated land use type is cultivated land for rice and wheat farming. The experimental site has a subtropical monsoon climate, and the long-term average annual air temperature, precipitation, relative humidity, sunshine duration, pan evaporation, and solar radiation are 14.9 °C, 969.2 mm, 79.6%, 1685.5 h, 1064 mm, and 1169 MJ m⁻¹, respectively (meteorological data series of 1953–2020 from the weather station of Dongtai, No. 58251). More than 60% of precipitation is concentrated between June and September. The measured basic physical soil properties at 0–300 cm depth in the experimental field are present in Table 1. The salinity of the 0–300 cm soil profile was averaged at 2.75 dS m⁻¹ (saturated electrical conductivity ECe), which is classified as a slightly saline soil [34].

Table 1. Soil properties in the experimental site.

Depth (cm)	Bulk Density (g cm ⁻³)	Field Capacity (cm ³ cm ⁻³)	Wilting Point (cm ⁻³ cm ⁻³)	Saturated Water Content (cm ⁻³ cm ⁻³)	Mechanical Composition (%)			Soil Texture
					Sand	Slit	Clay	
0–30	1.36 a	0.22 a	0.12 a	0.46 b	40.9	56.3	2.8	Silt loam
30–100	1.42 b	0.29 b	0.14 a	0.42 a	35.4	61.3	3.3	
100–200	1.44 b	0.31 b	0.15 a	0.42 a	35.5	60.4	4.1	
200–300	1.45 b	0.32 b	0.15 a	0.41 a	33.9	62.2	3.9	

Note: Data are means of five replications, and those followed without the same letter differ significantly at $p = 0.05$ level. Soil textures are determined by the USDA (United States Department of Agriculture) textural soil classification system.

At the research station (Figure 1), field observations of soil water–salt content and crop growth were conducted in two hydrologically independent rectangular fields (Field A: 80 m × 91 m; Field B: 80 m × 81 m) which were installed with parallel lateral subsurface drainpipes (a perforated plastic pipe of 50 mm diameter). The drain depth of the two fields was set at 0.9 m below the field surface, and the drain spacing was 22.75 and 8.9 m for fields A and B, respectively. The excess soil water collected by the drainpipes of the two fields was uniformly discharged into a nearby collector pond. During the study period, the rain-fed winter wheat (*Triticum aestivum* L.) variety Ningmai 13 was sown on 30 October 2020 and harvested on 5 June 2021 for both fields. Urea (225 kg ha⁻¹) was combined with 375 kg ha⁻¹ of compound fertilizer (N:P₂O₅:K₂O = 15:15:15) as the base fertilizer, and additional fertilization of 75 kg ha⁻¹ urea and 125 kg ha⁻¹ compound fertilizer was conducted on 24 January 2021, before the winter wheat reviving stage. Other agronomic measures, such as weed control and pest management, were practiced according to local experience.

Observation of soil moisture, salinity, and groundwater table fluctuations in the two fields began simultaneously in June 2020 and ended in July 2021. Soil samples (with five replicates) were obtained using a posthole auger at depths of 20, 50, 80, 110, and 140 cm to test the soil gravimetric water content and soil water electrical conductivity (EC_{1.5}, dS m⁻¹). Groundwater stage gauges (HOBO, U20-001 Onset) were installed in an observation well (depth of 3 m below the soil surface) located at the middle site between two parallel drainpipes to continuously measure the groundwater table variations in each field. Groundwater samples for salinity tests (EC, dS m⁻¹) were monthly collected by a 200-mL cylindrical bucket from three sampling wells (5 cm diameter, 3 m depth) located in the middle position of each field. The canopy cover (CC) and biomass of cultivated wheat were observed at the seedling stage (10 December 2020), tillering stage (1 January 2021), jointing stage (21 March 2021), boot stage (7 April 2021), ripening stage (21 May

2021), and harvest (5 June 2021) for both the two fields. An automatic color threshold image analysis package was used to estimate the CC values [35], and the image resources were captured at five random and non-overlapping observation plots (2×2 m for per plot) in each field using a digital camera (Alpha 6400 E18-135 APS-C 24 MP, SONY, Shanghai, China) fixed by a monopod (1.5 m) from the top of the canopy. Five non-adjacent wheat plant areas were selected in each field as the sampling plots (0.5×0.5 m per plot) to obtain the in-season aboveground biomass. The field-collected wheat samples were firstly oven-dried at 105°C for 30 min and then at 75°C for 48 h to obtain a constant dry weight for biomass measurement.

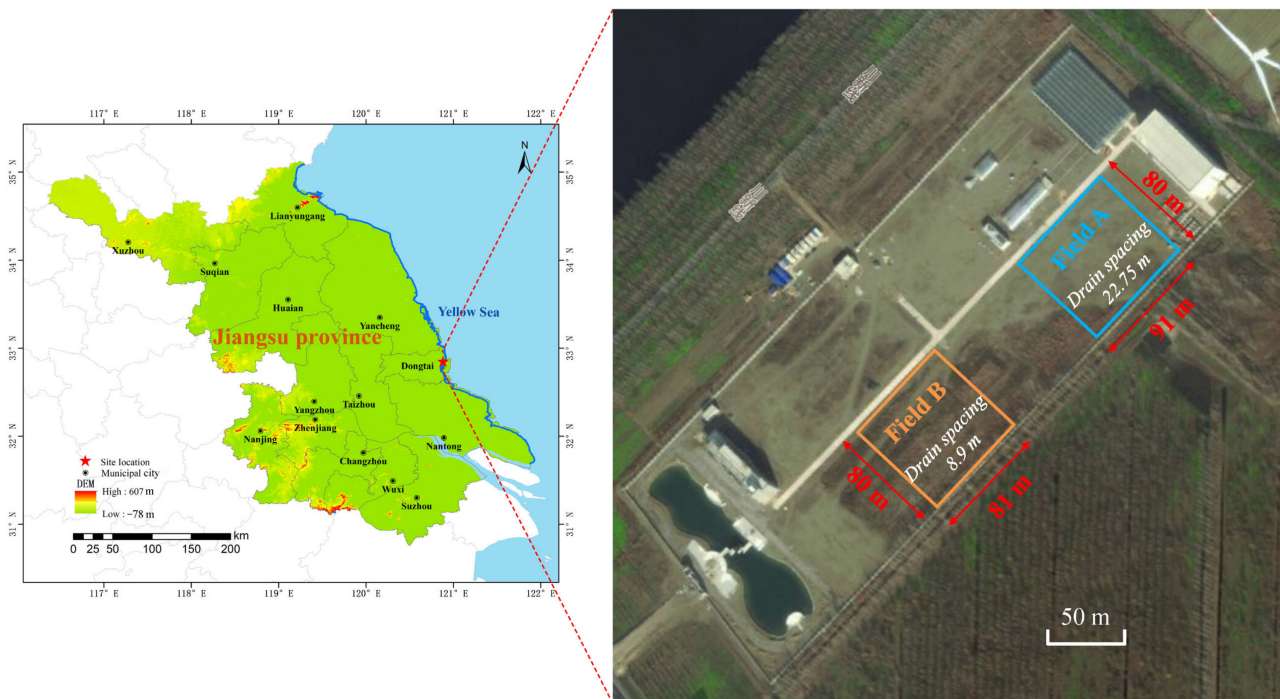


Figure 1. Location of the experimental site. Digital Elevation Model data source: National Earth System Science Data Centre, National science & Technology Infrastructure of China (<http://www.geodata.cn> (accessed on 11 December 2022)).

Weather data, including air temperature, precipitation, solar radiation, wind speed at 2.0 m height, and relative humidity, were recorded hourly by an automatic meteorological station inside the experimental site. Daily reference evapotranspiration (ET_0) derived from meteorological data was estimated using an FAO Penman–Monteith method-based ET_0 calculator [36]. The variations in precipitation and ET_0 during the study period (June 2020 to July 2021) are presented in Figure 2a.

2.2. Model Description

2.2.1. HYDRUS Model

The HYDRUS (2D/3D) software package used in this study is a finite element numerical model that simulates transient or cumulative water and solute transport in variably saturated porous media, based on the two- or three-dimensional form of Richards' equation [18] and convection–dispersion equation [37]. The van Genuchten–Mualem constitutive relationship was employed in HYDRUS to estimate the soil water retention curve and the unsaturated water conductivity function [38,39].

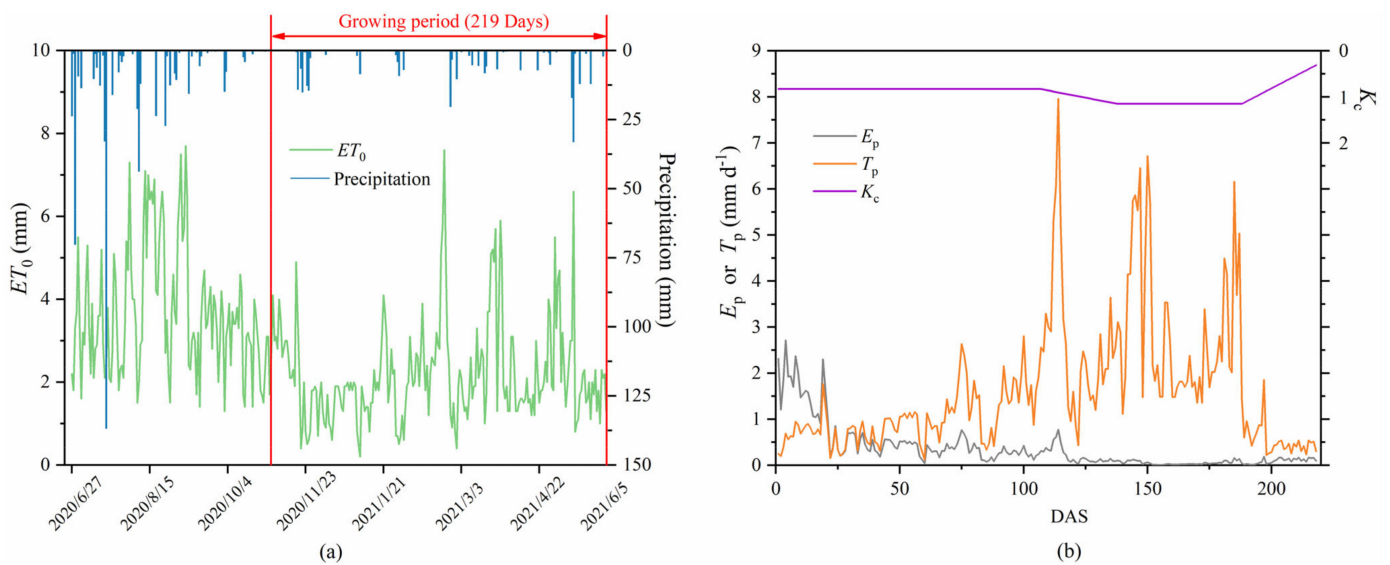


Figure 2. (a) Daily reference crop evapotranspiration (ET_0) and precipitation during the investigation. (b) Daily potential evaporation (E_p), transpiration (T_p), and crop coefficient (K_c) during the winter growing season. DAS refers to the days after wheat sowing.

The model setup of HYDRUS includes geometry establishment, boundary condition selection, and initial condition definition. In this study, a two-dimensional rectangular flow domain was designed for simulating the soil profile (vertical section perpendicular to the drainpipe) for fields A and B. The length of the flow domain corresponded to the actual field size with a depth of 300 cm. As there was no significant difference in soil properties within the 30–300 cm soil profile (Table 1), the model domain was divided into 0–30 cm for the surface plough layer and 30–300 cm for the sub-surface layer. The right and left sides of the flow domain were assigned to the no-flux boundary because an impermeable plastic film separated each field at this experimental site. The subsurface drainpipe was modelled by opening a series of 5 cm diameter circular holes on the flow domain at a depth of 90 cm with a horizontal spacing of 22.75 and 8.9 m for fields A and B, respectively. The boundary setting of this model domain is presented in Figure 3. A seepage face was imposed as the boundary condition for these opening holes, simulating the outflow through the drainpipe. An atmospheric boundary condition regarding time-variable rainfall, surface runoff, and evapotranspiration was specified at the soil surface. The bottom boundary was described by a variable pressure head condition, which represented a fluctuating water table (daily field-measured data). Notably, the rise of the field-measured water table is a response to rainfall infiltration, while the atmospheric boundary of HYDRSU also considers the rainfall events, which may accentuate the effect of rainfall events on the simulation results as the model operated under these two boundaries. Therefore, to reduce the water table rise caused by rainfall influencing the simulation of SPD performances, the data of water table depth less than the drain depth (0.9 m) was uniformly adjusted to 0.9 m before setting the bottom boundary condition. Furthermore, the total amount of dissolved salt in rainwater was disregarded because its average EC value was only 0.16 dS m^{-1} . The average groundwater salinity during the investigation period (3.16 g L^{-1}) was set at the bottom boundary to simulate the condition of saline groundwater. The initial conditions within the model domain were imposed by the measured soil water content and salt content at the beginning of the investigation, with a linear variable distribution from the soil surface to the bottom.

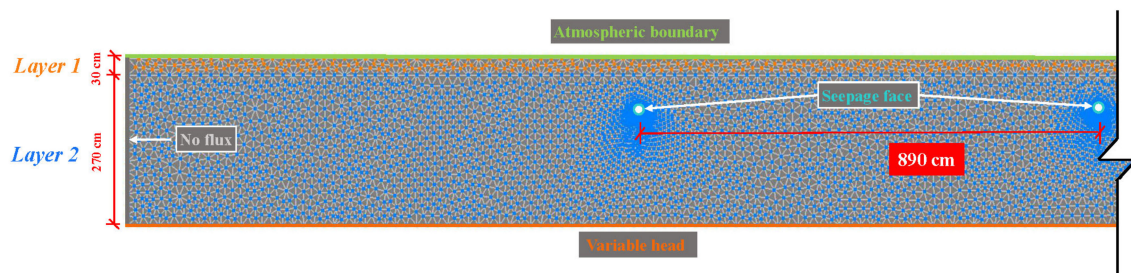


Figure 3. Two-dimensional modelling domain of Field B (part of the left side), including imposed boundary conditions and distribution of soil layers.

Daily potential evapotranspiration (ET_p) values derived from the daily ET_0 were calculated using crop coefficients at the early (0.7), middle (1.15), and late (0.4) stages of the winter wheat growing season [40] (Figure 2b). The estimated ET_p was further separated into potential daily evaporation (E_s) and transpiration (T_p) based on the variation in the leaf area index (LAI) [41]. The LAI variations in the studied winter wheat were estimated using an $LAI-CC$ relationship formula which is applicable to a wide range of field conditions [42]. The distribution of root growth defined in HYDRUS relies on the model reported by Vrugt et al. [43], and the root parameters of maximum depth and density were adopted from field observations at harvest assuming a linear root growth system for the model setting (0–40 cm region with a maximum root density at a 10 cm soil depth). A piecewise linear model proposed by Feddes [22] was implemented in the HYDRUS software package to describe the effect of soil water- or salt-stress on the root water uptake of winter wheat, and the associated threshold and function slopes of Feddes' model were set to the default values of the HYDRUS database.

Soil properties were essentially the same in the two studied fields. Therefore, the model was calibrated using soil moisture and salt content throughout the investigation of Field A, and validation was based on the corresponding data of soil water and salt content measured from Field B during the same period. Before calibration, the saturated and residual water contents inputted into the model were obtained from the soil samples at the beginning of the study period. The van Genuchten model parameters, including the residual and saturated water contents, the inverse of air-entry value, the dimensionless soil pore size distribution index, and the soil saturated hydraulic conductivity, were initially predicted using the ROSETTA neural network approach, which relies on the site-measured soil bulk density and particle size distributions [44]. Then, based on the dataset of measured water content in field A, the soil hydraulic parameters were verified by repeating model trials until an optimal calibration result was obtained (Table 2). In addition, the longitudinal dispersivity (D_L) and transverse dispersivity (D_T) related to solute transport properties were set according to the proposed relation of $D_L/D_T = 10$ [45], and D_L was set to one tenth of the model flow domain. Molecular diffusion in the soil solution was assumed to be negligible during the model simulation [46]. To suit the data input requirements of the HYDRUS model, the measured soil gravimetric water content was converted to volumetric water content based on the bulk density in different soil layers, and the measured soil salinity ($EC_{1.5}$) was described in terms of the liquid phase concentration ($g L^{-1}$). In this study, the saturated soil electrical conductivity (EC_e) was estimated using a linear relationship: $EC_e = 7.96EC_{1.5} + 0.33$, obtained in the laboratory. The estimated EC_e values were further converted to the electrical conductivity of the soil solution (EC_{sw}), based on the recommended assumption of $EC_{sw}/EC_e = 2$ [47,48]. The liquid phase concentration ($g L^{-1}$) of the simulated soil was obtained from the corresponding EC_{sw} values based on an empirical conversion equation suggested by Grattan [49].

Table 2. van Genuchten parameters describing soil hydraulic properties used in this model study.

Soil Layer (cm)	θ_r ($\text{cm}^3 \text{cm}^{-3}$)	θ_s ($\text{cm}^3 \text{cm}^{-3}$)	α	n	l	K_s (cm day^{-1})
0~30 cm	0.037	0.463	0.019	1.419	0.5	105.31
30~300 cm	0.041	0.415	0.013	1.453	0.5	58.52

NOTE: θ_r and θ_s denote the residual and saturated water contents; α is the inverse of the air-entry value; n is a pore size distribution index; l is a pore connectivity parameter, set to 0.5 as proved valid for most soil types [38]; and K_s is the saturated hydraulic conductivity.

2.2.2. AquaCrop Model

AquaCrop is a canopy-level and engineering type of crop model that is used to evaluate crop water productivity within a soil–plant–atmosphere continuum [50,51]. To describe the response of crop growth to field water availability, the data requirements of the AquaCrop model consist of irrigation and fertility regimes as well as groundwater conditions. In AquaCrop, the aboveground biomass was calculated as a function of daily crop transpiration and normalized water productivity associated with air CO_2 concentrations and atmospheric evaporative demand [31]. The grain yield (t ha^{-1}) as a component of the final crop biomass was estimated using the harvest index (HI), which linearly increased during the crop growing stages from yield formation to physiological maturity [52]. To describe the effect of salt stress on crop production, AquaCrop employs a computer routine called ‘BUDGET’ to dynamically simulate soil salt movement and retention [53]. Moreover, the effect of groundwater behavior on crop production was considered by estimating the capillary rise using a function of water table depth and soil hydraulic characteristics [28], because the upward flux from groundwater becomes pronounced as the water content ranges within the field capacity and wilting point [54].

The input parameters of the AquaCrop model pertain to the climate of the experimental site, soil characteristics, farm management, groundwater status, crop growth, and yield parameters. AquaCrop and HYDRUS share a set of climate data during the wheat growing season, and the mean annual CO_2 concentration was set at 0.39% according to the data from the Mauna Loa Observatory. The soil profile designed in the AquaCrop model was also divided into two layers (topsoil 0–30 cm; and subsoil 30–300 cm), with the input of the relevant soil information gathered before this study (Table 1). Surface runoff was not observed because the growing season was concentrated during the rainless period, and rainwater was expected to be totally converted to soil infiltration. Groundwater status was set under varying depth with constant water salinity, and the corresponding data of water table depth fluctuation were gathered from the HYDRUS modelling results of the pressure head distribution. Meanwhile, irrigation management was disregarded owing to rainfed cropping throughout the growing season, and adequate soil fertility in this study ensured few restrictions for crop development. The crop parameters in the AquaCrop model consist of conservative and non-conservative parameters (Table 3). The conservative parameters are generally crop-specific and show less response to time, field management, and climatic and geographic conditions, which are often obtained from the default values of the AquaCrop manual [55,56]. The non-conservative parameters associated with planting practices and crop phenology were mostly obtained from field measurement or adjusted by calibration and validation procedures.

Table 3. Input parameters of AquaCrop model used in this study.

Parameter Description	Value	Status
Non-conservative parameters		
Sowing rate	250 kg seed hm^{-2}	M
Cover per seeding	1.5 cm^2 plant	M
Initial canopy cover	5.2%	M
Canopy growth coefficient	3.2% day^{-1}	C
Canopy decline coefficient	6.9% day^{-1}	C
Maximum canopy cover	93%	C

Table 3. Cont.

Parameter Description	Value	Status
Time from sowing to emergence	12 day	M
Time from sowing to max canopy	175 day	M
Time from sowing to senescence	197 day	M
Time from sowing to maturity	219 day	M
Time from sowing to flowing	181 day	M
Minimum effective rooting depth	0.3 m	C
Maximum effective rooting depth	1.15	C
Time from sowing to maximum rooting depth	90 day	C
Sharp factor describing root zone expansion	1.5	D
Reference harvest index	41%	C
Minimum temperature of pollination fail	5 °C	D
Maximum temperature of pollination fail	35 °C	D
Salinity stress, lower thresholds	6 dS m ⁻¹	D
Salinity stress, upper thresholds	20 dS m ⁻¹	D
Conservative parameters		
Base temperature	0 °C	D
Upper temperature	26 °C	D
Canopy cover per seeding	1.5 cm ² Plant ⁻¹	D
Normalized crop water productivity	15 g m ⁻²	D
Canopy expansion, upper threshold	0.2%	D
Canopy expansion, lower threshold	0.65%	D
Stomatal conductance threshold	0.65%	D
Stomata stress coefficient curve shape	2.5	D
Senescence stress upper threshold	0.7%	D
Senescence stress coefficient curve shape	2.5	D

Note: Status M means the value of the parameter refers to the field measurement; Status D means the value of the parameter is taken from the model reference manual; Status C means the value was obtained by model calibration.

The calibration and validation procedures were conducted by evaluating the agreement between AquaCrop-simulated and field-measured data of the seasonal progression of canopy cover and crop biomass. The model under Field A was used for calibration, and the differences between simulated and measured data were minimized based on trial and error by repeatedly tuning the phenology-related parameters [55,57]. The calibrated model was then validated using the conditions of Field B, and the applicability of the model was verified only when the statistical error of the validation results ranged in an acceptable level.

2.3. Model Evaluation Criterion

The goodness of fit between the measured and model-simulated values was assessed using statistical indicators, including the mean error (*ME*), normalized root mean square error (*RMSEn*), Nash–Sutcliffe efficiency coefficient (*NSE*), and coefficient of determination (*R*²):

$$ME = \frac{\sum_{i=1}^N (S_i - M_i)}{N} \quad (1)$$

$$RMSEn = \frac{\sqrt{\frac{\sum_{i=1}^N (M_i - S_i)^2}{N}}}{\bar{S}} \quad (2)$$

$$NSE = 1 - \frac{\sum_{i=1}^N (M_i - S_i)^2}{\sum_{i=1}^N (M_i - \bar{S})^2} \quad (3)$$

$$R^2 = \left[\frac{\sum_{i=1}^N (M_i - \bar{M})(S_i - \bar{S})}{\sqrt{\sum_{i=1}^N (M_i - \bar{M})^2} \sqrt{\sum_{i=1}^N (S_i - \bar{S})^2}} \right]^2 \quad (4)$$

where M_i and S_i are the i th measured and simulated value, respectively. \bar{M} and \bar{S} are the means of the total N number data of the measured and simulated values, respectively. The positive or negative *ME* value indicates an overestimation or underestimation of the simulation results. The simulation result is considered reasonable when the *RMSEn* value

is less than 0.3 [58]. The model accuracy increases as R^2 and NSE approach 1.0, and the model simulation is remarkable if the NSE value is far less than 0.

2.4. Simulation Scenarios

In the scenario setting, the horizontal spacing was set at 10, 20, 30, and 40 m between two adjacent subsurface drainpipes, which refers to the actual and practical layout of the SPD system in fields subjected to a shallow groundwater table [14,59,60]. Furthermore, a scenario designed to simulate the absence of subsurface drainage was treated as the control (ND). Salinity levels of shallow groundwater were categorized under three levels: 30% (low level), 60% (medium level), and 90% (high level) of the average value of total dissolved solute (35.1 g L^{-1}) of porewater within 1.5–3.5 m soil depth in the local area [4]. For each scenario, the response of soil salt dynamics to the combined effect of SPD drain spacing and groundwater salinity were assessed through a long-term model operation, during which the historical climate data for 1990–2020 were obtained from the meteorological station in Dongtai (No. 58251). Regarding precipitation, years (1990–2020) were divided into three classes (wet, normal, dry) using the Weibull equation [61] with separating points of 25%, 50%, and 75% probability, respectively (Figure 4). The calibrated and validated HYDRUS model was employed to evaluate the long-term effect of SPD on soil salt dynamics under different drain spacings and groundwater salinity levels. Additionally, simulations of seasonal rain-fed crop grain yield (GY) and associated water productivity (WP) and groundwater supply (GS) in different precipitation years were conducted using the calibrated and validated AquaCrop model. The input data of water table depth fluctuations and initial soil water–salt distribution affected by SPD for AquaCrop operation in years with different precipitation levels were separately gathered from the HYDRUS results.

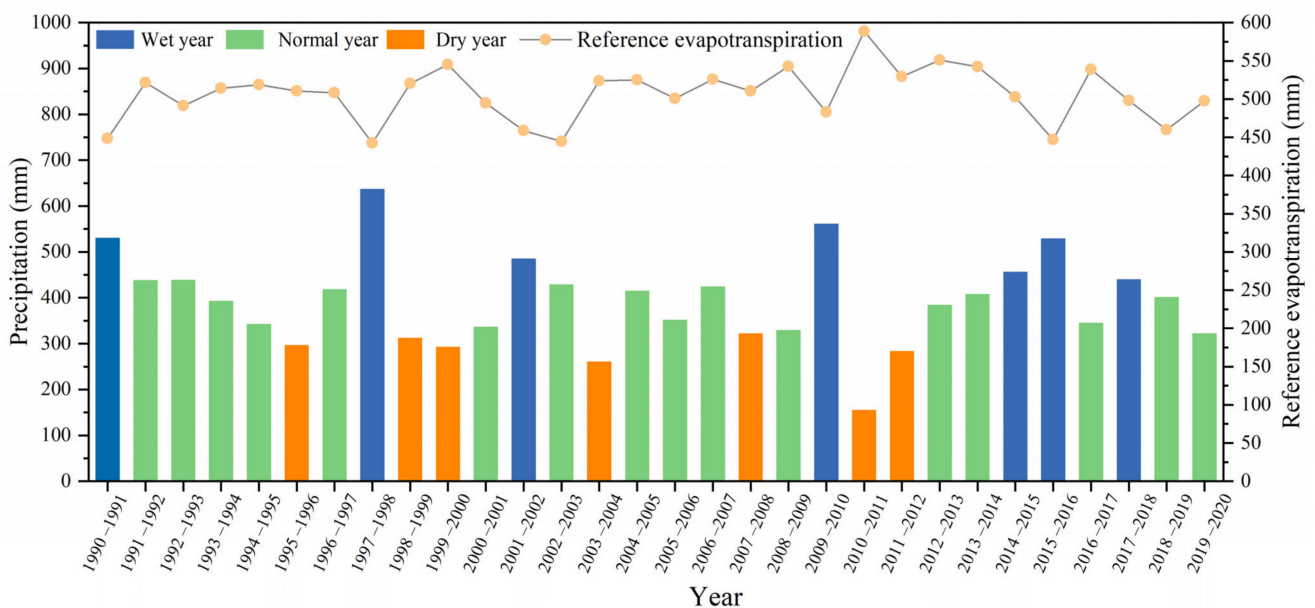


Figure 4. Variation in precipitation and reference evapotranspiration during winter wheat growing season in Dongtai County from 1990 to 2020.

3. Results and Discussion

3.1. Model Performance Evaluation

3.1.1. HYDRUS Model Calibration and Validation

The measured moisture and salt contents ($EC_{1:5}$) in the soil profiles of fields A and B throughout the investigation period were compared with the corresponding simulation values for model calibration (Figure 5) and further validation (Figure 6), respectively. The simulated data at different soil depths and dates adequately represented soil water and salt distribution under SPD, and captured the variation trend of the measured data during the

experimental period. The statistical indicators used to evaluate the differences between the measured and simulated values are presented in Table 4. Negative ME values were obtained for both soil moisture and salt content during calibration and validation, indicating a general underestimation during the simulation period. The extent of deviation in moisture content can be attributed to the assumption of constant root distribution characteristics, which likely increased crop water uptake and reduced the moisture content among root zones that involve the field sampling positions. By contrast, the over/underestimated salt content can be partly attributed to the model running at the daily step with the assumption that the rainfall amount is evenly varied daily, which potentially limits the occurrence of surface runoff caused by short-term (hourly or by the minute) heavy rainfall events and converts more rainwater to infiltration for soil leaching. Moreover, the statistical indicators suggest a lower model accuracy for representing soil salt dynamics than soil moisture because higher *RMSE_n* values and lower *NSE* and *R²* values were observed in both the calibration and validation stages. The explanation was that HYDRUS establishes the convection dispersion equation based on the solution of Richards' equation, and thus the simulation error of soil moisture will be added to the solute simulation. Although the statistical errors in the validation stage were generally larger than those in the calibration stage for both soil moisture and salt content simulations, the corresponding indicators of *RMSE_n*, *NSE*, and *R²* for evaluating the established model performance all ranged within an acceptable limit. Generally, despite certain deviations between the measured and simulated salt contents, the HYDRUS-simulated results showed reasonable agreement among field-measured values, and the estimation errors were on the lower side of the range reported in previous model studies related to subsurface pipe drainage [18,62].

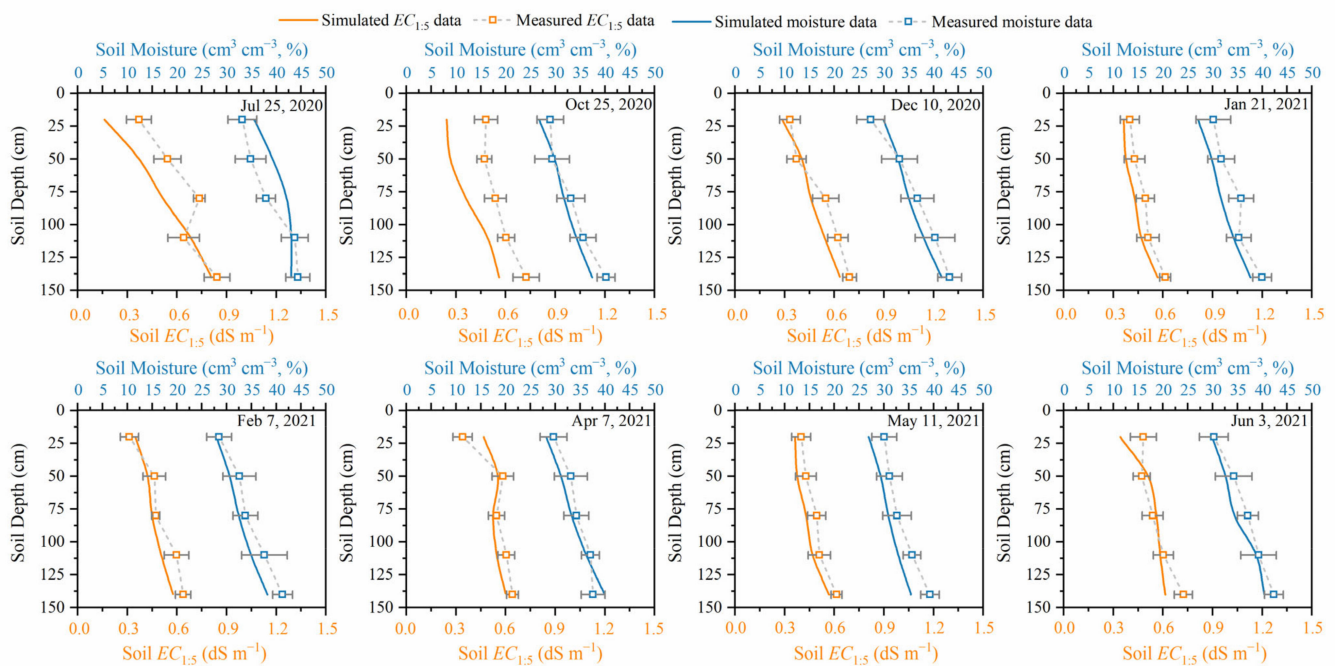


Figure 5. Comparison of field-measured and HYDRUS-simulated values of soil moisture and salinity ($EC_{1.5}$) in field A during the investigation period for model calibration. Note: The date and its corresponding stage are before sowing (25 July and 25 October 2020), overwintering stage (10 December 2020 and 21 January 2021), reviving green stage (7 February 2021), jointing stage (7 April 2021), grain-filling stage (11 May 2021), and maturity stage (3 June 2021). The error bars refer to the standard error of replicates as follows.

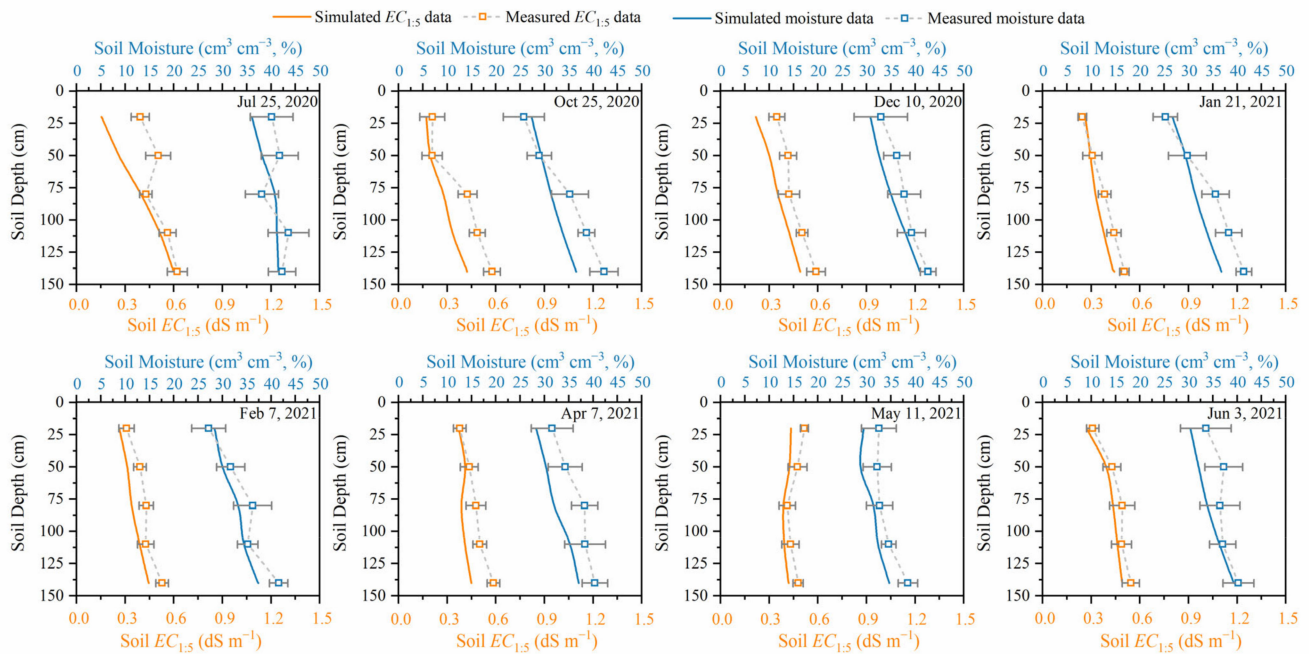


Figure 6. Comparison of field-measured and HYDRUS-simulated values of soil moisture and salinity ($EC_{1.5}$) in field B during the investigation period for model validation.

Table 4. Statistical evaluation of HYDRUS models for simulating soil moisture and salt content.

Stage	Data Series	ME	RMSEn	NSE	R ²
Calibration	Moisture ($cm^3\ cm^{-3}$)	−1.611	7.72%	0.749	0.822
	Salt content ($dS\ m^{-1}$)	−0.058	18.63%	0.677	0.764
Validation	Moisture ($cm^3\ cm^{-3}$)	−3.452	11.71%	0.595	0.778
	Salt content ($dS\ m^{-1}$)	−0.098	29.30%	0.434	0.690

3.1.2. AquaCrop Model Calibration and Validation

Figure 7 presents the difference between the field-measured and AquaCrop-simulated seasonal progression of winter wheat canopy cover and biomass. In the calibration stage, the negative ME values suggested that the AquaCrop model generally underestimated both canopy cover and biomass. The simulated values tended to be lower than the measured values during the middle growth stage of winter wheat. In the validation stage, the AquaCrop model results overestimated the canopy cover, and this tendency was more pronounced before reviving the green stage (approximately 100 DAS), while the biomass progression was slightly underestimated. Notably, the positive deviation of the simulated final biomass values from the corresponding measured values could result from the stable parameter setting of normalized water productivity ($15\ g\ m^{-2}$) throughout the wheat growing season, because water productivity represents the rate of crop transpiration converted to biomass production, which is expected to decline during the late growth stage [63,64]. Furthermore, the AquaCrop model estimates the flux of groundwater capillary transport to the soil surface based on the total water balance, resulting in the dynamic distributions of soil water being less extensively described [65]. By contrast, the HYDRUS model calculated the upward movement of soil water from the saturated zone of groundwater to the unsaturated zone based on the finite element method in a field-based model flow domain. Therefore, the inconsistent calculation pattern between these two models inevitably aggravates the prediction errors. Overall, despite certain occasional deviations between simulated and measured values of canopy cover and biomass, the corresponding RMSEn lower than 10%, and NSE and R² were close to 1 for both calibration and validation stages. These findings indicate that the established model presents a satisfactory simulation accuracy

and further proves the feasibility of using the AquaCrop model to evaluate crop growth in SPD-applied fields based on the HYDRUS-estimated water table behaviors.

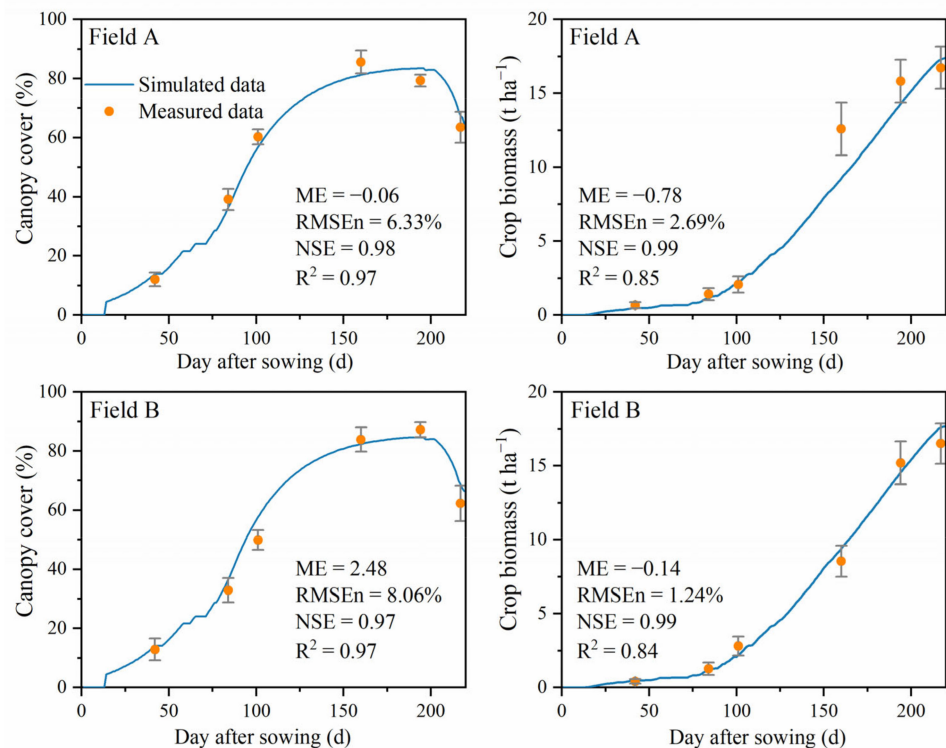


Figure 7. Comparison of field-measured and AquaCrop-simulated values of canopy cover and biomass during the winter wheat growth season for model calibration (Field A) and validation (Field B).

3.2. Scenario Evaluation and Analysis

3.2.1. Response of Drainage Performance to Groundwater Salinity

In Figure 8, the 30-year variation in solute concentration within the soil layer above the drain depth (0–0.9 m depth) is nearly in conformity with the annual precipitation, with high values of soil solute concentration in dry years and lower values in wet years. The groundwater salinity is the determinant of the range of soil solute concentration, because the average soil solute concentration under low groundwater salinity conditions for scenarios with different drainage spacings were 65.9% and 51.2% lower than those of high and medium salinity scenarios throughout the simulation period. Compared with the no-SPD scenario (ND), the 30-year average values of soil solute concentration of the four drainage spacing scenarios decreased by 11.1%, 13.8%, and 14.6% with groundwater salinity at low, medium, and high levels, respectively. However, there was no continuous downward trend of soil solute concentration during the long-term application of SPD, indicating that the desalination performance of SPD may not be relevant to its application time when rainfall is leached with a constant groundwater salinity. In fact, the average shoreline extension rate was approximately 200 m year⁻¹ during the last half century [66] in the coastal tidal flats of Jiangsu Province, and the salinity level of shallow groundwater generally declines as the distance from the shoreline increases [67]. Therefore, the salt content in the soil profile should gradually decrease during the long-term development of muddy deposition in nearshore areas, and the application of SPD can enhance such decreasing trends to improve the efficiency of land reclamation. Additionally, the discrepancies among the four drainage scenarios increased as the salinity level of the groundwater increased from low to high. For instance, the 30-year average value of the 10 m spacing scenario was only 0.22 g L⁻¹ lower than that of the 40 m spacing scenario under low groundwater salinity conditions, whereas under medium and high salinity levels, the difference between these two scenarios increased to 0.50 and 0.67 g L⁻¹, respectively. This phenomenon suggests that

the advantage of SPD with smaller drain spacing in controlling soil solute could be further pronounced as the field salinization is aggravated by increased groundwater salinity.

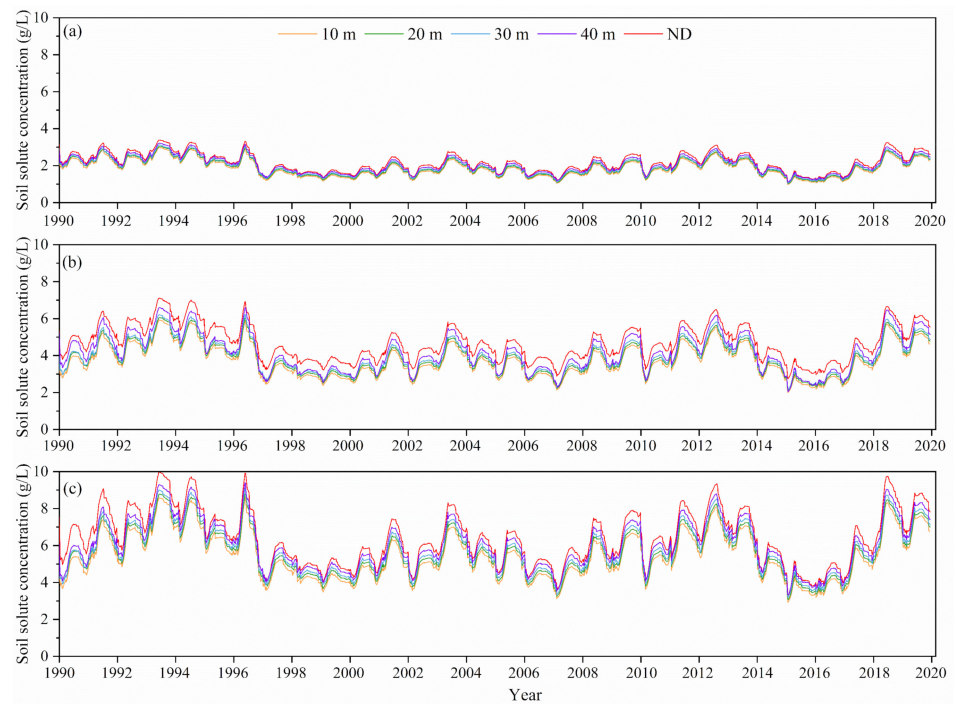


Figure 8. Temporal dynamics of soil solute concentrations at 0–0.9 m soil depth under low (a), medium (b), and high (c) groundwater salinity levels and five drain spacings in 30 years' meteorological condition (1990–2020). ND refers to the no-SPD scenario.

After applying SPD for 30 years under different groundwater salinity conditions, the total amount of discharged water and solute mass was estimated using the established field-size HYDRUS model, as shown in Figure 9. The cumulative water discharge amount was negatively related to the drain spacing and showed less response to the groundwater salinity. The scenarios with different drain spacings obtained the highest discharge amounts at high salinity levels, possibly due to the salt stress limiting the root water uptake and ensuring relatively high soil moisture [13]. In addition, for all the groundwater salinity levels, the values of the cumulative discharged solute mass of the 40 m spacing scenarios were 74.6%, 47.2%, and 29.3% lower than those of the scenarios with 10 m, 20 m, and 30 m spacing, respectively, suggesting that increased drainage spacing resulted in a reduction in salt discharge, while the extent of such reduction would gradually decrease with further increase in the drain spacing [15].

3.2.2. Response of Crop Yield, Water Productivity, and Groundwater Supply to Different Scenarios

Figure 10 presents the box plots of the AquaCrop-simulated grain yield (GY), water productivity (WP), and groundwater supply (GS) to winter wheat under different precipitation category years and SPD drain spacings. As precipitation is the dominant water source for rain-fed winter wheat growth, the GY and WP values generally varied in an accordant tendency, with higher values in wet years and lower values in dry years, which is in contrast to the variation in GS. Several studies reported similar results that shallow groundwater tends to move upward by capillary forces under deficit irrigation conditions to supply evapotranspiration, but such a supplement may not effectively improve crop production when crops are subject to the restricted water table in drained fields [54,68]. In terms of groundwater salinity, the values of GY, WP, and GS under low groundwater salinity almost varied in the same range in the same precipitation years. In contrast, under the medium and high groundwater salinity, the SPD-applied scenarios generally produced higher GY

and WP values compared to the no-SPD scenarios, and the corresponding increases in GY, WP, and GS were 0.81–1.65 t ha⁻¹, 0.13–0.35 kg m⁻³, and 6.06–31.03 mm, respectively.

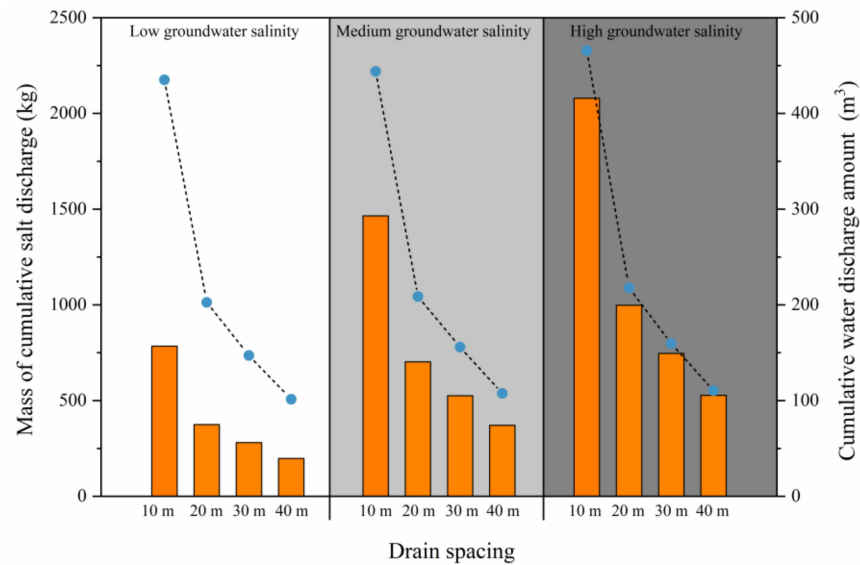


Figure 9. Simulation of 30 years cumulative discharge of water (point line) and solute mass (bar chart) by subsurface pipe drainage under low, medium, and high groundwater salinity condition.

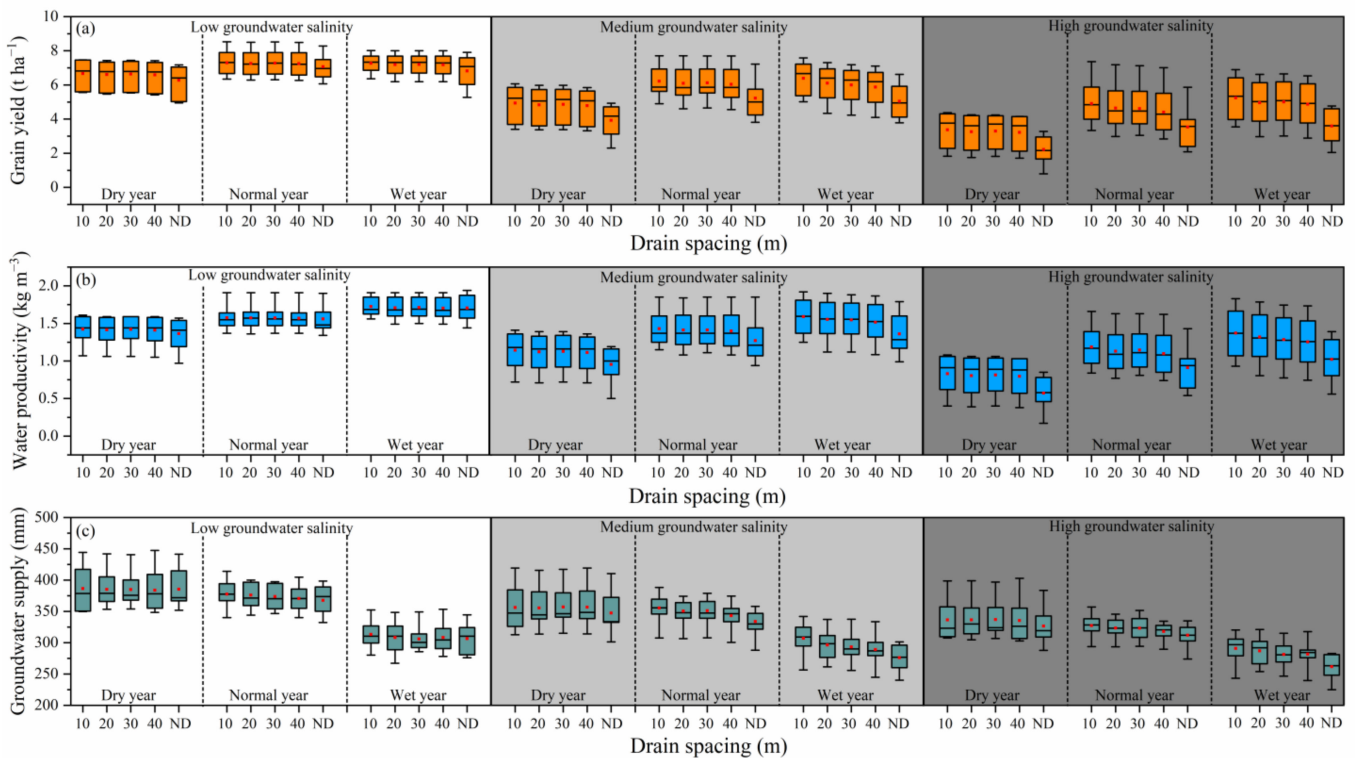


Figure 10. Comparison of simulated (a) grain yield, (b) water productivity, and (c) groundwater supply in a rain-fed winter wheat field under different groundwater salinity levels and drain spacings in wet, normal, and dry years. The top and bottom range of the box represent percentiles 25 and 75 of data. The box whisker represents an outlier range. The lines and red squares within the box represent median and mean values, respectively.

Additionally, among the four SPD-applied scenarios, the GY and WP values changed little with the drain spacing, and the maximum differences in GY and WP between the 10 m and 40 m drain spacing were only 0.37 t ha^{-1} and 0.11 kg m^{-3} , respectively. The GS values slightly decreased with increasing drain spacing in the normal and wet years under medium and high groundwater salinity, the average GS values of 10 m drain spacing scenarios increased by 2.16%, 3.47%, and 3.66% as compared to the 20 m, 30 m, and 40 m drain spacing scenarios, respectively. This is because the closer drain spacing allowed more of the infiltrated water to laterally discharge rather than undergo deep percolation for groundwater recharge [69], resulting in less upward flux of capillary supply for evapotranspiration [70,71].

4. Conclusions

This study demonstrated that the applicability of the AquaCrop model in simulating crop growth in fields with the SPD system could be improved by employing the HYDRUS model-predicted water table behaviors. The HYDRUS and AquaCrop were co-applied to assess the long-term influence of different precipitation years and groundwater salinity on the effect of the SPD systems with different drain spacings on soil water–salt transport, crop yield, water productivity, and groundwater upward supply. Results suggest that narrowing the drain spacing could facilitate soil solute discharge under rainfall leaching and restrict soil salinization caused by capillary-raised saline groundwater. However, there was no continuous downward trend of soil solute concentration during the long-term application of SPD when the drain fields were subjected to constant groundwater salinity. Additionally, the application of SPD could increase grain yield by $0.81\text{--}1.65 \text{ t ha}^{-1}$, water productivity by $0.13\text{--}0.35 \text{ kg m}^{-3}$, and groundwater supply by $6.06\text{--}31.03 \text{ mm}$ compared to the no-SPD scenarios, but such increases would be less pronounced in dry years with groundwater salinity at the low level. The present study's findings indicated that the cooperation of hydrologic and crop models can provide theoretical guidance for long-term agricultural salinity management in coastal areas, where rainwater is regarded as the primary resource for soil leaching and crop water uptake. Additionally, a small drain spacing layout pattern may lead to increased equipment installation and maintenance investment. Therefore, a trade-off between land reclamation performance and infrastructure expenditure of the SPD system should be investigated further.

Author Contributions: Conceptualization, P.L. and Z.J.; methodology, Y.Z.; software, P.L. and Y.Y.; validation, P.L., Z.J. and W.L.; formal analysis, P.L.; investigation, Y.Y. and W.L.; resources, P.L. and Y.Z.; data curation, P.L.; writing—original draft preparation, P.L. and Z.J.; writing—review and editing, P.L. and Z.J.; visualization, P.L. and Y.Y.; supervision, W.L.; project administration, P.L.; funding acquisition, P.L. and Z.J. All authors have read and agreed to the published version of the manuscript.

Funding: This research was funded by the National Natural Science Foundation of China, grant number 52109068; the China Postdoctoral Science Foundation, grant number 2022M712690; the Science and Technology Funding project of City-School Cooperation in Yangzhou, China, grant number YZU202101; the Postdoctoral Research Funding Program of Jiangsu province, China, grant number 2021K220B.

Data Availability Statement: The data that support this study cannot be publicly shared due to ethical or privacy reasons and may be shared upon reasonable request to the corresponding author if appropriate.

Acknowledgments: We are grateful to the editors and reviewers for their valuable suggestions on improving the manuscript.

Conflicts of Interest: The authors declare no conflict of interest.

References

1. Schuerch, M.; Spencer, T.; Temmerman, S.; Kirwan, M.L.; Wolff, C.; Lincke, D.; McOwen, C.J.; Pickering, M.D.; Reef, R.; Vafeidis, A.T.; et al. Future response of global coastal wetlands to sea-level rise. *Nature* **2018**, *561*, 231–234. [CrossRef]
2. Wu, W.T.; Yang, Z.Q.; Tian, B.; Huang, Y.; Zhou, Y.X.; Zhang, T. Impacts of coastal reclamation on wetlands: Loss, resilience, and sustainable management. *Estuar. Coast. Shelf Sci.* **2018**, *210*, 153–161. [CrossRef]
3. Robinson, C.E.; Xin, P.; Santos, I.R.; Charette, M.A.; Li, L.; Barry, D.A. Groundwater dynamics in subterranean estuaries of coastal unconfined aquifers: Controls on submarine groundwater discharge and chemical inputs to the ocean. *Adv. Water Resour.* **2018**, *115*, 315–331. [CrossRef]
4. Zhan, L.C.; Xin, P.; Chen, J.S. Subsurface salinity distribution and evolution in low-permeability coastal areas after land reclamation: Field investigation. *J. Hydrol.* **2022**, *612*, 128250. [CrossRef]
5. Long, X.H.; Liu, L.P.; Shao, T.Y.; Shao, H.B.; Liu, Z.P. Developing and sustainably utilize the coastal mudflat areas in China. *Sci. Total Environ.* **2016**, *569*, 1077–1086. [CrossRef]
6. Iost, S.; Landgraf, D.; Makeschin, F. Chemical soil properties of reclaimed marsh soil from Zhejiang Province PR China. *Geoderma* **2007**, *142*, 245–250. [CrossRef]
7. Velmurugan, A.; Swarnam, T.P.; Lal, R. Effect of land shaping on soil properties and crop yield in tsunami inundated coastal soils of Southern Andaman Island. *Agric. Ecosyst. Environ.* **2015**, *206*, 1–9. [CrossRef]
8. Setiawan, I.; Morgan, L.; Doscher, C.; Ng, K.; Bosserelle, A. Mapping shallow groundwater salinity in a coastal urban setting to assess exposure of municipal assets. *J. Hydrol. Reg. Stud.* **2022**, *40*, 100999. [CrossRef]
9. Forkutsa, I.; Sommer, R.; Shirokova, Y.I.; Lamers, J.P.A.; Kienzler, K.; Tischbein, B.; Martius, C.; Vlek, P.L.G. Modeling irrigated cotton with shallow groundwater in the Aral Sea Basin of Uzbekistan: I. Water dynamics. *Irrig. Sci.* **2009**, *27*, 331–346. [CrossRef]
10. Islam, M.N.; Bell, R.W.; Barrett-Lennard, E.G.; Maniruzzaman, M.J.A.f.S.D. Shallow surface and subsurface drains alleviate waterlogging and salinity in a clay-textured soil and improve the yield of sunflower in the Ganges Delta. *Agron. Sustain. Dev.* **2022**, *42*, 16. [CrossRef]
11. Fang, D.; Guo, K.; Ameen, A.; Wang, S.C.; Xie, J.; Liu, J.T.; Han, L.P. A Root Density Tradeoff in an Okra-Assisted Subsurface Pipe Drainage System for Amelioration of Saline Soil. *Agronomy* **2022**, *12*, 866. [CrossRef]
12. Sloan, B.P.; Basu, N.B.; Mantilla, R. Hydrologic impacts of subsurface drainage at the field scale: Climate, landscape and anthropogenic controls. *Agric. Water Manag.* **2016**, *165*, 1–10. [CrossRef]
13. Wang, Z.H.; Heng, T.; Li, W.H.; Zhang, J.Z.; Zhangzhong, L.L. Effects of subsurface pipe drainage on soil salinity in saline-sodic soil under mulched drip irrigation. *Irrig. Drain.* **2020**, *69*, 95–106. [CrossRef]
14. Nozari, H.; Azadi, S.; Zali, A. Experimental study of the temporal variation of drain water salinity at different drain depths and spacing in the presence of saline groundwater. *Sustain. Water Resour. Manag.* **2018**, *4*, 887–895. [CrossRef]
15. Shao, X.H.; Chang, T.T.; Cai, F.; Wang, Z.Y.; Huang, M.Y. Effects of subsurface drainage design on soil desalination in coastal resort of China. *J. Food Agric. Environ.* **2012**, *10*, 935–938.
16. Tuohy, P.; O’Loughlin, J.; Fenton, O. Modeling performance of a tile drainage system incorporating mole drainage. *Trans. Asabe* **2018**, *61*, 169–178. [CrossRef]
17. Bonaiti, G.; Borin, M. Efficiency of controlled drainage and subirrigation in reducing nitrogen losses from agricultural fields. *Agric. Water Manag.* **2010**, *98*, 343–352. [CrossRef]
18. Ebrahimian, H.; Noory, H. Modeling paddy field subsurface drainage using HYDRUS-2D. *Paddy Water Environ.* **2015**, *13*, 477–485. [CrossRef]
19. Lu, P.R.; Zhang, Z.Y.; Sheng, Z.; Huang, M.Y.; Zhang, Z.M. Assess Effectiveness of Salt Removal by a Subsurface Drainage with Bundled Crop Straws in Coastal Saline Soil Using HYDRUS-3D. *Water* **2019**, *11*, 943. [CrossRef]
20. Tao, Y.; Li, N.; Wang, S.L.; Chen, H.R.; Guan, X.Y.; Ji, M.Z. Simulation study on performance of nitrogen loss of an improved subsurface drainage system for one-time drainage using HYDRUS-2D. *Agric. Water Manag.* **2021**, *246*, 106698. [CrossRef]
21. Krevh, V.; Filipovic, V.; Filipovic, L.; Matekovic, V.; Petosic, D.; Mustac, I.; Ondrasek, G.; Bogunovic, I.; Kovac, Z.; Pereira, P.; et al. Modeling seasonal soil moisture dynamics in gley soils in relation to groundwater table oscillations in eastern Croatia. *Catena* **2022**, *211*, 105987. [CrossRef]
22. Feddes, R.A. Simulation of field water use and crop yield. *Soil Sci.* **1978**, *129*, 193.
23. Simunek, J.; Hopmans, J.W. Modeling compensated root water and nutrient uptake. *Ecol. Model.* **2009**, *220*, 505–521. [CrossRef]
24. Ranjbar, A.; Rahimikhoob, A.; Ebrahimian, H.; Varavipour, M. Simulation of nitrogen uptake and dry matter for estimation of nitrogen nutrition index during the maize growth period. *J. Plant Nutr.* **2022**, *45*, 920–936. [CrossRef]
25. Zhou, J.; Cheng, G.D.; Li, X.; Hu, B.X.; Wang, G.X. Numerical Modeling of Wheat Irrigation using Coupled HYDRUS and WOFOST Models. *Soil Sci. Soc. Am. J.* **2012**, *76*, 648–662. [CrossRef]
26. Roy, P.C.; Guber, A.; Abouali, M.; Nejadhashemi, A.P.; Deb, K.; Smucker, A.J.M. Crop yield simulation optimization using precision irrigation and subsurface water retention technology. *Environ. Model. Softw.* **2019**, *119*, 433–444. [CrossRef]
27. Zhao, J.; Han, T.; Wang, C.; Jia, H.; Worqlul, A.W.; Norelli, N.; Zeng, Z.H.; Chu, Q.Q. Optimizing irrigation strategies to synchronously improve the yield and water productivity of winter wheat under interannual precipitation variability in the North China Plain. *Agric. Water Manag.* **2020**, *240*, 106298. [CrossRef]
28. Goosheh, M.; Pazira, E.; Gholami, A.; Andarzian, B.; Panahpour, E. Improving Irrigation Scheduling of Wheat to Increase Water Productivity in Shallow Groundwater Conditions Using Aquacrop. *Irrig. Drain.* **2018**, *67*, 738–754. [CrossRef]

29. Zhang, C.; Xie, Z.A.; Wang, Q.J.; Tang, M.; Feng, S.Y.; Cai, H.J. AquaCrop modeling to explore optimal irrigation of winter wheat for improving grain yield and water productivity. *Agric. Water Manag.* **2022**, *266*, 107580. [CrossRef]
30. Hammami, Z.; Qureshi, A.S.; Sahli, A.; Gauffreteau, A.; Chamekh, Z.; Ben Azaiez, F.E.; Ayadi, S.; Trifa, Y. Modeling the Effects of Irrigation Water Salinity on Growth, Yield and Water Productivity of Barley in Three Contrasted Environments. *Agronomy* **2020**, *10*, 1459. [CrossRef]
31. Hsiao, T.C.; Heng, L.; Steduto, P.; Rojas-Lara, B.; Raes, D.; Fereres, E. AquaCrop-The FAO Crop Model to Simulate Yield Response to Water: III. Parameterization and Testing for Maize. *Agron. J.* **2009**, *101*, 448–459. [CrossRef]
32. Akhtar, F.; Tischbein, B.; Awan, U.K. Optimizing Deficit Irrigation Scheduling Under Shallow Groundwater Conditions in Lower Reaches of Amu Darya River Basin. *Water Resour. Manag.* **2013**, *27*, 3165–3178. [CrossRef]
33. Tenreiro, T.R.; Jerabek, J.; Gomez, J.A.; Zumr, D.; Martinez, G.; Garcia-Vila, M.; Fereres, E. Simulating water lateral inflow and its contribution to spatial variations of rainfed wheat yields. *Eur. J. Agron.* **2022**, *137*, 126515. [CrossRef]
34. Shirokova, Y.; Forkutsa, I.; Sharafutdinova, N. Use of Electrical Conductivity Instead of Soluble Salts for Soil Salinity Monitoring in Central Asia. *Irrig. Drain. Syst.* **2000**, *14*, 199–205. [CrossRef]
35. Patrignani, A.; Ochsner, T.E. Canopeo: A Powerful New Tool for Measuring Fractional Green Canopy Cover. *Agron. J.* **2015**, *107*, 2312–2320. [CrossRef]
36. Razzaghi, F.; Zhou, Z.J.; Andersen, M.N.; Plauborg, F. Simulation of potato yield in temperate condition by the AquaCrop model. *Agric. Water Manag.* **2017**, *191*, 113–123. [CrossRef]
37. Abbasi, F.; Simunek, J.; Feyen, J.; van Genuchten, M.T.; Shouse, P.J. Simultaneous inverse estimation of soil hydraulic and solute transport parameters from transient field experiments: Homogeneous soil. *Trans. ASAE* **2003**, *46*, 1085–1095. [CrossRef]
38. Mualem, Y. A new model for predicting the hydraulic conductivity of unsaturated porous media. *Water Resour. Res.* **1976**, *12*, 513–522. [CrossRef]
39. Genuchten, M.T.v. A Closed-form Equation for Predicting the Hydraulic Conductivity of Unsaturated Soils. *Soil Sci. Soc. Am. J.* **1980**, *44*, 892–898. [CrossRef]
40. Allen, R.G.; Pereira, L.S.; Raes, D.; Smith, M. *Crop Evapotranspiration—Guidelines for Computing Crop Water Requirements*; Food and Agriculture Organization of the United Nations (FAO): Rome, Italy, 1998.
41. Zhu, Y.H.; Ren, L.L.; Horton, R.; Lu, H.S.; Wang, Z.L.; Yuan, F. Estimating the Contribution of Groundwater to the Root Zone of Winter Wheat Using Root Density Distribution Functions. *Vadose Zone J.* **2018**, *17*, 1–15. [CrossRef]
42. Nielsen, D.C.; Miceli-Garcia, J.J.; Lyon, D.J. Canopy Cover and Leaf Area Index Relationships for Wheat, Triticale, and Corn. *Agron. J.* **2012**, *104*, 1569–1573. [CrossRef]
43. Vrugt, J.A.; van Wijk, M.T.; Hopmans, J.W.; Simunek, J. One-, two-, and three-dimensional root water uptake functions for transient modeling. *Water Resour. Res.* **2001**, *37*, 2457–2470. [CrossRef]
44. Schaap, M.G.; Leij, F.J.; van Genuchten, M.T. ROSETTA: A computer program for estimating soil hydraulic parameters with hierarchical pedotransfer functions. *J. Hydrol.* **2001**, *251*, 163–176. [CrossRef]
45. Ramos, T.B.; Simunek, J.; Goncalves, M.C.; Martins, J.C.; Prazeres, A.; Pereira, L.S. Two-dimensional modeling of water and nitrogen fate from sweet sorghum irrigated with fresh and blended saline waters. *Agric. Water Manag.* **2012**, *111*, 87–104. [CrossRef]
46. Radcliffe, D.E.; Šimůnek, J. *Soil Physics with HYDRUS*; CRC Press: Boca Raton, FL, USA; Taylor & Francis Group: Abingdon, UK, 2010.
47. Skaggs, T.H.; Shouse, P.J.; Poss, J.A. Irrigating forage crops with saline waters: 2. Modeling root uptake and drainage. *Vadose Zone J.* **2006**, *5*, 824–837. [CrossRef]
48. Karandish, F.; Simunek, J. An application of the water footprint assessment to optimize production of crops irrigated with saline water: A scenario assessment with HYDRUS. *Agric. Water Manag.* **2018**, *208*, 67–82. [CrossRef]
49. Grattan, S. *Irrigation Water Salinity and Crop Production*; UCANR Publications: Oakland, CA, USA, 2002; Volume 9.
50. Mondal, M.S.; Saleh, A.F.M.; Akanda, M.A.R.; Biswas, S.K.; Moslehuddin, A.Z.M.; Zaman, S.; Lazar, A.N.; Clarke, D. Simulating yield response of rice to salinity stress with the AquaCrop model. *Environ. Sci. -Process. Impacts* **2015**, *17*, 1118–1126. [CrossRef]
51. Foster, T.; Brozovic, N.; Butler, A.P.; Neale, C.M.U.; Raes, D.; Steduto, P.; Fereres, E.; Hsiao, T.C. AquaCrop-OS: An open source version of FAO's crop water productivity model. *Agric. Water Manag.* **2017**, *181*, 18–22. [CrossRef]
52. Saab, M.T.A.; Todorovic, M.; Albrizio, R. Comparing Aqua Crop and CropSyst models in simulating barley growth and yield under different water and nitrogen regimes. Does calibration year influence the performance of crop growth models? *Agric. Water Manag.* **2015**, *147*, 21–33. [CrossRef]
53. Raes, D.; Steduto, P.; Hsiao, T.C.; Fereres, E. AquaCrop-The FAO Crop Model to Simulate Yield Response to Water: II. Main Algorithms and Software Description. *Agron. J.* **2009**, *101*, 438–447. [CrossRef]
54. Pourgholam-Amiji, M.; Liaghat, A.; Ghameshlou, A.N.; Khoshravesh, M. The evaluation of DRAINMOD-S and AquaCrop models for simulating the salt concentration in soil profiles in areas with a saline and shallow water table. *J. Hydrol.* **2021**, *598*, 126259. [CrossRef]
55. Davarpanah, R.; Ahmadi, S.H. Modeling the effects of irrigation management scenarios on winter wheat yield and water use indicators in response to climate variations and water delivery systems. *J. Hydrol.* **2021**, *598*, 126269. [CrossRef]
56. Montoya, F.; Camargo, D.; Ortega, J.F.; Corcoles, J.I.; Dominguez, A. Evaluation of Aquacrop model for a potato crop under different irrigation conditions. *Agric. Water Manag.* **2016**, *164*, 267–280. [CrossRef]

57. Kumar, M.; Sarangi, A.; Singh, D.K.; Rao, A.R. Modelling the Grain Yield of Wheat in Irrigated Saline Environment with Foliar Potassium Fertilization. *Agric. Res.* **2018**, *7*, 321–337. [CrossRef]
58. Xu, J.Z.; Bai, W.H.; Li, Y.W.; Wang, H.Y.; Yang, S.H.; Wei, Z. Modeling rice development and field water balance using AquaCrop model under drying-wetting cycle condition in eastern China. *Agric. Water Manag.* **2019**, *213*, 289–297. [CrossRef]
59. Qian, Y.Z.; Zhu, Y.; Ye, M.; Huang, J.S.; Wu, J.W. Experiment and numerical simulation for designing layout parameters of subsurface drainage pipes in arid agricultural areas. *Agric. Water Manag.* **2021**, *243*, 106455. [CrossRef]
60. Tao, Y.; Wang, S.L.; Xu, D.; Guan, X.Y.; Ji, M.Z.; Liu, J. Theoretical analysis and experimental verification of the improved subsurface drainage discharge with ponded water. *Agric. Water Manag.* **2019**, *213*, 546–553. [CrossRef]
61. Chow, V.T.; Maidment, D.R.; Mays, L.W. *Handbook of Applied Hydrology*; McGraw-Hill: New York, NY, USA, 1988.
62. Liu, Y.; Ao, C.; Zeng, W.; Kumar Srivastava, A.; Gaiser, T.; Wu, J.; Huang, J. Simulating water and salt transport in subsurface pipe drainage systems with HYDRUS-2D. *J. Hydrol.* **2021**, *592*, 125823. [CrossRef]
63. Sandhu, R.; Irmak, S. Assessment of AquaCrop model in simulating maize canopy cover, soil-water, evapotranspiration, yield, and water productivity for different planting dates and densities under irrigated and rainfed conditions. *Agric. Water Manag.* **2019**, *224*, 105753. [CrossRef]
64. Huang, M.; Wang, C.; Qi, W.; Zhang, Z.; Xu, H. Modelling the integrated strategies of deficit irrigation, nitrogen fertilization, and biochar addition for winter wheat by AquaCrop based on a two-year field study. *Field Crops Res.* **2022**, *282*, 108510. [CrossRef]
65. Raes, D.; Steduto, P.; Hsiao, T.C.; Fereres, E. *Reference Manual AquaCrop*; FAO Land and Water Division: Rome, Italy, 2012.
66. Song, Y.; Shen, Y.M.; Xie, R.F.; Li, J.L. A DSAS-based study of central shoreline change in Jiangsu over 45 years. *Anthr. Coasts* **2021**, *4*, 115–128. [CrossRef]
67. Shang, T.X.; Xu, Z.W.; Gong, X.L.; Li, X.Q.; Tian, S.B.; Guan, Y.X. Application of electrical sounding to determine the spatial distribution of groundwater quality in the coastal area of Jiangsu Province, China. *J. Hydrol.* **2021**, *599*, 126348. [CrossRef]
68. Zhang, K.; Shao, G.C.; Wang, Z.Y.; Cui, J.T.; Lu, J.; Gao, Y. Modeling the impacts of groundwater depth and biochar addition on tomato production under climate change using RZWQM2. *Sci. Hortic.* **2022**, *302*, 111147. [CrossRef]
69. Aissa, I.B.; Bouarfa, S.; Vincent, B.; Chaumont, C.; Perrier, A. Drainage performance assessment in a modernized oasis system. *Irrig. Drain.* **2013**, *62*, 221–228. [CrossRef]
70. Gao, X.Y.; Bai, Y.N.; Huo, Z.L.; Xu, X.; Huang, G.H.; Xia, Y.H.; Steenhuis, T.S. Deficit irrigation enhances contribution of shallow groundwater to crop water consumption in arid area. *Agric. Water Manag.* **2017**, *185*, 116–125. [CrossRef]
71. Li, H.J.; Yi, J.; Zhang, J.G.; Zhao, Y.; Si, B.C.; Hill, R.L.; Cui, L.L.; Liu, X.Y. Modeling of Soil Water and Salt Dynamics and Its Effects on Root Water Uptake in Heihe Arid Wetland, Gansu, China. *Water* **2015**, *7*, 2382–2401. [CrossRef]

Disclaimer/Publisher’s Note: The statements, opinions and data contained in all publications are solely those of the individual author(s) and contributor(s) and not of MDPI and/or the editor(s). MDPI and/or the editor(s) disclaim responsibility for any injury to people or property resulting from any ideas, methods, instructions or products referred to in the content.

MDPI
St. Alban-Anlage 66
4052 Basel
Switzerland
www.mdpi.com

Agronomy Editorial Office
E-mail: agronomy@mdpi.com
www.mdpi.com/journal/agronomy



Disclaimer/Publisher's Note: The statements, opinions and data contained in all publications are solely those of the individual author(s) and contributor(s) and not of MDPI and/or the editor(s). MDPI and/or the editor(s) disclaim responsibility for any injury to people or property resulting from any ideas, methods, instructions or products referred to in the content.



Academic Open
Access Publishing

mdpi.com

ISBN 978-3-0365-9704-1